On the cross-sectional form of the patella in several primates

Christopher David Stanford Jones
MAppSc, BAppSc

A thesis submitted for the degree of Doctor of Philosophy at the University of Adelaide,
Department of Anatomical Sciences

June 2003

Table of Contents

List of Figures

List of Tables

Abstract

This study was performed to investigate the patterns of morphometric variation of the primate patella in cross-section, in an attempt to understand further the influences upon bone morphology. Specimens were selected from *Homo*, *Gorilla*, *Cercopithecus* and *Colobus*. These genera were chosen to investigate variation in patellar form in primates that are (1) bipedal and quadrupedal, (2) large and small, and (3) closely and distantly related. Therefore, there was the potential to uncover morphometric patterns that reflected such influences as function, body size, sex differences and phylogeny, and the aims of this study were formulated to investigate these influences. Variables chosen for this study were based on the patellar outline on cross-sectional computed tomography images: elliptic Fourier amplitudes, and also the outline perimeter length and the area contained within the outline.

Ordination using principal component analysis and cluster analysis showed continuous distributions of specimens, and it appeared that the bulk of intragenus variation was based on patellar size differences. Although cluster analysis showed patellae from *Homo* and *Gorilla* on one hand, and *Cercopithecus* and *Colobus* on the other, to be clearly separated, there was no clear separation among genera: specimens at extremes on PCA tended to be clustered with the next genus. Given the large disparities in average body weights for these genera, it was expected that patellar size would differ widely. This pattern was present in nonhuman primates; humans represented a deviation from this pattern, having large patellae relative to average body weight; it was likely that this was due to larger forces associated with bipedal locomotion. Principal component analysis showed that morphometric variables were correlated to varying extents; there were strong correlations between the conventional variables, so that the specimens were linearly arranged, with an effective reduction in phenotype space from two dimensions to one. Although the dimension of Fourier variables could be reduced, two dimensions were required, which was in part reflective of the dominance of two of the ten variables; only seldom was reduction to one dimension possible. An inference of geometric similarity was made in some cases; in other cases, size differences were associated with shape differences, but no clear pattern of shape differences was seen. Specimens within genera were found to show sexual size dimorphism. Occasionally sexual shape dimorphism was found, but not so that results could be related to an influential factor (function, for example). Published average body weights suggested that patellar size dimorphism was a reflection of body weight dimorphism.

Thus, patellar size differences dominated the picture of morphological variation, and this reflected genus body weight averages, although function also prevailed, and human patellae were large considering body weight averages for *Homo*. Clear sexual size dimorphism reflected body weight dimorphism, but results for shape dimorphism did not appear to reflect functional differences assumed to exist between smaller and larger individuals. Although size and shape differences did follow a pattern that did not contradict phylogenetic relations, this was also explicable in terms of body size and function.

Declaration

THIS WORK CONTAINS NO MATERIAL WHICH HAS BEEN ACCEPTED FOR THE AWARD OF ANY OTHER DEGREE OR DIPLOMA IN ANY UNIVERSITY OR OTHER TERTIARY INSTITUTION AND, TO THE BEST OF MY KNOWLEDGE AND BELIEF, CONTAINS NO MATERIAL PREVIOUSLY PUBLISHED OR WRITTEN BY ANOTHER PERSON, EXCEPT WHERE DUE REFERENCE HAS BEEN MADE IN THE TEXT.

I GIVE CONSENT TO THIS COPY OF MY THESIS, WHEN DEPOSITED IN THE UNIVERSITY LIBRARY, BEING AVAILABLE FOR LOAN AND PHOTOCOPYING.

CHRIS JONES

JUNE 2003

Acknowledgments

The author would like to extend his gratitude to the following people:

Dr Ray Tedman, Department of Anatomical Sciences, who supervised this study

Prof. Maciej Henneberg, Department of Anatomical Sciences, who gave advice regarding primate biology and reviewed the thesis

Prof. Grant Townsend, School of Dentistry, University of Adelaide, who gave advice regarding Fourier analysis and reviewed the thesis

Mr Wesley Fisk and **Mr Stelios Michas**, Department of Anatomical Sciences, who gave assistance in obtaining human specimens

Ms Gail Hermanis and **Mr Chris Leigh**, Department of Anatomical Sciences, who gave assistance in the preparation of specimens

Dr Paula Jenkins and staff, British Museum (Natural History), London, who gave access to the nonhuman specimens

Ms Marion Tregeagle, Department of Imaging, Adelaide Women's and Children's Hospital, who produced the CT images of the human specimens

The staff of the X-Ray Department, Chelsea and Westminster Hospital, London, who produced the CT images of the nonhuman specimens

Dr Pete Lestrel, formerly of the School of Dentistry, University of California at Los Angeles, who gave advice on elliptic Fourier methods

Prof. William Jungers, Department of Anatomical Sciences, State University of New York at Stony Brook, who gave advice on allometric investigations

Mr Tavik Morgenstern, Department of Anatomical Sciences, for assistance with photography

Mr Phil Leppard, formerly of the Department of Mathematics, University of Adelaide, who gave advice regarding statistical design and analysis

Dr Mauro Cavalcanti, Setor de Paleovertebrados, Departamento de Geologia e Paleontologia, Museu Nacional do Rio de Janeiro, Brazil, who gave advice regarding jackknifed principal component analysis

Dr James Rohlf, Department of Ecology and Evolution, State University of New York at Stony Brook, who gave general statistical advice

My family, **Annette** and **Robert**, who gave me a reason for doing this

Chapter 1 Introduction

This study was performed in response to a broad research question regarding the forces that mould the patella. The initial impetus for this research was an idea that human patellar morphology may reflect injurious biomechanics, and that patellar form on radiological investigation may be diagnostic of patellofemoral dysfunction. However, it became clear that data relating to patellar morphological variation were scant, and that a broad investigation into the patterns of variation was in order. Given that the primate knee has a very general morphological pattern, and that knees of different primate taxa function in different ways, and under greatly varying forces due to body weight, the focus of this study extended to the patellae of several different primates; accordingly, specimens from *Cercopithecus* and *Colobus* (small, quadrupedal monkeys), and *Gorilla* (large, quadrupedal apes) were also included.

Patellae from dissecting-room cadavera (human) and from a museum collection (nonhuman) were used to generate computed tomographic images in the horizontal plane. Data from the outlines of these specimens were captured, and were used to investigate patterns of morphological variation. Development of a skeletal element like the patella is an epigenetic phenomenon, directed by the genome to suit the functional circumstances of the element. Factors that may influence this development are extraneous (for example, mode of locomotion), but rather than being superimposed on a genetic blueprint, they *complete* the blueprint. Genetic variation may also produce phenotypic variation, although in such a study this cannot be controlled for. However, as each genus under investigation is more closely related to one genus than the other two, and as genes are inherited, it was also possible, although not very likely, that phylogenetic relations might also influence patellar morphology. A broad aim of this study was to view morphometric data of the patella such that interpretation regarding the influence of these factors was possible. It was of interest to peruse the distribution of these specimens in phenotype space, to detect any data heterogeneities and any outlying specimens. Given that much variation may stem from the simple fact that some specimens were larger than others (due to differences in overall size), it was of interest to repeat this after an attempt to remove the effects of differing specimen size, to focus more on specimen shape; bone shape was of interest due to its potential association with mechanical factors. As the mechanical circumstances of the weight-bearing bones of larger animals are likely to be different to those of smaller animals, it was also of interest to detect any relation of patellar size and shape; this was investigated in the section on allometry. A good deal of morphological variation may also be due to the fact that some specimens were from female

individuals, and some from males; some morphological features may appear peculiar to males or females, which although not directly involved with reproduction, are seen to confer reproductive benefits to that sex. Accordingly, data from males and females were compared in investigations into sexual dimorphism.

The potential significance of such a study lies in the fact that the morphology of a bone reflects its developmental (both ontogenetic and phylogenetic) and functional history. A bone must be able to successfully and economically sustain forces due to function, and mechanisms are in place to allow adaptation to forces the bone endures. Bone morphology must also reflect the genetic makeup of the individual, which carries with it a rich heritage; where two or more different taxa share in part that heritage, it may be expected that the specimens in these taxa show correlated morphologies. Consequently, interpretations may be made, where the data allow, of the contribution of potential influences, increasing the understanding of patellar morphology in particular, and skeletal morphology in general.

Chapter 2 Review of the Literature

2.1 Structure, Function, Development and Variation

In order to understand the morphological variation in the primate patella, it is important to consider first the typical structure and function of the patella and surrounding structures; these will be considered in the first two sections, §2.1.1 Gross Anatomy and §2.1.2. Biomechanics of the Patella. While literature specific to development of the patella is limited, research on limb bone development is of much greater breadth and depth, and on identifying general concepts it will be seen that there exists much potential for morphological variation at any step in the development of this bone; these aspects will be covered in §2.1.3 Development of the Patella. The literature regarding phenotypic variation in general will then be reviewed in §2.1.4 Phenotypic Variation, with the aim of presenting possible causes for patterns of variation that may be seen within and among individuals in a population, as well as among populations.

By far the bulk of relevant scientific work on the knee has been directed at the human state, and this review will reflect this. As a matter of convenience, the main parts of these sections will describe the human condition, with details relevant to nonhuman primates (where available) presented separately.

2.1.1 Gross Anatomy

The patella is located on the dorsal side of the primate knee, within the substance of the quadriceps femoris muscle group. The patella articulates with the distal aspect of the dorsal femur, and through its connection via the patellar ligament is functionally connected to the tibia. This review will outline what is currently known of the gross morphology of the patella, the quadriceps and distal femur, with an emphasis (where possible) on variation of these structures.

2.1.1.1 Patella

The patella consists of a shell of cortical bone encasing a trabecular core (Fulkerson, 1997), and possesses dorsal, ventral, lateral, medial, proximal and distal aspects. (Although the descriptions cited here are mostly of the human patella, the anterior and posterior surfaces are

here termed dorsal and ventral, respectively, to be inclusive of primates where the former terms may be inaccurate; otherwise, anterior and posterior will be used.) The convex dorsal surface is marked by vascular channels and grooves for the anterior fibres of quadriceps femoris (Dahhan et al., 1981; Williams et al., 1989). Dahhan (1981) further divided the dorsal surface into three regions: an upper, rugose third, providing the attachment for the quadriceps tendon; a middle third, marked by vascular openings; and a lower, *v*-shaped third, providing an attachment for the patellar ligament. The dorsal surface is subcutaneous, separated from the skin of the knee by the prepatellar bursa (Williams et al., 1989). The ventral surface comprises articular and non-articular areas. The articular area, for articulation with the distal femur, makes up three-quarters of the ventral surface (Dahhan et al., 1981); the articular area is divided into medial and lateral sides by a bony vertical ridge (Dahhan et al., 1981; Dye, 1993; Williams et al., 1989), the median (hereafter just patellar) crest. Wiberg (1941) further divided the articular surface into seven areas: an 'odd' medial, strip-shaped facet (the odd facet), and medial and lateral pairings of inferior, middle and superior facets. Reider et al. (1981) stated a different opinion, that the patella may exhibit a transverse ridge crossing the medial and lateral facets, dividing the patella into proximal (larger) and distal (smaller) segments. The non-articular area of the patella makes up the distal quarter of its ventral surface (Dahhan et al., 1981; Dye, 1993); it is marked by vascular openings and is in close relation to the infrapatellar fat pad of the knee (Dahhan et al., 1981). The proximal pole of the patella serves as an attachment for the quadriceps tendon dorsally (Dahhan et al., 1981; Williams et al., 1989), and is closely related to the suprapatellar fat pad of the knee (Dahhan et al., 1981). The distal pole forms an attachment for the patellar ligament (Dye, 1993). The medial and lateral borders of the patella serve as attachments for soft tissues: the aponeurosis of the vastus muscles, the knee joint capsule, and the fascia lata (Dahhan et al., 1981).

Systematic investigations (i.e. those dealing with diversity) of the patella are scant, with most focusing on the human condition; moreover, the focus of the human studies has mostly been correlation with clinical presentation, rather than a study of variability as such. In humans, Wiberg (1941) proposed a classification system based on the position of the patellar crest relative to the medial and lateral borders in the horizontal plane (alternatively, breadth of articular facets) (Figure 2.1). This classification refers only to osseous – not chondral – form, as the shape of the ventral osseous surface need not correspond to that of the chondral surface (Hehne, 1990). In Type I, the crest is positioned in the midline, in Type III it is placed quite medially, with Type II between these two extremes. The classification system was not based on objective measurements, the designations being defined by "approximately in the centre" (I), "slightly toward the medial border" (II) and "hardly any room...for the medial facet" (III) (pp 332-3). Brattström and Ahlgren (1960) measured lateral patellar facet width relative to

medial facet width, and although they provided neither data nor statistical evidence, found that females have a greater relative lateral facet width. Cross and Waldrop (1975) calculated the 'patellar index' in a large number of subjects, that being a ratio between total patellar breadth and the difference between lateral and medial facet breadth; only means were presented, so their conclusion that this index is greater in females and/or individuals with patellofemoral pathologies lacked regard for intragroup variation. Grelsamer et al. (1994) investigated vertical articular surface height versus that of the (distal) nonarticular surface with the aim of relating form and pathology; they found that anterior knee pain patients tended to have a ratio of articular length to patellar length at extremes of range. Trinkaus (1983) found patellar sagittal depth ('thickness') to be greater in a sample of Neanderthal specimens when compared to a sample of recent human patellae. This finding was interpreted as reflecting a greater quadriceps moment arm (see §2.1.2.2) in Neanderthals (Miller and Gross, 1998; Trinkaus, 1983), but was not increased when considered relative to body weight (Trinkaus and Rhoads, 1999). Trinkaus (2000) investigated variation of patellar measurements, specifically of the medial and lateral articular facets in a group of recent human specimens; in all but two of 247 specimens, the lateral facet was broader than the medial facet, but rarely extremely so: in only two specimens was the breadth of the medial facet less than half of that of the lateral facet.

Fewer comparative data on patellar variation were found. de Vriese (1909) described the monkey patella as an elongated ovoid plaque, that of apes as a rounded quadrilateral plaque, and that of humans as a broad triangular plaque. Haxton (1944) measured the 'patellar index' of various orders, that being the breadth relative to the total length of the patella (a different patellar index to the above); these data were only presented as means, and only one value was given for Primates (45, the same as Insectivora and one less than Edentata). Aiello and Dean (1990) listed three differences between human and African ape patellae: human patellae are absolutely and relatively larger, vastus medialis attaches more distally on the medial border of the human patella, and the nonhuman patella has a flatter articular surface.

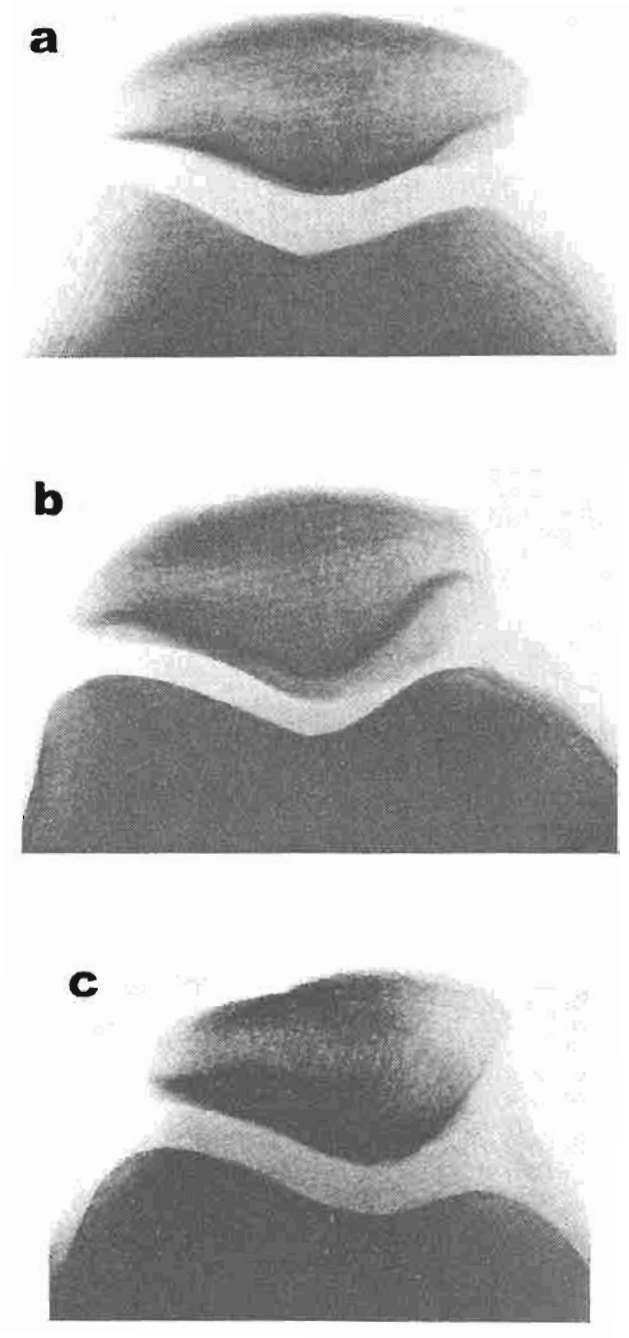

Figure 2.1. Wiberg's (a) Type I, (b) Type II and (c) Type III patellae (from Wiberg (1941))

2.1.1.2 Distal femur

The distal extremity of the femur is characterized by the lateral and medial femoral condyles. The lateral condyle is seen to be broader (in the coronal plane), and the medial condyle projects more distally (Brattström, 1964). This greater distal projection is due to the femoral bicondylar angle, which represents the obliquity of the femoral shaft relative to the plane of the condyles (Heiple and Lovejoy, 1971; Tardieu and Damsin, 1997; Walmsley, 1933) (see

Figure 2.2). Data for human bicondylar angles are given in Table 2.1. These data suggest a greater angle in females; whether this is related to sex-based differences in pelvic breadth (Tague, 1992) is not known (see Chapter 5).

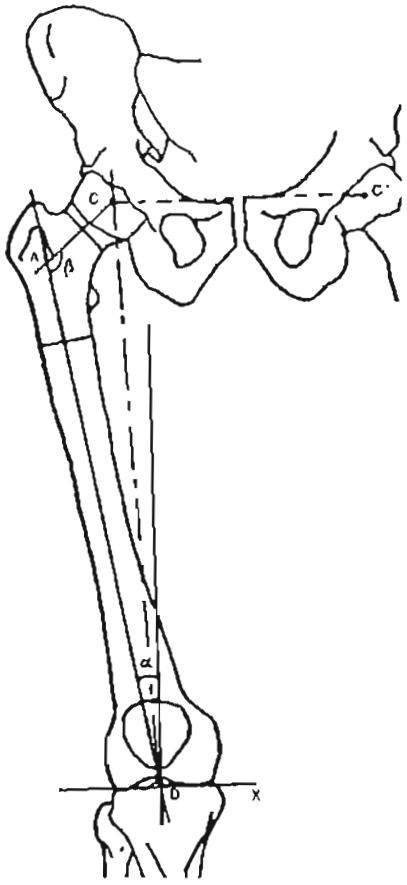

Figure 2.2. The bicondylar angle of the knee (α; from Tardieu and Damsin (1997))

Table 2.1. Mean human bicondylar angles

study	male	female
Parsons (1914)	9° (R), 9° (L)	10° (R), 11° (L)
Pearson and Bell (1919)	8.7° (R), 11.6° (L)	9.4° (R), 11.8° (L)
Kern and Straus (1949)	*8.1°	

*no data on sex or side

Few data exist for extant nonhuman primates. Kern and Straus (1949) gave an average for *Gorilla* of 4.4° (range −0.1° to 9.1°), and *Cercopithecus* species of 2.0° (−0.5° to 6.5°) (no data were given on sex or side). In general, there is an association between bicondylar angle value and degree of upright walking (Heiple and Lovejoy, 1971).

The dorsal (anterior) surface of the condylar part of the femur presents two facets, medial and lateral, for articulation with the patella (Dahhan et al., 1981). The lateral patellar facet is higher and broader, and projects dorsally more than the medial facet (Dahhan et al., 1981). The patellar surface is concave transversely and convex sagitally (Williams et al., 1989), forming what is known as the trochlea (Dahhan et al., 1981). The trochlea is separated from the tibial surfaces of the femoral condyles by two oblique grooves, medial and lateral (Williams et al., 1989). Human femora show a proximal extension of the lateral trochlear articular facet, whereas in apes the proximal extent of the articular surface is equal laterally and medially (Aiello and Dean, 1990).

The trochlea is concave side to side, but this concavity varies with position. The results of a computed tomography study (Schutzer et al., 1986), showed that the trochlea deepens, or becomes more concave, distally. The results of Farahmand and coworkers' (1998) study contradicted this, showing no such deepening. This discrepancy might have been due to method: in the former, cross-sections (in the transverse plane) were measured, while in the latter, tangential views (with changing planes) were measured. Nonetheless, these results bring to mind a statement by Wiberg, "the articular surface of the patella is in the main an exact cast of the femoral articular surface" (Wiberg, 1941 p320). As the patella translates on the trochlea, it is not necessarily clear which part of the femoral articular surface is aligned with which part of the patella. The ape femur shows a shallower trochlea when compared with that of humans, and in humans the lateral lip of the trochlea projects more dorsally (anteriorly) compared with the medial lip (Aiello and Dean, 1990; Heiple and Lovejoy, 1971; Wanner, 1977); it appears that the higher lateral lip buttresses the patella laterally (Heiple and Lovejoy, 1971).

2.1.1.3 Quadriceps femoris

The quadriceps is a four-part extensor of the knee, which attaches to the patella and proximal tibia. The distal aspects of this muscle will be discussed in greater depth than the proximal. The four parts of quadriceps arise as follows (Williams et al., 1989):

rectus femoris from the anterior inferior iliac spine (straight head) and just superior to the acetabulum and hip joint capsule (reflected head);

vastus lateralis from the femoral intertrochanteric line, anterior and distal borders of the greater trochanter, lateral lip of the gluteal tuberosity and proximal half of the lateral lip of the linea aspera of the femur;

vastus intermedius from the proximal two-thirds of the anterior and lateral aspects of the femoral shaft and distal part of the lateral intermuscular septum of the thigh; and

vastus medialis from the intertrochanteric line, spiral line, medial lip of the linea aspera, proximal aspect of the medial supracondylar line of the femur, the medial intermuscular septum of the thigh and from the tendons of adductors longus and magnus

This is the description as given in Gray's Anatomy; this description is not unchallenged, and arguments have been presented in favour of adding to the traditional description. In their study using amputated limbs, Lieb & Perry (1968) made a distinction between the proximal and distal fibres of vastus medialis. They designated the proximal, more vertical portion vastus medialis longus (VML), and the distal, more horizontal portion vastus medialis oblique – or obliquus – (VMO). Weinstabl et al. (1989) agreed with this terminology, and as a result of their cadaveric dissections they designated vastus lateralis accordingly – vastus lateralis longus (VLL), and vastus lateralis obliquus (VLO). Thus, to further add to the description of muscle origins:

vastus lateralis obliquus originates (at least partially) from the lateral intermuscular septum of the thigh (Hallisey et al., 1987); and

vastus medialis obliquus originates from the medial intermuscular septum of the thigh and adductor magnus tendon (Bose et al., 1980; Conlan et al., 1993), as well as the adductor longus tendon (Bose et al., 1980)

The muscles then converge on the patella as the quadriceps tendon. This has been shown to be a multilayered structure, having two, three or four laminations (Zeiss et al., 1992). The description given in Gray's Anatomy is that the fibrous tendon of quadriceps inserts into the tibial tuberosity, with the patella lying in the substance of the tendon (Williams et al., 1989). The tissue between patella and tibial tuberosity is therefore called the ligamentum patellae (or patellar ligament) (Williams et al., 1989). In other words, the patellar ligament is a continuation of the fibres of the quadriceps tendon; this has the implicit assumption that fibres surround, rather than attach to, the patella. This is a view shared by others: explicitly by

Dobbie and Ryerson (1942) and Hey Groves (1931) and implicitly by Ahmed et al. (1983) and Bennett et al. (1993). Anatomical dissection has shown a more complex state; there is much to say that the quadriceps tendon and the patellar ligament are not wholly continuous (Evans et al., 1990, 1991; Reider et al., 1981): this is due to the characteristic attachment (and thus termination) of ligament/tendon fibres (see below).

Rectus femoris becomes tendinous 5 to 8cm proximal to the patella (Reider et al., 1981), then either all (Reider et al., 1981) or only the more superficial fibres (Dahhan et al., 1981) pass over the patella to become continuous with the patellar ligament. Vastus lateralis and medialis become tendinous 3 to 6cm and only several millimetres proximal to the patella, respectively (Blauth and Tillmann, 1983; Reider et al., 1981) (no data were found for vastus intermedius). Fibres of the lateralis tendon attach to the proximolateral margin of the patella, or contribute to the patellar ligament and/or lateral patellar retinaculum (Blauth and Tillmann, 1983; Hallisey et al., 1987; Reider et al., 1981). Fibres of the medialis tendon either attach to the proximal half of the medial patellar border, or contribute to the medial patellar retinaculum (Blauth and Tillmann, 1983; Bose et al., 1980; Conlan et al., 1993; Farahmand et al., 1998; Reider et al., 1981). Vastus intermedius attaches to the proximal pole of the patella, or blends with the fibres of the other vasti, but "never" continues over the anterior patellar surface (Reider et al., 1981 p353). Thus it appears that the fibres of the quadriceps tendon do not simply continue as those of the patellar ligament. In a series of cadaveric dissections, Reider et al. (1981) found that only rectus femoris (and occasionally – and minimally – vastus lateralis) contributes fibres that continue distally over the dorsal aspect of the patella into the patellar ligament. The descriptions of the patellar ligament, as issuing from the distal pole of the patella given by Cooper and Misol (1970), Dahhan et al. (1981) and Dye (1993), accord with Reider and coworkers' findings.

Few data are available for the quadriceps muscles in nonhuman primates. The quadriceps muscles are generally the same in nonhuman primates as humans (Stern, 1971b). An interesting finding is that of the primate suprapatella, a cartilage-like (midway between hyaline cartilage and fibrocartilage) pad found in the vastus intermedius tendon just proximal to its attachment to the patella (Jungers et al., 1980; Stern, 1971b; Walji and Fasana, 1983). This has been found in Cebid monkeys (Stern, 1971b), *Lemur fulvus* (Jungers et al., 1980), *Cercopithecus aethiops* and *Papio cy. nocephalus* (Walji and Fasana, 1983). It is thought that the pad develops due to compressive stress in the quadriceps tendon during the initial (hyperflexed) phase of leaping (Jungers et al., 1980; Walji and Fasana, 1983). Stern (1971a) found differences in the extents of the origins of the vastus muscles between different species

of New World monkeys; he found that leaping species showed smaller areas of muscle origin, and longer muscle fibres.

2.1.1.4 Fibrous tissues

Fibrous tissues attaching to the patella may originate from other fibrous tissues (fascia lata, iliotibial tract), muscle/tendon units (vasti lateralis and medialis) and bone (femoral condyles and epicondyles). In the latter group are fibres from the knee joint capsule. A comprehensive review of different researchers' findings reveals either much structural variation and/or disagreement in descriptions, and in the case of the latter it is beyond the scope of this study to judge the merits of one description relative to another. One confounding factor in the naming of structures is that there appears to be no obvious distinction between retinacula and ligaments: both retinacula and ligaments are recognized, and while the former typically arise from soft-tissues and the latter from bone, some 'retinacula' arise from bone. It is important to note the extent to which fibrous tissues attach to the patella, as these will affect its function as well (potentially) as its morphology. Parapatellar retinacula issue from the vasti lateralis and medialis tendons (Brattström, 1964), the iliotibial band/fascia lata (Blauth and Tillmann, 1983); Fulkerson and Gossling, 1980; Hallisey et al., 1987; Reider et al., 1981), and the femoral epicondyles (Blauth & Tillmann, 1983; Kaplan, 1962). Fibres may then attach to the patella (Blauth and Tillmann, 1983; Brattström, 1964; Fulkerson and Gossling, 1980), the patellar ligament (Fulkerson and Gossling, 1980), or the tibia (Brattström, 1964). Patellar ligaments (patellofemoral, patellomeniscal and patellotibial) have been described as thickenings of the knee joint capsule (Dahhan et al., 1981; Kaplan, 1957; Reider et al., 1981), or as structures superficial (and distinct) from the capsule (Conlan et al., 1993; Fulkerson and Gossling, 1980; Seebacher et al., 1982;Warren and Marshall, 1979).

2.1.1.5 *Q*-angle

The human knee is located medial to the hip, so that the foot (and therefore the base of support) can be placed close to the line of gravity (Tardieu and Damsin, 1997; Tardieu and Trinkaus, 1994), so that less work is required to maintain balance during the single support phase of gait (Fulkerson, 1997). This adducted position of the femur, and therefore more efficient bipedal gait, is allowed (in part) by the femoral bicondylar angle (Heiple and Lovejoy, 1971; Tardieu and Damsin, 1997; Tardieu and Trinkaus, 1994) and the angle of inclination of the femoral neck (Anderson and Trinkaus, 1998). As the quadriceps act in line

with the shaft of the femur, (with an oblique alignment), the line of force from the bellies of the quadriceps muscles too lies obliquely (Fulkerson, 1997). In normal standing, with the knee extended (and tibia laterally rotated (Hungerford and Lennox, 1983) – but see §2.1.2.1), the tibial tuberosity lies lateral to the line of quadriceps force, such that an angle (open laterally) is formed between the line of the quadriceps, and the line of the patellar ligament. This angle is known as the *Q*-angle (Insall et al., 1976; Malkin, 1932) (Figure 2.3), and is of potential importance to the structure and function of the knee, as this angle produces a resultant lateral force vector when the quadriceps are active (Fulkerson, 1997) (Figure 2.4).

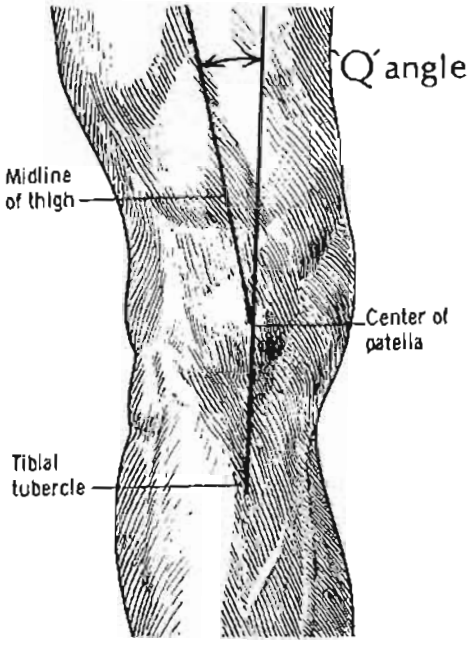

Figure 2.3. The clinical *Q*-angle defined (from Insall et al. (1976))

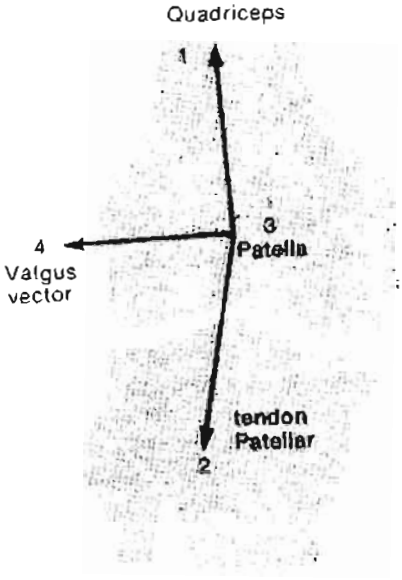

Figure 2.4. Quadriceps and patellar ligament (tendon) forces acting on the patella, with a resultant lateral (valgus) vector (from Fulkerson (1997))

Values of the *Q*-angle considered 'normal' are unclear. Malkin (1932) felt that the value for women is larger than that for men, but recorded no values. Supine values for males and females, respectively, have been recorded, as shown in Table 2.2.

Table 2.2. Mean human *Q*-angle values

study	male	female
Aglietti et al. (1983)	14°	17°
Fairbank et al. (1984)	10°	16°
Guerra et al. (1994)	8°	14°
Horton & Hall (1989)	11°	16°
Woodland & Francis (1992)	13°	16°

An explanation of wider female hips causing a greater knee valgus angle and *Q*-angle (Outerbridge, 1964) has been contradicted by Horton and Hall (1989), who indeed found sex-based differences in *Q*-angle, but failed to detect an increase in hip width (between greater trochanters) in females. These findings are supported by those of Kernozek and Greer (1993) who failed to detect any relationship between hip width and *Q*-angle. The *Q*-angle may be influenced by femoral neck anteversion and tibial extorsion (Fabry et al., 1994; Insall et al., 1976), hip rotation, foot position (Kernozek and Greer, 1993; Olerud and Berg, 1984), testing

posture (supine or standing) (Woodland & Francis, 1992), and whether the quadriceps are relaxed or contracted (Guerra et al., 1994).

Two points relevant to the present study must be emphasized here. Firstly, the *Q*-angle is of importance when considering the function and morphology of the patella; the oblique alignment of the quadriceps contributes to lateralization of forces acting on the patella (Fulkerson, 1997). Variations in this lateral force have been considered in experiments and calculations to determine forces in the patella and patellofemoral joint (see §2.1.2.3). Secondly, measurements using bony landmarks in lieu of muscle attachments suffer from inherent inaccuracies due to variability in location of attachment sites relative to these landmarks (Duda et al., 1996). Moreover, the proximal end of the quadriceps line is defined as the anterior superior iliac spine, which aside from being a readily palpable landmark forms no obvious relation with either the line of the quadriceps or that of the femur. Thus, the *precise* measurement of the *Q*-angle as directed by Insall et al. (1976) is probably meaningless, which should not overshadow the very meaningful concept of quadriceps obliquity as described by (Malkin, 1932).

From the above, it may be summarized that the human patella is likely to experience lateral forces which will vary both within individuals (through knee flexion, and with altered states of tibial rotation), and between individuals (due to variation in femoral and tibial angulation and torsion, as well as foot posture and movement patterns of the lower limb as a whole).

2.1.2 Biomechanics of the Patella

The patella is an integral part of the extensor mechanism of the knee, which may be active in both knee flexion and extension. How individuals in each species use their knee extensors will depend on their gait pattern. Almost all of a voluminous literature on knee function relates to the human state, and this bias will be reflected in this review. It will be of interest to consider both how the patella is displaced during knee function (kinematics), as well as the forces acting on the patella (kinetics). Discussion of the role of the patella will help to further elucidate the forces imposed on the patella, and will be presented as a preface to the section on kinetics. Some details of patellar stability will show that patellar forces are likely to be highly dependent on whether or not those forces displace the patella from the trochlea. Details of the primate knee (hindlimb, at least) will also be presented. Finally, the structural requirements of bones in general will be reviewed, with an attempt to state the requirements

of the patella and to provide some background for later discussion on bone morphology and function.

2.1.2.1 Kinematics of knee function

The patella moves in concert with the tibia (which moves on the femur), so it is of relevance here to consider the kinematics of the knee in general. Knee flexion and extension are achieved by a concurrent rolling and sliding of the femoral condyles on the tibial condyles: as flexion occurs, the femur rolls back and slides forwards, and vice versa for extension (O'Connor et al., 1990). Knee flexion has historically been considered to occur with concurrent tibial medial rotation (and extension with lateral rotation) (Hallén and Lindahl, 1966; Rajendran, 1985). However, kinematic studies have shown wide variation in tibial rotation during flexion and extension, such that concurrent rotations (for either flexion or extension) may be medial, lateral or no rotation at all (Hallén and Lindahl, 1965).

In full knee extension, the patella has not yet articulated with the trochlea (Elias et al., 1990). With knee flexion, the patella moves due to its attachment to the tibia via the patellar ligament (Fulkerson, 1997). From an initial position on the anterior distal femur it sinks into the intercondylar region of the femur (Hungerford and Barry, 1979; Kaufer, 1979); the path is complicated by medial and lateral tilt and translation of the patella, due to femoral condyle geometry and pull of medial and lateral soft-tissues (Heegaard et al., 1994; Hirokawa, 1991; Hungerford and Barry, 1979; Lin et al., 2003). The influence of these soft-tissues appears to be limited to early extension, prior to the patella engaging firmly with the trochlea (Heegaard et al., 1994). It also appears that tibial rotation affects patellar kinematics; (Hefzy et al., 1992) found that increasing lateral tibial rotation shifted the pattern of tilt and shift laterally (i.e. increased lateral tilt and shift and decreased medial tilt and shift) compared to that with medial tibial rotation.

As the knee flexes, the patellofemoral contact zone (on the patella) moves from a distal position in a proximal direction, and the area of contact increases in size (Goodfellow et al., 1976; Heegaard et al., 1995; Hehne, 1990; Huberti and Hayes, 1984; Hungerford and Barry, 1979). Medial and lateral contact areas have been shown to increase with medial and lateral tibial rotation, respectively (Hefzy et al., 1992). The odd facet has only been found to contact the femur near full flexion, where the patella articulates with the femoral condyles rather than the trochlea (Goodfellow et al., 1976; Hehne, 1990).

During human walking, the knee performs a sequence, starting in full extension, of flexion on heel strike (to approximately 20°), followed by a return to near-full extension, then flexion to around 60°, and back to full extension for the next stride (Perry, 1992) (Figure 2.5). The stance phase of gait is of more importance here (as this is the weightbearing phase). This is characterized by the first flexion-extension sequence (the remaining flexion-extension sequence takes place during the swing phase of gait) (Perry, 1992). There are very few data on the kinematics of gait for nonhuman primates. Vilensky and Gankiewicz (1990) found that a *Cercopithecus aethiops* individual, when running on a treadmill, showed a pattern of knee motion as follows: from 'extension' (approximately 45° flexion), the knee flexed (to approximately 70°), followed by extension (back to 45°), then a greater flexion (to approximately 85°), then back to 'full' extension for the next cycle. It was not clear which part of this was stance phase and which was swing phase, although like the human pattern this too followed a sequence of flexion-extension-flexion-extension. Notwithstanding this, it is clear that the knee of *C aethiops* typically flexes (during walking anyway) more than the human knee.

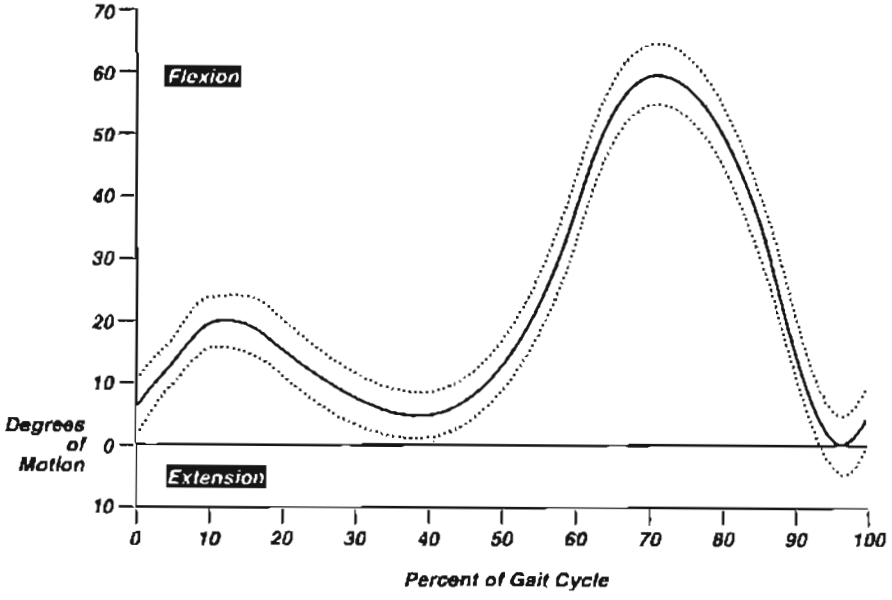

Figure 2.5. Range of sagittal plane tibiofemoral movement during the human gait cycle (0% represents heel-strike; from Perry (1992))

2.1.2.2 Role of the patella

A superficial view of the role of the patella is that it somehow aids action of the knee extensors, and that its presence is therefore beneficial to the individual; a popular view is that the knee acts as a simple lever acted upon by the pulley-like extensor mechanism, and that the anterior displacement of the line of the quadriceps caused by the patella increases the mechanical advantage of the quadriceps (DePalma, 1954; Hungerford and Barry, 1979; Kaufer, 1971; Nordin and Frankel, 1989; Smillie, 1971). The patella thus acts as a spacer, displacing the line of action of quadriceps anteriorly (Kaufer, 1971; Yamaguchi and Zajac, 1989). In this scenario, quadriceps tendon force should equal that of the patellar ligament (Alexander and Dimery, 1985; Fulkerson, 1997). However, rather than wrapping around the distal femur, the patella contacts the femur at a point, and this point varies through range; therefore tensions in the quadriceps tendon and in the patellar ligament vary relative to each other to balance their respective moments (Bishop, 1977; Bishop and Denham, 1977; Hehne, 1990; Huberti et al., 1984; Maquet, 1984; van Eijden et al., 1987). For this reason, the patella has been likened to a balance-beam, in that for a system to be in equilibrium, forces at either end of the beam must change with changing position of the pivot point (Buff et al., 1988) (Figure 2.6). If L/Q represents the ratio of patellar ligament force (L) to that of the quadriceps tendon (Q), it has been found (generally – differences exist between these studies, but these are beyond the scope of this review) that L/Q has its maximum (> 1) near full extension, and with increasing flexion L/Q decreases (< 1) (Ahmed et al., 1987; Buff et al., 1988; Grood et al., 1984; Hirokawa, 1991; Huberti et al., 1984; van Eijden et al., 1987). In terms of mechanical advantage, the quadriceps has greatest efficiency for a given patellar ligament tension in or near extension. In greater degrees of flexion (around 60° (Huberti et al., 1984)), L/Q equals less than unity, and a statement like "...[the patella] aids knee extension by producing anterior displacement of the quadriceps tendon throughout the entire range of motion..." (Nordin and Frankel, 1989 p128) missed this point. Furthermore, the spacer effect of the patella was calculated to only affect mechanical advantage of the quadriceps at flexion angles less than 35°, beyond which only the balance-beam effect is of influence (Yamaguchi and Zajac, 1989). The mechanical role of the patella is therefore as both a spacer and a lever (or balance-beam) (Yamaguchi and Zajac, 1989).

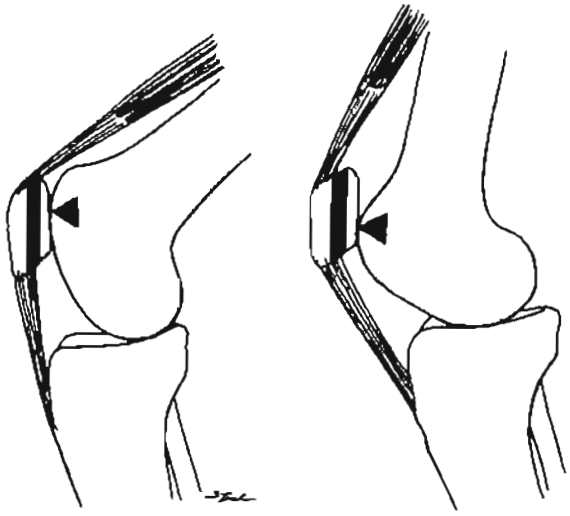

Figure 2.6. The patella as a 'balance-beam', showing point of patellofemoral contact (arrow head) (from Buff et al. (1988))

It must be asked whether an ideal mechanical advantage is simply as high as possible; a mechanical advantage greater than unity means that the force of effort may be reduced for a given load, but this comes with the trade-off of a slower joint rotation (Alexander and Dimery, 1985; Demes and Günther, 1989). Moreover, a greater quadriceps mechanical advantage does not necessarily result in more powerful extension (as supposed by Anemone (1993)), as power is the rate at which force is produced. If a rapid joint rotation is required, the speed of muscle contraction could be increased, but with increased metabolic cost to the individual (Alexander and Ker, 1990). The speed of rotation conferred by a mechanical advantage less than unity will not necessarily be a better solution for increased power (especially as muscle force would also need to increase), but there is no evidence to suggest that a high mechanical advantage is automatically advantageous.

2.1.2.3 Kinetics of patellar function

The forces experienced by the patella are of interest in the present study, as a theoretical link may be drawn between such forces and the morphology of the patella. The kinetics of the femur and tibia are not of relevance here, and will be omitted.

The patella may be represented in the sagittal plane (ignoring medial and lateral forces for now) as a beam that contacts the trochlea at a discrete point (Amis and Farahmand, 1996; Hayes and Snyder, 1981). The patella is subjected to forces from the pull of fibrous tissues

(quadriceps tendon and patellar ligament) as well as compression against the trochlea. Consequently, it is predicted that the stresses experienced by the patella consist of bending stresses with superimposed axial tension (Hayes and Snyder, 1981). It has been calculated that the most dorsal part of the patella should experience tensile stresses, with compressive stresses more ventrally with a maximum in the subchondral region (Carpenter et al., 1994; Goldstein et al., 1986; Han, 1999; Hayes and Snyder, 1981; Oxnard, 1971). Medial or lateral forces should also influence patellar stresses. Minns and associates (1979) calculated that, in addition to the compressive stresses occurring at the patellofemoral contact point, tensile stresses may also predominate depending on the direction of quadriceps forces; for example if the pull of quadriceps is lateralized, the medial aspect of the patella would experience tensile forces. The relatively distal attachment of vastus medialis should allow this muscle to exert a medially directed force on the patella (Hehne, 1990), but the contribution of vastus medialis to patellar stresses appears not to have been investigated.

During knee flexion, the patella is compressed against the trochlea by the tension in the quadriceps tendon and patellar ligament (Fu et al., 1993; Maquet, 1984). This compressive force is known as the patellofemoral joint reaction force (Hungerford and Lennox, 1983) (Figure 2.7) and for equilibrium to exist, this must equal the sum of the ventrally directed components of the quadriceps tendon and patellar ligament forces (Amis and Farahmand, 1996). In weightbearing activities, the limb segment that contacts the ground (or substrate) exerts a force on the ground, which by Newton's third law of motion exerts an equal and opposite force on the limb segment; this is known as the ground reaction force (LeVeau, 1992) (Figure 2.8). In weightbearing, the patellofemoral joint reaction force increases with increasing flexion, as the flexion moment (of body weight, or alternatively of the ground reaction force) moves increasingly posteriorly, and the quadriceps tendon and patellar ligament (especially the quadriceps tendon (van Eijden et al., 1985)), which serve to compress the patella against the trochlea, come to lie more perpendicular to the joint surface (Amis and Farahmand, 1996; Hungerford and Barry, 1979) (Figure 2.9). Thus, the compression force increases as the patellofemoral contact area too increases (§2.1.2.1), and therefore contact pressures (force per unit area) are kept lower than they otherwise would be during flexion (Hehne, 1990; Hungerford and Barry, 1979). Hehne (1990) investigated the forces on the medial and lateral patellar facets individually, and found a 60% increase in both contact force magnitude as well as area during flexion from full extension, such that contact pressures were equal. These findings echoed those of Huberti and Hayes (1984), who found contact pressures during flexion to be uniform over the whole contact area, although Heegaard et al. (1995) found higher lateral facet pressure in full extension. A limit to this pattern is the contact between the quadriceps tendon and the femur ('tendofemoral' contact) beyond 90° knee

flexion (Goodfellow et al., 1976; Huberti and Hayes, 1984). Such sharing of compression between the patellofemoral joint and the tendofemoral 'joint' thus decreases the stresses borne by the former (Ahmed et al., 1983; Huberti and Hayes, 1984). It is also likely that in primates that exhibit leaping, the suprapatella contacts the femur during extreme knee flexion (Jungers et al., 1980) and similarly shares the compressive load.

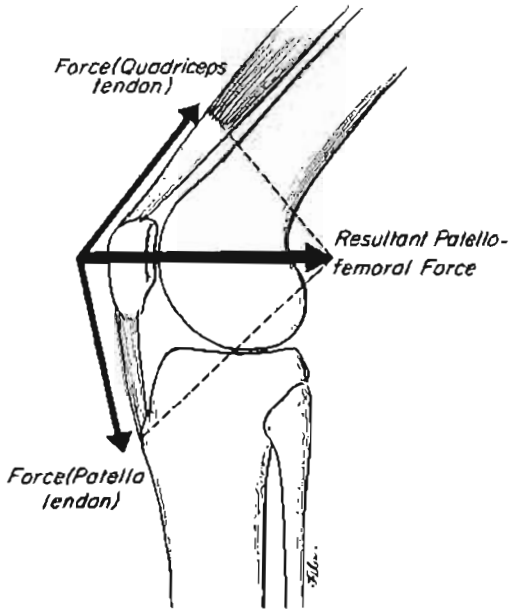

Figure 2.7. Patellofemoral joint reaction force as a resultant of quadriceps tendon and patellar ligament (tendon) forces (from Fu et al. (1993))

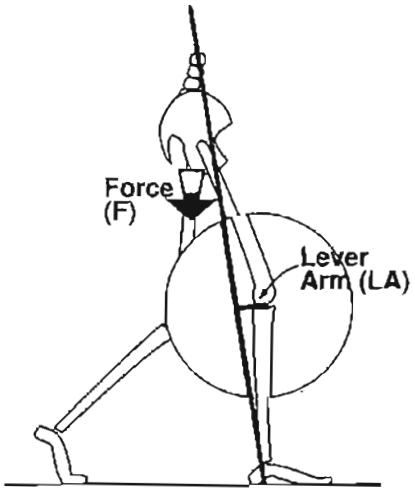

Figure 2.8. Ground reaction force (heavy line) due to force of body weight producing a knee flexion moment (acting through lever arm) (from Perry (1992))

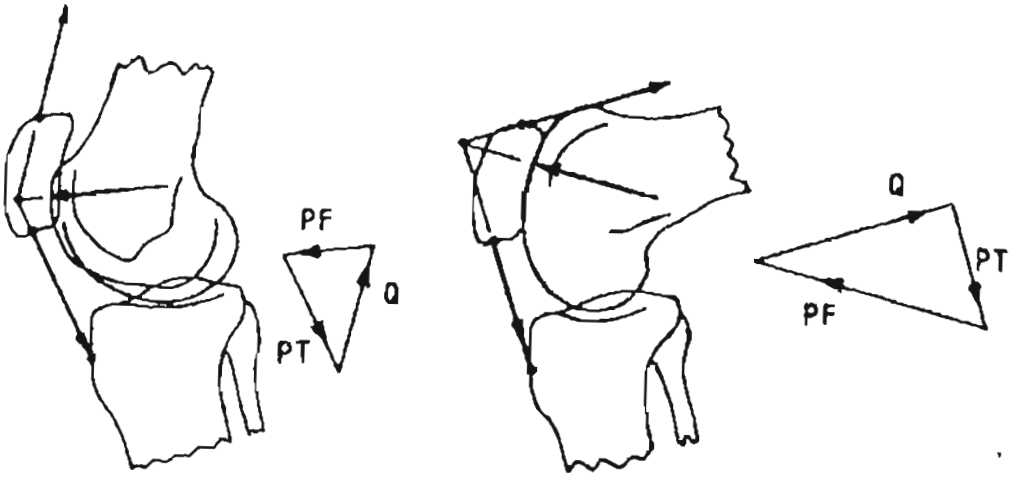

Figure 2.9. Patellofemoral joint reaction force (PF) as a function of knee flexion angle (quadriceps and patellar ligament forces, Q and PT, respectively) from Amis and Farahmand (1996))

Kinetic data on primate knee function appear scarce, and extrapolation from data on one taxon in one set of circumstances to different taxa in different circumstances may be imprudent. For example, Schmitt (1999) found that arboreal monkeys were able to make the direction of the ground reaction force vector more oblique by reducing the vertical force component; gross estimation of moments (for example, knee flexion always increases knee flexion moment, based on the human condition) would therefore be erroneous.

During human walking, the activity of the vasti differs markedly from that of rectus femoris. The vasti are active in the early part of the stance phase, where they work eccentrically to limit knee flexion (Perry, 1992). Rectus femoris is found to be active in the latter part of stance, again working eccentrically, to limit hip extension and knee flexion (Perry, 1992).

2.1.2.4 Stability of the patella

Patellofemoral stability is an important concept in this review, as it is likely that an inherently unstable patella will experience different stresses compared with one of normal stability. Factors that contribute to medial-lateral patellofemoral stability include bony factors (size of lateral femoral condyle, *Q*-angle, shape of articular surfaces) and soft-tissue factors (size and strength of vastus medialis obliquus, tightness of lateral retinaculum) (Halbrecht and Jackson,

1993). Lack of stability may present as an acutely dislocated patella (due to a single incident) (Halbrecht and Jackson, 1993), or as a chronic subluxation and/or dislocation (Fulkerson and Cautilli, 1993).

Three clinical presentations (two stable, one unstable) help to illustrate the unpredictable nature of the contribution of forces to the patella by certain structures. First is the normally stable knee: lower limb anatomy is normal, and the patella glides in the trochlea, experiencing stresses as outlined above. Second is the chronically subluxating/dislocating patella, which tracks abnormally in the trochlea due to a tight lateral retinaculum (Fulkerson and Cautilli, 1993). Third is the stable patella, with increased lateral pull (tight lateral retinaculum, weak vastus medialis obliquus), which presents with the lateral patellar compression syndrome (Merchant, 1993). This syndrome involves an increased lateralization of forces, but without subluxation or dislocation of the patella, to increase stress on the lateral facet (Ficat et al., 1975). Consequently, with increased lateral forces, the level of stress experienced by the lateral facet should depend on the stability of the joint.

2.1.2.5 Primate knee function

Function of the lower limb, and in particular the knee, is of great importance, as it will be seen that locomotor and postural influences have the potential to affect morphology (Fleagle, 1988; Oxnard, 1983a; Preuschoft, 1979). This review is an attempt to summarize important similarities and differences in locomotion and posture among the primates investigated here. Locomotion is the gross displacement of the individual's body mass with respect to the physical surroundings, with posture being the state of relative stability between one's mass and surroundings (Prost, 1965). The range of postural and locomotor activities exhibited by an animal makes up its positional repertoire (Rose, 1973).

As a means to efficiently describe an animal's locomotion, the investigator may use terms such as 'quadrupedal walker' and 'leaper'; the efficacy of such terminology depends in part on the purpose of its use (Oxnard, 1983a). While a descriptive term may be used legitimately for a diverse range of animals, the term may not encompass the diversity of these animals and would thus be insufficient if describing that diversity were the investigator's goal. Primates grouped together according to locomotor pattern may show striking locomotor differences (Ashton and Oxnard, 1964; Stern and Oxnard, 1973). For example, the designation 'arboreal quadruped' may encompass many diverse movement patterns, for example branch-running versus climbing (Oxnard, 1983a). Another term that may confound this diversity is that of

'leaper'. While no monkey is a true leaper (Rodman, 1979) (the term is usually reserved for certain prosimians), other primates do leap, but in different ways. Those primates designated as leapers may show differences in the amount of leaping they perform, and the functional pattern of leaping may differ between groups (Oxnard, 1983a). For example, the langur (*Presbytes*) has been found to leap with either a preceding run-up or 'pumps' up and down to increase the momentum of leaping (Ripley, 1967). Higher primates that leap tend to do so in descent, rather than the ascent common to prosimians, and show different patterns of leaping (Oxnard, 1983a). For example, the description given by Fleagle (1976) of the 'leap' of the siamang is one of a controlled fall, whereby the propulsive force is generated in part by the upper limbs and also the recoil of the supportive branches. Furthermore, primates tend not to move themselves by one mode of locomotion (Fleagle, 1988), and it will be seen that groups exhibit a number of different positional modes. In response to these inadequacies, Oxnard (1983a) derived the concept of a regional functional spectrum, whereby groups of animals may be represented along a continuum, and these groups are sited on this continuum according to the relative prevalence of a particular function. This enables the investigator to compare groups of animals according to the relative amounts of different functional modes.

In an effort to broadly describe similarities and differences at the genus level, the following locomotor classification has been adapted from Rose (1973). Quadrupedal primates typically walk, run and leap (locomotion) and sit, stand and suspend (posture), and these positional behaviours take place on the ground or in vegetation. *Colobus* and *Cercopithecus* exhibit arboreal quadrupedalism, the positional behaviour of which in general takes place in the small branch setting. They are both of large size, so that positional behaviour is specialized for equilibrium in relation to the small size of the branches. *Cercopithecus* fall into the category of branch sitting and walking, the general features of which are walking, running and leaping (locomotion) and mainly sitting (posture). *Colobus* are found in the category old world semibrachiation, which is similar to branch sitting and walking but includes specialization in regard to leaping and climbing. Gorillas on the other hand show terrestrial quadrupedalism with knuckle walking, the general features of which include quadrupedal walking, running and bipedalism (locomotion) and sitting, squatting and quadrupedal standing (posture). Humans will be summarized here as bipedal walkers (Fleagle, 1988).

Cercopithecus species operate in a diverse range of habitats, from terrestrial to arboreal (Manaster, 1979; Rollinson and Martin, 1981). Cercopithecines show varying degrees of walking, trotting, galloping and leaping (McGraw, 1996; Rollinson and Martin, 1981). *Cercopithecus aethiops* shows some terrestriality (20%) and leaping (10%), with others also engaging in leaping (Ashton and Oxnard, 1964; Fleagle, 1988; Manaster, 1979; McGraw,

1996; Oxnard, 1983a; Struhsaker, 1969). *Cercopithecus mitis* is semiarboreal, semiterrestrial (Ashton and Oxnard, 1964; Oxnard, 1983a). *Cercopithecus neglectus*, as one of the largest guenons, is a slow quadruped, and the most terrestrial (Fleagle, 1988; Rollinson and Martin, 1981), although Ashton and Oxnard (1964) found them to be more arboreal than *C. aethiops* when provided with the opportunity. *Cercopithecus mona* and *C. nicititans* typically move quadrupedally on small branches, and are able to make large leaps, landing on the hind limbs (Ashton and Oxnard, 1964; Struhsaker, 1969). *Cercopithecus campbelli* is mainly a quadrupedal walker, with decreasing levels, respectively, of climbing, running and leaping (McGraw, 1996).

Colobus monkeys spend most of their time resting or feeding, with locomotion occurring in short spurts (Mittermeier and Fleagle, 1976). Colobine monkeys are generally more arboreal, and better at leaping, than cercopithecines (Ashton and Oxnard, 1964; Fleagle, 1988; Mittermeier and Fleagle, 1976; Stern and Oxnard, 1973). The guerezas (the largest colobines – *C. guereza*, *C. polykomas*, *C. angolensis*) are more frequently quadrupedal walkers, but also run and leap (Fleagle, 1988; McGraw, 1996; Mittermeier and Fleagle, 1976). Leaping may be preceded by a run-up or recoil of bent branches, but they can also leap from a standing start; landing may be on hindlimbs only, or both hindlimbs and forelimbs, but they tend to favour flexible (impact-absorbing) landing spots (Mittermeier and Fleagle, 1976). *Colobus badius* is smaller than *C. guereza* (Fleagle, 1988), and shows more leaping than *C. polykomos* (McGraw, 1996).

Gorillas are among the most terrestrial of all primates, and move by quadrupedal walking and running (Ashton and Oxnard, 1964; Doran, 1997; Fleagle, 1988). Lowland gorillas (*Gorilla gorilla gorilla*), even the larger males, do spend some time in trees (Fleagle, 1988; Remis, 1995).

2.1.2.6 Mechanical properties of bones

The success of bones in fulfilling their role as mechanical supports is dependent on their mechanical properties, which are material and structural (Nigg and Grimston, 1994). Material properties are of bone tissue, and while they have the potential to affect mechanical properties (van der Meulen et al., 2001), they are not of direct relevance to this study. Structural properties, those peculiar to an individual bone, are of direct relevance here, as it may be expected that external gross form of a bone, in part at least, determines its structural properties (Currey, 2003; Frankel and Burstein, 1965; Jungers and Minns, 1979; Lovejoy et

al., 1976; Preuschoft and Weinmann, 1973; Ruff, 1990; Schaffler et al., 1985; van der Meulen et al., 2001).

A structure in engineering is a device that bears loads (Francis, 1980; Gere and Timoshenko, 1997), which is indeed what bones do. The general aims of structural design (and here this includes biological development) include producing a structure that is functional and economical (Francis, 1980; Schodek, 1980). The structure (bone) must perform its intended function, without failing due to normal loads. Therefore, a basic criterion which bones must meet is that they should not fail either by repetitive loading (fatigue failure) or by a single overload (monotonic failure) during normal functional loading (Biewener, 1990; Currey, 2003; Lanyon, 1981, 1987). The structure must also be economical – an excess of bone tissue may ensure functionality (at least structural stability), but will be expensive to produce and maintain, and to transport (Biewener, 1990; Currey, 2003; Dellanini, 2003).

Accordingly, the morphology of a bone should reflect the mechanical circumstances in which that bone functions (Ruff, 2000). Structures can typically bear the greatest load when this load is applied axially, as even quite trivial bending loads can engender dangerously high bending stresses (Currey, 1984; Lanyon and Rubin, 1985; Nigg and Grimston, 1994). Resistance to axial forces is proportional to the cross-sectional area of the bone (Preuschoft and Weinmann, 1973). Bending is best resisted when the mass of the bone is located as far as possible from the neutral axis of bending (where bone experiences neither compressive nor tensile stresses), in the direction of bending (Currey, 1984; Lanyon and Rubin, 1985; Lovejoy et al., 1976; Ruff and Hayes, 1983a). A measure of bending resistance relative to an arbitrary direction is known as the second moment of area, which is determined by the cross-sectional area of the bone and its distance from the centre (neutral axis) in the plane of bending (Jungers and Minns, 1979; Ruff and Hayes, 1983a). Therefore for bending in a specific direction (i.e. habitual bending loads), it is not simply the cross-sectional area that determines the bone's ability to resist these loads, but the spatial distribution of this area (Frankel and Burstein, 1965; Preuschoft and Weinmann, 1973; Ruff, 1990). The spatial distribution of the most external cortex is more critical than that of the internal cortex (Jee et al., 1981), and although external cortical measurements are likely to reflect the structural properties of a bone, both internal and external cortical measurements convey more structural information (Ruff, 2002). A structural approach has been used to advantage by numerous researchers, finding that the geometrical aspects of bones correlate with functional use (Burr et al., 1982; Demes and Jungers, 1989; Schaffler et al., 1985) and risk of failure (Augat et al., 1996; Faulkner et al., 1993; Nakamura et al., 1994).

Are bones then built to minimize stress or strain, while keeping the mass of tissue to a minimum? Loading a bone in bending creates dangerously high stresses compared with axial loading, so minimizing stress or strain could therefore be achieved by reducing bending forces (Currey, 1984). However, this is belied by the formation of bone curves that should increase rather than decrease bending forces (Lanyon, 1987; Lanyon and Rubin, 1985). The latter authors have suggested that bending strains (rather than pure compression) better enable the bone to adapt to gradual changes in strain. It therefore appears that simply minimizing peak strain is not the main design objective in bone architecture (Lanyon and Rubin, 1985). Instead it is theorized that adaptation works to keep strains within physiological limits (Burr and Martin, 1992; Frost, 1983; Jee and Frost, 1992).

What is an appropriate structural model for the patella? The bulk of structural design research in bones has been directed at long bones, for example the femur and tibia (Jungers and Minns, 1979; Ruff and Hayes, 1983a). Ruff and Hayes (1983a,b) considered the femoral shaft a hollow beam, and related cortical cross-sectional geometry to imposed bending loads. There are two main morphological differences between the patella and a hollow beam. Firstly, the patella is not hollow, but filled with a trabecular core. The patella is more like a composite beam, where the mechanical properties of the beam depend on both inner and outer components (Gere and Timoshenko, 1997); both cortical and trabecular bone contribute to the mechanical properties of such bones (Carter and Hayes, 1976; Gibson, 1985; Rafferty, 1998), and the mechanical properties of trabecular bone vary with its architecture (Brown and Ferguson, 1980; Fox and Keaveny, 2001; Hayes et al., 1978).

In the sagittal plane, the patella is principally loaded (1) axially (in tension), and (2) in three-point bending (§2.1.2.3). Therefore, patellar depth should relate to bending forces experienced, such that leaping animals may be expected to have deeper patellae (Ward et al., 1995), although trabecular adaptations may confound this. It should be noted that the bending load applied to the bone, or bending moment, is dependent on the length of the bone (Lovejoy et al., 1976). Therefore, a bone's cross-sectional geometry should ideally be considered as relative to the length of the bone (Lovejoy et al., 1976; Ward et al., 1995). Trinkaus (1983) and Trinkaus and Rhoads (1999) interpreted patellar depth as reflecting the quadriceps moment arm, but focused on the role of the patella as a spacer. Quite possibly, patellar depth reflects other properties. It is likely that depth reflects quadriceps moment arm via the balance-beam effect, in that patellar length must be accompanied by appropriate depth and trabecular architecture to withstand bending forces (Ward et al., 1995). Secondly, the ventral surface of the patella is largely articular, so the cross-sectional form of the patella includes an arch of subchondral bone, which is compressed against the femur. Arches, when subject to

loads, sustain bending stresses (Schodek, 1980). While subchondral bone shows adaptive responses to mechanical use (at least cortical thickness (Eckstein et al., 1999; Milz et al., 1995, 1997), presumably also trabecular architecture), the adaptive ability of subchondral bone may be limited due to articular function (preservation of congruity, for example) (Ruff and Runestad, 1992) (see §2.1.3.3.2. for a discussion on adaptations of bones). Thus, external cortical form in the articular region may be constrained by the form of the trochlea.

With these findings and assumptions, it is possible to stipulate theoretical mechanical design criteria for the patella, which are as follows. Firstly, the patella should have sufficient cross-sectional area at fibrous attachment sites (to resist axial tension, due to pull of the quadriceps tendon and patellar ligament, as well as transverse tension, from vasti and retinacula). Secondly, this area should be appropriately distributed in the appropriate direction so that the patella has sufficient depth with respect to its length, to resist bending moments in the sagittal plane. As the patella is also compressed against the trochlea by the (postero-) medial and (postero-) lateral pull of quadriceps, i.e. the pull of vastus medialis working to counteract the lateralization of the other components of quadriceps, it is envisaged that the patella also sustains three-point bending in the horizontal plane. Such bending would also be resisted by patellar depth, but this is likely to be of lesser morphological importance than bending in the sagittal plane. Finally, the patella should have appropriate breadth to provide sufficient articular surface area, to attenuate patellofemoral compression force.

2.1.3 Development of the Patella

The patella ossifies endochondrally (Mérida-Velasco et al., 1997; Ogden, 1984), so in a study of variation it is important to be aware of factors that may influence mesenchymal condensation, chondrification and ossification (in the present study all three are referred to as morphogenesis), especially if such influences result in altered morphology. Superimposed on such morphogenetic process are other processes that further modify the form of a bone: these are growth, modelling and remodelling. The details of patellar morphogenesis will be presented, but the limited scope of studies specific to the patella will contribute little to the understanding of limb bone variation. Therefore, the review of patellar morphogenesis will be preceded by a review of limb bone development in general. Finally, aspects of evolution of the knee joint will be addressed.

2.1.3.1 Limb bone morphogenesis

Morphogenesis of skeletal elements involves the processes of mesenchymal condensation (forming a blastema), chondrification (forming a primordium) and ossification (Jee, 1983). Formation of a blastema is initiated by a condensation of mesenchymal cells (Solursh, 1983; Wolpert, 1982). Differentiation of this mesenchyme into a cartilage primordium involves the secretion of cartilage-specific molecules (for example, type II collagen) and an increase in cell size (Tickle, 1994). The development of the cartilaginous primordium is an important step in the development of limb bone morphology, as it serves as a template for the future bone (Erlebacher et al., 1995; Reddi, 1994; Thorogood, 1983; Tickle, 1994; Wolpert, 1982). Thus, in a primary sense, the shape of the patella is determined by the shape of the primordium. The outer perichondrium may form mechanically when more central cells secrete matrix and push the peripheral cells outward (Wolpert, 1982). Alternatively, perichondral cells are predetermined, and drive the chondrification of the more central cells (Tickle, 1994). In diaphyseal ossification, chondrocytes in the growth plate typically proliferate, mature and hypertrophy, followed by matrix calcification, which causes death of the chondrocytes (Caplan and Boyan, 1994; Jee, 1983). This process is accompanied by an invasion of resorptive cells and vascular tissue (Caplan and Boyan, 1994). Pluripotential cells from the vascular tissue then differentiate into osteoblasts, which form bone (Jee, 1983).

In the growth plate, the process by which proliferating chondrocytes mature and then hypertrophy, leading to terminal differentiation, appears to be under the control of Indian hedgehog protein and parathyroid hormone-related protein (PTHrP). Specifically, a model has been proposed (Lanske et al., 1996; Vortkamp et al., 1996) which places expression of PTHrP under the control of Indian hedgehog protein in a negative feedback loop: hypertrophic chondrocytes express Indian hedgehog protein, which directly or indirectly upregulates PTHrP in the perichondrium (Karp et al., 2000; St-Jacques et al., 1999). Maturation and hypertrophy of proliferating chondrocytes expressing the PTH/PTHrP receptor is either delayed or prevented by PTHrP (St-Jacques et al., 1999); this then reduces the number of cells expressing Indian hedgehog protein (Kronenberg et al., 1997). Thus, PTHrP, expressed from the perichondrium acts as a spatial determinant of the ossification front (Karp et al., 2000; St-Jacques et al., 1999); the spatial distribution of bone was seen to be of interest in bone mechanics (§2.1.2.6.).

However, ossification of the patella proceeds along the lines of epiphyseal, not diaphyseal, ossification (Ogden, 1984). In typical epiphyses, the invasion of vascular tissue occurs in the form of vascular cartilage canals, which extend from the perichondrium and penetrate the centre of the primordium (Burkus et al., 1993). It appears that the presence of cartilage canals are related to the onset of chondrocyte hypertrophy, matrix calcification and chondrocyte death, resorption and ossification, although they precede ossification by a number of months in the human femur (Burkus et al., 1993; Roach et al., 1998). Ossification proceeds radially (rather than longitudinally), from the centre out to the perichondrium (periosteum will only exist when ossification is complete) (Jee, 1983). Ogden and coworkers (1987) have called such an ossification field a 'spherical physis'. The immature mammalian epiphysis shows a band of mitotic chondrocytes ('mitotic annulus'; Hinchliffe and Johnson, 1983) surrounding the ossific nucleus, forming the proliferative (= growth) zone for the ossifying epiphysis (Harris and Russell, 1933; Mankin, 1962; Rigal, 1962). The mitotic zone represents the spherical physis, so that epiphyses grow radially (in contrast to the longitudinal growth at the metaphysis). A mitotic annulus also runs parallel to the articular surface, presumably for growth of the articular surface (Mankin, 1962). It has been postulated that chondrocyte hypertrophy is induced by factors released from cartilage canals, initiating the above sequence (Roach et al., 1998). While the Indian hedgehog protein-parathyroid-related peptide feedback loop looks promising for diaphyses, Iwasaki et al. (1997) did not find expression of Indian hedgehog protein in developing epiphyses.

2.1.3.2 Patellar morphogenesis

There is evidence that the patellar blastema branches off from the femoral blastema; Doskocil (1985) found the patellar blastema arising from the area of the future femoral condyles. Other researchers' findings are less clear. Bardeen's (1905) views on the provenance of the initial condensation of the patellar blastema are not known; he did claim (p289) that "in [the quadriceps tendon] the patella becomes differentiated", but this only accounted for the primordium, not the blastema. Walmsley's (1940) study commenced at the 20mm stage, when the condensation of the patellar blastema had already occurred on a background of cartilaginous femur and tibia; he found the patella was developing within the substance of the quadriceps tendon, but again had no evidence of its development prior to this stage. The studies of Haines (1947) and Mérida-Velasco et al. (1997) state that the patellar blastema developed anterior to the femur, but neither explicitly expressed any views on its provenance.

It is in the development of the patellofemoral joint that a strong argument for a femoral origin of the patella resides. Walmsley (1940) found loose tissue between the deep aspect of the patellar element and the femur, which with chondrification of the patellar primordium, condensed to form a perichondrium on the patella. This perichondrium then appeared to fuse with that of the patellar aspect of the distal femur, such that the two elements were separated only by a double layer of flattened cells. Such a secondary fusion, then cavitation, of joint partners is not suggestive of the process described for primarily connected elements, such as the presumptive long bones. Walmsley's study commenced at the 20mm stage, when there was (1) a mesenchymal patella; (2) a cartilaginous femur; and (3) 'loose tissue' between the two. It is conceivable that Walmsley did not recognize the intervening loose tissue as a primary connection between the patella and femur. Haines (1947) reviewed Walmsley's study, and felt that the 'fused' appearance of the patellar and femoral chondrogenous layers was artefactual. The evidence of Andersen (1961) is more convincing. Andersen found that the presumptive patella develops "in the blastema behind the quadriceps tendon" (p282) i.e. in the region of the (blastemal) distal femur and proximal tibia and fibula. There was an even transition from the blastemal patella into loose interzone mesenchyme, with sharp demarcation anteriorly between the patella and quadriceps. Agreeing with Haines (1947), Andersen (1961) found at later stages that the patellofemoral interzone had trilaminated. The findings of Doskocil (1985) also supported this. Several authors have observed this cavitation at around eight to nine postovulatory weeks (Gardner and O'Rahilly, 1968; Gray and Gardner, 1950; Mérida-Velasco et al., 1997). The development of the relation between the patella and the quadriceps tendon are also unclear. Walmsley (1940) found the blastema to be forming in the substance of quadriceps, whereas Doskocil (1985) found (i) vastus intermedius attached to the patella, (ii) vasti lateralis and medialis attached to connective tissue next to the patella, and (iii) rectus femoris continued over the anterior aspect of the patella. Andersen (1961) found the patella to be invading the quadriceps tendon, although the details of this 'invasion' are not clear.

Prenatally, the mesenchymal condensation for the future patella has been reported in the range from around the seventh (Gardner and O'Rahilly, 1968; Gray and Gardner, 1950; Mérida-Velasco et al., 1997; O'Rahilly and Gardner, 1975) to the eighth (McDermott, 1943) postovulatory weeks. Chondrification of this mesenchymal element is described as occurring at as early as 7.5 weeks (Gardner and O'Rahilly, 1968; Mérida-Velasco et al., 1997); O'Rahilly and Gardner, 1975), or as late as 10 weeks (Gray and Gardner, 1950; McDermott, 1943). Prior to the onset of ossification, the cartilaginous patella expands (Ogden, 1984). The patella first undergoes multifocal ossification (Ogden, 1984), and these multiple ossific centres soon coalesce to form a single centre. Ossification is usually described as

commencing postnatally, in the first few years of life (Jo-Osvatic et al., 1993; Ogden, 1984). However, Mérida-Velasco et al. (1997) described the first signs of ossification as occurring at 14 postovulatory weeks. This quite different result is due to Mérida-Velasco et al. (1997) regarding the initial presence of cartilage canals as an indication of ossification.

2.1.3.3 Growth, modelling and remodelling

As limb bones change in nature from mesenchyme to cartilage and then to bone, they will also increase in size. A simple increase in size will here be called growth. It will be seen that certain parts of a bone may increase in size at different rates to others (Thompson, 1946); such differential growth causes nonuniform changes across the bone and here will be called modelling (that is, modelling is a specific process of growth). A very different process, by which bone is continually turned over, is remodelling. Remodelling will be considered here as bones may undergo slight changes in shape over the course of the individual's life. Notwithstanding this, it is growth and especially modelling which will determine the form of the definitive bone (Frost, 1997; Smit and Burger, 2000).

2.1.3.3.1 growth

Growth of a chondral element (in this case the patellar primordium) may occur interstitially, from cell division, cell volume increase, and/or matrix secretion, and appositionally, by accretion of matrix and cells from the perichondrium (Hinchliffe and Johnson, 1983; Ogden, 1990; Thorogood, 1983). The primordium is only purely cartilage for a limited time, after which an ossific nucleus forms. Growth may then proceed at the spherical physis/mitotic annulus.

2.1.3.3.2 modelling

The adult form of a bone will be the result of growth within the bone (Thorogood, 1983) and may be regarded as the outcome of relative (differential, i.e. not uniform) growth directed according to a number of criteria. The specific adult form of a bone is appropriate for the functional influences that acted on it during its development (Lanyon, 1981), from as early as the in-utero phase (Amtmann, 1979). It is generally accepted that skeletal tissues can (by

various means) respond to the forces they experience, and alter their morphology to suit those mechanical circumstances (Carter et al., 1991; McLeod et al., 1998; Ruff et al., 1993, 1994; Trinkaus et al., 1994). Thus, functional forces help to shape the bones such that they mature into structural supports that, except for reasonably rare fractures, are able to sustain those forces (Carter et al., 1996; Lanyon, 1987). Changes in bone form during growth (and possibly beyond maturity) to meet these biomechanical demands occur via processes of modelling (Frost, 1990c).

The developing patella consists of a trabecular osseous core, surrounded by hyaline cartilage. Bone is essentially laid down according to the cartilage template, so that during skeletal maturation changes to the outline shape of the patella occur via cartilage modelling (Frost, 1990c) (but see below). To explain the process of chondral modelling is to explain responses of chondral tissue to mechanical stimuli such that aspects of growth (cell proliferation, matrix synthesis etc.) are directed to alter the element's architecture, with the result that this architecture is appropriate to the mechanical circumstances. Frost proffered a chondral modelling theory (Frost, 1979, 1990c) as a proposal that cartilage tissue responds to forces depending on their nature (tension or compression) and intensity. This response is to alter the form of the element, such that strain within the tissue is kept at an acceptable level (see §4.1.2.2). No attempt was made to explain the cellular mechanisms involved. Frost's theory nevertheless is supported by studies investigating the responses of chondrocytes to mechanical forces (Hamrick, 1999). For example, chondrocyte metabolism has been found to alter with applied force (Urban, 1994), and that the metabolic response is contingent on the amplitude and frequency of dynamic forces (Kim et al., 1994).

This chondral modelling theory was developed to explain articular cartilage development, and as such omitted the fact that cartilage primordia also undergo ossification. When chondrocytes mature and hypertrophy, chondral modelling will cease; the definitive shape of an endochondral bone will therefore, in part, be determined by the relative amounts of chondrocyte proliferation on one hand, and chondrocyte maturation and hypertrophy on the other (Karp et al., 2000; Vortkamp et al., 1996; Wallis, 1996). If chondrocyte proliferation is maintained in one part of the mitotic annulus, but another part of the annulus is directed toward chondrocyte maturation, differential growth should result. In §2.1.3.1, the proposed effect of perichondral PTHrP as a spatial determinant of the ossification front was outlined; whether the feedback loop mentioned there influences epiphyseal ossification is not known. It is of interest to note that mechanical deformation of certain tissues increases their expression of PTHrP (in lung fibroblasts and pneumocytes (Torday and Sanchez-Esteban, 1998), and in vascular smooth muscle cells (Pirola et al., 1994)). It is tempting to speculate on a role for

mechanical deformation of the perichondrium (for example from muscle attachments) in directing chondral modelling via PTHrP, although lack of evidence of Indian hedgehog protein in epiphyses (§2.1.3.1) must temper one's speculation.

Modelling of bone is also of relevance here. Bone modelling is characterized by uncoupled resorption and/or formation (Frost, 1990a) – that is, formation at a site is not preceded by resorption (cf. remodelling). While it is considered that bone modelling normally ceases at skeletal maturity (Frost, 1990a), bone modelling may change external bone form beyond maturity; it has been found in mature skeletons that application of increased mechanical loads can lead to bone formation at the periosteum (i.e. modelling; Burr et al., 1989a,b; Jee et al., 1981; Lanyon et al., 1982; Pead et al., 1988; Raab et al., 1991). Also, trabecular bone can model both prior to (Iwamoto et al., 1999) and after skeletal maturity (Johnson et al., 2000; Radin et al., 1982), and potentially in preference to cortical bone (Iwamoto et al., 1999; Rubin et al., 2002).

Specific bony features that develop with the onset of upright walking provide illustrations of modelling: two such examples are the development of the femoral bicondylar angle (Preuschoft and Tardieu, 1996; Tardieu, 1993; Tardieu and Damsin, 1997) and the femoral neck-shaft angle (Anderson and Trinkaus, 1998; Houston and Zaleski, 1967). At birth, the femoral shaft lies perpendicular to the plane of the condyles; with the onset of walking, the alignment becomes oblique, thus allowing the knees to be medial to the hips (cf. *Q*-angle), and the feet as close to the line of gravity as possible (Lovejoy et al., 1973). Children who do not progress to walking retain a vertical alignment (Tardieu and Damsin, 1997). It is apparent that the oblique alignment is due to differential growth due to upright walking (Shefelbine et al., 2002). A similar pattern is seen with the femoral neck-shaft angle, which at birth has a relatively high value (vertical neck issuing from the shaft), which decreases (neck lies more horizontally) with weightbearing (Anderson and Trinkaus, 1998; Houston and Zaleski, 1967).

The patella probably also models according to biomechanical demands. It is tempting to regard the characteristically larger lateral patellar facet in humans as a result of modelling, due to the influences of lateral forces. Walmsley (1940) stated that the patella initially develops as a symmetrical bone (articular facets of equal size), but with increasing lateral force of the quadriceps it assumes its typical shape with a dominant lateral facet. Doskocil (1985) contradicted this, declaring that before the quadriceps muscles are able to exert force on the patella (before significant connections are seen between the two), the patella has already assumed this lateral bias. Ogden (1984) imputed this asymmetrical appearance to maltracking of the patella in utero, but it is unlikely that a normal morphological feature

would result from pathological function. Hehne (1990) has supported the notion that the form of the patella develops according to mechanical influences, and has cited Hellmer's (1935) findings that the immature form of the patella is quite different to its adult form. Other examples of apparent patellar modelling exist. Carey et al. (1927) removed the right patella from a series of puppies, and found the left patella to be 'hypernormally developed'. This may be explained by increased forces through the left knee due to favouring the right when walking. The patellar odd facet is thought to be produced by contact of the patella against the medial femoral condyle (Fulkerson, 1997; Hehne, 1990). A large medial facet (possibly corresponding to the odd facet, but apparently larger) has been found in individuals in whom squatting (knees in full flexion) is habitually performed (Lamont, 1910). Thus, the odd facet appears similar to squatting facets found elsewhere (for example, on the talus (Baba, 1975)).

2.1.3.3.3 remodelling

Lifelong turnover of bone, involving a sequence of osteoclastic resorption and osteoblastic formation, is known as remodelling (Jee, 1983). Action of the osteoclasts and osteoblasts is coupled: resorption precedes formation in the one site (Jee, 1983). Remodelling occurs on bone surfaces, and these are of four types: periosteum, osteons, cortical endosteum and trabecular endosteum (Frost, 1990b; Jee, 1983). In this study only the external morphology of the patella will be considered, so only periosteal remodelling is of direct relevance to this review.

It is well accepted that mechanical factors influence bone remodelling (Beaupré et al., 1990; Burr and Martin, 1992; Frost, 1990b; Jee and Frost, 1992; Rubin and Lanyon, 1987). The difference between the amount of bone resorbed and that formed (i.e. resorbed – formed) is known as the bone balance (Frost, 1990b; Jee and Frost, 1992). While it appears that in general decreased mechanical use increases remodelling and increases negative bone balance, increased mechanical use decreases remodelling and bone balance approaches zero (Jee and Frost, 1992). In general, and unlike modelling, increased mechanical use merely conserves bone (Frost, 1997; Jee and Frost, 1992). Specifically considering the periosteum, it is considered that over time normal remodelling creates a positive bone balance, such that the girth of a bone may increase during this time (Epker and Frost, 1965; Garn et al., 1967; Humphrey, 1998; Martin and Atkinson, 1977; Ruff and Hayes, 1982; van der Meulen et al., 1993). This is in contrast to bone in contact with marrow (for example trabecular endosteum), where bone balance is typically negative (Frost, 1990b).

2.1.3.4 Knee joint evolution

Little information was found on the subject of knee joint evolution. The primitive pattern of tibiofemoral and femorofibular articulations was present around 350 million years ago, with the recession of the fibula from the knee joint (as shown by most mammals, certainly all primates) occurring at least 70 million years ago (Dye, 1987). It appears that the patella developed independently in birds, lizards and mammals 65 to 70 million years ago (Dye, 1987). Therefore, the current pattern of knee joint osteology had been in place well before the advent of higher primates in the late Eocene (i.e. at least 38 million years ago) (Fleagle, 1988).

2.1.4 Phenotypic Variation

A morphometric study will inevitably show differences in form among individuals within a population, and among populations. This phenotypic variation, or the state of being varied, is as a result of variability, or potential to vary (Wagner and Altenberg, 1996). Variability arises from genetic and epigenetic variation; the relative contributions from these influences will be discussed, and it will be reinforced that developing bones are quite sensitive to their functional environment. A broader association between function and structure exists which can probably not be explained wholly by the ability of bone to respond to these functional demands; this association will also be discussed.

2.1.4.1 Genetic, epigenetic and environmental influences

The final form of a structure is influenced by both genetic and environmental factors during development (Atchley and Hall, 1991). Development of an organ is directed by the interactions between the genome and its environment (both hereditary, or epigenetic, and external, or environmental) (Atchley and Hall, 1991), so that these processes together determine the form (size and shape) of the organ. However, ranges of phenotypic variation are not limitless, and it is seen in comparative studies that taxa tend to form clusters where not all theoretically possible phenotypes are represented (Alberch, 1982). Phenotypic variation usually results from a mix of selective and developmental constraints (Maynard Smith et al., 1985; Raff, 1996). Natural selection may be invoked to explain phenotypic limitations (Maynard Smith et al., 1985; Raff, 1996), as selective pressures may favour one patellar form over another according to functional demands, with the elimination of nonadaptive forms

(Alberch, 1982). Developmental constraints are also likely to influence the patterns of phenotypic variation; these are defined as limits on phenotypic variability due to the structure, character, composition or dynamics of the developmental process (Maynard Smith et al., 1985). For example, bones must satisfy certain architectural requirements beyond any other criteria (Gould and Lewontin, 1979). Developmental constraints limit the variability on which natural selection acts by limiting the possible phenotypes (Alberch, 1982; Raff, 1996). Alberch (1982) proposed the useful concept of 'phenotype space', wherein phenotypes are positioned along coordinate axes according to variable measurements; constraints lead to areas within phenotype space where specimens may lie, and others where they may not. For limb bones, illustrations of these two constraints are (1) survival of individuals with optimal bone architecture as a selective constraint, and (2) the deposition of bone where mechanical influences demand as a developmental constraint (Preuschoft, 1970). These two processes become intertwined with the knowledge that, while the adaptation to one's environment is not heritable (and consequently not subject to selection), the capacity to adapt is (Gould and Lewontin, 1979). It is difficult to separate selective from developmental constraints, and adult phenotypic variation can only suggest the contributions of selection and development (Maynard Smith et al., 1985). For example, whereas some may argue that an allometric relation (Chapter 4) shows evidence of a developmental constraint, there may be equally good arguments for the morphological pattern resulting from a selective constraint (Maynard Smith et al., 1985). Phenotypic departures from predictions made on selective grounds may indicate the presence of developmental constraints (Levinton, 1986; Maynard Smith et al., 1985).

Despite the potential diversity due to genetic as well as epigenetic influences among individuals (Clarke, 1998; Hartman et al., 2001; Rendel, 1979), there is a tendency (to varying extents) of individuals to produce somewhat identical structures. This tendency is known as canalization, and was defined by Waddington (1959) as the ability to attain "the normal adult condition" despite disturbances (p1654). The converse of canalization, plasticity, refers to the extent to which the adult phenotype is altered by environmental influences on the developmental process (Smith-Gill, 1983). Plasticity may be defined as a low degree of canalization where minor fluctuations have a lasting effect on the adult phenotype (Waddington, 1957). In Waddington's model, canalized phenotypes approximate an ideal ("the standard end-product" (Waddington, 1942 p563)), and environmental influences serve to redirect the developmental pathway from this ideal (Waddington, 1942, 1957). However, phenotypes do not exist outside the environments in which they have developed (Pigliucci et al., 1996): the form of limb bones may alter, via a process of modelling, to meet mechanical demands (§2.1.3.3.2). Functional demands are also brought to bear in early development; results of immobilization studies show that normal limb bone and joint development is

dependent on mechanical stimulation from the cells' environment. Data from experimental and clinical investigations in vertebrates show that immobilization leads to gross changes such as a decrease in long bone dimension and bone malformations, and histological changes such as a decrease in rate of cartilage resorption and ossification (Hall and Herring, 1990; Hosseini and Hogg, 1991; Rális et al., 1976; Rodríguez et al., 1992). Normal articular morphology has also been shown to be strongly dependent on intrauterine mobility (Drachman and Sokoloff, 1966).

Due to genetic influences, morphological variation, in addition to its reflection of functional variation, is also likely to be influenced by heredity, or phylogeny. In general, closely related taxa tend to be more morphologically similar than distantly related taxa (Harvey and Pagel, 1991). Therefore heritable aspects of morphology may confound expectations of a one-to-one mapping of form and function (Polk, 2002); however, to deviate far from sound mechanical principles even on the basis of heredity would risk skeletal failure (Biewener, 1989). To help elucidate phylogenetic influences on morphology, it is useful to compare phylogenetically related subjects against those more distantly related (Harvey and Pagel, 1991; Polk, 2002). Ideally, the traits measured should be strongly influenced by genetic information (and therefore heritable) (Lieberman, 1997). The value of osteometric variables in reflecting phylogenetic information has been questioned, due to the influences of nongenetic factors on bone morphology, especially mechanical load (Collard and Wood, 2000; Lieberman, 1997). That cranial measures were poor reflections of phylogenetic relations (in hominoids and papionins) (Collard and Wood, 2000) suggests that the patella, with its role as a conduit for extensor force, would be an even less useful indicator of morphological heredity. Phenotypically plastic structures such as bones are more likely to be better indicators of those influences that manifest this plasticity, mechanical load for example (Lieberman, 1997).

Whether a bias towards canalization or plasticity is in theory beneficial depends on the character in question. In general, if there is an advantage to the individual to develop a structure irrespective of the degree of environmental stimulus, canalization is advantageous (Waddington, 1942). This is not so for limb bones, as they require a modelling response to meet specific mechanical needs, especially altered mechanical needs in the transition from early development (in-utero) to later development (onset of adult-style gait). It has been shown that maximal peak strains in different bones in different species are consistent (see below); this consistency is aided by an ability of bones to model appropriately. This is a form of 'physiological homeostasis' (Waddington, 1957), rather than of the morphological kind. In the face of potentially varied environments, low canalization is an advantage where the system requires physiological homeostasis (Waddington, 1957). It is therefore appropriate to

adopt McLachlan's (1999) concept of an incomplete morphological attractor whereby genes direct morphogenesis according to environmental input, and a standard morphological end product does not exist. This is due to the prevailing standard physiological end product, as evidenced by dynamic strain similarity (see §4.1.2.2). The likely role of genes is in the production of a bone capable of responding to mechanical influences (Oxnard, 1979).

While it is likely that the patella has a certain degree of variability due to plasticity, it must be remembered that it does not develop in isolation. The forces sustained by the patella are in part due to the femur, the quadriceps femoris and the various other soft tissues of the knee; the patella is thus part of a complex, and a factor influential in the development of one part of a complex has the potential to also influence that of another. This concept of correlated development is known as morphological integration (Cheverud, 1996; Hallgrímsson et al., 2002). Integration within the individual may be due to function (functional links between structures demand structural integration) or development (an external factor drives the development of more than one structure) (Cheverud, 1996). Thus, development of these other structures could potentially constrain the development of the patella; the excision and investigation of the patella in isolation should not cloud one's perceptions about what, morphologically, is possible.

2.1.4.2 Structure-function association

As locomotion (function) is performed by the skeleton (structure), it is reasonable to expect that function and structure do not vary independently (Preuschoft, 1979; Schaffler et al., 1985). It has been noted that function may cause morphological changes (i.e. modelling); there is also an association between structure and function where the direction of cause to effect is not as plain. Thus, phenotypic constraints may have a functional element, such that phenotypic variation may reflect functional differences. Overall, certain morphological traits are associated with broad locomotor divisions; for instance, long lower limbs have been related to leaping as well as running. Leapers have relatively long lower limbs (relative to body length) to maximize leaping distance (Demes and Günther, 1989; Fleagle, 1988; Jungers, 1979; Napier and Walker, 1967; Oxnard, 1983a). Terrestrial quadrupeds also have long limbs, for speed of locomotion (Fleagle, 1988). These associations may be explained biomechanically, as adaptations to maximize the distance over which the body may be accelerated (Bennet-Clark, 1977; Demes and Günther, 1989); terminal velocity of limb movement is therefore increased with increased limb length (Gambaryan, 1974). Leapers propel themselves via a rapid extension of a flexed knee (Fleagle, 1988), for example the

lesser galago, *Galago senegalensis* (Hall-Craggs, 1965). For runners, the length of the limb relative to body size is increased to increase stride length and speed (Hildebrand, 1988). However, similarities and differences in function between groups may not necessarily be reflected morphologically – for instance, different species may respond to similar biomechanical demands in different ways (Fleagle, 1988). Also, functional differences may be overshadowed structurally by functional similarities (Burr et al., 1981). It may also be the case that the function investigated may simply not be a sufficient reflection of that animal's function in general (Schaffler et al., 1985). Skeletal morphology probably reflects some sort of average of function, but it is likely that certain functions (especially those involving large forces) may influence morphology more than others (Oxnard, 1983a), and that awareness of some aspects of function is more important than of others when considering any link between structure and function (Oxnard, 1979). Conversely, some aspects of bone morphology may be related to lower intensity loading, and may reflect other characteristics, such as muscle morphology (Rubin et al., 2002).

Thus, both lesser galagos and humans have relatively long limbs, but humans cannot leap effectively. To suggest that longer limbs in larger animals may make them efficient leapers would ignore that, although there would be greater distance over which muscles could accelerate the limb segments, the muscle force available is insufficient to accelerate body weight effectively (Demes and Günther, 1989). Leaping primates are exposed to very high forces during leaping, which are related to the propulsion of body weight (Demes and Günther, 1989). As will be seen in Chapter 4, larger animals have different biomechanical needs compared to smaller animals. Large animals may have less muscle force per unit weight to propel themselves relative to smaller animals functioning in the same way (Demes and Günther, 1989). To decrease locomotor forces (relative to body weight), larger animals may reduce the accelerations of the proximal limb ends (Gambaryan, 1974). This would be reflected in the tendency for larger animals to show less leaping behaviour. Table 2.3 shows the body weights for the species under investigation where these details were available.

Table 2.3. Average body weights (kg) for several primate species

	male	female	source
Homo sapiens	68	55	Fleagle (1988)
Cercopithecus aethiops	5.37	3.36	Fleagle (1988)
	5.31	3.30	Plavcan & van Schaik (1992)
	4.21	2.74	Anapol et al. (1995)
C. ascanius	4.17	3	Fleagle (1988)
	4.21	2.90	Plavcan & van Schaik (1992)
C. campbelli	4.5	2.7	Oates et al. (1990)
C. mitis	7.36	4.23	Plavcan & van Schaik (1992)
	7.93	4.25	Anapol et al. (1995)
C. mona	4.40	2.50	Plavcan & van Schaik (1992)
	5.1	–	Smith & Jungers (1997)
C. neglectus	6.32	3.96	Fleagle (1988)
	8.03	4.46	Plavcan & van Schaik (1992)
C. nictitans	6.5	4	Fleagle (1988)
	6.58	4.22	Plavcan & van Schaik (1992)
C. solatus	6.29	3.64	Harrison (1988)
Colobus angolensis	9.69	7.4	Plavcan & van Schaik (1992)
C. badius	8.25	8.24	Fleagle (1988)
	9.34	6.77	Plavcan & van Schaik (1992)
	*8.36	*8.21	Smith & Jungers (1997)
	†9.67	†7.21	Smith & Jungers (1997)
	8.3	8.2	Oates et al. (1990)
C. guereza	10.1	8.04	Fleagle (1988)
	9.32	7.83	Plavcan & van Schaik (1992)
	9.89	7.90	Smith & Jungers (1997)
C. polykomas	10.7	7	Fleagle (1988)
	8.41	7.43	Plavcan & van Schaik (1992)
	9.9	8.3	Oates et al. (1990)
C. satanas	–	9	Fleagle (1988)
	11.97	9.5	Plavcan & van Schaik (1992)
Gorilla gorilla	159.6	95	Plavcan & van Schaik (1992)
	**169.5	**71.5	Fleagle (1988)
			Jungers & Susman (1984)
	**169	**80.25	Leigh & Shea (1996)
	‡175.2	‡80	Fleagle (1988)
	‡159.2	‡97.7	Jungers & Susman (1984)

**C. b. badius*

†*C. b. rufomitratus*

***G. g. gorilla*

‡*G. g. beringei*

Broadly speaking, body weight is reflected in the locomotor habits the primates under consideration. It can be seen that the two genera that never leap (*Homo* and *Gorilla*), are on average much bigger than the two that variably leap (*Cercopithecus* and *Colobus*). *Homo* and *Gorilla* are also terrestrial genera, whereas *Cercopithecus* and *Colobus* range from arboreality to terrestriality. In §2.1.2.5, it was seen that colobines are generally better leapers than cercopithecines (Ashton and Oxnard, 1964; Fleagle, 1988; Mittermeier and Fleagle, 1976; Stern and Oxnard, 1973). This appears to be despite the greater average weight of *Colobus* compared to *Cercopithecus*. This apparent paradox is most likely due to larger cercopithecine genera not included under *Cercopithecus* – *Papio* and *Mandrillus*, for example. Within *Cercopithecus*, *C. neglectus* is a large terrestrial species, whereas *C. mona* is smaller, arboreal and employs leaping. Within *Colobus*, *C. badius* is smaller than the guereza (Fleagle, 1988), and shows more leaping than *C. polykomos* (McGraw, 1996).

Environment also plays a part in the structure-function association, mainly via the substrate on which the animal functions. Arboreal quadrupeds must propel themselves on an unstable medium (Fleagle, 1988); they may increase their stability by flexing and abducting their limbs, so that their centre of gravity is brought closer to their base of support (Fleagle, 1988; Schmitt, 1999). Jungers (1979) found that patterns of relative limb length in prosimians reflected functional differences: for example, relative lower limb length was preserved with body weight changes for leapers, but quadrupedal walkers showed decreased relative lower limb length with increased body weight, presumably to allow larger individuals to bring their centre of gravity closer to the supporting branch. Environment and body weight may interact in a somewhat isolated manner, i.e. body weight may limit the substrates upon which an animal may walk, or vice versa. For example, terrestrial cercopithecines tend to be heavier than arboreal species (Rollinson and Martin, 1981).

2.1.5 Summary

The patella is an integral part of the extensor mechanism of the primate knee; it serves as a spacer, shifting the line of pull of the knee extensors dorsally or anteriorly, and as a lever or 'balance-beam', further altering the mechanical advantage of the knee extensors. However, a precise function is difficult to state; the popular view of the patella increasing the moment arm of the knee extensors is tempered by the fact that, especially in knee flexion, the presence of the human patella at least serves to decrease the efficiency of the extensors. The morphological pattern of the patella articulating with the femur, and the four components of the quadriceps femoris muscles attaching to the proximal patella appears constant across

primates; the main differences appear to be between human and nonhuman knees (increased femoral bicondylar angle, more distal attachment of vastus medialis), which are likely related to the bipedal locomotion of humans.

During locomotion, the line of action of body weight falls behind the knee and exerts a flexor moment; in response, the quadriceps exert an extensor moment. When the quadriceps muscles are contracted, tension in the quadriceps tendon and patellar ligament pull the patella posteriorly against the distal femur. Mechanically, the patella is loaded in three-point bending, with typically tensile stresses dorsally and compressive forces ventrally. The role of the patella, beyond influencing knee extensor moment arms, is also to endure the forces imposed on it. To resist bending forces, the patella can increase its depth perpendicular to its contact planes; skeletal elements have the ability to change their shape during (and possibly after) skeletal growth, so that they are able to function safely within the environments in which they developed. The individual animal is also able to avoid large bending forces, for example by adopting a more extended limb position and avoiding forceful activities like leaping.

Morphological variation in the patella is a reflection of the variability in the morphogenetic process; this variability emanates not only from genetic variation, but also variation in mechanical circumstances, to which developing bones are sensitive. Genetic variation may be reflected in results of comparative analyses, where closely related taxa are expected to show more morphological similarity than more distantly related taxa. However, functional differences among taxa (especially those imposed by body weight) are likely to cloud this picture, so that bony morphology will provide only limited information relating to phylogenetic development. Patellar morphometric variation may reflect these influences, although past studies relevant to this topic are few and have not taken a broad approach to sources of variation.

2.2 Mathematical and Statistical Concepts

In this section, the principles underlying the methods used in this study will be reviewed. It will be seen that, presented with objects to be investigated, the morphometric investigator will potentially have many morphometric methods at his or her disposal. Some methods relate to the way data are gathered, others to how those data are assessed and interpreted as a second step. Accordingly, this section will comprise two parts: §2.2.1 Morphometric Methods and §2.2.2 Mathematical and Statistical Methods. This is a general review: mathematical and statistical concepts specific to certain chapters will be reviewed in those chapters.

2.2.1 Morphometric Methods

Morphometrics is the science of measuring form; in this study, 'form' refers to a combination of both size and shape of an object (Sprent, 1972). Rohlf and Marcus (1993) defined morphometrics as (in part) "...the description and statistical analysis of shape variation within and among samples of organisms...". This definition appears to ignore the size of the objects under investigation. This is not a simple omission – what constitutes size and what shape is anything but clear (Jungers et al., 1995). For the purposes of this study the above definition will be amended to read "...analysis of form variation...", and discussion of size and shape will be suspended until Chapter 4.

When planning a morphometric study, the investigator may, depending on the specimens under investigation, choose from a wide variety of data types, ranging from simple metrical data (for example distances and areas) to more mathematically complex data. While metrical data are conceptually appealing, an investigation may require more complex data to adequately describe a specimen's form. Therefore, the choice of data to be gathered will be governed by the nature of the specimens to be studied, as well as the intentions of the researcher. The morphometrician will need to, when gathering data for a morphometric investigation, take various factors into account which may influence the performance as well as the result of the investigation. Such factors may include the ability to uniquely describe the aspects of form, being computationally efficient, and separating global from local form features (Lestrel, 1997a). Although modern computing power may make computational efficiency less of a priority, the ability to describe an object's form in simple terms may still be advantageous. For instance, if the objects under investigation are reasonably regular,

simple measurements may suffice (Lestrel, 1997a; Oxnard, 1978). Less regular forms may require more complex data for an adequate description.

The many different types of data that may be generated for morphometric investigation may be divided into three categories; the broad field of morphometrics thus comprises: (1) multivariate morphometrics; (2) coordinate (or landmark) morphometrics; and (3) boundary (or outline) morphometrics (Lestrel, 1997a).

2.2.1.1 Multivariate morphometrics

The field of morphometrics that yields data as metrical measurements (for example Ashton and associates (1965) and Corruccini (1975)) fall under the umbrella of 'multivariate' morphometrics (Lestrel, 1997a; Reyment et al., 1984). The typical 'multivariate' morphometric study uses metrical data, which are typically entered into multivariate (occasionally univariate) statistical methods. The main difference between the 'multivariate' methods and others is the type of data that are inputted into the various multivariate analyses. A more useful term then for this style of investigation is the conventional metrical approach (Lestrel, 1997a).

Conventional metrical data have the advantage that they may be easily generated (using a ruler or callipers), but they do have the disadvantage that selection of measurements is likely to omit information about the object's form (Lestrel, 1997a). Such data also may not be used to reconstruct the original form of the specimen, and therefore may not uniquely describe the form of the specimen (Bookstein, 1990).

2.2.1.2 Coordinate morphometrics

The use of coordinate (or landmark) morphometric methods is contingent on the ability of the investigator to reliably register the position of homologous landmarks relative to Cartesian axes. Objects may be investigated using such methods as Procrustes superposition (Rohlf, 1990), Bookstein's shape coordinates (Bookstein, 1991), and various thin-plate spline methods (Bookstein, 1996a). The outline of a typical cross-sectional image of the patella, especially the nonhuman patella, does not obviously lend itself to reliable landmark registration, so these methods will not be considered here.

2.2.1.3 Boundary morphometrics

Another group of morphometric methods uses boundary, or outline, data. Popular methods include eigenshape analysis (Lohmann, 1983; Rohlf, 1986) and Fourier methods (Ferson et al., 1985; Rohlf, 1986); in this section, Fourier methods will be discussed.

In conventional metrical analyses, as well as coordinate analyses, the choice of metrics or landmarks (i.e. the decision of which distances or landmarks to include) is subjective, and data thus generated will not necessarily encompass the entire form. Information between metrics or landmarks is lost, which might have otherwise been of importance (Ehrlich et al., 1983; Lestrel, 1997a; Oxnard, 1978). The more complex the form, the more data are required (Healy-Williams et al., 1997). The advantage of outline methods is that data from the entire outline are used in the analysis. However, data analysis does not proceed simply from initial data capture: an object's outline may be represented accurately by a series of Cartesian coordinates, but outlines of different objects cannot be compared directly using this information (Johnson, 1997); this is due to differences in outline representation (distribution of points, orientation of object). The outline methods (including Fourier methods) involve a transformation of data taken around the perimeter of the object being investigated, so that it may be more readily analysed using multivariate statistics (Foster and Kaesler, 1988).

Fourier analysis is a method by which a complex spatial series (for example, the outline of a biological specimen) is expressed as the sum of regular sinusoidal curves of differing amplitude, wavelength and starting point (phase), which are statistically independent (Davis, 1986). In a reverse fashion, Fourier methods output instructions for successively deforming a relatively simple shape into a more complex one (Healy-Williams et al., 1997; Johnson, 1997).

The term 'conventional' is used in this study to distinguish between the method used originally to investigate shapes (Lestrel et al., 1977; Lu, 1965), and the later development, elliptic Fourier analysis (Kuhl and Giardina, 1982). (The term 'conventional' here is not to be confused with its use in later chapters in relation to conventional metrical data.) The conventional method will be reviewed first, with the elliptic method presented (as much as possible) in similar terms.

2.2.1.3.1 the conventional Fourier method

Fourier methods require that the outline of an object be represented as a series of points in space; the Fourier transformation transforms these data from the spatial domain to the frequency domain, by expressing the outline as a sum of waveforms (Lestrel, 1997b). Each resultant waveform is called a harmonic. These harmonics are represented by a series of cosine and sine terms, weighted by amplitude coefficients (a_n and b_n, respectively – two coefficients per harmonic) (Rohlf and Archie, 1984). In addition, there is a zero-harmonic, where the constant term (a_0) represents the mean of all the observations, while b_o always equals zero (Davis, 1986; Lestrel, 1997b). Successive harmonics generated by Fourier transformation are orthogonal, that is statistically independent (not correlated) (Crampton, 1995). The lower-order harmonics describe large-scale aspects of form, whereas higher-order harmonics describe smaller aspects, due to the wavelength of higher-order harmonics being shorter than those of a lower order (see below). In biological morphometrics, it is expected that the first few harmonics will reflect global shape aspects, with higher harmonics reflecting more local aspects (Lestrel, 1989). In this case it may be found that the first harmonics of a series of objects will not differ greatly unless larger disparities in shape are present (Crampton, 1995).

The data resulting from a Fourier transformation are referred to as Fourier descriptors (Lestrel, 1997b). Fourier descriptors are useful in morphometrics, as they allow re-creation of the object outline in the absence of the original object (Healy-Williams et al., 1997; Lestrel, 1997b). As they do not involve omission of interlandmark shape factors (where much important information may reside (Lestrel, 1997b)), they do not require a priori assumptions regarding the importance of isolated points in describing an object's shape (Healy-Williams et al., 1997), unlike landmark methods. Three values (descriptors) may be computed from the Fourier transform directly: period, amplitude, and phase (Lestrel, 1997b), and these three parameters completely describe the waveform (Davis, 1986). These three descriptors are illustrated in Figure 2.10.

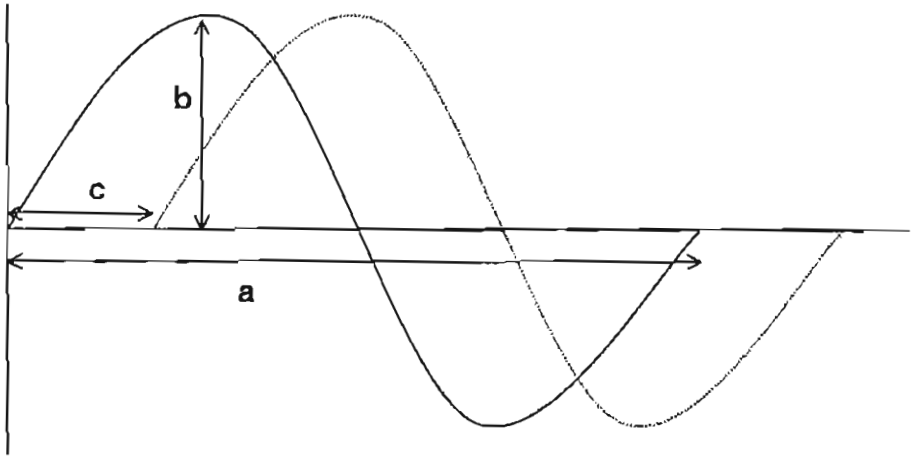

Figure 2.10. Waveform showing (a) period, (b) amplitude and (c) phase

The period of a harmonic is equivalent to its wavelength (Davis, 1986), that is, the distance over which the waveform exists. The period of the first harmonic is from 0 to 2π radians; the frequency of each harmonic is inversely proportional to its period. Successive harmonics are represented by successive fractions of the period of the first harmonic (Lestrel, 1997b) (i.e. 2π, $2\pi/2$, $2\pi/3$,...,$2\pi/n$), so that higher harmonics display a shorter wavelength, consequently accounting for small-scale aspects of form. The amplitude of a harmonic can be thought of as half the distance from the crest to the trough of a waveform (Davis, 1986). The contributions of each harmonic to the outline shape are represented by their amplitudes – the larger the amplitude, the larger the contribution of that harmonic to the outline approximation (Lestrel, 1997b). A power spectrum may be calculated using the amplitudes of successive harmonics, showing the relative contribution of each harmonic to the outline (Lestrel, 1989). The power, or amount of variation accounted for by each harmonic, can be represented as a proportion of the total variation (Davis, 1986; Lestrel, 1997b). Finally, phase refers to the starting point, or offset, of the waveform (Davis, 1986; Lestrel, 1997b). Studies using Fourier methods may leave themselves open to criticism if phase information is discarded (Foster and Kaesler, 1988). As Rohlf (1986) pointed out, different shapes can have the same amplitudes, so discarding phase information may leave the investigator with a false picture. However, Healy-Williams et al. (1997) considered that shape information may exist in the amplitudes and/or phase angles, and advocated the initial use of amplitudes, followed by inclusion of phase

information if necessary. The initial phase angle is affected by choice of alignment procedure (see below) (Lestrel, 1997b).

2.2.1.3.2 the elliptic Fourier method

The elliptic Fourier transformation (Giardina and Kuhl, 1977; Kuhl and Giardina, 1982) is a more flexible application to the analysis of object outlines. This transformation uses an orthogonal decomposition of a curve into a sum of harmonically related ellipses, which when combined approximate a closed curve (Ferson et al., 1985). In contrast to the conventional Fourier method, elliptic Fourier transformation requires the calculation of two waveforms. If a point is considered to be travelling around the outline over time t, the outline can be expressed as (1) deviation of the point in the x-direction, and (2) deviation in the y-direction; the two resultant waveforms then represent the change in the x-value as t increases, and correspondingly for such changes in y (Ferson et al., 1985; Giardina and Kuhl, 1977). In calculating the n^{th} harmonic, the measure Δx_p (the displacement of the curve along the x-axis between points $p-1$ and p) is used to compute two coefficients for the x-projection of the curve (a_n and b_n). This is also done for Δy_p (coefficients c_n and b_n), such that now four coefficients are computed per harmonic (Ferson et al., 1985).

The contributions of successive harmonics may be illustrated in terms of ellipses. The zero-coefficients (the bias terms, a_0 and c_0) represent the centroid of the original outline (Kuhl and Giardina, 1982) (coefficients b_0 and d_0 equal zero). The first harmonic approximates the outline of the object using a single ellipse (Diaz et al., 1997). The successive harmonics also represent ellipses, which modify the shape of the first. Elliptic Fourier descriptors analogous to those from the conventional method may be calculated (Rohlf, 1986-1998).

2.2.1.3.3 methodological considerations

Conventional Fourier descriptors are typically calculated from an outline represented by coordinate points which lie on the object outline at the ends of a series of radii emanating from the centroid of each shape, the lines being a uniform number of degrees apart (Lestrel, 1997b). Two constraints attached to this method are that points must be equidistant, and each radius must connect with only one outline point (Rohlf and Archie, 1984). That is, with complex shapes, where the radius intersects the outline at more than point, conventional Fourier methods are either not appropriate, or the complex region of the outline must be

omitted from the investigation. Elliptic Fourier transformation has certain advantages over the conventional form, as it can be used with complex outlines, and also does not require equidistant points (Rohlf and Archie, 1984). Points may be sampled in higher concentrations (around sharp curves) to increase accuracy of approximation (Lestrel and Kerr, 1993). Elliptic Fourier transforms in particular are capable of detecting subtle differences among very similar, nearly oval shapes (Ferson et al., 1985). As for disadvantages, elliptic Fourier analysis requires approximately twice the number of coefficients (Ferson et al., 1985). Therefore, for a small sample size, the number of harmonics retained may have to be reduced.

A Fourier series is convergent, i.e. by increasing the number of harmonics the outline approximation draws ever closer to the original outline (Lestrel, 1997b). However, the investigator is not free to simply increase the number of harmonics calculated for a given outline; the maximum number of harmonics that can be computed is limited by the Nyquist frequency (Davis, 1986). Harmonics with a wavelength less than twice the spacing between points cannot be detected – the maximal number of harmonics is then half the number of outline points. Even so, retaining the $p/2$ (for an even number of points, or $(p-1)/2$ for an odd number) harmonics is not without its drawbacks. The interesting information in an object's outline may reside in less than the total amount of shape information, so by retaining all harmonics one may retain too much information for the size of study sample (Healy-Williams et al., 1997). Higher-order harmonics may represent shape elements, but they may also represent noise, for example from digitizing error (Rohlf, 1986). As Fourier descriptors are generated for use in statistical analyses, one must also take into account that the number of objects investigated should ideally far outweigh the number of variables (by a factor of roughly 2.5 (Johnson, 1997)). There are a number of ways of determining the optimal number of harmonics. Crampton (1995) suggested limiting the number of harmonics to those that account for a figure, for example 99%, of the power spectrum. Residual distances, between the original and approximated outlines, may also be calculated (Lestrel, 1997b). O'Higgins (1989) found when investigating multiple groups of objects the discriminatory ability of the Fourier data was optimal when using a limited number of harmonics (in his study, 15 out of 128), but that this discriminatory ability lessened with fewer, and also more, harmonics.

Once the original data are transformed, the investigation may be carried out as for conventional metrical data, the Fourier descriptors being entered into statistical analyses (Johnson, 1997). Due to the orthogonality of successive harmonics, it is possible to analyse the contribution of each harmonic separately (Ohtsuki et al., 1997). Elliptic Fourier coefficients may be used directly in multivariate analysis (for example Crampton (1995), Ferrario et al. (1994), Ferson et al. (1985), Liu et al. (1996), Premoli (1996) and Rohlf and

Archie (1984)). However, amplitudes from the x-coefficients (a_n, b_n) and y-coefficients (c_n, d_n) have also been used (for example Lestrel (1989), Lowe et al. (1994) and McLellan and Endler (1998)). As a more advanced application, Lestrel et al. (1993), Lestrel and Kerr (1993) and Tanaka (1999) have used a method based on the distances between expected points on the outline and the centroid.

2.2.1.4 Comparison of methods – landmark versus outline methods

It is certain that no morphometric method is free of pitfalls, such that there is no intrinsically 'appropriate' method (Read and Lestrel, 1986). With regard to the nature of the specimens involved, Read and Lestrel (1986) proposed that, rather than asking *which method is better?*, the question should be rephrased, to ask *which method is sensitive to, and provides a direct measure of, biologically meaningful aspects of shape?* However, the concept of biological meaning is also subjective, to a degree. For example, Bookstein (1991) claimed that only landmark methods can localize shape difference, thus leading to meaningful biological explanations. This assumed that the process of identifying obvious landmarks and subjecting these to mathematical algorithms reliably mirrors biological processes. Bookstein has also been a critic of Fourier methods in particular. He has criticized these methods, stating that one cannot draw the change of shape of an object, using a vector, from a Fourier decomposition of outline data ("there is no place to put the arrowheads...at which end does the arrowhead go?" (Bookstein, 1991 p62)). Bookstein (1991) lamented that Fourier methods do not allow the overlay of vectors to illustrate shape change. The assertion that one method is better than another for a series of objects depends on knowledge of how the objects develop such shapes (Lestrel, 1989; Read and Lestrel, 1986). Bookstein's argument implies that the positioning of landmarks drives the development of the object as a whole; certainly this is not the case with the patella, as interstitial chondral growth and epiphyseal ossification (expanding radially from the centre) will result in the position of the outline being determined by what has occurred in the interior of the bone. It is certain that the outline is not dragged along by points that, by a pleasing coincidence, are developmentally motile as well as easily identifiable. To suggest that one point along a smooth outline is more important than any other in this case requires more support than ease in placing vectors. In answer to Bookstein's (1990) criticism of Fourier coefficients, that "they are no reliable guide to understanding ... the biological processes that have modified form", it could be argued that neither are a collection of arrowheads on landmarks that have been chosen for the principal reason that they are easily located.

As a means of illustrating how outline methods that ignore homologous landmarks are 'inadequate', Bookstein et al. (1982) included a hypothetical example (Figure 2.11), which shows two objects with the same outline shape (circular), but with differing positions of homologous landmarks. Rohlf and Archie (1984) refuted this argument, by pointing out that if one's objective is to measure shape, then the Fourier methods will detect this. In Bookstein and coworkers' (1982) example, the shape of the object had not changed, only the relative positions of the landmarks. Read and Lestrel (1986) agreed with Bookstein and associates, on the point that Fourier methods cannot detect changes in landmark position that are independent of outline shape. Read and Lestrel (1986) provided a hypothetical example to counter that of Bookstein et al. (1982) (Figure 2.12). Here, homologous landmarks have maintained their positions, while the outline shape of the object has obviously changed: landmark methods would not detect such a shape change. This disparity is a result of the subjective nature of what is important in a study; to the investigator more interested in what the outline of an object looks like than the relative positions of arbitrary points on the outline (the present study included), Bookstein's criticisms are surmountable.

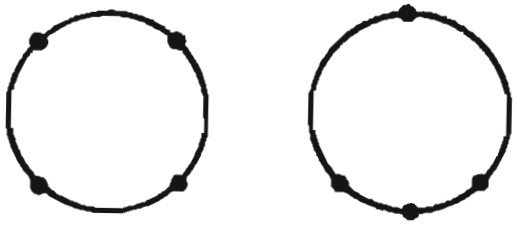

Figure 2.11. Change of landmark position, keeping outline shape constant (from Read and Lestrel (1986))

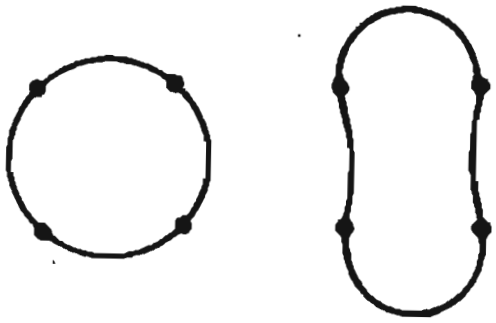

Figure 2.12. Change of outline shape, keeping landmark position constant (from Read and Lestrel (1986))

2.2.2 Mathematical and Statistical Methods

In a morphometric study, it is of value to initially view the data on a univariate basis to gain an idea of the distributions of each of the measurements (Flury and Riedwyl, 1988). However, having recourse to only univariate methods may be inadequate, as the data may well be uninformative, and the statistics generated by such data will not be independent, as such data should tend to show correlations between the variables (Flury and Riedwyl, 1988; Oxnard, 1983a). Therefore, the morphometrician is called upon to make use of multivariate statistical methods; two popular methods of some generality are principal component analysis and cluster analysis, and these methods will be used (directly or indirectly) in each chapter of this study. Despite the popularity (and reasonable familiarity amongst morphometricians) of these methods, the author will provide a review of these methods, as their use is anything but uniform, and the interpretations of the analyses are contingent on decisions made during analysis.

2.2.2.1 Principal component analysis

A widely used multivariate procedure, principal component analysis (PCA), is a popular method by which morphometric data may be explored (Jolliffe, 1986; Marcus, 1990). There are many decisions to be made by the investigator when performing a PCA, and interpretation of the results of such an application need not be straightforward. Accordingly, the mechanisms underlying the application and interpretation of PCA will be reviewed, with an emphasis on methods to be used in this study.

2.2.2.1.1 description

A typical PCA inputs the p original variables (X_i) of a study sample (n), which usually show some intervariable correlation, and forms p new 'variables' (principal components, U_j) that represent weighted linear combinations of the original variables. These principal components are of the form (Flury and Riedwyl, 1988; Marcus, 1990):

$$U_1 = b_{11}X_1 + b_{12}X_2 + \ldots + b_{1p}X_p$$

$$U_2 = b_{21}X_1 + b_{22}X_2 + \ldots + b_{2p}X_p$$

$$\vdots$$

$$U_p = b_{p1}X_1 + b_{p2}X_2 + \ldots + b_{pp}X_p$$

The resulting principal components are chosen to be both uncorrelated, and to successively represent the scatter (variance) of the original variables most effectively (Flury and Riedwyl, 1988). Principal component analysis involves calculation of axes that pass through the (hyper-) ellipsoidal scatterplot, these axes lying in directions of maximal variation of the points (Campbell and Atchley, 1981; Reyment et al., 1984). Thus, the first principal component axis represents a line passing through a cloud of data points such that the spread of points is greatest along that line, and such that the sum of the squared lengths of perpendicular lines joining this line and the individual points is minimal (Campbell and Atchley, 1981; Marcus, 1990). Successive principal components each account for successively smaller proportions of the remaining variance (Marcus, 1990; Reyment et al., 1984). There is also the constraint in PCA that the axes be normalized – that is, of unit length, or (Flury and Riedwyl, 1988; Marcus, 1990)

$$b_{11}^2 + b_{12}^2 + \ldots + b_{1p}^2 = 1.$$

Principal component analysis represents an eigenanalysis, whereby eigenvectors and eigenvalues result. It is beyond the scope of this review to discuss the mathematics of eigenanalyses, but aspects of eigenvectors and eigenvalues of relevance to the morphometrician will be discussed. The eigenvectors of the PCA, or the axes of the above description, are the principal components (hereafter sometimes just components, U_i), such that the vector elements represent the coefficients (b_i) (Marcus, 1990). The magnitudes of the coefficients reflect the importance of those variables to that component (Morrison, 1976). Eigenvectors with coefficients of the same sign are known as general components, those of

mixed sign, bipolar (Pimentel, 1992). The coefficients of a single eigenvector may be multiplied by the corresponding original variables, the linear combination resulting in a principal component score (u_i) (Reyment et al., 1984). By plotting component scores (u_1 versus u_2), one may obtain visual information regarding structure of the data; this will be an important procedure in Chapter 3. The eigenvalues (l_i) represent the variances of the scores along a principal component axis (Campbell and Atchley, 1981; Marcus, 1990; Reyment et al., 1984). The importance of each component is reflected by the proportion of variance accounted for by that component, and may be calculated as the ratio of the eigenvalue to the total variance (Flury and Riedwyl, 1988; Morrison, 1976).

The dimensionality or rank of a data matrix is of importance in this study. The rank of a matrix, or the number of dimensions in which the data vectors lie, is the lesser of n (rows, or individuals) or p (columns, or variables) (Cliff, 1987). For rank $< p$, zero eigenvalues (i.e. equal to zero) are the result; it will be seen that zero eigenvalues may be of interest, as they indicate linear relations between variables. Zero eigenvalues will also result from data matrices where $n < p$, where the number of variables exceeds the sample size; in this particular case, zero eigenvalues are of no interest, so ideally principal component analysis should only be used where $n > p$ (Flury and Riedwyl, 1988).

The effectiveness of PCA resides in the intervariable correlation typically present in morphometric data. In situations where correlation is high, PCA is especially useful, but makes little sense in cases with weak correlation (Flury and Riedwyl, 1988). As PCA involves a transformation of correlated to uncorrelated data, the resulting components may be interpreted independently (Flury, 1988). If sufficient variation is explained by the first q ($< p$) components, it may be possible to represent the p-variate data in a lower dimension (q) (Flury and Riedwyl, 1988; Rao, 1964). Such dimension-reduction may be useful in three cases. Firstly, the number of variables under investigation, if large, may be difficult to manage (Anderson, 1958). Secondly, dimension-reduction may allow the data to be plotted in two or three dimensions to allow inspection of data scatter (Chapters 3 and 4). Thirdly, principal components with (near-) zero eigenvalues may be of interest, as these represent linear combinations of variables that vary little (if at all) throughout the study sample (Jolliffe, 1986).

2.2.2.1.2 methodological issues

Use of principal component analysis is not straightforward; the investigator will be required to make certain decisions that will affect the interpretation of the results. These relate to the input matrix used (covariance or correlation), whether to use raw or log-transformed data, how many principal components should be retained, and distinctness of eigenvalues.

2.2.2.1.2.1 covariance or correlation matrix?

Principal component analysis is performed by extracting eigenvectors and eigenvalues from either the covariance or correlation matrix. As PCA is a scale-dependent method, components resulting from a covariance matrix will be different to those arising from the correlation matrix (Flury and Riedwyl, 1988); the choice of matrix therefore depends on the nature of the data. The covariance matrix is preferred if variables are measured in the same units (Flury and Riedwyl, 1988). If variables are measured in different units, the choice of unit may affect the variance of that variable, which will drive the transformation (Seal, 1964). If the measurements are of different units, and interpretations of linear combinations of these would be difficult, then the correlation matrix should be used (Flury and Riedwyl, 1988; Morrison, 1976). If it cannot be assumed that variances are the same for all variables, Reyment et al. (1984) recommended using the correlation matrix (but see next paragraph), especially for exploratory work. In an allometric investigation, scaling of variables is important, and therefore the covariance matrix is recommended (Klingenberg, 1996).

2.2.2.1.2.2 raw or logarithmic data?

The use of either raw or logarithmic data must also be considered; from a statistical viewpoint, the choice may not be obvious (Jolicoeur, 1963a). One advantage to using logarithms is that results tend to be independent of the order of magnitude of the variables, and variances are made more homogeneous (Jolicoeur, 1963a; Klingenberg, 1996; Smith, 1980). Jolicoeur (1963a,b) advocated the use of the covariance matrix of the log-transformed raw data, in preference to the correlation matrix (of raw data), the latter option he felt "would merely make final interpretation more difficult" (Jolicoeur, 1963a p12). Log-transformation may also be useful if the statistical methods used carry with them distributional assumptions. If log-normality is approximated, log-transformation in this case makes obvious sense (Ebert

and Russell, 1994). However, routine log-transformation may not be an anodyne procedure; while Smith (1980) acknowledged the usefulness of log-transformed variables, he warned against the "exclusive and uncritical use" of such variables (p99). Such use, he stated, could lead to problems with interpretation of results.

2.2.2.1.2.3 how many principal components?

It may be that the investigator has performed a PCA in order to reduce the dimensionality of the data. Discarding components with small eigenvalues aids in interpretation of a PCA, but how small is small enough? Conceptually, the problem relates to the ratio of the sum of the eigenvalues of the components retained to that of all components (Rao, 1964). How much variance explained (relative to the total variance) is sufficient to ignore the remaining eigenvectors is subjective. Numerous methods exist that attempt to objectively calculate the necessary number of components retained (Jolliffe, 1986). It is common to have an approximate cut-off point, for example at 80-90% variance explained (Flury and Riedwyl, 1988). It was Morrison's (1976) view that if one needed to keep more than the first four or five components, interpretation may become impractically difficult.

2.2.2.1.2.4 distinctness of eigenvalues

Flury and Riedwyl (1988) recommended preceding investigation of standard errors with an investigation of sphericity, i.e. whether neighbouring eigenvalues are sufficiently different, or distinct. Principal components are only uniquely defined if the eigenvalues are not identical (Flury and Riedwyl, 1988); if neighbouring eigenvalues are found to be distinct, the corresponding components are necessarily orthogonal. However, if they are found not to be distinct, the components may be chosen to be orthogonal, but an infinite number of orthogonal components may be calculated (Morrison, 1976). Consequently, in the case of 'identical' eigenvalues, the associated components are not uniquely defined (Flury, 1988). Geometrically, such a scatter of points would be of the form of a circle, rather than an ellipse (Morrison, 1976). Should equality of eigenvalues exist, interpretation of the spherical components would not make sense (Seal, 1964).

2.2.2.1.3 interpretation of principal components

As the resultant principal components are uncorrelated, one may interpret the components separately (Flury and Riedwyl, 1988). For whichever reason the investigator has performed the PCA, it will often be of interest to see which of the original variables contribute strongly (or otherwise) to the principal component of interest (as measured by the size of the coefficients). This interpretation may uncover patterns or relationships not evident with the original data (Jolliffe, 1986).

The first principal component in a morphometric study is often referred to as the 'size' component, as the coefficients tend to be of the same sign (i.e. general) (Jolicoeur, 1963a; Jolicoeur and Mosimann, 1960; Marcus, 1990). The remaining components, with mixed sign (bipolar), reflect contrasts in measurement and are designated the 'shape' components (Jolicoeur and Mosimann, 1960; Marcus, 1990). There is, however, no a priori reason that this should be so, although this appears to be a common interpretation (Reyment et al., 1984). Bookstein's (1989) statement, "...one hopes that this linear combination is congenial to interpretation as "size"..." (p175), suggests that he was not convinced. This issue will be discussed further in Chapters 3 and 4.

While attention in the literature has focused on the eigenvalues with the greatest variance, the eigenvectors with the smallest eigenvalues may also be of interest (Gnanadesikan and Wilk, 1969; Gower, 1967; Rencher, 1995). The eigenvector associated with the smallest eigenvalue should reflect a direction of relative invariance, which may be biologically meaningful (Jolicoeur, 1963a; Reyment et al., 1984). This eigenvector is a combination of variables that remains relatively constant, and such eigenvectors may be compared across samples, provided that measurements are made in the same metric (Rencher, 1995; Reyment, 1980). The last components may also provide information about outliers and extreme values (Flury and Riedwyl, 1988). If the last components have small and similar magnitudes, it may be that these components reflect sampling error (Flury and Riedwyl, 1988). Should these components reflect such error, one would expect them to be spherical, as random (uncorrelated) error variables should be distributed in a circular fashion (Bookstein, 1991).

2.2.2.2 Cluster analysis

Cluster analysis, in its different forms, appears to have been used to a lesser extent in morphometric studies, but has general properties which should be of use in this study. This review will encompass the foundations and methodological considerations that may affect interpretation of the results of a cluster analysis.

2.2.2.2.1 description

In general (as methods are numerous), clustering analysis takes a set of data based on a sample of specimens, and organizes these specimens into "relatively homogeneous groups" (Aldenderfer and Blashfield, 1984 p7). Such groups, or clusters, are vaguely defined (if at all), and may be indicated by such properties as an increased density of points in phenotype space (Aldenderfer and Blashfield, 1984; Sneath and Sokal, 1973). Starting with a matrix of similarity (or dissimilarity) data, specimens are clustered first with those most similar, with successively larger clusters containing less similar specimens (Boyce, 1969; Sneath and Sokal, 1973). How successive specimens are compared to smaller clusters differs from method to method, and in NTSYSpc this is the only way the various clustering methods differ (Rohlf, 1986-1998). A tree diagram is then constructed, which links specimens based on phenetic similarity (i.e. of appearance, based on the available data) (Aldenderfer and Blashfield, 1984; Sokal and Rohlf, 1962). Specimens are clustered relative to a horizontal scale based on the measure of similarity, one end representing maximal similarity, the other maximal dissimilarity (Sokal and Rohlf, 1962). The limit of dissimilarity is reached when all specimens are clustered in one group (Aldenderfer and Blashfield, 1984; Sokal and Rohlf, 1962).

2.2.2.2.2 methodological issues

A summary of steps taken during a cluster analysis is as follows: (1) select sample; (2) measure variables; (3) compute similarities (or dissimilarities); (4) perform cluster analysis; and (5) validate the analysis (Aldenderfer and Blashfield, 1984). Steps (1) and (2) are self-explanatory, and will not be discussed here; the remaining steps deserve some attention, as these will affect interpretation of results.

The choice of similarity measure, step (3), may include distance measures (Euclidean distance, average taxonomic distance) which are measures of dissimilarity (i.e. increase with increasing dissimilarity), and correlation measures (product moment correlation coefficient, direction cosine) which are measures of similarity (Sneath and Sokal, 1973).

Summarizing step (4), choice of method, is not straightforward. Methods that fall under the umbrella of cluster analysis are many and widely varied (Sneath and Sokal, 1973), and it is beyond the scope of this review to be comprehensive when discussing these methods. It will be helpful here to consider what defines a method that is popular with morphometricians (Daegling and Jungers, 2000; Lague and Jungers, 1996; Seiffert and Kappelman, 2001; van Dam, 1996), the unweighted pair-group method using arithmetic averages (UPGMA) (Sneath and Sokal, 1973). UPGMA is a pair-group method in that only one specimen is allowed to join a cluster per iteration of the method, that is, a most similar pair of individual specimens will be clustered first, and in the second iteration, a third specimen will be clustered with the first-level cluster (Sneath and Sokal, 1973). It is unweighted in that a specimen joining a cluster of several specimens carries the same weight as if it were joining another single specimen. Finally, UPGMA uses arithmetic averages, in that when comparing a single specimen against a cluster of several specimens, the arithmetic average of similarity between specimens in a cluster and the next specimen is calculated (Sneath and Sokal, 1973).

The success of a clustering method, step (5), may be measured by how well the final tree diagram reflects the similarities presented in the similarity matrix (Sneath and Sokal, 1973). Such concordance is not guaranteed – for example, the UPGMA method compares average similarities, so information on the individual similarities is lost (Sokal and Rohlf, 1962). A measure of concordance is the cophenetic correlation (Rohlf and Sokal, 1981; Sokal and Rohlf, 1962). Cophenetic correlation is calculated as the product-moment correlation coefficient between the original similarity matrix and a matrix derived from the tree diagram structure, and the greater the value of this correlation, the more appropriate the classification (with respect to the similarity matrix) (Aldenderfer and Blashfield, 1984; Rohlf, 1986-1998; Rohlf and Sokal, 1981; Sokal and Rohlf, 1962).

2.2.3 Summary

The morphometrician must make a number of decisions in an investigation; even the act of gathering basic data comes only after considering certain factors such as the nature of the specimens and the aims of the investigation. Specimens may lend themselves to detection of landmarks, or may be so devoid of recognizable features such that the smooth outline of the form is the object of interest. In this investigation, elliptic Fourier analysis will be used to quantify the outline form of the patella. The choice of analytical tools is wide, and two such tools are principal component analysis and cluster analysis. These methods allow for easier observation of data structure and outlying specimens than would the raw data alone. Principal component analysis also provides 'new' variables, derived from the raw data, that are uncorrelated and allow for further univariate analysis.

Chapter 3 Preliminary Investigations

In this section, preliminary investigations of the data were recorded; these investigations included determining reliability prior to further analysis of the data. The number of Fourier descriptors that was most appropriate to use in the later investigations was also determined, and was included under 'preliminary investigations'. Lastly, ordination of data from each group was performed, which had the potential to influence the more advanced investigations.

3.1 Background

Investigation of data structure within a large data set may begin with a visual assessment of the spread of data points, so as to give information regarding heterogeneities (grouping and separation within phenotype space) as well as outlying data points (Foottit and Sorensen, 1992; Gower, 1987; Pielou, 1984; Pimentel, 1992). This is of interest in a study of patellar morphology, as Wiberg (1941) has suggested that patellae present as one of three types (page 4); Moreover, it is of interest to view the patterns of specimens in phenotype space, to uncover possible constraints of phenotypes (§2.1.4.1). In the bivariate case ($p = 2$), such an assessment may be done simply by plotting one variable against the other and perusing the scatterplot (Gower, 1987). In the multivariate case, the simple representation of data points along Cartesian axes is difficult when $p = 3$, and impossible when $p > 3$, and other methods must be called upon to meaningfully reduce the information from p dimensions into two (at most three) (Gower, 1987). Such a reduction should be meaningful in the sense of minimizing the loss of information with such a manoeuvre (Foottit and Sorensen, 1992; Pimentel, 1992). The use of such methods, and the subsequent plotting in reduced dimension, is known as ordination (Gower, 1987; Pimentel, 1992).

Principal component analysis, as an ordination method, capitalizes on redundancy in data sets, such that redundant dimensions of the transformed data may be ignored, and the investigator may concentrate on the data set of reduced dimension (Foottit and Sorensen, 1992; Pielou, 1984). If the data set can be reduced to two or three dimensions (i.e. sufficient proportion of total variance accounted for – §2.2.2.1.2.3), the transformed data may be graphically represented and can thus be used to gain information regarding data patterns (Reyment et al., 1984). Examples of the PCA approach to morphometric ordination include Jolicoeur (1963a) (limb bones in martens), Jolicoeur and Mosimann (1960) (turtle carapaces), Klingenberg et al. (2001) (mouse mandibles) and Rincón (2000) (whole fish) and. The appropriateness of PCA

as an ordination method depends on its ability to account for the spread of the data points in reduced dimension. Therefore, the eigenvalues associated with the retained components must represent a large amount of the total variance of the data points (Marcus, 1990). Certain details of data structure may be gleaned from plotting principal component scores; for instance, information regarding nonlinearity of the data and multivariate outliers (Flury and Riedwyl, 1988).

Alternatively, cluster analysis results in a tree diagram that relates specimens on a one-dimensional axis of morphometric similarity, so specimens with greater morphometric similarity are placed closer together than specimens with less similarity (Boyce, 1969; Sneath and Sokal, 1973). For example, heterogeneities in the data would be represented by a tree that shows clustering of some specimens within a short range of dissimilarity, with a greater measure of dissimilarity required to cluster these with other specimens or clusters (Sokal and Rohlf, 1962). A uniform distribution of specimens on the other hand would be indicated by a uniform distribution of dissimilarities between specimens. The appropriateness of interpreting the tree diagram for ordination is reflected in the cophenetic correlation (§2.2.2.2.2). Examples of UPGMA cluster analysis for morphometric ordination include Lague and Jungers (1996) (fossil hominid humeri), Seiffert and Kappelman (2001) (primate orbits) and van Dam (1996) (fossil murid teeth).

Before using these ordination methods, an issue that needs to be addressed is reliability. Reliability relates to the repeatability of the data capturing methods, as opposed to validity, or the ability of the methods to measure what they are supposed to measure (Currier, 1990); it was assumed here that the validity of the methods was acceptable. The variables measured will be a reflection of (1) the 'true' value of the variable, and (2) measurement error (Bailey and Byrnes, 1990; Fleiss, 1986). It will be of value to estimate the degree of measurement error in a data set, as substantial error may attenuate correlations (and therefore covariances), which will potentially affect principal component analysis (Bailey and Byrnes, 1990; Fleiss, 1986). There is also the potential, more relevant to Chapters 4 and 5, for measurement error to reduce the power of inferential methods (Bailey and Byrnes, 1990; Fleiss, 1986).

3.2 Aims and Hypotheses

The aims and hypotheses of this chapter were:

Aim 1: to investigate the reliability of the conventional (perimeter length and square root of area) and Fourier (amplitudes) variables, by means of Model II analyses of variance of data (from *Homo*) collected on two separate occasions

Aims 2 and 3 related to ordination.

Aim 2: to uncover any patterns in the data (including identification of outliers and the influence of such specimens, and any grouping of specimens) using principal component analysis based on conventional and Fourier data and plotting data points according to scores on the first two principal components

Aim 3: to investigate clustering of all specimens using UPGMA cluster analysis based on average taxonomic distance between specimens using conventional and Fourier data

Aims 2 and 3 required that the number of Fourier variables be modified according to the contribution of each harmonic, so it was necessary to state

Aim 4: to investigate the power spectra of the Fourier amplitudes, to identify which harmonics accounted for the bulk of form information, and should therefore be retained for further use

3.3 Materials and Methods

3.3.1 Materials

Human patellae were harvested from dissecting-room cadavera from the Department of Anatomical Sciences, University of Adelaide (Table A.1, page 297). Use of this material was allowed for by the Transplantation and Anatomy Act, 1983 (South Australia). Patellae were excised from all available cadavera, male and female, from right and left sides. All individuals were skeletally mature. Patellae were excluded if the knees showed signs of surgery (for example knee arthroplasty) or of advanced cartilage degeneration (for example bony eburnation).

Nonhuman specimens were obtained from the Mammal Collection at the British Museum (Natural History), London (Table A.2, page 301). Specimens used were any available loose (not mounted) bones from individuals of the genera *Cercopithecus*, *Colobus* or *Gorilla*. Patellae from both sexes were included. It was not possible to judge from which side each bone came, as the author was not aware of any data which might elucidate this in nonhuman primates (as opposed to humans (Trinkaus, 2000)). Patellae were excluded if there was any indication that the individual had not reached skeletal maturity (nonfused physes), or if they showed signs of articular degeneration (bony erosion).

3.3.2 Methods

3.3.2.1 Specimen preparation/data capture

In the human cadavera, skin and superficial fascia were dissected from the anterior aspect of the knee in a flap, hinged medially or laterally, which extended 1 or 2cm above and below the patella. The extensor mechanism soft-tissues were incised around the periphery of the patella, and the patella was removed. Each patella was wrapped in wire mesh, which allowed each bone to be accompanied by a metal disc, upon which a unique identifying alphanumeric code had been punched. Thus it was possible to identify each bone during the next stage of processing. Patellae were rinsed in running tap water for at least an hour, before being placed in a beaker in a solution of 2% potassium hydroxide. The beaker was placed on a hotplate and brought to the boil (typically taking approximately 45 minutes). The solution was kept boiling for a further 15 minutes, after which the beaker and its contents were rinsed under running tap water for an hour. Bones were then individually cleaned of any remaining soft-tissue, and

dried in a drying oven for at least 24 hours. Once dried, the identification code was written on the dorsal surface of each bone in black marker.

Patellae were taken to the Imaging Department of the Adelaide Women's and Children's Hospital. Two computed tomographic (CT) images were taken horizontally across each patella. Imaging locations on each bone had been marked at the junction of the first and second quarters (proximal image) and the third and fourth quarters (distal image) of the articular surface. These locations were found by (i) drawing a pencil line across the greatest breadth of the articular surface, (ii) drawing a vertical pencil line perpendicular to the first, (iii) measuring the greatest vertical distance of the articular surface along this vertical line, (iv) marking points at 25% and 75% of this distance along this vertical line, and (v) drawing horizontal pencil lines perpendicular to the vertical line at these points (Figure 3.1). Patellae were placed on their dorsal sides on the CT scanning bench (articular surface facing upwards) in a foam rubber cradle, which was used to minimize tilting of the bones around sagittal or coronal axes. Bones were aligned using a horizontal laser guiding light, so that the proximal pencil line was aligned with the guiding light. Images were then taken at this point and the point where the guiding light met the distal pencil line. Hard copies of images were then produced. An electronic copy of each image was produced using a desktop scanner capable of scanning transparencies, and saving the image as a bitmap file.

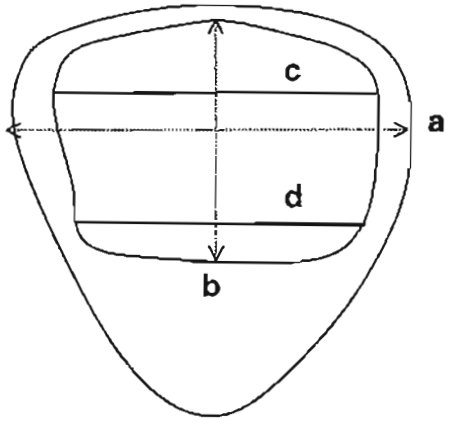

Figure 3.1. Diagram showing the lines drawn on the articular surface of the patella (**a** maximum horizontal patellar breadth, **b** perpendicular to a along articular surface, **c** and **d** at 25% and 75% length of **b**, respectively)

For the nonhuman specimens, CT images were made in the X-Ray Department of the Chelsea and Westminster Hospital, London. Locations of proximal and distal image sites were determined differently with these specimens, as they could not be marked. Instead, the greatest vertical distance was measured on each articular surface, parallel to the longitudinal axis of the bone. Each bone was placed on the scanning bench in a foam cradle. The CT scanner was equipped with both vertical and horizontal guiding lights, so the longitudinal axis of each bone was aligned with the vertical guiding light. Images were then taken at the appropriate distances (calculated using the length of the articular surface, measured with callipers to 0.1mm) from the most proximal articular margin. Hard copies were produced, and electronic copies were made (as above).

Outline data for each image were captured using WinDig software (Lovy, 1994-1996), by pointing the mouse cursor to points of arbitrary distance along the specimen outline. It was intended that left and right specimens that were mirror images of each other (i.e. were the same up to a horizontal reflection), would be deemed identical. In *Homo*, images from right-sided bones were reflected in a horizontal plane, so that all specimens could be considered as left-sided (i.e. all treated alike). This could not be done with the nonhuman specimens (§3.3.1). At least 60 points were captured on each outline, with point data stored in a ascii text file as (x, y) pairs. Measurements were made in pixels: at a screen resolution of 72 pixels per inch, each pixel was equivalent to 0.35mm. The first point was digitized at the tip of the patellar crest, and successive points were digitized in an anticlockwise direction (i.e. initially moving medially). Some specimens (mostly *Homo*) showed very irregular exostoses on their dorsal sides, which were not considered important aspects of bone shape, and outline digitizing ignored these features. Nonhuman specimens were only digitized once. Each data file was transformed to elliptic Fourier coefficients using the Fourier option in NTSYSpc (Rohlf, 1986-1998). Data were left unscaled (*Standardize by – NONE*), and outlines were oriented by rotating so that the long axis of the first harmonic came to lie horizontally, and the starting point of each outline lay at the tip of this long axis (*Orientation adj. – BOTH*). As the minimum number of outline points was 60, 30 harmonics were generated for each outline. Outline lengths were also generated using this procedure, and outline areas were obtained by repeating the process using scaled data (*Standardize by – AREA*). For *Homo* specimens, the process from digitizing onwards was performed three times, for reliability purposes as well as increasing the validity of the data (due to approximation of some dorsal outlines).

Data used in this study were both conventional (perimeter length (***P***), the square root of area (***A***) – the square root was used to keep ***P*** and ***A*** in the same dimension) and Fourier variables. Elliptic Fourier coefficients detect right-left differences, and it was not possible to tell which side each nonhuman specimen was from. This was important, as these differences determined the direction of digitizing. However, amplitudes do not detect side differences (due to squaring of coefficients), so all coefficients (including *Homo*) were transformed to amplitudes. This was done using the method of McLellan and Endler (1998), that is:

$$Xn = \sqrt{a_n^2 + b_n^2} \text{ and } Yn = \sqrt{c_n^2 + d_n^2} .$$

There being two amplitudes per harmonic (***Xn*** and ***Yn***), 60 amplitudes were generated per specimen (***X1***, ***Y1***, ***X2***, ***Y2***,..., ***X30***, ***Y30***). Conventional and Fourier variables were also transformed to their natural logarithms (**ln*P***, **ln*A***, **ln*X*1**, **ln*Y*1** etc.).

3.3.2.2 Reliability

Reliability of data used in this study was estimated using Model II analysis of variance (anova) (Fleiss, 1986; Sokal and Rohlf, 1995). This entailed the computation of the following percentage:

$$\frac{s_A^2}{(s^2 + s_A^2)} \times 100,$$

where s_A^2 is the added variance component among groups, s^2 is the within-groups variance, and

$$s_A^2 = \frac{1}{n}(\textit{among-groups variance} - \textit{within-groups variance}).$$

This percentage reflects the variance among specimens relative to that within specimens (i.e. among repeats) with 100% reflecting perfect reliability. The variance components were computed as follows (Sokal and Rohlf, 1995):

$$\textit{among-groups variance} = \frac{\Sigma(\bar{Y} - \bar{\bar{Y}})^2}{a-1} \times n,$$

where $\bar{Y}$ equals the individual means (from repeated measures), $\bar{\bar{Y}}$ is the grand mean (of individual means), a is the number of groups (individuals), and n equals the number of measurements on each individual; and

$$within\text{-}groups\ variance = \frac{\sum\left(\sum y^2\right)}{\sum(n-1)},$$

where $\sum y^2$ is the sum of squared deviations from the group (individual) mean.

Data were gathered from specimens on two separate occasions at least one week apart. Due to the time constraints of overseas travel, no repeat data could be gathered for the nonhuman groups. Therefore, repeat data were gathered for a series of human specimens only. Reliability specimens were selected arbitrarily, such that there were specimens from 10 individuals, right and left sides, both male and female i.e. 40 bones from 20 individuals. Repeat data were generated by painting over the original orientation lines using an opaque white enamel paint, and the process was repeated (marking, scanning and digitizing, including averaging three sets of data). All conventional and Fourier variables were assessed, in their raw state.

3.3.2.3 Power spectra

As a means of reducing the number of Fourier amplitudes used in this study, power spectra were constructed using the definition of power from Lestrel (1997b),

$$power = \frac{amplitude^2}{2},$$

and graphs were plotted to allow interpretation of this information (consequently, there were two powers per harmonic). Decisions regarding the number of amplitudes to retain were made on the subjective basis of a substantial proportion of power.

3.3.2.4 Ordination

Ordination was performed on each data set using (1) principal component analysis and (2) UPGMA cluster analysis. The data sets used were of conventional data (***P*** and ***A***), and Fourier data (amplitudes selected from §3.4.3). For principal component analysis, covariance matrices of raw and logarithmic data were used, as the variables were measured in the same units (§2.2.2.1.2.1). Principal component analyses were performed by first generating covariance and correlation matrices, using the Simint program in NTSYSpc. Eigenanalyses were then performed using the Eigen program in NTSYSpc using the covariance matrices. The decision regarding the type of data used for ordination was made in view of the distribution of variances of variables (preferably all of similar magnitude) and the amount of variance accounted for by the first two (three if necessary) eigenvectors; the ability to plot data in only two dimensions was weighted highly when making this decision. Principal component scores were calculated using Projection, and data scatters were produced using 2D plot. Outlying data points were detected by perusing the data scatters and identifying any points that lay noticeably away from the majority of points. As a means of detecting the influence of any outlying specimens uncovered, analyses were repeated with the omission of these individuals. Influences on eigenvectors were expressed as angles between the original and repeat eigenvectors, and on eigenvalues as differences in variance proportions. Angles were calculated first as the cosines of these angles, which were calculated as follows (Sneath and Sokal, 1973):

$$\cos\theta_{jk} = \frac{\sum_{i=1}^{n} X_{ij} X_{ik}}{\sqrt{\sum_{i=1}^{n} X_{ij}^2} \sqrt{\sum_{i=1}^{n} X_{ik}^2}},$$

where j and k were the two eigenvectors, inclusive and exclusive of these specimens respectively.

Cluster analysis was performed using NTSYSpc by first calculating average taxonomic distance (ATD) between all specimen pairs using SimInt (*coefficient – DIST*). Average taxonomic distance between specimens a and b based on p measurements was calculated as follows (Rohlf, 1986-1998; Sneath and Sokal, 1973):

$$ATD_{ab} = \sqrt{\sum_{i=1}^{p} \frac{1}{p}(x_{ia} - x_{ib})^2} .$$

The clustering procedure was carried out using SAHN (*clustering method – UPGMA*). Tree diagrams were produced using Tree plot. Cophenetic correlations were calculated by submitting each tree diagram to Coph, then comparing the matrix generated by Coph with the original dissimilarity matrix using MxComp. Interpretation of cophenetic correlation was based on Rohlf's (1986-1998) criteria.

As the tree diagram resulting from cluster analysis reflects the relative phenetic similarity between specimens, it was decided to repeat the analyses using the females distal data with the inclusion of specimens from a vastly different (structurally and functionally) taxon, to gain some perspective. Thus, these data also featured those from two patellae (expressed as an average) from the museum skeleton of a 46-years-old Asian elephant (*Elephas maximus*). The (distal) images were generated using the method for the nonhuman primates in the Imaging Department of the Adelaide Women's and Children's Hospital.

3.4 Results

3.4.1 Specimens

The sample sizes of human and nonhuman patellae are presented in Table 3.1. *Cercopithecus* comprised specimens from the species *C. aethiops* (22 specimens), *C. solatus* (one), *C. mona* (12), *C. campbelli* (two), *C. neglectus* (nine), *C. ascanius* (six), *C. nictitans* (five), *C. mitis* (39), and nonspecific *Cercopithecus* (three). *Colobus* included the species *C. badius* (15 specimens), *C. preussi* (two), *C. angolensis* (four), *C. guereza* (23), *C. satanus* (two) and *C. polykomas* (one). Five *Gorilla* specimens from three individuals were marked *G. g. gorilla*, and no further subspecies details were given. Beyond exclusion of whole bones, one outline on certain bones (proximal *or* distal) was not deemed acceptable for use in this study (outline was not clear), and was excluded. Figure 3.1 shows photographs of selected specimens from each genus.

Table 3.1. Study sample sizes – specimens (individuals)

	n_{female}	n_{male}	n_{total}
Homo	[a]106 (59)	[b]103 (60)	209 (119)
Cercopithecus	49 (27)	[c]50 (28)	99 (55)
Colobus	26 (14)	21 (13)	47 (27)
Gorilla	16 (10)	9 (5)	25 (15)

[a]4 specimens excluded from distal data
[b]2 specimens excluded from proximal data
[c]1 specimen excluded from distal data

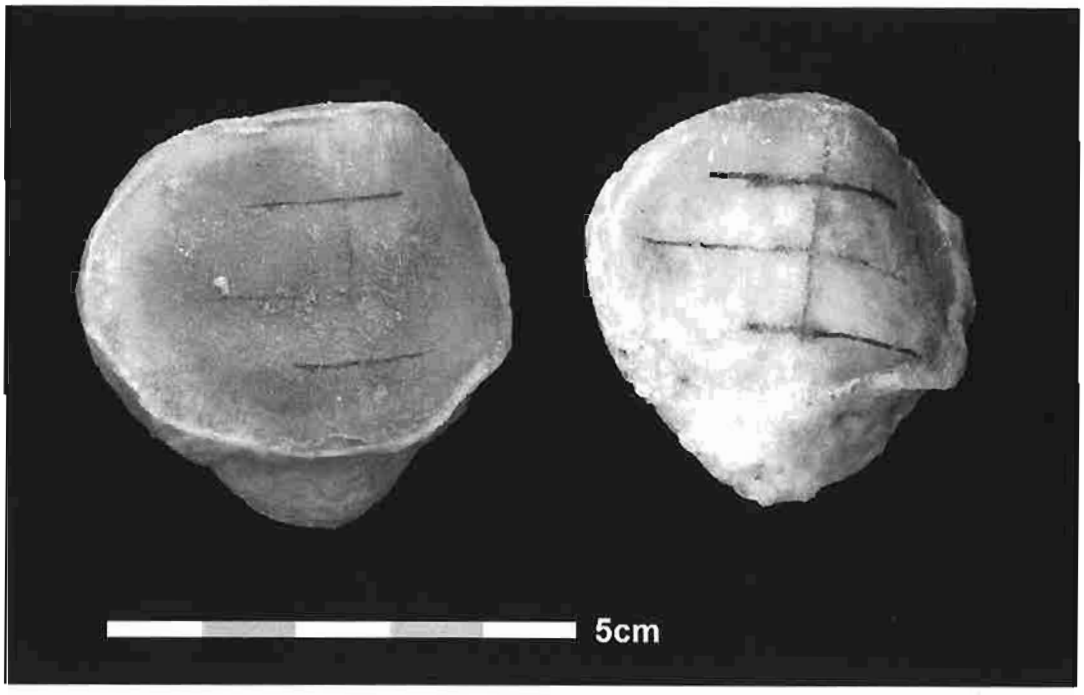

(a) *Homo* (specimens 113 and 97, left to right)

(b) *Cercopithecus* (specimens 505, 543 and 588, left to right)

Figure 3.2. Photographs of selected patellae (proximal pole uppermost, ventral side facing; nonhuman scales in mm)

(c) *Colobus* (specimens 628 and 606, left to right)

(d) *Gorilla* (specimens 648 and 662, left to right)

Figure 3.2 (continued)

3.4.2 Reliability

3.4.2.1 Conventional data

Results from the estimations of reliability for *Homo* data are presented in Table A.3 (page 303), and reproduced in Table 3.2. Percentages of reliability for ***P*** and ***A*** ranged from very good (***P***, females distal – 96.98%) to only moderate (***P***, males proximal – 79.64%). As the bulk of variance here was due to among-specimen variance, these variables were retained for analysis.

Table 3.2. Reliability percentages – *Homo*, conventional data

	P	***A***
females distal	96.98	96.57
females proximal	92.71	90.15
males distal	88.27	94.06
males proximal	79.64	89.40

Error in measuring these variables (beyond random variation) might have been introduced in generating the images and in the digitizing of outline points. In the former, error might have resulted from the marking of the image lines and the placement of the bones on the scanning bench. In the latter, error might have resulted from the placement of the cursor on the outline. Digitizing error might also have arisen due to the number of points digitized: the outlines were digitized not as smooth curves but many-sided polygons; slightly different results might have resulted due to the difference between (say) a 60-sided polygon and a 65-sided polygon, even though these shapes approximated the same smooth outline. Error was also potentially increased in this study due to the 'estimation' of the dorsal outline for some specimens (mostly *Homo*). In order to estimate the size of these error components (imaging and digitizing), the three outlines per specimen were used. The reliability of these variables in absence of imaging error (as the images did not change) was calculated in a similar manner (using all specimens, rather than the reliability subset), and these results are presented in Table A.4 (page 303) and reproduced in Table 3.3. The excellent reliability for the conventional data (all > 98%), when considering digitizing error only, indicated that the bulk of the measurement error lay in the imaging methods. These results also suggested that the estimation of the dorsal outline in some cases was performed reliably.

Table 3.3. Reliability percentages (digitizing error only) – *Homo*, conventional data

	P	*A*
females distal	99.65	98.24
females proximal	99.62	98.65
males distal	99.50	98.58
males proximal	99.43	98.30

3.4.2.2 Fourier data

Results from the estimation of reliability for Fourier data for *Homo* are presented in Table A.5 (page 305) and reproduced in Figure 3.3. Reliabilities were fair to excellent for the first five harmonics (67.95% to 97.24%), with two major exceptions: ***Y*3** from the females distal data showed a very poor reliability of only 43.90%, and ***X*2** from the males distal data was only marginally better at 55.84%. Therefore, although most variables had acceptable reliability (around 80% to close to 100%), these two variables were conspicuously unreliable. Inspection of the higher-order harmonics revealed that much of the interspecimen variation was overshadowed by intraspecimen variation, sometimes to the extent that reliabilities took on negative values.

As for the conventional data, the error due to digitizing was estimated by using the three digitized outlines per specimen (again, using all specimens). As this was for illustration purposes only, these calculations were only performed on the males proximal data (the group with the lowest consistent reliabilities), and only for the first 10 harmonics. These results are presented in Table A.5(c) (page 306), and reproduced in Table 3.4. Again, there was very little in the way of measurement error (all reliabilities exceeded 96%), so that the bulk of the error related to the imaging method.

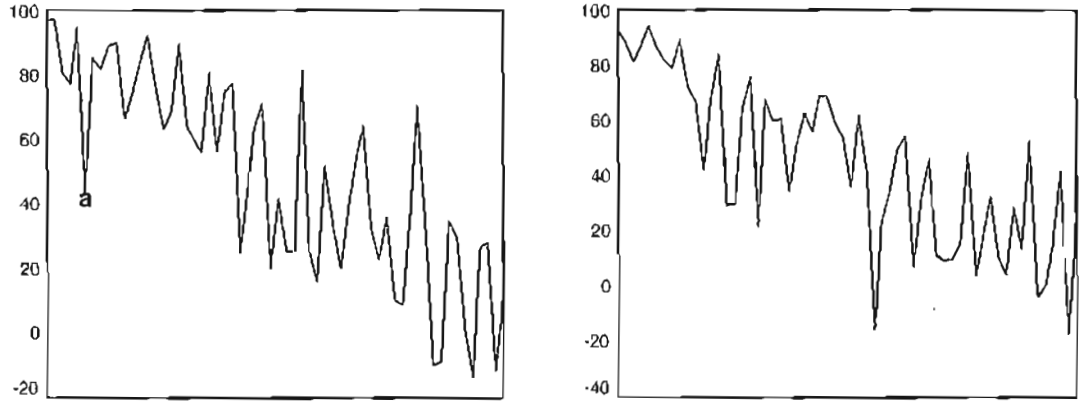

(a) females distal (b) females proximal

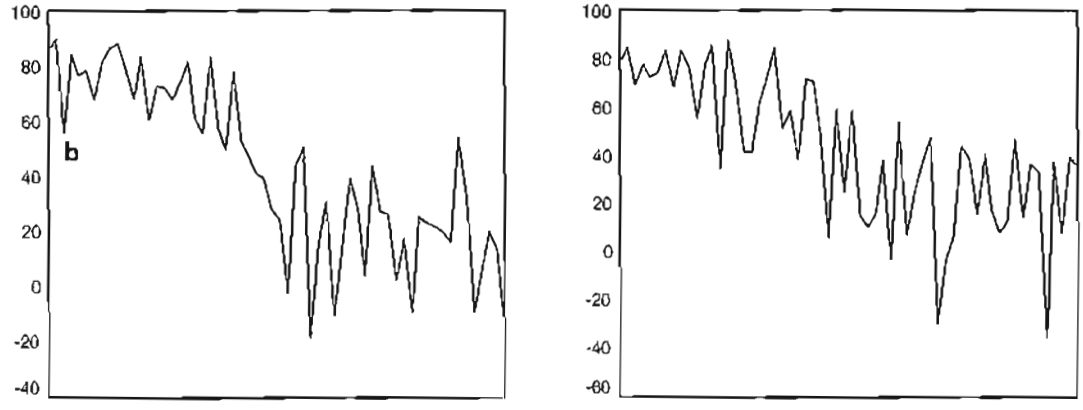

(c) males distal (d) males proximal

Figure 3.3. Graphs of reliability percentages (y-axis) for variables $X1$, $Y1$,..., $X30$, $Y30$ (x-axis) – *Homo* (a and b indicate amplitudes $Y3$ and $X2$, respectively)

Table 3.4. Digitizing reliability – *Homo* males proximal, Fourier data

amplitude	$X1$	$Y1$	$X2$	$Y2$	$X3$	$Y3$	$X4$	$Y4$	$X5$	$Y5$
rel %	98.99	98.98	98.93	98.87	98.99	98.96	98.95	98.96	98.98	98.76
amplitude	$X6$	$Y6$	$X7$	$Y7$	$X8$	$Y8$	$X9$	$Y9$	$X10$	$Y10$
rel %	98.91	98.91	98.92	98.89	98.93	98.93	98.90	98.85	96.67	98.75

3.4.3 Power

The powers of amplitudes ***X*1** to ***X*30** and ***Y*1** to ***Y*30** for each group are presented in Table A.6 (page 307). The first harmonic greatly dominated for all groups. The percentages of total power (separately for *X* and *Y*) for each amplitude were calculated and are presented in Table A.6 in cumulative form for the first 10 harmonics. The power spectra are charted cumulatively for the first 10 harmonics in Figure 3.4. The minimum power (as a proportion of total power) accounted for by the first five harmonics was 99.92%. Dominance of the first harmonic was reflected well in these figures: the minimum percentage of total power accounted for by either ***X*1** or ***Y*1** was 97.92%. As such, further investigations only included data from the first five harmonics.

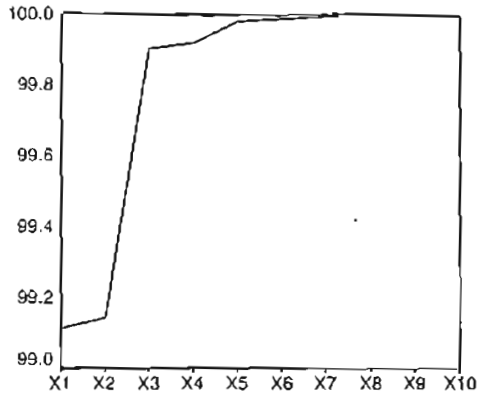

(i) females distal, *X*-amplitudes

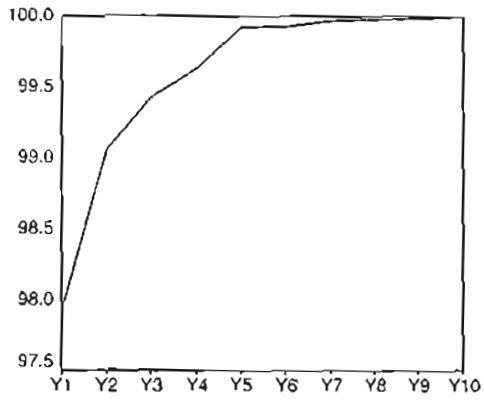

(ii) females distal, *Y*-amplitudes

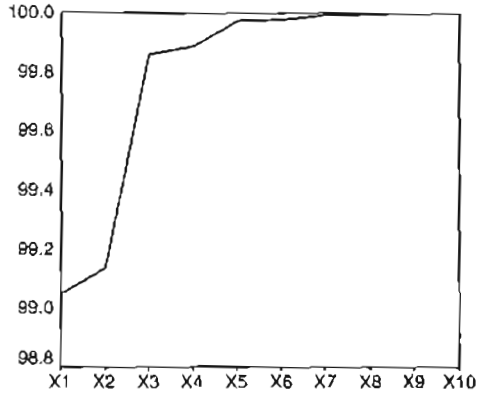

(iii) females proximal, *X*-amplitudes

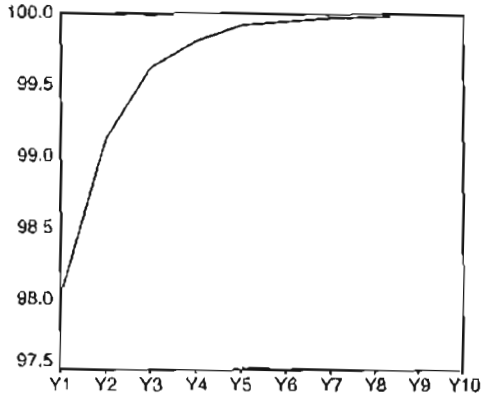

(iv) females proximal, *Y*-amplitudes

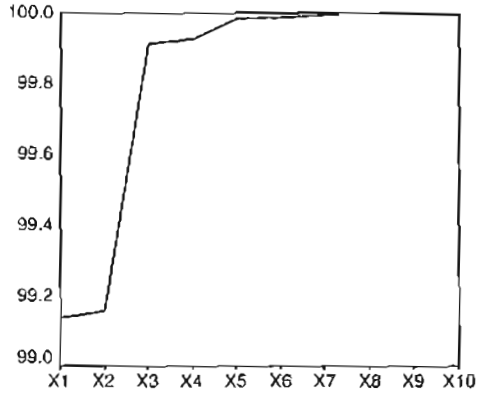

(v) males distal, *X*-amplitudes

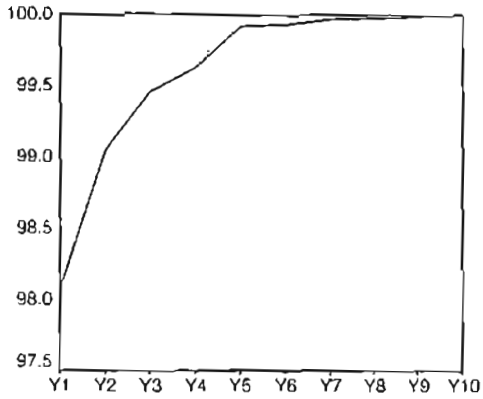

(vi) males distal, *Y*-amplitudes

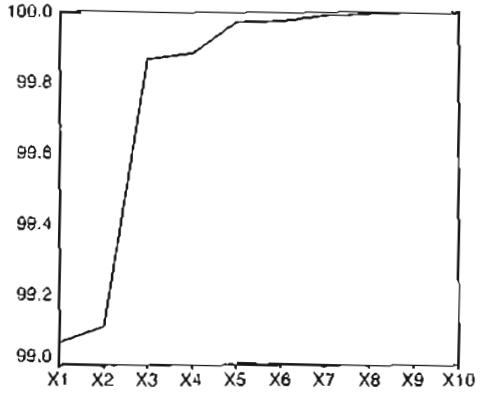

(vii) males proximal, *X*-amplitudes

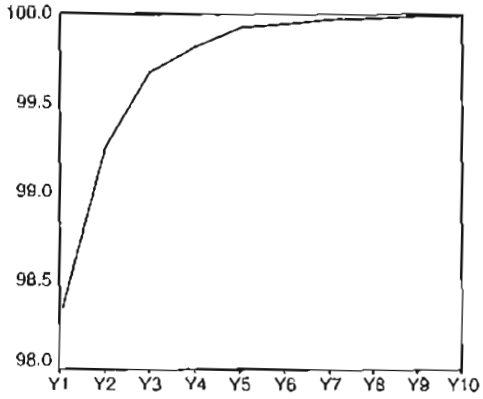

(viii) males proximal, *Y*-amplitudes

Figure 3.4. Cumulative percentages (*y*-axis) of total power for harmonics 1 to 10 (*x*-axis)

(a) *Homo*

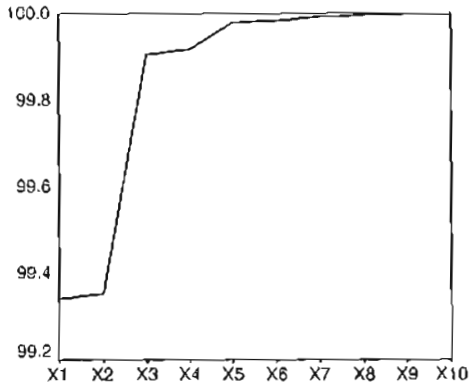

(i) females distal, *X*-amplitudes

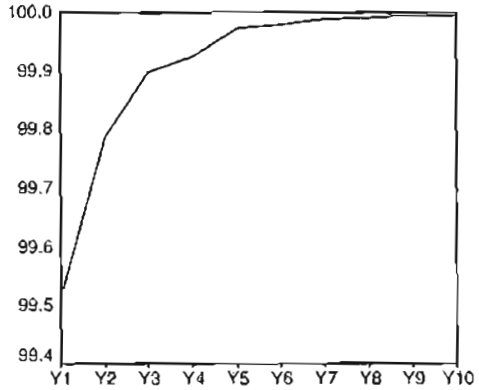

(ii) females distal, *Y*-amplitudes

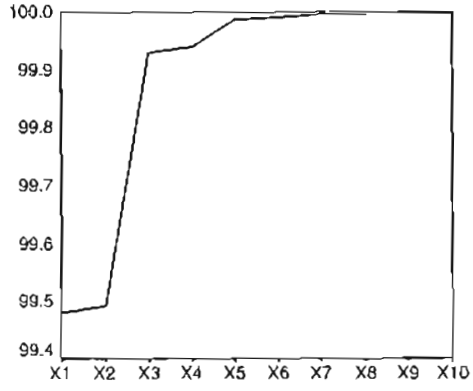

(iii) females proximal, *X*-amplitudes

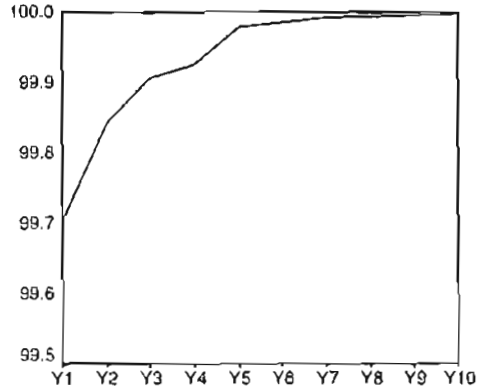

(iv) females proximal, *Y*-amplitudes

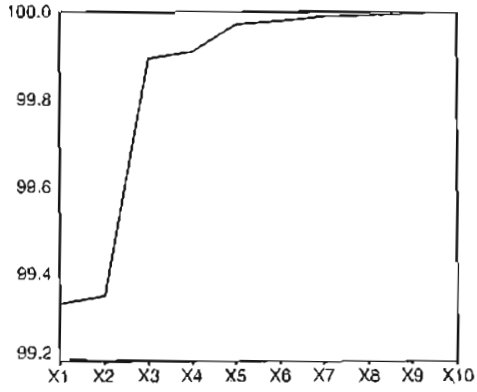

(v) males distal, *X*-amplitudes

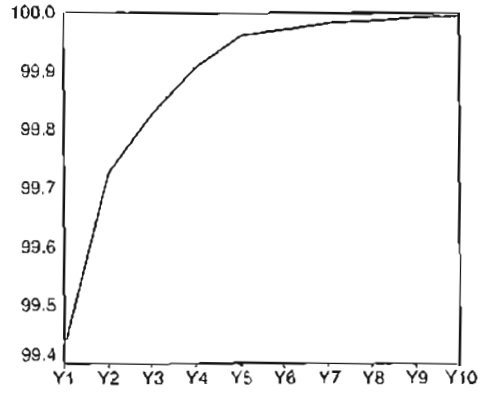

(vi) males distal, *Y*-amplitudes

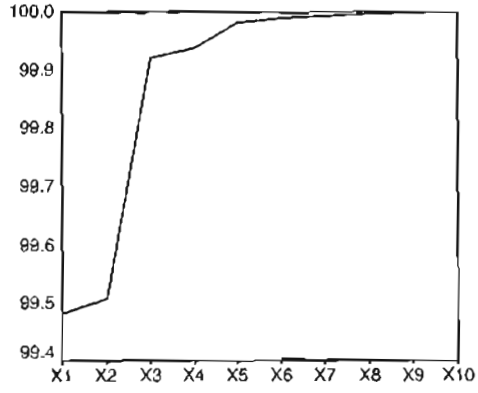

(vii) males proximal, *X*-amplitudes

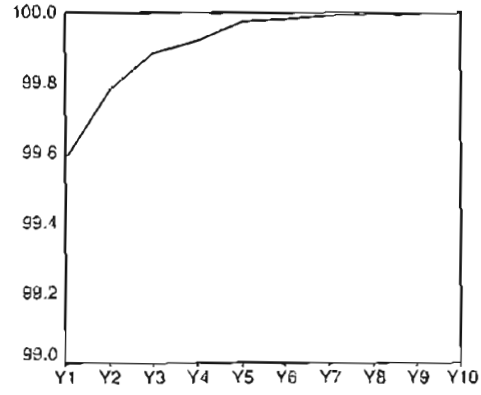

(viii) males proximal, *Y*-amplitudes

Figure 3.4. (**b**) *Cercopithecus*

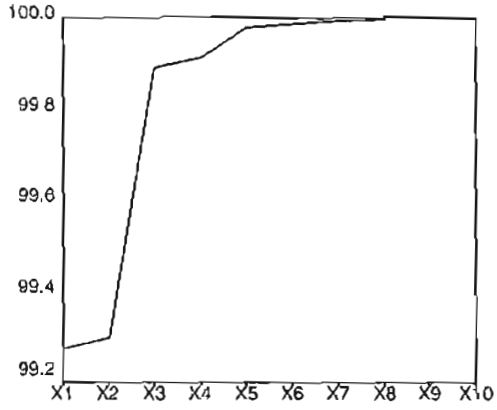

(i) females distal, *X*-amplitudes

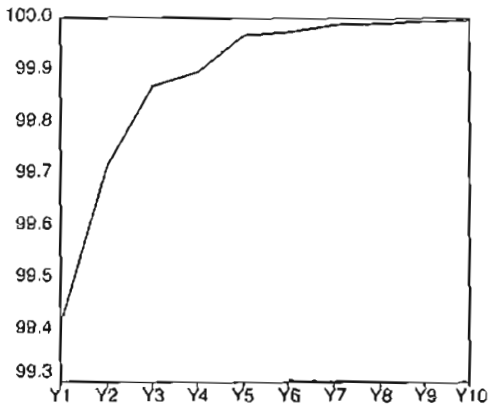

(ii) females distal, *Y*-amplitudes

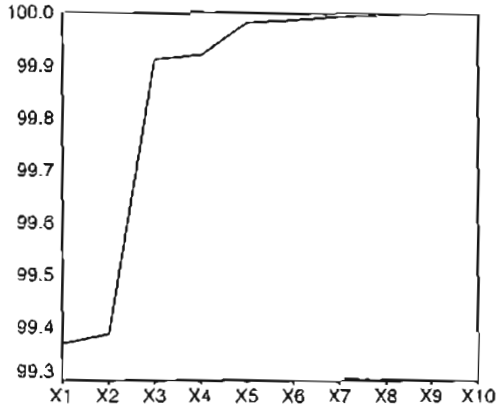

(iii) females proximal, *X*-amplitudes

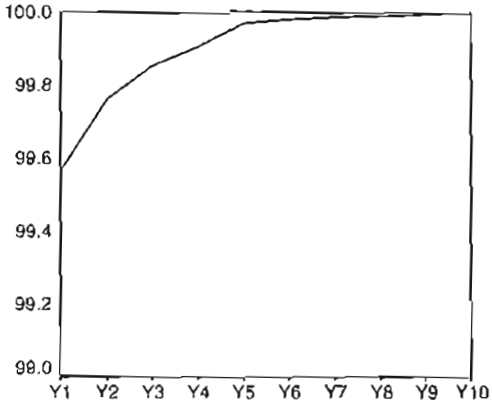

(iv) females proximal, *Y*-amplitudes

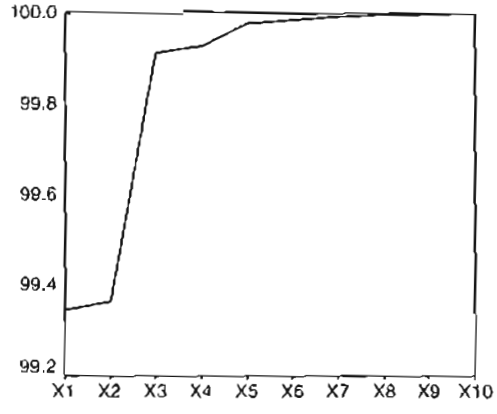

(v) males distal, *X*-amplitudes

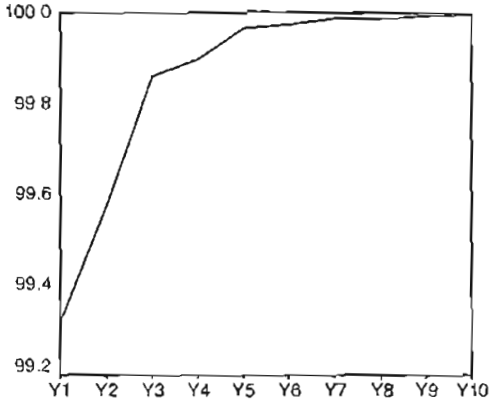

(vi) males distal, *Y*-amplitudes

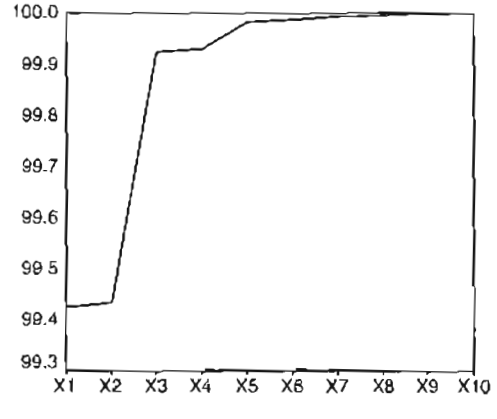

(vii) males proximal, *X*-amplitudes

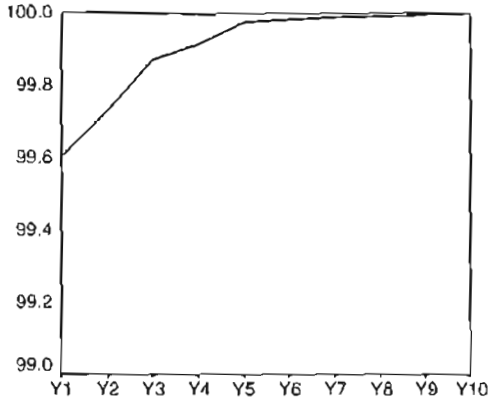

(viii) males proximal, *Y*-amplitudes

Figure 3.4. (c) *Colobus*

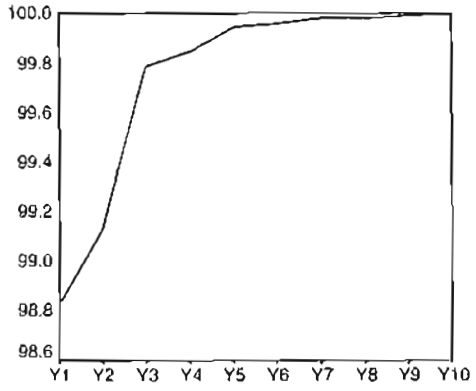

(i) females distal, *X*-amplitudes

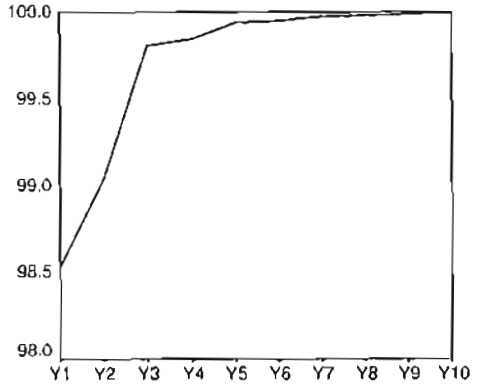

(ii) females distal, *Y*-amplitudes

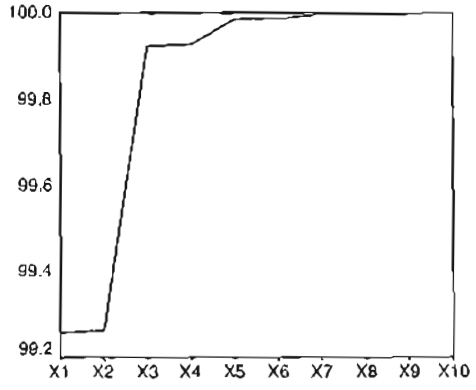

(iii) females proximal, *X*-amplitudes

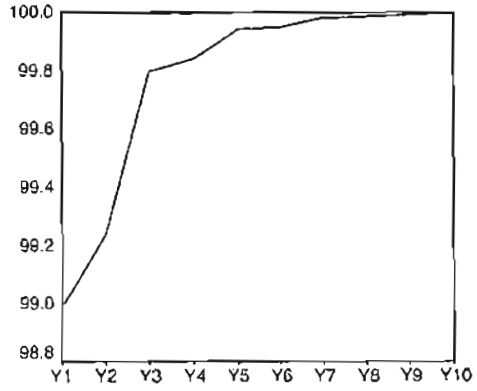

(iv) females proximal, *Y*-amplitudes

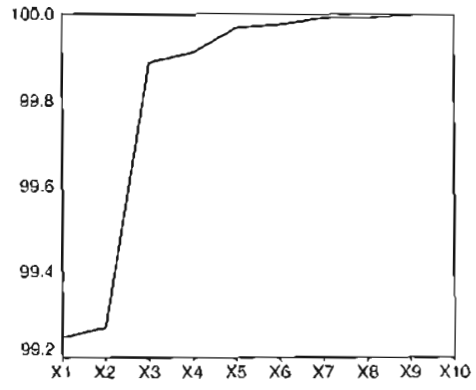

(v) males distal, *X*-amplitudes

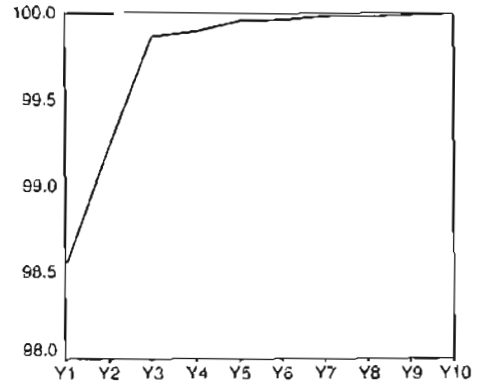

(vi) males distal, *Y*-amplitudes

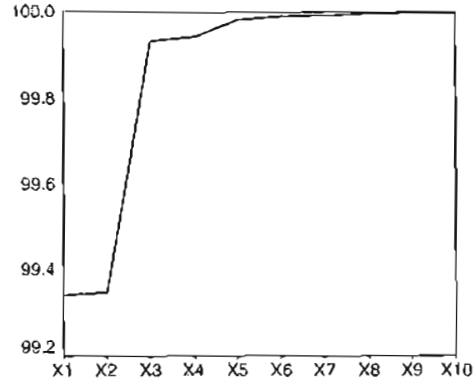

(vii) males proximal, *X*-amplitudes

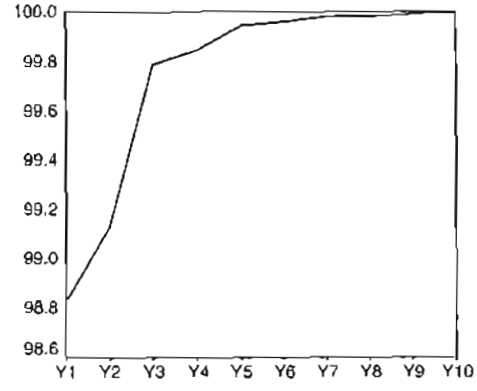

(viii) males proximal, *Y*-amplitudes

Figure 3.4. (**d**) *Gorilla*

3.4.4 Ordination

3.4.4.1 Principal component analysis

3.4.4.1.1 *Homo*

3.4.4.1.1.1 conventional data

Means and standard deviations of these variables are presented in Table A.7(a,b) (page 315). The covariance-correlation matrices of $\boldsymbol{P}$ and $\boldsymbol{A}$ are presented in Table A.9(a) (page 321). Inspection of these matrices revealed consistently that variances of $\boldsymbol{P}$ outweighed those of $\boldsymbol{A}$ by one to two orders of magnitude, and intervariable correlations were strong (0.9296 to 0.9743). Due to the large differences in variance within each group, the logarithmic data were also assessed. This transformation resulted in almost equal variances within each group, and correlations were again strong (0.9311 to 0.9742) (Table A.9(a)). Consequently, logarithmic data were used for ordination. The eigenvectors and eigenvalues of principal component analyses using the covariance matrices of logarithmic variables are presented in Table A.11(a) (page 331), and the eigenvalues (as a percentage of total variation) have been reproduced in Table 3.5. Throughout, the eigenvalues for the first principal component far outweighed those for the second, values (as percentages of total variance) ranging from 96.57% to 98.73%. This reflected the high intervariable correlations.

Table 3.5. First eigenvalues as a percentage of total variation – *Homo*, conventional data (ln)

	l_1 (%)
females distal	96.57
females proximal	98.73
males distal	97.15
males proximal	97.15

The principal components were as follows:

females distal

$\boldsymbol{U}_1 = [0.7332, 0.6800]$

$\boldsymbol{U}_2 = [0.6800, -0.7332]$

females proximal

$\boldsymbol{U}_1 = [0.7298, 0.6837]$

$\boldsymbol{U}_2 = [0.6837, -0.7298]$

males distal	**males proximal**
$\boldsymbol{U}_1$ = [0.7147, 0.6994]	$\boldsymbol{U}_1$ = [0.7242, 0.6896]
$\boldsymbol{U}_2$ = [0.6994, −0.7147]	$\boldsymbol{U}_2$ = [0.6896, −0.7242].

Principal component scores for the two principal component axes were computed by projecting the data points on to the two principal axes. The scatterplots of these PC scores are presented in Figure 3.5(a) (at end of §3.4.4.1); it should be noted that axes 1 and 2 are of different scales, and that variation in the direction of the second component was relatively expanded. The scatterplots showed reasonably even distributions of points, and only one specimen was found to be an outlier – specimen 87 in the females proximal group. This specimen lay to the right from the main group in the direction of the first PC axis. As this was an unpaired specimen, there was no opportunity to compare the position of this data point with that of the contralateral specimen. To investigate the effect of this specimen on the PCA, it was omitted and the above process was repeated (Table A.13(a), page 341). Table 3.6 shows the angles between PC1 of the whole sample and that of the sample with the omission of specimen 87 ($\theta_{1,-i}$). Table 3.6 also shows the first eigenvalue after omission as a percentage of the first eigenvalue from the whole sample ($l_{1,-i}$). The correlation and variance components decreased slightly, which was expected: correlation is dependent on the variable range (Smith, 1980), which decreased with the omission of this specimen, and variance reflected the decreased spread of points in the direction of PC1. From the latter it was not surprising that the first eigenvalue decreased in size, the new first eigenvalue shrinking to 88.86% of the original value, although the first eigenvalue still clearly dominated the second. This omission only caused a very slight change in direction of the first component, by 0.29°.

Table 3.6. Effects of outlier omission on first eigenvectors ($\theta_{1,-i}$) and first eigenvalues ($l_{1,-i}$) – *Homo*, conventional data

specimen omitted	$\theta_{1,-i}$ (°)	$l_{1,-i}$ (%)
87 (females proximal)	0.29	88.86

3.4.4.1.1.2 Fourier data

Table A.8(a-d) (page 317) shows the means and standard deviations for these variables. The covariance-correlation matrices are presented in Table A10(a) (page 323). The sizes of the variances were qualitatively correlated with the mean values, such that the variables with the larger means had larger variances than variables with smaller means (for example in females distal ***X1*** mean = 106.82, variance = 62.9961 versus ***X2*** mean = 1.70, variance = 0.5484). Correlations were of mixed size and sign. Transformation to natural logarithms altered the variances, but with a strong bias in favour of variables with smaller means (females distal **ln*X1*** mean = 4.668, variance = 0.0055 versus **ln*X2*** mean = 0.420, variance = 0.2556).

Results from principal component analyses using the covariance matrix (raw and logarithmic data) are presented in Table A.12(a,b) (page 333), and the percentages of total variance for eigenvalues 1 to 3 have been reproduced in Table 3.7. Eigenvalues from PCA of the covariance matrix of raw data showed a clear dominance of the first and second principal components: the first eigenvalue as a percentage of total variance ranged from 79.63% to 82.60%. The first two components accounted for the bulk of the variance (92.83% to 95.00%). Transformation of the raw variables to their natural logarithms did not, for ordination purposes, prove advantageous: the first two eigenvalues accounted for much less variance (65.76% to 75.20%), and the addition of the third component only brought the variance explained to 78.07% to 87.80%. While approximately 80% of variance was reasonable for ordination, this came at the expense of visibility by introducing a third dimension. Moreover, the component coefficients were greatest for variables such as ***X2*** and ***Y2***, which contributed little to the power spectrum, and whose variances were amplified by transformation due to low values (see page 111). For ordination, the covariance matrix of raw data was used, for reasons of (1) variance explained, and (2) dominance of ***X1*** and ***Y1*** was reasonable considering their contribution to the power spectrum.

Table 3.7. Eigenvalues 1 to 3 – *Homo*, Fourier data

	l_1	l_2	l_3
females distal (raw)	79.63	93.10	97.39
females distal (ln)	48.16	67.38	78.07
females proximal (raw)	88.55	95.00	98.32
females proximal (ln)	53.46	75.20	87.36
males distal (raw)	82.60	94.33	97.19
males distal (ln)	32.84	58.74	74.34
males proximal (raw)	83.48	93.96	97.76
males proximal (ln)	35.55	65.76	80.80

Inspection of the coefficients of these two components reveals that these were, as expected, dominated by the variables with the highest means, viz. ***X*1** and ***Y*1**. These principal components were as follows:

females distal

U_1 = [0.9401, 0.3166, 0.0156, 0.0065, 0.1050, 0.0292, –0.0072, 0.0323, 0.0336, 0.0405]

U_2 = [0.2979, –0.9352, –0.0905, –0.0672, 0.1257, 0.0276, –0.0557, 0.0208, 0.0598, 0.0186]

females proximal

U_1 = [0.9117, 0.3923, 0.0211, –0.0053, 0.1011, 0.0014, 0.0002, 0.0394, 0.0417, 0.0312]

U_2 = [0.3538, –0.8651, –0.1539, –0.2494, 0.1456, –0.0510, –0.1108, 0.0296, 0.0354, 0.0480]

males distal

U_1 = [0.9171, 0.3807, 0.0088, 0.0281, 0.0974, 0.0311, –0.0037, 0.0270, 0.0337, 0.0284]

U_2 = [0.3565, –0.9139, –0.0100, –0.0081, 0.1571, 0.0388, –0.0414, 0.0593, 0.0769, 0.0140]

males proximal

U_1 = [0.9165, 0.3816, 0.0239, 0.0336, 0.0952, 0.0240, 0.0038, 0.0332, 0.0297, 0.0328]

U_2 = [0.3540, –0.9063, 0.0549, 0.0363, 0.1759, –0.0887, 0.0268, 0.0109, 0.0909, 0.0326].

Scatterplots of component scores are presented in Figure 3.6(a) (following Figure 3.5 at end of §3.4.4.1). It can be seen that distributions of specimens were reasonably even, showing no heterogeneities, and only one outlier – specimen 87 in the females proximal group (again). This specimen had a high value on the first PC axis, which reflected the findings using conventional data. Repeating the PCA led to the results presented in Table A.14(a) (page 342). Again, the correlation-covariance matrix was not greatly altered. The effects on the first eigenvector and eigenvalue are presented in Table 3.8. Comparison of eigenvalues showed a decrease of over 15% of variance in the direction of PC1. The angle between the original PC1 and the new PC1 was only 1.11°. Thus, omission of this specimen altered the first eigenvalue by shortening the data spread along PC1 (although the first two eigenvalues still accounted for 94.21% of the total variance), and left the direction of PC1 virtually unchanged.

Table 3.8. Effects of outlier omission on first eigenvectors ($\theta_{1,-i}$) and first eigenvalues ($l_{1,-i}$) – *Homo*, Fourier data

specimen omitted	$\theta_{1,-i}$ (°)	$l_{1,-i}$ (%)
87 (females proximal)	1.11	84.83

3.4.4.1.2 *Cercopithecus*

3.4.4.1.2.1 conventional data

The means and standard deviations for these variables are presented in Table A.7(c,d) (page 315). The covariance-correlation matrices are presented in Table A.9(b) (page 321). The variances of $\boldsymbol{P}$ outweighed those for $\boldsymbol{A}$ by more than one order of magnitude. Intervariable correlations were strong, in the range of 0.9746 to 0.9931. Logarithmic transformation of these data almost equalized these variances, and correlations were strong (0.9727 to 0.9937). The results of principal component analyses using the covariance matrices of logarithmic variables are presented in Table A.11(b) (page 331). Table 3.9 shows the first eigenvalues as proportions of total variance; proportions were very large, ranging from 98.64% to 99.69%

Table 3.9. First eigenvalues as a percentage of total variation – *Cercopithecus*, conventional data (ln)

	l_1 (%)
females distal	98.64
females proximal	99.25
males distal	99.31
males proximal	99.69

These eigenvalues showed that almost all variation lay in one direction, and that this direction was again weighted almost equally between the two variables, as follows:

females distal

$U_1 = [0.7276, 0.6860]$

$U_2 = [0.6860, -0.7276]$

females proximal

$U_1 = [0.6939, 0.7200]$

$U_2 = [0.7200, -0.6939]$

males distal

$U_1 = [0.6914, 0.7225]$

$U_2 = [0.7225, -0.6914]$

males proximal

$U_1 = [0.6973, 0.7167]$

$U_2 = [0.7167, -0.6973]$.

Principal component scores were computed, and the scatterplots of these scores are presented in Figure 3.5(b). The distribution of data points was even, and no obvious outliers were seen.

3.4.4.1.2.2 Fourier data

Table A.8(e-h) (page 318) shows the means and standard deviations of these variables. The covariance-correlation matrices are presented in Table A.10(b) (page 325). The variances of variables ***X1*** and ***Y1*** dominated, sometimes by more than two orders of magnitude; correlations were of mixed size and sign. Logarithmic transformation led to variables with smaller means to have comparatively higher variances, as was seen for the *Homo* data, and again there was a wide range of variances.

Table A.12(c,d) (page 335) shows results from principal component analyses using the covariance matrix of raw and logarithmic data, and percentages of total variation for eigenvalues 1 to 3 have been reproduced in Table 3.10.

Table 3.10. Eigenvalues 1 to 3 – *Cercopithecus*, Fourier data

	l_1	l_2	l_3
females distal (raw)	87.20	96.75	98.87
females distal (ln)	46.17	72.27	83.40
females proximal (raw)	87.27	97.58	98.91
females proximal (ln)	53.57	74.89	86.36
males distal (raw)	93.03	98.94	99.53
males distal (ln)	44.13	66.50	77.11
males proximal (raw)	94.68	98.86	99.40
males proximal (ln)	38.69	58.33	74.70

Eigenvalues from the PCA (raw data) showed dominance of the first two principal components: the first eigenvalue as a percentage of total variance was in the range 87.20% to 94.68%, and the addition of the second component brought this percentage up to 96.75% to 98.96%. Inspection of the first eigenvectors showed that almost all weighting was divided between variables ***X1*** and ***Y1***, as expected given their individual variances. Use of logarithmic data did not show advantages when compared to the above results. The first two eigenvalues accounted for only moderate percentages of total variance, and the addition of the third component did not always raise the explained variance to an acceptable level. For logarithmic data, the first two and three components accounted for 58.33% to 74.89% and 74.70% to 86.36%, respectively. Accordingly, principal component analysis using the covariance matrix of raw variables was used for ordination for the same reasons expounded for *Homo*. These principal components were as follows:

females distal

$\boldsymbol{U}_1$ = [0.8987, 0.4247, 0.0046, 0.0203, 0.0970, –0.0065, 0.0019, 0.0208, 0.0370, 0.0194]

$\boldsymbol{U}_2$ = [0.4004, –0.8937, 0.0130, –0.0342, 0.1775, 0.0257, –0.0222, 0.0234, 0.0800, –0.0060]

females proximal

$\boldsymbol{U}_1$ = [0.7872, 0.6146, 0.0112, –0.1011, 0.0422, 0.0033, –0.0047, 0.0101, 0.0169, 0.0111]

$\boldsymbol{U}_2$ = [0.5906, –0.7720, 0.0028, 0.0669, 0.2051, 0.0518, 0.0230, 0.0046, 0.0548, 0.0495]

males distal

U_1 = [0.8135, 0.5762, 0.0125, 0.0501, 0.0518, 0.0046, 0.0184, 0.0089, 0.0187, 0.0101]

U_2 = [0.5447, –0.7984, 0.0270, 0.0865, 0.1866, 0.0565, –0.0104, 0.1202, 0.0691,0.0146]

males proximal

U_1 = [0.8109, 0.5817, 0.0019, 0.0043, 0.0551, 0.0080, 0.0075, 0.0191, 0.0186, 0.0160]

U_2 = [0.5486, –0.7925, –0.0015, 0.0308, 0.2329, 0.0613, –0.0060, 0.0069, 0.1002,0.0429].

Scatterplots of component scores are presented in Figure 3.6(b). The distributions of data points were even and with no heterogeneities; no obvious outlying specimens were seen.

3.4.4.1.3 *Colobus*

3.4.4.1.3.1 conventional data

Table A.7(e,f) (page 316) shows the means and standard deviations for these variables. The covariance-correlation matrices are presented in Table A.9(c) (page 322). The variances of ***P*** far outweighed those of ***A***, by more than an order of magnitude. Correlations were strong, in the range of 0.9327 to 0.9935. The bias in variances was remedied by logarithmic transformation, and correlations were strong (0.9675 to 0.9939). Principal component analyses were performed on the covariance matrices of logarithmic data, and the results are presented in A.11(c) (page 332). Table 3.11 shows the proportions of total variance accounted for by the first eigenvalues, which were very large (98.38% to 99.70%).

Table 3.11. First eigenvalues as a percentage of total variation – *Colobus*, conventional data (ln)

	l_1 (%)
females distal	99.44
females proximal	99.70
males distal	98.44
males proximal	98.38

Again, dominance of the first eigenvalues revealed that most of the variation occurred in one direction, as follows:

females distal	**females proximal**
$\boldsymbol{U}_1$ = [0.6777, 0.7353]	$\boldsymbol{U}_1$ = [0.6619, 0.7496]
$\boldsymbol{U}_2$ = [0.7353, –0.6777]	$\boldsymbol{U}_2$ = [0.7496, –0.6619]
males distal	**males proximal**
$\boldsymbol{U}_1$ = [0.7023, 0.7119]	$\boldsymbol{U}_1$ = [0.6924, 0.7215]
$\boldsymbol{U}_2$ = [0.7119, –0.7023]	$\boldsymbol{U}_2$ = [0.7215, –0.6924].

Principal component scores were computed, and the scatterplots of these scores are presented in Figure 3.5(c). Lower sample sizes meant the data points were scattered more sparsely, but still evenly, and with no obvious outliers.

3.4.4.1.3.2 Fourier data

The means and standard deviations of these variables are presented in Table A.8(i-m) (page 319). The covariance-correlation matrices are presented in Table A.10(c) (page 327). Variances of variables ***X1*** and ***Y1*** dominated, being larger than some by more than two orders of magnitude. Correlations were of varied size and sign. Logarithmic transformation showed a similar picture seen above, where variables with small means showed much larger variances. Table A.12(e,f) (page 337) shows the results from principal component analyses using the covariance matrix of raw and logarithmic data, and the percentages of total variation for eigenvalues 1 to 3 have been reproduced in Table 3.12. Inspection of the eigenvalues from the PCA of raw data showed again that the first two eigenvalues accounted for the bulk of the variance: l_1 lay in the range 81.68% to 94.64%, and the combination of l_1 and l_2 accounted for between 97.12% and 98.58%. The option of using the covariance matrix of logarithmic data did not result in an improvement for ordination. The first two eigenvalues from logarithmic data accounted for between 60.89% and 77.49% of the total variance, with the first three eigenvalues accounting for 79.46% to 90.52%. Ordination was therefore performed using PCA of the covariance matrix of raw variables, for the same reasons as in *Homo* and *Cercopithecus*.

Table 3.12. Eigenvalues 1 to 3 – *Colobus*, Fourier data

	l_1	l_2	l_3
females distal (raw)	89.83	97.33	99.08
females distal (ln)	53.13	77.49	90.52
females proximal (raw)	94.64	97.78	99.16
females proximal (ln)	50.68	68.71	83.44
males distal (raw)	82.96	97.12	98.92
males distal (ln)	52.10	73.54	83.80
males proximal (raw)	81.68	98.58	99.33
males proximal (ln)	40.62	60.89	79.46

The component coefficients showed that the first two principal components were dominated by ***X*1** and ***X*2**; these components were as follows:

females distal

$\boldsymbol{U}_1$ = [0.7499, 0.6521, 0.0554, 0.0522, 0.0401, –0.0437, 0.0421, 0.0105, 0.0317, 0.0091]

$\boldsymbol{U}_2$ = [0.6141, –0.6683, –0.2021, –0.2136, 0.2005, 0.1046, –0.1805, 0.0066, 0.0336, 0.0699]

females proximal

$\boldsymbol{U}_1$ = [0.6777, 0.7349, 0.0035, 0.0077, 0.0199, –0.0014, 0.0060, 0.0057, 0.0117, 0.0080]

$\boldsymbol{U}_2$ = [0.6765, –0.6322, 0.1643, 0.2494, 0.1201, 0.0345, 0.0657, 0.1677, 0.0379, –0.0627]

males distal

$\boldsymbol{U}_1$ = [0.8429, 0.5302, 0.0025, –0.0058, 0.0720, –0.0353, 0.1139, 0.0091, 0.0367, 0.2100]

$\boldsymbol{U}_2$ = [0.4992, –0.8308, –0.0242, 0.0535, 0.2168, –0.0314, –0.0280, –0.0104, 0.0869, 0.0285]

males proximal

$\boldsymbol{U}_1$ = [0.7891, 0.6110, 0.0038, 0.0270, 0.0344, 0.0347, 0.0057, 0.0212, 0.0021, 0.0214]

$\boldsymbol{U}_2$ = [0.5877, –0.7743, –0.0172, 0.0076, 0.2076, 0.0492, –0.0350, –0.0071, 0.0851, 0.0266].

Scatterplots of these component scores are presented in Figure 3.6(c). Data points were distributed in a somewhat homogeneous manner, but sample sizes were quite small, reducing confidence in such an interpretation; nonetheless, no specimens were seen to be outliers.

3.4.4.1.4 *Gorilla*

3.4.4.1.4.1 conventional data

Table A.7(g,h) (page 316) shows the means and standard deviations of these variables. The covariance-correlation matrices are presented in Table A.9(d) (page 322). Variances of ***P*** exceeded those of ***A*** by more than one order of magnitude. The correlations were strong and lay in the range 0.9692 to 0.9967. The bias in variances was ameliorated by logarithmic transformation, and correlations were again strong (0.9662 to 0.9968). Principal component analysis results for the covariance matrices of the logarithmic data can be found in Table A.11(d) (page 332) and Table 3.13. First eigenvalues accounted for 98.31% to 99.84% of total variance.

Table 3.13. First eigenvalues as a percentage of total variation – *Gorilla*, conventional data (ln)

	l_1 (%)
females distal	99.09
females proximal	98.31
males distal	99.05
males proximal	99.84

Once more, the bulk of the variation lay roughly in the direction of [0.7071, 0.7071], as follows:

females distal

$\boldsymbol{U}_1$ = [0.6645, 0.7473]

$\boldsymbol{U}_2$ = [0.7473, –0.6645]

females proximal

$\boldsymbol{U}_1$ = [0.7172, 0.6969]

$\boldsymbol{U}_2$ = [0.6969, –0.7172]

males distal

$\boldsymbol{U}_1$ = [0.7028, 0.7114]

$\boldsymbol{U}_2$ = [0.7114, –0.7028]

males proximal

$\boldsymbol{U}_1$ = [0.7319, 0.6815]

$\boldsymbol{U}_2$ = [0.6815, –0.7319].

Principal component scores were computed, and the scatterplots of these scores are presented in Figure 3.5(d). With such low numbers, inspection of the scatterplots had limited value in regard to heterogeneities. In the females distal data, there were two pairs of distinctly outlying points – specimens 671 and 672 on PC1, and specimens 657 and 658 on PC2 – from two individuals (no subspecies information). Due to the small sample size, further analysis with omission of these four specimens was not pursued. Specimens 671 and 672 were also outliers on PC1 in the females proximal data. These specimens were omitted from the proximal data (given the close proximity of each specimen to the other, it was appropriate to omit these together), and the data were reanalysed (Table A.13(b), page 341). Correlation decreased from 0.9939 to 0.9235; a decrease was expected, due to the effect on the correlation coefficient of the variable range. Omission resulted in a substantial decrease in variance and covariance, and this was reflected in a 66.13% decrease in the size of the first eigenvalue (Table 3.14). Notwithstanding this decrease, the first eigenvalue still accounted for almost all variance. The angle between the original PC1 and the recalculated PC1 (with omissions) was 7.13° (Table 3.14). Therefore, these two specimens (from the same individual) appeared as extreme relative to the rest of the group, but extreme in the direction of maximal variance (size), and without unduly affecting the direction of the component axes.

Table 3.14. Effects of outlier omission on first eigenvectors ($\theta_{1,-i}$) and first eigenvalues ($l_{1,-i}$) – *Gorilla*, conventional data

specimen omitted	$\theta_{1,-i}$ (°)	$l_{1,-i}$ (%)
671, 672 (females proximal)	7.13	33.87

3.4.4.1.4.2 Fourier data

Table A.8(m-p) (page 320) shows the means and standard deviations for these variables. The covariance-correlation matrices for these data are presented in Table A.10(d) (page 329). Variances of variables ***X1*** and ***Y1*** were sometimes more than two orders of magnitude greater than variances for other variables. Correlations were of mixed size and sign. Transformation to logarithms showed a similar result as seen earlier, that of smaller variables having much greater variances than larger variables. Results from principal component analyses using the covariance matrix of raw and logarithmic data are presented in Table A.12(g,h) (page 339), and the percentages of total variance for eigenvalues 1 to 3 have been reproduced in Table 3.15. The males data consisted of 10 variables but only nine individuals, so the covariance

matrices were not of full rank (rank nine rather than rank 10), so at least one eigenvalue had to equal zero. The pattern of the first two eigenvalues of raw variables continued here: as a percentage of total variance, the first eigenvalue accounted for between 89.43% and 97.59%, and the combination of the first two eigenvalues accounted for between 95.62% and 99.23% of the total. There was no advantage in using logarithmic data for ordination, as three axes were required to account for 90% or more of variation for most groups (92.88% to 98.95% for these three axes). Therefore, the raw data were used for ordination.

Table 3.15. Eigenvalues 1 to 3 – *Gorilla*, Fourier data

	l_1	l_2	l_3
females distal (raw)	95.96	99.23	99.80
females distal (ln)	55.53	85.51	93.01
females proximal (raw)	90.73	99.20	99.61
females proximal (ln)	61.70	85.01	94.38
males distal (raw)	89.43	95.62	99.70
males distal (ln)	92.54	96.25	98.95
males proximal (raw)	97.59	99.04	99.58
males proximal (ln)	58.41	76.68	92.88

In the first two principal components (raw data), the coefficient weightings were divided mainly between ***X*1** and ***Y*1**, almost to the exclusion of other variables. An exception here was the males distal data: the second principal component, while having substantial weightings for ***X*1** and ***Y*1**, also had a strong weighting for ***Y*2**. These principal components were as follows:

females distal

$\boldsymbol{U}_1$ = [0.8477. 0.5240, –0.0117, –0.2356, 0.0712, –0.0092, –0.0036, 0.0096, 0.0286, 0.1171]

$\boldsymbol{U}_2$ = [0.4863, –0.7937, 0.0729, 0.2880, 0.1644, –0.0754, 0.0478, –0.0672, 0.0960, 0.0044]

females proximal

$\boldsymbol{U}_1$ = [0.8872, 0.4390, 0.0260, 0.0816, 0.0619, 0.0720, 0.0244, 0.0399, 0.0011, 0.0404]

$\boldsymbol{U}_2$ = [0.4300, –0.8759, –0.0542, –0.1134, 0.1543, 0.0571, –0.0447, –0.0031, 0.0473, 0.0271]

males distal

$\boldsymbol{U}_1$ = [0.8293, 0.5224, 0.0617, 0.1716, 0.0338, 0.0228, 0.0642, 0.0077, 0.0163, 0.0053]

$\boldsymbol{U}_2$ = [0.4866, –0.5501, –0.2304, –0.5638, 0.1721, 0.0773, –0.2140, 0.0352, 0.0639, –0.0533]

males proximal

$\boldsymbol{U}_1$ = [0.9406, 0.4122, 0.0068, 0.0598, 0.0653, 0.0426, 0.0335, 0.0147, 0.0113, 0.0261]

$\boldsymbol{U}_2$ = [0.3802, –0.8385, –0.0470, –0.1703, 0.2002, 0.1097, –0.1222, –0.2084, 0.1014, 0.0187].

Scatterplots of these component scores are presented in Figure 3.6(d). Interpretation of these plots was hampered by the small sample sizes. In the females distal group, two pairs of specimens (671 and 672, and 657 and 658) from two individuals were seen to lie away from the main group on the first and second component axes, respectively. As these four specimens represented a quarter of the sample, they were not investigated further. The former pair of specimens was also seen to lie away from the main group in the females proximal group, again on the first axis. These two specimens were omitted for a repeat PCA (Table A.14(b), page 342), as again they were in close proximity to each other. From Table 3.16 it can be seen that omission of these specimens shortened the data scatter along the line of the first principal axis (to 37.09% of the original first eigenvalue), and that the new direction of PC1 deviated strongly (20.46°) from the original PC1. These specimens therefore strongly influenced the original PCA. In the males distal group, specimen 656 was seen to be an outlier on the second axis, as it had a markedly greater difference between $\boldsymbol{X1}$ and $\boldsymbol{Y1}$. Omission of specimen 656 from males distal had predictable results on the PCA (Table A14(c), page 342; Table 3.16): the new PC1 deviated only a small amount from the original PC1 (2.46°), and had the effect of increasing the new first eigenvalue (to 111.13% of the original).

Table 3.16. Effects of outlier omission on first eigenvectors (θ_1) and first eigenvalues ($l_{1,-i}$) – *Gorilla*, Fourier data

specimen omitted	θ_1 (°)	$l_{1,-i}$ (%)
671, 672 (females proximal)	20.46	37.09
656 (males distal)	2.46	111.13

Figure 3.5. Scatterplots of PC2 scores (y-axis) versus PC1 scores (x-axis) – conventional data

(**a**) *Homo*

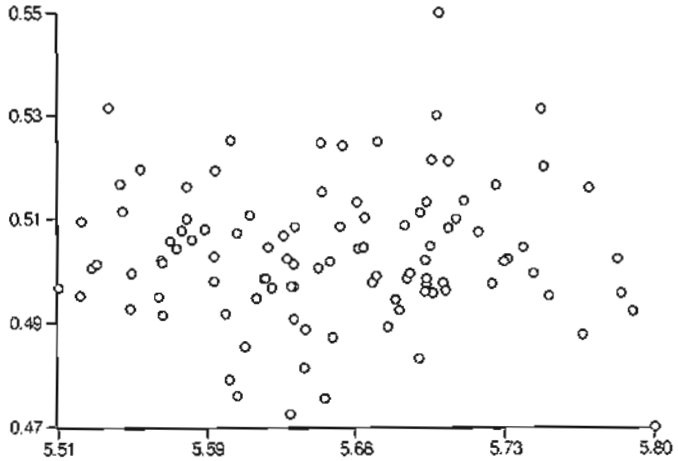

(i) females distal

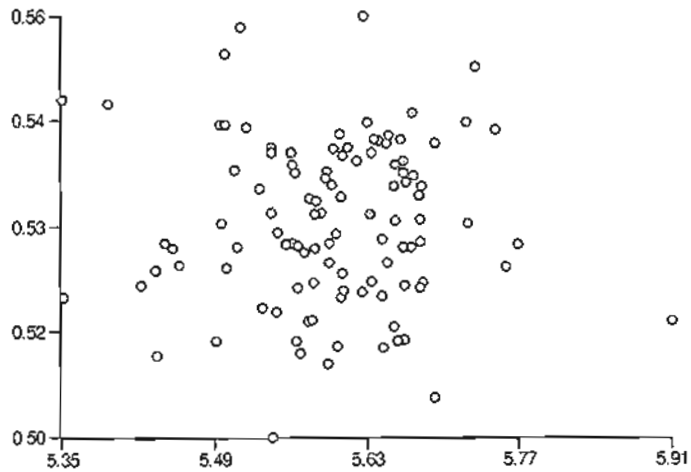

(ii) females proximal

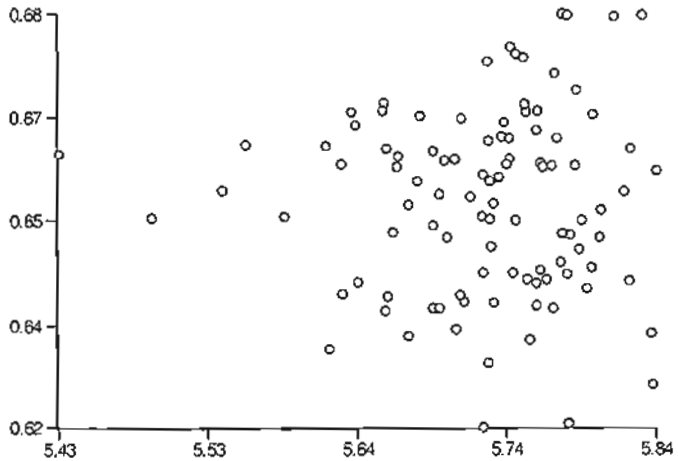

(iii) males distal

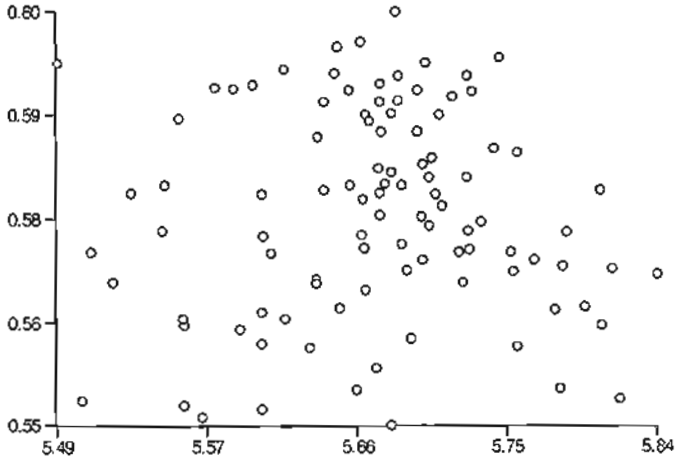

(iv) males proximal

Figure 3.5. (**b**) *Cercopithecus*

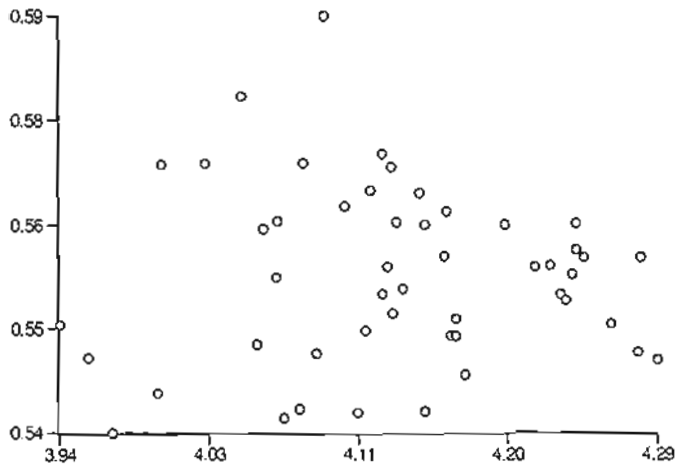

(i) females distal

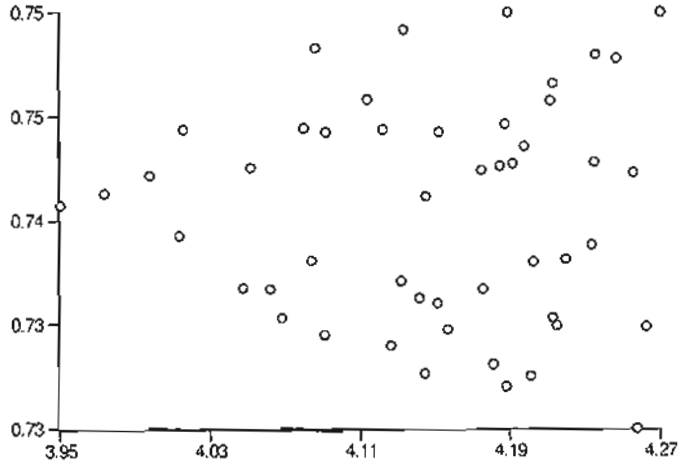

(ii) females proximal

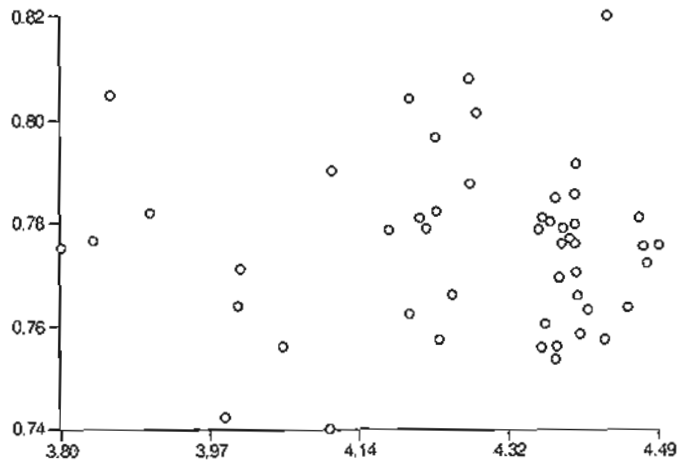

(iii) males distal

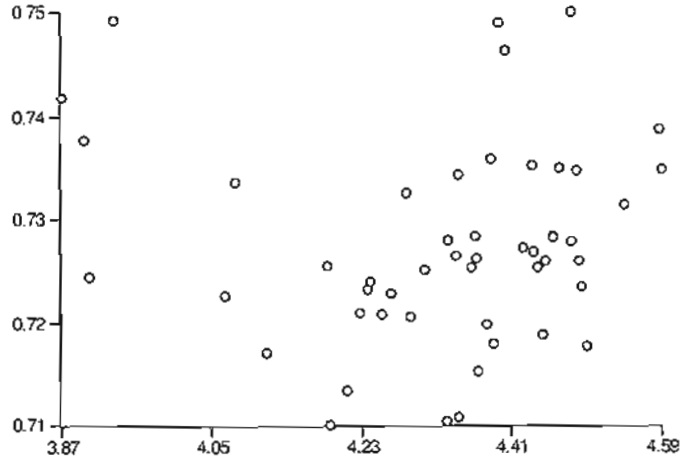

(iv) males proximal

Figure 3.5. (c) *Colobus*

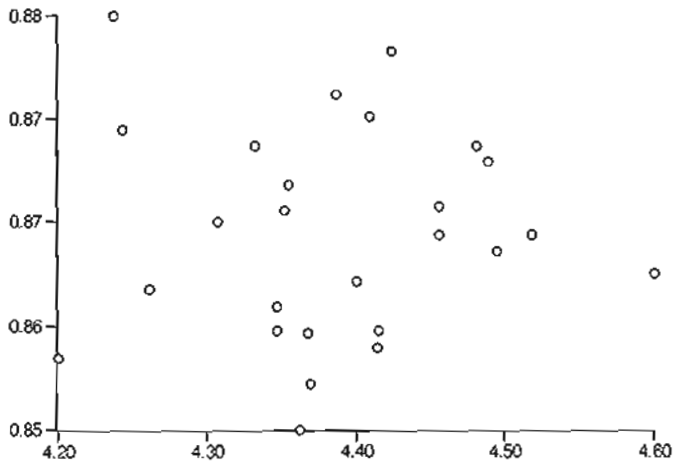

(i) females distal

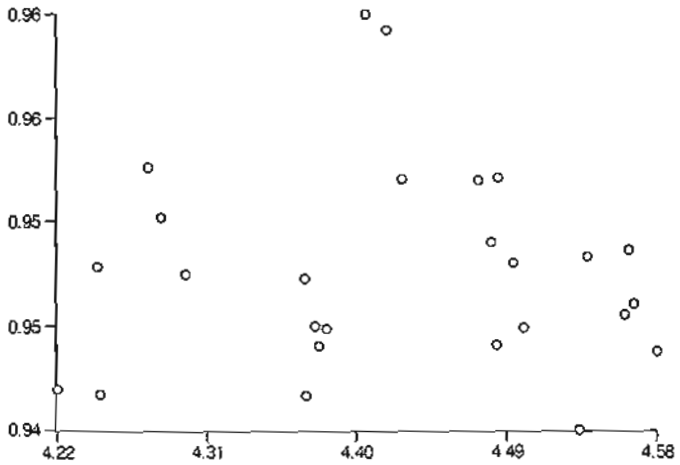

(ii) females proximal

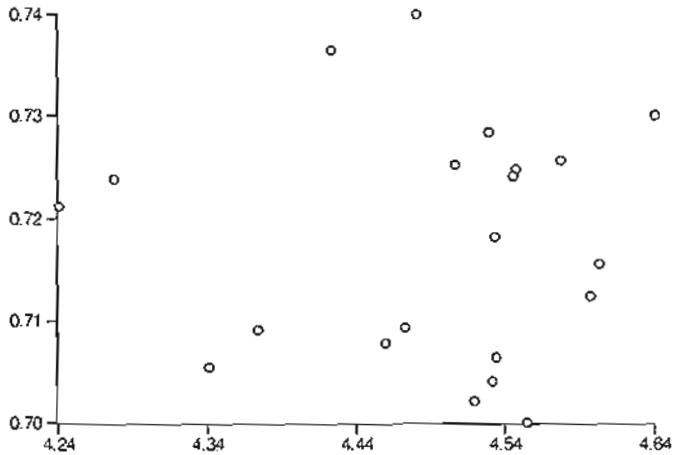

(iii) males distal

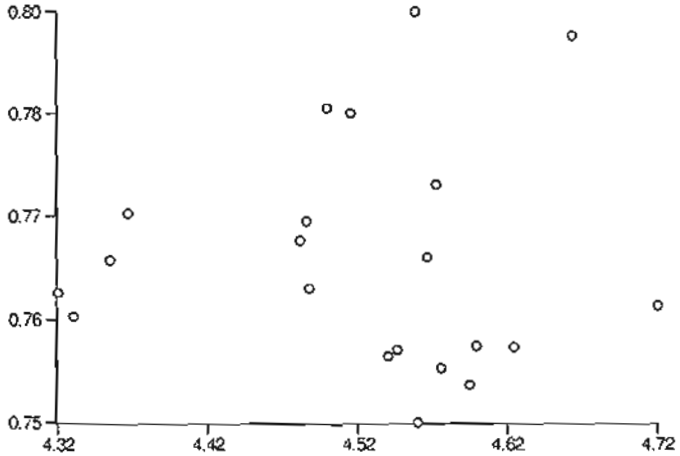

(iv) males proximal

Figure 3.5. (**d**) *Gorilla*

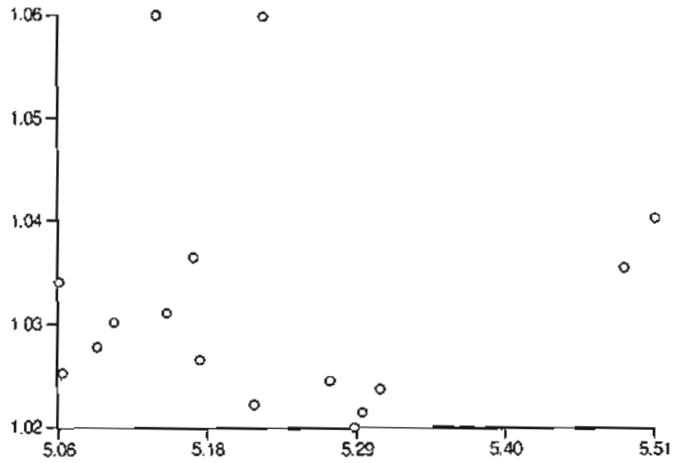

(i) females distal

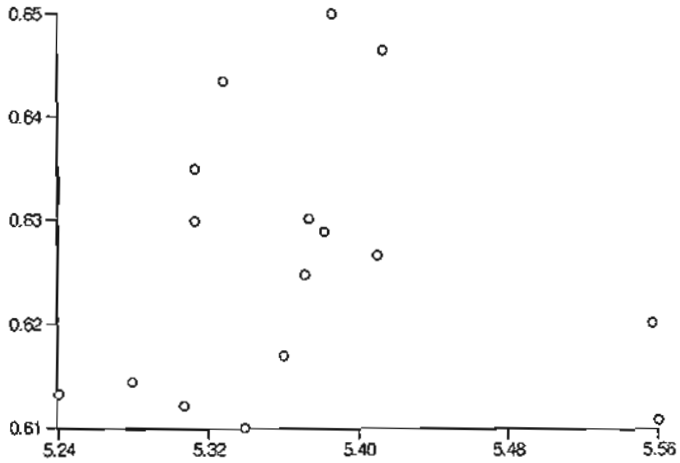

(ii) females proximal

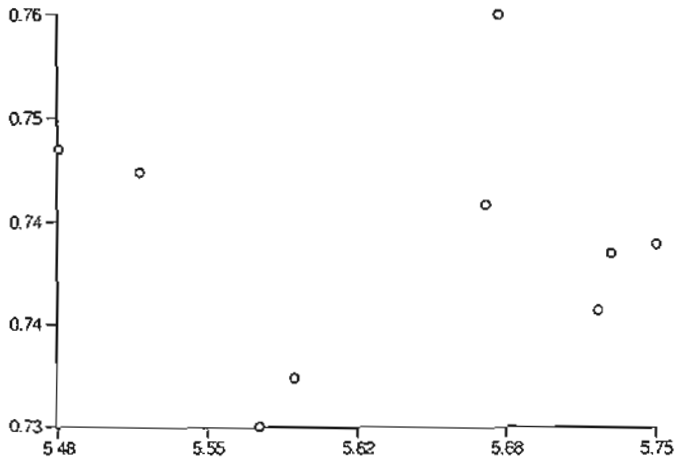

(iii) males distal

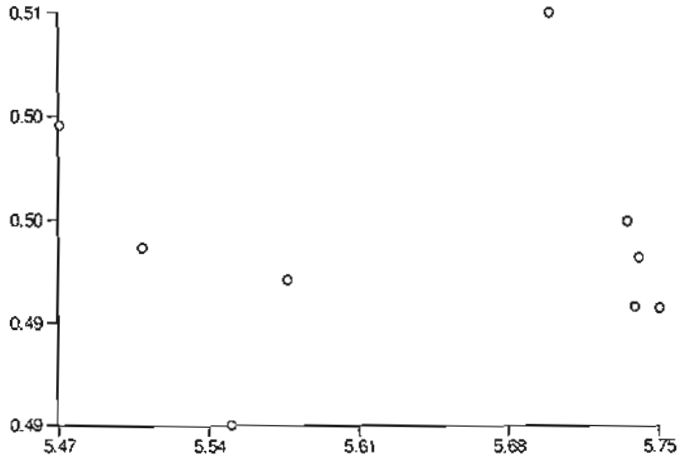

(iv) males proximal

Figure 3.6. Scatterplots of PC2 scores (y-axis) versus PC1 scores (x-axis) – Fourier data

(**a**) *Homo*

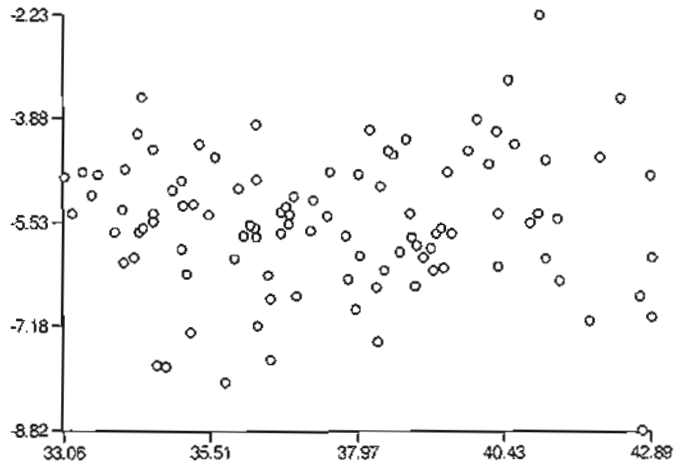

(i) females distal

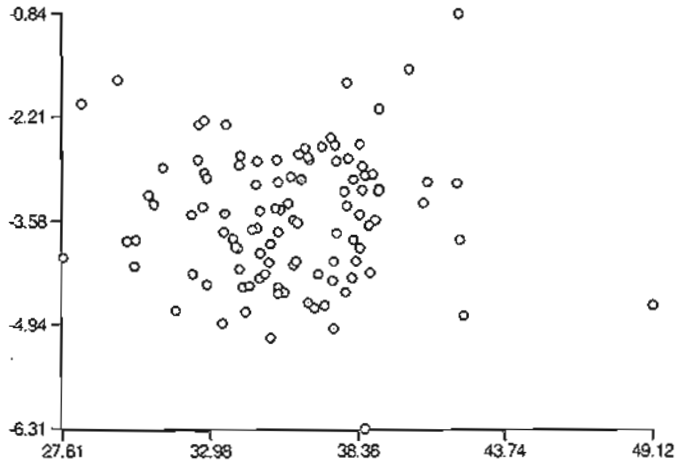

(ii) females proximal

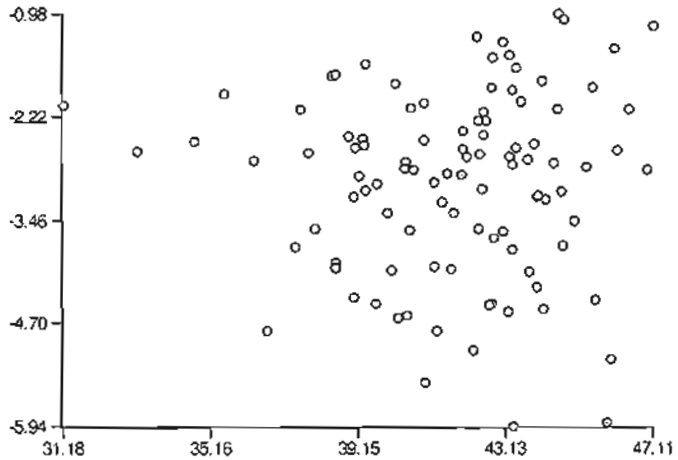

(iii) males distal

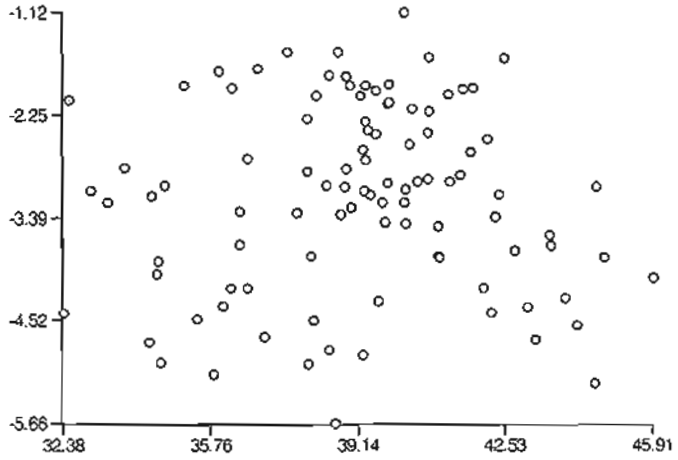

(iv) males proximal

Figure 3.6. (**b**) *Cercopithecus*

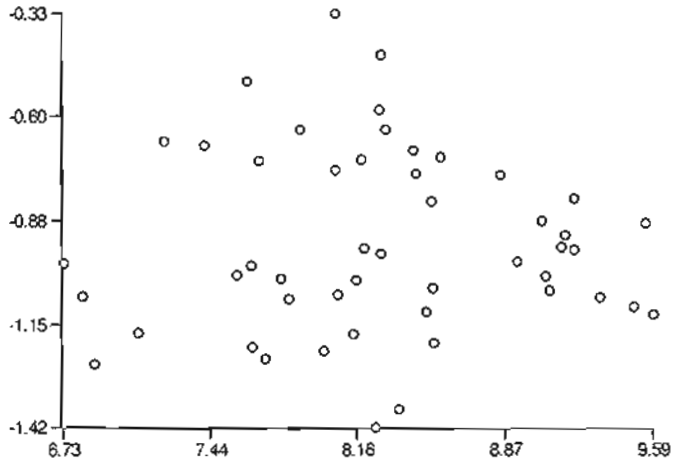

(i) females distal

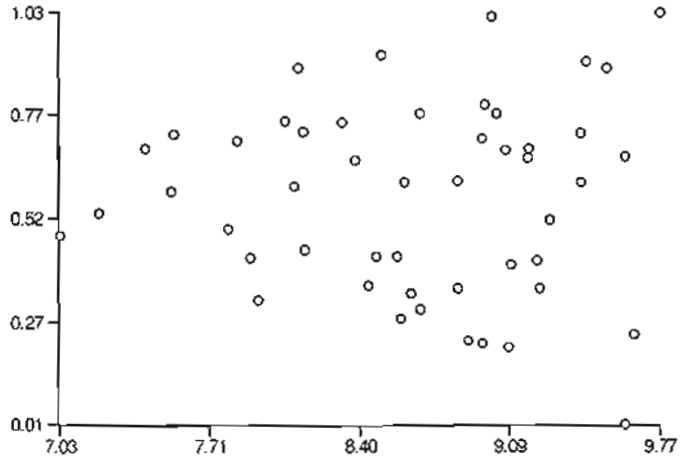

(ii) females proximal

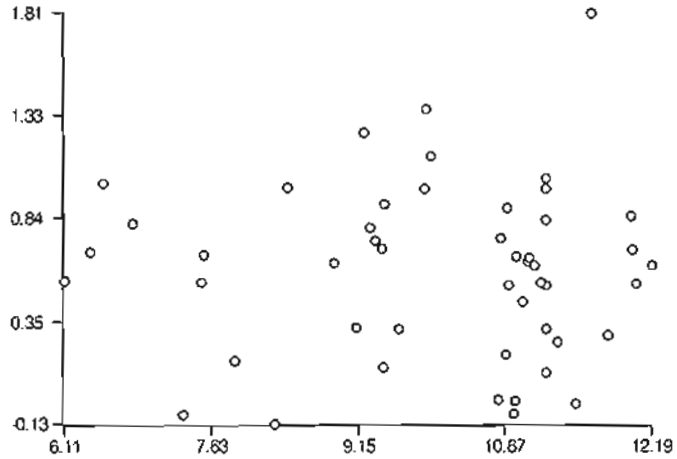

(iii) males distal

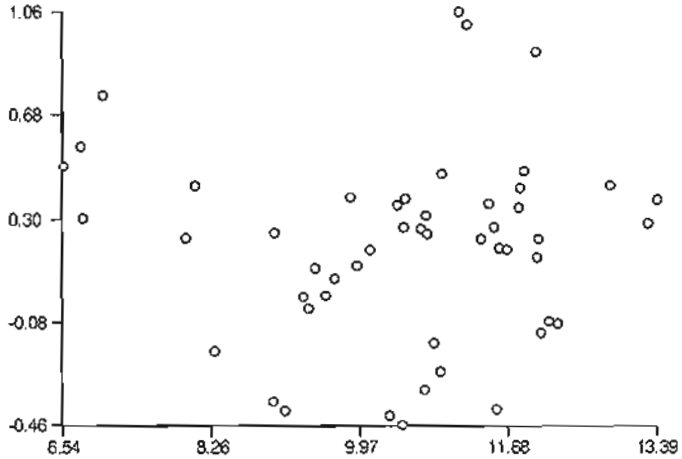

(iv) males proximal

Figure 3.6. (c) *Colobus*

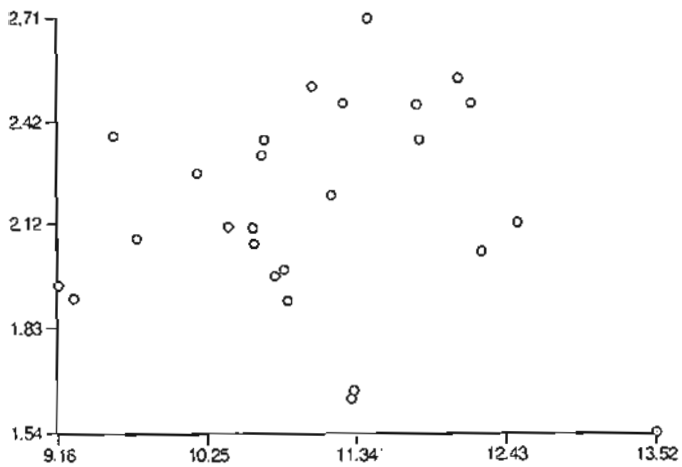

(i) females distal

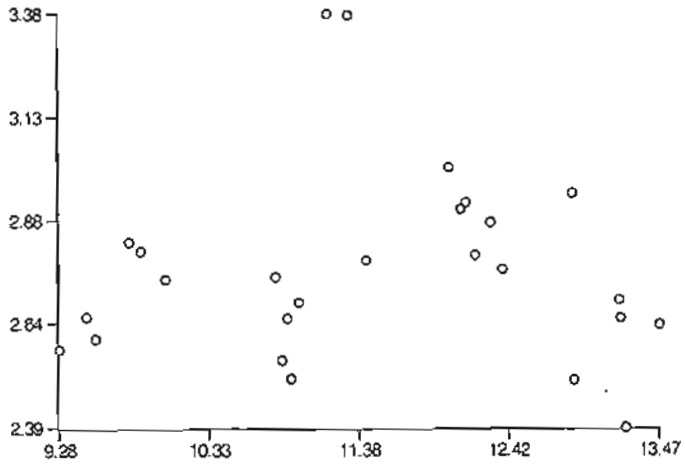

(ii) females proximal

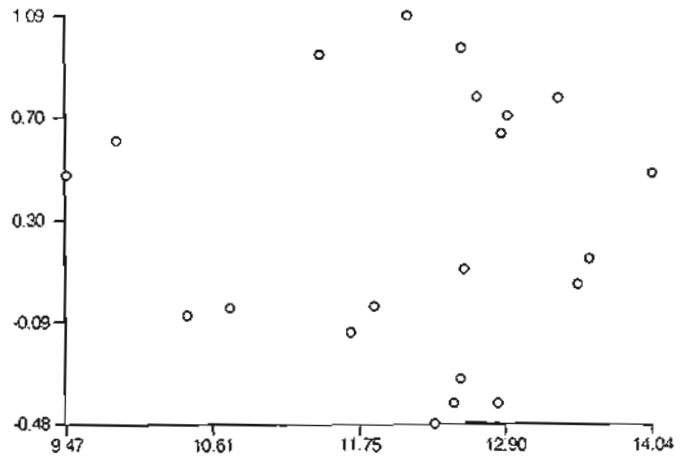

(iii) males distal

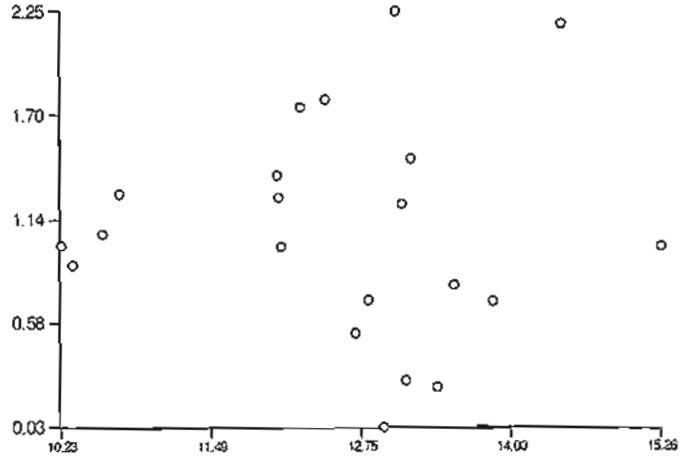

(iv) males proximal

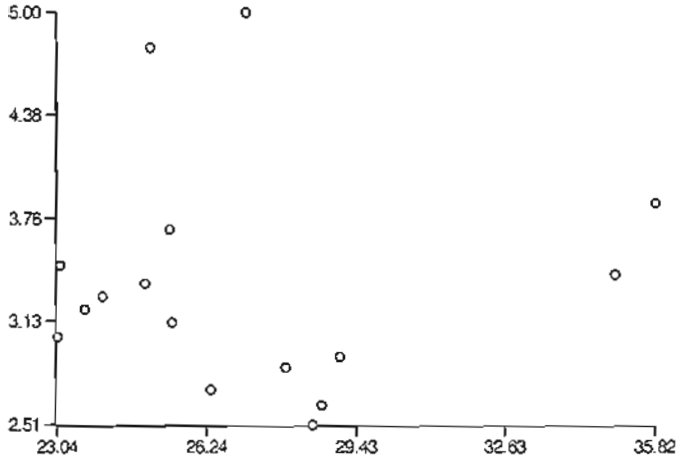

(i) females distal

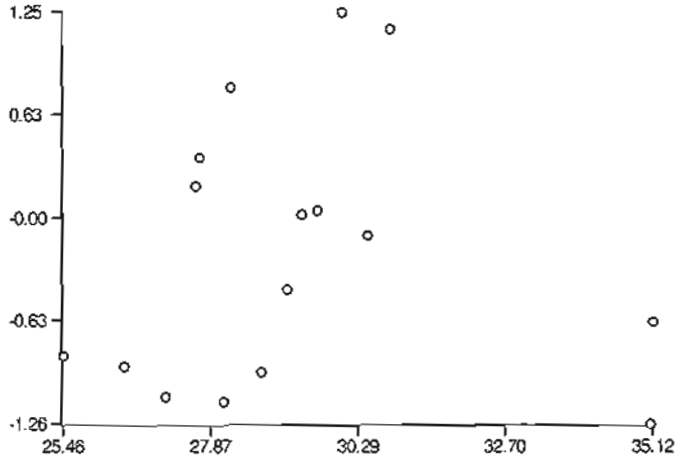

(ii) females proximal

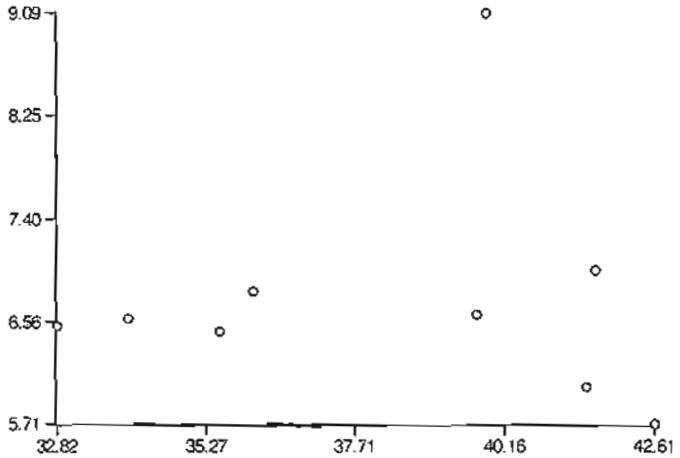

(iii) males distal

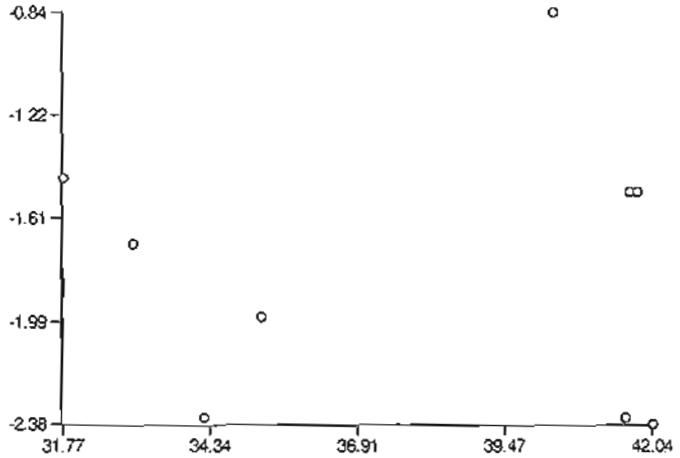

(iv) males proximal

3.4.4.2 Cluster analysis

The results of the UPGMA cluster analyses based on average taxonomic distance (ATD) for all specimens are presented in tree diagram form in Figures A.1 to A.8 and are summarized in Figure 3.7 and Figure 3.8. Cluster points marked by letters on the latter two diagrams correspond to those letters in the text.

3.4.4.2.1 conventional data

The cophenetic correlations calculated for the cluster analyses using average taxonomic distance based on the conventional data are presented in Table 3.17. Correlations were all very good, ranging from 0.9564 to 0.9818. Therefore, it was appropriate to interpret the cluster analyses using these data.

Table 3.17. Cophenetic correlations – conventional data

	r_{COPH}
females distal	0.9564
females proximal	0.9593
males distal	0.9818
males proximal	0.9775

3.4.4.2.1.1 females distal

Two clearly separated clusters were seen here (Figure A.1, page 376; Figure 3.7(a)): (a) comprising only *Homo* and *Gorilla*, and (b) comprising only *Cercopithecus* and *Colobus*. As (a) and (b) represented the superfamilies Hominoidea and Cercopithecoidea, the clusters were named hominoids and cercopithecoids, respectively. A relatively great distance was required to cluster these two groups (compared to the distance required to cluster specimens into either of these two groups), so they were clearly separate. The hominoid cluster was further divided almost perfectly into (c) *Homo* and (d) *Gorilla*; the only deviation from this was that *Gorilla* specimens 671 and 672 were clustered with *Homo*. The cercopithecoid cluster was also almost perfectly divided into genera, (e) *Cercopithecus* and (f) *Colobus*; the only deviation from this was that *Colobus* specimen 632 was grouped with *Cercopithecus*.

3.4.4.2.1.2 females proximal

The specimens were divided into two clusters (Figure A.2, page 380; Figure 3.7(b)), (a) hominoids and (b) cercopithecoids. The hominoid cluster was clearly divided into (c) *Homo* specimen 87 and (d) all other hominoids. Cluster (d) was further divided into (e) *Homo* plus *Gorilla* specimens 671 and 672, and (f) *Gorilla* plus *Homo* specimens 12, 46, 47, 123, 124, 148, 149, 212 and 213. The cercopithecoid cluster was divided into two clusters, (g) *Cercopithecus* plus *Colobus* specimens 601, 602, 610, 611, 622 and 623, and (h) the rest of *Colobus*.

3.4.4.2.1.3 males distal

The specimens were divided into two clusters (Figure A.3, page 384; Figure 3.7(c)), (a) hominoids and (b) cercopithecoids. The hominoid cluster was not divided clearly into *Homo* and *Gorilla* at all. Two clusters seen were populated by both genera, with a larger cluster, (c), and a smaller cluster, (d). The cercopithecoids were divided into two clusters, (e) a subset of *Cercopithecus* (specimens 514, 515, 516, 519, 520, 529, 530, 533, 534 and 553), and (f) the rest of *Cercopithecus* and all of *Colobus*.

3.4.4.2.1.4 males proximal

The specimens were divided into two clusters (Figure A.4, page 388; Figure 3.7(d)), (a) hominoids and (b) cercopithecoids. The hominoid cluster was not in turn made up of clusters based on genera. Two hominoid clusters were seen, one larger, (c) and one smaller, (d), both comprising *Homo* and *Gorilla* specimens. The cercopithecoid cluster was also not clustered according to genera. Two main clusters, (e) and (f) comprised a subset of *Cercopithecus*, and *Colobus* plus the remaining *Cercopithecus* specimens, respectively.

Figure 3.7. Summary UPGMA tree diagrams – conventional data (average taxonomic distance, letters correspond to specific clusters on the full diagrams in Figures A.1 to A.4)

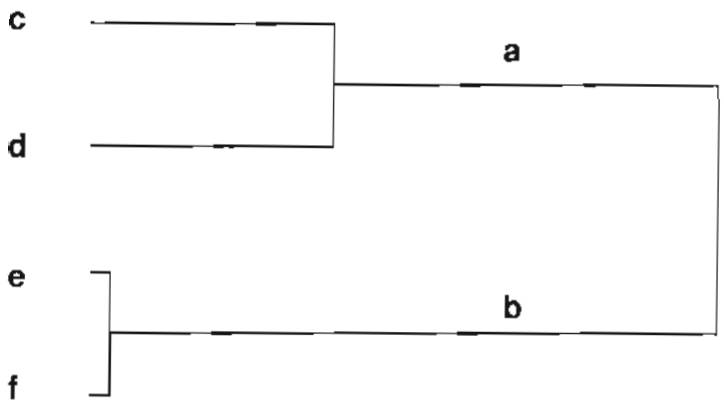

(a) females distal

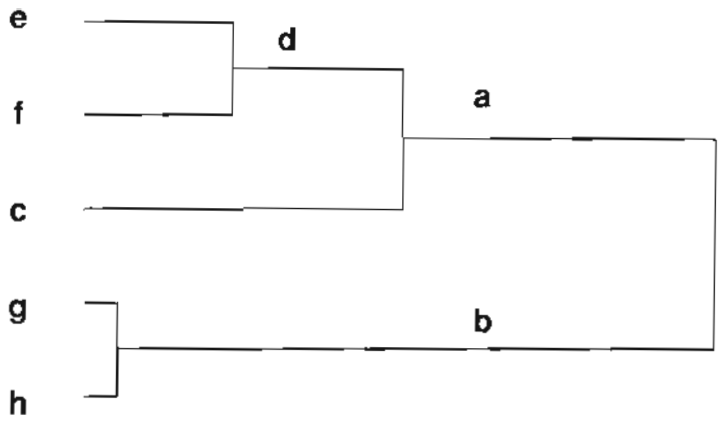

(b) females proximal

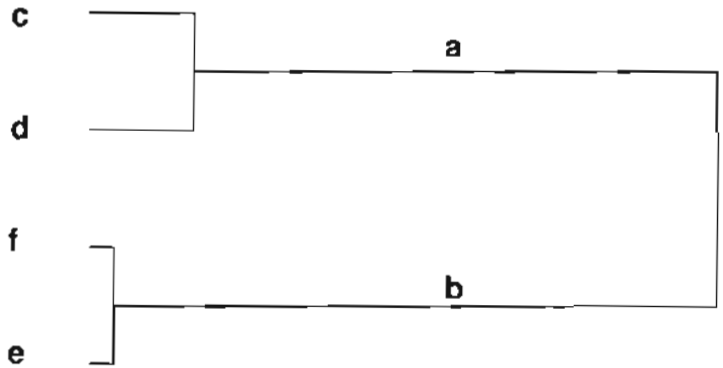

(c) males distal

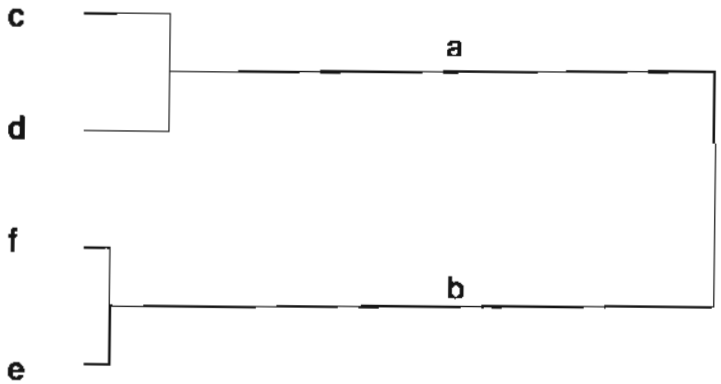

(d) males proximal

3.4.4.2.2 Fourier data

The cophenetic correlations for cluster analysis using average taxonomic distance for Fourier amplitudes are presented in Table 3.18. Correlations were all high (0.9564 to 0.9818), and very similar to those seen for conventional data. It was therefore appropriate to interpret the cluster analyses.

Table 3.18. Cophenetic correlations – Fourier data

	r_{COPH}
females distal	0.9564
females proximal	0.9594
males distal	0.9818
males proximal	0.9777

3.4.4.2.2.1 females distal

Two large clusters were seen here (Figure A.5, page 392; Figure 3.8(a)): (a) *Homo* and *Gorilla* (hominoids), and (b) *Cercopithecus* and *Colobus*, (cercopithecoids). The hominoids cluster was almost separated into its two genera, (c) *Homo* and (d) *Gorilla*. The only overlap was found in the *Homo* cluster, where specimens 671 and 672 were found to be more similar to *Homo* than to other *Gorilla* specimens. The *Homo* cluster was in turn found to consist of two clusters, (e) and (f). The cercopithecoid cluster was separated into two clusters, (g) which consisted mostly of *Cercopithecus*, but with *Colobus* specimens 622, 623, 632 and 633, and (h) which consisted of *Colobus*.

3.4.4.2.2.2 females proximal

Two clusters identified as (a) hominoid and (b) cercopithecoid were seen (Figure A.6, page 396; Figure 3.8(b)). The hominoid cluster was further divided into (c) *Homo* specimen 87 and (d) all other hominoids. Cluster (d) was not separated into *Homo* and *Gorilla* clusters: while cluster (e) contained *Homo* specimens as well as *Gorilla* specimens 671 and 672, cluster (f) contained a mix of both *Homo* and *Gorilla*. The cercopithecoid cluster consisted of two

clusters, with (g) consisting of all *Cercopithecus* specimens, plus six *Colobus* specimens (601, 602, 610, 611, 622 and 623) and (h) all other *Colobus* specimens.

3.4.4.2.2.3 males distal

The clustering of all specimens was again into two main groups (Figure A.7, page 400; Figure 3.8(c)): (a) hominoids and (b) cercopithecoids. The hominoid cluster was further subdivided into two clusters, (c) *Homo* specimens 28, 29, 58 and 59 and *Gorilla* specimens 664 and 665, and (d) all other hominoids. Cluster (d) was divided into two mixed groups ((e) and (f)) of *Homo* and *Gorilla*. The cercopithecoid cluster was devoid of any obvious clustering into *Cercopithecus* and *Colobus*, as the two genera were interspersed. Two clusters formed were (g) *Cercopithecus* specimens 514, 515, 516, 519, 520, 529, 530, 533, 534 and 553 and (h) the other *Cercopithecus* specimens plus *Colobus*.

3.4.4.2.2.4 males proximal

These specimens were also clustered into two main groups (Figure A.8, page 404; Figure 3.8(d)): (a) hominoids and (b) cercopithecoids. The hominoids cluster, as with the males distal data, was further subdivided into two clusters, (c) and (d), with unknown significance, with mixed *Homo* and *Gorilla* specimens. The picture was similar for the cercopithecoids. Cluster (e) represented a group of seven *Cercopithecus* specimens (515, 516, 530, 533, 534, 555 and 556), well segregated from the rest of this genus. The rest of *Cercopithecus* and all of *Colobus* made up cluster (f).

Figure 3.8. Summary UPGMA tree diagrams – Fourier data (average taxonomic distance, letters correspond to specific clusters on the full diagrams in Figures A.5 to A.8)

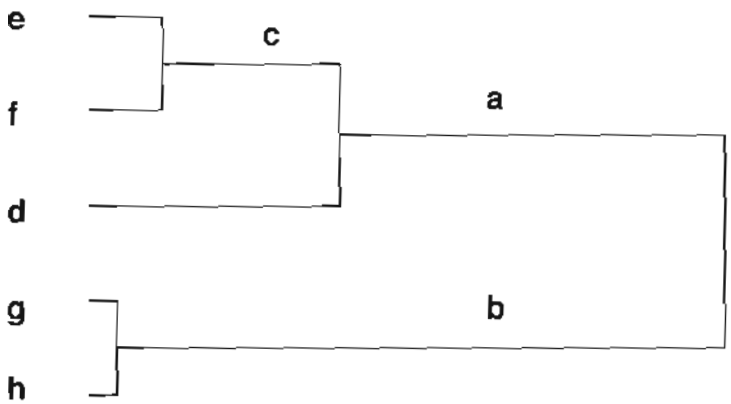

(a) females distal

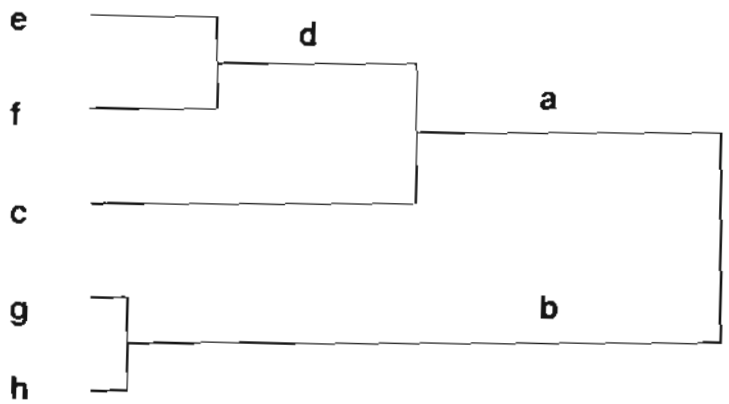

(b) females proximal

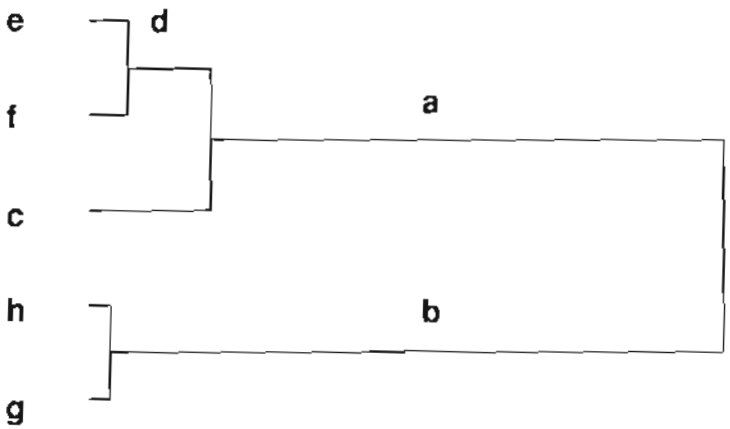

(c) males distal

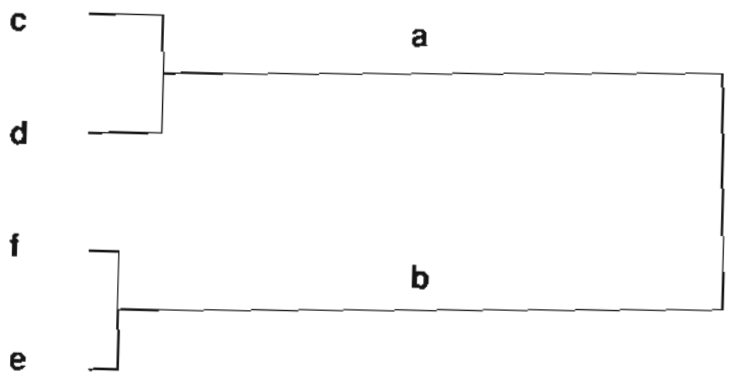

(d) males proximal

3.5. Discussion

3.5.1 Reliability

The results of the investigation into reliability (repeatability) showed that (1) the conventional variables were measured with moderate to very good reliability, and (2) that Fourier variables were measured with varied reliability. In the lower-order harmonics, it was found that ***Y3*** (females distal) and ***X2*** (males distal) were quite unreliable, with reliability percentages of just below and above 50%, respectively. Measurement error might have stemmed from placement of the pencil lines on the specimens, positioning the specimens on the scanning bench, positioning the scanner for taking the images, and/or from digitizing the outlines, although it was found that the bulk of the error arose from all but the latter influence. The interpretation of results of the principal component analysis, and really any investigations using these variables, would be affected by this lack of reliability.

These poor results warranted further inspection. The within-specimen variance of ***Y3*** in the females distal group (0.30) was similar to those for the other groups (0.19 to 0.43), but its among-specimen variability (0.76) was comparatively low (2.71 to 2.95). The same could not be said of ***X2*** from the males distal data: in comparison with the females distal ***X2***, the among-specimen variance was similar (0.38 versus 0.39, for males and females, respectively), but the males' within-specimen variance was almost three times the size (0.11 versus 0.04). Notwithstanding these two exceptions, such low reliabilities were not systemic through the same variables, so these variables were retained.

3.5.2 Power

The power spectra showed an almost complete dominance by the first harmonic (***X1*** and ***Y1***), i.e. the best-fitting ellipse to the outlines; this reflected the nearly elliptic shape of the patellar outline. It could be judged from these results that only the first harmonic amplitudes were of interest. However, this would have ignored the possibility that overall the outlines were largely elliptic but that outline differences, however small, were local and thus represented by higher-order harmonics. It was clear that, notwithstanding the dominance of the first harmonic, only harmonics 1 to 5 had any noticeable contribution. Only these five harmonics were used in the succeeding ordinations, and in further investigations.

3.5.3 Ordination

3.5.3.1 Principal component analysis

Principal component analysis results showed certain general features across and within the genera. Conventional data were transformed to natural logarithms for ordination, as variances were far from equal using raw data. This was likely due to differences in scale between ***P*** and ***A***, and was ameliorated by transformation. First eigenvalues accounted for the bulk of total variance, all such proportions exceeding 96%. Eigenvalue proportions were not critical for conventional data, as two dimensions always accounted for 100% of total variance. However, the strong correlations suggested that these specimens occupied a limited region of phenotype space. Coefficients on the first component approximated 0.71 in all data sets, which reflected the nearly equal variances. To score highly on this axis, specimens needed to have large values for both ***P*** and ***A***; that is, specimens needed to be large, and this is the basis for imputing the quality of size to the first principal component (Jolicoeur, 1963a; Jolicoeur and Mosimann, 1960; Marcus, 1990) (§2.2.2.1.3). As will be seen in Chapter 4, the PCA definition of size also includes size-related shape; any conclusions regarding the representation of specimen size by the first principal component must allow for this component to also convey shape information. The second principal component approximated [0.7071, −0.7071]. To score highly on this axis, specimens needed to show a relatively great contrast between ***P*** and ***A***. Consequently, this axis represented the difference between ***P*** and ***A***, or specimen shape. The issues of size and shape will be further addressed in Chapter 4.

For Fourier data, transformation to logarithms did not improve variance inequalities; for raw data, variances were dominated by ***X1*** and ***Y1***, presumably due to variable size, but for ln-transformed data variables accounting for relatively low power showed much greater variances. This was contrary to the goal of transformation, i.e. making variances independent of the magnitudes of the variables (Jolicoeur, 1963a; Smith, 1980) (§2.2.2.1.2.2) although it must be noted that transformation only "tends to" equate variances (Jolicoeur, 1963a p10). Figure 3.9 elucidates this phenomenon, by plotting the values of variables and their logarithms. The curve $X_2 = \ln X_1$ must necessarily be nonlinear, although variable scatters were narrow enough to be practically linear. Contrasting the plot of ***lnX1*** versus ***X1*** with that of ***lnX2*** versus ***X2*** for *Homo* females distal, it was apparent that the scatters of points were on different limbs of the curve, and the variance reflected this. As these lines of scatter were merely different segments of the curve $X_2 = \ln X_1$, the variances of the smaller variables were greatly magnified, rather than equalized with those of the larger variables; this was primarily due to the differences in magnitude (and to a lesser extent, the ranges) of the variables.

Therefore raw data were used for ordination, as it was better that the PCAs were driven by variables contributing more power than those contributing less, although performing a PCA with such disparities in variances meant that specimens may appear to be artificially constrained in phenotype space (this was not the case with conventional data). Nevertheless, this decision was (independently) supported by the proportions of variance accounted for by the first few eigenvalues. The first two eigenvalues for the raw data exceeded 90% of total variance in all data sets, a figure seldom reached from three eigenvalues for transformed data. It was therefore appropriate to treat the first two components (raw) as a representation of the whole data suite (Flury and Riedwyl, 1988). In general, the first two principal components were dominated by ***X1*** and ***Y1***. Given that the first principal component (PC1) had substantial loadings for ***X1*** and ***Y1*** (and both the same sign), the first component could be interpreted as representing size. Furthermore, PC2 showed substantial loadings for these variables, but of different sign. Thus, PC2 represented a contrast between ***X1*** (half the breadth of the best-fitting ellipse) and ***Y1*** (half the depth of the same ellipse), or shape (not related to size). These concepts will be discussed further in Chapter 4. That ***X1*** and ***Y1*** dominated the first two principal components was expected, as the variances of these variables were substantially greater than those of the remaining variables.

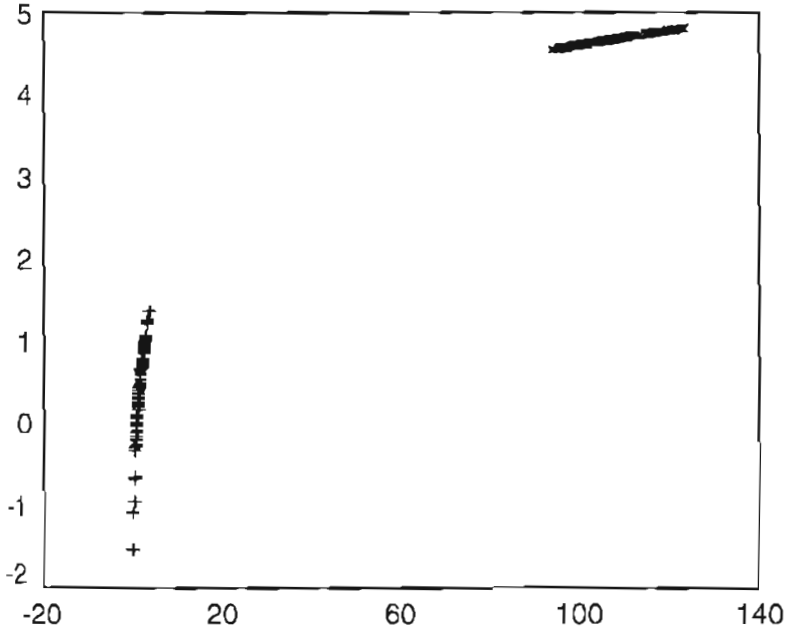

Figure 3.9. Graphs of **ln*X1*** versus ***X1*** (×) and **ln*X2*** versus ***X2*** (+), *Homo* females distal

The scatterplots of principal component scores showed several specimens that lay moderately away from the main groups, and it was of interest to investigate the effect of such specimens. In *Homo*, female specimen 87 (proximal only) was found to be such a specimen using both conventional and Fourier data. This specimen was outstanding by being at the positive extreme on PC1, so it could be interpreted as being a noticeably large specimen. Similarly, female *Gorilla* specimens 671 and 672 were at the positive extreme on PC1 for both sets of data, and were considered larger specimens. A likely explanation for *Gorilla* is that the sample size was too small, that more intermediate specimens happened not to be available, and that this heterogeneity was artefactual. As *Homo* and *Gorilla* males tend to be larger than females, another explanation was that these large female specimens might have been mislabelled, and were male. *Gorilla* female specimens 657 and 658 were found to be at the positive extreme on PC2 in both data sets, and *Gorilla* male specimen 656 was at the positive extreme on PC2 only using Fourier data. These specimens showed a noticeably large contrast between $\boldsymbol{X1}$ and $\boldsymbol{Y1}$, so were outstanding on shape.

That the data matrices for *Gorilla* males were only of rank nine ($p = 10$, $n = 9$) was of concern; Flury and Riedwyl (1988) recommended not performing PCA when the data matrix is not of full rank. However, this recommendation appeared to be related to interpretation of the last $(p - n)$ components, which was not attempted in this chapter; therefore, ordination proceeded with these data as with the others.

Repeat analysis with omission of the above specimens showed greater differences in *Gorilla* than in *Homo*. This could largely be attributed to sample sizes – specimen 87 was only one of 106 specimens in *Homo*, but specimens 671 and 672 were the equivalent of one out of eight in *Gorilla*. Omission of these specimens mostly shortened the length of the first principal component (i.e. reduced first eigenvalue), with little effect on its direction. Omission of specimen 656, the only 'shape' omission, did little to affect the direction of spread of specimens, but reduced the length of PC2, thus increasing the relative length of PC1.

In no data set was there any suggestion that patellar phenotypes were grouped into discrete types, for example Wiberg's (1941) three types in humans. While Wiberg hinted that patellae exist on a morphological continuum ("the transition between these types was gradual"), the conclusion of this sentence ("...in general there was no difficulty in differentiating between them") contradicted this. Morphological types proposed as clinical tools presumably require that intermediate phenotypes (between types) are lacking. Without a rationale couched in terms of developmental or selective constraints (§2.1.4.1) to explain lack of intermediate

forms between two or more types (Alberch, 1982), it is more reasonable to expect a continuum of phenotypes, which was found here. Notwithstanding this, patellar outline form was constrained: using either conventional or Fourier data, there were strong correlations between variables within genera (greater with conventional data than with Fourier data), such that there were not widely disparate forms filling phenotype space uniformly. For example, correlation between ***X1*** and ***Y1*** meant that it was unlikely that there were any very broad but very shallow (i.e. very flat) patellar outlines; such a phenotype would presumably offer little resistance to bending forces, and if natural selection had not excluded it, modelling processes would have. These correlations showed that constraints with Fourier data were not artificial.

3.5.3.2 Cluster analysis

UPGMA cluster analysis was performed using both conventional and Fourier data from both distal and proximal images, based on average taxonomic distance. Cophenetic correlations closely approximated unity, which supported interpretation of the resultant tree diagrams.

The general feature of all analyses was that *Homo* and *Gorilla* (hominoids) and *Cercopithecus* and *Colobus* (cercopithecoids) were clearly separated. Separation within these two major clusters based on genus was mixed. For example, in females distal (conventional and Fourier data), the separation of *Homo* and *Gorilla* was almost perfect, save for the clustering of *Gorilla* specimens 671 and 672 into the *Homo* cluster. These specimens were interpreted in §3.5.3.1 as the largest female *Gorilla* specimens, and the cluster analyses have seen these as more *Homo*-like than *Gorilla*-like. Data (conventional and Fourier) from the female proximal images gave quite different results. Here, *Homo* specimen 87, seen in §3.5.3.1 to be an outstandingly large specimen, was found to be so unlike the other *Homo* specimens that even all the *Gorilla* specimens were seen to be more *Homo*-like. Notwithstanding this remarkable specimen, *Homo* and *Gorilla* still showed more overlap than found in the distal data set, with some *Homo* specimens clustered with *Gorilla*. To view these data in a different way and better understand these results, the PCA scatterplots for several arbitrary data sets have been superimposed to allow for comparison of groups (Figure 3.10). This method of comparison was not technically correct – the proper method would have been to use common principal component analysis (Flury, 1988), as the one-group method rotates data independently of any other data set. Inspection of the principal components of these data sets showed that the coefficients were slightly different (especially for Fourier data), so there was a degree of inaccuracy here. In Figure 3.10(a) it can be seen that the nine '*Gorilla*-like' specimens from

Homo were seen to occupy the negative end of PC1 (although they were not all that extreme). The two *Homo*-like *Gorilla* specimens were at the large end of PC1. Thus, large *Gorilla* specimens were *Homo*-like, and small *Homo* specimens were *Gorilla*-like. Figure 3.10(b) shows the PCA scatterplots for *Homo* males distal (Fourier data). The *Homo* and *Gorilla* specimens in cluster (d) were at the small end of their respective PC1s. Similarly, *Homo* and *Gorilla* specimens in clusters (e) and (f) had intermediate and high scores on PC1, respectively. One exception to this was *Homo* specimen 54 in cluster (e), which, based on its PC1 score, would have been placed in cluster (f). The scatterplot shows that the closest specimen to 54 was specimen 27 (cluster (e)), and the tree diagram shows that these two specimens were clustered together. Therefore, despite its relatively high score on PC1, specimen 54 was grouped according to its nearest neighbour. This was not a case where larger *Gorilla* specimens were grouped with smaller *Homo* specimens – smaller *Gorilla* specimens were grouped with smaller *Homo* specimens, and the same for intermediate and larger specimens. Figure 3.10(c) shows the scatterplots of *Cercopithecus* and *Colobus* females proximal (Fourier data); small *Colobus* specimens were seen as *Cercopithecus*-like. Figure 3.10(d) shows the scatterplots of *Cercopithecus* and *Colobus* males distal (conventional data). Here, large *Cercopithecus* specimens were seen as *Colobus*-like.

Figure 3.10. Selected scatterplots reproduced from Figures 3.5 and 3.6

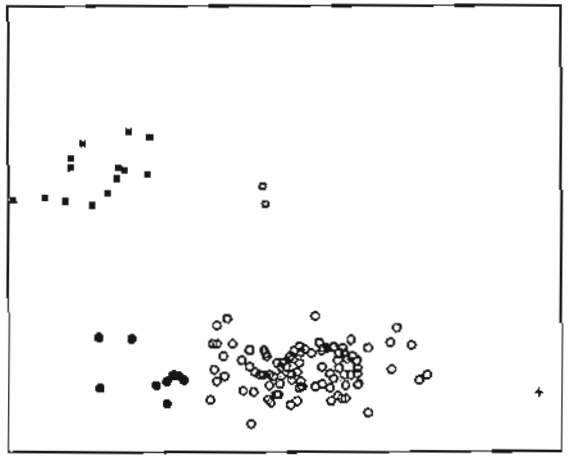

(a) *Homo* (cluster f ●, cluster e ○, specimen 87 +) and *Gorilla* (cluster f ■, cluster e □) females proximal – conventional data

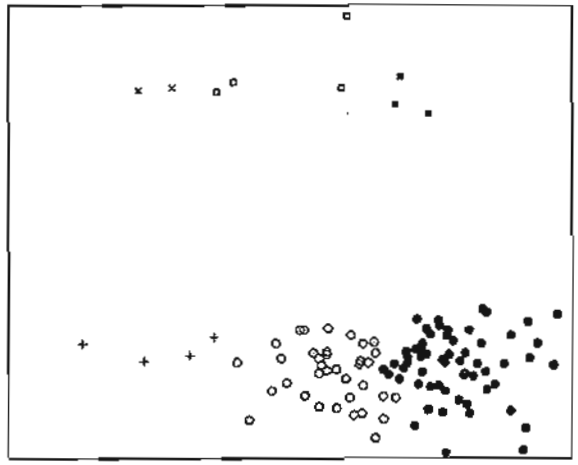

(b) *Homo* (cluster f ●, cluster e ○, cluster c +) and *Gorilla* (cluster f ■, cluster e □, cluster c ×) males distal – Fourier data

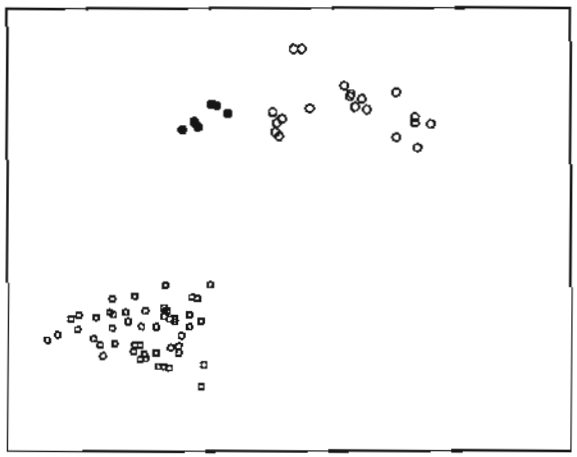

(c) *Cercopithecus* (□) and *Colobus* (cluster g ●, cluster h ○) females proximal – Fourier data

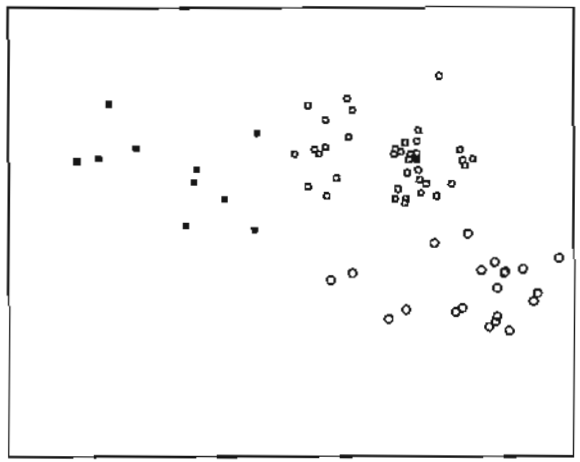

(d) *Cercopithecus* (cluster e ■, cluster f □) and *Colobus* (○)males distal – conventional data

There was the potential with the cercopithecoids for the overlap of genera to be species-related, and these details were available; however, there was no evidence that this was the case. For example, in females proximal (Fourier data) six *Colobus* specimens were clustered with *Cercopithecus*. These six specimens were from *Colobus badius* and *C. guereza*, and both species were represented in the main *Colobus* cluster.

Figure 3.11 shows the tree diagrams from the repeat cluster analysis using the *Elephas* specimens. It is clear that the primate specimens, both hominoid and cercopithecoid, had substantially greater phenetic similarity than the much larger elephant specimens.

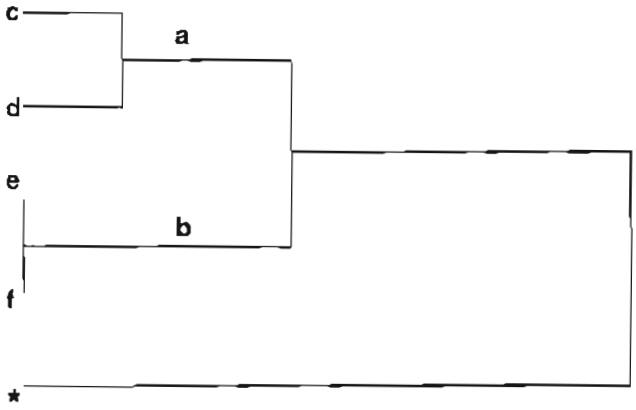

(**a**) conventional data

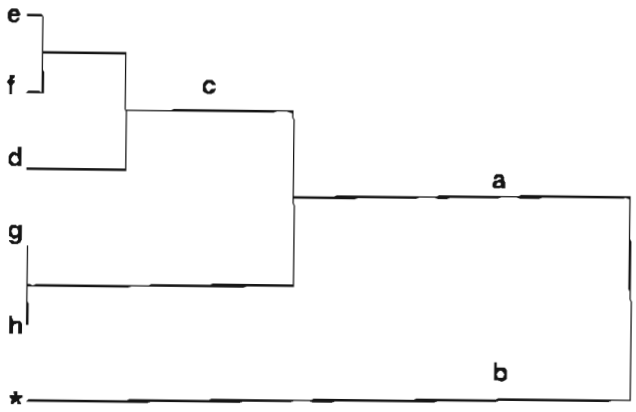

(**b**) Fourier data

Figure 3.11. UPGMA tree diagrams from Figures 3.7 and 3.8, with the addition of mean *Elephas* data (*) – females distal (letters refer to clusters in text)

There was no suggestion of discrete phenotypes within genera found using cluster analysis, which supported the findings using principal component analysis.

3.5.4 Comparative Discussion

3.5.4.1 Principal component analysis versus cluster analysis

The two aims of ordination in this study, those of identification of (1) outlying or influential specimens, and (2) heterogeneities within the data, were well met by principal component analysis and cluster analysis. Principal component analysis was useful as it gave clear indication, by the dominance of the first few eigenvalues, that overall the scatter of data was constrained, rather than filling phenotype space uniformly. This was seen more with conventional data; Fourier data could only be reasonably reduced to two dimensions, and these dimensions were dominated by the two variables whose variance far outstripped that of any other variable. It also allowed for tentative interpretation of principal component axes as representing the concepts of size and shape, and furthermore allowed interpretation of size and shape differences, especially in relation to outlying specimens. The influence on PCA of the several outlying specimens was found to not be great, and therefore these did not drive the analyses. The main advantage offered by UPGMA cluster analysis in this investigation was the ability to place the different genera side by side and detect relative similarities (or differences) within and among the four genera, as opposed to the one-group PCA. Cluster analysis showed that there was a substantial gap in phenotype space between hominoids and cercopithecoids, but not between the genera within these two groups. These gaps (or, indeed, overlaps) were defined by size and shape information, but it was likely that size was the dominating influence. The tree-plots produced by cluster analysis combined with the PCA scatterplots showed that similarities and differences found appeared largely due to specimen size. It was also apparent that at the genus level similarities within clusters were of the same magnitude as similarities among clusters; that is the data scatters were homogeneous, which supported the interpretations of the scatters of principal component scores. Thus, the two methods combined allowed for greater interpretation than either method alone would have provided.

There was one major discrepancy between PCA and cluster analysis: *Homo* specimen 87. The proximal outline was shown to be an outlier using both methods, but its degree of separation from the main group using cluster analysis was much greater than using PCA – indeed, the

other *Homo* specimens were more similar to *Gorilla* than to specimen 87. The results of the PCA with omission of this specimen showed only a slight alteration in length and direction of the first component. One possible reason for this was that the principal component scores reflected the bulk of the original morphometric information, and in reducing the dimension of the data substantial information might have been lost (Flury and Riedwyl, 1988); cluster analysis, using the full data suite, would not have lost this information, although information certainly would have been lost due to the use of average similarities (§2.2.2.2.2). Consequently, the choice of clustering method might have had some influence on the results (Aldenderfer and Blashfield, 1984).

3.5.4.2 Proximal versus distal outlines

An important question in this study was whether taking data from two outlines per specimen introduced redundancy in the data; this was not the case. In *Homo* females, for example, specimen 87 was found to be a striking outlier only in the proximal data set; it was reasonable to suspect that data from one level (most likely proximal) were erroneous. Two explanations for such an error were that the image outline was (1) poorly digitized, and (2) magnified relative to the other images. It was unlikely that the outline had been so poorly digitized that the average of three outlines was so different to the others. If this had been the case, then it would be expected that the outline shape would also be conspicuous – this will be addressed in Chapter 4. Image magnification was also unlikely, as the proximal and distal images were produced in the same CT session, and these images were scanned in the same session; if the proximal image had been magnified, it would be expected that the distal image would also have been magnified. A third possibility was that the image had been mislabelled (i.e. given another *Homo* specimen number); this also seemed unlikely, as the proximal and distal outlines were not simply different – the proximal outline made *Gorilla* specimens look *Homo*-like in comparison. Certain specimens were found to overlap in the cluster analysis in both proximal and distal data sets, but others were found only in proximal or in distal data sets (for example in *Cercopithecus* males). While neither proximal nor distal data sets consistently carried more information than the other, and as the intention was to conduct a thorough investigation, gathering two sets of data did not simply duplicate the data and was justified.

3.5.4.3 Conventional versus Fourier data

Both conventional and Fourier data were derived from the same outlines, so it was expected that there should be some consistency in the results; any discrepancies could have been due to the differences in morphometric information included using 10-dimensional Fourier data compared to 2-dimensional conventional data. Only in *Gorilla* males distal was there any clear difference between the two principal component scatterplots, but only relating to the position of specimen 656 relative to the rest of the sample. Otherwise, there were strong similarities between scatterplots for the two data sets. For example, the conventional and Fourier scatterplots from *Gorilla* females (both distal and proximal) appeared to be (axis values aside) almost perfect copies of each other. Thus, the use of both conventional and Fourier data (as opposed to either type alone) did not greatly aid ordination.

That specimens were arranged on a line using conventional data and on a plane using Fourier data suggested that the fairly simple picture of morphometric variation along a line belied a slightly richer pattern of variation. Therefore, the constraints apparent from conventional data were in part due to the simplicity of the data, so the data appeared less constrained, filling a greater part of possible phenotype space, when Fourier data were used.

3.5.4.4 Comparison among genera

In all genera, it appeared that specimen size dominated ordination. Furthermore, outlying specimens tended to differ from the other specimens due to size differences. One clear exception to this was specimen 656 in *Gorilla* males distal (Fourier data): this specimen was unremarkable on its score for PC1, but was markedly different to the rest on PC2.

While the great size differences between hominoids (*Homo* and *Gorilla*) and cercopithecoids (*Cercopithecus* and *Colobus*) kept these two groups separate in the cluster analysis, size similarities within each of these two groups caused overlaps between genera. For females, smaller *Homo* specimens tended to be clustered with *Gorilla*, while larger *Gorilla* specimens tended to be clustered with *Homo*. Similarly, small *Colobus* specimens were clustered with *Cercopithecus*, and large *Cercopithecus* with *Colobus*. This pattern was seen for male *Cercopithecus* and *Colobus* (large *Cercopithecus* clustered with *Colobus*), but not for *Homo* and *Gorilla*. Male *Gorilla* specimens with low, intermediate and high scores on PC1 clustered

with male *Homo* specimens which had low, intermediate and high scores on PC1, respectively. These different patterns are reflected in Figure 3.12, which shows error bar plots of |x| (measurement vector lengths – this will be seen in Chapter 4 to be a measure of specimen size). There was a clear increase in patellar size from *Cercopithecus* to *Colobus* and then to *Gorilla* to *Homo*. The means of *Homo* and *Gorilla* were more similar for males than females, which possibly explained the almost complete overlap of these genera seen in the cluster analysis (§3.5.3.2). This suggested different degrees of sexual dimorphism in *Homo* and *Gorilla* – that is, there were greater morphological differences between female *Homo* and *Gorilla* than for males. This issue will be taken up in Chapter 5.

It was expected that patellar size would differ between genera, due to body size differences. Presumably, the functional circumstances of these patellae differed both within and among these genera, although differences in shape (which should reflect function) were overshadowed by size differences. Choosing specimens from genera such as *Gorilla* and *Cercopithecus* contributed to this: unless functional differences among these two genera were at least as remarkable as the size differences, size differences were always going to dominate. Aspects of shape will be investigated further in Chapter 4.

Figure 3.12. Error bars (y-axis) for $|x|$ – conventional data (values on y-axis, squares at means, bars represent $\pm$ 2 standard errors)

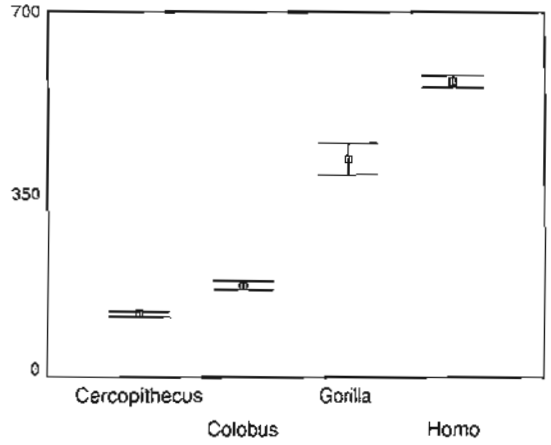

(a) females distal

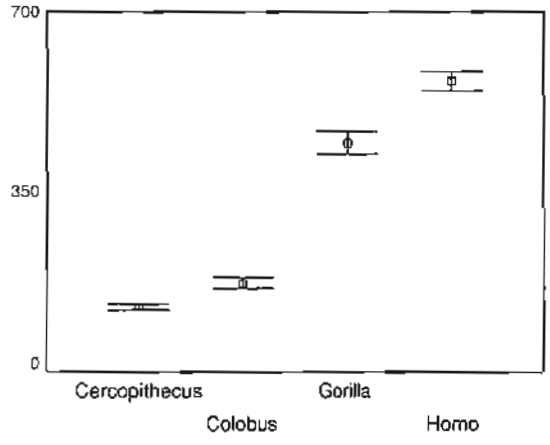

(b) females proximal

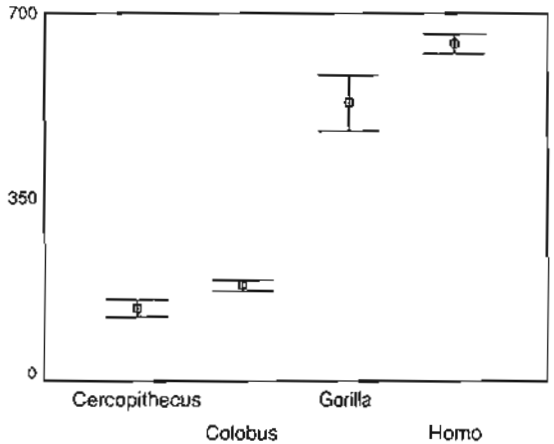

(c) males distal

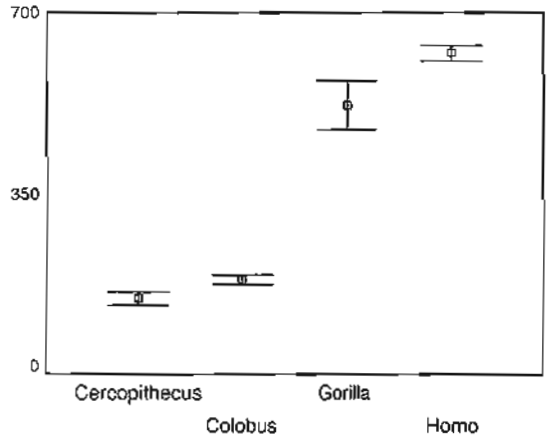

(d) males proximal

3.6 Conclusions

3.6.1 Reliability

Overall, the reliability of data, as estimated by Model II anova, was acceptable. That is, variances of error in the methods were small relative to overall variation, and unlikely to bias the results. Two exceptions to this were the Fourier amplitudes ***X2*** and ***Y3***, which had poor reliability. Consequently, results featuring these variables required care in interpretation.

3.6.2 Power

Power spectra from the Fourier data showed that harmonics 6 to 30 contributed very little to the patellar outlines in each group. Consequently, only amplitudes from harmonics 1 to 5 were to be used further in this study.

3.6.3 Ordination

Principal component analysis revealed that there were constraints to the scatter of data in phenotype space. Using the conventional data, most of the scatter of specimens could be explained by a single factor, which translated roughly as size (which included some shape information). The variation between specimens based on (a rough definition of) shape differences was relatively minor. When using Fourier amplitudes, the bulk of variation existed in only two (of a possible 10) dimensions, and those two dimensions were largely defined by two variables (***X1*** and ***Y1***), due to the dominance of their variation. In general, there was a continuous spread of data points in each group, with no convincing grouping of specimens found; there were, in some groups, insufficient data to conclude this with confidence, although it was more reasonable to assume that gaps in the data scatters were due to absences due to sampling, rather than separation of phenotypes. Some specimens were conspicuous by their relative positions in the scatterplots, but such specimens were not typically seen as overly influential in respect to ordination.

Cluster analysis showed that there was clear separation, based on average taxonomic distance derived from both conventional and Fourier data, between hominoids (*Homo* and *Gorilla*) and cercopithecoids (*Cercopithecus* and *Colobus*). However, there typically was not clear

separation into the relevant genera, and there was overlapping between *Homo* and *Gorilla*, and between *Cercopithecus* and *Colobus*. For females, overlapping specimens were found to be those that had extreme scores on the first principal components, i.e. largest or smallest specimens in the samples. For males, there was practically complete overlap between *Homo* and *Gorilla*. Thus, from principal component analysis and cluster analysis it was concluded that morphometric variation was dominated by interspecimen size differences, and that shape differences were comparatively minor.

Chapter 4 Size, Shape and Allometry

In this chapter, the broad concepts of specimen form, size and shape were considered. While object form is represented by a vector of raw measurements, the concepts of size and shape are not concretely defined in the literature, and there exist multiple pathways for investigation of such issues. The concepts of size and shape, briefly touched on in Chapter 3, raise two issues relevant to this study. Firstly, the form of an object is often separated into a shape component and a size component, so that shape alone (sometimes size alone) may be studied (the process of size-adjustment). It will be seen that such a practice may ignore some conceptual difficulties, particularly the rather abstract notions of size and shape, and the blurred boundary between the two. Secondly, given an increase (or decrease) in size, form measurements may change in equal proportion to each other (maintaining the same shape), or in different proportions, producing shape differences. The concept of intervariable relations, (which encompasses the relation between size and shape), belongs to the realm of allometry. In this chapter, size-shape separation and allometry will be investigated.

4.1 Background

The raw data recorded by the morphometrician reflects the form of each object. Object form may be conceptually broken down into two components, those of (1) size and (2) shape (Sprent, 1972). In colloquial use, the terms size and shape prima facie present little difficulty: size may be thought of as representing the magnitude of one or more dimensions, and shape as likeness to a regular geometric figure (circle, square, etc.), or relative measurements in different directions. Therefore, *unique* definitions of patellar size and shape in this study are not immediately obvious.

In the scientific literature, size and shape are in general not well defined, and this introduces arbitrariness to decisions as to what precisely is meant by them (Bookstein, 1989; Jungers et al., 1995; Rao, 1964). What the investigator chooses to call 'size' may depend on the nature of the specimens and the objectives of the investigation (Jungers et al., 1995). The size of an object may be represented by one or more measurements made on the object – for example breadth, length, perimeter, area, geometric mean, vector length (Mosimann, 1970; Rohlf and Sokal, 1965) – or on the organism as a whole – for example body weight (Jungers, 1984). This list is not exhaustive, but shows the diversity among choices as to what may be called

size. As size is subjective, the use of this term in this study will refer to a nonspecific concept of general magnitude, unless otherwise stated.

A general definition of shape has been provided by (Healy-Williams et al., 1997): the spatial configuration of area or volume. This definition recalls the concept of second moment of area (§2.1.2.6) – that is, the relative distribution of bone in a certain direction – and as such, bone shape is more likely to reflect mechanical circumstances than a measure of size alone (Ruff, 1987). Thompson (1946) defined form as the collection of actual or relative magnitudes in various directions. In this study, the actual measurements will be termed 'form', and the relative measurements (or proportions), 'shape' (Jungers et al., 1995; Klingenberg, 1998). Another definition of shape is widely used: the characteristic of an object that remains unchanged following scaling, translation, reflection and rotation (Bookstein, 1996b; Lele, 1991). While translation, reflection and rotation are en bloc relocations of the object and are easily defined, scaling may have many definitions (Jungers et al., 1995; Mosimann and Malley, 1979), although the choice here is arbitrary.

4.1.1 Size-adjustment

As the difference in form (as measured) between objects may reside at least partly in size differences, it has been recommended that shape be separated from size to assess the variation of the former (Blackith, 1960; Corruccini, 1977; Jungers et al., 1995; Rohlf and Sokal, 1965; Steudel, 1981). Such a differentiation is artificial (Shea, 1985a), as Bookstein (1986) has pointed out that size and shape are "inextricably entangled" (p185). This entanglement is due to an overlap between size and shape, that which is referred to as size-related shape (Klingenberg, 1998). Size-related shape is the basis of allometry (§4.1.2), and for now it will suffice to define this as the alteration in shape due to an alteration in size. The decision to adjust data for size may stem from one of two motivations: either the investigator wishes to define shape as the relative dimensions, or proportions, of an object (Corruccini, 1995), or to remove from the data both size as well as size-related shape (Albrecht et al., 1993). With regard to the latter, the effect of size on shape can be no straightforward matter biologically; in terms of patellar form, general size presumably has its effects during development, but this is at the level of the chondrocyte (proliferation, matrix deposition), and it is unlikely that a relatively simple mathematical procedure will necessarily reflect these effects. Moreover, what is left behind following such a procedure may have little meaning biologically (Jungers, 1984; Shea, 1985b; Sprent, 1972); Oxnard, 1978), and presumably must reflect any shortcomings of the procedure.

The aim of adjusting data for size in this study will be to render data as shape measurements or proportions (i.e. relative measurements). Ideally, following such a procedure, two specimens with the same shape will be shown to be identical (Mosimann and James, 1979; Mosimann and Malley, 1979). In other words, geometric similarity is respected. Two specimens, with measurement vectors $\boldsymbol{a}$ and $\boldsymbol{b}$, if geometrically similar (they have the same shape), will show measurements which are directly proportional, or $\boldsymbol{a} = c\boldsymbol{b}$ (Boyce, 1969; Godfrey et al., 1991; Mosimann, 1970). These two specimens will be represented as points on the same ray (a line passing through the origin (0, 0) in phenotype space) (Boyce, 1969; Mosimann and Malley, 1979). Shape is then represented by the direction of this ray, and size reflects the distance of each specimen from the origin (Mosimann and James, 1979); specimens on such a line have the same shape, and different rays reflect different shapes (Bookstein, 1989; Jungers et al., 1995). Specimens on lines not passing through the origin, when raw data are being assessed, cannot be geometrically similar (Jungers et al., 1995).

There are several approaches to separate shape from size, and within each general approach there have been many methods devised to achieve this goal. Some of these approaches will be reviewed here, with the aim of identifying methods that are sensitive to geometric similarity (equality of proportions). Broad philosophies include (1) treating the first principal component as size and the remaining $(p - 1)$ components as shape, and (2) rendering original data as shape data via ratios with size. In (3), the method(s) used in this investigation (as well as the rationale for this choice) will be stated.

4.1.1.1 Principal component analysis

A popular size-adjustment method uses the theory that a general (often the first) principal component represents the size difference between specimens (Marcus, 1990; Mosimann and Malley, 1979). Following removal of this size component, what is left (the other $(p - 1)$ components) represents shape variables (Jolicoeur, 1963a; Mosimann and Malley, 1979).

Two general objections to this approach limit its usefulness. Firstly, as the remaining shape components are orthogonal to the size component (Sprent, 1972), shape is statistically independent of size, so that size-related shape is necessarily included in the size component (Bookstein, 1989; Flessa and Bray, 1977; Klingenberg, 1998). As Oxnard (1978) stated, "the fact that some aspects of shape are correlated with size does not mean they are size" (p233). Secondly, principal component analysis is not explicitly designed to extract size and shape components, and so the assignation of size to the first component is not built on firm

foundations (Bookstein, 1989; Jungers et al., 1995; Rao, 1964). The expectation that size will account for the greatest variation in the data is not a justification for heralding the component with the largest eigenvalue as size, nor conversely concluding that "shape...is much more constant than...size" (Jolicoeur, 1963a p25). This reasoning is circular: (1) assume that size variation will overshadow shape variation, then (2) based on this assumption, call the first eigenvector 'size', then (3) determine the variation of size by the dominance of its eigenvalue. Such a method is not immediately appropriate in this study, as it is not necessarily sensitive to geometric similarity; this is not to say that PCA need not reflect geometric similarity, merely that this can only be stated in retrospect. Data are transformed by shifting the mean of variables to the origin, such that the principal components pass through the origin, but such transformations do not preserve geometrically similar relations between specimens (Mosimann and Malley, 1979). Figure 4.1 shows that as geometric similarity is defined here as specimens lying on the same ray (from the origin), shifting the position of the origin means that information on the original origin is lost. Thus, specimens 1 and 2, and specimens 5 and 6, which originally showed geometric similarity, show shape differences due to the shifting of the origin; only specimens 3 and 4 continue to show geometric similarity.

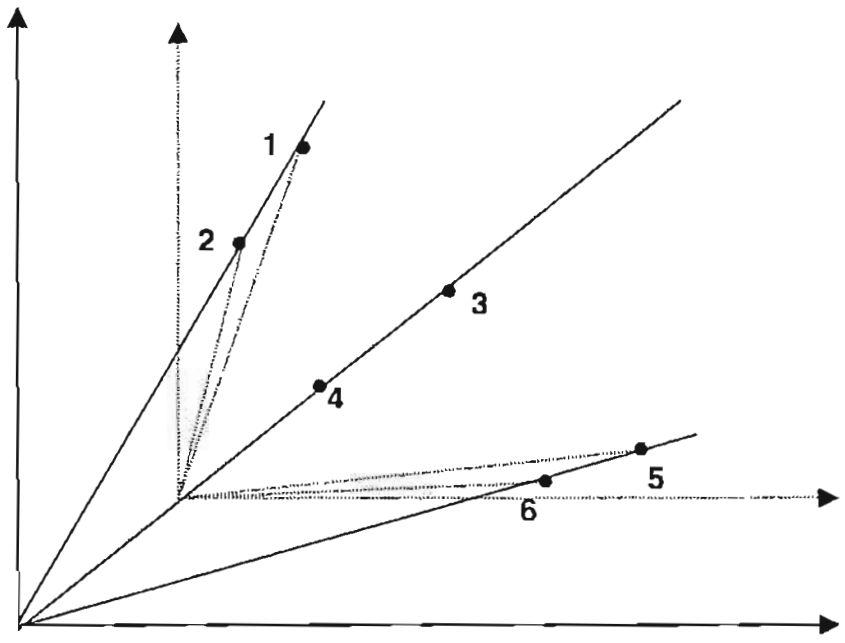

Figure 4.1. Illustration showing effect of shifting mean on geometric similarity (pairs of geometrically similar specimens [solid lines] are not necessarily on the same ray from a new origin [dashed lines]) (adapted from (Mosimann and Malley, 1979))

4.1.1.2 Ratios

It is possible to present raw data as ratios: one variable is derived from two ($X_3 = X_1/X_2$), and the ratio records the relation between them (Sokal and Rohlf, 1995). One approach that uses ratios of data to quantify shape is that of Mosimann (1970). Each set of p values contains information regarding both object shape and size. As stated earlier, shape corresponds to the direction of the vector, while the length of the vector reflects the size of the individual. Using vector length, size may be calculated as $(\Sigma X_i^2)^{1/2}$ (Boyce, 1969) (as seen in Chapter 3); other suitable size variables may include ΣX_i, $(\Pi X_i)^{1/p}$, X_k etc. (Mosimann, 1970; Mosimann and Malley, 1979). Shape is then defined as the ratio of the original form vector and the size measurement. As illustrated in Figure 4.2, it is the relative proportion of the original variables that determines the resultant shape variable, not the choice of size variable; when the relation between variables is constant, shape is constant. This, importantly, reflects the concept of shape as relative size or proportion. The choice of size variable is thus academic for the purpose of expressing shape (Corruccini, 1995). For example, the following two ratios (from O'Higgins (1997) and Young et al. (1974))

$$F_1 = \frac{length}{breadth} \text{ and } F_2 = \frac{4\pi \times area}{perimeter^2},$$

simply express one variable in terms of another. F_1 and F_2 reflect the likeness of an object to a square or circle, respectively.

Mosimann's approach has the benefit of preserving geometric similarity: if two specimens A (form vector $\boldsymbol{a} = (X_{1\,1}, X_{2\,1})$) and B ($\boldsymbol{b} = (X_{1\,2}, X_{2\,2})$) are geometrically similar, then the ratio $X_{1\,1}/X_{2\,1}$ must equal $X_{1\,2}/X_{2\,2}$, and these two ratios must equal a (as in $X_2 = aX_1$ – see §4.1.2.1). Dividing each vector by a scalar does not change the vector proportions – that is, the two shapes are the same if one form vector is a multiple of the other.

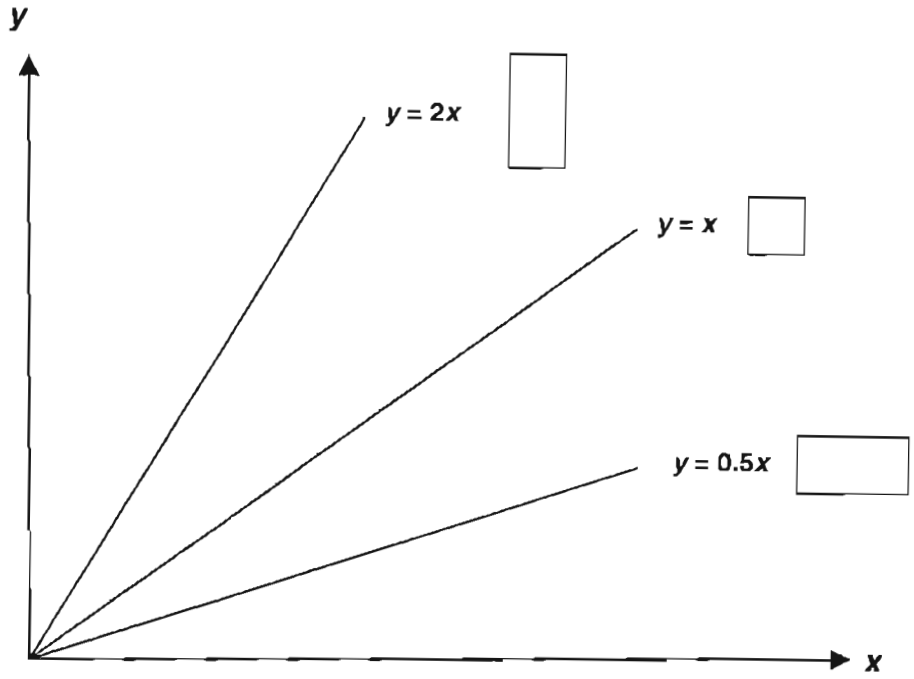

Figure 4.2. Diagram showing that proportional measurements are the same along each line of geometric similarity from the origin (x = breadth, y = depth)

The use of ratio, or index, data in morphometric studies has received some criticism. Atchley and coworkers (1976) have criticized the use of ratios to 'correct' for size differences, due to statistical concerns. For example, they found that the distributions of ratio variables tended towards nonnormality. Further problems may arise depending on the aims of the investigator. If it is intended to investigate the relation between the two original variables among specimens, information regarding the nature of the relation is lost when only a ratio is used (Sokal and Rohlf, 1995), and both numerator and denominator variables must be retained (Ross and Ward, 1982). If the variables within the ratio do not scale (increase or decrease together) in equal proportion, this relation is confounded (Aiello, 1981). However, ratio data need not always be seen as invalid, and can be useful depending on the investigator's intentions. These values are merely proportions, and their use need not be mutually exclusive to that of the original (nonratio) data. For example, Biegert and Maurer (1972) plotted the scatter of limb length/skeletal trunk length versus skeletal trunk length; that the scatter of points was not disposed along a horizontal line reflected the lack of isometry between limb length and skeletal trunk length. That some genera were found to lie along a line, and some noticeably away from this line, allowed Biegert and Maurer (1972) to infer relative morphological differences between the former and the latter. Use of the ratio denominator as the abscissa variable meant that the relation was not lost.

4.1.1.3 Methods for this investigation

Data may be size-adjusted prior to any number of further investigations. For example, size-adjusted data may be used for ordination purposes, to compare results due to raw data with those from which size has been 'removed' (Corruccini, 1987; Grine et al., 1996; Jolicoeur and Mosimann, 1960; Jungers et al., 1988, 1995; Lague and Jungers, 1996). They may also be used in allometric investigations, to investigate relations between size and shape (see §4.1.2.3.1.4) (Mosimann and James, 1979). The purpose of size-adjustment in this investigation will be for ordination, to detect any data structure based on specimen shape.

With the intention of identifying geometric similarity, the present study used Mosimann's approach, with the interpretation of object shape as represented by the direction of the measurement vector (reflecting relative proportions of variables), and size by the length of that vector; this approach accords with the concept of phenotype space. The two ordination methods used in Chapter 3 allow for two different approaches to size-adjustment. Firstly, dividing each measurement vector by its length renders a vector of unit length (a normalized vector); specimens can then be plotted according to their normalized measurement vector using PCA. Secondly, rather than render a measurement vector as a shape vector by dividing the former by an arbitrary size variable, the present study also used the concept of shape difference between specimens being reflected by the difference in direction of measurement vectors; this difference may thus be measured by direction cosines (Boyce, 1969; Reyment and Jöreskog, 1993; Sneath and Sokal, 1973). Calculating the cosine of the angle between each of n specimens allows the construction of an $n \times n$ matrix of values that effectively ignore the length of the data vector, and these similarity coefficients may then be used for cluster analysis. For example, Grine and coworkers (1996) and Lague and Jungers (1996) used the UPGMA method on average taxonomic distance coefficients from both raw data, and data rendered as shape variables by division by the geometric mean. Such an approach allowed these authors to make inferences regarding relative size and shape differences. A multigroup method such as cluster analysis also allows a comparison of the separation of different groups with size-included and size-free data: different groups may be clearly separated initially, but indistinguishable following size adjustment (Darroch and Mosimann, 1985).

4.1.2 Allometry

The field of allometry depends on relations between variables, and it is the strength and nature of such relations that is investigated in an allometric study. Why there may be such relations, what such relations should look like in view of biological knowledge, and how they may be uncovered will be reviewed in the succeeding paragraphs.

4.1.2.1 Functional relations

When two variables (X_1 and X_2) are measured on a series of objects, and these objects are plotted according to these measurements, it may be found that there is some correlation between the variables; that is, the values of these measurements may be interdependent (Sokal and Rohlf, 1995). This may be of interest to the investigator, as there may be good biological reasons why there should be such interdependence. If there is such strong correlation that the specimen points lie along a line, there is (more or less) a unique value of X_2 for each value of X_1 – that is, there is a functional relation between these variables (Rice and Strange, 1977). The functional relation is the basis of allometry, be it Huxley's (explicit) model of interrelated measurements (below), or Mosimann's (implicit) model of size-shape associations (§4.1.2.3.1.4). In this investigation, allometry will be defined as relations between measurements (perimeter length and square root of area, or Fourier amplitudes). Any such relations (as they may not exist – see §4.1.2.3.2) within a group will reflect the shape of the sample specimens. Relations describing constant proportion between measurements will indicate constant shape, whereas shape differences will be indicated by relations describing differing proportions. Bivariate relations may be described by a number of functions, both linear and nonlinear (Albrecht et al., 1993). The simplest relation is of the form

$$X_2 = aX_1,$$

where the two variables vary directly (Rice and Strange, 1977) throughout the sample. Implicit in this model is that (hypothetically), when $X_1 = 0$, $X_2 = 0$. If this is not the case, an intercept must be included, that is

$$X_2 = aX_1 + c,\ c \neq 0.$$

The relation between X_2 and X_1 might not be linear. For instance, the relation

$$X_2 = aX_1^k,\ k \neq 1$$

may better describe the spread of points. Also a nonzero intercept may have to be included, that is

$$X_2 = aX_1^k + c.$$

The field of modern allometric research was founded by Huxley (Huxley, 1932; Huxley and Teissier, 1936), who defined allometry in terms of growth of an organ relative to that of the whole body (typically, measurements used were of weight). If an organ increases in size at a rate different to that of the body, this relation is allometric. Huxley's allometric relation is of the form $X_2 = aX_1^k$, where k is called the allometric coefficient, which is related to growth rates and final proportions (Huxley and Teissier, 1936). The allometric equation seeks to relate one measurement to another: in the context of growth, the allometric coefficient represents the ratio of growth rates of X_1 and X_2 (Shea, 1985a), but in a static allometric context (for example measurements made on adults), no inferences regarding growth may be made (Leamy and Bradley, 1982; Shea, 1981, 1985a). The allometric coefficient therefore reflects the degree to which one measure changes (in a nonlinear fashion if $k \neq 1$) in relation to another. Positive allometry ($k > 1$) occurs when the rate of increase of size of the part represented by the dependent variable exceeds that of the independent, and vice versa for negative allometry ($k < 1$) (Huxley and Teissier, 1936). In the case of a sample where variables are kept proportional over a size range (i.e. the objects are geometrically similar, $k = 1$), the relationship is isometric (Jungers et al., 1995; Rayner, 1985; Sprent, 1972) (but see below).

A perusal of the relevant literature shows that the principal objective in many allometric studies is to identify k, the allometric exponent (Alexander, 1977; Bennett, 1996; Biewener, 1983; McMahon, 1975; Pollock and Shadwick, 1994; Strasser, 1992). Indeed, it appears little regard is given to the value of a, and Huxley's classic model did not even allow for an intercept (c). That is not to say that Huxley ignored the possibility of a nonzero intercept, but he did consider that intercept values tend to be small when allometry is marked (Huxley, 1932); furthermore, he objected to the use of a constant as a means to simply improve the fit of the regression line, and could justify its use only subject to adequate physiological explanation (Huxley, 1932). Measuring relations in logarithmic space is not the only means of

determining relations between variables, as data may be left in the untransformed state, using the linear model $X_2 = aX_1 + c$ (Godfrey et al., 1991; Scammon and Calkins, 1929; Smith, 1980; Thompson, 1946). What, then, is the significance of each of these models?

Linear models allow for a constant increment in X_2 for a given increment in X_1. For the model $X_2 = aX_1$, all specimens show geometric similarity, at least as shown by the two variables (Jungers et al., 1995; Ranta et al., 1994). The constant of proportionality, a (Rice and Strange, 1977), represents the slope of the linear relation, and defines the shape of the specimens, as $a = X_2/X_1$ (Jungers et al., 1995). For example, if X_2 represents breadth and X_1 represents depth and $a = 1$, the specimens would resemble squares, but if $a = 5$ they would resemble broad rectangles. If an intercept must be included ($X_2 = aX_1 + c$), a represents the change in X_2 for a given change in X_1, but the specimens cannot be geometrically similar (Ranta et al., 1994), as X_2/X_1 will not equal a, but $a + c/X_1$, which will vary with X_1 and therefore will not be a constant proportion. Despite this, the relation still reflects a constant relative increment in variables. In nonlinear models the value of k is seen as critical in allometric studies, especially if X_1 and X_2 can be predicted, on biological grounds, to increase at different rates across the population (see below). In the model $X_2 = aX_1^k$ geometric similarity is indicated when $k = 1$, but not otherwise (Jungers et al., 1995). In the model allowing a nonzero intercept ($X_2 = aX_1^k + c$) geometric similarity is not indicated even if $k = 1$ (Godfrey et al., 1991).

This last point is at odds with the notion that isometry ($k = 1$) reflects geometric similarity; Gould (1971) drew this parallel with the implicit assumption of a zero intercept. The importance of the intercept is as explained as follows: Huxley's (1932) nonlinear relation may be written in linear form (for linear regression analysis – see §4.1.2.3.1) by transforming the original variables to their logarithms (Sprent, 1972), so that

$$\log X_2 = \log\left(aX_1^k\right) = k \log aX_1 = \log a + k \log X_1 .$$

Regression may proceed by ignoring the log a term and estimating k, as omitting the intercept does not interfere with regression calculations (Lindley, 1947). However, if the original relation includes a nonzero intercept, the logarithmic form, i.e.

$$\log X_2 = \log\left(aX_1^k + c\right),$$

does not simplify, and analysis is not straightforward. Figure 4.3 shows the result of a simulation study, where 20 data points were derived using an arbitrary choice for X_1 as an argument for a power function with (X_2') and without (X_2) a nonzero intercept. Major axis regression of ln-transformed data was performed on both data sets (see §4.1.2.3.1.2), and slopes were calculated. It can be seen that the slope of the regression of X_2 on X_1 correctly estimated the allometric coefficient (0.67), but the slope of the regression of X_2' on X_1 was a substantial underestimate (0.39). Thus, a nonzero intercept confounds estimation of the allometric coefficient.

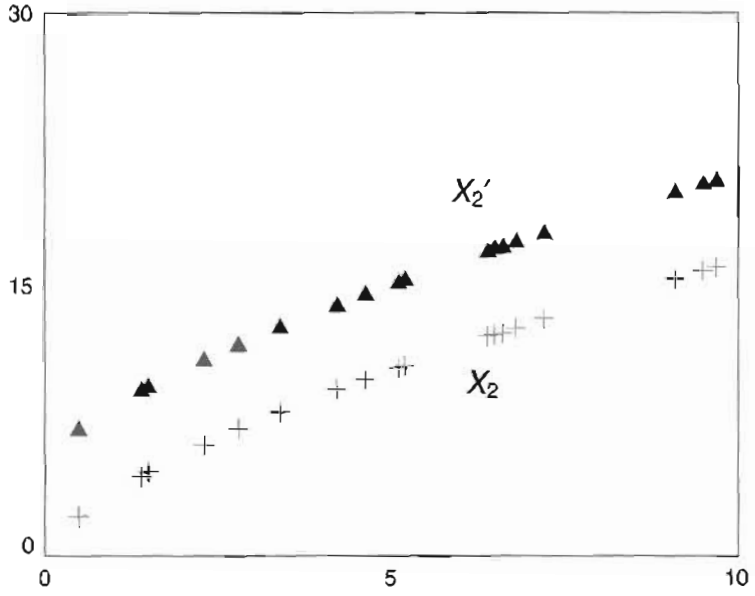

$$X_2' = 3.5X_1^{0.67} + 4.7 \qquad X_2 = 3.5X_1^{0.67}$$

$$a_1 = \frac{0.3656}{0.9308} = 0.39 \qquad a_2 = \frac{0.5566}{0.8308} = 0.67$$

Figure 4.3. Diagram showing the graphs of functions X_2 and X_2' (above) and major axis regressions on these functions (below), illustrating the confounding factor of a nonzero intercept

4.1.2.2 Biological scaling

For various reasons one may expect to see functional relations between morphometric variables – should such relations be expected to be linear or nonlinear? There are many reasons why such a relation may be nonlinear. Nonaquatic animals face a potential problem

when faced with increasing overall size (Biewener, 1990; Jolicoeur, 1963a). An animal's body weight is proportional to its volume (a cubic dimension, X^3), and the ability to withstand the force that the weight produces is dependent on the cross-sectional area of its limb bones (a squared dimension, X^2). Maintaining dimensions across size ranges and keeping function constant should lead to an increase in stress (force per unit area) – therefore stress should increase proportional to $X^{3/2}$. For stress to be dependent on body weight should mean that heavier animals operate with dangerously high stresses, and lighter animals operate with uneconomically low stresses, due to too little and too much bone, respectively (Biewener, 1982). The material properties of bone tissue could be altered to withstand greater stresses (Currey, 1977), although Biewener (1982) found these properties to not vary. For bones from animals of different sizes to experience similar stresses (see below), an increase in body weight would be accompanied by a faster increase in bone diameter (related to area) than for bone length. Therefore, different-sized individuals should show a change in bone shape to keep stresses constant (Galileo Gailei, 1638; Jolicoeur, 1963a; Sprent, 1972). Accordingly, linear dimensions should scale greater than the cube root of body weight (W) (or proportional to $W^{>0.33}$), and areas proportional to $W^{>0.67}$ (Biewener, 1982). This is the basis of McMahon's (1973) theory of elastic similarity: that is, long bones should become stouter (greater width/length ratio) with increased body weight. An investigator may predict such a relation, which is usually grounded in terms of preservation of function, or functional equivalence (Fleagle, 1985; Gould, 1975). It may be calculated that over a size range, within a population, for functional characteristics to remain more or less identical, geometric similarity in a structure would be biomechanically inappropriate. McMahon (1973, 1975) cited evidence from primate and ungulate limbs to support his theory. It must be noted here that elastic similarity is indicated by a functional relation that shows (1) lack of geometric similarity, and (2) a nonconstant slope (which depends on X).

Although Alexander (1977) found that limb bones of Bovidae tend to scale with elastic similarity, Alexander and associates' (1979) data from 37 species with a body weight range of 2.9g to 2.5t, and Biewener's (1983) data from 32 species (20g to 3.5t) did not support McMahon's theory. These data appeared to support the theory of geometric similarity, by which bone width/length is preserved over a range of body weights. In other words, the bones of different individuals can be made to appear the same if all linear dimensions of these bones are multiplied by a scaling factor (Alexander, 1985a). Such scaling implies a relation with a constant slope (which does not depend on X). Thus, while ungulates showed elastic similarity, more general data showed geometric similarity.

The theory of elastic similarity was derived to explain the observations that maximal functional limb bone stresses and strains tend to be independent of body weight, and moreover tend to be remarkably similar over diverse size ranges (Biewener, 1983; Lanyon, 1996; Rubin and Lanyon, 1984). This constancy of maximal strain has been termed 'dynamic strain similarity' (Rubin and Lanyon, 1984). All else being equal, geometric similarity should result in bone stresses increasing with increasing body weight (Biewener, 1983; Currey, 1977), as force should outstrip cross-sectional area. There are two main reasons why dynamic strain similarity exists in the absence of elastic similarity. Firstly, focusing on cross-sectional area ignores the contribution of cross-sectional shape – that is, second moment of area (Ruff and Hayes, 1983a). For example, in the femoral necks of a series of anthropoid primates, second moment of area (cortical bone only) scaled with positive allometry with respect to body weight, whereas cortical area scaled isometrically (Rafferty, 1998). This is probably site- and taxon-specific, as Demes and associates (1991) found that cortical area and second moment of area of the femoral midshaft in a series of indriid primates scaled isometrically with respect to body weight. Secondly, mechanisms to reduce the forces that bones of larger animals should otherwise experience also reduce stresses; as bending forces create high stresses, reducing bending forces should be an effective strategy (Biewener, 1983). These mechanisms appear to be both mechanical (structural) and functional. As an example of the former, bone curvature may be altered to decrease bending strains (Biewener, 1983) (but see §2.1.2.6). Functional mechanisms include increasing duty factor (time during which the foot is grounded in gait, in order to reduce peak force), as well as aligning the limb with the ground reaction force vector (limb more extended) to increase axial loading and decrease the bending moment (Alexander, 1977; Biewener, 1983; Polk, 2002). To illustrate the importance of functional modifications, Jungers and Burr (1994) measured the bending strength of primate femora (midshaft), which was derived from second moment of area as well as the length of the bone, and found negative allometry with respect to body weight. Consequently, second moment of area was not sufficient to counter the increased bending stress otherwise induced by increased bone length. Jungers and Burr (1994) concluded that functional modifications (extended limbs, for example) must countervail this relative decrease in strength.

Body size can thus influence function (Biewener, 1990; Demes and Günther, 1989; Lindstedt and Calder, 1981), such that smaller animals may experience greater accelerations than larger animals (Biewener, 1982) (cf. §2.1.4.2). For example, leaping tends to be found in smaller primates, while an activity such as suspension is more likely to be performed by larger primates (Fleagle, 1985). Fleagle (1985) suggested a practical reason for this: a smaller

animal will exert less force on a support (with only a limited resilience), and a larger animal will fall more heavily than a smaller one. This may also be explained in terms of scaling of muscle force: muscle force (proportional to muscle cross-sectional area), is used to propel body weight (proportional to volume), so muscle force should be expected to scale proportional to $W^{0.67}$ in geometrically similar animals (Alexander, 1985b; Demes and Günther, 1989). Therefore, geometrically similar animals of greater body weight would be expected to move more slowly (Demes and Günther, 1989) (§2.1.4.2). Alexander (1985b) found muscle force to scale approximately thus across diverse body weight ranges. Günther et al. (1991) found greater ground reaction forces, relative to body weight, in smaller primates compared with larger primates during jumping; this was thought to be related to greater acceleration of the smaller animals. However, it appears that muscles are not wholly constrained by geometric similarity: hindlimb muscle cross-sectional area has been found to scale with positive allometry ($\propto W^{>0.67}$) in quadrupedal mammals (Alexander et al., 1981; Pollock and Shadwick, 1994). In addition, Biewener (1983, 1989, 1990) introduced the concept of effective mechanical advantage, that being the ratio of moments of extensor muscles and ground reaction forces. He found that effective mechanical advantage in the hindlimbs of several species of quadrupedal mammals scaled with positive allometry (Biewener, 1990). This was found to be due to both an increase in extensor moment and a decrease in ground reaction moment: muscle moment arms scaled with positive allometry (proportional to $W^{0.43}$, versus $W^{0.33}$ for geometric similarity), as did ground reaction moments (proportional to $W^{0.26}$, versus $W^{0.43}/W^{0.33}$, or $W^{0.10}$ for geometric similarity of joint position). As effective mechanical advantage increases with increasing body size, forces on bones due to muscle contractions should therefore decrease relative to body weight (Biewener, 1983, 1989). These results mirror those of Demes and Günther (1989), who found an increase in effective mechanical advantage at the knee joint with increasing body weight for prosimian primates. Interestingly, they treated the patella as a spacer, not a balance-beam. Thus, effective mechanical advantage scaled with positive allometry not only due to adopting a more extended limb position (Biewener, 1990), but also by increasing the muscle moment arm (i.e. distance from muscle to centre of joint).

Limbs of larger individuals need not always function in a more extended posture than those of smaller animals; limbs may be held in more flexed postures if cross-sectional properties are adapted to cope with the increased forces (Polk, 2002). As seen in §2.1.4.2, arboreal primates need to flex their limbs to decrease their centre of gravity and therefore aid stability. Such limb flexion would in theory lead to higher bending stresses and higher ground (or substrate) reaction force moments. Arboreal primates appear to overcome the potential problems of

instability-increased forces by adopting a compliant gait (Schmitt, 1999). A compliant gait features spring-like flexion of the limbs on contact with the substrate, which serves to increase the time over which body weight acts on the limb, and thus decreases force (Schmitt, 1999). Schmitt (1999) also found that arboreal primates make ground reaction force direction approximate that of the flexed limb by decreasing the vertical component of force while maintaining the horizontal component of force, making the vector more oblique and more in line with the limb.

Scaling relations between articular surface dimensions have received much less attention in the literature than those of whole bones, but the story of articular scaling reflects that for long bones; as a sizeable portion of the patellar outline is articular surface, it is relevant to consider scaling effects on articular morphology. It is again reasonable to expect that over size ranges the maximal stresses or strains experienced by articular cartilage would be kept somewhat constant (Swartz, 1989). If forces transmitted by articular surfaces are proportional to body weight, then it may be expected that articular surface area scales proportional to $W^{1.0}$ (as opposed to $W^{0.67}$ for geometric similarity), to maintain constant stresses over diverse size ranges (Godfrey et al., 1991; Jungers, 1988; Swartz, 1989). Alternatively, geometric similarity and constant joint stresses could be maintained if joint *forces* scaled proportional to $W^{0.67}$. Indeed, joint forces have been found to be roughly proportional to $W^{0.67}$ over a range of sizes (Alexander, 1980, 1981), and geometric similarity of articular surfaces has been inferred (Godfrey et al., 1991).

Thus, functional factors may again confound the expectation of elastic similarity, and these may or may not be related to body size. Presumably, maximal articular forces may be modified by avoiding postures and activities that would otherwise result in dangerously high stresses, in much the same way that heavier animals reduce diaphyseal bending stresses by aligning their limbs to the lines of force. Morphological differences may also exist due to differences in manoeuvrability and posture which may directly relate to body size, but which are separate from articular surface scaling (Godfrey et al., 1991): articular surface area may be increased to allow for greater range of movement (Godfrey et al., 1991; Swartz, 1989), and also to cope with the highly unusual forces of a novel function. An example of the latter is the increased size of hind limb articular surfaces in humans relative to nonhuman primates: this increased joint size is not related solely to body size, but also the unique forces peculiar to bipedal gait (Jungers, 1988; Ruff, 1988). Therefore, a scaling relation along a size range (as concluded by Swartz (1989)) may in fact be indirectly due to size-related and/or non-size-related functional differences (Godfrey et al., 1991).

Thus, organisms need not maintain precise functional characteristics along a range of sizes. As Fleagle (1985) has summarized, animals may adapt to scaling imposed on them by (1) deviating from geometric similarity, or (2) adopting different functions at different sizes to make best use of this scaling. Given this flexibility, it is difficult to argue against linear relations, where the slope of the relation is constant across a size range. However, it is also difficult to argue in favour of an a priori expectation of a linear relation. Indeed, what may prompt the prediction of the specific linear relation of geometric similarity? Gould (1971), in light of pressures biased against preservation of shape, concluded that "geometric similarity is a problem, not an expectation" (p129). It is therefore difficult to predict the relation of bone dimensions with a change in body size (Jungers and Burr, 1994), as individuals both within and among taxa have more means to constrain bone stresses at their disposal than to merely make bones thicker.

Very few data were found regarding patellar allometry. Work carried out by Jungers (1990, personal communication), showed that nonhuman primate patellar articular breadth scaled with negative allometry with respect to body weight ($k = 0.275$). When grouped with humans, the relation appeared to be close to geometric similarity ($k = 0.322$). Two interpretations are possible here. Firstly, a decrease in patellar articular breadth relative to body weight in nonhuman primates presumably reflects relatively decreased patellar articular surface area. Therefore, not only was there not the positive articular allometry predicted by Swartz (1989), there also was not the isometry as seen by Godfrey and coworkers (1991). Given that constancy of function and functional modification is the basis of positive allometry and isometry, respectively, it is possible that functional modification has 'overcorrected' in terms of patellar articular breadth. That is, functional modifications might not exist along a continuum; rather the choices an animal has to decrease forces on its skeleton may be more discrete. Thus, larger animals might have had the choice of adopting Function *A*, which overstressed its bones, or Function *B*, which understressed them. Secondly, the breadth of a convex surface like the articular surface of the patella might not reflect articular surface area at all, especially if the convexity of the articular surface (patellar crest) is marked, such that the importance of the breadth would then be unclear. Allometric relations in primate patellae were also investigated by Ward et al. (1995), who primarily compared allometric coefficients and intercepts of patellar measurements monkeys and great apes. Differences in allometric coefficients were not statistically significant, but they did find significant differences in intercepts, allowing them to conclude that monkey patellae had greater length and depth than those of great apes. Furthermore, human specimens were aligned with great ape specimens. Ward and associates (1995) inferred from these results that (1) relatively longer patellae in

monkeys reflected their more prevalent use of running and leaping than larger apes and humans, and (2) that patellar depth was relatively increased as a means of resisting the greater bending forces resulting from increased length.

4.1.2.3 Allometric methods

4.1.2.3.1 bivariate allometry

Efforts to uncover linear relations (or linearized relations as represented by Huxley's (1932) allometric equation), seek to elucidate functional relations (Kendall and Stuart, 1973; Sprent, 1969) whereby two mathematical variables X_1 and X_2 are related via a parameter α such that (Sprent, 1972)

$$X_2 = \alpha X_1 . \qquad (1)$$

Although an additive constant term (α_0) may be included in this equation, it may be omitted if the origin is shifted to the mean of observations (Sprent, 1969); here, α refers to either a or k. The investigator then seeks to identify α from a set of observations. If these (mathematical) variables could be observed without error, solving for α would be a mathematical problem (Kendall and Stuart, 1973). However, in practice the 'true' values X_1 and X_2 are not observable due to an element of error, or departure from this true value. The departures inherent in random variables are erroneous in the sense that they prevent the investigator from observing the true variables and their functional relation (Rayner, 1985). Such departures may represent both individual variation and measurement error (Jolicoeur, 1990; Sprent, 1972). Accordingly, α must be derived from the observed variables, subject to error, such that the exercise becomes a statistical one (Kendall and Stuart, 1973).

As X_1 and X_2 cannot be observed, the investigator must estimate α from the random variables ξ_1 and ξ_2, which include error variables δ and ε respectively:

$$\xi_1 = X_1 + \delta$$
$$\xi_2 = X_2 + \varepsilon .$$

Substituting for X_1 and X_2 in equation (1) results in

$$\xi_2 = \alpha\xi_1 - \alpha\delta + \varepsilon .$$

This equation (in random variables) is known as the structural relation, which results from the lack of observability of the functional relation between mathematical variables (Kendall and Stuart, 1973; Sprent, 1969). Therefore, the methods reviewed here estimate the structural, not functional, relation.

In an allometric study, α (a or k) must be estimated from the structural relation using the random variables measured. However, the structural relation does not lend itself to easy computation: in a structural relation, α is unidentifiable, and the investigator must make an assumption regarding error variances (Kendall and Stuart, 1973). Two methods commonly used to estimate the structural relation are the least-squares and major axis methods. These are special cases of the structural relation model, with different assumptions regarding error distributions (Kuhry and Marcus, 1977; Mattfeldt and Mall, 1987; Rayner, 1985; Seim and Sæther, 1983).

4.1.2.3.1.1 Model I (least-squares) regression

Least-squares regression has not uncommonly been used to estimate the structural relation (Biewener, 1983; Jungers, 1984; Wolpoff, 1983), but those researchers have done so in the face of criticism. Least-squares regression is a Model I regression method (Sokal and Rohlf, 1995), which carries with it the assumption that the regressor variable is measured without error (Leamy and Bradley, 1982; Gould, 1966; Sprent, 1972; Steudel, 1982). Therefore, when both variables are subject to error (a more likely situation), least-squares regression slopes are biased (Sokal and Rohlf, 1995; Sprent, 1969), such that the slope is underestimated (Rayner, 1985). Because in this situation this important assumption is not met, least-squares is an asymmetric method, in that the regression of X_2 on X_1 is different to the inverse of that of X_1 on X_2 (Martin and Barbour, 1989). It is also often difficult to justify the choice of dependent and independent variables (Hens et al., 1998). In theory, least squares should only be used if the independent variable is controlled (Mattfeldt and Mall, 1987; Rayner, 1985; Williams, 1959) (but see §4.1.2.3.1.3).

4.1.2.3.1.2 Model II (major axis) regression

Choice of a Model II method, where both variables show random variation, depends on the aims of the investigator and the nature of the data (Sokal and Rohlf, 1995); one Model II method is major axis regression. In comparison to the least-squares method, the major axis method carries the assumption that the error variance ratio equals unity (Jolicoeur, 1990). This is often sensible when the variables are measured in the same units (Kimura, 1992; Sprent and Dolby, 1980), especially after log-transformation (Kuhry and Marcus, 1977; Martin and Barbour, 1989).

The major axis method is a special case of principal component analysis, where $p = 2$ (Kuhry and Marcus, 1977; Sokal and Rohlf, 1995). The slope of the structural relation (α) thus estimated is equal to the tangent of the angle that the first principal component makes with the x-axis, (Sprent and Dolby, 1980), or the ratio of principal component coefficients, i.e.

$$\alpha = \frac{b_{2,1}}{b_{1,1}},$$

(Jolicoeur and Mosimann, 1968; Kuhry and Marcus, 1977). As PCA shifts the origin to the mean of observations (Marcus, 1990), intercept information is lost, but can be regained (Legendre and Legendre, 1998) (see page 153).

4.1.2.3.1.3 comparison of methods

Rayner (1985) has criticized the use of the major axis method due to its lack of scale-invariance, as a different scale between variables would alter the estimate of the functional relation. However, the criticisms regarding the scale-invariance of the major axis method are not considered to be valid when the variables are measured in the same units, especially when they are log-transformed (Jolicoeur, 1990; Jolicoeur and Heusner, 1971; Kuhry and Marcus, 1977; Sokal and Rohlf, 1995).

In practice, the behaviour of these regression slopes in relation to intervariable correlation may make the choice of regression method academic. As the correlation coefficient approaches unity, the least-squares and major axis methods converge (Aiello, 1981, 1992; Leamy and Bradley, 1982; Seim and Sæther, 1983). Therefore, a decision to strongly favour

one method over another is questionable, as on one hand the three methods converge with a highly correlated data set, and on the other, a low correlation makes use of any method to estimate a functional relation somewhat meaningless (Jungers, 1984).

4.1.2.3.1.4 Mosimann's method

Mosimann (Mosimann, 1970; Mosimann and James, 1979) proposed an allometric method that was based on the concept of an association of shape with size. Allometry was then defined as statistical dependence of a shape vector on a size variable, with isometry being the lack of such dependence (Mosimann, 1970; Mosimann and James, 1979). This method requires an explicit definition of size prior to analysis (Mosimann, 1970), and as such did not come under initial consideration for use in this investigation. However, if two variables (X_1, X_2) are linearly related, the shape variable X_2/X_1 and the size variable X_1 can only be uncorrelated if the linear relation includes a zero intercept: i.e. isometry is indicated by a zero intercept (Allison et al., 1995).

4.1.2.3.2 multivariate allometry

Allometry has hitherto been described here in terms of relations between two measured variables; allometry may also be investigated in the case of $p > 2$ variables. The multivariate extrapolation of the major axis method, principal component analysis, still allows one to measure relations between variables without explicitly defining size. The principal component approach to allometry is essentially an extension of the classic bivariate method (Jolicoeur, 1963a,b; Jolicoeur and Mosimann, 1960; Klingenberg, 1996), and typically uses the general (usually first) eigenvector as a measure of size (and size-related shape) (Mosimann and Malley, 1979). In this approach, the first principal component of the covariance matrix of log-transformed variables is used as an allometric equation (Flessa and Bray, 1977; Jolicoeur, 1963b), with relative differences in coefficients of the first component indicating proportional differences in measurements (Shea, 1985a). The equation, relating any two variables X_i and X_j, is of the form

$$\log X_i = \alpha \log X_j \text{ or } X_i = X_j^{\alpha},$$

where α equals the ratio $b_{i,1}/b_{j,1}$, as before (Jolicoeur, 1963b).

For example, in the context of a growth study, (Jolicoeur, 1963a,b) developed a method for testing for isometry between individuals. His definition of isometry stated that among individuals, through growth, "relative growth rates ... would then be equal" (Jolicoeur, 1963a p16). In other words, the component that is being called size has equal values for all variables: the individuals are increasing their dimensions at a uniform rate. Isometry is then indicated by the coefficients of PC1 taking the values of $p^{-1/2}$ (Jolicoeur, 1963a). This approach ignores the influence of a nonzero intercept, as PCA shifts the origin to the mean of observations. Therefore, the above expression should also allow for an intercept.

As outlined in §2.2.2.1.3, eigenvectors with close-to-zero eigenvalues reflect combinations of variables within a population that vary little (if at all). One may therefore turn to the principal component with a close-to-zero eigenvalue in the multivariate case to uncover linear relations in the data (Jolliffe, 1986; Rencher, 1995). A functional relation between several variables X_i satisfies at least one relation of the form

$$\sum b_i X_i = c,$$

where c is a constant (i.e. it doesn't vary) (Sprent, 1969). Such a relation is satisfied by the principal component associated with a (close-to) zero eigenvalue. This equation may be rewritten as

$$X_p = \alpha_1 X_1 + \alpha_2 X_2 + \ldots + \alpha_{p-1} X_{p-1} + c,$$

where the selection of X_p as the variable expressed as a weighted sum of the others is arbitrary, and any such X could be chosen (Sprent, 1969). (In this case, α_i is calculated as the ratio b_i/b_p.) Having made that choice, one variable can be described in terms of a weighted combination of other variables, which when the variables have previously been log-transformed, may then be written in the antilogarithmic form

$$X_p = X_1^{\alpha_1} + X_2^{\alpha_2} + \ldots X_{p-1}^{\alpha_{p-1}} + c$$

which is a multivariate form of Huxley's original allometric formula, with the addition of a constant intercept. This is different to equations relating two variables at a time, but not all the principal component coefficients need have a substantial weighting for any relation.

In the multivariate case, more than one linear relation may be found. In a linearly independent data set, the data points lie in p-dimensional hyperspace. One linear relation defines a $p-1$ hyperplane, $p-1$ relations define a straight line (Sprent, 1969). More generally, q relations specify a hyperplane of $p-q$ dimensions (Sprent, 1968). Thus, the condition of simple allometry (i.e. a straight line) is represented by $q = p-1$ (Sprent, 1968). This is the case in major axis regression – the second eigenvalue, if (close-to) zero, defines a linear distribution of data points.

Performing a PCA (in two or more dimensions) does not automatically reveal simple allometry, as simple allometry need not exist (Aiello, 1981). A general component only reveals the axis on which all variables increase or decrease together, and possibly the axis of greatest variance. The ability of the PCA approach to indicate simple allometry depends on the correlations between measurements (Leamy and Bradley, 1982). If the data scatter is too great, there may be no point in attempting to fit a relationship (Sprent, 1972; Sprent and Dolby, 1980; Wood, 1985).

In theory, if simple allometry does exist (i.e. data scatter is explained by a single weighted combination of variables), and is uncovered by PCA, then the first component should account for practically all variance (Klingenberg, 1996), that is the covariance matrix should be of rank one (Hopkins, 1966; Sprent, 1972). In practice, under the condition of simple allometry there may be fewer than $p-1$ zero eigenvalues; for simple allometry to exist, these $p-1$ eigenvalues should not be significantly different (Hopkins, 1966), and small enough to still reasonably allow for a simple linear relation (Sprent, 1972). In such a case, variation in all measured variables would be overwhelmingly due to size variation – size variation alone in the case of isometry, or in addition to size-related shape for allometry. Therefore, in a PCA approach, if eigenvalues other than the first are not zero (or close to), this implies a greater deal of data scatter orthogonal to the 'line of allometry', and thus should invalidate the hypothesis of simple allometry (Sprent, 1972). The investigator should first determine whether any dimension-reduction can be justified, and if so, whether the data can be represented as occurring on a line, or in a plane, etc. (Klingenberg, 1996; Sprent, 1972). However, the presence of more than one linear relation may well not be interpretable, as multiple eigenvalues with a value of close to zero would indicate sphericity.

4.1.3 Summary

Unless one is highly restrictive (and fortunate) in selecting specimens for morphometric investigation, at least some morphometric variation will be attributable to the fact that some individuals are bigger than others, and the biological importance of such a size difference may be greatly overshadowed by its effect on the pattern of variation of morphometric variables. It was seen in the previous chapter that size of specimens played a substantial role in determining the distribution of specimens in ordination, and given the dominance of size, other interesting features of data structure may have been overlooked. It is reasonable in this case to seek methods of adjusting the raw data, such that this potentially great influence is not brought to bear, or at least is minimized, so the remaining variation may therefore be deemed to be due to shape differences. As shape is likely to be reflective of the mechanical circumstances of the specimen, this is of great interest, and warrants some effort in elucidation. Some methods have been presented in the literature, each having different qualities. Ideally, for this investigation a method that can identify specimens with identical proportions as the same, and preferably one that does not hinge on a definition of size is desired; the general method used in this investigation was that of Mosimann (1970) and Mosimann and Malley (1979). Although Mosimann defined shape as a ratio with (a choice of) size as the denominator, it can be seen that this choice does not affect the relative proportions of variables, which is the definition of shape in this study.

Despite the potential for increasing stresses or strains on the bones of larger individuals, it appears that a number of options are available to larger individuals to reduce the effects of functional forces. These options include (functionally) avoiding inappropriate activities to decrease forces, and also morphologically adapting to greater body weight-related forces. Exactly how larger individuals will reduce stresses and strains is difficult to predict. A collection of dry bones tells one little directly about body size, and nothing about functional or mechanical modifications. However, the shape of the bones is likely to reflect mechanical demands, and as such these bones may differ in shape according to the size of the individual. The question then arises, *how do shape and size vary?* The relation between size and shape is known as allometry; allometry may be more broadly defined as interdependence between variables. A more general question, then, is *how do morphometric variables vary*? Allometry is most meaningful when such interdependence explains the bulk of the morphological variation, such that relations exist between variables where one variable can be expressed in terms of another. If the relation is such that all specimens are merely enlarged or reduced copies of each other, the relation is isometric, and indicates geometric similarity. If a relation

is identified, but reflects shape differences, the relation is allometric, and shape variation is considered due to size differences. Relations may be nonlinear, where the dependent variable is expressed as a power (exponent $\neq 1$) of the independent variable, or linear (exponent = 1). Nonlinear relations must reflect allometry, and the slope of the relation varies with the independent variable. For geometric similarity, the relation must be linear (if variables are measured in the same dimension), but must also pass through the point (0, 0). The presence of a nonzero intercept indicates an allometric relation, but one where the slope of the relation is constant and doesn't vary with the independent variable (the choice of independent variable is arbitrary). Where variables are of different dimension (for example area and volume), and where there are biological reasons for interdependence, a nonlinear relation may be predicted. However, as animals are capable of structural and functional flexibility, relations may result which diverge markedly with those predicted. Such divergence may then become the target of the investigation.

4.2 Aims and Hypotheses

Aims 1 and 2 of this chapter related to size-adjustment; the rationale for these aims was that, if overall size of specimens could be ignored, then patterns of variation of shape could be investigated, with the notion that shape variables reflect the mechanical properties of a bone more than overall size.

Aim 1: to transform data vectors (both conventional and Fourier data) to unit length, and examine the structure of the transformed data using principal component analysis in view of results using raw (nonnormalized) data

Aim 2: to perform UPGMA cluster analyses based on size-excluded similarities by using cosines of angles between specimens and also between genera in view of results using raw data; this required expanding the cluster analyses of Chapter 3 (using average taxonomic distance) to include generalized distance between means of genera

Aim 3 related to allometry, i.e. could patterns of covariation between variables be uncovered, which would reflect the simultaneous change of variables in the sample with a change in overall size?

Aim 3: to investigate the presence and nature of structural relations between variables (between conventional variables as well as between Fourier variables), within each data set using the method of major axis regression/principal component analysis

As the major axis regressions using conventional data were supplemented by calculation of confidence limits for slopes and intercepts, it was necessary to investigate the normality of the data used in these regressions; this necessitated

Aim 4: to investigate the normality of the conventional variables by calculating Kolmogorov-Smirnov *Z*-statistics by comparing distributions against the normal distribution

and

Hypothesis 1: that $\boldsymbol{A}$ and $\boldsymbol{P}$ were distributed normally (H_0: that distributions were normal)

To investigate allometry using the last eigenvector from principal component analysis of Fourier data, it was necessary to state

Aim 5: to determine whether ninth and tenth eigenvalues were distinct, to allow for reliable interpretation of eigenvector coefficients, by calculating sphericity statistics for these two eigenvalues

and

Hypothesis 1: that ninth and tenth eigenvalues from principal component analysis of Fourier data were distinct ($H_0 : l_9 = l_{10}$)

4.3 Materials and Methods

4.3.1 Materials

The outline data were the same as for Chapter 3.

4.3.2 Methods

4.3.2.1 Size-adjustment

Attempts to remove size from the raw measurement data were performed by (a) dividing each measurement vector by its length, and performing principal component analysis ordination as in Chapter 3, and (b) inputting matrices of similarity coefficients (cosines, or rather transformed cosines) into cluster analyses as in Chapter 3.

4.3.2.1.1 principal component analysis

Data vectors were standardized for size by dividing each row (i.e. measurement vector of each specimen) of each data matrix by the square root of the sum of squared values for that row. This was performed using the *DIVSY2* option in Transf in NTSYSpc, and rendered each specimen data vector to unit length (i.e. vectors were normalized). The effect of this normalization can more readily be seen in two dimensions: forcing the vectors to have unit length, that is

$$\sqrt{X_1^2 + X_2^2} = 1 \text{, or just } X_1^2 + X_2^2 = 1,$$

removes one degree of freedom – that is, once one variable is defined, the other is defined also. The graph of these points then must be aligned on the circumference of a unit circle defined by $X_1^2 + X_2^2 = 1$. The distribution of points along the circumference will then be a reflection of shape variation. For proportionally identical forms with different size (i.e. different points along the same ray), normalization will give these points identical placement. Although points will be distributed in two dimensions on a curved line, if the spread of points is not substantial a straight line is approximated. A similar situation exists with $p > 2$ variables, except that points will be arranged on the surface of a sphere ($p = 3$) or ($p - 1$)-

dimensional hypersphere. Principal component analysis is not appropriate for curvilinear data (Pimentel, 1992), but the assumption was made that the spread of points was sufficiently compact so that the data were linear. For bivariate data, PCA of normalized data gave the direction of the resultant arc. If PC1 of the raw (nonnormalized) data lay in the direction of geometric similarity (i.e. passed through the origin), PC2 of raw data would correspond with PC1 of the normalized data.

Principal component analysis of these normalized data was performed as for Chapter 3. It was intended that only raw data would be used for Fourier variables due to the problems of variance encountered in Chapter 3. Results of these PCAs were then compared to those using raw data: angles between PC1 and PC2 of raw data, and PC1 of normalized data were calculated from the cosines of these angles, which were calculated as in §3.3.2.4.

4.3.2.1.2 cluster analysis

Dissimilarity matrices were constructed from raw data matrices using the SimInt module of NTSYSpc. All specimens were included initially. Matrices were constructed based on interspecimen average taxonomic distance (ATD) and cosines. Cosines were calculated using the method used in §3.3.2.4. Cosines were changed, for ease of comparison with distances, using the Transf module of NTSYSpc, to $(1 - \cos)_S$ (by negating all coefficients, then adding 1, i.e. to dissimilarities). Coefficients were also computed based on genera: intergenus generalized distance and cosines (transformed to $(1 - \cos)_G$) based on variable averages per genus. Generalized distances were computed using NTSYSpc by constructing a pooled variance covariance matrix (PoolVCV), and generating a matrix of generalized distances (CVA).

UPGMA cluster analyses were performed using the SAHN module of NTSYSpc as in Chapter 3; cophenetic correlations were computed using the Coph module as in Chapter 3. As in Chapter 3, the outline data from the two *Elephas* specimens were included for repeat analysis in the females distal data to give perspective.

4.3.2.2 Allometry

The first step in the investigation of allometry was to establish whether the data satisfied the criteria of the functional relation $X_2 = aX_1$ (here $\boldsymbol{A} = a\boldsymbol{P}$). This meant seeking evidence of a relation (measured by variance residual to the purported relation), and whether there was a zero intercept. If so, then isometry was indicated, and the slope a reflected the ratio of variables (or shape). If not, it may have been that an allometric model either of the form $\boldsymbol{A} = a\boldsymbol{P} + c$ or $\boldsymbol{A} = a\boldsymbol{P}^k + c$ was appropriate, again depending on evidence of a relation. It might also have been that the data did not follow a relation (either of the above types, or at all, as the methods of allometry need not uncover evidence of richer biological relations), which would have been indicated by an unacceptable amount of variance residual to the posited relation.

The specific methods to meet these objectives were carried out as follows. Major axis regression was performed on the covariance matrices from the raw data sets (principal component analysis for Fourier amplitudes) as in Chapter 3. For a relation to be indicated, the first eigenvalue must have accounted for the bulk of total variance. This was a subjective decision, but the first eigenvalue must have equalled at least 90% for the Fourier data, and even higher (approximating 100%) for the bivariate conventional data (there being only two eigenvalues). The product-moment correlation coefficient was also calculated for conventional data, and functional relations were indicated if this closely approximated 1.00 (≥ 0.90). For the conventional data, the slope a of the (linear) relation was given by the ratio $b_{2\,1}/b_{1\,1}$. The intercept c was given by the following (Legendre and Legendre, 1998):

$$c = \overline{A} - a\overline{P}\,.$$

To obtain 95% confidence limits for c (c_1 and c_2), the confidence limits a_1 and a_2 of the slope were first computed (Legendre and Legendre, 1998) using the method of Sokal and Rohlf (1995), which carried the assumption of bivariate normality (Jolicoeur, 1968; Sokal and Rohlf, 1995). Kolmogorov-Smirnov Z-statistics were calculated for these data using SPSS (SPSS Inc, 1989-1999), and distributions were considered significantly different to zero at the two-tailed 5% level. The 95% confidence intervals a_1 and a_2 were calculated as:

$$a_1 = \tan\left(\tan^{-1} a - \frac{1}{2}\sin^{-1} 2\sqrt{H}\right) \text{and } a_2 = \tan\left(\tan^{-1} a + \frac{1}{2}\sin^{-1} 2\sqrt{H}\right),$$

where

$$H = \frac{F_{0.05[1,n-2]}}{\left[l_1/l_2 + l_2/l_1 - 2\right](n-2)}.$$

The intercept limits were then computed as follows (Legendre and Legendre, 1998):

$$c_1 = \overline{A} - a_2\overline{P} \text{ and } c_2 = \overline{A} - a_1\overline{P}.$$

For Fourier amplitudes (where $p = 10$), pairwise relations between variables were similarly defined, for example $\boldsymbol{X1} = a_{\boldsymbol{X1},\boldsymbol{Y1}}\boldsymbol{Y1} + c$, where $a_{\boldsymbol{X1},\boldsymbol{Y1}}$ equalled $b_{2\,1}/b_{1\,1}$, and this relation indicated geometric similarity if $c = 0$. Values of c for each relation between arbitrary variables (candidates for investigation were judged according to their coefficients on the first principal component) were calculated as for the conventional data. In the absence of any equations for calculating confidence limits for c in the multivariate case, confidence limits were calculated based on standard error estimates using jackknifed principal component analysis. The jackknife is a method that may reduce bias in the estimation of a statistic, that may be used for a great variety of statistics and enables the estimation of the variance of that statistic (Efron and Gong, 1983; Bissell and Ferguson, 1975). The method for obtaining the jackknifed estimate of slope a was as follows (Sokal and Rohlf, 1995):

- compute $a_{\boldsymbol{X1},\boldsymbol{Y1}}$ as above (hereafter just a)
- for each of n iterations, delete the n^{th} row from the data matrix, repeat PCA and compute a_{-i}
- calculate pseudovalues, ϕ_i as follows

$$\phi_i = n \cdot a - (n-1)a_{-i}$$

- the jackknifed estimate of a is then

$$\hat{a} = \frac{\sum a_i}{n} = \overline{\phi},$$

and the approximate standard error is

$$s_{\hat{a}} = \sqrt{\frac{\sum\left(\phi_i - \bar{\phi}\right)^2}{n(n-1)}}$$

- 95% confidence limits were calculated as follows:

$$a_1 = a - t_{0.05[n-1]}s \text{ and } a_2 = a + t_{0.05[n-1]}s$$

The intercept limits c_1 and c_2 were calculated as above. An assumption implicit in the use of these two methods was that the data had been sampled randomly (Klingenberg, 1996).

Functional relations were also investigated using any eigenvectors associated with a close-to-zero eigenvalue. 'Close-to-zero' was defined ideally as a value that could be rounded to 0.00% of total variance. In order to interpret the corresponding eigenvector, sphericity statistics were calculated (Flury, 1988; Flury and Riedwyl, 1988) to determine whether that eigenvalue and any neighbouring eigenvalues were distinct. To determine the distinctness of two neighbouring eigenvalues, l_{h-1} and l_h, the following sphericity statistic was calculated:

$$S(l_{h-1}, l_h) = 2n \log \frac{l_{h-1} + l}{2\sqrt{l_{h-1} l_h}},$$

which was distributed as χ^2 on two degrees of freedom, and carried the assumption of large n.

To determine whether nonlinear relations were appropriate, the above procedures were repeated using the logarithmic data from Chapter 3. If the results using these data (correlation coefficients, eigenvalue proportions) suggested a stronger functional relation than for the nontransformed data, then major axis regression/principal component analysis results were further investigated. Here, the relation model was $\ln X_2 = \ln a + k \log X_1$, or by taking antilogarithms, $X_2 = aX_1^k$. However, as it was shown in §3.5.3.1, transforming Fourier data to logarithms resulted in an unacceptable bias in variance to variables that contributed little information to outline form. Therefore, nonlinear relations were not investigated using Fourier data.

4.4 Results

4.4.1 Size-adjustment

4.4.1.1 Principal component analysis

4.4.1.1.1 *Homo*

4.4.1.1.1.1 conventional data

The covariance-correlation matrices are presented in Table A.15(a) (page 343). There were almost perfect negative correlations between variables (–0.9998 to –0.9999). The correlations were only *almost* perfect as this relation was necessarily a nonlinear one; that the correlations were so close to –1.00 supported the decision to treat these data as linear. Variances were unequal, although here the bias was toward ***A*** rather than ***P***. For example, in females distal the variances of ***P*** and ***A*** were 1.7969 and 31.7917, respectively. Transforming these data to their natural logarithms did not ameliorate this bias (Table A.15(a)); indeed, the variances of ***A*** were only further inflated. In females distal again, the variances of ***P*** and ***A*** were 1.8988 and 595.7819, respectively. Therefore, only nontransformed (i.e. not to logarithms) data were used for ordination, despite log-transformed data being used in Chapter 3.

The results of the principal component analyses are presented in Table A.17(a) (page 349) and the results for the first component are reproduced in Table 4.1. First eigenvalues accounted for 100% of total variance (values were rounded to two decimal places), which again supported the assumption of linearity. As expected, the eigenvectors showed a high loading for ***A***. Also, the principal component coefficients were all very similar. These principal components were contrasts between ***P*** and ***A***.

Table 4.1. Principal component 1 – *Homo*, conventional data (normalized)

	females distal	females proximal	males distal	males proximal
	U_1	U_1	U_1	U_1
P	0.2312	0.2344	0.2324	0.2335
A	–0.9729	–0.9721	–0.9726	–0.9724
l	33.5878	22.6718	31.1702	34.2302
%	100.00	100.00	100.00	100.00

The scatterplots of scores on the two principal axes are shown in Figure 4.4 (end of §4.4.1.1). The apparently highly curved distributions were an artefact of scale differences between the axes; from Figure 4.5 the effect of the axis scale differences on the distribution of specimens can be seen. In general, specimens were grouped along a short part of the curve, with several specimens at the fringes. In some cases, specimens were conspicuous by their distance from the main group, although this tended to be on PC2. It was difficult to judge the position of specimen 87 (females proximal), but this was not an outlier.

Table 4.2 shows the angles calculated between the first principal component from the normalized data, and the first (θ_1) and second (θ_2) principal components from the raw data. It can be seen that PC1 (normalized) was (1) almost perpendicular to the direction of PC1 (raw), and (2) almost parallel with PC2 (raw).

Table 4.2. Angles between normalized PC1 and raw PC1 (θ_1) and PC2 (θ_2) – *Homo*, conventional data

	θ_1	θ_2
females distal	88.41	1.88
females proximal	88.91	1.24
males distal	88.96	1.04
males proximal	88.90	0.81

4.4.1.1.1.2 Fourier data

The covariance-correlation matrices of the normalized data are presented in Table A.16(a) (page 345). Inspection of these matrices showed consistently strong negative correlations (–0.9955 to –0.9971) between ***X1*** and ***Y1***; other correlations were less strong. Variances were consistently not uniform across all variables, as those of ***X1***, ***Y1*** and ***Y2*** were consistently greater than the others, some by an order of magnitude.

Eigenvectors and eigenvalues from principal component analysis (covariance matrix) are presented in Table A.18(a) (page 350), and the results for the first two components are reproduced in Table 4.3. First principal components consistently showed that the direction of greatest variance was explained by a contrast between ***X1*** and ***Y1***. However, the first eigenvalues showed that this was not the only substantial pattern of variation, as l_1 accounted for only 57.72% to 66.82% of total variance. Second eigenvalues accounted for 16.79% to

27.74% of total variance; the first two eigenvalues accounted for 83.61% to 87.70% of total variance. The second principal component was dominated more or less by ***Y2***. Interestingly, for females ***Y2*** had a positive weighting (0.9078 and 0.7508 for distal and proximal, respectively), whereas for males the weighting was negative (–0.9182 and –0.8199).

Table 4.3. Principal components 1 and 2 – *Homo*, Fourier data (normalized)

	females distal		females proximal		males distal		males proximal	
	U_1	U_2	U_1	U_2	U_1	U_2	U_1	U_2
X1	0.4318	0.0116	0.4354	0.1191	0.4246	0.0229	0.4323	0.0193
Y1	–0.8775	–0.1206	–0.8118	–0.3205	–0.8804	0.0493	–0.8691	0.0626
X2	–0.0774	0.1114	–0.1323	0.2158	–0.0112	–0.1821	0.0568	–0.1539
Y2	–0.0819	0.9078	–0.2787	0.7508	–0.0172	–0.9182	0.0127	–0.8199
X3	0.1429	–0.0998	0.1702	–0.0369	0.1705	0.0672	0.1875	0.0668
Y3	0.0333	0.2734	–0.0693	0.4576	0.0369	–0.2242	–0.0858	–0.4897
X4	–0.0599	0.2144	–0.1111	0.2134	–0.0478	–0.2063	0.0183	–0.1772
Y4	0.0254	–0.0149	0.0518	–0.0900	0.0648	–0.1004	0.0230	0.1102
X5	0.0626	–0.1234	0.0579	–0.0548	0.0835	0.0985	0.0932	0.0890
Y5	0.0339	–0.0524	0.0638	–0.0733	0.0185	0.0597	0.0477	0.0635
I	0.8767	0.2798	0.6493	0.3121	0.6957	0.1748	0.7649	0.2438
%	66.48	21.22	57.72	27.74	66.82	16.79	65.81	20.98

Scatterplots of principal component scores on first and second components are presented in Figure 4.6 (end of §4.4.1.1). No obvious outliers were found, and specimens were distributed evenly.

Table 4.4 shows for each data group θ_1, the angle between the PC1 (raw) and PC1 (normalized). These angles were varied, coming close to 90°. Table 4.4 also shows angles between PC2 (raw) and PC1 (normalized), θ_2. It can be seen that the directions of these two vectors deviated by minor amounts.

Table 4.4. Angles between normalized PC1 and raw PC1 (θ_1) and PC2 (θ_2) – *Homo*, Fourier data

	θ_1	θ_2
females distal	81.54	8.54
females proximal	81.27	6.55
males distal	85.60	4.49
males proximal	84.99	5.35

4.4.1.1.2 *Cercopithecus*

4.4.1.1.2.1 conventional data

Covariance-correlation matrices are presented in Table A.15(b) (page 343). Again, correlations approximated −1.00 (−0.9998 to −1.0000), which supported the assumption of linearity. Variances of ***A*** were an order of magnitude greater than those of ***P*** using raw data (for example females distal – s^2_P = 1.5780, s^2_A = 23.8737), and transformation to natural logarithms increased this to two orders of magnitude (females distal – s^2_P = 1.6824, s^2_A = 385.5215). Consequently, data were left in their untransformed state for ordination.

Results of the principal component analyses are presented in Table A.17(b) (page 349), with the PC1 results shown in Table 4.5. Again, the first eigenvalue accounted for practically all variance of the normalized data. Eigenvector coefficients were all similar.

Table 4.5. Principal component 1 – *Cercopithecus*, conventional data (normalized)

	females distal	females proximal	males distal	males proximal
	U_1	U_1	U_1	U_1
P	0.2490	0.2565	0.2466	0.2539
A	−0.9685	−0.9666	−0.9691	−0.9672
l	25.4513	12.6632	55.1571	24.5533
%	100.00	100.00	100.00	100.00

The scatterplots of the principal component scores are presented in Figure 4.4. As in the *Homo* data, most specimens were grouped together, with one or two at the periphery, but none was outstanding.

The angles θ_1 and θ_2 were calculated and are presented in Table 4.6. The first principal component (normalized) was almost parallel with PC2 (raw), and perpendicular to PC1 (raw); the deviations from 90° and 0°, respectively, were smaller than those for *Homo*.

Table 4.6. Angles between normalized PC1 and raw PC1 (θ_1) and PC2 (θ_2) – *Cercopithecus*, conventional data

	θ_1	θ_2
females distal	89.66	1.05
females proximal	90.25	*0.00
males distal	90.44	0.57
males proximal	90.14	0.44

*not defined ($\cos^{-1} > 1.00$)

4.4.1.1.2.2 Fourier data

The covariance-correlation matrices for these data are presented in Table A.16(b) (page 346). The pattern of strongly negative correlation between ***X*1** and ***Y*1** was repeated here, values being in the range –0.9983 to –0.9992; all other correlations were less strong. Variances were consistently nonuniform, being substantially larger for ***X*1**, ***Y*1**, and to a lesser extent, ***Y*2**.

Results from the principal component analyses are presented in Table A.18(b) (page 351) and Table 4.7. The first principal component represented a contrast between ***X*1** and ***Y*1** and the proportion of variance explained was in the range 77.07% to 85.24%, with second eigenvalues accounting for 8.06% to 14.50% of total variance. The first two eigenvalues accounted for 89.97% to 91.57% of total variance. The second principal component was dominated to varying extents by ***Y*2**, but here the weightings were negative for females (–0.9210 and –0.8818 for distal and proximal, respectively), but of mixed sign for males (–0.9016 and 0.7276).

Table 4.7. Principal components 1 and 2 – *Cercopithecus*, Fourier data (normalized)

	females distal		females proximal		males distal		males proximal	
	U_1	U_2	U_1	U_2	U_1	U_2	U_1	U_2
X1	0.4984	0.0309	0.5387	0.0827	0.4932	0.0275	0.5316	0.0150
Y1	−0.8378	0.0085	−0.8071	−0.0730	−0.8384	−0.0094	−0.8083	−0.0370
X2	0.0173	−0.2557	0.0027	−0.3188	0.0153	−0.2980	−0.0080	0.3582
Y2	0.0043	−0.9210	0.0972	−0.8818	0.0360	−0.9016	0.0297	0.7276
X3	0.1999	−0.0202	0.1994	−0.0067	0.1861	0.0757	0.2233	−0.2218
Y3	0.0040	0.0327	0.0575	−0.0211	0.0520	−0.1432	0.0492	0.3814
X4	−0.0143	−0.2881	0.0344	−0.3097	−0.0207	−0.2411	−0.0119	0.3108
Y4	0.0332	0.0266	−0.0010	−0.0374	0.0985	−0.0369	−0.0049	−0.0372
X5	0.0901	−0.0098	0.0512	0.0194	0.0672	0.1043	0.1004	−0.2058
Y5	0.0066	−0.0096	0.0462	−0.1026	0.0186	0.0289	0.0225	−0.0756
l	1.0015	0.1884	0.7182	0.1076	1.8985	0.1796	1.2803	0.1706
%	77.07	14.50	79.39	11.89	85.24	8.06	79.39	10.58

Scatterplots of principal component scores on the first two components are presented in Figure 4.6. No outliers were seen, and individuals were distributed evenly.

Table 4.8 shows the angles θ_1 and θ_2. In each group the first principal component of raw data deviated from PC1 (normalized) by nearly 90°. Also, PC2 (raw) deviated from PC1 (normalized) by several degrees only.

Table 4.8. Angles between normalized PC1 and raw PC1 (θ_1) and PC2 (θ_2) – *Cercopithecus*, Fourier data

	θ_1	θ_2
females distal	83.35	7.15
females proximal	94.13	4.05
males distal	93.90	5.01
males proximal	91.39	2.25

4.4.1.1.3 *Colobus*

4.4.1.1.3.1 conventional data

The covariance-correlation matrices are presented in Table A.15(c) (page 344). The correlations approximated −1.00 very closely (−0.9999 to −1.0000), which supported the assumption of linearity of the normalized data. Variances of ***A*** were greater than those of ***P*** by at least an order of magnitude (for example females distal – s^2_P = 0.8913, s^2_A = 12.8645), a bias only amplified by transformation to natural logarithms (females distal – s^2_P = 0.8715, s^2_A = 214.9887). Therefore, nontransformed data were used in this ordination.

The results of the principal component analyses are presented in Table A.17(c) (page 349). The results from the first components are presented in Table 4.9. Results were very similar to those of *Homo* and *Cercopithecus*, in that the first eigenvalues accounted for approximately 100% of total variance, and the eigenvector coefficients were relatively uniform among groups.

Table 4.9. Principal component 1 – *Colobus*, conventional data (normalized)

	females distal	females proximal	males distal	males proximal
	U_1	U_1	U_1	U_1
P	0.2447	0.2519	0.2459	0.2505
A	−0.9696	−0.9678	−0.9693	−0.9681
l	13.6837	20.4869	39.9048	45.2566
%	100.00	100.00	100.00	100.00

Scatterplots of principal component scores are presented in Figure 4.4. Despite smaller sample sizes, most specimens were grouped together, with only a few specimens at the fringes.

The angles θ_1 and θ_2 were calculated and are presented in Table 4.10. Again, PC1 (normalized) was almost perpendicular to PC1 (raw) and parallel with PC2 (raw).

Table 4.10. Angles between normalized PC1 and raw PC1 (θ_1) and PC2 (θ_2) – *Colobus*, conventional data

	θ_1	θ_2
females distal	91.07	1.21
females proximal	91.83	1.76
males distal	89.69	0.25
males proximal	90.21	0.42

4.4.1.1.3.2 Fourier data

The covariance-correlation matrices for these data are presented in Table A.16(c) (page 347). There was a consistent pattern of strongly negative correlations between ***X1*** and ***Y1*** (–0.9959 to –0.9993); other correlations were less strong. Variances of ***X1*** and ***Y1***, and to a lesser extent, ***Y2***, were consistently and substantially greater than those of other variables. First principal components (Table A.18(c), page 352) and Table 4.11) were consistently dominated by a contrast between ***X1*** and ***Y1***, and the corresponding eigenvalues accounted for large proportions of the total variance (76.41% to 91.52%). Second eigenvalues accounted for 4.18% to 15.07% of total variance. The first two eigenvalues accounted for 91.00% to 95.70% of total variance. Second principal components were dominated by ***Y2***, but coefficient sign showed no clear pattern: 0.7732 and –0.7860 for females (distal and proximal, respectively), and –0.8472 and 0.6771 for males.

Table 4.11. Principal components 1 and 2 – *Colobus*, Fourier data (normalized)

	females distal		females proximal		males distal		males proximal	
	U_1	U_2	U_1	U_2	U_1	U_2	U_1	U_2
X1	0.4713	0.0637	0.5276	0.0651	0.4792	0.0279	0.5190	0.0046
Y1	–0.7825	–0.1653	–0.8294	–0.0524	–0.8451	–0.0079	–0.8226	–0.0240
X2	–0.2034	0.2551	0.0405	–0.4370	–0.2587	–0.4441	–0.0149	0.1220
Y2	–0.1668	0.7732	0.0636	–0.7860	0.0575	–0.8472	–0.0027	0.6771
X3	0.1698	–0.1242	0.1461	0.0707	0.2104	0.0265	0.2076	–0.1637
Y3	0.1855	0.4420	0.0504	–0.0679	–0.0121	–0.0347	0.0356	0.5629
X4	–0.1719	0.2275	0.0049	–0.2561	–0.0278	–0.2832	–0.0334	0.0265
Y4	–0.0101	0.0603	0.0534	–0.3186	–0.0091	0.0171	–0.0116	–0.4046
X5	0.0007	–0.1985	0.0356	0.0428	0.0797	0.0383	0.0875	–0.0659
Y5	0.0589	0.0069	–0.0039	0.0766	0.0265	0.0157	0.0219	–0.1164
l	0.8631	0.1702	1.0539	0.1826	1.6755	0.1980	2.0944	0.0958
%	76.41	15.07	78.23	13.55	81.38	9.62	91.52	4.18

Scatterplots of principal component scores on the first and second components are presented in Figure 4.6. Due to small samples, it was difficult to judge data structure visually, but no specimens were outlying.

Angles between size-adjusted first principal components and the first two components of raw data are presented in Table 4.12. There were roughly 90° deviations between PC1 (raw) and PC1 (normalized), and only slight deviations between PC2 (raw) and PC1 (normalized) in males. These deviations were much greater in females (20.94° in the distal data set).

Table 4.12. Angles between normalized PC1 and raw PC1 (θ_1) and PC2 (θ_2) – *Colobus*, Fourier data

	θ_1	θ_2
females distal	100.66	12.13
females proximal	104.35	20.94
males distal	91.39	*0.00
males proximal	94.85	4.92

*not defined ($\cos^{-1} > 1.00$)

4.4.1.1.4 *Gorilla*

4.4.1.1.4.1 conventional data

The covariance-correlation matrices are presented in Table A.15(d) (page 344). The correlations very closely approximated −1.00 (−0.9999 to −1.0000), which supported the assumption of linearity of the data. A similar pattern to the other genera was seen with the variances: those of ***A*** were at least one (nontransformed: females distal – $s^2_P = 2.2608$, $s^2_A = 41.8590$) or two (logarithms: females distal – $s^2_P = 2.3833$, $s^2_A = 818.3427$) orders of magnitude greater than those of ***P***. Consequently, nontransformed data were used in this ordination.

The results of the principal component analyses are presented in Table A.17(d) (page 349), and the results from the first component are reproduced in Table 4.13. Again, first eigenvalues accounted for practically 100% of total variance, and principal component coefficients were relatively uniform among the groups (see below).

Table 4.13. Principal component 1 – *Gorilla*, conventional data (normalized)

	females distal	females proximal	males distal	males proximal
	U_1	U_1	U_1	U_1
P	0.2263	0.2369	0.2358	0.2405
A	–0.9740	–0.9715	–0.9718	–0.9707
l	44.1193	28.0521	19.0965	8.1716
%	100.00	100.00	100.00	100.00

Scatterplots of the principal component scores are presented in Figure 4.4. Due to the very small sample sizes, specimens were scattered loosely, and no attempt was made to locate outliers. Specimens 15 and 16, which were obvious outliers in Chapter 3 were located inconspicuously on these plots.

Angles θ_1 and θ_2 were calculated and are presented in Table 4.14. The first principal component (normalized) was very nearly perpendicular to and parallel with PC1 (raw) and PC2 (raw), respectively.

Table 4.14. Angles between normalized PC1 and raw PC1 (θ_1) and PC2 (θ_2) – *Gorilla*, conventional data

	θ_1	θ_2
females distal	91.54	1.70
females proximal	89.61	0.70
males distal	89.89	0.50
males proximal	89.05	0.84

4.4.1.1.4.2 Fourier data

The covariance-correlation matrices for these data are presented in Table A.16(d) (page 348). There was a pattern of strong negative correlations between ***X1*** and ***Y1*** (–0.9970 to –0.9995). All other correlations were less strong. Variances were consistently nonuniform, being substantially greater for ***X1*** and ***Y1***. The variance of ***Y2***, which was seen in other groups to be relatively large, had the greatest variance of any variable in the males distal data.

The principal component analysis results are presented in Table A.18(d) (page 353). Table 4.15 shows the results from the first two components. The first principal components largely represented a contrast between ***X1*** and ***Y1***, except for the males distal data. In males distal ***X1*** was contrasted with ***Y1***, ***X2***, ***Y2*** and ***X4***. The first eigenvalue accounted for variable proportions of total variance, from 58.34% to 85.77%. The second eigenvalue accounted for 8.09% to 35.76% of total variance; together, the first two eigenvalues accounted for 81.43% to 97.62% of total variance. The second principal components were weighted heavily towards ***Y2***, except in the males distal data, which represented a contrast between ***X1*** and ***Y1*** as well as between ***Y2*** and ***Y1***.

Table 4.15. Principal components 1 and 2 – *Gorilla*, Fourier data (normalized)

	females distal		females proximal		males distal		males proximal	
	U_1	U_2	U_1	U_2	U_1	U_2	U_1	U_2
X1	0.3643	0.1029	0.4328	0.0074	0.2773	0.3293	0.4436	0.0244
Y1	−0.8606	−0.1964	−0.8772	−0.0503	−0.5172	−0.7101	−0.8685	−0.0262
X2	0.0897	−0.1799	−0.0474	0.2258	−0.2629	0.1429	−0.0160	−0.1667
Y2	0.3031	−0.6839	−0.0880	0.7034	−0.6954	0.5658	0.0858	−0.7313
X3	0.1280	0.2508	0.1456	−0.1077	0.1670	0.0963	0.1181	0.2698
Y3	0.0399	−0.4900	0.0869	0.4423	0.0653	0.0331	0.1333	−0.2025
X4	0.0538	−0.2779	−0.0371	0.1851	−0.2584	0.1703	0.0440	−0.3590
Y4	−0.0506	−0.1156	0.0139	0.2921	0.0176	0.0420	−0.0794	−0.3466
X5	0.0568	0.2387	0.0336	−0.2026	0.0504	−0.0004	0.0248	0.2242
Y5	0.0042	−0.0151	0.0418	0.2894	−0.0334	0.0758	0.0286	0.1523
l	0.9367	0.1341	0.7710	0.0728	0.7807	0.4513	0.2244	0.0888
%	82.50	11.81	85.77	8.09	61.86	35.76	58.34	23.09

Scatterplots of principal component scores on the first two components are presented in Figure 4.6. Again small samples made assessing data structure difficult, but no outlying points were found.

Table 4.16 shows the angles θ_1 and θ_2. For the proximal specimen outlines, θ_1 was close to 90°, but at least 100° for distal outlines. These results were reflected in the values of θ_2, except for males proximal. Although θ_1 was very close to 90° (86.39°), θ_2 was comparatively quite far from 0° (20.69°).

Table 4.16. Angles between normalized PC1 and raw PC1 (θ_1) and PC2 (θ_2) – *Gorilla*, Fourier data

	θ_1	θ_2
females distal	101.80	10.41
females proximal	89.59	2.86
males distal	100.63	14.81
males proximal	86.39	20.69

Figure 4.4. Scatterplots of scores on PC2 (y-axis) versus PC1 (x-axis) – conventional data (normalized)

(a) *Homo*

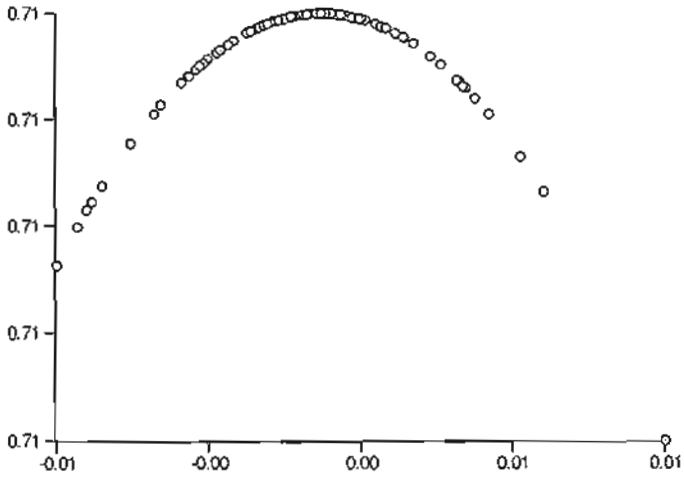

(i) females distal

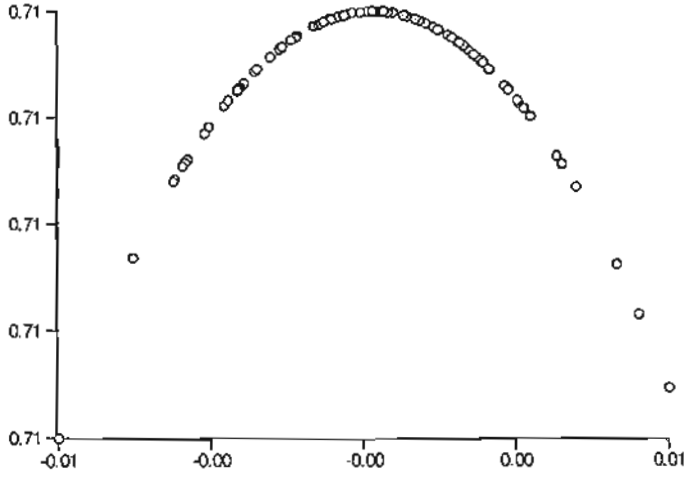

(ii) females proximal

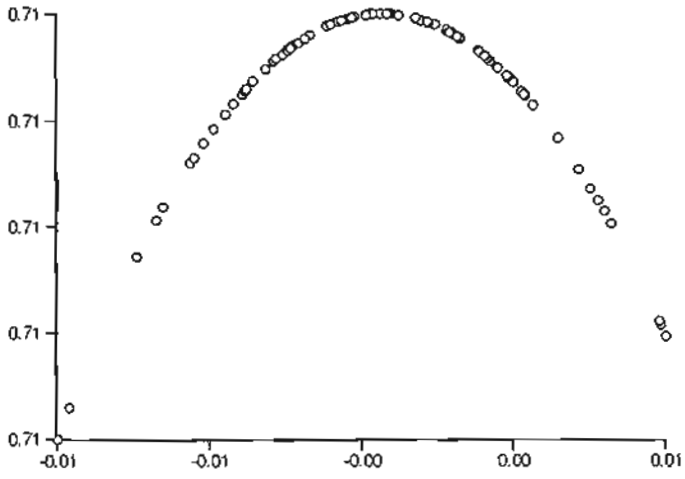

(iii) males distal

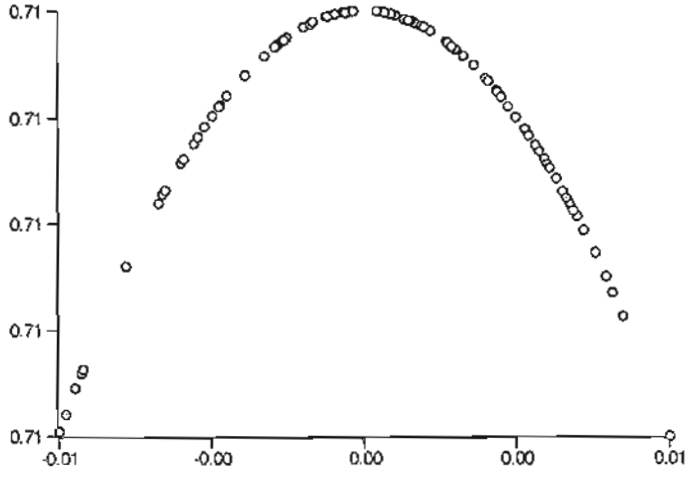

(iv) males proximal

Figure 4.4. (b) *Cercopithecus*

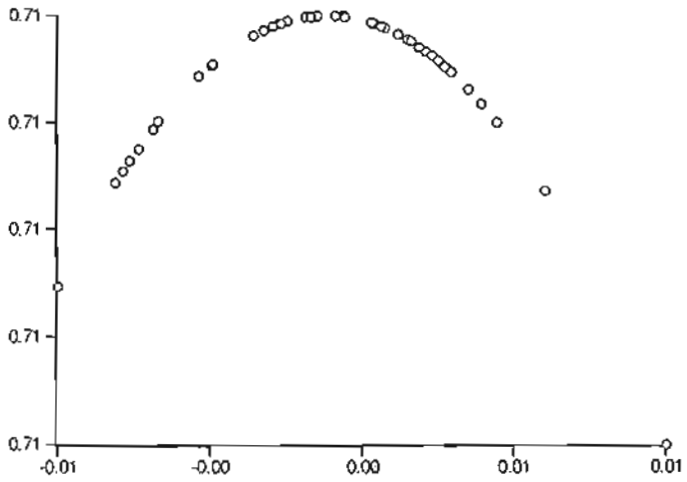

(i) females distal

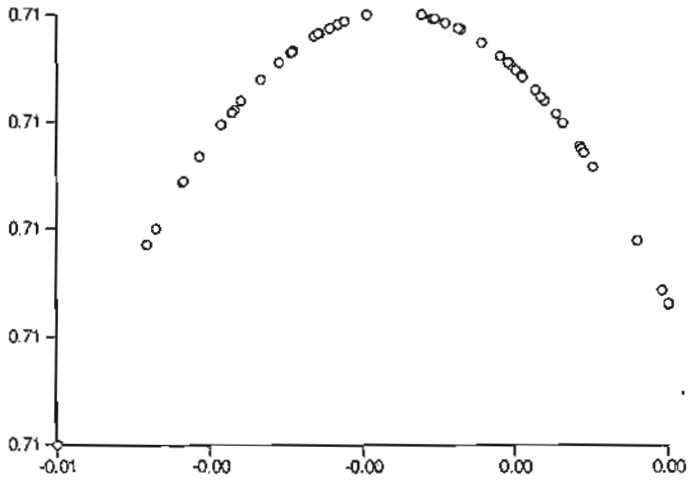

(ii) females proximal

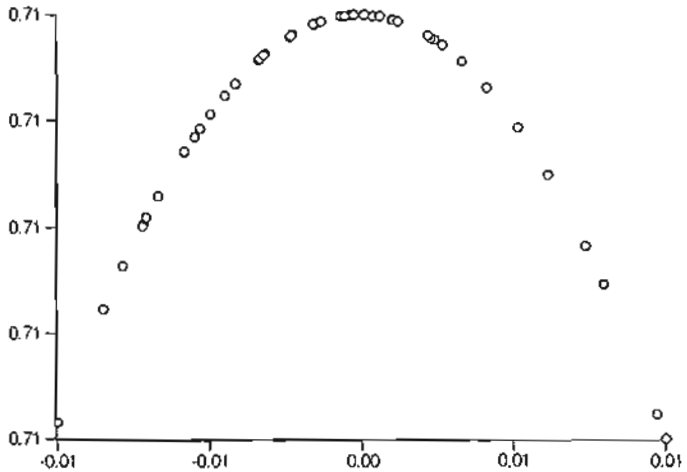

(iii) males distal

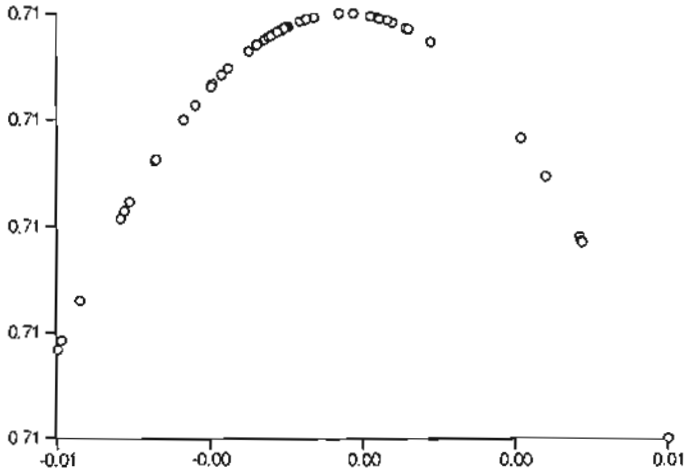

(iv) males proximal

Figure 4.4. (c) *Colobus*

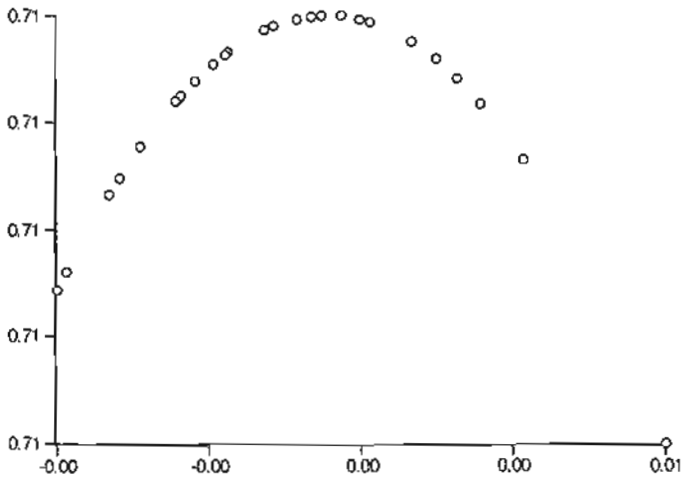

(**i**) females distal

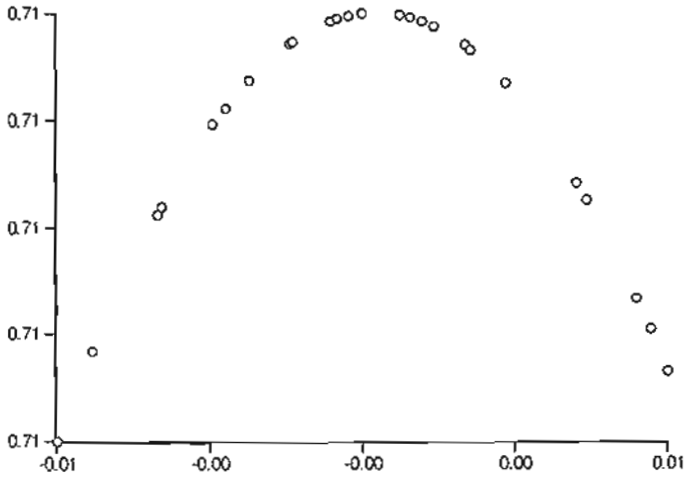

(**ii**) females proximal

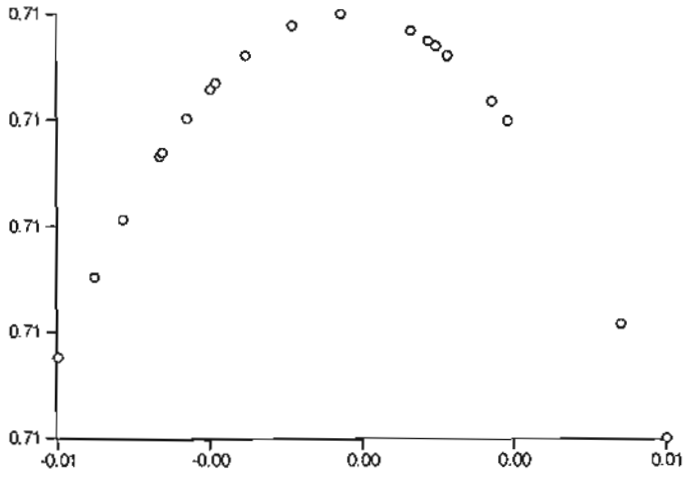

(**iii**) males distal

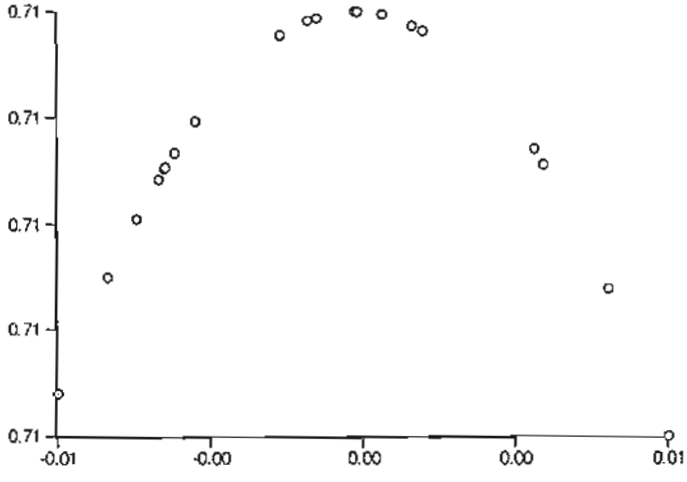

(**iv**) males proximal

Figure 4.4. (**d**) *Gorilla* (specimens **a** 671, **b** 672)

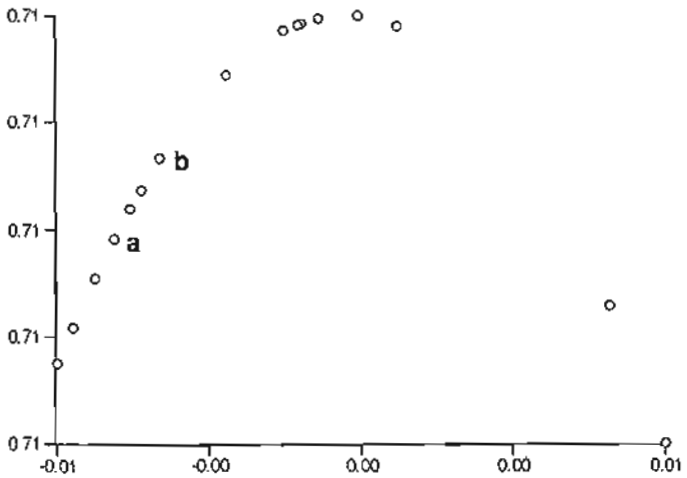

(i) females distal

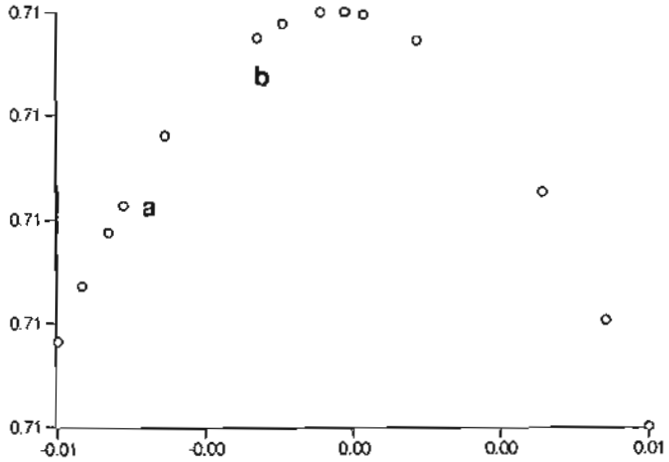

(ii) females proximal

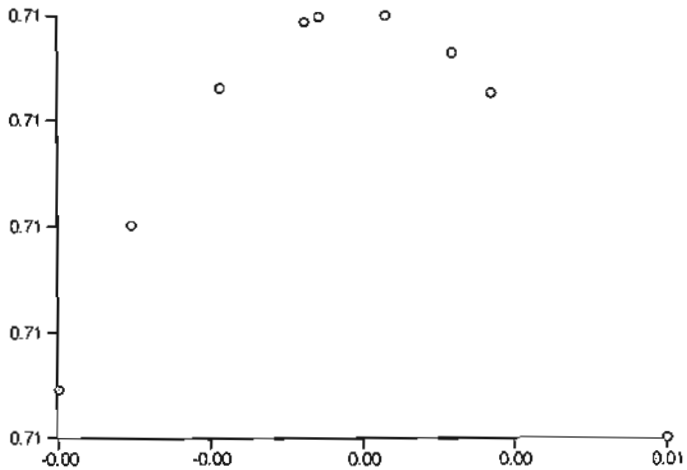

(iii) males distal

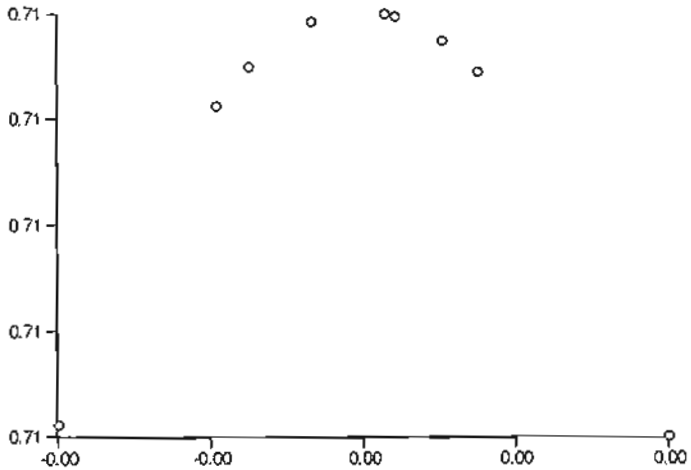

(iv) males proximal

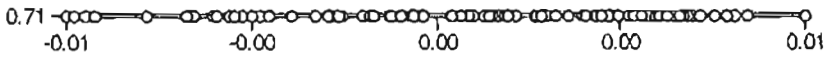

Figure 4.5. PCA scatterplot of *Homo* males proximal from Figure 4.4, with component axes of equal scale

Figure 4.6. Scatterplots of scores on PC2 (y-axis) versus PC1 (x-axis) – Fourier data (normalized)

(a) *Homo* (specimen 87 **a**)

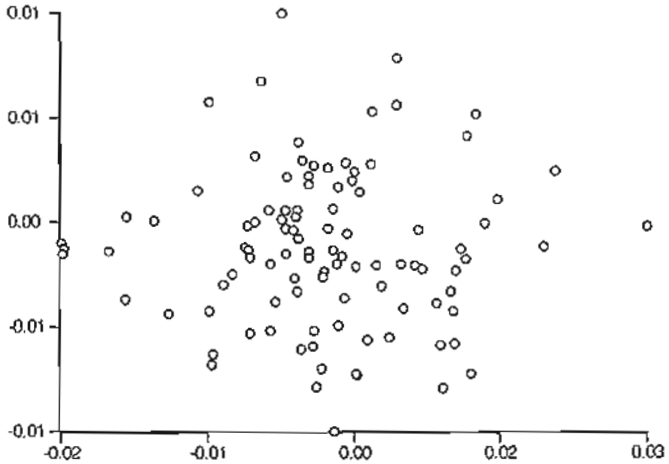

(i) females distal

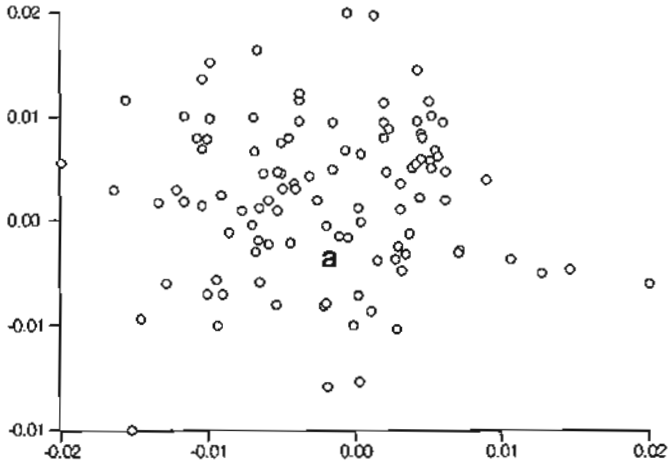

(ii) females proximal

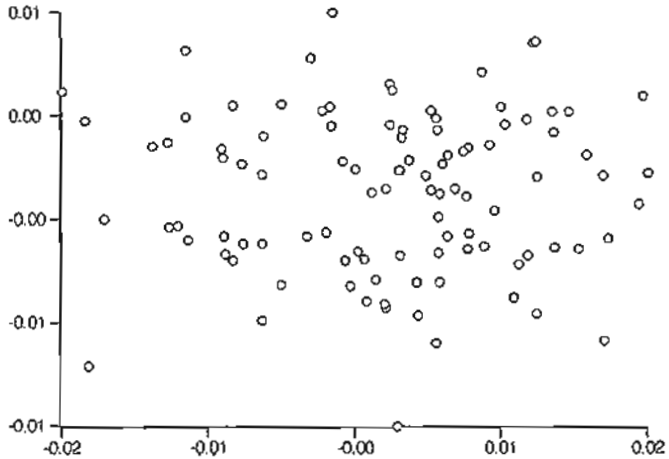

(iii) males distal

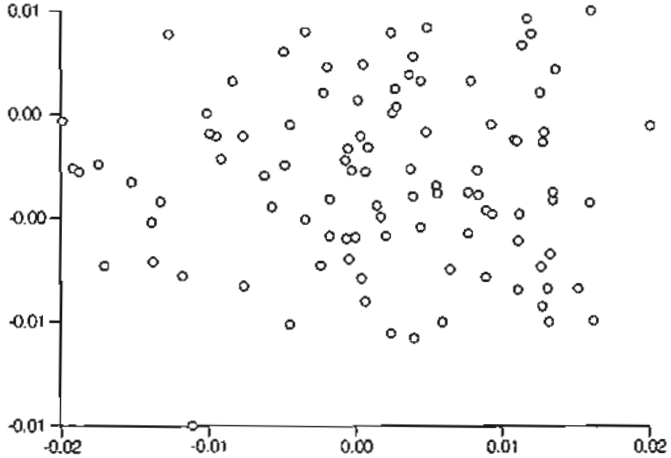

(iv) males proximal

Figure 4.6. (b) *Cercopithecus*

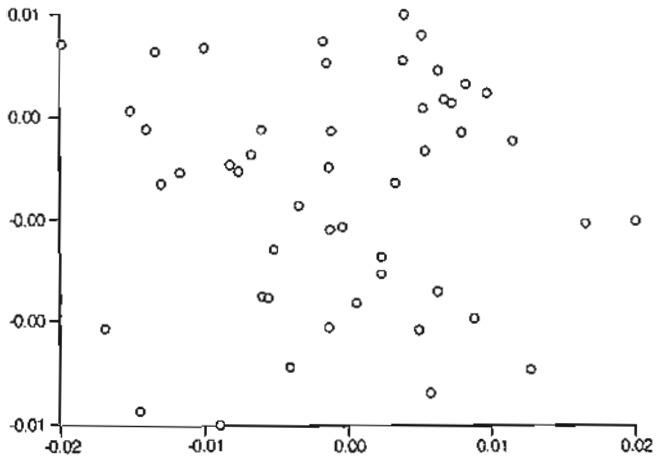

(i) females distal

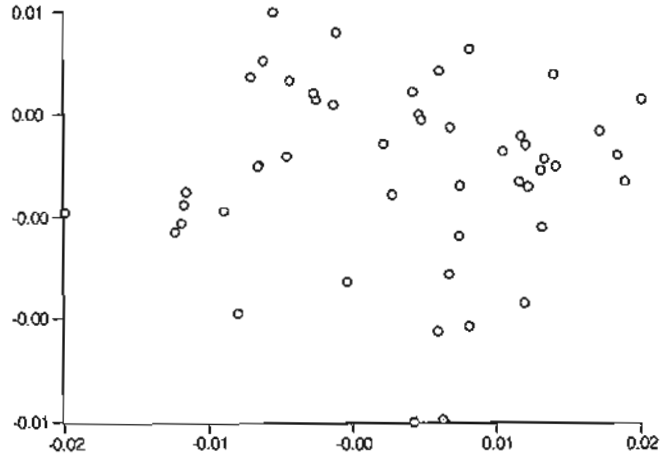

(ii) females proximal

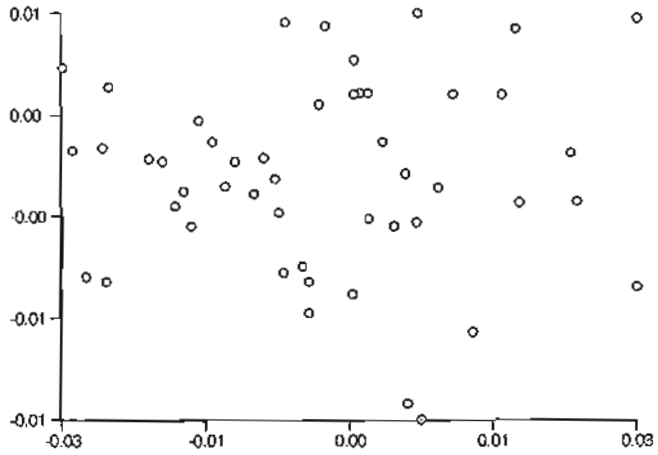

(iii) males distal

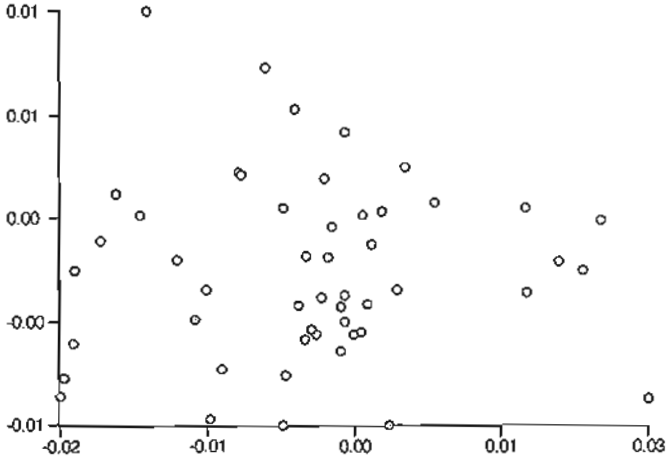

(iv) males proximal

Figure 4.6. (c) *Colobus*

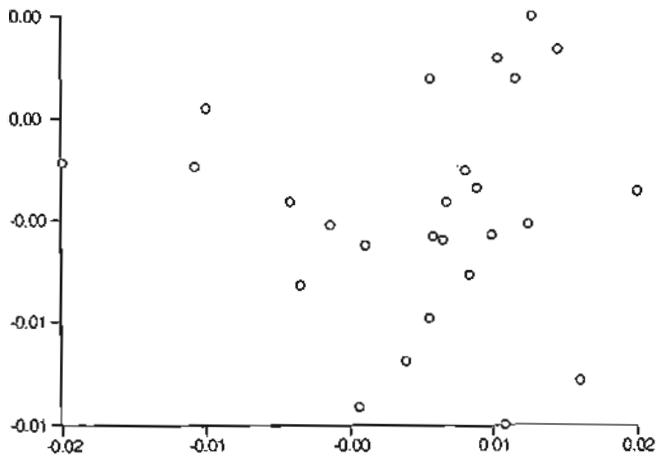

(i) females distal

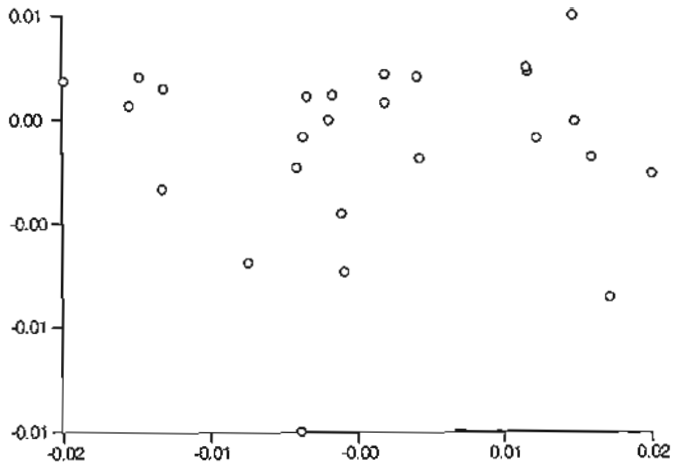

(ii) females proximal

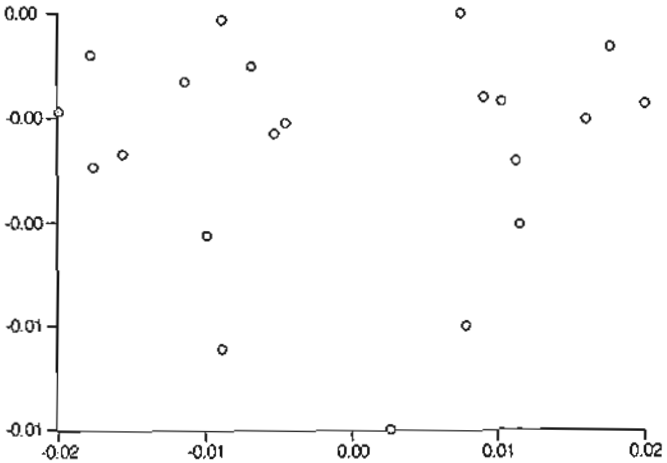

(iii) males distal

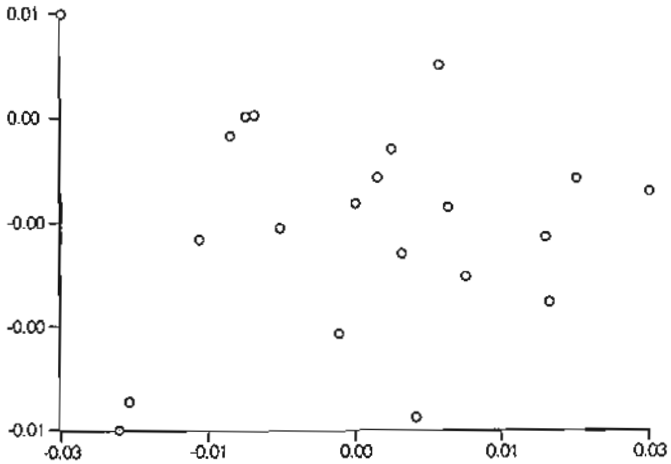

(iv) males proximal

Figure 4.6. (d) *Gorilla* (female specimens **a** 671, **b** 672, **c** 657, **d** 658; male specimen **a** 656)

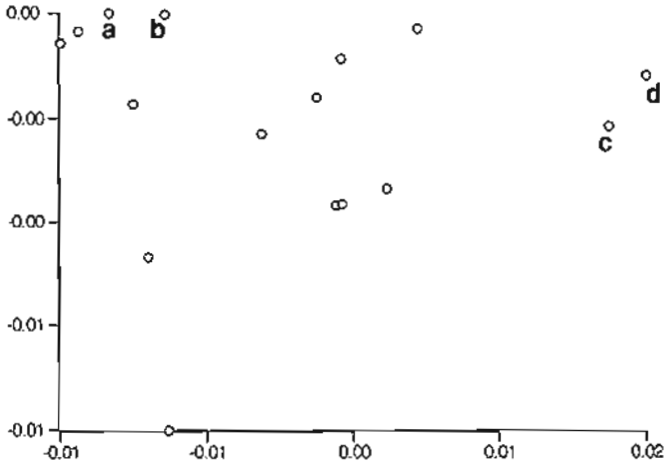

(i) females distal

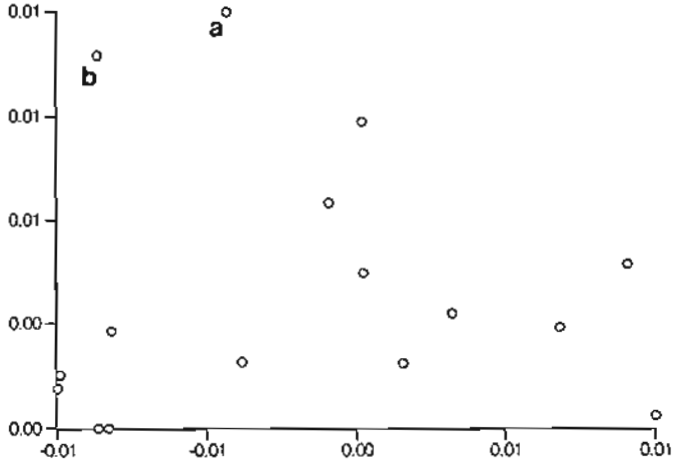

(ii) females proximal

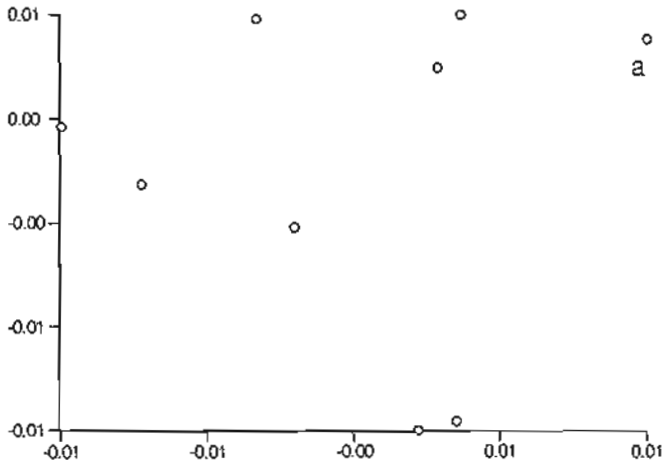

(iii) males distal

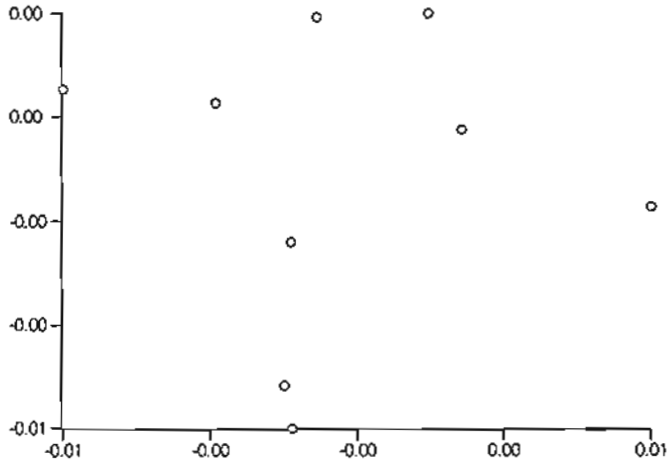

(iv) males proximal

4.4.1.2 Cluster analysis

4.4.1.2.1 conventional data

Cophenetic correlations from the UPGMA cluster analyses are presented in Table 4.17. It can be seen that when individual specimens were considered, average taxonomic distance showed very good correlations (0.9564 to 0.9818), but $(1-\cos)_S$ showed some very poor to poor correlations (0.5984 to 0.7542). Correlations were more consistent when only genera were considered, ranging from 0.8542 to 0.8601 (good) for generalized distance and from 0.7404 to 0.9305 (poor to very good) for $(1-\cos)_G$. Therefore, only clustering at the genera level was considered in this investigation.

Table 4.17. Cophenetic correlations – conventional data

	d	$(1-\cos)_S$	D^2	$(1-\cos)_G$
females distal	0.9564	0.5984	0.8564	0.9305
females proximal	0.9593	0.7542	0.8542	0.8856
males distal	0.9818	0.6582	0.8601	0.8507
males proximal	0.9775	0.7192	0.8597	0.7404

Figure 4.7 shows the tree diagrams for females and males, for both generalized distance (including details of size) and $(1-\cos)_G$ (ignoring size). In both females and males, there was a consistent pattern of *Cercopithecus* and *Colobus* (cercopithecoids) clustering at slightly greater than 1 (generalized distance), and *Homo* and *Gorilla* (hominoids) clustering between 4 and 5. These two clusters were finally clustered around 9 to 10. With the dissimilarity coefficient of $(1-\cos)$, the situation was quite different. Cercopithecoids and hominoids were clustered together consistently (around 10^{-4}), but other cluster points varied both within and among females and males. A consistent feature with these data was that the clustering of the cercopithecoids and of the hominoids was at a comparatively closer point (relative to the generalized distance clustering), and this was more marked in females than males.

4.4.1.2.2 Fourier data

Cophenetic correlations from cluster analyses using Fourier amplitudes are presented in Table 4.18. A pattern of correlations similar to that of the conventional data was seen here. There was again an inconsistency between matrices based on ATD (0.9564 to 0.9818) and $(1-\cos)_S$

(0.5775 to 0.7248) for individual specimens. At the genera level, greater consistency was found between generalized distance (0.9152 to 0.9957) and $(1 - \cos)_G$ (0.8652 to 0.9489). Again, only clustering at the genera level was considered here.

Table 4.18. Cophenetic correlations – Fourier data

	d	$(1 - \cos)_S$	D^2	$(1 - \cos)_S$
females distal	0.9564	0.5775	0.9152	0.8610
females proximal	0.9594	0.7283	0.9802	0.9489
males distal	0.9818	0.6794	0.9951	0.8652
males proximal	0.9777	0.7428	0.9957	0.8823

Clustering based on generalized distance was consistent among males and females Figure 4.8: *Cercopithecus* and *Colobus* were clustered around 1, *Homo* and *Gorilla* at 5 or 6, and all genera at around 11 or 12. While the hominoids were clustered at a level more similar to that of the cercopithecoids using $(1 - \cos)_G$, this time it was in the males that this effect was more marked.

Figure 4.7. UPGMA tree diagrams – conventional data (size-adjusted)

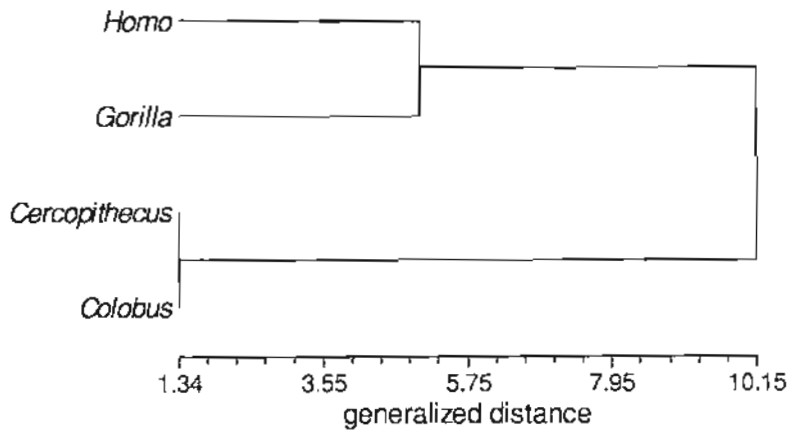

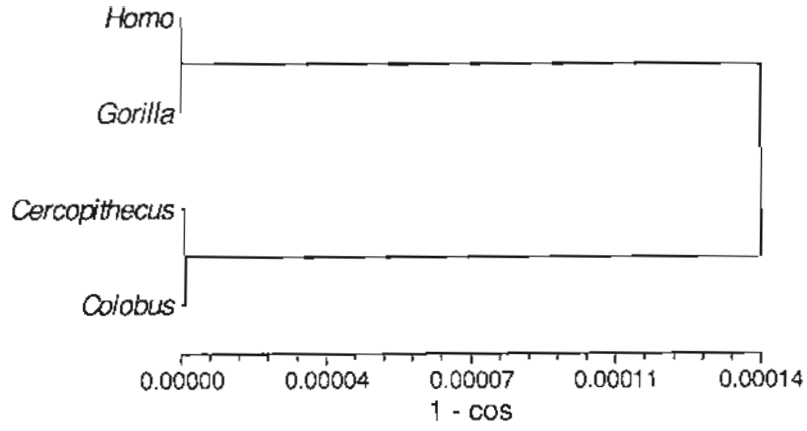

(i) distal

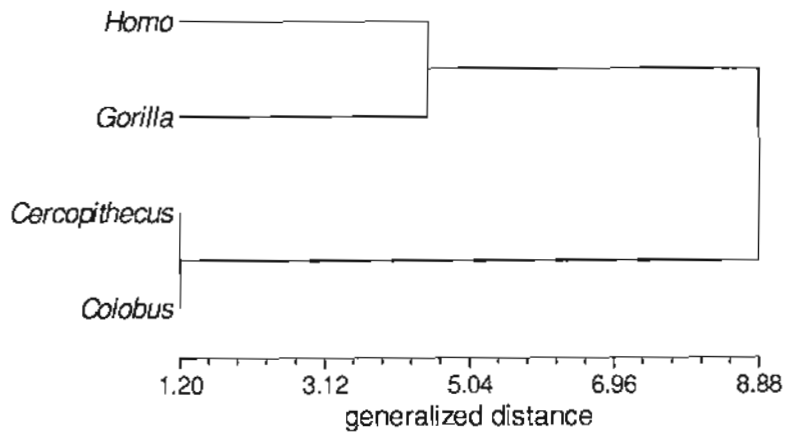

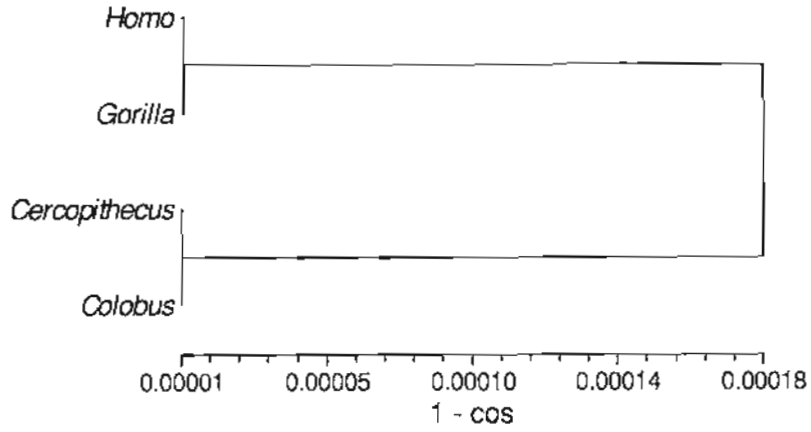

(ii) proximal

(a) females

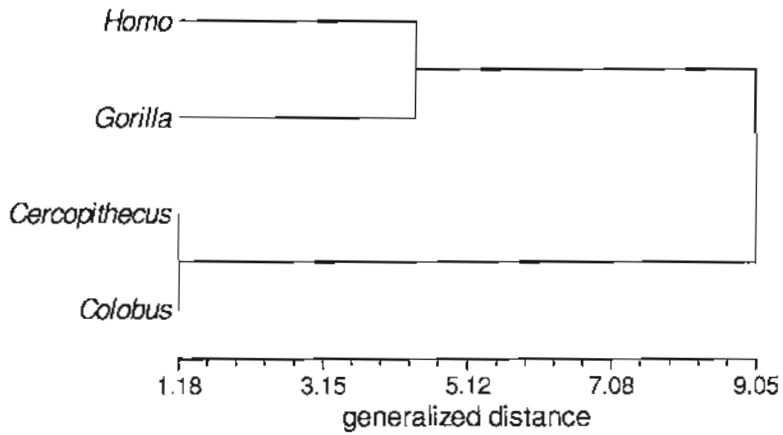

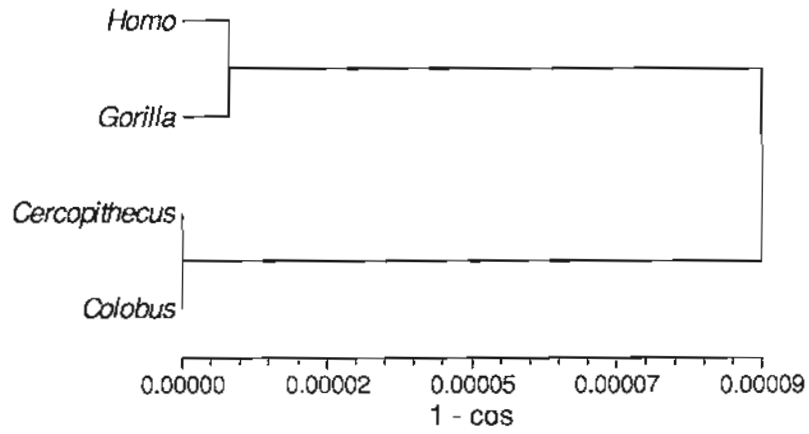

(i) distal

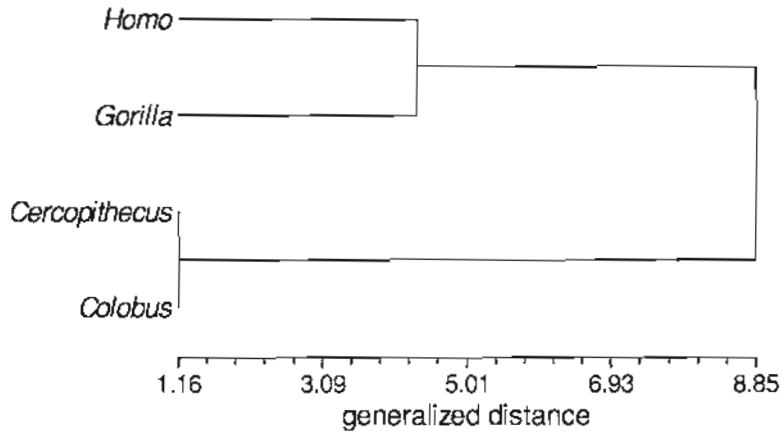

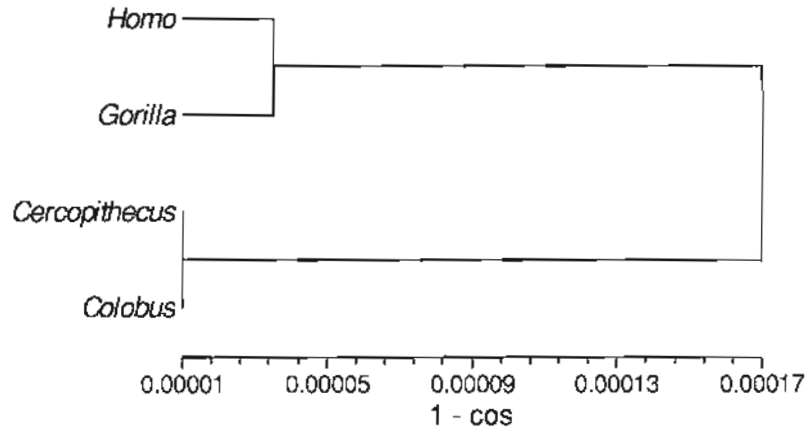

(ii) proximal

(b) males

Figure 4.8. UPGMA tree diagrams – Fourier data (size-adjusted)

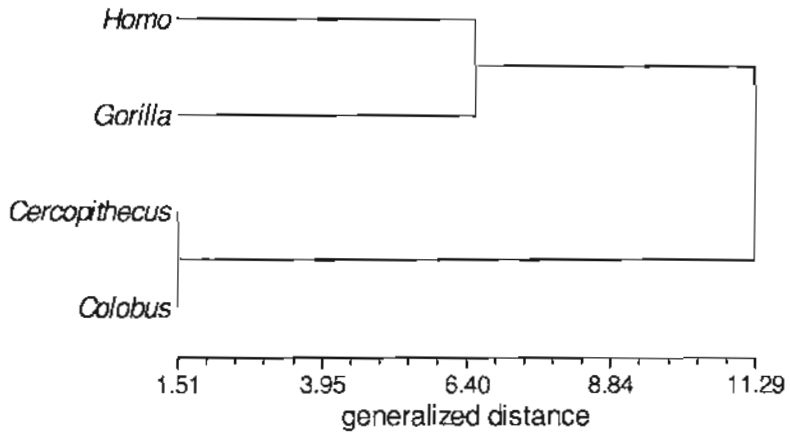

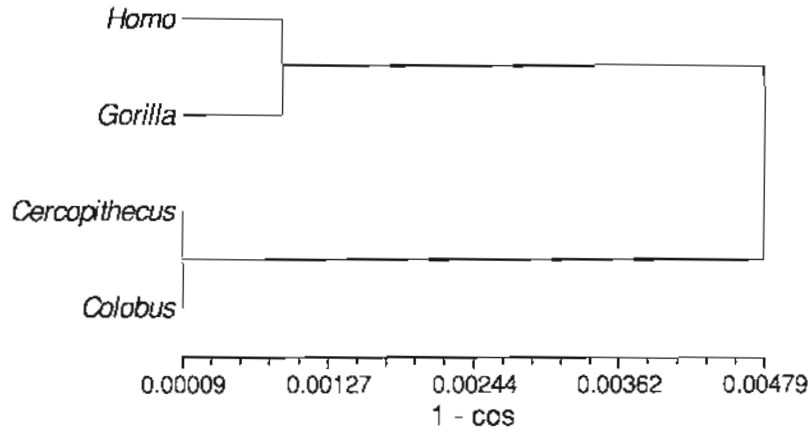

(i) distal

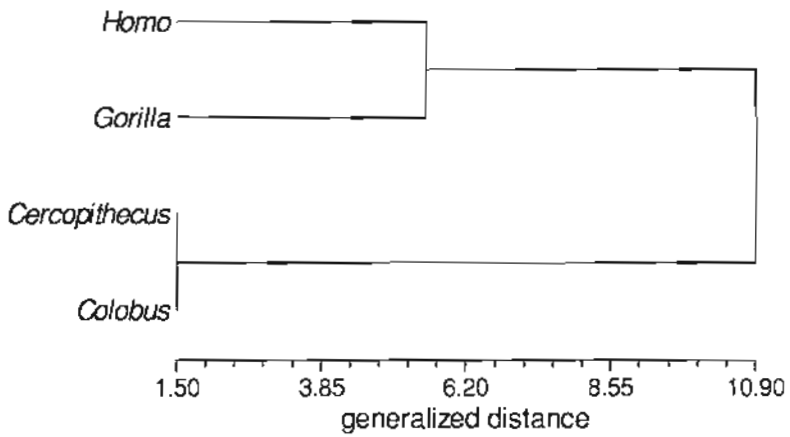

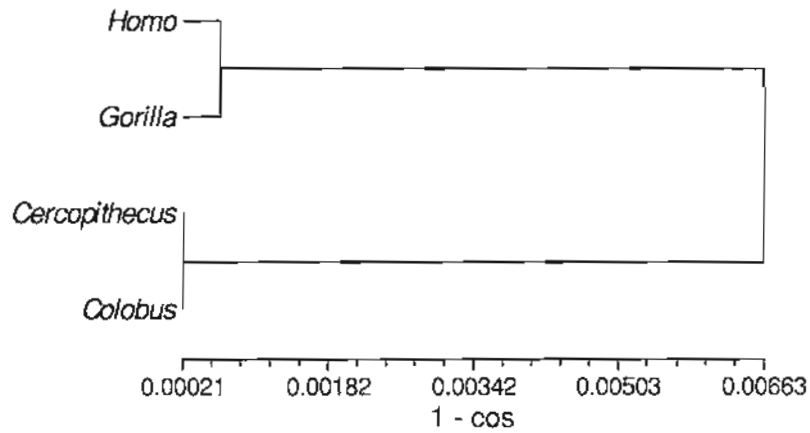

(ii) proximal

(a) females

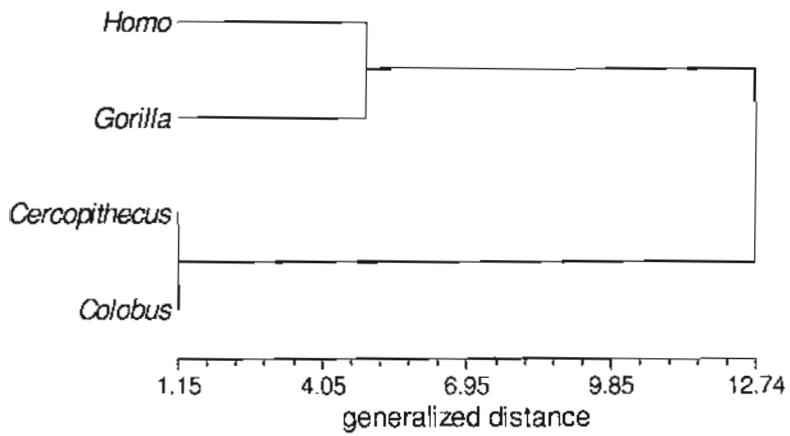

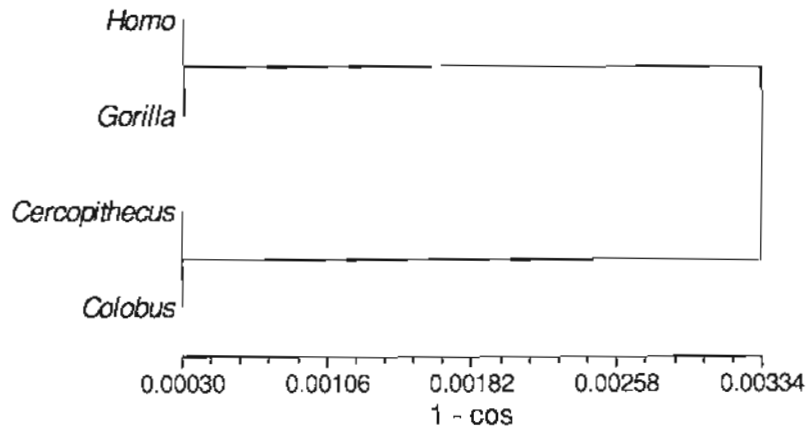

(i) distal

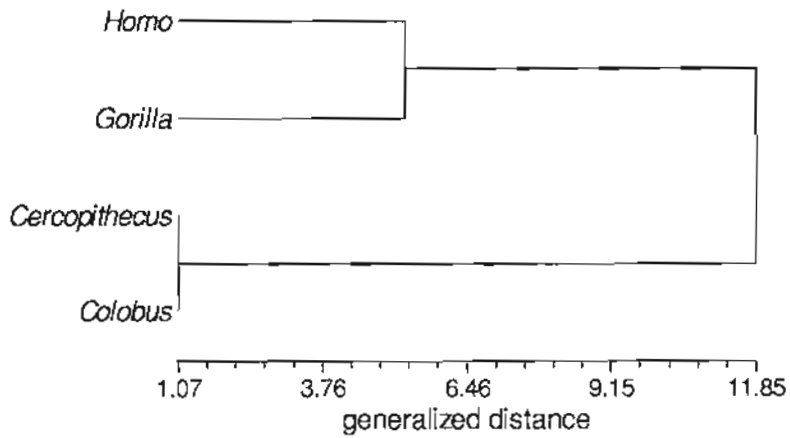

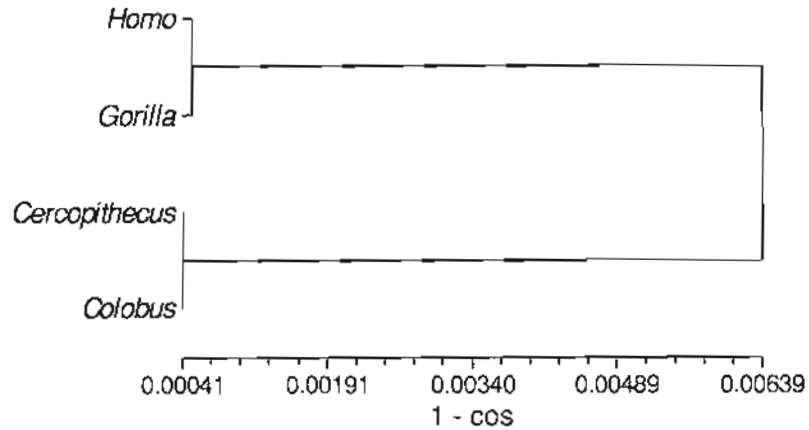

(ii) proximal

(b) males

4.4.2 Allometry

4.4.2.1 *Homo*

4.4.2.1.1 conventional data

Correlation coefficients and percentages of total variance explained by first eigenvalues of raw data are reproduced in Table 4.19. Correlation coefficients were all high (0.9296 to 0.9743), and first eigenvalues accounted for at least 99% of total variance (99.38% to 99.77%). It was therefore concluded that linear functional relations existed.

Table 4.19. Product-moment correlation coefficients (r) and percentages of total variance accounted for by eigenvalue 1 – *Homo*, conventional data

	r	$100 \times l_1/l_{tot}$
females distal	0.9296	99.38
females proximal	0.9743	99.76
males distal	0.9359	99.39
males proximal	0.9433	99.46

No significant deviations from the normal distribution were found for these data (Table A.19(a), page 354), and the null hypothesis of normality was accepted. Table 4.20 shows the values for a, the major axis regression slope, and c, the A-intercept, and their confidence limits. All intercept estimates were positive (10.5507 to 17.0304), and the 95% confidence limits for c did not include 0.00 in any data set.

Table 4.20. Major axis regression slopes (a), intercepts (c) and their 95% confidence limits – *Homo*, conventional data

	a	a_1	a_2	c	c_1	c_2
females distal	0.2085	0.2250	0.1921	17.0304	7.6730	26.3311
females proximal	0.2211	0.2311	0.2112	10.5507	5.1386	15.9087
males distal	0.2198	0.2364	0.2033	11.6645	1.3263	21.9403
males proximal	0.2199	0.2356	0.2043	11.1570	1.9533	20.3021

The best estimates for the linear functional relations between P and A in these samples were:

females distal	$A = 0.2085P + 17.0304$
females proximal	$A = 0.2211P + 10.5507$
males distal	$A = 0.2198P + 11.6645$
males proximal	$A = 0.2199P + 11.1570$.

The correlation coefficients and percentages of total variance explained by the first eigenvalue for the logarithmic variables are presented in Table 4.21. These results were very similar to those of the nontransformed data. There was consequently no clear advantage in estimating nonlinear relations. Moreover, due to the nonzero intercepts (and the resultant difficulties in estimating nonlinear relations), it was decided to not proceed to estimate nonlinear relations.

Table 4.21. Product-moment correlation coefficients (r) and percentages of total variance accounted for by eigenvalue 1 – *Homo*, conventional data (ln)

	r	$100 \times l_1 / l_{tot}$
females distal	0.9311	96.57
females proximal	0.9742	98.73
males distal	0.9430	99.15
males proximal	0.9428	99.15

4.4.2.1.2 Fourier data

The results of the principal component analyses of covariance matrices of raw data are presented in Table A.12(a,b) (page 333). The proportions of total variance explained by the first and last three eigenvalues are reproduced in Table 4.22. First eigenvalues accounted for between 79.63% and 88.55% of total variance, and the range for second eigenvalues was 6.45% to 13.47%. Therefore, the dominance of the first eigenvalue was not overwhelming, especially over the second eigenvalue, and the first principal components were not judged to represent allometric equations in the sense that they accounted for the bulk of character variance, as the second component accounted for a still substantial proportion of variance.

Table 4.22. Proportions of total variance accounted for by eigenvalues 1 to 3 and 8 to 10 – *Homo*, Fourier data

	l_1	l_2	l_3	l_8	l_9	l_{10}
females distal	79.63	13.47	4.29	0.17	0.04	0.01
females proximal	88.55	6.45	3.32	0.09	0.02	0.00
males distal	82.60	11.73	2.86	0.12	0.03	0.01
males proximal	83.48	10.48	3.80	0.11	0.03	0.01

Functional relations were then investigated by considering eigenvectors with eigenvalues close to zero. While tenth eigenvalues were small (0.00% to 0.01% of total variance), ninth eigenvalues were also quite small (0.02% to 0.04%), which suggested circularity of the eigenvectors. Sphericity statistics were calculated for ninth and tenth eigenvalues, and these results are presented in Table 4.23. These values exceeded the critical value of $\chi^2_{0.05[2]}$ (5.991), so that the null hypothesis was rejected: tenth eigenvalues were distinct from ninth, and tenth principal components were therefore interpreted as functional relations.

Table 4.23. Sphericity statistics (S) for eigenvalues 9 and 10 – *Homo*, Fourier data

	l_9	l_{10}	$S(l_9, l_{10})$
females distal	0.0380	0.0075	26.46
females proximal	0.0198	0.0050	20.40
males distal	0.0352	0.0092	18.35
males proximal	0.0302	0.0058	26.29

The tenth principal components were as follows:

females distal

U_{10} = [0.0477, –0.0286, 0.0892, 0.0581, –0.6698, –0.0151, –0.3130, –0.0321, 0.5863, 0.3001]

females proximal

U_{10} = [0.0639, –0.0479, 0.2041, 0.1150, –0.6189, –0.0671, –0.5453, –0.1380, 0.4210, 0.2400]

males distal

U_{10} = [0.0426, –0.0248, 0.0597, 0.0843, –0.6478, 0.0019, –0.2544, 0.0038, 0.6608, 0.2566]

males proximal

U_{10} = [0.0623, −0.0449, 0.0715, 0.0894, −0.7413, −0.0379, −0.2787, −0.0149, 0.5600, 0.2790].

The eigenvectors consistently showed high loadings for ***X*3** and ***X*5**, and to a lesser extent, ***X*4** and ***Y*5**.

4.4.2.2 *Cercopithecus*

4.4.2.2.1 conventional data

Correlation coefficients and percentages of total variance explained by first eigenvalues are reproduced in Table 4.24. The correlation coefficients were high (0.9746 to 0.9931), and first eigenvalues accounted for at least 99.7% of total variance (99.73% to 99.81%). It was concluded that linear functional relations existed.

Table 4.24. Product-moment correlation coefficients (r) and percentages of total variance accounted for by eigenvalue 1 – *Cercopithecus*, conventional data

	r	$100 \times l_1/l_{tot}$
females distal	0.9746	99.73
females proximal	0.9834	99.79
males distal	0.9840	99.80
males proximal	0.9931	99.91

Table A.19(b) (page 354) shows the Kolmogorov-Smirnov Z-statistics for these data: in males distal, the distribution of A was found to be significantly different to normal, and the null hypothesis of normality was rejected; otherwise the null was accepted. As the results here for males distal did not obviously deviate, it seemed appropriate to interpret them. Table 4.25 shows the slope and intercept estimates with their respective confidence limits. In females distal, there was a positive intercept, with the other groups showing small negative intercepts (range of 2.1575 to −0.9344). Only in females distal did the confidence limits for c exclude zero, and only barely.

Table 4.25. Major axis regression slopes (a), intercepts (c) and their 95% confidence limits – *Cercopithecus*, conventional data

	a	a_1	a_2	c	c_1	c_2
females distal	0.2389	0.2551	0.2228	2.1575	0.1911	4.1117
females proximal	0.2700	0.2847	0.2554	–0.6244	–2.4661	1.2047
males distal*	0.2626	0.2766	0.2487	–0.9344	–2.9754	1.0921
males proximal	0.2652	0.2743	0.2561	–0.0642	–1.4391	1.3108

*A nonnormal

The best estimates for the linear functional relations were as follows:

females distal $A = 0.2389P + 2.1575$

females proximal $A = 0.2700P - 0.6244$

males distal $A = 0.2626P - 0.9344$

males proximal $A = 0.2652P - 0.0642$.

The correlation coefficients and percentages of variance for the logarithmic data are presented in Table 4.26. While the correlation coefficients were similar for nontransformed data (0.8727 to 0.9937), the first eigenvalues of the logarithmic data accounted for slightly less variance (98.64% to 99.69). While there were disadvantages to estimating nonlinear relations, these were only slight.

Table 4.26. Product-moment correlation coefficients (r) and percentages of total variance accounted for by eigenvalue 1 – *Cercopithecus*, conventional data (ln)

	r	$100 \times l_1/l_{tot}$
females distal	0.9727	98.64
females proximal	0.9850	99.25
males distal	0.9862	99.31
males proximal	0.9937	99.69

Since intercepts were small, especially for males proximal, nonlinear relations were estimated (excepting females distal). Kolmogorov-Smirnov Z-statistics (Table A.19(b), page 354) showed that $\ln A$ in males distal data set was non-normal, and the null was rejected; for the other data sets, the null was accepted. Again, as the results were not obviously different to those of the others, they were interpreted. The slope and intercept results are shown in Table

4.27. Not surprisingly, the confidence limits for the slope included 1.00, as the linear estimates were at least as good as the nonlinear estimates.

Table 4.27. Major axis regression slopes (k), intercepts (a) and their 95% confidence limits – *Cercopithecus*, conventional data (ln)

	k	k_1	k_2	a	a_1	a_2
females proximal	1.0376	1.0923	0.9857	−1.5180	−1.7824	−1.2671
males distal*	1.0450	1.0978	0.9948	−1.5866	−1.8489	−1.3373
males proximal	1.0278	1.0620	0.9947	−1.4687	−1.6399	−1.3031

*ln$A$ nonnormal

The best nonlinear estimates of these relations were thus:

females proximal $A = 0.2191P^{1.0376}$

males distal $A = 0.2046P^{1.0450}$

males proximal $A = 0.2302P^{1.0278}$,

which were not greatly different to the linear estimates.

4.4.2.2.2 Fourier data

The results of the principal component analyses using the covariance matrices of raw data are presented in Table A.12(c,d) (page 335), and eigenvalue proportions (first and last three) are reproduced in Table 4.28. For females, the first eigenvalue accounted for less than 90% of total variance (87.20% and 87.27% for distal and proximal, respectively), and for males the corresponding proportions were greater than 90% (93.03% and 94.68%). Therefore, for males the first principal component was more convincing as an allometric equation than for females.

Table 4.28. Proportions of total variance accounted for by eigenvalues 1 to 3 and 8 to 10 – *Cercopithecus*, Fourier data

	l_1	l_2	l_3	l_8	l_9	l_{10}
females distal	87.20	9.55	2.12	0.03	0.02	0.00
females proximal	87.27	10.31	1.33	0.03	0.02	0.00
males distal	93.03	5.91	0.59	0.02	0.02	0.00
males proximal	94.68	4.18	0.54	0.02	0.01	0.00

As can be seen from the principal component coefficients,

males distal

U_1 = [0.8315, 0.5762, 0.0125, 0.0501, 0.0518, 0.0046, 0.0184, 0.0089, 0.0187, 0.0101]

males proximal

U_1 = [0.8109, 0.5817, 0.0019, 0.0043, 0.0551, 0.0080, 0.0075, 0.0191, 0.0186, 0.0160],

the first principal component was mostly a combination of ***X1*** and ***Y1***. This, and the dominance of PC1, led to the conclusion that there was a functional relation between ***X1*** and ***Y1***. Table 4.29 shows the jackknifed estimates of the slope and intercept for the relation $\boldsymbol{Y1} = a\boldsymbol{X1} + c$.

Table 4.29. Major axis regression slopes (a), intercepts (c) and their 95% confidence limits – *Cercopithecus*, Fourier data

	a	a_1	a_2	c	c_1	c_2
males distal	0.7132	0.8178	0.6096	–2.4824	–5.2753	0.2837
males proximal	0.7157	0.8077	0.6237	–0.7484	–3.2471	1.7503

Intercepts were both negative. The confidence intervals were narrow, and included 0.00. Best (jackknifed) estimates for the functional relations were as follows:

males distal $Y1 = 0.7132X1 - 2.4824$

males proximal $Y1 = 0.7157X1 - 0.7484$

From the principal component analysis results, it was clear that the tenth eigenvalues accounted for almost no variance (all 0.00%), and the ninth eigenvalues accounted for only a minuscule amount of variance (0.01% to 0.02%). Therefore, the tenth eigenvectors were suitable for interpreting functional relations, as long as the ninth and tenth eigenvalues were distinct. Sphericity statistics were calculated for these groups and are presented in Table 4.30. These statistics were all greater than the critical value (5.991), so the null hypothesis was rejected, and it was concluded that tenth eigenvalues were distinct.

Table 4.30. Sphericity statistics (S) for eigenvalues 9 and 10 – *Cercopithecus*, Fourier data

	l_9	l_{10}	$S(l_9, l_{10})$
females distal	0.0009	0.0002	13.84
females proximal	0.0011	0.0002	12.02
males distal	0.0055	0.0007	18.78
males proximal	0.0038	0.0007	13.15

Tenth principal component coefficients were as follows:

females distal

U_{10} = [0.0717, –0.0559, 0.0681, 0.0599, –0.7050, –0.0100, –0.2363, –0.0368, 0.5679, 0.3266]

females proximal

U_{10} = [0.0873, –0.0079, –0.0438, 0.0533, –0.7550, –0.0650, –0.1563, –0.0100, 0.4727, 0.3990]

males distal

U_{10} = [0.0782, –0.0670, –0.0132, 0.0539, –0.7572, –0.0134, –0.0894, –0.0170, 0.5530, 0.3142]

males proximal

U_{10} = [0.0910, –0.0790, –0.0020, 0.0585, –0.7496, –0.0925, –0.1517, –0.0111, 0.4791, 0.3986].

The tenth eigenvectors consistently featured high loadings for ***X3***, ***X5*** and ***Y5***.

4.4.2.3 *Colobus*

4.4.2.3.1 conventional data

Table 4.31 shows the correlation coefficients and percentages of total variance explained by the first eigenvalues. Correlations were strongly positive (0.9327 to 0.9935), and first eigenvalues accounted for at least 99.5% of total variance (99.53% to 99.90%). It was therefore appropriate to investigate linear functional relations.

Table 4.31. Product-moment correlation coefficients (r) and percentages of total variance accounted for by eigenvalue 1 – *Colobus*, conventional data

	r	$100 \times l_1/l_{tot}$
females distal	0.9897	99.87
females proximal	0.9935	99.90
males distal	0.9654	99.61
males proximal	0.9327	99.53

Kolmogorov-Smirnov Z-statistics (Table A.19(c), page 354) showed that distributions were not significantly different to normal, and the null hypothesis of normality was accepted. The slope and intercept data are presented in Table 4.32. Intercepts were of varying sign and strength. Both confidence intervals for females did not allow for a zero intercept. The corresponding limits for males did include 0.00, although the confidence intervals were relatively wider than for females.

Table 4.32. Major axis regression slopes (a), intercepts (c) and their 95% confidence limits – *Colobus*, conventional data

	a	a_1	a_2	c	c_1	c_2
females distal	0.2724	0.2891	0.2558	–3.0980	–5.8523	–0.3601
females proximal	0.2947	0.3089	0.2806	–5.8185	–8.2623	–3.3919
males distal	0.2480	0.2805	0.2160	1.1037	–4.6964	6.8145
males proximal	0.2626	0.2984	0.2274	–0.3906	–6.9615	6.0702

The best estimates of these linear functional relations were as follows:

females distal	$A = 0.2724P - 3.0980$
females proximal	$A = 0.2947P - 5.8185$
males distal	$A = 0.2480P + 1.1037$
males proximal	$A = 0.2626P - 0.3906$.

Table 4.33 shows the correlation coefficients and percentages of total variance for the ln-transformed data. While the differences (compared to nontransformed data) in correlations varied, each first eigenvalue accounted for slightly less total variance. As there was no clear disadvantage, and since intercepts were close to zero, it was decided to investigate nonlinear relations in males.

Table 4.33. Product-moment correlation coefficients (r) and percentages of total variance accounted for by eigenvalue 1 – *Colobus*, conventional data (ln)

	r	$100 \times l_1/l_{tot}$
females distal	0.9888	99.44
females proximal	0.9939	99.70
males distal	0.9688	98.44
males proximal	0.9675	98.38

Distributions of these data were distributed normally (Table A.19(c), page 354), and the null hypothesis of normality was accepted. Estimates of k and a (and their confidence intervals) for the males data are presented in Table 4.34. Regression slopes were close to 1.00 (1.01 and 1.04, distal and proximal respectively), and confidence intervals included 1.00.

Table 4.34. Major axis regression slopes (k), intercepts (a) and their 95% confidence limits – *Colobus*, conventional data (ln)

	k	k_1	k_2	a	a_1	a_2
males distal	1.0137	1.1470	0.8961	−1.4408	−2.1312	−0.8317
males proximal	1.0420	1.1825	0.9188	−1.5644	−2.2960	−0.9229

The best estimates of these nonlinear relations were as follows:

males distal $A = 0.2367P^{1.0137}$

males proximal $A = 0.2092P^{1.0420}$.

4.4.2.3.2 Fourier data

Results of the principal component analyses on covariance matrices from raw data are presented in Table A.12(e,f) (page 337). Table 4.35 shows the eigenvalue proportions for the first and last three eigenvalues. Only in the females proximal group did the first eigenvalue account for over 90% of total variance (94.64%). For the other groups, this value ranged from 81.68% to 89.93%. Therefore, only in the females proximal group was PC1 used as an allometric equation.

Table 4.35. Proportions of total variance accounted for by eigenvalues 1 to 3 and 8 to 10 – *Colobus*, Fourier data

	l_1	l_2	l_3	l_8	l_9	l_{10}
females distal	89.83	7.50	1.75	0.03	0.01	0.00
females proximal	94.64	3.14	1.38	0.04	0.02	0.00
males distal	82.96	14.16	1.80	0.02	0.01	0.00
males proximal	81.68	16.90	0.75	0.01	0.01	0.00

The first eigenvector coefficients for females proximal were as follows:

$\boldsymbol{U}_1$ = [0.6777, 0.7349, 0.0035, 0.0077, 0.0199, –0.0014, 0.0060, 0.0057, 0.0117, 0.0080].

Again, this was dominated by ***X*1** and ***Y*1**. The slope and intercept data (jackknifed estimates) of the linear relation between ***X*1** and ***Y*1** are presented in Table 4.36. The intercept was negative, and the confidence limits (wider than those for *Cercopithecus*, in part due to smaller sample size) excluded 0.00.

Table 4.36. Major axis regression slopes (a), intercepts (c) and their 95% confidence limits – *Colobus*, Fourier data

	a	a_1	a_2	c	c_1	c_2
females proximal	1.0826	1.2099	0.9553	−13.2655	−17.2347	−9.2963

The best (jackknifed) estimate of the functional relation was

$$Y1 = 1.0826X1 - 13.2655 .$$

Tenth eigenvalues accounted for almost no variance (all rounded to 0.00%), and ninth eigenvalues accounted for little more than this (0.01% to 0.02%). Sphericity statistics were calculated for ninth versus tenth eigenvalues, and the results are presented in Table 4.37. In males distal, S did not exceed 5.991, so the null hypothesis was accepted: ninth and tenth eigenvalues were not distinct, and these results were considered no further. For the other data sets, S exceeded this figure, so the null hypothesis was rejected. Keeping in mind that the computation of S assumed large sample sizes, and these samples were small (26 female and 21 male specimens), only S for females proximal was clearly above the critical level of 5.991.

Table 4.37. Sphericity statistics (S) for eigenvalues 9 and 10 – *Colobus*, Fourier data

	l_9	l_{10}	$S(l_9, l_{10})$
females distal	0.0013	0.0003	6.70
females proximal	0.0029	0.0003	11.50
males distal	0.0023	0.0005	4.60
males proximal	0.0023	0.0004	6.04

The coefficients of the tenth eigenvectors were as follows:

females distal

U_{10} = [0.0813, −0.0687, −0.0644, 0.0980, −0.7703, −0.0681, −0.2066, 0.0348, 0.5111, 0.2677]

females proximal

U_{10} = [0.0713, −0.0583, 0.0431, 0.0524, −0.7221, −0.0255, −0.1328, −0.0537, 0.5710, 0.3440]

males proximal

U_{10} = [0.1285, –0.1120, 0.2545, –0.1128, –0.8295, –0.1916, 0.1152, –0.1365, 0.2365, 0.2843].

The tenth eigenvectors all had high coefficients for ***X3***, and to lesser extents, ***X5*** and ***Y5***.

4.4.2.4 *Gorilla*

4.4.2.4.1 conventional data

Correlation coefficients and percentages of total variance explained by the first eigenvalue are presented in Table 4.38. These approximated 1.00 (0.9692 to 0.9967) and 100% (99.68% to 99.97%), respectively, very closely, so it was appropriate to investigate linear relations.

Table 4.38. Product-moment correlation coefficients (r) and percentages of total variance accounted for by eigenvalue 1 – *Gorilla*, conventional data

	r	$100 \times l_1/l_{tot}$
females distal	0.9844	99.81
females proximal	0.9692	99.68
males distal	0.9810	99.80
males proximal	0.9967	99.97

Table A.19(d) (page 354) shows that data were distributed normally, and the null hypothesis of normality was accepted. The slope and intercept values, together with their respective confidence limits, are presented in Table 4.39. Intercepts varied in sign and strength (–10.08 to 9.75). A zero intercept was only excluded by the confidence limits in males proximal, and only barely (0.34 to 19.10). In the other groups, 0.00 was included in the confidence limits.

Table 4.39. Major axis regression slopes (a), intercepts (c) and their 95% confidence limits – *Gorilla*, conventional data

	a	a_1	a_2	c	c_1	c_2
females distal	0.2609	0.2878	0.2344	–10.0971	–20.9715	0.6156
females proximal	0.2367	0.2715	0.2024	3.5465	–11.4938	18.3707
males distal	0.2407	0.2837	0.1985	1.3611	–23.2729	25.5349
males proximal	0.2302	0.2471	0.2135	9.7343	0.0928	19.0574

The best estimates of these linear relations were thus:

females distal	$A = 0.2609P - 10.0971$
females proximal	$A = 0.2367P + 3.5465$
males distal	$A = 0.2407P + 1.3611$
males proximal	$A = 0.2302P + 9.7343$.

Correlation coefficients and percentages of total variance explained by the first eigenvalue (logarithmic data) are presented in Table 4.40. Nearly all of these values suggested that the linear functional relation was more appropriate than the nonlinear relation, and as intercepts were large, nonlinear relations were not estimated.

Table 4.40. Product-moment correlation coefficients (r) and percentages of total variance accounted for by eigenvalue 1 – *Gorilla*, conventional data (ln)

	r	$100 \times l_1/l_{tot}$
females distal	0.9815	99.09
females proximal	0.9662	98.31
males distal	0.9809	99.05
males proximal	0.9968	99.84

4.4.2.4.2 Fourier data

Table A.12(g,h) (page 339) shows the results of the principal component analyses on covariance matrices from raw data. Eigenvalue proportions for the first and last three eigenvalues are presented in Table 4.41. In females distal and males proximal the first eigenvalue exceeded 90% of total variance (95.96% and 97.59%, respectively). Therefore, simple allometry was detected in these two groups. The first eigenvector coefficients for females distal and males proximal were

$\boldsymbol{U}_1$ = [0.8477, 0.5240, –0.0117, –0.2356, 0.0712, –0.0092, –0.0036, 0.0096, 0.0286, 0.1171],

and

$\boldsymbol{U}_1$ = [0.9046, 0.4122, 0.0068, 0.0598, 0.0653, 0.0426, 0.0335, 0.0147, 0.0113, 0.0261],

respectively.

Table 4.41. Proportions of total variance accounted for by eigenvalues 1 to 3 and 8 to 10 – *Gorilla*, Fourier data

	l_1	l_2	l_3	l_8	l_9	l_{10}
females distal	95.96	3.27	0.57	0.00	0.00	0.00
females proximal	90.73	8.47	0.41	0.00	0.00	0.00
males distal	89.43	6.19	4.08	0.00	0.00	0.00
males proximal	97.59	1.45	0.54	0.00	0.00	0.00

The jackknifed slope and intercept data for these two groups are presented in Table 4.42 for the relation $Y1 = aX1 + c$. The intercept was negative for females distal, positive for males proximal. In males proximal, but not females distal, the intercept confidence limits included 0.00.

Table 4.42. Major axis regression slopes (a), intercepts (c) and their 95% confidence limits – *Gorilla*, Fourier data

	a	a_1	a_2	c	c_1	c_2
females distal	0.5975	0.7121	0.4829	−10.3710	−19.3109	−1.4310
males proximal	0.4623	0.5678	0.3568	7.4894	−3.6746	18.6534

The best estimates of these functional relations were

females distal $Y1 = 0.5975X1 - 10.3710$

males proximal $Y1 = 0.4623X1 + 7.4984$.

Tenth eigenvalues for females accounted for almost zero variance (in fact, the last three eigenvalues – rounded – accounted for 0.00%). Tenth eigenvalues for the males had to account for exactly zero variance, as the covariance matrix was not of full rank ($n = 9$, $p = 10$). Functional relation estimation using the tenth eigenvector was therefore only appropriate for female specimens. Sphericity statistics were calculated to determine the distinctness of the tenth eigenvalues, and these results are presented in Table 4.43. These statistics fell well short of the critical value (5.991), so the null hypothesis was accepted, and functional relations were not pursued.

Table 4.43. Sphericity statistics (S) for eigenvalues 9 and 10 – *Gorilla*, Fourier data

	l_9	l_{10}	$S(l_9, l_{10})$
females distal	0.0010	0.0003	2.95
females proximal	0.0010	0.0004	1.21

4.5 Discussion

4.5.1 Size-adjustment

4.5.1.1 Principal component analysis

Normalization of data vectors led to some general results. With the conventional data, variances of variables were unequal, but this time it was the variance of A that dominated (cf. Chapter 3). The reason for this can be seen in Figure 4.9: due to the greater magnitude of P in the raw data set, the specimens in the normalized data set came to lie on the lower part of the upper right quadrant of the circle $A^2 + P^2 = 1$, so that the data scatter approximated the vertical line $P = 1$. In other words, the dominance of P in the raw data set meant that removing the effect of size largely removed variance of P; the variance of A was at least an order of magnitude greater than that of P (normalized data). Transformation to natural logarithms only amplified these differences, so raw data were used for ordination. Correlations between variables approximated −1.00; the negative correlation was due to the fact that, as the vector lengths were constrained to unity, a relative increase in one variable was met with a relative decrease in the other. First eigenvalues accounted for 100% of variance of these normalized vectors (when rounded to two decimal places), which confirmed that the arc of scatter of these points approximated a straight line. The first principal component of the normalized data represented a contrast between P and A – that is, higher values of one variable, say P, were accompanied by lower values of A, and vice versa. The value of A relative to that of P reflected the likeness of the outline to a circle: a circle has the greatest area per unit perimeter length, less circular forms having less relative area. The ratio A/P then expressed the proportion of the square root of area relative to perimeter length, which was of the form of Mosimann's shape variables (§4.1.1.2); a perfectly circular specimen would have a ratio of A/P of

$$\frac{\sqrt{\pi \cdot r^2}}{2\pi \cdot r} \approx 0.28 .$$

The first principal component thus reflected the circularity, or shape, of the specimen outlines; this was an example of the concept of shape as relative measurements (§4.1). Figure 4.10 (at end of §4.5.1.1) shows the CT images of the specimens lying at the extremes of these scatters, as well as those specimens closest to the mean score on PC1 (normalized), and illustrates the contrast between A and P. Specimens on the left had the lowest score on PC1 (normalized),

and were relatively circular (this was supported by their respective values of ***A/P***, the highest in each group). Specimens on the right had the highest scores on PC1 (normalized), and were less circular specimens (with lowest values of ***A/P***). A less circular specimen could have deviated from circularity globally (was flatter, or more elliptic), or more locally (showed a local concavity or convexity – a hollow or a bulge). For instance, the proximal image from specimen 75 (*Homo* females) appeared less flat than other less circular specimens, but showed a slightly recurved outline on its lateral articular facet, which would have accounted in part for the low value of ***A/P***. The distal outline of specimen 513 (*Cercopithecus* males) showed both a generally flat outline, which also featured local irregularities (although the dorsal exostosis on the right of the image was not included in the outline). Of note also was *Cercopithecus* males specimen 504, whose proximal outline approximated very closely the figure of 0.28 (0.2736), and provided an effective illustration of a circular outline. The central specimens in each case showed that these 'mean' specimens did occupy a midpoint between the two extremes in terms of shape. It is clear from Figure 4.10, as it was suggested in Chapter 3, that shape variation was constrained: the extreme shapes, while different, still resembled each other, and did not vary remarkably.

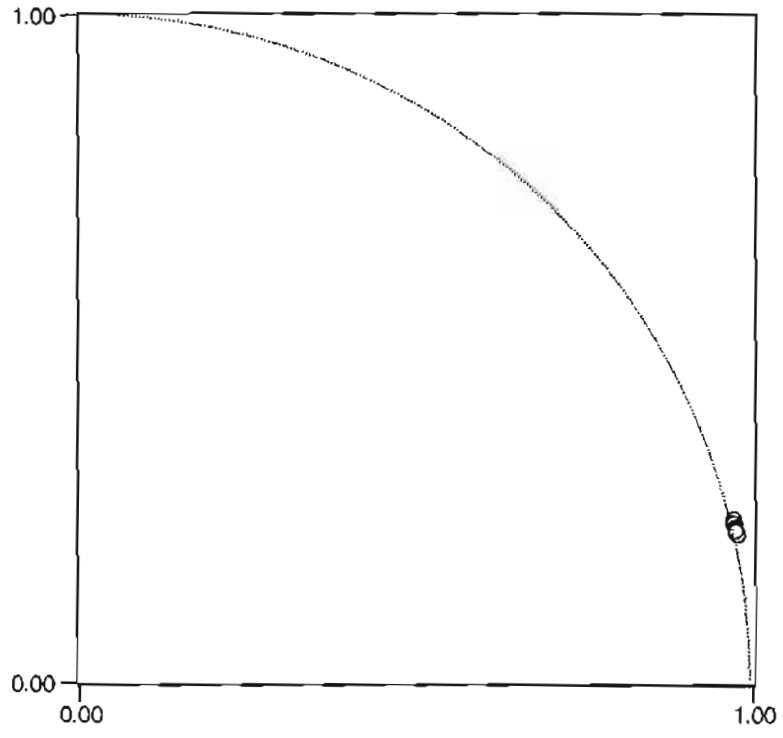

Figure 4.9. Scatterplot of ***A*** (*y*-axis) versus ***P*** (*x*-axis) for *Homo* females proximal, also showing the upper right quadrant of circle $A^2 + P^2 = 1$

For Fourier data, variances were larger for ***X1*** and ***Y1***, and also for ***Y2***, than for other variables. Almost perfect negative correlations were seen between ***X1*** and ***Y1***, which reflected their magnitudes – as, say, ***X1*** increased across the sample, ***Y1*** had to decrease to produce a vector of unit length (alterations in other variables would not have been sufficient). First eigenvalues of these normalized data accounted for widely varying amounts of variance, and in general the dominance of the first eigenvalue was not overwhelming. The addition of a second eigenvalue brought the variance accounted for to at least 80% of the total, so plotting the scores on the first two axes was justified. The coefficients of PC1 (normalized) mostly reflected a contrast between ***X1*** and ***Y1***; thus, PC1 (normalized) reflected a contrast between patellar breadth (***X1***) and depth (***Y1***). This recalled the notion of circularity seen with the conventional data – contrasts between ***X1*** and ***Y1*** ranged from small (breadth and depth more similar, therefore a more circular patella) to large (disparate breadth and depth, therefore more elliptic). Less circular patellae in this respect must have been elliptic, as the first harmonic could only measure the most global aspects of patellar outline form. Also, these specimens were elliptic in that they were broader than they were deep, as no specimen was seen that was deeper than it was broad. That this component was not overwhelming suggested a substantial proportion of morphometric variance in directions away from this pattern. This was not unexpected, since from the conventional data it was seen that less circular forms could show more local deviations from circularity. (An advantage to using Fourier data over the simple conventional variables was that more complex patterns of variation might be uncovered. This advantage was tempered by the knowledge that interpretation of the Fourier data was much more difficult.) This might have been the interpretation of PC2 (normalized); this component was dominated by higher-order amplitudes, especially ***Y2***, and was not interpreted. An exception to this pattern was found in *Gorilla* males distal, where the first component represented a contrast between ***X1*** on one hand and ***Y1***, ***X2***, ***Y2*** and ***X4*** on the other; interpretation of this component was again not attempted. To gain further insight into the patterns of variation, Figure 4.11 (following Figure 4.10) shows the specimens at the extremes of these two components, as well as specimens closest to the mean scores on these components. The first component overall reflected shape differences from circular to elliptic. Indeed, in most cases the specimens at the negative and positive extremes of this component were those with maximal and minimal values for the ratio ***Y1/X1***; in several cases there were specimens with more extreme values of this ratio. In *Homo* females distal, specimen 78 had a value of 0.6000. In *Homo* males proximal, specimen 177 had a value of 0.5931. In *Cercopithecus* males distal, specimen 534 had a value of 0.4978. This merely showed that PC1 (normalized) was not completely explained by ***X1*** and ***Y1***, and that other variables contributed to principal component scores. However, this did not contradict the general

finding of an axis spanning the range from circular to elliptic shapes, which explained the bulk of morphometric variation excluding size. As PC2 (normalized) featured high weightings for higher-order harmonics (especially amplitude ***Y2***), this must have reflected more local morphological features. However, the contribution of the second eigenvector to total variance was low compared to that of the first, so such local features were expected to be more subtle. The largest relative second eigenvalues tended to be found in *Homo*, which suggested greater local morphological variation where Figure 4.11 shows articular concavities at the positive and negative extremes for females and males, respectively; these articular concavities could have been related to PC2 (normalized), but the present study did not speculate on the likelihood of this.

The results of Chapter 3 suggested that the first and second principal components of raw data might have been suitable measures of size and shape, respectively, despite concerns raised in §2.2.2.1.3. To elucidate this theory, angles were measured between the first two principal components of raw data and the first principal component of normalized data. Angles between PC1 (raw) and PC1 (normalized) were typically close to 90°, and those between PC2 (raw) and PC1 (normalized) were typically close to zero (but see §4.5.1.3.2 for a comparison of conventional and Fourier data). For conventional data there were only two dimensions, so θ_2 was expected to have equalled $90 - \theta_1$; presumably the slight nonlinearity of the normalized data sometimes caused subtle deviations from this. For PC1 (raw) to be a measure of size it must also have been a measure of size-related shape (Bookstein, 1989; Flessa and Bray, 1977; Klingenberg, 1998; Oxnard, 1978); PC2 (raw) should then have been a measure of size-unrelated shape. That PC1 (normalized) was nearly parallel with PC2 (raw), suggested that size-related shape was a relatively minor contributor to morphometric variation, as the former and the latter should have reflected shape (size-related and -unrelated) and size-unrelated shape, respectively. If, say, PC2 (raw) were perfectly correlated with PC1 (normalized), size-related shape (allometry) would have been absent. For linear relations, allometry is signified by a nonzero intercept: this intercept means that the linear relation does not pass through (0, 0), and therefore specimens along this line differ in terms of proportional measurements. Shifting the mean of observations to the origin does not alter this, but information about rays from the origin is lost. The only way for PC2 (raw) to coincide with PC1 (normalized) was therefore for the linear relation to have passed through the origin, i.e. geometric similarity must have existed. That these components differed (albeit slightly in some cases) reflected a deviation from geometric similarity i.e. allometry. The results from the distal images for *Gorilla* females and males went against this trend, as substantial angles were found between PC2 (raw) and PC1 (normalized) in the distal sets of Fourier data.

Also in Chapter 3, several specimens were conspicuous due to their position on principal component axes. Specimens 87 (*Homo* females proximal), and 671 and 672 (*Gorilla* females distal and proximal) were seen as extreme on PC1 (raw) (both conventional and Fourier data), and it was suggested that these specimens were extreme on size, i.e. they were conspicuously large. Specimens 657 and 658 (*Gorilla* females distal) on both sets of data, and specimen 656 (*Gorilla* males distal) were extreme (at the positive end) on PC2 (raw), and it was suggested that these specimens showed conspicuously different shape to the rest of the specimens. Perusal of the scatterplots of normalized variables supported these conclusions: specimens 87, 671 and 672 were not found at extremes on these scatterplots. Figure 4.6 shows the positions of these specimens on the Fourier plots (it was impossible to locate the specimens on the conventional plots, as they were grouped with most of the other specimens, and therefore not in extreme positions), which confirmed that, when size was not considered, these specimens were not outstanding. Figure 4.6 also shows the positions of specimens 656, 657 and 658, which, while not necessarily outstanding, were in extreme positions on PC1 (normalized), the 'shape' axis.

Figure 4.10. Computed tomography images from specimens with the lowest (left), highest (right), and closest to mean (centre) scores on PC1 (normalized) – conventional data (***A/P*** value in parentheses)

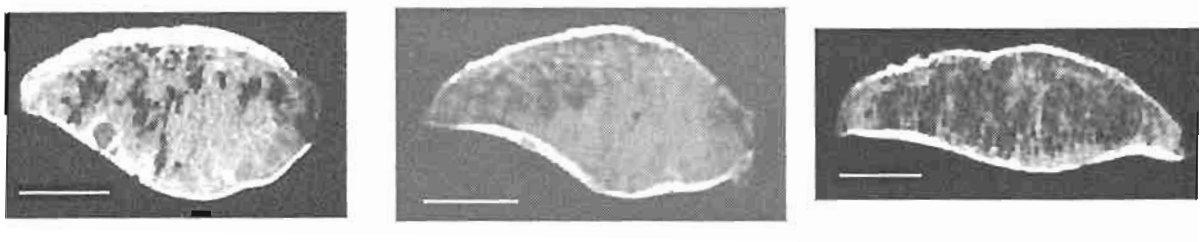

106 (0.2535) **8 (0.2388)** **136 (0.2174)**

(**i**) females distal (mean = 0.2387)

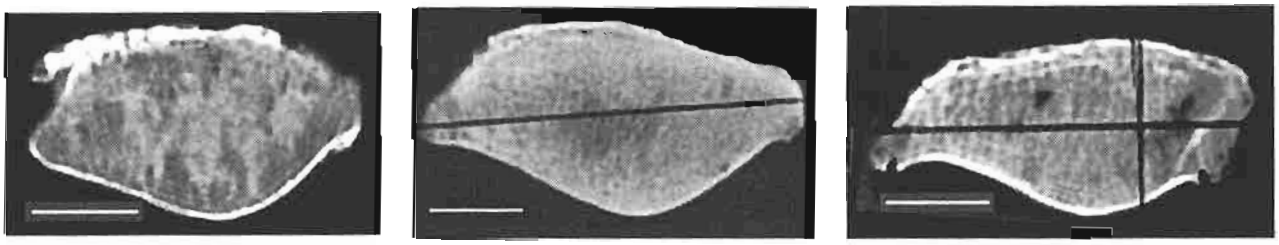

206 0.2547 **24 (0.2409)** **75 (0.2284)**

(**ii**) females proximal (mean = 2408)

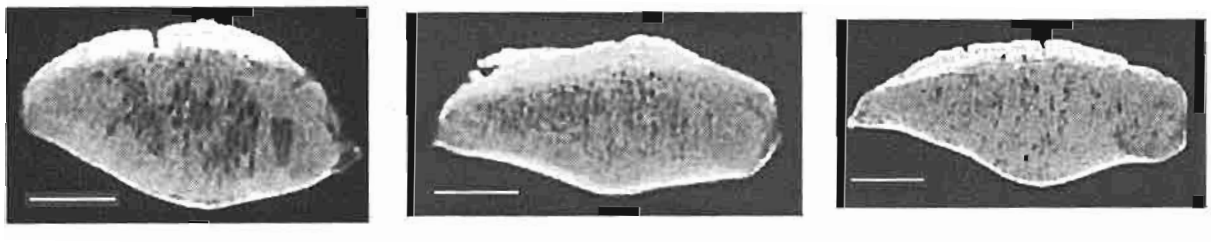

194 (0.2536) **122 (0.2386)** **215 (0.2263)**

(**iii**) males distal (mean = 0.2386)

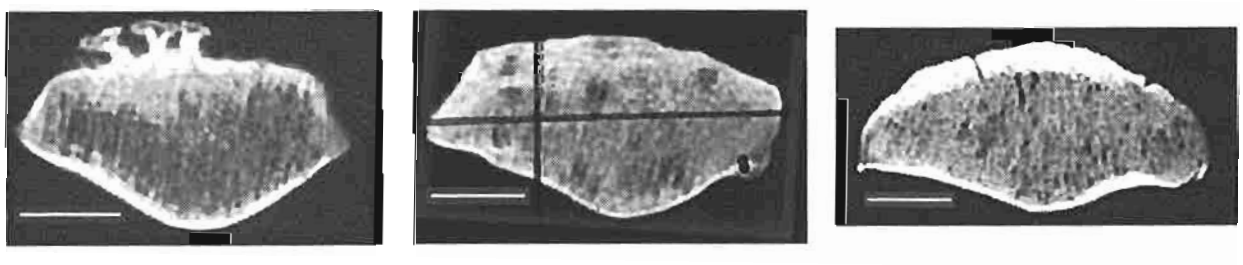

177 (0.2529) **81 (0.2393)** **134 (0.2274)**

(**iv**) males proximal (mean = 0.2393)

(**a**) *Homo* (bar = 10mm)

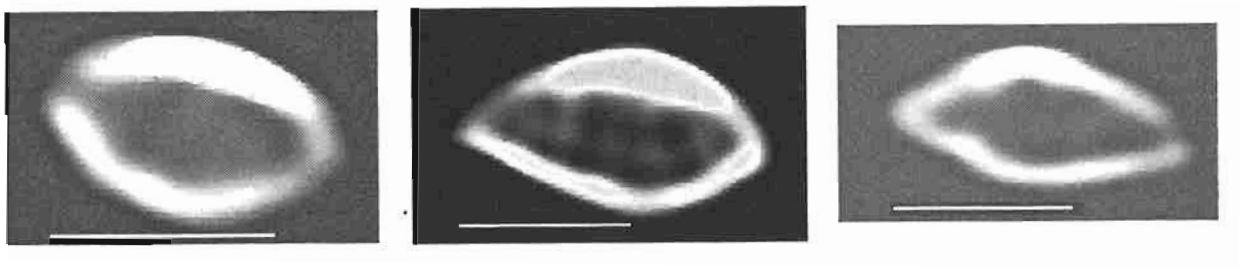

502 (0.2687) 570 (0.2567) 551 (0.2425)

(i) females distal (mean = 0.2568)

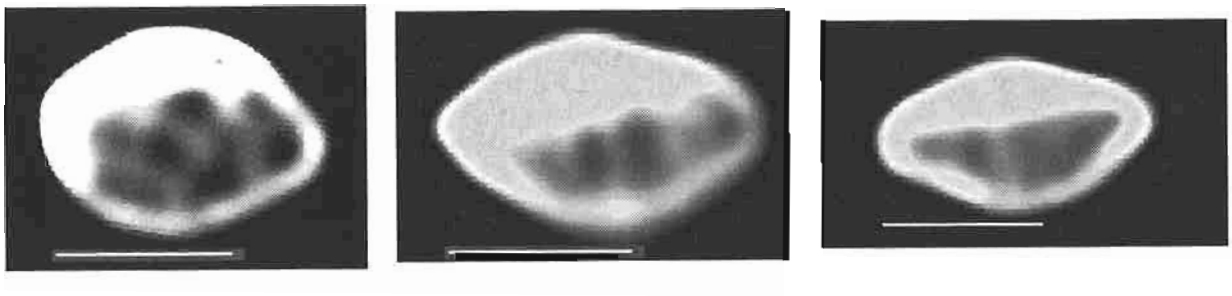

593 (0.2734) 522 (0.2647) 525 (0.2587)

(ii) females proximal (mean = 0.2650)

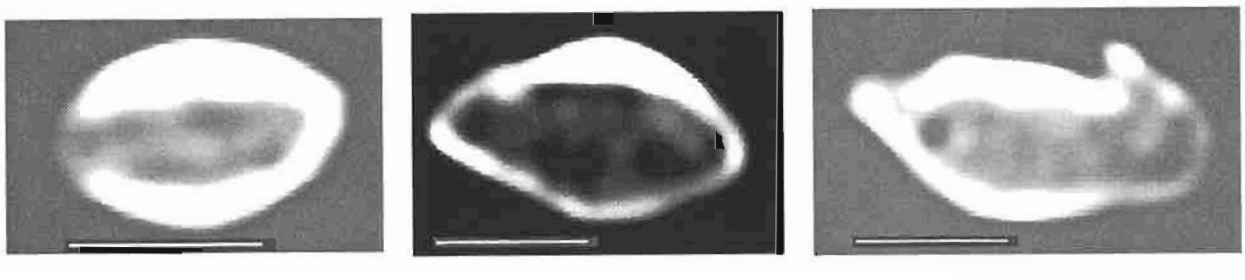

514 (0.2711) 590 (0.2565) 513 (0.2375)

(iii) males distal (mean = 0.2560)

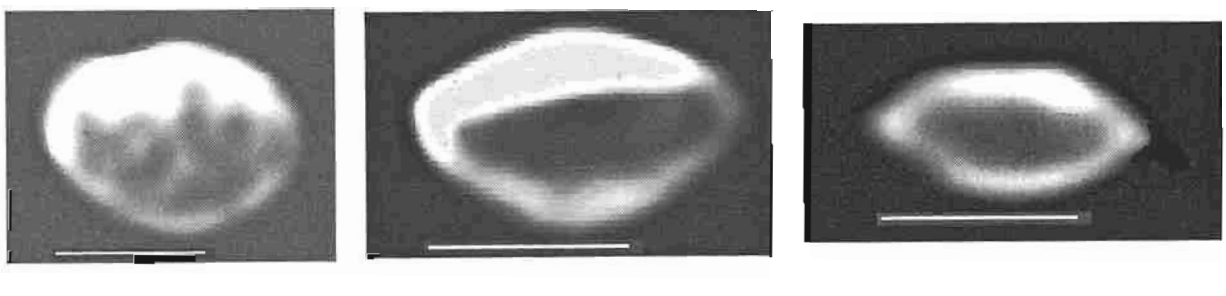

504 (0.2736) 529 (0.2643) 533 (0.2501)

(iv) males proximal (mean = 0.2642)

(b) *Cercopithecus* (bar = 10mm)

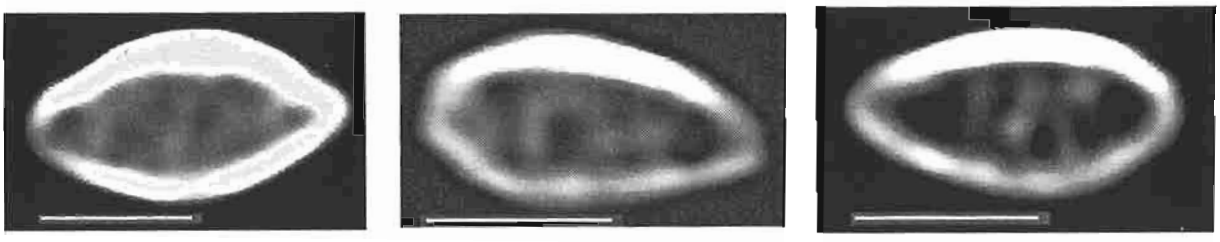

644 (0.2595) 632 (0.2538) 633 (0.2435)

(i) females distal (mean = 0.2535)

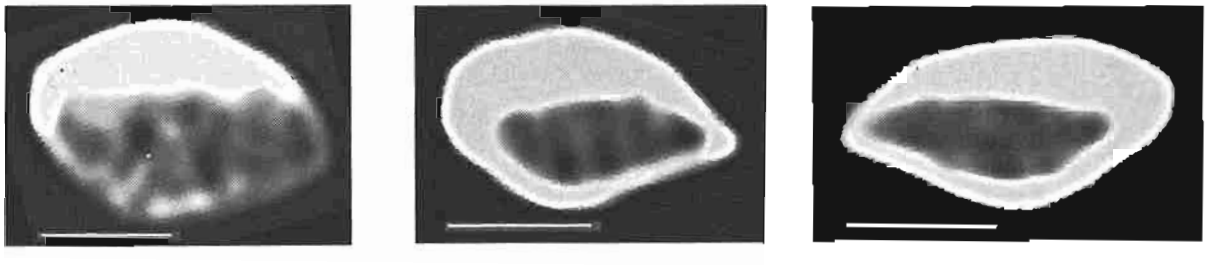

619 (0.2693) 615 (0.2607) 605 (0.2521)

(ii) females proximal (mean = 0.2605)

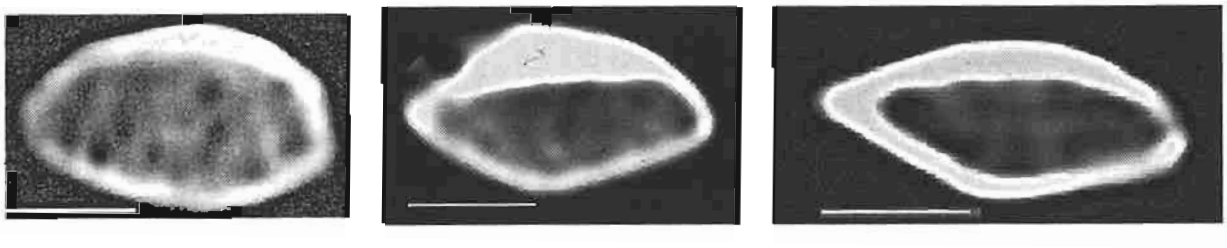

640 (0.2649) 613 (0.2540) 609 (0.2414)

(iii) males distal (mean = 0.2542)

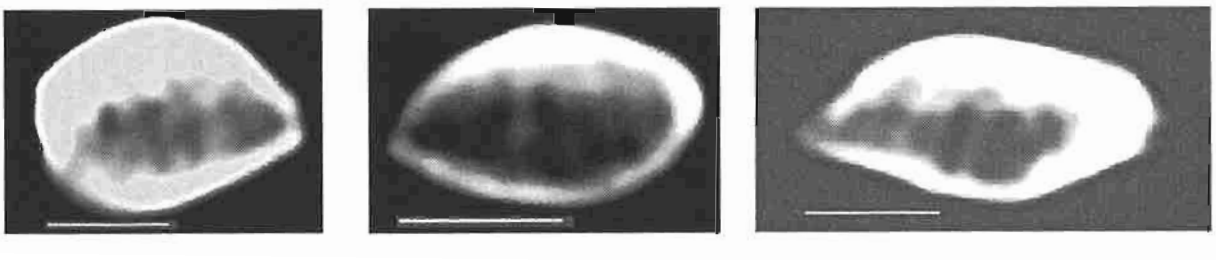

627 (0.2713) 624 (0.2604) 607 (0.2457)

(iv) males proximal (mean = 0.2605)

(c) *Colobus* (bar = 10mm)

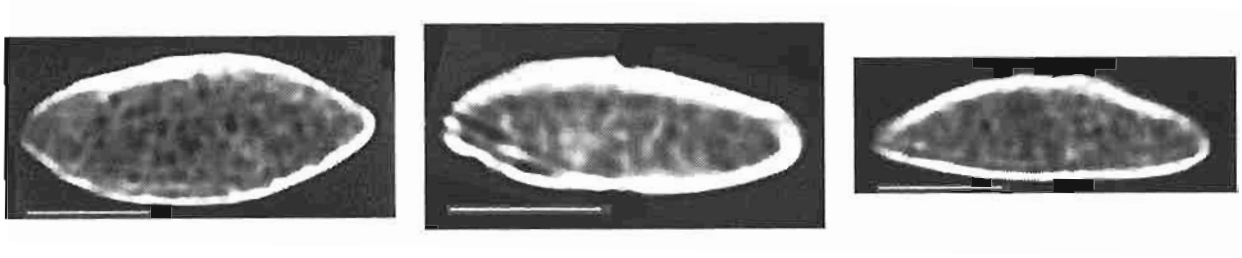

662 (0.2436) 650 (0.2348) 658 (0.2200)

(i) females distal (mean = 0.2355)

663 (0.2521) 668 (0.2454) 658 (0.2346)

(ii) females proximal (mean = 0.2450)

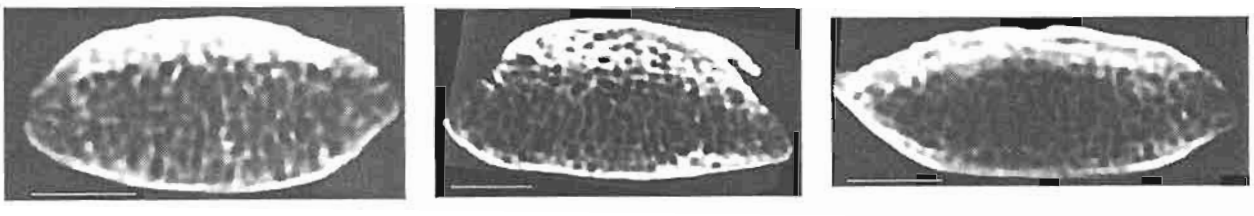

659 (0.2499) 651 (0.2435) 656 (0.2350)

(iii) males distal (mean = 0.2431)

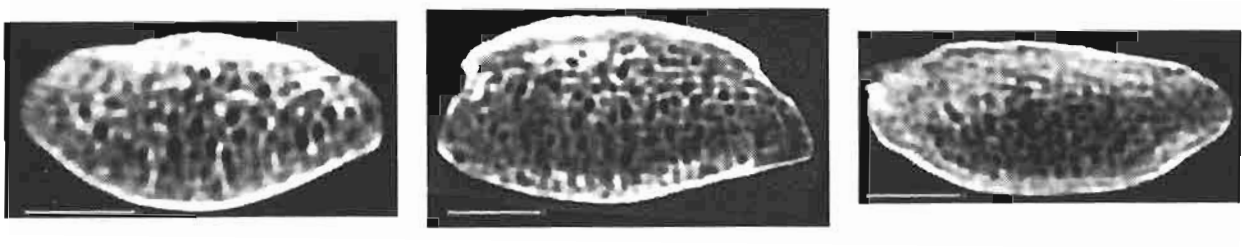

660 (0.2530) 651 (0.2473) 656 (0.2424)

(iv) males proximal (mean = 0.2479)

(d) *Gorilla* (bar = 10mm)

Figure 4.11. Computed tomography images from specimens with the lowest (left) and highest (right) scores on PC1 (normalized), highest (top) and lowest (bottom) scores on PC2 (normalized), with the specimen closest to the mean of both axes (centre) – Fourier data (***Y1/X1*** value in parentheses)

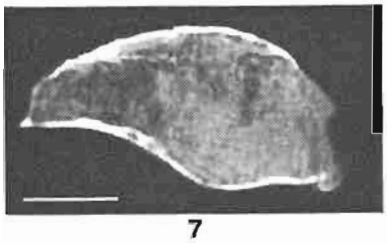

7

106 (0.5992)

66 (0.4838)

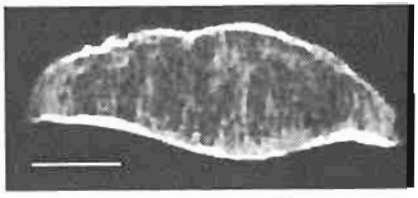

136 (0.3927)

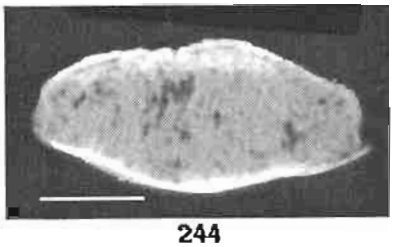

244

(i) females distal

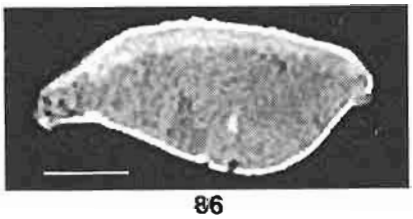

86

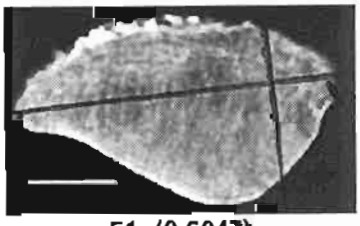

51 (0.6047)

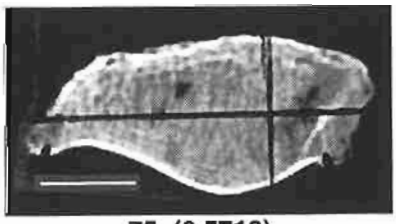

75 (0.5713)

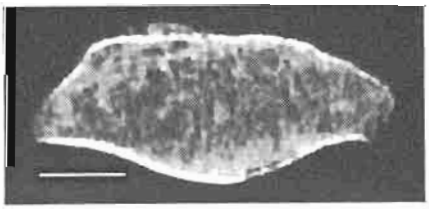

136 (0.4474)

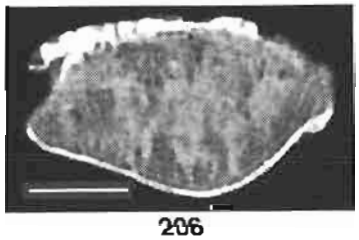

206

(ii) females proximal

(a) *Homo* (bar = 10mm)

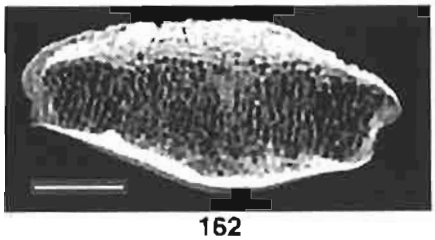

162

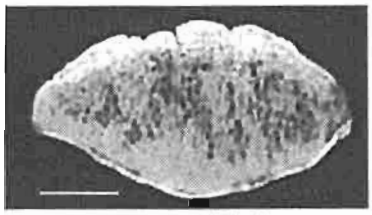

195 (0.5794)

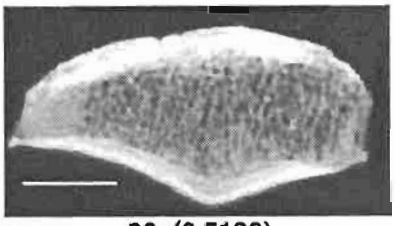

98 (0.5133)

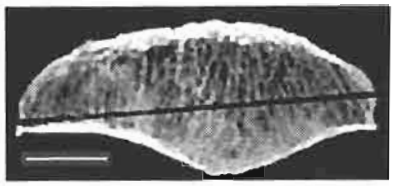

52 (0.4386)

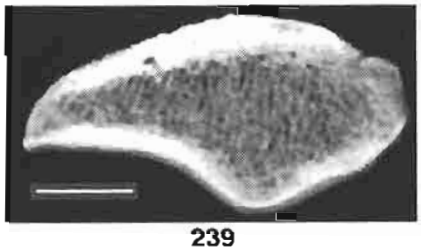

239

(iii) males distal

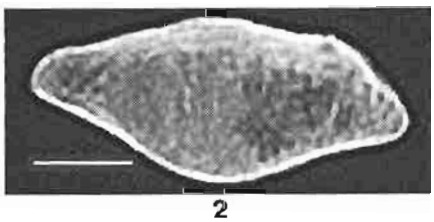

2

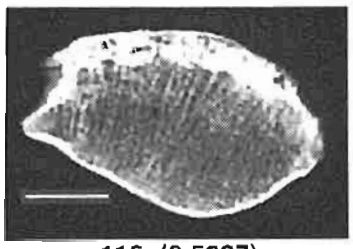

116 (0.5927)

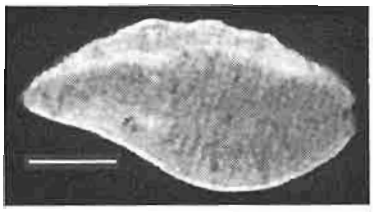

214 (0.5179)

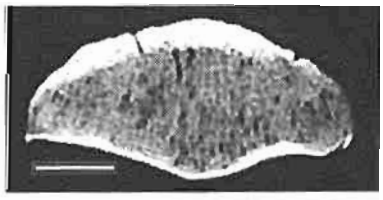

134 (0.4472)

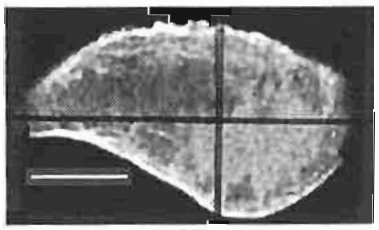

37

(iv) males proximal

(a) (continued)

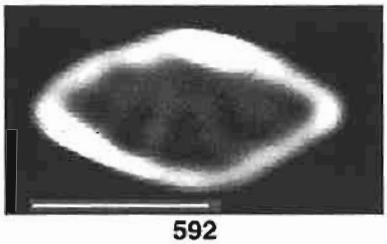

592

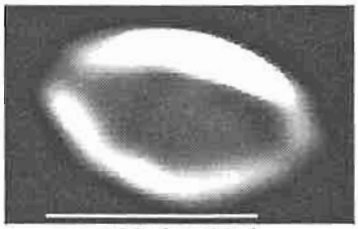

502 (0.7068)

561 (0.6120)

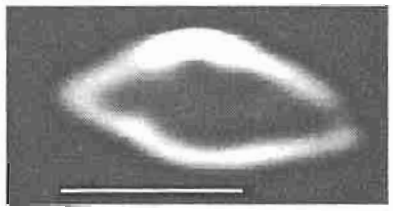

551 (0.5200)

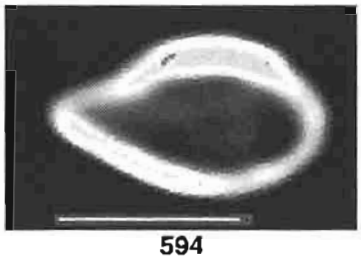

594

(i) females distal

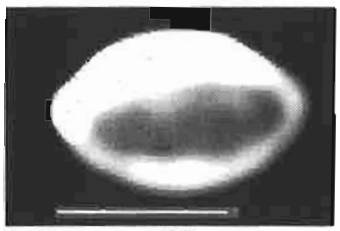

596

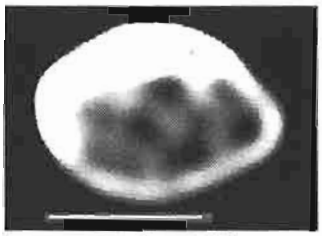

593 (0.7819)

570 (0.6862)

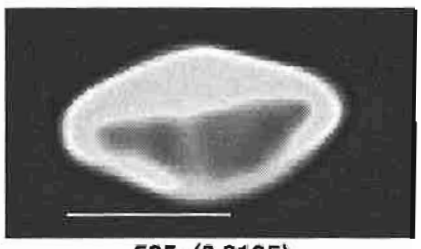

525 (0.6195)

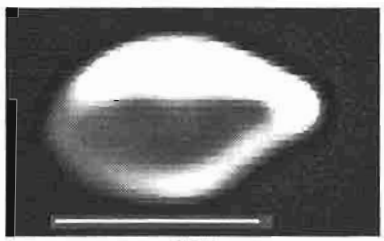

537

(ii) females proximal

(b) *Cercopithecus* (bar = 10mm)

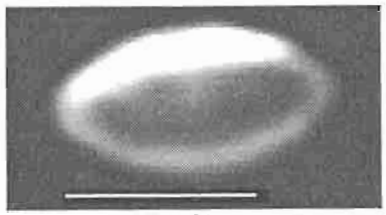

516

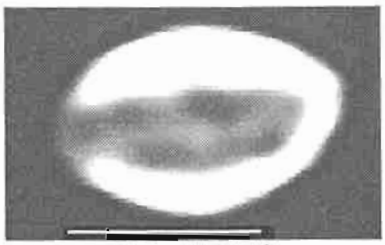

514 (0.7238)

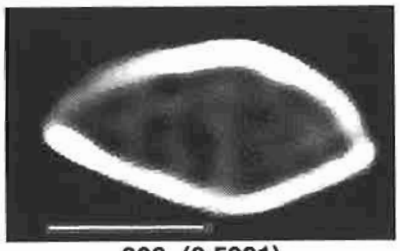

600 (0.5991)

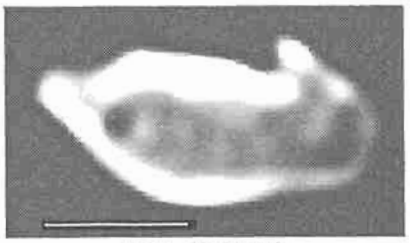

513 (0.4999)

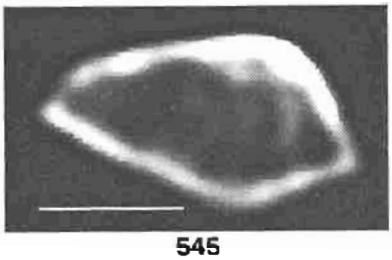

545

(iii) males distal

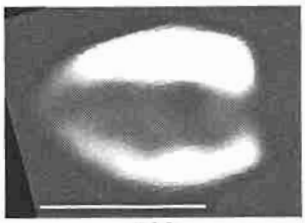

530

532 (0.7854)

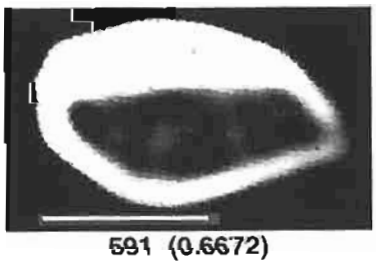

591 (0.6672)

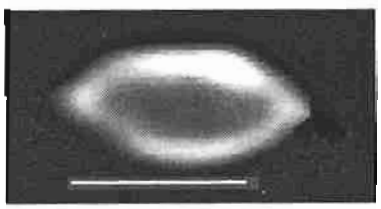

533 (0.5656)

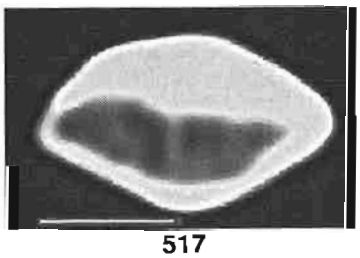

517

(iv) males proximal

(b) (continued)

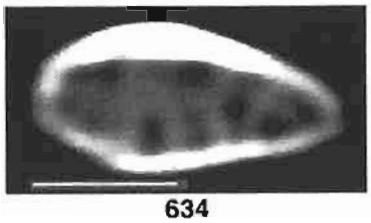

634

621 (0.6987)

610 (0.6213)

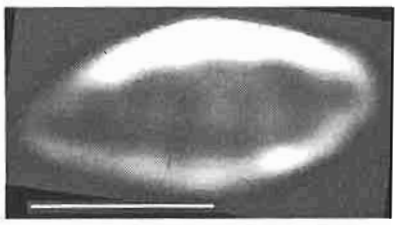

622 (0.5307)

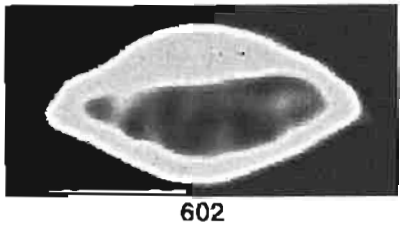

602

(i) females distal

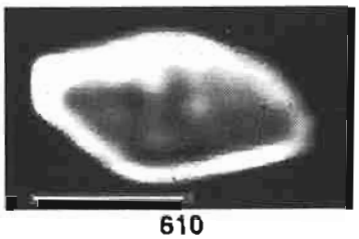

610

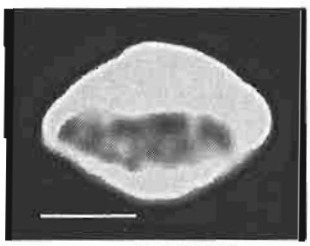

644 (0.7423)

621 (0.6623)

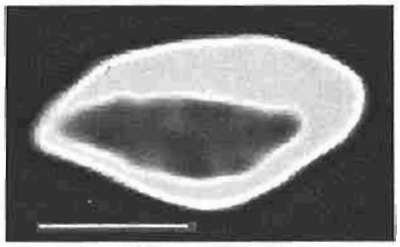

605 (0.5791)

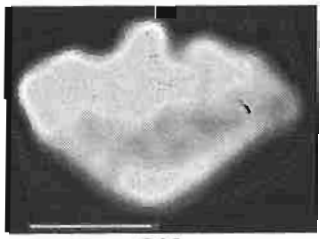

616

(ii) females proximal

(c) *Colobus* (bar = 10mm)

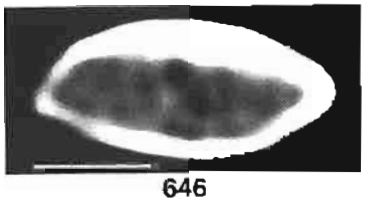

646

604 (0.6726)

no close-to-mean specimen

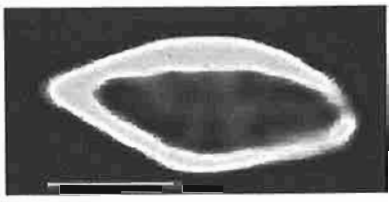

609 (0.5069)

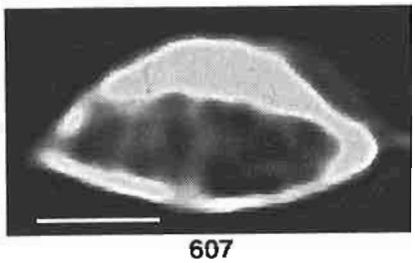

607

(iii) males distal

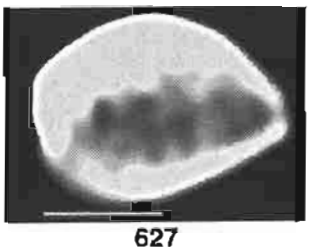

627

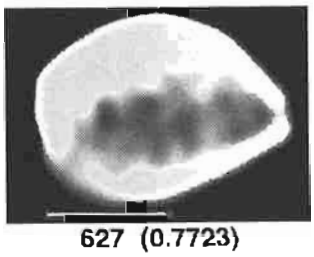

627 (0.7723)

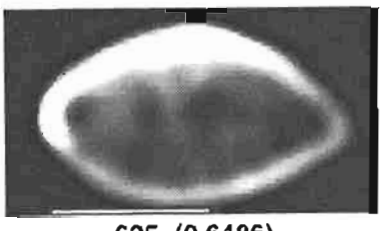

625 (0.6486)

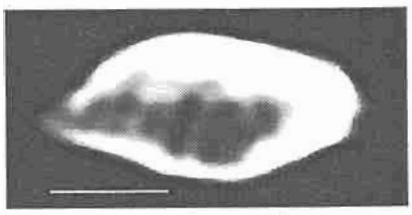

607 (0.5357)

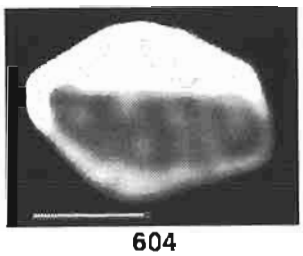

604

(iv) males proximal

(c) (continued)

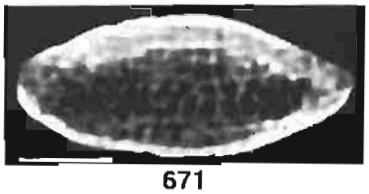

671

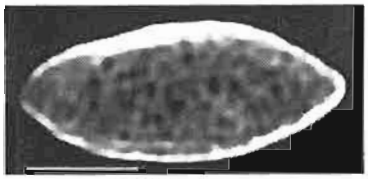

662 (0.5037)

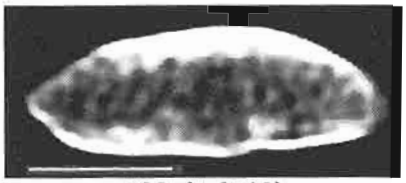

666 (0.4518)

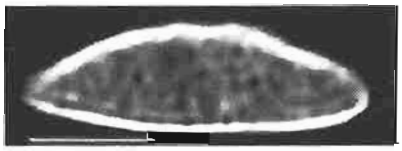

658 (0.3914)

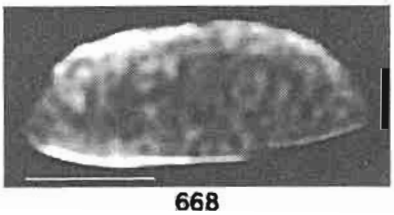

668

(**i**) females distal

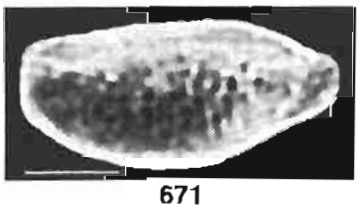

671

661 (0.5569)

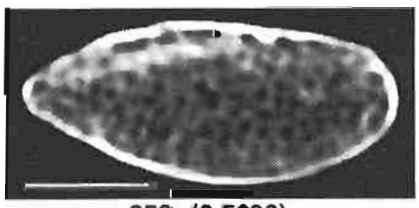

653 (0.5090)

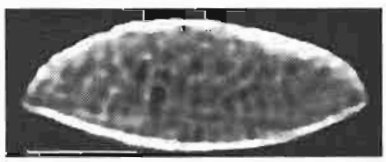

658 (0.4559)

654

(**ii**) females proximal

(**d**) *Gorilla* (bar = 10mm)

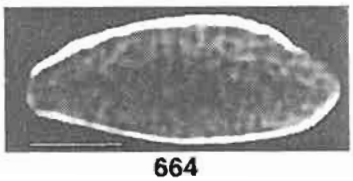

664

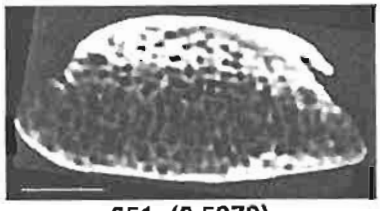

651 (0.5379)

648 (0.4882)

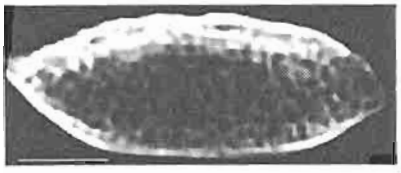

656 (0.4604)

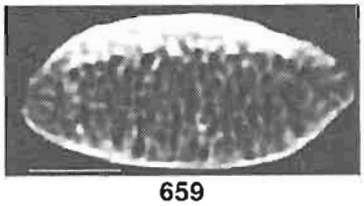

659

(**iii**) males distal

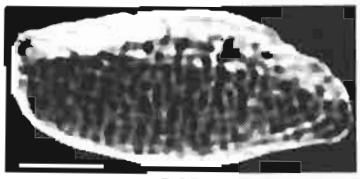

649

660 (0.5657)

665 (0.5402)

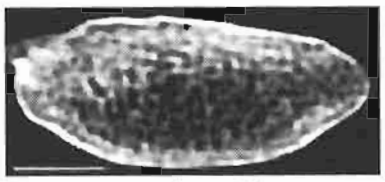

656 (0.4987)

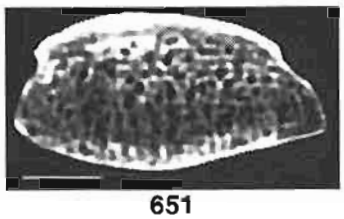

651

(**iv**) males proximal

(**d**) (continued)

4.5.1.2 Cluster analysis

To gain insight into the effects of size and shape on cluster analysis, it was necessary to repeat the size-included analyses, this time based on genus average measurements, as cophenetic correlations could not justify interpreting size-adjusted cluster analyses based on individual specimens. Generalized distance was used as a measure of total morphometric dissimilarity (both size and shape differences) among genera. The measure $(1-\cos)_G$ reflected the separation of genera based on direction (shape, both size-related and -unrelated). The cluster analysis tree plots only gave information about relative separation (or clustering), and did not allow for distinguishing between size-related and size-unrelated shape differences.

In general, *Homo* and *Gorilla* (hominoids) on one hand, and *Cercopithecus* and *Colobus* (cercopithecoids) on the other, were more similar (requiring less dissimilarity to cluster) to each other than to any other genus, based on either dissimilarity measure. Thus, despite cancellation of the great size differences among these genera, cercopithecoids were never clustered with hominoids until the final (all-inclusive) step. Consequently, the gap in phenotype space between cercopithecoids and hominoids seen in Chapter 3 comprised a substantial amount of shape information. Relative to the cercopithecoids, hominoids showed greater dissimilarity based on generalized distance, which was much reduced when $(1-\cos)_G$ was used. That is, size differences cancelled, there was still a relatively greater difference (i.e. in shape) between *Homo* and *Gorilla* than between the cercopithecoids. Therefore, relative to the cercopithecoids, the morphometric dissimilarity between *Homo* and *Gorilla* was largely due to size. Alternatively, relative to the hominoids, the dissimilarities between *Cercopithecus* and *Colobus* were largely not of size, but of shape. This effect was less pronounced for males using conventional data; using Fourier data, the effect was less pronounced for females. It was not known why this finding ensued. It was logical that Fourier data might have carried more morphometric information than conventional data, as there were eight more Fourier variables than conventional; after all, this was the main reason for using a greater number of variables, as increased information (hopefully) made up for the attendant inconvenience. It could have been that there simply was less morphometric information to be gathered from males, especially regarding outline shape.

Figure 4.12 shows the tree diagrams for females distal data with the inclusion of the *Elephas* specimens. The results for conventional data and for Fourier data were vastly different: Fourier data showed that there was great dissimilarity between the primate and elephant

specimens, a difference not detected using conventional data, which showed the latter to be relatively close in phenetic similarity to the cercopithecine specimens.

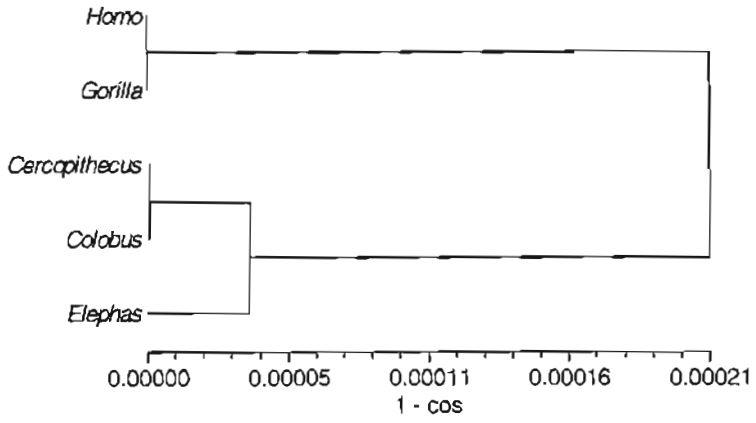

(**a**) conventional data

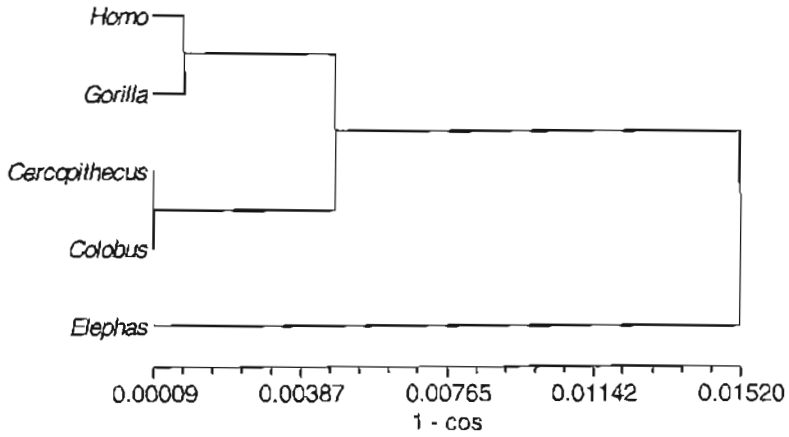

(**b**) Fourier data

Figure 4.12. UPGMA tree diagrams from Figures 4.7 and 4.8 with the addition of mean *Elephas* data – females distal data

Figure 4.13 is a companion to Fig 3.12, in that it shows error-bar graphs for males and females, this time for ***A/P*** (a measure of shape). Comparing the two sets of graphs, it can be seen that the means for both ***A*** and ***A/P*** were reasonably similar for *Cercopithecus* and *Colobus*, so these two genera provided an appropriate reference point. In relation then to the cercopithecoids, *Homo* and *Gorilla* females were more different in terms of size than shape. Conversely, and again in relation to the cercopithecoids, *Homo* and *Gorilla* males were more

different in terms of shape than size. These graphs then support the findings of the cluster analyses.

Figure 4.13. Error bars (y-axis) for A/P (values on y-axis, squares at means, bars represent ± 2 standard errors)

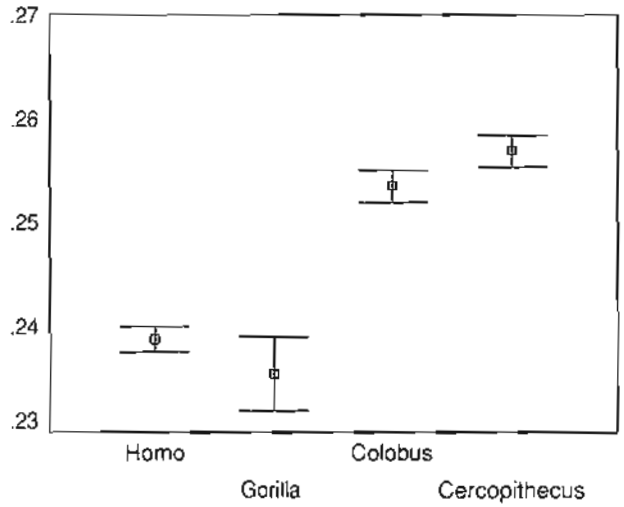

(a) females distal

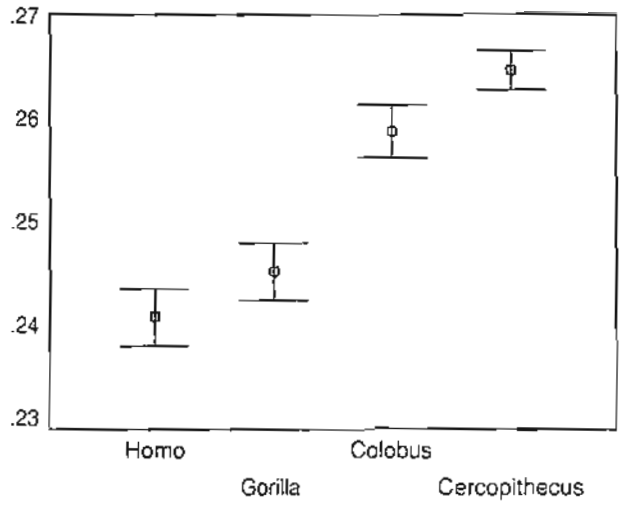

(b) females proximal

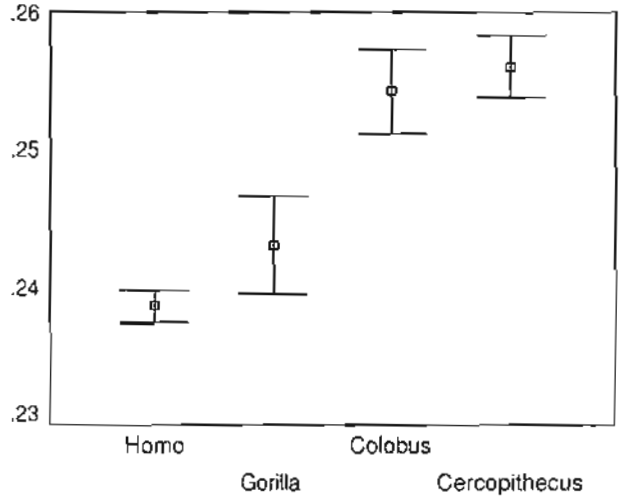

(c) males distal

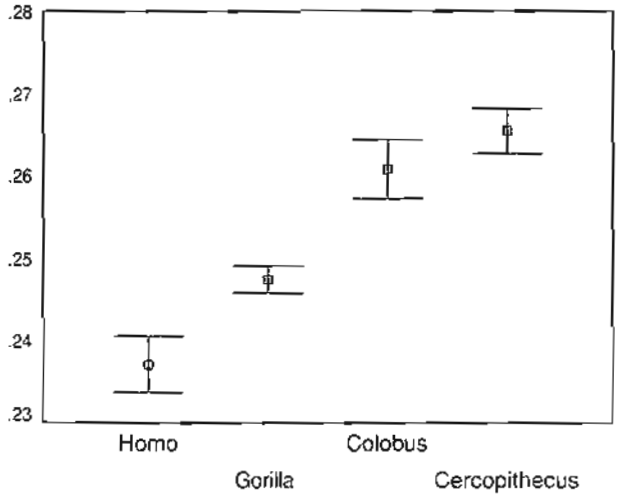

(d) males proximal

4.5.1.3 Comparative discussion

4.5.1.3.1 proximal versus distal outlines

This investigation into size-standardization showed little difference in results for proximal and distal outlines; mostly, findings were very similar for both data sets. The only exceptions to this general finding were found in *Gorilla*: here, the proximal outlines showed that normalized PC1s were almost perpendicular to raw PC1s, whereas the deviations for the distal outlines were around 10°. It was then expected that proximal PC1s (normalized) would be nearly parallel to PC2s (raw), and this was found for females. In males, a strange finding resulted: with the expectation that the deviation between PC1 (normalized) and PC2 (raw) would be slight, a value of 20.69° ensued. These findings were confirmed by computing the product-moment correlation coefficients for scores on PC2 (normalized) and PC1 (raw) (Table 4.44); while the females proximal data set showed a strong correlation between scores (0.9940), the correlation was weaker for males proximal (0.8370). There was therefore a difference between these two 'shape' axes, which by definition could not be explained by size-related shape, as PC1 (normalized) and PC2 (raw) were almost uncorrelated. A possible reason for this discrepancy is shown in Figure 4.14. The discrepancies between component scores for males proximal were greater than for females proximal, but it could not be said that they were outstandingly so. The difference appeared to be in the range of scores: the range of scores for males appeared to be comparatively quite short, which would have had the effect of blunting the scatter ellipse, and therefore the effects on the direction of PC1 (normalized) of these deviations would have been relatively amplified.

Table 4.44. Product-moment correlation coefficients between PC2 (normalized) and PC1 (raw) scores – *Gorilla*, Fourier data

	$r_{PC2, PC1}$
females distal	0.8932
females proximal	0.9940
males distal	0.7893
males proximal	0.8370

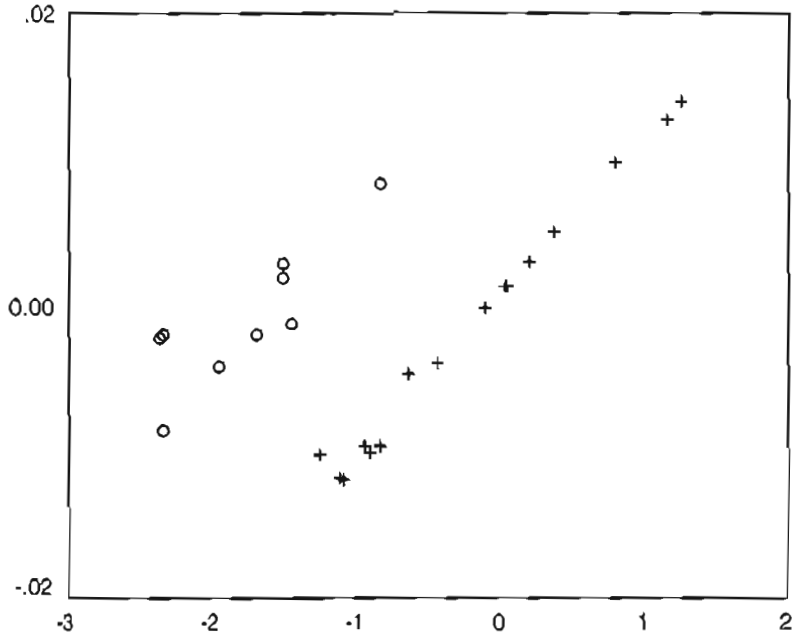

Figure 4.14. Scatterplots of PC1 (normalized, *y*-axis) versus PC2 (raw, *x*-axis) (males ○, females +) – *Gorilla*

There were no qualitative differences between results for proximal and distal outlines using cluster analysis.

4.5.1.3.2 conventional versus Fourier data

Principal component analysis of normalized variables showed similar results for both conventional and Fourier data. For conventional data shape variation occurred along a range from more circular to less circular outlines. For Fourier data the range was from narrow and deep to broad and shallow outlines; uncorrelated with this direction of variation was a not insubstantial (although variable) component of shape variation, which was not interpretable, but being of higher harmonic order than one must have reflected local shape variation, for example articular concavities.

Angles calculated between PC1 (normalized), and PC1 (raw) and PC2 (raw) showed that typically PC2 (raw) (representing size-unrelated shape) was less correlated with PC1 (normalized) (size-related and -unrelated shape) for Fourier data than for conventional data. That is, there appeared to be greater size-related shape among these specimens when measured using Fourier amplitudes. An exception to this was *Colobus* males distal. With the exception of this data set, there was the expectation that the results of the allometry

investigation would show greater size-related shape variation using Fourier rather than conventional data.

Were two sets of data redundant? Given that the ratios ***A/P*** and ***Y1/X1*** reflected similar aspects of shape, it was expected that there would be strong correlations between the two. However, ***Y1/X1*** measured only the best-fitting ellipse, and it was expected that any specimens lying away from a line of best fit through this correlated scatter would reflect disparities between ***A/P*** and ***Y1/X1***; that is, these specimens would show more local deviations from circularity. For example, the proximal outline of *Homo* female specimen 75 was the least circular of the sample, but clearly was not a shallow specimen. Product-moment correlations were calculated between ***A/P*** and ***Y1/X1*** for each data set, and these values are presented in Table 4.45. Correlation coefficients exceeded 0.9, with the exceptions of *Homo* females proximal ($r = 0.857$) and *Colobus* females distal ($r = 0.776$).

Table 4.45. Product-moment correlation coefficient of *A/P* and *Y1/X1*

	$r_{Y1,X1}$
***Homo* females distal**	0.955
***Homo* females proximal**	0.857
***Homo* males distal**	0.959
***Homo* males proximal**	0.957
***Cercopithecus* females distal**	0.937
***Cercopithecus* females proximal**	0.957
***Cercopithecus* males distal**	0.973
***Cercopithecus* males proximal**	0.945
***Colobus* females distal**	0.776
***Colobus* females proximal**	0.940
***Colobus* males distal**	0.955
***Colobus* males proximal**	0.970
***Gorilla* females distal**	0.992
***Gorilla* females proximal**	0.993
***Gorilla* males distal**	0.910
***Gorilla* males proximal**	0.951

Figure 4.15 shows the scatterplots for the latter two data sets. For *Homo* females proximal, it can be seen that specimen 75 lay away from the rest of the sample, which was arranged in a narrow ellipse. Specimen 75 therefore had a conspicuously high value for ***Y1/X1*** given its value of ***A/P***; that is, the dimensions of the best-fitting ellipse to this specimen did not take into account a substantial lack of circularity due to its local nature (see Figure 4.10(a)(ii), showing the proximal image of specimen 75, with its concave lateral facet). In *Colobus* females distal, it would appear that two specimens were responsible for the low correlation.

Specimens 621 and 633 were conspicuous by relatively high values of ***Y1/X1***. Specimen 621 had an outline marked with irregularities, notwithstanding that the two dorsal prominences on the image were not included in the digitized outline (Figure 4.11(c)(i)). The irregularities in specimen 633 (Figure 4.10(c)(i)) were much more subtle, as the outline was smooth and relatively featureless. It would appear that deviations here were of a scale too large to be obvious, but not large enough to affect the first harmonic. However, it is likely that the effect of these two specimens on the strength of the correlation had much to do with the small sample size, as well as their deviations from the main group. For principal component analysis, using both forms of data helped elucidate patellar shape variation than either alone.

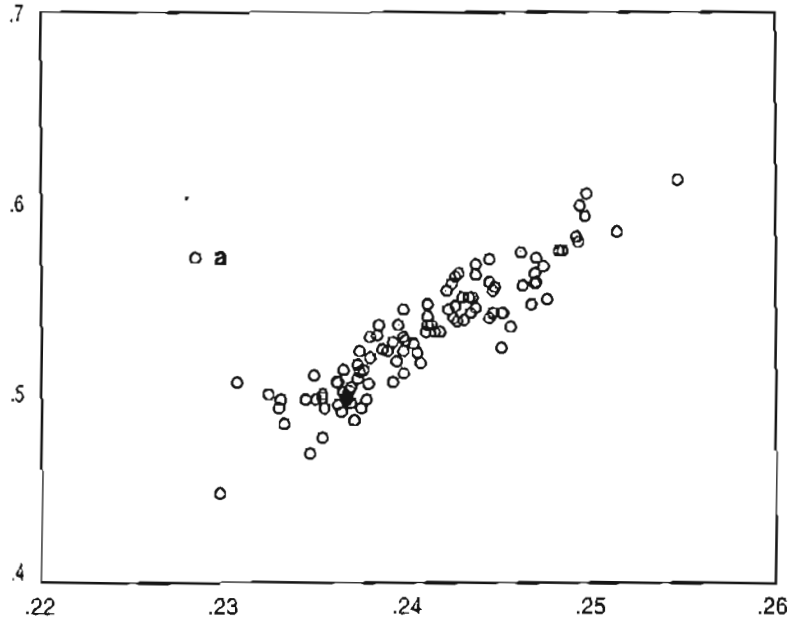

(a) *Homo* females proximal

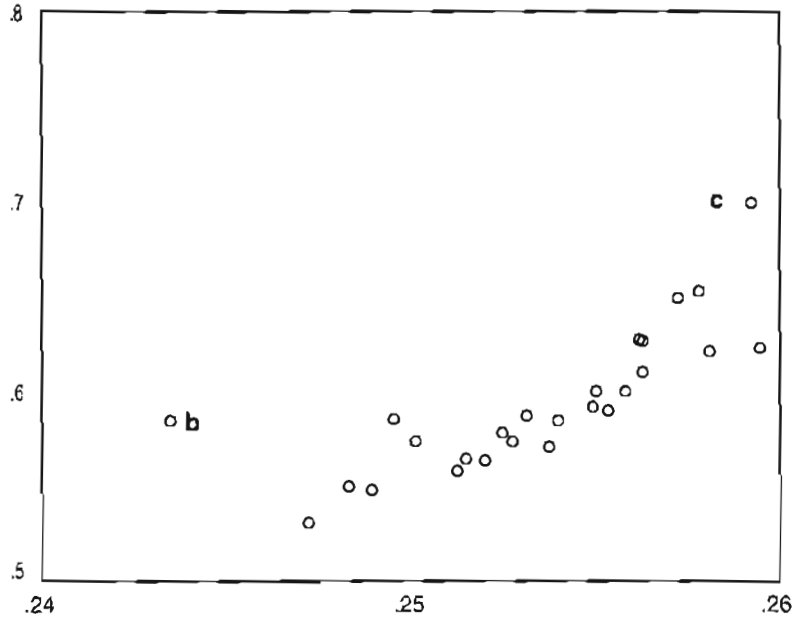

(b) *Colobus* females distal

Figure 4.15. Scatterplots of ***Y1/X1*** (*y*-axis) versus ***A/P*** (*x*-axis) (**a** specimen 75, **b** specimen 633, **c** specimen 621)

A comparison of the cluster analyses using conventional and Fourier data showed that in females, size-adjustment showed greater shape difference between *Homo* and *Gorilla* (relative to *Cercopithecus* and *Colobus*) using the Fourier data. This was presumably due to the increased information carried by the Fourier amplitudes. In contrast, in males the opposite pattern prevailed: Fourier data showed less shape difference between *Homo* and *Gorilla*. The important point here was that this was relative to the clustering of *Cercopithecus* and *Colobus*. As it was unlikely that the Fourier amplitudes would convey less shape information than the conventional variables, it was more likely that the Fourier data showed relatively greater shape difference between *Cercopithecus* and *Colobus*.

4.5.1.3.3 principal component analysis versus cluster analysis

Ideally, these two methods would have been compared on equal terms (data reflecting individual specimens, and within-group covariance retained). This was not possible, as the cophenetic correlations for clustering based on interindividual cosines were poor, and it was not appropriate to interpret the resulting tree diagrams. However, it was appropriate to interpret the results based on intergenus cosines, which had the advantage of relating differences among genera. These showed that there were greater form differences (based on generalized distance) between *Homo* and *Gorilla* than between *Cercopithecus* and *Colobus*, but that these differences were largely based on size. It was also clear that results differed among sexes (to be discussed in Chapter 5). Thus, although information stemming from these analyses was necessarily scant, performing cluster analyses was beneficial as they allowed a direct comparison of genera.

4.5.1.3.4 comparison among genera

There were no outstanding differences in ordination among genera using principal component analysis. From the results of the cluster analyses, there were shape differences between *Gorilla* and *Homo* on one hand, and *Cercopithecus* and *Colobus* on the other. It can be seen in Figure 4.13 that, on average, *Cercopithecus* and *Colobus* specimens were more circular than those of *Homo* and *Gorilla*. *Cercopithecus* specimens were on average more circular than *Colobus* specimens, although the relative shape of *Homo* and *Gorilla* was not constant – in females distal, *Homo* was on average more circular than *Gorilla*, but conversely in the other data sets.

4.5.2 Allometry

4.5.2.1 Allometry

The first step in the process of detecting allometry was to estimate linear relations among variables; prior to such estimation, it was necessary to first determine whether such relations were appropriate. This was done using eigenvalues derived from principal component analysis (major axis regression). For conventional data, there was a general finding that estimation of linear relations was appropriate, as the first eigenvectors accounted for over 99% of total variance of $\boldsymbol{P}$ and $\boldsymbol{A}$. Accordingly, the correlations closely approximated unity (≥ 0.93). These strong correlations meant that the choice of regression method was of minor importance (Aiello, 1981, 1992; Leamy and Bradley, 1982; Seim and Sæther, 1983). Major axis slopes and intercept values were then calculated to complete the relation $X_2 = aX_1 + c$. The value of the intercept was of great interest here: an intercept of zero would have reflected geometric similarity, or isometry, within the sample, a nonzero intercept reflecting size-related shape variation, or allometry.

None of the calculated intercepts equalled zero, so each sample showed shape change across the size range. Intercepts calculated ranged from −10.08 to 17.04. The morphological meaning of the intercept value, especially its sign, can be determined simply. For example, the linear relation calculated for *Colobus* females proximal outlines was $\boldsymbol{A} = 0.29\boldsymbol{P} - 5.82$. The slope tells that for every unit increment of $\boldsymbol{P}$, there was a 0.29 increment in $\boldsymbol{A}$. The inclusion of a negative intercept meant that this slope was offset 5.82 units of (square root of) area; less area for a given perimeter length reflected a less circular specimen. The shape of the specimen in terms of these variables can be measured by

$$\frac{A}{P} = 0.29 - \frac{5.82}{P}.$$

That is, for smaller values of $\boldsymbol{P}$, the value of $\boldsymbol{A/P}$ was more affected by the intercept – smaller specimens were less circular. For larger values of $\boldsymbol{P}$, the value of $\boldsymbol{A/P}$ approximated 0.29, and larger specimens were more circular. (The value of $\boldsymbol{A/P}$ could only *approximate* 0.29, as a perfect circle has a value of ~0.28.) To contrast, *Gorilla* males proximal outlines showed the linear relation $\boldsymbol{A} = 0.23\boldsymbol{P} + 9.75$. The positive intercept meant a relative increase in the square root of area, so the effect was that smaller specimens, being more affected by the intercept, were more circular than larger specimens. These effects can be seen for all conventional data sets in Figure 4.16 (toward the end of §4.5.2.1), which plots $\boldsymbol{A/P}$ versus $\ln$ (the length of the

measurement vector, as a measure of size). Samples with positive intercepts showed a negative correlation, and those with negative values showed a positive correlation; thus the measure of shape was variably correlated with that of size. This recalls Mosimann's concept of allometry (Mosimann, 1970; Mosimann and James, 1979). The data sets where correlations were not significantly different to zero were also those where 95% confidence intervals for intercepts included zero. The presence of the nonzero intercept required that there be a nonzero correlation between these two variables (Allison et al., 1995), which confirmed that a nonzero intercept reflected allometry.

Where zero was included in the confidence intervals, isometry (geometric similarity) could not be ruled out. In *Homo*, these intervals excluded zero; as an example, in the males distal data set the interval was 1.38 to 21.85, which, compared to other genera, included relatively small to relatively large intercepts. Therefore, despite moderately large sample sizes, the confidence intervals for *Homo* were wide, and while the data did not allow for the conclusion of isometry, the estimation of intercepts was otherwise done with little precision. In *Cercopithecus*, only in females distal did the intervals not include zero. Confidence intervals were relatively narrow, in all cases only allowing for small intercepts. In *Colobus*, the intervals excluded zero for females and included it for males. The intervals were wider than for *Cercopithecus* (probably due, in part, to the smaller sample sizes), and allowed for larger intercept both sides of zero. For example, in males proximal the interval included zero but also 6.93 and 6.04. In *Gorilla*, only the males proximal interval did not include zero. However, in the remaining *Gorilla* data sets, the intervals were very wide, and included relatively large positive and negative intercepts as well as a zero intercept. Consequently, to infer isometry from these data sets also demanded that some fairly large negative and positive intercepts also be inferred; for example, in males distal the interval spanned from –23.24 to 25.50.

Transformation of these data to natural logarithms did not provide compelling evidence that nonlinear relations were more appropriate; although the correlations were very strong and first eigenvalues accounted for almost all variance, only in three data sets (*Homo* males distal and proximal, and *Gorilla* males proximal) did the first eigenvalue account for a greater proportion of variance than with nontransformed data. Even then, the proportional increases were small. Nevertheless, nonlinear relations were estimated where zero intercepts were included in confidence intervals for nontransformed data. This was to try to avoid the complicating factor of the intercept when transforming to logarithms (page 134). *Gorilla* specimens were not included, since the confidence intervals were so wide. The results mostly

appeared to mirror those using nontransformed data: allometry coefficients greater than 1.00 could be interpreted as the square root of area outstripping perimeter length, such that larger specimens showed greater (square root of) area per unit perimeter length. That is, they were more circular, which reflected the negative intercepts found using nontransformed data. The exception here was *Colobus* males distal, where a positive intercept had been found. This was possibly due to the confounding effect of a nonzero intercept, although this factor potentially affected all data sets. In each case where nonlinear relations were estimated, the confidence intervals included 1.00, so the findings here of isometry accorded with those using nontransformed data. In general, there was no advantage to estimating nonlinear, over linear, relations.

The results for the analyses using Fourier data were mixed. In only five data sets (*Cercopithecus* males distal and proximal, *Colobus* females proximal, and *Gorilla* females distal and males proximal) did the first eigenvalue account for clearly greater than 90% of total variance; only in these data sets was the first principal component judged to reflect simple allometry. Principal component coefficients showed that these components were dominated by $\boldsymbol{X1}$ and $\boldsymbol{Y1}$. Accordingly, allometric relations were estimated of the form $\boldsymbol{Y1} = a\boldsymbol{X1} + c$. No intercept was zero, so shape change across a size range was shown by these data. All intercepts estimated were negative, excepting *Gorilla* males proximal. As $\boldsymbol{X1}$ represented the semimajor axis of the best-fitting ellipse for each outline, and $\boldsymbol{Y1}$ represented the corresponding semiminor axis, the relations estimated reflected relations between patellar breadth ($\boldsymbol{X1}$) and depth ($\boldsymbol{Y1}$). However, where intercepts were negative these relations were offset by small negative values of $\boldsymbol{Y1}$ i.e. less depth. This recalled the concept of outline circularity with the conventional data – a shallower patella (relative to its breadth) would, all else being equal, be a less circular patella. Smaller specimens would have shown this offset more than larger specimens, so that larger specimens were deeper (larger value of $\boldsymbol{Y1/X1}$). The opposite would be true of relations including a positive intercept – a relative increase in depth would be seen in smaller specimens, with larger specimens being shallower. This was reflected in Figure 4.17 (following Figure 4.16), which shows scatterplots of the ratio $\boldsymbol{Y1/X1}$ versus $\boldsymbol{X1}$. Where intercepts were negative, correlations between $\boldsymbol{Y1/X1}$ and $\boldsymbol{X1}$ were positive, and conversely, a positive intercept reflected a negative correlation.

Figure 4.16. Scatterplots of ***A/P*** (y-axis) versus $|\mathbf{x}|$ (x-axis), including values for regression intercept (c) and correlation (r, significant at $p < 0.05$*, $p < 0.01$**)

(**a**) *Homo*

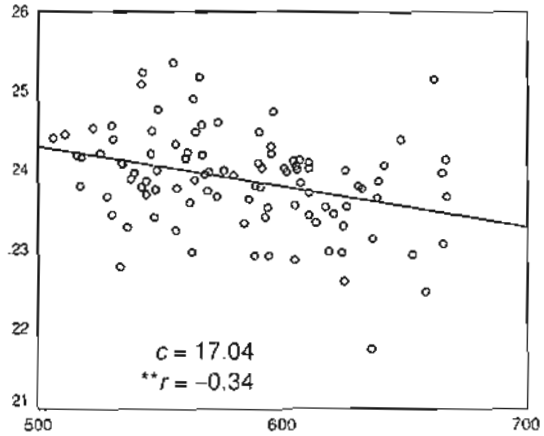

(i) females distal

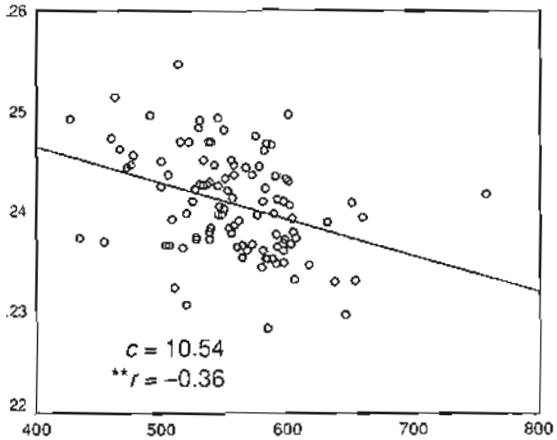

(ii) females proximal

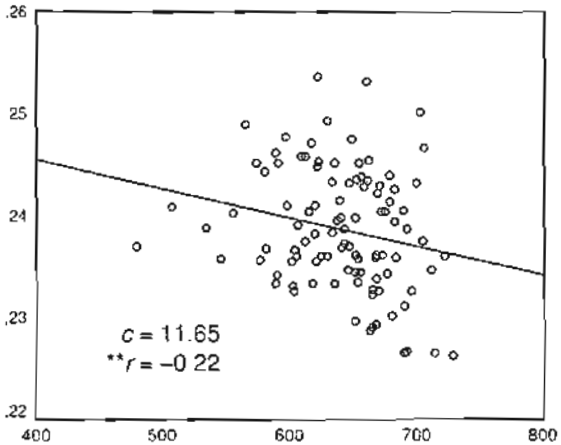

(iii) males distal

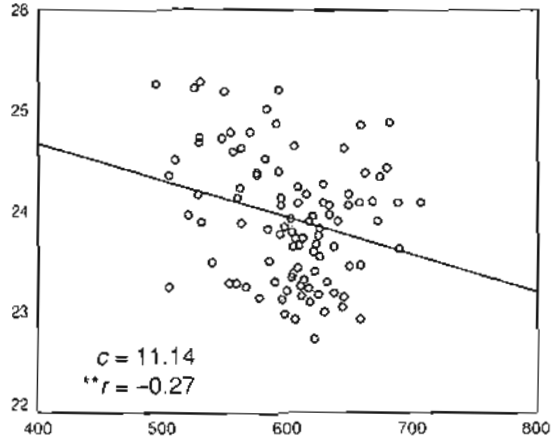

(iv) males proximal

Figure 4.16. (b) *Cercopithecus* (*Cercopithecus* sp. +, *C. aethiops* ◇, *C. solatus* ●, *C. mona* ○, *C. campbelli* ■, *C. neglectus* ×, *C. ascanius* ▷, *C. nictitans* △, *C. mitis* □)

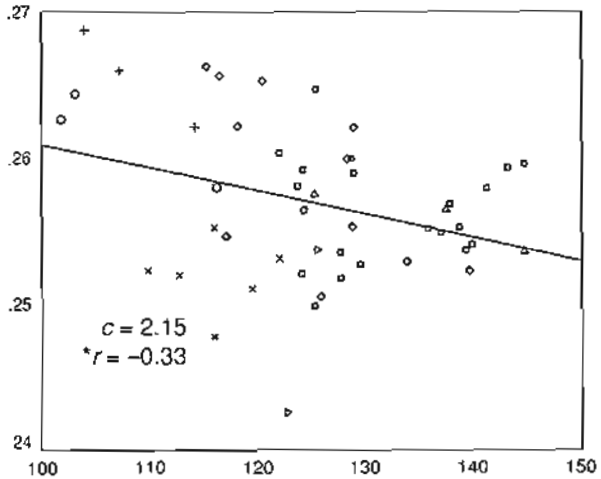

(i) females distal

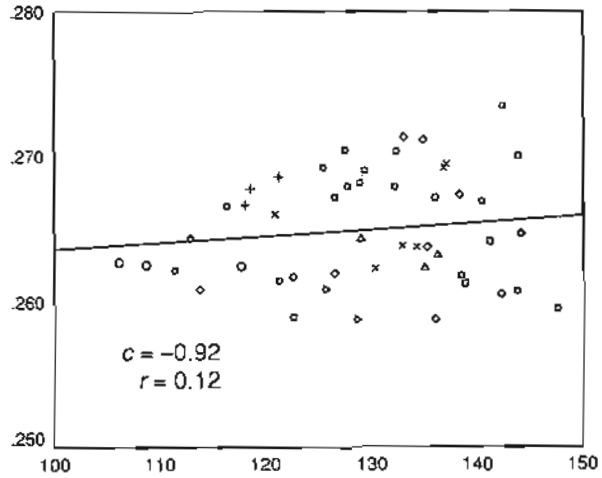

(ii) females proximal

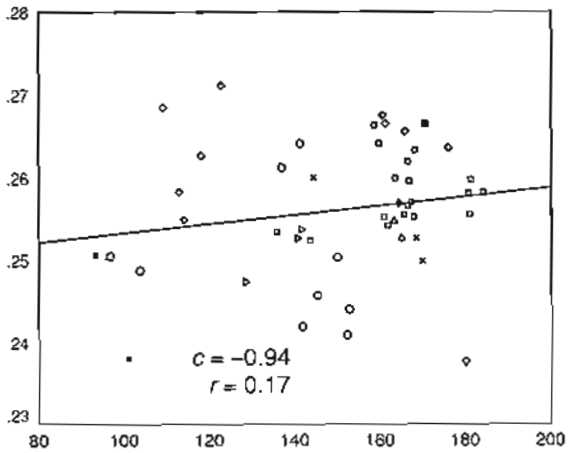

(iii) males distal

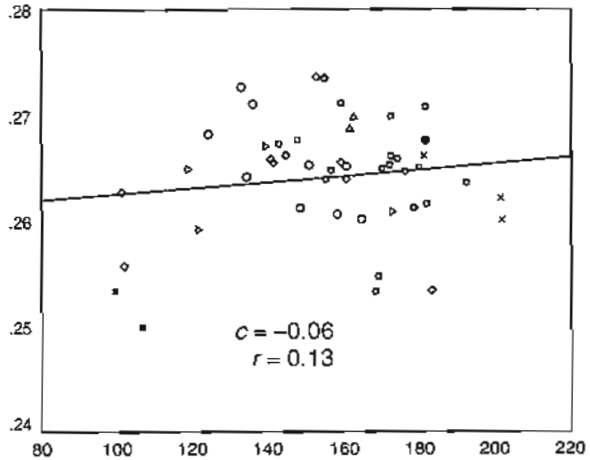

(iv) males proximal

Figure 4.16. (c) *Colobus* (*Colobus badius* ×, *C. preussi* +, *C. angolensis* □, *C. guereza* ○, *C. satanus* △, *C. polykomas* ▷)

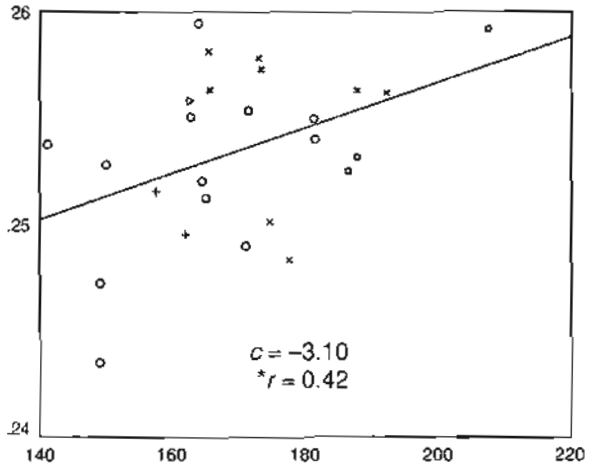

(i) females distal

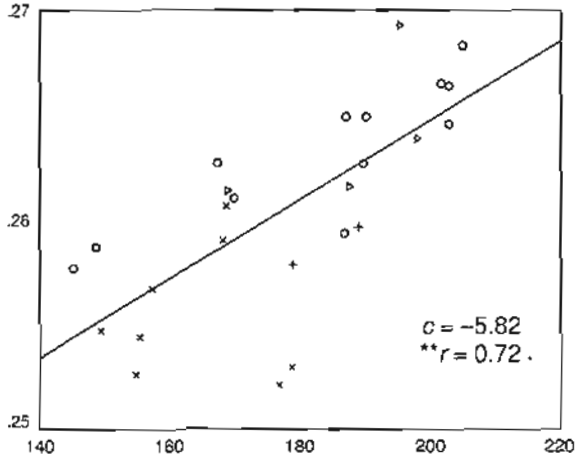

(ii) females proximal

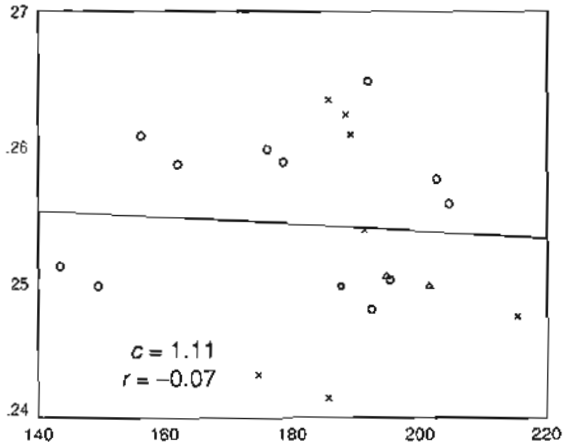

(iii) males distal

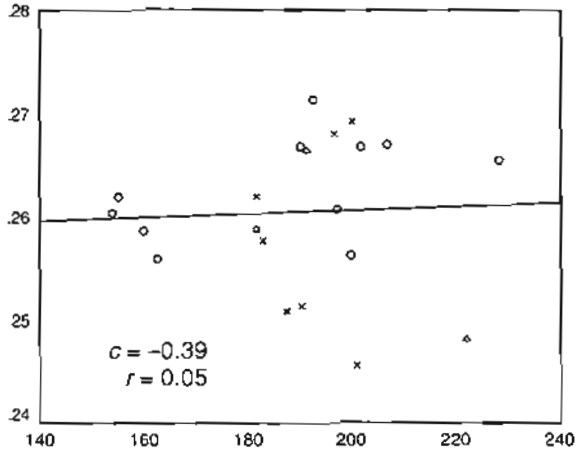

(iv) males proximal

Figure 4.16. (**d**) *Gorilla*

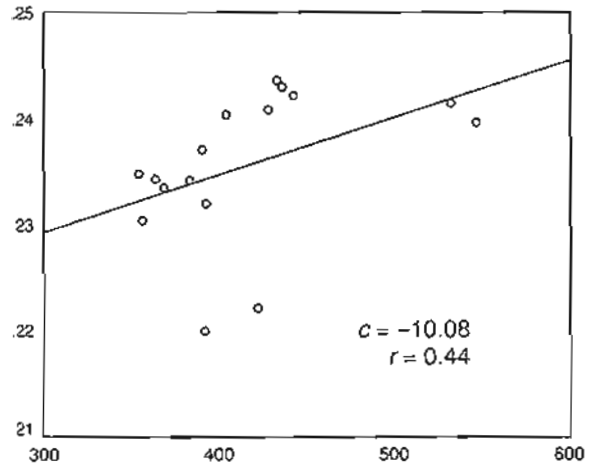

(**i**) females distal

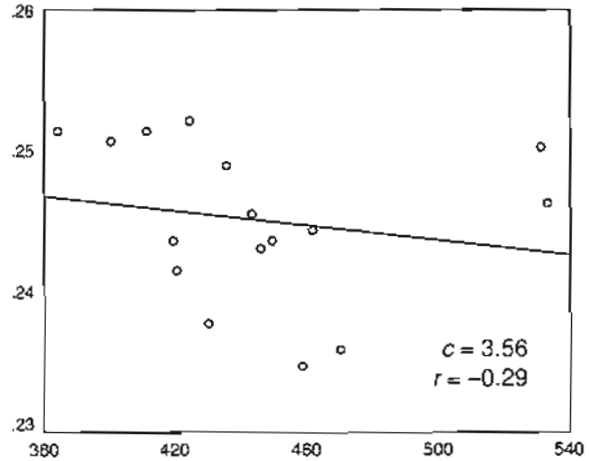

(**ii**) females proximal

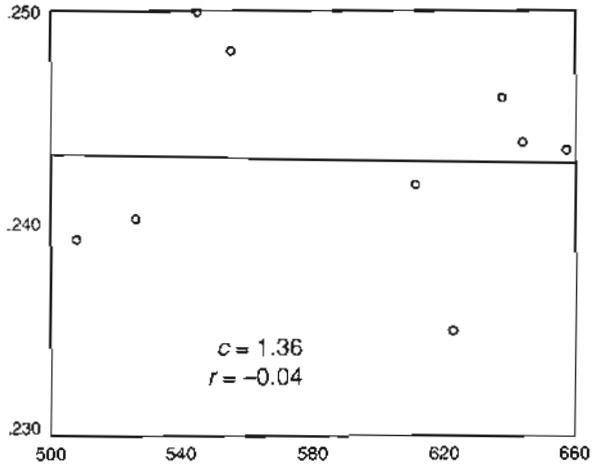

(**iii**) males distal

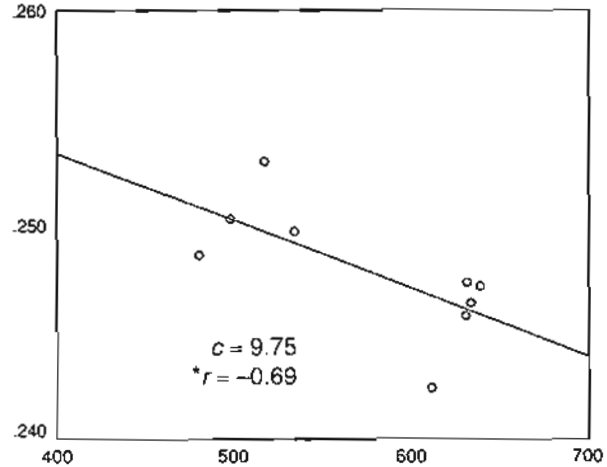

(**iv**) males proximal

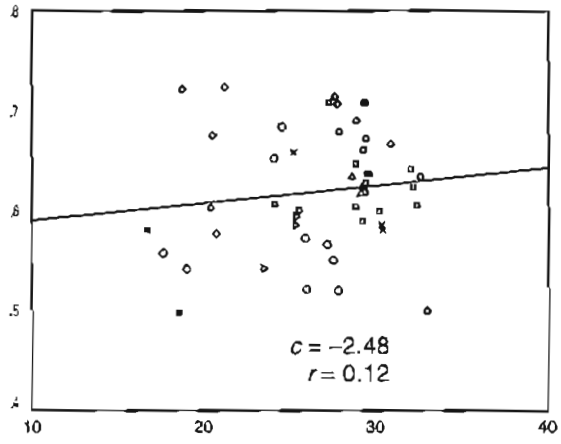

(a) *Cercopithecus* males distal (*C. aethiops* ◊, *C. solatus* ●, *C. mona* ○, *C. campbelli* ■, *C. neglectus* ×, *C. ascanius* ▷, *C. nictitans* △, *C. mitis* □)

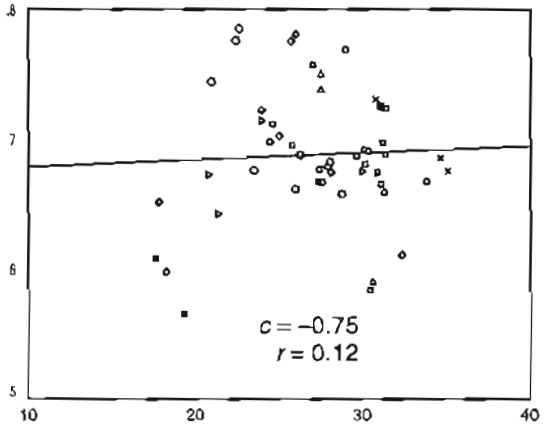

(b) *Cercopithecus* males proximal (symbols as in (a))

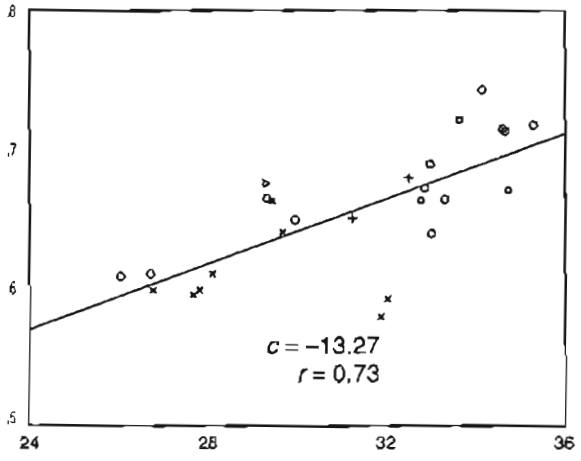

(c) *Colobus* females proximal (*C. badius* ×, *C. preussi* +, *C. angolensis* □, *C. guereza* ○, *C. polykomas* ▷)

Figure 4.17. Scatterplots of ***Y1/X1*** (*y*-axis) versus ***X1*** (*x*-axis) , including values for regression intercept (*c*) and correlation (*r*)

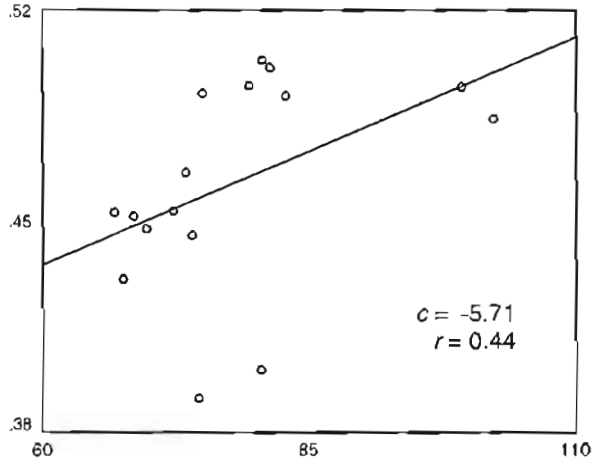

(**d**) *Gorilla* females distal

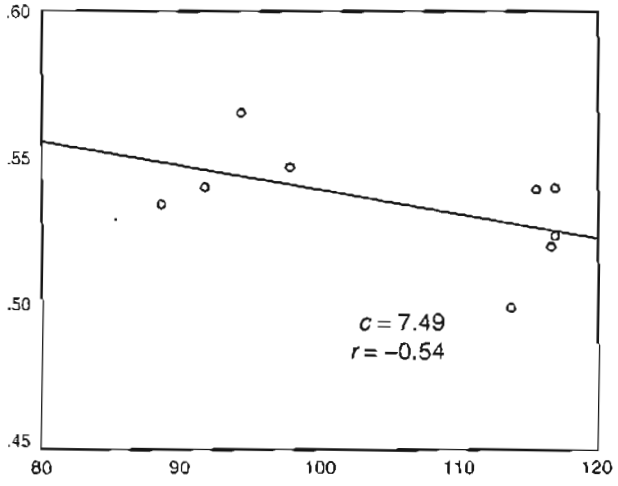

(**e**) *Gorilla* males proximal

Figure 4.17. (continued)

The procedure of determining whether functional relations existed between Fourier variables was less clear than that for the conventional variables: the correlations between ***A*** and ***P*** were very strong, and clearly showed relations. The judging of relations using Fourier data was based on the idea that first eigenvalues should account for at least 90% of total variance. Figure 4.18 shows the scatterplot of the correlation between ***X*1** and ***Y*1** versus the percentage of total variation accounted for by the first eigenvalue for all data sets. Clearly, this plot supported the denying of functional relations where the first eigenvalue accounted for less variance: for example, in *Homo* females distal, the low percentage (79.63%) was reflected in the low correlation between ***X*1** and ***Y*1** (0.53). The plot shows a line at $r = 0.9$, below which the conclusion of functional relations is less convincing: it would appear that the finding of a

functional relation for *Cercopithecus* males proximal (marked **a**, r = 0.88, 93.03%) might have been imprudent

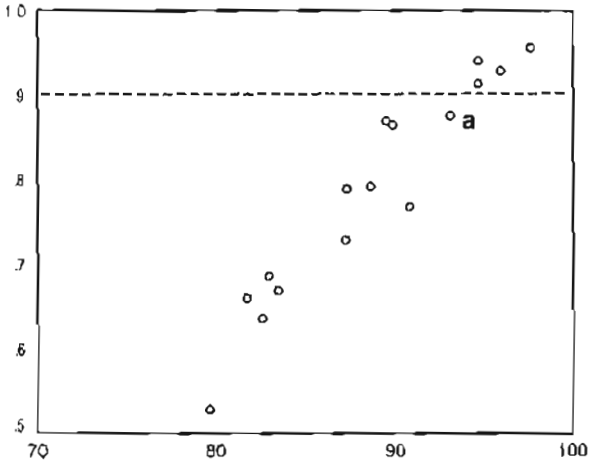

Figure 4.18. Scatterplot of product-moment correlation of ***X*1** and ***Y*1** (y-axis) versus percentage of total variance of 1st eigenvalue for all genera (x-axis) (**a** represents *Cercopithecus* males proximal; dashed line represents correlation of 0.9)

The method of elucidating allometry by inspecting principal components with close-to-zero eigenvalues produced very limited findings. In general, tenth eigenvalues were sufficiently close to zero; values for *Gorilla* males *were* zero, as the covariances matrices were only of rank nine. These data were not interpreted further. For *Homo* and *Cercopithecus*, tenth eigenvalues were statistically distinct. In *Colobus* males distal, the ninth and tenth eigenvalues were not found to be distinct. Furthermore, in *Colobus* females distal and males proximal, the sphericity statistic only barely reached significance, and even then with the assumption of large n violated. The ninth and tenth eigenvalues for *Gorilla* females were not found to be distinct. Where interpretation of tenth principal component coefficients was appropriate, little meaning was found: these coefficients were typically weighted highly for small-power amplitudes like ***X*3** and ***X*5**, which defied interpretation. This did not vitiate the method as such, but merely showed that the success of the method was dependent on the nature (in this case, its morphological meaning) of the data.

4.5.2.2 Comparative discussion

4.5.2.2.1 proximal versus distal outlines

In general, the results for proximal and distal outlines were mixed: relations were found that reflected associations of shape with size in different directions between levels in the same sample. Moreover, there was no consistency within either proximal or distal data sets, such that some proximal data sets showed positive correlations of shape with size, others showing negative correlations, and the same for the distal data sets. Given that bone morphology is sensitive to mechanical circumstances, it could have been argued that these different associations of shape and size were related to functional demands, but there were inadequate kinetic data on the patella in the literature to suggest precisely why such differences were seen. Furthermore, the present study has been unable to suggest why size-shape associations would differ at proximal and distal levels.

4.5.2.2.2 conventional versus Fourier data

The conventional data showed that across each sample the variables ***A*** and ***P*** were closely related. As seen above, relations between ***A*** and ***P*** reflected shape variation, specifically either an increase or decrease of outline circularity with outline size. A decrease in circularity could have been global (elliptic outline), and/or local (smaller-scale deviations, for example articular surface concavities). It was also seen from the Fourier data that relations between ***X1*** and ***Y1*** would also reflect shape differences, but this time shape as represented by the best-fitting ellipse to the outline (the only variation here could have been from more circular to more elliptic). Although the first principal components were dominated by ***X1*** and ***Y1***, more often than not simple allometry was not found with the Fourier data; in these cases (where variation accounted for by the first eigenvalue was relatively low), morphometric variation was richer than explicable by a single weighted combination of variables; despite the dominance of ***X1*** and ***Y1***, these two variables were insufficient to explain shape variation in these cases. Where simple allometry was judged to have prevailed, there was agreement between results for conventional and Fourier data (pattern of outline circularity reflected pattern of relative outline depth). If relations between ***X1*** and ***Y1*** had agreed completely with those between ***A*** and ***P***, the shape variation in patellar outlines would simply have been along the range of circular to elliptic outlines. That there was not such duplication in results

reflected that shape variation in patellar outlines was more complex than this, and that it was worthwhile analysing both conventional and Fourier data.

4.5.2.2.3 comparison among genera

The estimates of the functional relations showed widely varying values of slope and intercept; these values told of the nature of size-related shape variation, but not its extent. However, comparing slope and intercept values for these data sets would not elucidate the morphometric effect of these values. Table 4.46 shows the coefficients of variation of A/P for all data sets; most values were around 2%. The maximum and minimum values were for *Cercopithecus* males distal (3.09%) and *Gorilla* males proximal (1.22%), respectively. The effect of the intercept depends on the abscissa variable (here, P), so that larger values of P reflected less of an effect, and is nonlinear due to the c/X_1 term. Figure 4.19 shows the graphs of $1/P$ versus P for *Cercopithecus* males distal (circles) and *Gorilla* males proximal (crosses). Notwithstanding that the absolute value of the intercept for *Cercopithecus* was much smaller than that for *Gorilla* (0.94 versus 9.75), the difference in ranges and values of P made A/P more susceptible to P in the former data set. This effect was not solely due to the overall magnitude of P, as *Homo* showed larger coefficients of variation than some other data sets despite larger values of P, but due to its range as well.

Table 4.46. Coefficients of variation for A/P

	V (%)
***Homo* females distal**	2.57
***Homo* females proximal**	2.09
***Homo* males distal**	2.47
***Homo* males distal**	2.59
***Cercopithecus* females distal**	2.09
***Cercopithecus* females proximal**	1.44
***Cercopithecus* males distal**	3.09
***Cercopithecus* males proximal**	2.00
***Colobus* females distal**	1.55
***Colobus* females proximal**	1.86
***Colobus* males distal**	2.65
***Colobus* males proximal**	2.76
***Gorilla* females distal**	2.97
***Gorilla* females proximal**	2.29
***Gorilla* males distal**	1.90
***Gorilla* males proximal**	1.22

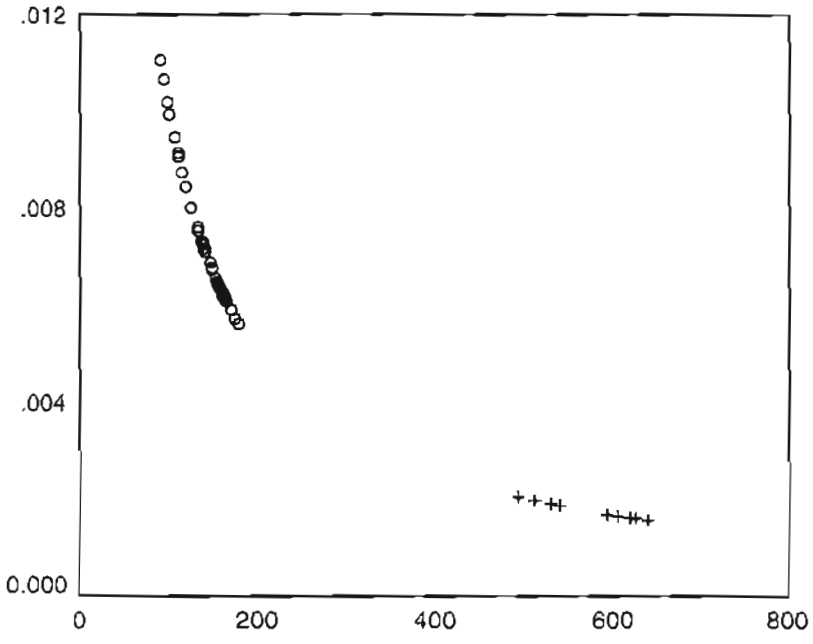

Figure 4.19. Scatterplots of $1/\boldsymbol{P}$ (y-axis) versus $\boldsymbol{P}$ (x-axis) for *Cercopithecus* males distal (○) and *Gorilla* males proximal (+)

Discussion in §4.5.1.3.4 alluded to a possible allometric relation between size and shape among the genera. To elucidate this further, Figure 4.20 shows the scatterplots of $\boldsymbol{A/P}$ versus $|x|$ (genus averages only). Any association between shape and size was stronger for data sets other than females distal, which was reflected in Figure 4.13 – *Homo* and *Gorilla* represented a clear deviation from the line of best fit, due to *Homo* being more circular than *Gorilla* in this data set only. All correlations were lower (stronger) than –0.9, although that for females distal was substantially lower than those for the other data sets. It must be noted that the range of values would have made a substantial contribution to the strength of these correlations (Smith, 1980), although it is clear that there was an overall association between size and shape, with a slight deviation in females distal.

Figure 4.20. Scatterplots of mean A/P (y-axis) versus mean $|x|$ (x-axis) (*Homo* ○, *Cercopithecus* +, *Colobus* △, *Gorilla* □)

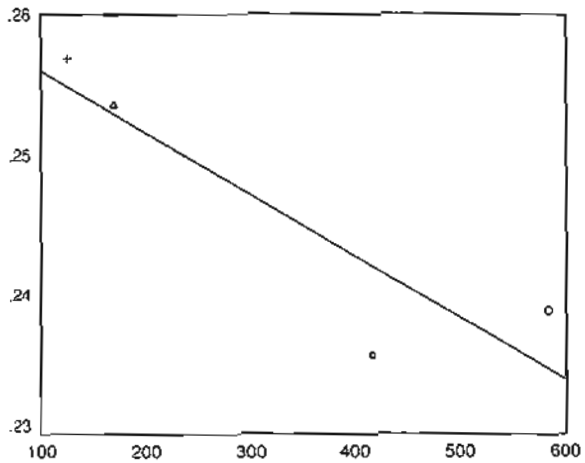

(a) females distal

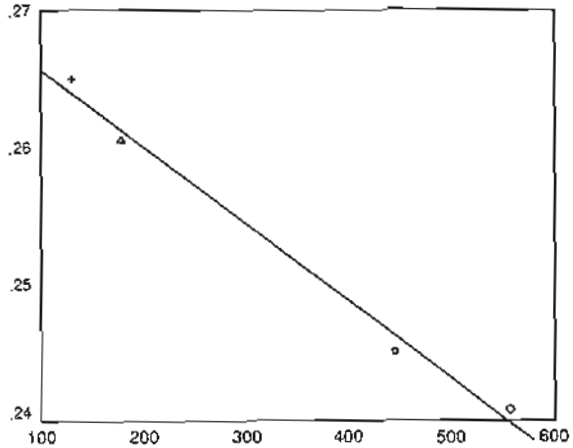

(b) females proximal

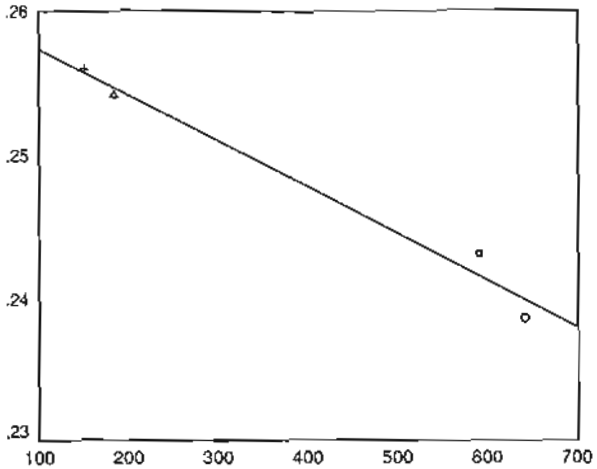

(c) males distal

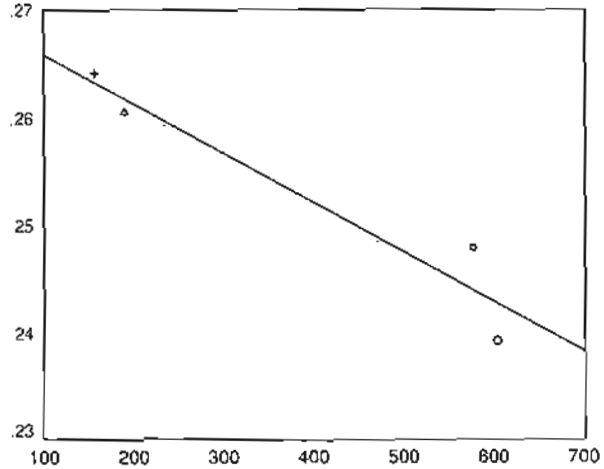

(d) males proximal

4.6 Conclusions

4.6.1 Size-adjustment

Ordination using principal component analyses of normalized conventional data showed that these shape data were highly constrained in phenotype space; unless the range of variables had been sufficiently wide, this was a necessary artefact of the normalization process. The first principal components defined the direction of shape variation (as measured by normalized data), and the spread of data points was sufficiently small for this vector to account for approximately 100% of shape variation. This direction defined a contrast between ***P*** and ***A***, which was interpreted as proximity to, or deviation from, outline circularity. The results using Fourier data showed that one weighted combination of normalized variables did not in general account for a similar amount of variance: often, two principal components were necessary to account for an acceptable amount of variance. However, the direction of greatest variance was defined by a contrast between ***X*1** and ***Y*1**, or the breadth and depth of the best fitting ellipse, respectively. These vectors tended to be orthogonal to the first principal components of raw data, which gave credence to the opinion that the latter component was a measure of size. On scatterplots, no outlying specimens were found, and the specimens found in Chapter 3 to be conspicuously large were found here to be located inconspicuously. The specimen that in Chapter 3 was seen to be at an extreme of shape was also found to lie in a similar position with the normalized data.

Cluster analysis of raw and size-adjusted data was performed on genus averages; in general, the hominoids (*Homo* and *Gorilla*) and the cercopithecoids (*Cercopithecus* and *Colobus*) were still clearly separated after size-adjustment. Following size-adjustment, *Cercopithecus* and *Colobus* specimens were more alike (showed greater shape similarity) than specimens of *Homo* and *Gorilla*.

4.6.2 Allometry

Functional relations were found between ***P*** and ***A*** in each data set: in all cases, it was appropriate to estimate linear relations, and in certain cases nonlinear relations were also estimated. Where nonlinear relations were estimated the results were typically in agreement with the linear relations. In only a few cases were linear relations found to be appropriate using Fourier data, and nonlinear relations were not considered. Calculation of 95%

confidence intervals of intercept values showed that isometry was not excluded by these results in some data sets (conventional data). Where isometry was excluded, there was no clear pattern of shape and size variation, although the few results using Fourier data agreed with corresponding results using conventional data. Furthermore, it was shown that the approach investigating relations between variables agreed with results using Mosimann's approach of investigating size-shape correlations, an approach not initially considered in the study. The approach of investigating the coefficients of principal components with close-to-zero eigenvalues was not effective, due to the lack of interpretability of the Fourier variables with large weightings in these components.

Chapter 5 Sexual Dimorphism

In this chapter, morphological distinctions between male and female patellae will be investigated. The literature reviewed in this section relates to animals in general, and where primates have been the subjects of study, this is indicated. It will be seen that in general there are differences between male and female primate body size means within taxa, and such body size differences have the potential to lead to (or at least be associated with) morphological differences in the patella. Beyond this association, there may be other reasons, especially functional influences, that lead to morphological differences. Influential factors, which may affect phenotypic differences between the sexes, are many and varied, and the results of this investigation may lead to conclusions about such factors; for example, patellar size differences may be related to body size differences, which in turn may or may not be related to patellar shape differences. Leading on from the preceding chapter, such size-related shape differences may be due to allometric relations between variables. There may also be functional differences between males and females that are related to morphological differences between the sexes, but which may or may not be related to body size.

5.1 Background

Intraspecific morphological variation may be due, at least in part, to differences between males and females (Wood, 1985). Consistent differences in morphological features between the sexes is known as sexual dimorphism (Martin et al., 1994; Wood, 1985), and in primates such morphological dimorphisms include body size as well as dimensions of limb bones (Leutenegger, 1982; Leutenegger and Cheverud, 1985; Martin et al., 1994; Oxnard, 1983b; Ralls, 1977; Willner and Martin, 1985). The focus of the sexual dimorphism literature is body size dimorphism, and this review will reflect this focus.

5.1.1. Definitions

Sexual dimorphism refers to the presentation of "morphological differentiation of sexually mature males and females" (Fairbairn, 1997 p659). Sexual size dimorphism is defined as statistically significant differences among the sexes based on an arbitrary size measure (Lovich and Gibbons, 1992). In the literature some species are deemed 'dimorphic' where the male/female or female/male size ratio is greater than an arbitrary dimorphism critical value of

1.15 (Martin et al., 1994; Willner and Martin, 1985), although this ignores the concept of statistical significance. If it is assumed that size may meaningfully be segregated from shape, then it is also possible to describe shape dimorphism (Lague and Jungers, 1999; Oxnard, 1983b; Wood, 1976; Wood and Lynch, 1996). Shape dimorphisms may include simple proportional shape measurements (for example bone robusticity – thickness relative to length (Martin et al., 1994; Oxnard, 1984)) as well as more complex shape measurements (for example landmark-derived craniofacial shape (O'Higgins and Dryden, 1993) and conventional metrical shape of the pelvis (Arsuaga and Carretero, 1994)). Shape dimorphism may result from size dimorphism (due to allometric scaling), or may be non-size-related (Arsuaga and Carretero, 1994; Oxnard, 1983b, 1984; Wood, 1976, 1985).

5.1.2 Causality

Differences among sexes are the evolutionary results of differential pressures of natural and sexual selection (Reynolds and Harvey, 1994), although presumably developmental constraints (§2.1.4.1) are also at play. It is most likely that dimorphisms are multifactorial, and in general it is not possible to provide a simple explanation (Leutenegger, 1982; Martin et al., 1994; Oxnard, 1984; Ralls, 1977; Wood, 1976); furthermore, cause and effect may sometimes be confounded (Martin et al., 1994). When discussing causes of sexual dimorphism it may be convenient to assume that selection acts to increase size of the larger sex (often male). Nevertheless, the obverse of this must also be considered, i.e. selection acts on females to decrease size, or furthermore that both sexes respond (Martin et al., 1994; Reynolds and Harvey, 1994; Willner and Martin, 1985). Two popular theories of evolutionary causation relate to (1) sexual selection, and (2) protection from predators. Two other factors also appear to be associated with dimorphism in primates, those of (3) energetic constraints, and (4) ecology. These factors appear to be not mutually exclusive.

The sexual selection theory suggests that traits giving males mating access to females are selected for (Leutenegger, 1982; Ralls, 1977; Reynolds and Harvey, 1994). Sexual selection can be divided into two processes, intrasexual selection (competition with members of same sex for mating access), and intersexual selection (choice of mating partner) (Ralls, 1977). In terms of body size, large size would in theory be beneficial (a) in fighting off rivals, and (b) attracting the notice of a potential mating partner, if it be deemed that larger body size is advantageous, for predator protection as an example (Reynolds and Harvey, 1994) (see below). If so, dimorphism would be expected in taxa where males must compete for this

access, but not necessarily in those where they do not. In general, polygynous primates range from monomorphic to dimorphic (with respect to body size), with monogamous species tending towards monomorphism (Clutton-Brock et al., 1977; Leutenegger, 1982; Martin et al., 1994; Willner and Martin, 1985), although prediction from mating system to degree of dimorphism is notoriously difficult (Ralls, 1977).

The predator protection theory suggests that selection may favour traits that enable individuals to protect their group against predators (Martin et al., 1994), for example increased male body size (Anderson, 1986; DeVore and Washburn, 1963). By definition, the two influences of sexual selection and predator protection may also be combined (Harvey et al., 1978).

It may also be helpful to consider that each sex has an optimal size for their energetic and physiological needs, and that these optima differ (Willner and Martin, 1985). For instance, females have energetic needs in addition to those for daily living – those relating to pregnancy, lactation and childcare (Key and Ross, 1999). Reducing body weight, which is correlated with energy expenditure (Key and Ross, 1999), may be a strategy to reduce energy expenditure in females. For males, the benefits of reduced body weight would have to be compared to the benefits of high body weight in protecting against predators, or in acquiring mates (Clutton-Brock et al., 1977; Key and Ross, 1999).

Ecological circumstances may also influence the development of dimorphism (Reynolds and Harvey, 1994). Clutton-Brock et al. (1977), Gautier-Hion and Gautier (1985), Lindenfors and Tullberg (1998) and Martin et al. (1994) noted a general association between terrestrial habits and body size dimorphism in Old World monkeys. This may be due to a link between terrestriality and predator attack behaviours (Martin et al., 1994), but overall this link is not convincing (Harvey et al., 1978). Alternatively and/or in addition to this, this association may be due to a lack of dimorphism in arboreal species as an arboreal habitat may limit size increases (Leigh, 1995), for example an increase in body size may restrict food availability (Clutton-Brock et al., 1977; Remis, 1995). There are deviations from this association (Oxnard, 1983b; Struhsaker, 1969), which again illustrates that one factor generally is insufficient to explain a pattern of variation.

The question has been raised whether the degree (not presence) of dimorphism is dependent on body size – specifically that larger taxa are more dimorphic (Fairbairn, 1997). For primates, an association between body size and body size dimorphism has been found

(Clutton-Brock et al., 1977; Gautier-Hion and Gautier, 1985; Leutenegger, 1978; Leutenegger and Cheverud, 1985). The increase in dimorphism with increasing body weight is reflected in an allometric relation between male and female body weight: in male primates, body weight scales proportional to female $W^{>1.00}$ (Clutton-Brock et al., 1977; Leutenegger, 1978, 1982; Martin et al., 1994). Leutenegger (1978, 1982) further qualified his results, finding that this allometric body size scaling occurred only in polygynous taxa.

5.1.3 Body-part Dimorphism

The subject of this investigation is sexual dimorphism of the patella; in the absence of any data on body size; it is of interest to know whether patellar size dimorphism may be imputed to dimorphism of body size, i.e. whether body-part size dimorphism is expected to follow body size dimorphism. (For now it may be ignored that the magnitude of body size may influence body size dimorphism.) From what is known of the effect of body size (directly or indirectly) on morphology (§4.1.2.2), it is also of interest to know what effect body size dimorphism may have on patellar shape dimorphism. In general, dimorphisms of different characters vary independently (Leutenegger, 1982; Martin et al., 1994; Masterson and Hartwig, 1998; Oxnard, 1983b; Ralls, 1977; Wood, 1976). For example, a character linked with competition (in this case body size) may be expected, under some circumstances, to be strongly dimorphic, but another character, showing no link with competition, may show less or no dimorphism (Martin et al., 1994). However, if greater body size requires greater body-part size (for example, as a morphological adaptation to different mechanical demands (Ruff, 2000)), dimorphism in the latter would be a consequence of that in the former (Harvey et al., 1978; Lague and Jungers, 1999). For example, Leutenegger and Larson (1985) attributed limb bone size dimorphism in a series of primates to a factor of overall size; in addition, Plavcan (2002) found in a study of primate craniofacial dimorphism that muscle attachment sites tended to be more dimorphic than areas such as the orbits and cranial vault. Thus, size dimorphism in the patella, its main function being to provide an extension moment (largely) against body weight, is likely to follow dimorphism in body size.

Patellar size differences (due to body size differences) alongside allometric relations among variables, the latter at least partly due to functional influences, should in theory also lead to shape dimorphism (Arsuaga and Carretero, 1994; Lague, 2003; Oxnard, 1984; Wood, 1976). Thus, due to functional demands, dimorphic body size can lead to dimorphism in related body parts, although individuals may use functional modifications to avoid increased stresses

(§4.1.2.2). Lague (2003) appeared unconvinced that individuals of different size within a species use such functional modifications, citing a lack of kinematic evidence. It must be appreciated that the possibilities for functionally reducing forces are numerous and diverse: not only may joints be kept more extended, but bone curvature may alter, as may duty factor (§4.1.2.2), and as such sufficient functional modifications may be difficult to detect. Body size, via function, may also influence structure slightly more indirectly; here, dimorphic function is promoted by body size dimorphism – an example is the association between body size and locomotor function in primates (Fleagle and Mittermeier, 1980).

Dimorphic function (and, possibly, structure) may also be independent of body size; pelvic dimensions illustrate this well – while some dimensions have been found to show allometry, other dimensions relating to the pelvic inlet show non-size-related differences between males and females, relating to the specialized function of parturition (Arsuaga and Carretero, 1994; Leutenegger and Larson, 1985). Human skeletal samples have been found to show a range of degree of dimorphism that is related to subsistence strategy: greater dimorphism is found in hunter-gatherer communities than in agricultural communities, due to sexual division of labour (Ruff, 1987, 2000). Therefore it is sensible to consider the existence of sexual functional dimorphisms (as found in chimpanzee locomotion and posture (Doran, 1993)), as some association with structural dimorphisms would be expected (Oxnard, 1984).

Beyond body size dimorphism, are there any clues to aid prediction of patellar dimorphism? Patellar dimorphism could, in theory, arise from differences between the sexes in the types of positional behaviour – locomotion and posture – that individuals adopt. For example, if one sex were more or less likely to engage in leaping, or climbing, or running etc., hindlimb structure may be expected to reflect these differences. As reviewed earlier, heavier animals are less likely to engage in leaping than lighter animals, and so are more likely to climb or walk (§2.1.4.2). However, there is probably a range of body weights for which leaping does not cause prohibitively large forces, and it could be conceived that in this range, the patellae of heavier animals sustain larger forces. In addition, larger terrestrial animals may reduce forces by keeping their limbs extended, but arboreal animals may do this by adopting a more flexed, compliant gait. Another way a force difference could be introduced is by a sexual difference in joint position – that is, kinematic data could indicate, say, an habitual increase in knee flexion in one sex, which would tend to increase patellofemoral joint reaction force. As even basic kinematic data on the nonhuman species investigated here is lacking, this must remain an unelucidated theory.

Structural factors, again applying different forces to the patella, could include dimorphisms of any part of the extensor mechanism (including related bones) via morphological integration (§2.1.4.1), due to all parts of this complex being functionally interrelated. Sexual structural dimorphism in the human extensor mechanism has received some attention in the literature, for example *Q*-angle, bicondylar angle and pelvic width (§2.1.1). The *Q*-angle, or obliquity of the quadriceps relative to the patellar tendon, theoretically reflects the lateralization of quadriceps force on the patella. Studies have consistently found larger *Q*-angles in females (Aglietti et al., 1983; Fairbank et al., 1984; Guerra et al., 1994; Horton and Hall, 1989; Woodland and Francis, 1992). A larger *Q*-angle may reflect higher forces pulling the patella laterally, which may in turn be reflected by a laterally larger patella (for example a larger lateral articular facet) to cope with larger lateral forces. Bicondylar angle could also play a role in increasing the forces acting on the patella in a lateral direction, by reflecting the obliquity of the femur, from which the three vasti arise. Parsons (1914) and Pearson and Bell (1919) found a trend toward greater bicondylar angle in females. The structure of the pelvis should not be ignored, as the pelvis and femur (and therefore the patella) form a functional complex (Lovejoy et al., 1973; Ruff, 1995; Ruff and Hayes, 1983b). Measures of pelvic width (for example biacetabular diameter (Tague, 1992; Tardieu and Preuschoft, 1996)) may be associated with patellar morphology, via an association with femoral obliquity (Tardieu and Preuschoft, 1996); Tague (1992) has found statistical sexual dimorphism in biacetabular diameter in humans. With more of a view to dynamic relations between hind limb bones, Ferber et al. (2003) found sex-based differences in running humans: females were found to show greater hip adduction and knee abduction during the stance phase of running than males.

5.1.4 Ontogeny

It is of interest here to consider the ontogeny of sexual dimorphism. In general there are no recognized selection pressures for neonatal body size dimorphism (Willner and Martin, 1985), and Martin et al. (1994) considered primate species to differ "little, if at all" in neonatal body weight (p168). Nevertheless, Smith and Leigh (1998) found, among a large number of primate species, that neonatal body size is dimorphic (males heavier than females), and that this dimorphism is correlated with adult body size dimorphism. Beyond neonatal size dimorphism, adult sexual size dimorphism is imputed to different rates of growth and/or different durations of growth postnatally (Humphrey, 1998; Leigh, 1995; Leigh and Shea, 1996; Martin et al., 1994; Willner and Martin, 1985). In the case of males having greater body weight, two explanations may be proposed. Firstly, females may show a shorter growth period

(and therefore lower body weight) if there is selection for earlier reproductive age (more rapid reproduction) (Martin et al., 1994; Willner and Martin, 1985); the time of sexual maturity in females is associated with a slowing of skeletal growth, due to sex hormones (Nettle, 2002; Sinclair and Dangerfield, 1998). Specifically, oestrogen has been found to have the effect of decreasing the size of the proliferative and hypertrophic zones in growth plates (van der Eerden et al., 2002). Alternatively, males may have a longer growth period, making them larger and more able to fight off other males, but also making them attain sexual maturity at a later time (Lieberman, 1982; Martin et al., 1994; Willner and Martin, 1985). Males of taxa with seasonal breeding patterns (and which would therefore suffer from delays in sexual maturity) may show less of a tendency to lengthen their growth period: lemurs, which lack body size dimorphism, fit this picture (Martin et al., 1994).

5.1.5 Primate Sexual Dimorphism

Primate sexual dimorphism shows great variation among species (Leutenegger and Cheverud, 1985); not all primate groups are dimorphic, and primate body size dimorphism is not always biased towards males (Martin et al., 1994). Among the primates, sexual dimorphism is most common in monkeys, apes and humans, and most pronounced in the former two groups (Martin et al., 1994). Divergences from predictions of dimorphism occur (Martin et al., 1994), presumably due to the multifactorial nature of dimorphisms. Table 5.1 (an adaptation of Table 2.3) shows values for body weight dimorphism, presented in its 'common' form (Smith, 1999), i.e. as a ratio of male weight/female weight.

Table 5.1. Primate body weight dimorphism values (male weight/female weight)

	m/f	source
Homo sapiens	1.24	Fleagle (1988)
Cercopithecus aethiops	1.60	Fleagle (1988)
	1.61	Plavcan & van Schaik (1992)
	1.54	Anapol et al. (1995)
C. ascanius	1.39	Fleagle (1988)
	1.45	Plavcan & van Schaik (1992)
C. campbelli	1.67	Oates et al. (1990)
C. mitis	1.74	Plavcan & van Schaik (1992)
	1.87	Anapol et al. (1995)
C. mona	1.76	Plavcan & van Schaik (1992)
C. neglectus	1.60	Fleagle (1988)
	1.80	Plavcan & van Schaik (1992)
C. nictitans	1.63	Fleagle (1988)
	1.56	Plavcan & van Schaik (1992)
C. solatus	1.73	Harrison (1988)
Colobus angolensis	1.31	Plavcan & van Schaik (1992)
C. badius	1.00	Fleagle (1988)
	1.38	Plavcan & van Schaik (1992)
	*1.02	Smith & Jungers (1997)
	†1.34	Smith & Jungers (1997)
	1.01	Oates et al. (1990)
C. guereza	1.26	Fleagle (1988)
	1.19	Plavcan & van Schaik (1992)
	1.25	Smith & Jungers (1997)
C. polykomas	1.53	Fleagle (1988)
	1.13	Plavcan & van Schaik (1992)
	1.19	Oates et al. (1990)
C. satanas	1.26	Plavcan & van Schaik (1992)
Gorilla gorilla	1.68	Plavcan & van Schaik (1992)
	**2.37	Fleagle (1988)
		Jungers & Susman (1984)
	**2.11	Leigh and Shea (1996)
	‡2.19	Fleagle (1988)
	‡1.63	Jungers & Susman (1984)

C. b. badius

†C. b. rufomitratus

**G. g. gorilla

‡G. g. beringei

Below is a summary of information relevant to dimorphism in the taxa under investigation, which is patchy due to incompleteness of the scientific record.

Guenons (*Cercopithecus*) are moderately sexually dimorphic, with *C. neglectus* showing strong body size dimorphism (Fleagle, 1988; Gautier-Hion and Gautier, 1985), despite being almost monogamous (Leutenegger and Lubach, 1987). *Cercopithecus aethiops* is an unusual guenon in that it lives in large groups with several adult (hierarchical) males, and is sexually dimorphic, both in total body size and body segment size (Fleagle, 1988; Turner et al., 1997). *Cercopithecus nictitans* is also body size dimorphic (Gautier-Hion and Gautier, 1985). Within *Cercopithecus*, it has been found that only terrestrial species (for example *C. aethiops*) live in multimale groups, with forest-dwellers (for example *C. nictitans*, *C. neglectus*) having only one male per group (Gautier-Hion and Gautier, 1985; Struhsaker, 1969). Ontogenetically, *C. mitis* and *C. neglectus* are considered dimorphic through growth rate differences (Leigh, 1995). Gautier-Hion and Gautier (1985) found *C. neglectus* and *C. nictitans* to show no neonatal body size dimorphism, and that body size dimorphism arose through both increased rate and duration of growth in males. Turner and coworkers (1997) found a pattern of greater rate and duration of growth in *C. aethiops*, although Leigh (1995) listed *C. aethiops* as a species that achieves dimorphism mainly through growth duration. A study performed by Isbell (1990) showed no protective behaviour of *C. aethiops* against predators. In general, Struhsaker (1969) found no evidence that male *Cercopithecus* have a role in protecting against predators, preferring to attribute sexual dimorphism to sexual selection.

Guerezas (*Colobus guereza*, *C. polykomas*, *C. angolensis*) are body size dimorphic (Fleagle, 1988). Guerezas typically live in small groups with one male and one or two females, with *C. satanas* living in multimale groups (Fleagle, 1988). *Colobus badius* lives in large groups with numerous male and female adults, but nonetheless shows less body size dimorphism than guerezas (Fleagle, 1988). In a study in the Gombe National Park (Tanzania), it was found that *C. badius* was heavily preyed upon by chimpanzees (Stanford et al., 1994), although it was not clear whether there were strategies for protecting the group against this predation. It is of interest to note that, overall, *Colobus* monkeys appear to be less dimorphic in body weight than *Cercopithecus* monkeys, despite greater body size Table 5.1.

Gorillas are strongly body size dimorphic (Dixson, 1981; Fleagle, 1988; Leutenegger, 1982; Martin et al., 1994; Taylor, 1997; Willner and Martin, 1985) and this is more pronounced in mountain gorillas (*Gorilla gorilla beringei*) (Taylor, 1997). Mountain gorillas are reported to be more arboreal than lowland gorillas (*G. g. gorilla*) (Taylor, 1997). Gorillas typically live in

groups of around a dozen, with one mature male and several younger males (Fleagle, 1988; Yamagiwa, 2001). Competition for mating partners occurs between males of a group (Watts, 1996). Large adult male gorillas play a role in protecting the smaller members of the group from predators (Watts, 1996; Yamagiwa, 2001), including (possibly) leopards (Fay et al., 1995). Gorillas are not seasonal breeders, and can reproduce throughout the year (Dixson, 1981). Gorillas have been found to show both a greater rate of weight gain in males at adolescence, as well as an extended growth period (Dixson, 1981; Gijzen and Tijskens, 1971; Leigh and Shea, 1996; Shea, 1983, 1985c; Taylor, 1997), when compared to females.

Adult human males are about 20% heavier on average than females (Martin et al., 1994). Sexual selection is believed to have played a part in the evolution of stature dimorphism in humans, with taller men having greater reproductive success than shorter men, presumably due to mate choice (i.e. intersexual selection) (Nettle, 2002; Pawlowski et al., 2000). Human sexual dimorphism is thought to be the result of increased rate and duration of growth in males during adolescence (Harrison et al., 1988; Humphrey, 1998; Lieberman, 1982), although at birth (on average), males are slightly heavier and longer than females (Lieberman, 1982).

The above is a useful illustration that dimorphisms arise due to a complex interaction of factors, and prediction of dimorphism cannot be made with great confidence when only single (even a few) factors are considered.

5.1.6 Review of Methods

5.1.6.1 Size dimorphism

Methods used by researchers in the field of sexual size dimorphism are designed to uncover the presence and/or degree of dimorphism. Popular general approaches include the derivation of ratios and differences (Lovich and Gibbons, 1992; Marini et al., 1999), and in this section such approaches will be reviewed for applicability in this investigation.

5.1.6.1.1 ratios

A widely used index of sexual size dimorphism is the ratio of mean sizes of the sexes (Lovich and Gibbons, 1992); such ratios have been used by Clutton-Brock et al. (1977), Leutenegger (1982), Macchiarelli and Sperduti (1998), Masterson and Hartwig (1998), Plavcan (2002) and Post et al. (1978). Rather than an end in themselves, these ratios have formed the first step in, for example, comparative taxonomic analyses of dimorphism (Clutton-Brock et al., 1977; Masterson and Hartwig, 1998; Plavcan, 2002; Post et al., 1978).

5.1.6.1.2 differences

Other indices of sexual size dimorphism have been derived from the differences between size measures (for example $\overline{X}_{male} - \overline{X}_{female}$) (Lovich and Gibbons, 1992; Smith, 1999); an example of this approach is in Cheverud et al. (1985). However, differences between mean sizes of males and females, like any other mean difference, lack absolute meaning due to intrasexual variation (Bennett, 1981; Marini et al., 1999; Smith, 1999); as only mean values are used in deriving the simple ratios above, this criticism applies to these indices as well. As an alternative, the univariate *t*-test considers the mean difference relative to the standard deviation of the variable. Such an approach has been used by Anderson and Trinkaus (1998), Arsuaga and Carretero (1994), Igbigbi and Msamati (2002), King et al. (1998), Lazenby (2002), Leutenegger and Larson (1985), Steudel (1981), Tague (1992) and Wood and Lynch (1996). Marini et al. (1999) found *t* to be a useful intersex distance, not only as it takes account of intrasexual variability, but as it may also be modified for cases of heteroscedasticity. Examples of such alternatives are Welch's approximate *t*-test (Sokal and Rohlf, 1995) and the nonparametric Mann-Whitney-Wilcoxon test (used in lieu of the *t*-test (Sokal and Rohlf, 1995), the latter used by Demes and associates (1991) and Prescher and Klümpen (1995). The Kolmogorov-Smirnov distance was also suggested, as it has the advantage of being applicable to non-normal distributions (Marini et al., 1999). The latter two methods are nonparametric – in comparison to parametric methods, such as the *t*-test, and where the assumptions of the parametric methods are met, nonparametric methods tend to lack power (Sokal and Rohlf, 1995).

5.1.6.2 Shape dimorphism

Having derived shape data from the original multivariate form vector, the investigator may then use statistical methods to judge the separation of males and females. In the case of the shape data being univariate, the *t*-test may again be used. For example Ruff (1987) measured *t* from data based on bending moment of inertia measurements; Daegling and Jungers (2000) performed analyses of variance (with two sexes, this is equivalent to the *t*-test) on principal coordinate analysis scores (one axis at a time), based on size-standardized data to investigate sexual shape dimorphism in mandibles using elliptic Fourier descriptors. Multivariate methods are appropriate when shape data are multivariate. For example, Daegling and Jungers (2000) performed multivariate analyses of variance on combinations of axis scores; multivariate analysis of variance was also used by Wood and Lynch (1996) on coordinate shape data.

5.1.6.3 Methods for this investigation

Methods to be used in this investigation will ideally express the degree of dimorphism with respect to intrasexual variance. This will have additional importance in this investigation, as the sample sizes differed markedly, and it will be important to gauge the precision with which results are interpreted. Student's *t*-test (here its equivalent, the single-classification analysis of variance), as reviewed above, is a univariate method that meets this criterion. Nonparametric methods may also be used where the appropriate assumptions are not met. In the multivariate case, analysis of variance can be extended to the multivariate analysis of variance.

5.1.7 Summary

Sexual dimorphism can be a rich source of morphological variation within a taxon. Dimorphism may be associated with social structure, for example it is more likely in polygynous groups, and/or where one sex (principally males) are required to defend the group against predators. Dimorphism may be associated with dimorphic physiological requirements; for example, females may have a shorter growth period due to reproductive roles. Dimorphism may also be associated with ecological characteristics – for example, an arboreal habit may place an upper limit on body size, due to the strength of tree branches. Differences in function (especially positional behaviours), which may or may not be related to body size, may also be associated with structural dimorphism. It is likely that the associative factors

interrelate, and a priori conclusions about the likelihood of dimorphism might therefore be inaccurate.

Dimorphism in body size (males larger than females) is a frequent, but not invariable, finding in primates. In the case of size dimorphism, males and females (or their body parts) may not simply be scaled versions of each other due to allometric relations between variables, causing shape dimorphism. Sex-based differences in form may manifest in terms of body weight, but also in size and shape of body parts, and dimorphism in one region of interest need not predict dimorphism in another. However, there may be factors that relate dimorphism in two or more regions of interest. For weight-bearing limb bones, such as the patella, dimorphism is likely to be entrained by body weight dimorphism, as the patella must endure the forces of body weight.

By investigating sexual dimorphism in the patella (especially shape dimorphism), it may be possible to reflect on the social and functional circumstances of the taxa, and thus understand better the variation in morphology seen in earlier chapters. For example, size differences may reflect overall size differences in the genus *Gorilla*, which are important in gaining access to mates and for protecting the group against predators. Size dimorphism may also reflect ecology – for example, arboreal taxa (some *Cercopithecus*) may show less dimorphism than a terrestrial taxon (*Gorilla*). Shape dimorphism may reflect biomechanical differences between sexes, possibly due to the superimposition of size dimorphism on intervariable allometric relations, or for reasons not directly associated with size, for example sexual division of labour.

5.2 Aims and Hypotheses

The aims and hypotheses for this chapter were:

Aim 1 related to size dimorphism, i.e. were the patellae of one sex, on average, larger than those of the other sex?

Aim 1: to investigate the presence of statistical size dimorphism of the patella in each genus based on the lengths (|**x**|) of the measurement vectors (1) (***A***, ***P***) and (2) (***X*1**, ***Y*1**...***X*5**, ***Y*5**) using single classification analysis of variance

Analysis of variance assumed both normality of variables and homoscedasticity of variables between the sexes, so Aim 1 first required the statement of

Aim 2: to investigate the normality of the distributions of |**x**| for conventional and Fourier data by calculating Kolmogorov-Smirnov *Z*-statistics, comparing the data distributions against the normal distribution

and

Aim 3: to investigate the homoscedasticity of |**x**| for conventional and Fourier data between the sexes using *F*-ratios (ratios of variances)

Accordingly, Aim 2 and Aim 3 gave rise to, respectively

Hypothesis 1: that |**x**| for conventional and Fourier data was normally distributed (H_0 : that distributions were normal)

and

Hypothesis 2: that variances of |**x**| for conventional and Fourier data in males and females were not homoscedastic ($H_0 : s_m^2 = s_f^2$)

Aim 1 then gave rise to

Hypothesis 3: that there was statistically significant size difference between male and female patellae as measured by |x| for conventional and Fourier data ($H_0 : \overline{X}_m = \overline{X}_f$)

The following aims and hypotheses related to shape dimorphism. That is, did the patellae of one sex differ, on average, based on shape variables? This would imply the presence of functional difference between males and females.

Aim 4: to investigate the presence of statistical shape dimorphism of the patella in each genus based on (1) the ratio of the square root of area and the perimeter length (***A/P***) and (2) the scores on first and second principal components of Fourier data (normalized data, covariance matrix) ($\boldsymbol{u}_1$, $\boldsymbol{u}_2$) using single classification analysis of variance

As Aim 1 gave rise to Aim 2 and Aim 3, so Aim 4 gave rise to

Aim 5: to investigate the normality of distributions of $\boldsymbol{u}_1$ and $\boldsymbol{u}_2$ by calculating Kolmogorov-Smirnov Z-statistics, comparing the data distributions against the normal distribution

and

Aim 6: to investigate the homoscedasticity of $\boldsymbol{u}_1$ and $\boldsymbol{u}_2$ between the sexes using *F*-ratios

(Due to possible statistical problems, the ratio ***A/P*** was omitted from these analyses, as it was assumed that distributions were nonnormal – see below.)

Aim 5 and Aim 6 gave rise to, respectively

Hypothesis 3: that $\boldsymbol{u}_1$ and $\boldsymbol{u}_2$ were distributed normally (H_0 : that distributions were normal)

and

Hypothesis 4: that variances of ***A/P*** and $\boldsymbol{u}_1$ and $\boldsymbol{u}_2$ in males and females were not homoscedastic ($H_0 : s_m^2 = s_f^2$)

Hypothesis 5: that there was statistically significant shape difference between male and female patellae as measured by ***A/P*** and $\boldsymbol{u}_1$ and $\boldsymbol{u}_2$ ($H_0 : \overline{X}_m = \overline{X}_f$)

It must be noted that where the assumption of normality was violated for the single classification anova, the appropriate test was the Wilcoxon two-sample test, and that instead of a comparison of means, the test was one of a difference in location in rank-ordered positions of males and females (Sokal and Rohlf, 1995).

5.3 Materials and Methods

5.3.1 Size Dimorphism

Data from both conventional and Fourier variables were used in this investigation; the choice was to use the size variables from Chapters 3 and 4, the length of the specimen measurement vectors, |x|.

Mean differences among sexes based on size data were investigated using the single classification analysis of variance (anova) (Sokal and Rohlf, 1995). In this analysis, the following values were calculated:

- the sums of squares among groups, $SS_{among} = \sum^{a} n_i \left(\overline{X}_i - \overline{\overline{X}}\right)^2$, where n_i was the sample size for each sex
- the sums of squares within groups, $SS_{within} = \sum^{a}\sum^{n}\left(X - \overline{X}_i\right)$
- the mean squares among groups, $MS_{among} = \frac{SS_{among}}{a-1}$, where $a - 1$ was the among-groups degrees of freedom, and equalled 1 here
- the mean squares within groups, $MS_{within} = \frac{SS_{within}}{\sum^{a} n_i - a}$, where $\sum^{a} n_i - a$ was the within-groups degrees of freedom

The null hypothesis, that $\overline{X}_{male} = \overline{X}_{female}$, was rejected at the 5% level if the F-value exceeded $F_{0.025[1,\nu_2]}$, where ν_2 was the within groups degrees of freedom (Rohlf and Sokal, 1995). The α-value of 0.025 represented a two-tailed test with an overall α of 0.05; a two-tailed test was used despite the expectation of $\overline{X}_{male} > \overline{X}_{female}$, as the reverse (a) could not be discounted, and (b) would have been a finding of great interest. Ninety-five per cent confidence limits, L_1 and L_2, for the mean differences were calculated using the method of Sokal and Rohlf (1995), as follows.

$$L_1 = \left(\overline{X}_1 - \overline{X}_2\right) - t_{\alpha/2[\nu]} s_{\overline{Y}_1 - \overline{Y}_2} \text{ and } L_2 = \left(\overline{X}_1 - \overline{X}_2\right) + t_{\alpha/2[\nu]} s_{\overline{Y}_1 - \overline{Y}_2},$$

where

$$s_{\bar{Y}_1-\bar{Y}_2} = \sqrt{\left[\frac{(n_1-1)s_1^2+(n_2-1)s_2^2}{n_1+n_2-2}\right]\left(\frac{n_1+n_2}{n_1 n_2}\right)}.$$

A second assumption of anova (in addition to normality) was homoscedasticity, or homogeneity of variances (Sokal and Rohlf, 1995). Consequently, before the single classification anova was performed, sex differences of variances of the size variables were investigated by generating F-ratios, where (Armitage and Berry, 1994; Sokal and Rohlf, 1995)

$$F = \frac{s_1^2}{s_2^2},\ s_1^2 > s_2^2.$$

The null hypothesis that $s^2_{male} = s^2_{female}$ was rejected at the 5% level if F exceeded $F_{0.025[\nu_1,\nu_2]}$. Ninety-five per cent confidence intervals for the ratios were constructed using the method of Armitage and Berry (1994), as follows.

$$L_1 = \frac{F}{F_1} \text{ and } L_2 = F.F_2,$$

where

$$F_1 = F_{0.025[\nu_1,\nu_2]} \text{ and } F_2 = F_{0.025[\nu_2,\nu_1]}.$$

Where assumptions were violated, alternative analyses were performed. In the case of heteroscedasticity, Welch's approximate t-test was used (Sokal and Rohlf, 1995). The calculation was as follows:

$$t' = \frac{(\bar{X}_1-\bar{X}_2)-(\mu_1-\mu_2)}{\sqrt{\frac{s_1^2}{n_1}+\frac{s_2^2}{n_2}}}.$$

The critical value of t'_α was calculated as

$$t'_\alpha = \frac{t_{\alpha[\nu_1]}\frac{s_1^2}{n_1} + t_{\alpha[\nu_2]}\frac{s_2^2}{n_2}}{\frac{s_1^2}{n_1} + \frac{s_2^2}{n_2}}.$$

Where the assumption of normality was violated, the nonparametric Wilcoxon two-sample test was used (Sokal and Rohlf, 1995). This entailed the ranking of all observations from lowest to highest, followed by summing the ranks of the smaller sample. These steps were performed using SPSS. The Wilcoxon statistic was calculated as

$$C = n_1 n_2 + \frac{n_2(n_2+1)}{2} - \sum^{n_2} R,$$

where n_1 and n_2 were the sizes of the larger and smaller samples, respectively, and $\sum^{n_2} R$ was the sum of ranks as above. The test statistic U was determined as the larger of C and $n_1 n_2 - C$. When $n_1 \leq 20$, U was compared directly (Rohlf and Sokal, 1995); when $n_1 > 20$ a t-statistic was computed as follows:

$$t = \frac{U - \frac{n_1 n_2}{2}}{\sqrt{\frac{n_1 n_2 (n_1 + n_2 + 1)}{12}}}.$$

5.3.2 Shape Dimorphism

Shape dimorphism was also investigated using data from conventional and Fourier variables. For the conventional data, the ratio ***A/P*** was used; this was seen to be an appropriate shape measure in Chapter 4, although the scores on PC1 (normalized) could also have been used. Results using the latter should have been similar, as both measures represented a contrast between ***P*** and ***A***. As outlined in §4.1.1.2, ratios derived from normal variables may show serious departures from normality. With that in mind, it was decided to investigate sexual shape differences using the nonparametric method of the Wilcoxon two-sample test (Demes et al., 1991; Sokal and Rohlf, 1995). From the Fourier data, it was seen that the first two principal components of the size-adjusted data (§4.5.1.1) described shape variation, so scores

on these two components were used in this investigation. As these scores were by definition orthogonal (statistically independent), the component scores were analysed separately using single-classification anovas.

5.4 Results

5.4.1 Size Dimorphism

5.4.1.1 *Homo*

5.4.1.1.1 conventional data

Table A.20(a) (page 355) shows the values of Kolmogorov-Smirnov *Z*; no statistically significant deviations from normality were detected, and the null hypothesis of normal distribution was accepted. The results of the analyses of homoscedasticity are presented in Table A.21(a,b) (page 356); the ratios of the variances were not significantly different to 1.00 at the 0.05 level, and therefore the null hypothesis of homoscedasticity was accepted.

The results of the anovas testing the mean differences between sexes are presented in Table A.22(a,b) (page 358) and Table 5.2. The *F*-ratios were very large, and indicated that the differences between means of males and females were significantly different to zero at the $p < 0.0001$ level; the 95% confidence intervals for the mean differences illustrated this well. As measured by the length of the specimen measurement vectors, the null hypothesis of equal means was rejected, with a finding of sexual size dimorphism.

Table 5.2. *F*-values for mean sex size differences and 95% confidence intervals – *Homo*, conventional data

	$\overline{X}_m - \overline{X}_f$	*F*	95% CI
distal	57.23	*88.72	45.35 to 69.10
proximal	46.10	*46.82	32.81 to 59.38

*significant at $p = 0.00$

5.4.1.1.2 Fourier data

Kolmogorov-Smirnov Z-statistics were computed (Table A.23(a), page 361), and in no data set was any deviation from normal detected; the null hypothesis of normal distribution of data was accepted. The homoscedasticity results are presented in Table A.24(a,b) (page 362). No deviation from a ratio of unity was found, and the null hypothesis of homoscedasticity was accepted.

The results of the anovas testing mean differences between sexes are presented in Table A.25(a,b) (page 364) and Table 5.3. Very large *F*-ratios again led to a rejection of the null hypothesis of no mean differences in size between the sexes.

Table 5.3. *F*-values for mean sex size differences and 95% confidence intervals – *Homo*, Fourier data

	$\overline{X}_m - \overline{X}_f$	*F*	95% CI
distal	12.04	*95.13	9.60 to 14.47
proximal	9.90	*52.70	7.21 to 12.59

*significant at $p = 0.00$

5.4.1.2 *Cercopithecus*

5.4.1.2.1 conventional data

Kolmogorov-Smirnov *Z*-statistics are presented in Table A.20(b) (page 355); no statistically significant deviations from normality were detected, and the null hypothesis of normality was accepted. The results of the homoscedasticity tests are presented in Table A.21(c,d) (page 356); the ratios of the variances were significantly different to 1.00 at the $p < 0.0001$ level, with 1.00 well out of the 95% confidence intervals for both distal and proximal levels. The null hypothesis was rejected, with a finding of heteroscedasticity.

The results of the analyses of variance are presented in Table A.22(c,d) (page 358) and Table 5.4. The *F*-ratios were again very large, and the mean differences were significantly different to zero at the $p < 0.0001$ level. The null hypothesis of zero mean size difference was rejected.

Table 5.4. *F*-values for mean sex size differences and 95% confidence intervals – *Cercopithecus*, conventional data

	$\overline{X}_m - \overline{X}_f$	*F*	95% CI
distal	25.18	*43.69	17.62 to 32.75
proximal	26.93	*48.98	19.29 to 34.57

*significant at $p = 0.0000$

However, the assumption of homoscedasticity was violated for these data. As an alternative test, Welch's approximate *t*-test was used, which did not assume homoscedasticity (Sokal and Rohlf, 1995). The results of these tests are presented in Table 5.5. Again, at the two-tailed 5% level of significance, the null hypothesis was rejected in both data sets: the means were significantly different, and there was sexual size dimorphism.

Table 5.5. Welch's approximate *t* statistics for mean sex size difference – *Cercopithecus*, conventional data

	t'	$t'_{0.025}$
distal	6.61	2.01
proximal	7.05	2.01

5.4.1.2.2 Fourier data

Table A.23(b) (page 361) presents the Kolmogorov-Smirnov *Z*-statistics for these data; a statistically significant departure from normality was seen in the males distal data set. For males distal, the null hypothesis of normal distribution of data was rejected; the null hypothesis was accepted for the other data sets. The results of the homoscedasticity tests are presented in Table A.24(c,d) (page 362). In both distal and proximal data sets, statistically significant departures from variance ratios of unity were found, and the null hypothesis of homoscedasticity was rejected.

The results of the tests of mean size differences are presented in Table A.25(c,d) (page 364) and Table 5.6. *F*-ratios were strongly significant, and the null hypothesis of no mean size difference was rejected.

Table 5.6. *F*-values for mean sex size differences and 95% confidence intervals – *Cercopithecus*, Fourier data

	$\overline{X}_m - \overline{X}_f$	*F*	95% CI
distal	5.20	*42.53	3.62 to 6.79
proximal	5.63	*48.41	4.02 to 7.23

*significant at $p = 0.00$

As with the conventional data, the assumption of homoscedasticity was violated. In addition, the males distal data was not normally distributed, a normal distribution of data being another assumption of anova (Sokal and Rohlf, 1995). Therefore, these analyses were repeated using the nonparametric Wilcoxon two-sample test, and the results are presented in Table 5.7. In both cases, the *U*-values were statistically significant and the null hypothesis of zero mean size difference was rejected.

Table 5.7. Wilcoxon two-sample test statistics for mean sex size difference – *Cercopithecus*, Fourier data

	U	*t*
distal	1954.0	*5.35
proximal	2058.5	*5.83

*significant at $p < 0.001$

5.4.1.3 *Colobus*

5.4.1.3.1 conventional data

Table A.20(c) (page 355) shows the Kolmogorov-Smirnov *Z*-statistics for these data; in no data set was any deviation from normality detected, and the null hypothesis of normality was accepted. The results of the homoscedasticity tests are presented in Table A.21(e,f) (page 356). The variance ratios were not significantly different to 1.00 at the 5% level, and the null hypothesis of homoscedasticity was accepted.

The results of the tests of mean differences are presented in Table A.22(e,f) (page 359) and Table 5.8. The *F*-ratios were smaller than for *Homo* and *Cercopithecus*, but showed the mean differences to be nonzero at the $p < 0.01$ and $p < 0.05$ levels for distal and proximal datasets, respectively; the null hypothesis of no size difference was rejected. The lower limit for the proximal data (0.59) was very close to zero, and showed that here zero was only just rejected.

Table 5.8. *F*-values for mean sex size differences and 95% confidence intervals – *Colobus*, conventional data

	$\overline{X}_m - \overline{X}_f$	*F*	95% CI
distal	13.99	*8.14	4.11 to 23.86
proximal	11.81	†4.50	0.59 to 23.02

*significant at $p = 0.0066$ †significant at $p = 0.0384$

5.4.1.3.2 Fourier data

Kolmogorov-Smirnov *Z*-statistics for these data are presented in Table A.23c (page 361). No significant deviations from the normal distribution were found for any data sets, and the null hypothesis of normal data distribution was accepted. The results of the tests for homoscedasticity are presented in Table A.24(e,f) (page 362); no statistically significant deviations from variance ratios of unity were found, and the hypothesis of homoscedasticity was accepted.

Table A.25(e,f) (page 365) and Table 5.9 show the results of the tests of mean size differences. Distal and proximal data sets were significant at the $p < 0.001$ and $p < 0.01$ levels, respectively: the null hypothesis of zero mean size difference was rejected, with a finding of sexual size dimorphism.

Table 5.9. *F*-values for mean sex size differences and 95% confidence intervals – *Colobus*, Fourier data

	$\overline{X}_m - \overline{X}_f$	*F*	95% CI
distal	3.06	*9.02	1.01 to 5.12
proximal	2.53	†4.56	0.14 to 4.93

*significant at $p = 0.0043$ †significant at $p = 0.0382$

5.4.1.4 *Gorilla*

5.4.1.4.1 conventional data

Kolmogorov-Smirnov Z-statistics are presented in Table A.20(d) (page 355); there were no statistically significant deviations from normality, and the null hypothesis of normal data distribution was accepted. The results from the tests for homoscedasticity are presented in Table A.21(g,h) (page 357). The ratios of variances were not significantly different to 1.00 at the 5% level, and the null hypothesis of homoscedasticity was accepted.

The results of the tests of mean size differences are presented in Table A.22(g,h) (page 360) and Table 5.10. The *F*-ratios were very large, and mean differences were significantly different to zero at the $p < 0.0001$ level. The null hypothesis of zero mean difference was rejected, with a finding of sexual size dimorphism.

Table 5.10. *F*-values for mean sex size differences and 95% confidence intervals – *Gorilla*, conventional data

	$\overline{X}_m - \overline{X}_f$	*F*	95% CI
distal	174.22	*55.14	125.68 to 222.76
proximal	130.16	*37.29	86.06 to 174.26

*significant at $p = 0.00$

5.4.1.4.2 Fourier data

Kolmogorov-Smirnov *Z*-statistics are presented in Table A.23(d) (page 361), where it can be seen that there were no significant departures from normality. The null hypothesis of normal data distribution was accepted for these data. Results from the tests for homoscedasticity are presented in Table A.24(g,h) (page 363); variance ratios were not significantly different to unity, and the null hypothesis of homoscedasticity was accepted.

Results from the tests of mean differences are presented in Table A.25(g,h) (page 366) and Table 5.11. *F*-values were large, and means were significantly different at the $p = 0.00$ level; the null hypothesis of zero mean size difference was rejected.

Table 5.11. *F*-values for mean sex size differences and 95% confidence intervals – *Gorilla*, Fourier data

	$\overline{X}_m - \overline{X}_f$	*F*	95% CI
distal	36.43	*55.81	26.34 to 46.52
proximal	27.29	*38.94	18.24 to 36.33

*significant at $p = 0.00$

5.4.2 Shape Dimorphism

5.4.2.1 *Homo*

5.4.2.1.1 conventional data

The results of the Wilcoxon two-sample tests are presented in Table 5.12. The null hypothesis of no shape differences between the sexes was accepted for distal data, but rejected for proximal data. Therefore, shape dimorphism was found using proximal data.

Table 5.12. Wilcoxon two-sample test statistics for sex shape difference – *Homo*, conventional data

	$\overline{X}_f$	$\overline{X}_m$	*U*	*t*
distal	0.2387	0.2386	5306	0.37
proximal	0.2392	0.2407	6100	*2.01

*significant at $0.05 > p > 0.02$

5.4.2.1.2 Fourier data

Kolmogorov-Smirnov Z-statistics for these data are presented in Table A.26(a) (page 367); no significant deviations from normality were detected. In the distal data set, the variance ratio for u_2 was significantly different to unity at the $p < 0.01$ level (Table A.27(a,b), page 368), so the null hypothesis of homoscedasticity was rejected; otherwise, the null hypothesis was accepted.

The results of the analyses of variance for mean shape differences are presented in Table A.28(a,b) (page 370) and Table 5.13. For each data set and for both u_1 and u_2, the null hypothesis of zero mean shape difference was accepted: no statistical shape dimorphism was detected.

Table 5.13. *F*-values for mean sex shape differences and 95% confidence intervals – *Homo*, Fourier data

		$\bar{u}_m - \bar{u}_f$ [a]	*F*	95% CI
distal	u_1	1.25	1.01	–1.20 to 3.71
	u_2	1.10	2.71	–2.19 to 2.42
proximal	u_1	1.79	2.32	–0.53 to 4.10
	u_2	–1.14	2.37	–3.08 to 0.80

[a]mean differences x 10^{-3}

However, due to the assumption of homoscedasticity being violated for u_2 in the distal data set, these data were submitted to Welch's approximate *t*-test. These results are presented in Table 5.14, and confirm that no shape dimorphism was detected.

Table 5.14. Welch's approximate *t* statistics for mean sex shape difference – *Homo*, Fourier data

	t'	$t_{0.025}$
distal u_2	1.65	1.98

5.4.2.2 *Cercopithecus*

5.4.2.2.1 conventional data

The results of the Wilcoxon two-sample tests for shape differences between sexes are presented in Table 5.15. The null hypothesis of no shape difference among the sexes was accepted, so no sexual shape dimorphism was found.

Table 5.15. Wilcoxon two-sample test statistics for sex shape difference – *Cercopithecus*, conventional data

	$\overline{X}_f$	$\overline{X}_m$	*U*	*t*
distal	0.2568	0.2560	1225	0.17
proximal	0.2650	0.2642	1263	0.27

5.4.2.2.2 Fourier data

Table A.26(b) (page 367) and Table A.27(c,d) (page 368) show the results of the tests of normality and homoscedasticity, respectively; no significant deviations from normality were detected, and the null hypothesis of normality was accepted. In both distal and proximal data sets, variance ratios for u_1 were significantly different to unity, and the null hypothesis of homoscedasticity was rejected. The null was accepted for the variances of u_2.

The results of the tests of mean shape differences are presented in Table A.28(c,d) (page 371) and Table 5.16. In the distal data set, the mean difference for u_2 between sexes was significantly different to zero at the $p < 0.01$ level, and the null hypothesis of zero mean shape difference was rejected; otherwise, the null hypothesis was accepted.

Table 5.16. *F*-values for mean sex shape differences and 95% confidence intervals – *Cercopithecus*, Fourier data

		$\bar{u}_m - \bar{u}_f$ [a]	*F*	95% CI
distal	u_1	–2.08	0.73	–6.35 to 3.31
	u_2	–2.57	*8.79	–4.29 to –0.85
proximal	u_1	–2.65	1.73	–6.64 to 1.35
	u_2	0.25	0.11	–1.24 to 1.74

*significant at $p = 0.0038$
[a]mean differences $\times 10^{-3}$

The u_1 data were analysed again using Welch's approximate *t*-test due to heteroscedasticity – these results are presented in Table 5.17. The zero mean shape differences were confirmed by these results.

Table 5.17. Welch's approximate *t* statistics for mean sex shape difference – *Cercopithecus*, Fourier data

	t'	$t_{0.025}$
distal u_1	−0.86	2.01
proximal u_1	−1.32	2.01

5.4.2.3 *Colobus*

5.4.2.3.1 conventional data

The results from the Wilcoxon two-sample tests for shape differences between the sexes are presented in Table 5.18; the null hypothesis of no shape difference between the sexes was accepted

Table 5.18. Wilcoxon two-sample test statistics for sex shape difference – *Colobus*, conventional data

	$\overline{X}_f$	$\overline{X}_m$	U'	t
distal	0.2535	0.2542	294	0.45
proximal	0.2605	0.2605	284	0.24

5.4.2.3.2 Fourier data

Table A.26(c) (page 367) and Table A.27(e,f) (page 369) show the results of the tests for normality and homoscedasticity, respectively; no significant deviations from normality were seen, and the null hypothesis of normality was accepted. None of the variance ratios was significantly different to unity, so the null hypothesis of homoscedasticity was accepted.

The results of the tests for mean differences among sexes are presented in Table A.28(e,f) (page 372) and Table 5.19. In all cases the mean shape difference was not significantly different to zero, so the null hypothesis of no mean shape difference between the sexes was accepted.

Table 5.19. *F*-values for mean sex shape differences and 95% confidence intervals – *Colobus*, Fourier data

		$\bar{u}_m - \bar{u}_f$ [a]	*F*	95% CI
distal	u_1	−4.35	1.80	−10.89 to 2.18
	u_2	1.50	1.43	−1.02 to 4.03
proximal	u_1	0.61	0.03	−6.21 to 7.42
	u_2	2.33	4.39	−4.90 to 0.24

[a]mean differences x 10^{-3}

5.4.2.4 *Gorilla*

5.4.2.4.1 conventional data

The results of the Wilcoxon two-sample tests for difference between sexes are presented in Table 5.20; as the larger sample size did not exceed 20, the significance of *U* was assessed directly. In the distal data set, the difference between the sexes was statistically significant, and the null hypothesis of zero shape difference was rejected; there was therefore sexual shape dimorphism in these specimens. The null hypothesis was accepted in the proximal data set.

Table 5.20. Wilcoxon two-sample test statistics for sex shape difference – *Gorilla*, conventional data

	$\bar{X}_f$	$\bar{X}_m$	*U*
distal	0.2431	0.2355	*116
proximal	0.2450	0.2479	92

*significant at $0.02 > p > 0.01$

5.4.2.4.2 Fourier data

The results from the tests for normality and homoscedasticity are presented in Table A.26(d) (page 367) and Table A.27(g,h) (page 369), respectively; no significant deviations from normality were detected. In the distal data set, the variance ratio for u_2 was found to be significantly different to unity, so the null hypothesis of homoscedasticity was rejected; otherwise, the null was accepted.

Table A.28(g,h) (page 373) and Table 5.21 show the results for the tests for mean differences between the sexes. In the proximal data set, the difference between means of u_2 was significant at the $p < 0.01$ level, and the null hypothesis of no mean shape difference was rejected; otherwise, the null hypothesis was accepted.

Table 5.21. *F*-values for mean sex shape differences and 95% confidence intervals – *Gorilla*, Fourier data

		$\bar{u}_m - \bar{u}_f$ [a]	*F*	95% CI
distal	u_1	2.29	0.34	–5.81 to 10.39
	u_2	1.40	0.46	–2.86 to 5.66
proximal	u_1	0.78	0.02	–5.79 to 7.35
	u_2	–3.68	*12.05	–6.09 to –1.27

*significant at $p = 0.0021$ [a]mean differences $\times 10^{-3}$

The assumption of homoscedasticity was violated for u_2 in the distal data set, so these data were submitted to Welch's approximate *t*-test (Table 5.22); the results confirmed that the null hypothesis should have been accepted.

Table 5.22. Welch's approximate *t* statistics for mean sex shape difference – *Gorilla*, Fourier data

	t'	$t_{0.25}$
distal u_2	0.58	2.28

5.5 Discussion

5.5.1 Size Dimorphism

This investigation found statistically significant sexual dimorphism in patellar outline size as measured by the length of the specimen measurement vectors (1) (***A***, ***P***) and (2) (***X1***, ***Y1***,...,***X5***, ***Y5***) in all of the data sets. Furthermore, in all data sets the male specimens were on average larger than the female specimens. The degree of size dimorphism was reflected in the 95% confidence intervals for mean size differences: for example, using conventional data, in *Homo* distal the mean difference was at least 45.35 units, whereas in *Colobus* proximal the lower limit was only 0.59 (in *Colobus* proximal). The confidence intervals for *Gorilla* were relatively wide, and although the estimates of mean size differences were imprecise, that they were not zero was clear.

Earlier it was stated that body size can influence body size dimorphism due to allometry (§5.1.3) – that is larger species show greater body weight dimorphism than smaller species due to a nonlinear relation between male and female body weight. It was interesting to ask whether, in a similar vein, patellar size was associated with patellar size dimorphism. Firstly, it must be asked whether a relation existed between male and female patellar size (i.e. means of genera), a question that was not addressed in Chapter 4. Figure 5.1 shows, on the left side, scatterplots of female versus male size ($|x|$, for both conventional and Fourier data). On the right side in Figure 5.1 are scatterplots of the ratio of average male and average female size (as a measure of dimorphism), versus the grand mean of each size variable (as an overall measure of specimen size). The plots of mean female versus mean male size revealed consistently that there was no relation between means; the points for *Gorilla* and *Homo* deviated substantially from the line of best fit, being below and above it, respectively. Therefore, *Gorilla* showed, on average, greater size dimorphism than *Homo*. On a lesser scale, *Cercopithecus* showed greater dimorphism than *Colobus*. Therefore, there was no allometric relation between male patellar size and female patellar size. When plotting the dimorphism ratio against the size grand mean for each genus, it was clear that there was no association between patellar size dimorphism and patellar size, which reflected the lack of allometry. On average, *Cercopithecus* and *Gorilla* patellae consistently showed greater dimorphism, despite being smaller, than *Colobus* and *Homo*, respectively.

Figure 5.1. Scatterplots of female (y-axis) versus male (x-axis) mean patellar size (left) and male/female mean size ratio (y-axis) versus mean patellar size (x-axis) (right) (*Cercopithecus* ○, *Colobus* +, *Gorilla* △, *Homo* □)

(a) distal, conventional data

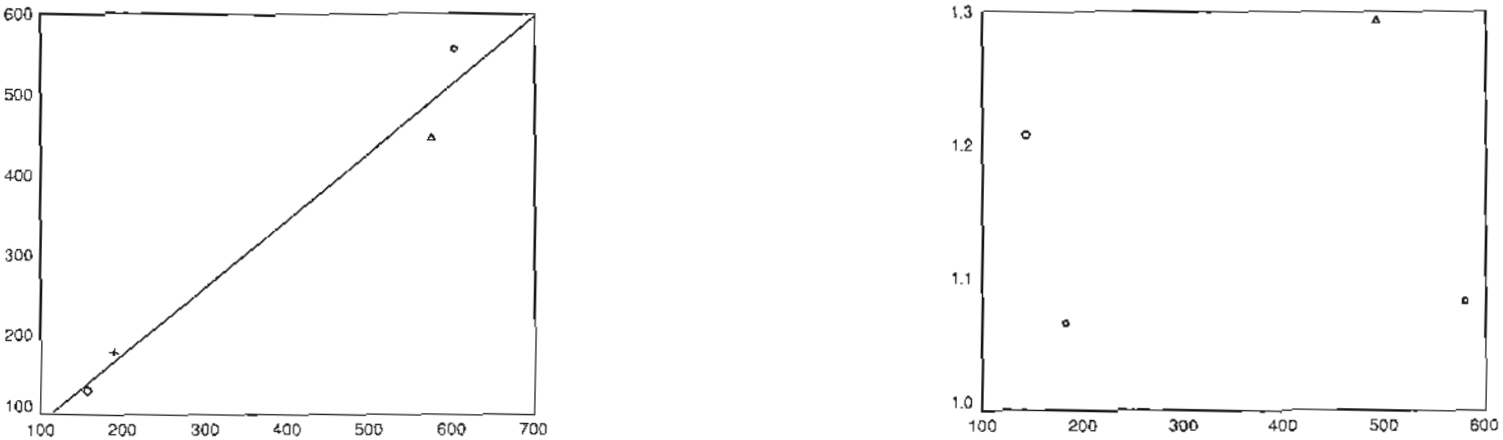

(b) proximal, conventional data

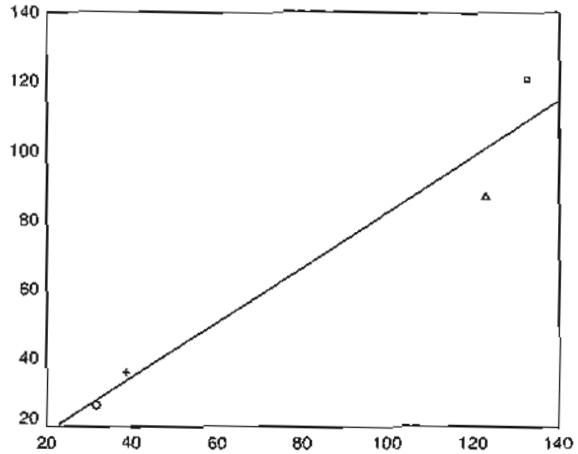

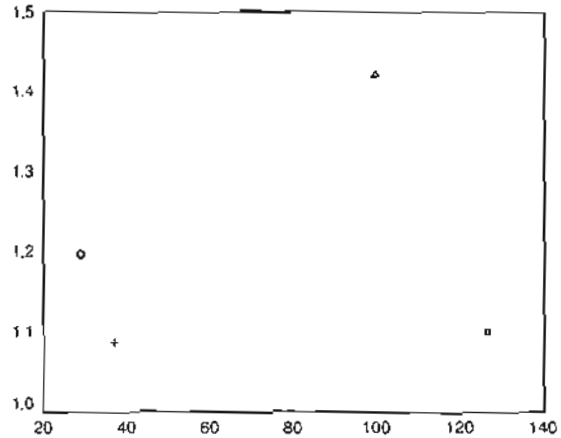

(**c**) distal, Fourier data

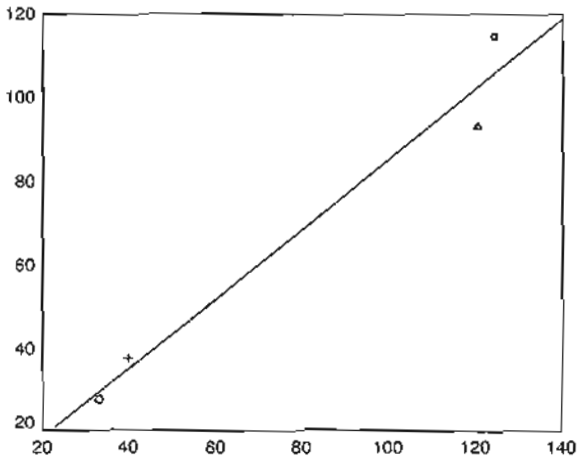

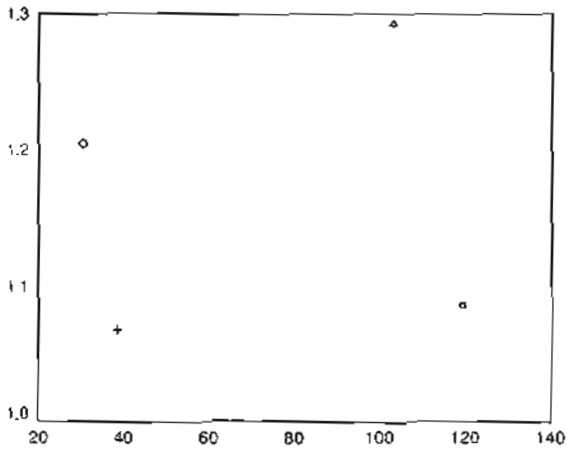

(**d**) proximal, Fourier data

5.5.2 Shape Dimorphism

In general, there was a lack of clear sexual shape dimorphism. As measured by ***A/P***, only in *Homo* proximal and *Gorilla* distal was statistical shape dimorphism found, and using Fourier data, dimorphism was only found in *Cercopithecus* distal and *Gorilla* proximal for u_2. Where significant shape dimorphism was found, there was no apparent pattern of shape difference: for *Homo* proximal and *Gorilla* distal, females had a lower and a higher mean value of ***A/P*** than males, respectively. The findings of shape dimorphism in *Cercopithecus* distal and *Gorilla* proximal using u_2 reflected larger values of u_2 for females in each case.

Shape dimorphism may arise due to a combination of (1) an allometric relation between variables, and (2) size dimorphism (Arsuaga and Carretero, 1994; Oxnard, 1984; Wood, 1976); that is, due to size-related shape differences and size differences. Sexual size dimorphism was detected in all data sets, and from Chapter 4 there were findings of allometry between ***P*** and ***A*** in data sets where shape dimorphism was not found (*Homo* males and females distal, *Cercopithecus* females distal, *Colobus* females distal and proximal, and *Gorilla* males proximal). It could be that lack of shape difference in this section (i.e. null hypothesis of geometric similarity accepted) was due to isometry in the combined (male and female) data sets. Table A.29 (page 374) and Table 5.23 show the allometry results for these combined data sets (as these analyses were not performed in Chapter 4). With the exception of *Homo* distal, the findings relating to shape difference reflected the combined allometry results – where shape difference was found (*Homo* proximal and *Gorilla* distal), the 95% confidence interval for the intercept did not include zero, and zero was included where shape difference was not found. Therefore, shape difference was due to allometry and size dimorphism, and lack of shape difference was due to isometry (despite size dimorphism). *Homo* distal was the exception to this pattern – there was a combination of combined allometry between ***P*** and ***A***, and there was strong size dimorphism. Figure 5.2 explains the lack of shape difference: despite overall allometry between ***P*** and ***A***, with respect to the male and female *means* there was isometry – a line linking the two means passed very close to the origin (calculated as passing through (0.002, 0.000) from the mean values). This meant that, despite expectations of shape differences, the means of ***A/P*** (0.2386 for females, 0.2387 for males) were almost identical.

Table 5.23. Intercepts and 95% confidence limits from combined allometric investigation

	c	c_1	c_2
***Homo* distal**	9.83	4.00	15.60
***Homo* proximal**	10.73	6.22	15.17
***Cercopithecus* distal**	−0.09	−1.20	1.02
***Cercopithecus* proximal**	0.06	−0.73	0.85
***Colobus* distal**	−0.91	−3.65	1.79
***Colobus* proximal**	−2.94	−5.95	0.05
***Gorilla* distal**	−8.93	−14.18	−3.68
***Gorilla* proximal**	−0.83	−6.66	4.99

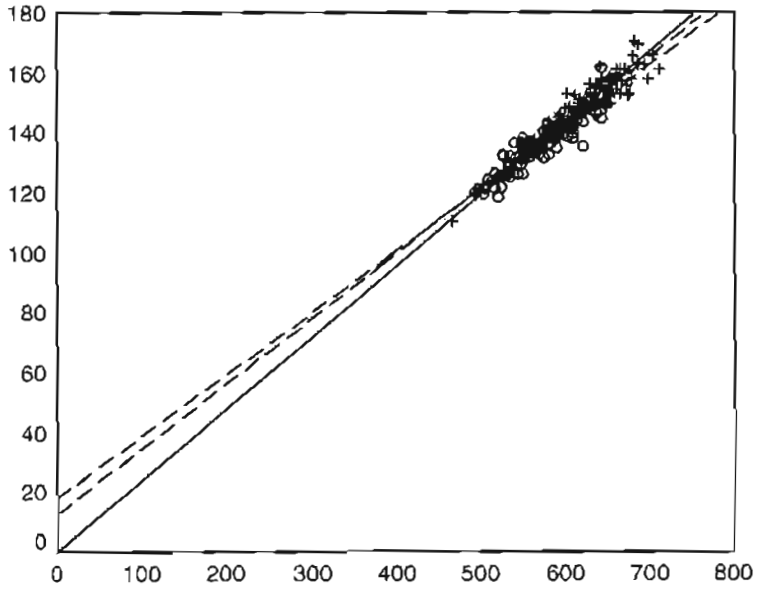

Figure 5.2. Scatterplots of *A* versus *P* (female ○, male +), with lines of best fit for female and male specimens (dashed) and for female and male means (solid) – *Homo* distal, conventional data

How may these shape dimorphisms be interpreted? As seen in Chapter 4, the ratio ***A/P*** reflected the likeness of the outline to a circle – the closer to 0.28 this value was, the closer the outline approximated a circle; deviations from this value (always decreasing) indicated either that the outline was less circular globally (i.e. more elliptic), or locally (articular concavities, for example). In the *Homo* proximal data set, the mean value for ***A/P*** was 0.2408 for females and 0.2393 for males. Therefore, on average, female patellae were more circular than male patellae. In the *Gorilla* distal data set, this situation was reversed – values for ***A/P***

were 0.2355 for females and 0.2431 for males, so on average males were more circular than females.

A difference in the value of ***A/P*** would have reflected a difference in the degree of circularity of the patellar outlines, which may be due to global or local deviations. Global deviations, or ellipticity of outlines, would be reflected in differences in $\boldsymbol{u}_1$, which from §4.5.1.1 was seen to represent a contrast in the semimajor and semiminor axes of the best-fitting ellipse to the outline. No data sets showed dimorphism in $\boldsymbol{u}_1$, which suggested that shape dimorphisms found with conventional data were not due to global deviations. However, sexual dimorphism in $\boldsymbol{u}_2$ was found only in *Cercopithecus* distal and *Gorilla* proximal, and not in *Homo* proximal or *Gorilla* distal, where shape dimorphism with conventional data had been found. Interpretation of $\boldsymbol{u}_2$ was not attempted, but it was probable that it accounted for local outline deviations, as it was dominated by ***Y2***.

It was important to consider why shape dimorphism was not found. Sample sizes ranged from nine to 106, but there was no association between sample size and shape dimorphism – *Homo* and *Gorilla* were at the extremes of sample sizes. Conventional data were analysed using a nonparametric method, Fourier data by a parametric method. In general, and only if parametric method assumptions are met, nonparametric methods have lower power than parametric methods (Sokal and Rohlf, 1995). However, there was no clear pattern of results when comparing conventional and Fourier data. In addition, while the assumption of homoscedasticity was violated for some data sets, reanalysing using Welch's approximate *t*-test did not change the findings. In Chapter 3, the Fourier amplitudes ***X2*** (males distal) and ***Y3*** (females distal) were found to be unreliable. As unreliability can reduce the power of inferential statistical methods (Bailey and Byrnes, 1990; Fleiss, 1986), it was possible that the lack of shape difference was due in part to this unreliability; as these amplitudes contributed only a small part to the shape variables, this was unlikely to have been of importance.

5.5.3 Comparative Discussion

5.5.3.1 Proximal versus distal outlines

In general, there were no substantial differences between the results for proximal and distal outlines for size dimorphism, in that all data sets showed dimorphism. There was no consistent difference between levels for shape dimorphism: in most data sets, no dimorphism was found, and was found in only a few cases, where distal outlines were found to be as

dimorphic as proximal outlines. There was consequently no advantage to using images from one level over the other, but there was also no obvious redundancy.

5.5.3.2 Conventional versus Fourier data

Sexual size dimorphism was found equally using conventional and Fourier data. Sexual shape dimorphism was only found in two data sets using conventional data, and in another two sets using Fourier data. It could be argued that where shape dimorphism was found with conventional data, but not Fourier data, the reduction of power in nonparametric methods when compared to parametric methods (Sokal and Rohlf, 1995) might have explained the results. That shape dimorphism was also found using Fourier data, where it had not been found using conventional data, would refute this argument.

5.5.3.3 Comparison among genera

All genera were found to be sexually dimorphic in terms of patellar size. In Chapter 3 it was suggested that patellar size dimorphism should be greater in *Gorilla* than *Homo*. This was supported by the results of this chapter: Figure 5.1 clearly shows that sexual size dimorphism was greater for *Gorilla* than *Homo*, and furthermore that this was not simply due to patellar size. Whether body size could have been influential here, as well as over all genera, will be discussed in Chapter 6. There appeared to be no genus-specific pattern of sexual shape dimorphism, dimorphism being found in *Homo*, *Cercopithecus* and *Gorilla*, but not in *Colobus*; even within the former three genera there were mixed results, which could not be reconciled with function.

5.6 Conclusions

There were statistically significant differences between males and females in terms of size of the patella, as measured by measurement vector lengths of both (***A***, ***P***) and (***X1***, ***Y1***,...,***X5***, ***Y5***).

In only a minority of cases was there found any shape dimorphism, either by the ratio of the square root of specimen cross-sectional area or by the scores on the first and second principle components of normalized (size-adjusted) data. There were no clear patterns of shape dimorphism, as (1) where dimorphism was found at one level of the patellae, it was not found at the other, and (2) dimorphism could not be related to functional types.

Chapter 6 General Discussion, Limitations of This Study and Areas for Further Research, and Concluding Remarks

6.1 General Discussion

In Chapters 2, 4 and 5, background information was reviewed which showed potential interrelations among such influences on morphology as function, body size and sex differences. A general aim of this study was to elucidate these effects on patellar morphology; here, the findings from Chapters 3, 4 and 5 will be summarized, and then discussed as a means of elucidating these interrelations.

6.1.1 Summary of Findings

The results of Chapter 3 related to patellar outline form (the 'actual' measurements) and while they related information about data structure, it was not generally possible to associate the findings from each genus with functional influences. Data were constrained in phenotype space, and it appeared that the spread of specimens, based on the variables measured, was described by combinations of these variables in fewer than the total number of dimensions. It was clear that specimen size was helped to explain such limitations to morphometric variation, and shape variation was comparatively overshadowed by size. One finding that was clear was that *Homo* specimens were larger than otherwise expected based on published average body weights. The first part of Chapter 4 (size-adjustment), showed that the patellar outlines (the 'relative' measurements) occupied a place on the shape range from more circular to less circular: this was the only interpretation possible from the bivariate conventional data. The Fourier data allowed for two general interpretations of 'less circular': more elliptic, and/or with local deviations (articular concavities, for example). The somewhat abstract nature of the Fourier amplitudes, especially of harmonic > 1, limited interpretation of the findings. The results from the second part of the chapter (allometry), elucidated the size-associated variation of shape. For conventional data, functional relations were shown to exist between A and P, but the nature of these relations varied; results showed that, with an increase in size, the specimens under investigation became either more or less circular. On occasions, the data allowed for a statistical inference of geometric similarity, but there was no clear pattern: interpretations differed between genera, sexes, and even levels within the same genera. The results using Fourier data were much less clear, and in only a minority of cases was there found a relation between variables; where relations were found between $X1$ and $Y1$,

they concurred with the findings using conventional data. Otherwise, the relations were not interpretable. The results of Chapter 5 showed that, on average, male patellae (at least by their outlines) were larger than female patellae. Species with larger patellae did not necessarily show greater patellar size dimorphism. More often than not, the results did not show shape differences between the sexes. That there were (a) size differences between the sexes, and (b) allometric relations among variables (especially ***A*** and ***P***) suggested that there should have been more shape differences; this expectation was shown to be wrong, as male and female specimens together often showed geometric similarity along the size range.

6.1.2 Function

Figure 6.1 shows the relations between specimen morphology and function, body size and sexual dimorphism, as discussed in Chapters 2, 4 and 5. (Phylogeny, also assumed to have some influence on morphology, probably acts via the above influences, as well as directly.) There is seen to be a two-way flow of influence between morphology and function. That is, function can alter morphology, but morphology may also determine function. The outline form of the patella should have an association with function, as bone shape is determined in part by functional factors, although not necessarily function that admits of ready interpretation. Bone morphology arises according to constraints of development and natural selection; some morphologies may be due to architectural constraints, meaning that avoiding such a morphology is impossible (Gould and Lewontin, 1979), but this does not necessarily give a clear functional interpretation. Other features might arise through modelling, to meet structural criteria, or through inheritance, due to an advantage conferred on the individual. While features arising from modelling are explicitly mechanically competent, those inherited via natural selection are still beholden to structural criteria. That is, a feature of a bone may be (1) as a consequence of mechanical demands placed on the bone, and/or (2) an inherited feature which increases the fitness of the animal, but which still exists within the bounds of structural competence.

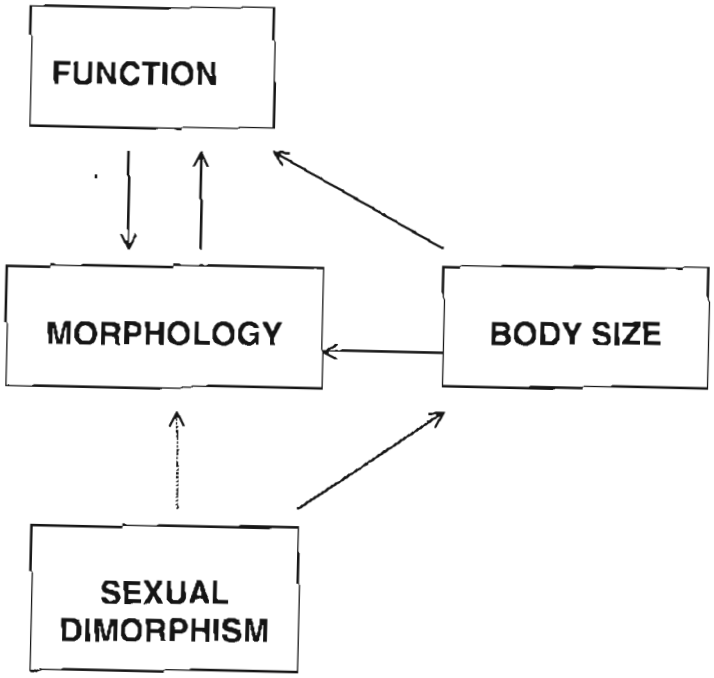

Figure 6.1. Diagram showing the interrelations between specimen morphology, function, body size and sexual dimorphism (dashed arrow signifies that a direct effect of sex differences on morphology is unlikely with the patella)

The functional and biomechanical information from §2.1.2.2, §2.1.2.3 and §2.1.2.6 may be useful in interpreting the patterns of patellar cross-sectional morphological variation. The cross-sectional area enclosed within the outline could have reflected applied axial forces, but as the patella mainly endures bending and compression (of the ventral surface against the trochlea), this was unlikely to be directly relevant. If the cross-sectional area of the patella reflected anything directly, it was likely to be as a measure of fibrous tissue (quadriceps tendon, patellar ligament) attachment area. Sagittal depth of the patellar outline might have reflected the resistance to applied bending forces in the sagittal plane; given that all specimens had greater breadth than depth, deeper patellae were often more circular, but not always. This would be an example of a developmental constraint: the developing bone, sensitive to stress and/or strain, was obliged to increase the sagittal diameter to attenuate bending stress or strain to achieve physiological homeostasis. Patellar depth might alternatively be a selected character: that is, this diameter might be an inherited feature, selected for due to its spacer effect. It would appear from §2.1.2.2 that the spacer effect is of limited utility, which would suggest that patellar depth is largely governed by the sagittal bending forces applied to the

patella (Ward et al., 1995); that patellar depth is available for the secondary function (Gould and Lewontin, 1979) of spacing would not contradict this. However, an argument against this must remain: the mechanical properties of the patella, as a composite beam, derive not only from cortical architecture, but also from that of the inner trabecular framework, and bending resistance is not solely due to cortical form. The sagittal depth of the patella may also resist horizontal plane bending, a feature likely to be of greater need in *Homo*. Coronal breadth of the patellar outline most likely reflected patellofemoral contact area; although is indirectly related to patellar breadth (as the base relates to the other two sides of a triangle), but a broader patella would tend to have greater articular area available for contact.

From Figure 4.13 and Figure 4.20, it is clear that there was a separation of *Cercopithecus* and *Colobus*, on one hand, and *Homo* and *Gorilla*, on the other, in terms of shape (at least as represented by ***A/P***). Therefore, the cercopithecoids showed more circular patellar outlines than the hominoids; that is, the patellae of primates that overall engage in more leaping and climbing activities were more circular. This can be explained mechanically: species that move using large accelerations through a highly flexed knee should apply greater bending forces (relative to body weight) than species that move with smaller accelerations through a more extended knee. Therefore, separation of hominoids and cercopithecoids in phenotype space was not purely due to patellar size, but also shape; patellar shape likely reflected function, but it must also be accepted that size influenced shape.

Figure 4.16, showing the scatterplots of ***A/P*** versus |x|, allowed for a possible functional interpretation of shape within *Cercopithecus* and also *Colobus*. To gain a functional interpretation of shape, functionally disparate species should ideally have shown some separation on the *y*-axis. Defining primate function in a simple manner is difficult (§2.1.2.5) – hence Oxnard's regional functional spectrum – although considering species at relative functional extremes should be meaningful. *Cercopithecus mona* was seen in §2.1.2.5 to exhibit some leaping, and *C. neglectus* to be a slow, terrestrial monkey. Projecting these points on the females distal plot to the *y*-axis showed that the *C. mona* specimens occupied a position higher up the *y*-axis (greater values of ***A/P***) than the *C. neglectus* specimens. That is, leapers showed more circular patellar outlines than did the slow terrestrial individuals. The projections of the *C. aethiops* specimens confounded this: these specimens covered a range from more circular than *C. mona* to as circular as most *C. neglectus* specimens. Therefore, there was no clear functional interpretation of these shape data; that there was no separation even between *C. mona* and *C. neglectus* on the other scatterplots confirmed this. In the *Colobus* scatterplots, there was no clear separation of any species; *C. badius*, which appeared in §2.1.2.5 to leap the most, was certainly not separate from *C. guereza*, a walker.

It was anticipated that shape differences would have reflected functional differences. Overall size differences also appeared to reflect functional differences, namely those between quadrupeds and bipeds. As found by Jungers (1988) and Ruff (1988), hindlimb articular area, relative to body weight, was greater for humans than other primates. The results of this study (Chapter 3) showed that human patellae were of greater size than average body weight would have predicted, at least relative to the other genera. That Jungers (1988) and Ruff (1988) found this divergence for articular surfaces (not cross-sections of bones) did not affect the conclusion of this study, as slightly under half of the patellar outline in cross-section is articular. It is interesting to consider the divergence of human hindlimb joint size relative to that of nonhumans; that humans are likely to use greater joint surface area to attenuate otherwise increased stresses is intuitive. However, did joint size increase relative to body weight with evolution, or did body weight decrease relative to joint size? The latter possibility is given credence by studies into human brain evolution (Aiello and Wheeler, 1995; Henneberg, 1998). These authors have suggested that a decrease in gut size may have allowed a relative increase in brain size; may it be possible, perhaps, to suggest that this may also have allowed hind limb bones to remain large relative to body weight, and therefore able to cope with the increased forces?

6.1.3 Body Size

Body size is likely to affect limb bone morphology in two ways: via overall size (large individuals have large skeletons), and via body size-related morphological requirements. The latter influence is mediated by function – large individuals are likely to place different functional demands on their bones than smaller individuals, and may be manifested by allometric relations (Chapter 4). Body size also may influence morphology via function by determining the actual mode of function; smaller animals are more likely than larger animals to engage in large-acceleration activities such as leaping (this was discussed in §2.1.4.2).

In nonhuman primates, larger genera had larger patellae (Chapter 3); for example, Figure 4.20 showed that *Homo* patellae were larger than *Gorilla* specimens, but Table 2.3 quite clearly showed that average body weights were greater for *Gorilla* than *Homo* (in Figure 4.20, genera were ordered on the *x*-axis according to increasing *patellar* size). Patellar size reflected average body weight (qualitatively) in *Cercopithecus* and *Colobus*. The morphological divergence in *Homo* probably reflected the functional divergence of human bipedalism versus nonhuman quadrupedalism as seen in §4.1.2.2.

The theoretical basis for allometry is that the mechanical demands placed on the skeletons of individuals of different body sizes should differ. An association found between size and specimen shape could be in terms of (1) body size, and/or (2) specimen size; allometric associations were determined between patellar shape and patellar size, in the absence of body size data. For the theoretical basis for allometry to hold, it must be assumed that patellar size, within genera, reflected body size – that patellar size did not appear to reflect body size among genera did not contradict this assumption. The allometric patterns found may be better understood by first discussing expected patterns, although to predict the pattern of size-related morphological variation in a sample of animals is difficult. As a starting point, it is useful to consider the morphological ramifications of assuming constant function with increasing body size (the elastic similarity theory). Body weight produces a flexor moment of the knee, so the flexor moment to be opposed by quadriceps femoris should increase proportional to $W^{1.00}$. The ability to produce an extensor moment is dependent on extensor force multiplied by the extensor moment arm; this could be achieved by increasing muscle cross-sectional area and/or increasing the extensor moment arm, both relative to body weight. Increasing the cross-sectional area of the quadriceps relative to body weight would require a commensurate increase in the cross-sectional area of the patella, simply to provide the necessary area for attachment of the quadriceps tendon. However, as seen in §2.1.2.2, the extensor moment arm is not simply the distance of the patella from the tibiofemoral joint as assumed implicitly by Biewener (1983, 1990) and explicitly by Demes and Günther (1989). Due to the balance-beam effect, the extensor moment arm is also dependent on the distances to both the proximal and distal patellar poles from the point of contact with the femur. Therefore, extensor moment arm may be increased by increasing the patellar ligament moment arm; increasing the patellar ligament arm could be achieved by adopting a more extended position of the knee, but for now function is being kept constant. Morphological adaptations could include increasing the dorsal projection of the patella (spacer effect), as well as increasing the 'distal length' (the distance between the point of femoral contact and the distal pole) by lengthening the patella (balance-beam effect). An increase in the quadriceps force (via increased cross-sectional area) would increase bending in the sagittal plane, so the increase in area should be such that the sagittal second moment of area (via patellar depth) is increased relative to body weight. This should also be increased if the patella is lengthened, as length alone would increase the bending moment on the bone. Patellofemoral joint reaction force should also increase proportional to $W^{1.00}$; the articular surface area of the patella should then increase proportional to $W^{>0.67}$ to attenuate the otherwise increased chondral stresses. Consequently, patellar breadth should also increase relative to body weight, to increase contact area. However, to predict that there should be increases relative to body weight in patellar (1)

cross-sectional area, (2) depth and (3) breadth does not allow for a confident prediction of shape (especially relative increases in breadth and depth) in the absence of body size data.

Is there experimental evidence to support these predictions? There is evidence that hindlimb muscle cross-sectional area increases relative to increasing body weight (Alexander et al., 1981; Pollock and Shadwick, 1994), so this prediction for quadriceps allometry is supported. The prediction of morphological changes to increase the extensor moment arm is partially supported by the evidence of Biewener (1983, 1989, 1990), who found that hindlimb muscle moment arms also increase relative to body weight. However, this was only in concert with a decrease in ground reaction moment arms, due to a more extended position of the limb, which illustrates the incompleteness of the elastic similarity theory. Therefore, the aforementioned morphological adaptations could be avoided at least partly by functional modifications. Patellar depth, as a measure of bending strength (via second moment of area in the sagittal plane) could increase or remain the same with respect to body weight based on evidence from the primate femur (Demes et al., 1991; Rafferty, 1998). Demes and Günther (1989) provided possible evidence (albeit indirect), of patellar depth increasing relative to body weight in larger animals, by measuring knee extensor moment arm (treating the extensor mechanism as a pulley, not a balance-beam); it could be inferred that the finding of increased moment arm was at least in part due to increased patellar depth. However, in an investigation similar to the current study, Ward et al. (1995) found decreased patellar depth relative to patellar breadth in larger primates (humans and apes, as compared to monkeys), and related this to decreased leaping in the larger primates. The expectation of increased articular surface area relative to body weight, as predicted by Swartz (1989), may be avoided by modifying the forces imposed on the joint so that forces increase proportional not to $W^{1.00}$, but to $W^{0.67}$ (Alexander, 1980, 1981), and then geometric similarity may prevail (Godfrey et al., 1991). Such functional modifications presumably include keeping the knee more extended (Biewener, 1990; Jungers and Burr, 1994), and by a relative avoidance of large-acceleration behaviours such as leaping (Demes and Günther, 1989; Günther et al., 1991). Therefore, this study did not support Gould's (1971) contention that geometric similarity is a problem, and while geometric similarity might not be an expectation, it should not be a wholly surprising finding. Nevertheless, of the only data addressing patellar scaling relative to body size (Jungers, 1990; personal communication), nonhuman primate patellar articular breadth was found to scale with negative allometry with respect to body weight; that is, larger individuals had relatively narrower patellae. When humans were grouped with these nonhumans, the relation approximated geometric similarity. However, the latter result appears artefactual, as human hindlimb joints have been found to have greater surface area relative to body weight (Jungers,

1990; Ruff, 1990). This deviation of humans from nonhumans was probably related to the differences between bipedal and quadrupedal locomotion, and the addition of humans to a nonhuman sample confounded the finding of negative allometry. This was supported by the findings that suggested average patellar outline size (relative to body weight) was increased in humans relative to nonhumans.

As the patella is roughly elliptic with a coronal major axis, an increase in depth relative to breadth (by itself) should increase circularity, i.e. an increase in square root of area per unit perimeter length; a relative increase in breadth should do the opposite. There was no clear pattern of shape variation seen here: in *Homo*, all data sets showed negative correlation between ***A/P*** and |x|, but in other genera correlation signs were mixed, both among and within sexes. In *Homo*, by the above assumption, larger animals may sustain greater medial-lateral tensile forces (due to lateralization of forces) and/or benefit from greater articular surface area. How to reconcile the findings in nonhumans with mechanical concepts was unclear, as in some cases correlation signs were opposite in distal and proximal data sets. Was it possible to explain different mechanical circumstances between the different levels of the articular surfaces? Presumably there was a biological explanation, but one that could not be determined by this study. In §2.1.2.1 it was shown that the distal part of the patellar articular surface contacts the femur in extension, and that this contact zone moves proximally with flexion. It is possible that the descent of the patella into the femoral intercondylar notch and the medial-lateral movement of the patella in knee flexion, at least in humans (also §2.1.2.1), create different mechanical circumstances for the proximal and distal articular regions of the patella.

There appeared to be an overall departure from circularity of patellar outlines in larger genera (Figure 4.20). Correlations between ***A/P*** and |x| were likely to be strong due to value ranges, but with exception of female distal, all outlines qualitatively showed strong negative correlations between these size and shape variables. That this was the case might have been unexpected in light of the divergence between body weight and patellar size. The expectation of skeletal allometry is based on an expectation that different body sizes cause different levels of stress or strain in the skeleton, and although this is likely to occur in all genera (including *Homo*), specimens from bipedal humans showed larger patella than would have been expected by body size alone. That patellar shape in *Homo* (mostly) followed the trend set by the nonhuman genera supported the idea that human patellae sustain greater forces relative to body weight than those of nonhumans.

Homo individuals are relatively large bipeds, and *Cercopithecus* and *Colobus* individuals are relatively small quadrupeds; consequently, it was expected that morphological differences would be found between humans and monkeys. However, gorillas are large (larger than humans), and quadrupedal. That *Gorilla* specimens were grouped with bipedal *Homo* rather than the quadrupedal monkey species (even using size-adjusted data) supported the notion that patellar morphology was primarily influenced (in terms of extraneous factors) by body weight, even if body weight acted through function.

6.1.4 Sexual Dimorphism

It was unlikely that sexual dimorphism in patellar outlines would have arisen by the direct route in Figure 6.1 – that is, patellar form is unlikely to confer a special reproductive advantage to one sex beyond that accounted for by dimorphic body size.

In Chapter 5 it was postulated that patellar size dimorphism should reflect body weight dimorphism as found by Leutenegger and Larson (1985). This was based on an earlier expectation, only partially realized, that patellar size would reflect body size (Chapter 3): a deviation from this association was found when *Homo* were considered, presumably due to the different mechanical circumstances of a biped. From Figure 6.1 it can be seen that sexual body size dimorphism could lead to patellar dimorphism by (1) a simple difference in patellar size, as well as (via function) (2) size-related shape difference. As body weight measurements were not available with these specimens it was not possible to directly measure the association between body size dimorphism and patellar dimorphism, but this association between body size dimorphism and patellar size dimorphism may be assessed indirectly using the body weight dimorphism data presented earlier (Table 5.1). This table did not list *Colobus preussi*, although it was unlikely that this species would have altered the results greatly, as there were only two such specimens. Figure 6.2 shows graphs indicating the 95% confidence intervals of the mean size sex difference for each genus, in order of least dimorphic to most dimorphic on the *x*-axis. Due to interspecies variation within *Cercopithecus* and *Colobus*, separation of these two genera was not clear, but *Cercopithecus* was considered more dimorphic than *Colobus* for this purpose. For both conventional and Fourier data, there was a clear pattern of increasing patellar size dimorphism with increasing body size dimorphism. The inclusion of bipedal *Homo* to the other quadrupedal genera did not qualitatively affect this finding. Nevertheless, the combination of allometry and sexual size dimorphism did not lead to the findings of consequent sexual shape dimorphism as expected. Where a negative

finding of sexual shape dimorphism appeared to contradict expectations, it was found that male and female specimens grouped together showed isometry; in *Homo* proximal, there was only isometry between the means, but this was sufficient to prevent mean shape sex difference. Overall, there was little found in the way of shape dimorphism, which suggested that, within these taxa, biomechanical demands were similar between sexes despite body size differences. Even within taxa where shape dimorphism was found, dimorphism at one level was not accompanied by dimorphism at the other. While in theory shape dimorphism was not found due to small sample sizes, that shape dimorphism was found only variably in *Homo* suggested that lack of power was not a primary influence. Consequently, it may be interpreted that, with several exceptions, patellar stress differences that would have been a potential result of sexual size differences were not met with a change in external patellar shape; alternatives to shape changes include internal morphological differences and functional modifications. Internal differences might include geometry of endosteal cortex, and functional modifications might include maintaining a more extended position of limb joints, and avoiding activities such as leaping.

In Chapter 5, it was seen that *Cercopithecus* and *Gorilla* showed greater patellar size dimorphism than *Colobus* and *Gorilla*, yet showed smaller patellae than *Colobus* and *Gorilla*, respectively. From the above it was clear that patellar size dimorphism followed body weight dimorphism. *Homo* patellae were larger, relative to body weight, than those of *Gorilla* (Chapter 3), but gorillas on average show greater body weight dimorphism. *Colobus*, despite greater body size, appear to show less body size dimorphism than *Cercopithecus*; *Colobus* still had larger patellae than *Cercopithecus*, as on average they weigh more.

Figure 6.2. Error bars (y-axis) for mean patellar sex size difference – conventional data (values on y-axis, bars represent 95% confidence intervals)

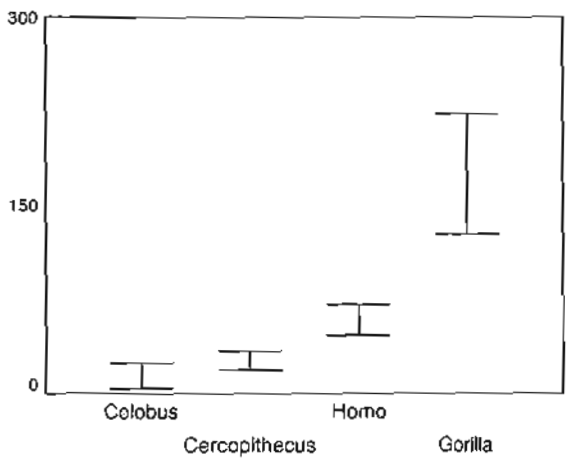

(a) distal, conventional data

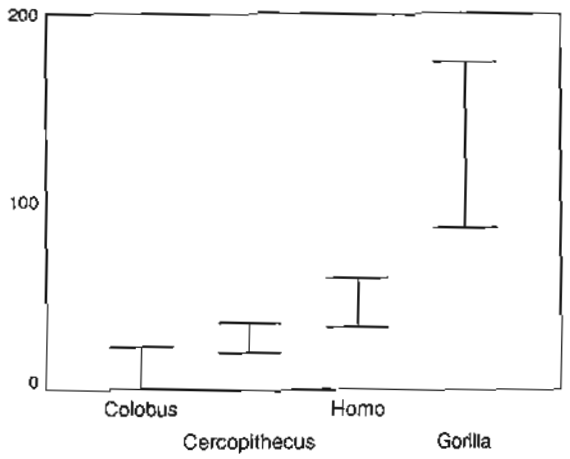

(b) proximal, conventional data

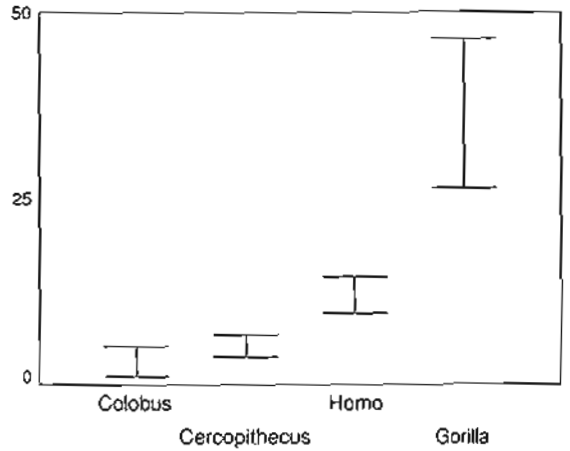

(c) distal, Fourier data

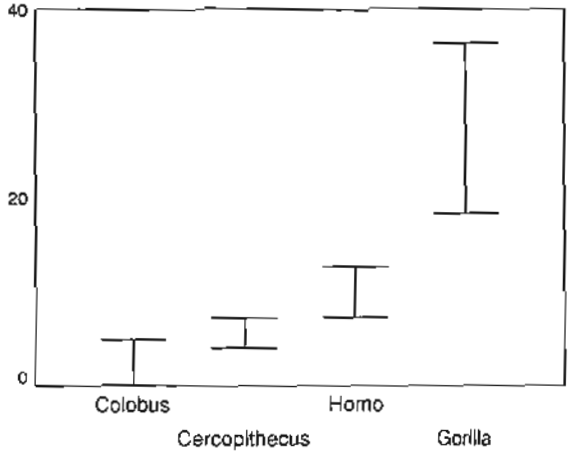

(d) proximal, Fourier data

6.1.5 Phylogeny

It was stated in Chapter 2 that phylogenetic relations among taxa may influence morphology. *Homo* and *Gorilla* are members of the superfamily Hominoidea, and *Cercopithecus* and *Colobus* are members of the superfamily Cercopithecoidea. Relative phylogenetic proximity had the potential, via inheritance, to produce relative morphological similarity within each superfamily. Despite this, it is thought that the potential for phenotypic plasticity means that functional influences may overshadow phylogeny (Collard and Wood, 2000; Lieberman, 1997). In Chapters 3 and 4 it was shown that the hominoid specimens were separated from the cercopithecoid specimens not only by size but also by shape. Separation by size was an expected finding, given the wide disparities in body weights between cercopithecoids and hominoids (Table 2.3); separation in body weight need not reflect phylogenetic history, as closely-related taxa may show extreme size differences (for example, gorillas and bonobos, (Henneberg, personal communication)). Shape differences (as measured by ***A/P***) were found between cercopithecoid and hominoid specimens, which might have been in part due to phylogenetic history: after all, quadrupedal gorillas and bipedal humans differ functionally. However, *Gorilla* and *Homo* are alike in terms of body size, at least in comparison to the much smaller cercopithecoids. The smaller cercopithecoids are more likely to engage in high-speed activities, including leaping, than the hominoids, and as such the patellae of the former are structured to resist sagittal plane bending. It is likely that shape similarity between *Gorilla* and *Homo* was a reflection on the avoidance in both taxa of large bending stresses and strains, as body size is too great to even perform such activities as leaping, let alone resist the forces engendered.

6.2 Limitations of this Study and Areas for Further Research

6.2.1 Limitations of This Study

Reliability of measurements was determined using only *Homo* specimens (Chapter 3). If time had permitted, it would have been of use to use nonhuman specimens, since the method of data capture was different to that used for the human specimens; this was due to the fact that pencil lines could not be drawn on the nonhuman museum specimens, and could have introduced further error into the data.

Having access to body weight data would have added useful information to this study, especially in areas where published body weight averages were used to only suggest the influence of body weight (for example, allometry and sexual dimorphism). From the published averages it appeared that body weight had a large role to play in determining patellar outline form; actual body weight data would have allowed for stronger conclusions, although it was also possible that the actual data might have contradicted the body weight-patellar form association.

The lengths of the specimens would have been useful data: that cross-sectional measurements reflect a bone's ability to resist bending forces only tells part of the story. Patellar length would influence the bending forces applied to the bone, and would have made the cross-sectional measurements much more informative. Unfortunately, during (or after) processing, the thin cortical shell of the distal pole of the patella in *Homo* and *Gorilla* (less so in the other genera) was damaged, to the extent that with many specimens there was a partial distal pole, making accurate measurement of length impossible.

The external cortical morphology of a bone can only tell part of the story of that bone's strategy to cope with mechanical demands: this study investigated data from neither the internal aspect of the cortex nor the trabecular core of the patella. In theory, information was thus ignored, although in the absence of methods to capture information (1) from the cortex such that resistance to bending in two (not necessarily collinear) planes (from medial and lateral facet contact) simultaneously can be calculated, and (2) from the trabecular core, to be used in conjunction with cortical data.

6.2.2 Areas for Further Research

A simple extension to this study would have been to include specimens from a brachiating genus (especially *Hylobates*, but also *Pongo*) and from a leaping taxon (one of the leaping prosimians). The distal patellar poles of smaller primates (especially prosimians) seemed to remain intact after processing, so a study could be performed which also takes into account the length of the patella, and therefore also information on bending moment.

It was hoped that an investigation into patellar asymmetry might have been possible; unfortunately the nonhuman collection did not record the side of the specimens, but other collections not accessed by the author may have this information, so that such a study could be performed.

The work of several researchers has shown that bone morphology may be successfully related to functional history using an engineering approach; using such an approach would in theory be beneficial in aiding understanding of the patella and the way its morphology relates to its function (see above). Two ways that this could add to current knowledge are (1) to integrate morphological information from two planes of bending as well as from trabecular bone (as above), and (2) to investigate the kinetics of the patella, specifically to calculate stresses acting on the patella in knee flexion as well as extension.

It was assumed that part of the patellar outline form in humans was due to lateralization of quadriceps force; it would therefore be of interest to investigate form again, but with extra data relating to, say, femoral bicondylar angle or pelvic width, to directly assess the influences of these factors.

6.3 Concluding Remarks

This study used elliptic Fourier descriptors and simpler outline length and area data to quantify the outline form of patellar cross-sectional images. The Fourier data were used to capture the complexity of the patellar outline, with the trade-off that specimens were registered in 10-dimensional phenotype space. As an alternative, the length and (square root of) area data (2-dimensional) were used to compare results from both types of data. Where size dominated the investigation (raw data ordination, sexual size dimorphism), results were essentially identical: the Fourier variables and the conventional variables conveyed size information equally well. Where the focus was on shape (size-adjusted data ordination, allometry, sexual shape dimorphism), there were divergences between Fourier and conventional variables. For example, the conventional variables could detect approximations to and deviations from outline circularity, although the data were insensitive to whether a deviation from circularity was due to a global (elliptic) widening of the patella or more local deviations (for example, articular concavities), or both. The Fourier variables had the potential to distinguish between global and local deviations, although the nature of the descriptors was that the variables were often not interpretable. Notwithstanding this, the results using the

Fourier variables showed that the morphological variation of the patella was richer than described by the terms 'circular' and 'elliptic'.

It was anticipated, based on the work of a number of other researchers, that results of the shape analyses would have had a functional interpretation; among the genera, larger patellae were less circular patellae, which might have been a reflection of avoidance of activities which would create dangerous stresses and strains in the patella – leaping, for example. Within genera, associations of size and shape were found, but not which allowed a clear functional interpretation. In particular, the results from proximal and distal outlines sometimes differed; for example, proximal and distal outlines sometimes showed opposing trends in terms of shape change with size change. Although it must be expected that the morphology of each specimen suited its function, how closely structure maps with function is not known. Even if this were known, the function of the primate patella appears so complex that it is difficult to attribute one part of this function with structure; this study has been an attempt to quantify structure – future work on function may allow further interpretation of these results.

Appendix

Table A.1. Details of human specimens

specimen no.	reference no.	side	sex	age
1	3110	left	male	73
2	3110	right	"	"
5	3105	left	female	82
6	3105	right	"	"
7	3139	right	female	97
8	3139	left	"	"
10	3134	right	female	83
11	3153	left	female	68
12	3153	right	"	"
13	3111	left	male	60
14	3111	right	"	"
17	3152	left	male	72
18	3152	right	"	"
19	3101	right	male	78
20	3101	left	"	"
21	3102	left	female	62
22	3102	right	"	"
23	3103	left	female	78
24	3103	right	"	"
27	3108	right	male	83
28	3107	left	male	74
29	3107	right	"	"
30	3097	right	female	97
31	3097	left	"	"
32	3098	right	male	60
35	3129	left	male	60
37	3132	left	male	85
38	2875	right	female	82
39	2875	left	"	"
40	3130	left	male	88
41	3130	right	"	"
42	3104	right	male	67
43	3104	left	"	"
44	3067	left	female	99
45	3067	right	"	"
46	3100	right	female	55
47	3100	left	"	"
48	3043	right	female	89
49	3043	left	"	"
50	3055	right	female	78
51	3055	left	"	"
52	3128	right	male	81
53	3128	left	"	"
54	2999	left	male	69
55	2999	right	"	"
56	3120	left	female	88
57	3120	right	"	"
58	3070	left	male	83
59	3070	right	"	"
60	3081	left	male	73
61	3081	right	"	"
62	3087	left	male	86
63	3087	right	"	"
64	3047	right	male	48
65	3047	left	"	"
66	3125	left	female	76
70	3078	left	female	84

Table A.1. (continued)

specimen no.	reference no.	side	sex	age
72	2971	right	male	68
73	2971	left	"	"
75	3083	left	female	82
76	3089	right	male	65
77	3089	left	"	"
78	3085	right	female	60
79	3085	left	"	"
81	3076	right	male	74
82	3058	left	female	43
83	3058	right	"	"
84	2926	right	male	79
85	3073	left	male	81
86	3073	right	"	"
87	3079	right	female	81
88	3057	right	male	86
90	3039	left	female	72
91	3039	right	"	"
92	3029	right	female	80
93	3029	left	"	"
94	3061	right	female	55
95	3061	left	"	"
96	3113	right	female	60
97	3113	left	"	"
98	3115	right	male	83
100	3117	right	female	79
101	3117	left	"	"
102	3119	left	female	84
103	3119	right	"	"
104	3126	right	female	84
105	3126	left	"	"
106	3127	right	female	74
107	3127	left	"	"
108	3131	right	male	68
109	3131	left	"	"
110	3135	left	female	68
111	3135	right	"	"
112	3136	right	male	86
113	3136	left	"	"
116	3141	right	male	59
117	3141	left	"	"
118	3142	right	male	76
119	3142	left	"	"
120	3143	left	female	67
121	3143	right	"	"
122	3145	left	male	73
123	3146	right	female	71
124	3146	left	"	"
125	3151	right	female	99
126	3151	left	"	"
127	3154	right	male	74
128	3154	left	"	"
130	3161	left	female	95
131	3161	right	"	"
133	3201	left	male	79
134	3203	right	male	77
135	3203	left	"	"
136	3206	right	female	91
137	3206	left	"	"
138	3208	right	male	76
139	3208	left	"	"
140	3172	right	female	78

Table A.1. (continued)

specimen no.	reference no.	side	sex	age
141	3172	left	female	"
142	3177	right	female	47
143	3177	left	female	47
144	3181	right	male	54
145	3181	left	"	"
146	3242	right	male	97
147	3242	left	"	"
148	3063	right	female	70
149	3063	left	"	"
150	2994	right	female	81
151	2994	left	"	"
152	3066	right	male	78
153	3066	left	"	"
154	3092	right	male	72
155	3092	left	"	"
156	3093	right	male	80
157	3093	left	"	"
158	3114	right	male	70
159	3114	left	"	"
160	3118	right	female	88
161	3118	left	"	"
162	3150	right	male	63
163	3150	left	"	"
164	3149	right	female	73
165	3149	left	"	"
166	3160	right	male	83
168	3163	right	female	87
169	3163	left	"	"
170	3123	right	female	95
171	3123	left	"	"
172	3228	left	female	100
173	3228	right	"	"
174	3230	right	female	87
175	3230	left	"	"
176	3095	left	male	92
177	3095	right	"	"
178	3233	left	female	62
179	3233	right	"	"
180	3231	right	male	72
181	3231	left	"	"
182	3207	right	male	82
183	3207	left	"	"
184	3183	right	female	90
185	3183	left	"	"
186	3094	right	male	77
187	3094	left	"	"
188	3180	right	male	84
189	3180	left	"	"
190	3184	left	male	81
191	3184	right	"	"
192	3188	left	male	73
194	3248	right	male	88
195	3248	left	"	"
196	3166	left	male	70
197	3166	right	"	"
198	3147	left	male	74
199	3147	right	"	"
200	3164	right	female	83
201	3164	left	"	"
202	3168	left	female	91
203	3168	right	"	"

Table A.1. (continued)

specimen no.	reference no.	side	sex	age
204	3170	right	female	57
205	3170	left	"	"
206	3192	left	female	84
209	3238	right	male	83
210	3189	right	male	74
212	3236	right	female	93
213	3236	left	"	"
214	3221	left	male	84
215	3221	right	"	"
216	3178	left	female	79
218	3193	left	male	81
222	3227	left	female	72
223	3227	right	"	"
224	3204	right	female	52
225	3204	left	"	"
226	3167	left	female	85
228	3165	right	male	88
230	3247	left	female	67
232	3197	right	male	84
234	3176	left	female	87
236	3179	left	male	74
237	3179	right	"	"
238	3190	right	male	79
239	3190	left	"	"
240	3199	right	female	65
241	3199	left	"	"
242	3240	left	male	76
243	3240	right	"	"
244	3149	left	female	73
245	3213	right	female	64

Table A.2. Details of nonhuman specimens

specimen no.	reference no.	sex	species
501	72.119	female	*Cercopithecus sp.*
502, 503	72.120	female	"
504, 505	1977.3148	male	*C. aethiops*
506	1930.8.1.15	female	"
507, 508	72.25	male	"
509, 510	1977.3149	female	"
511, 512	1849.12.6	female	"
513, 514	72.29	male	"
515, 516	72.28	male	"
517	72.31	male	"
519, 520	72.33	male	"
521, 522	72.27	female	"
523, 524	72.23	female	"
525, 526	72.30	female	"
527	87.19	male	*C. solatus*
528	1948.481	male	*C. mona*
529, 530	1938.7.7.6	male	"
531, 532	1938.7.7.11	male	"
533, 534	1977.200	male	*C. campbelli*
535	1948.463	female	*C. mona*
536, 537	1859.2.8.3	female	"
538, 539	1948.475	male	"
540, 541	1948.469	male	"
542	72.47	male	*C. neglectus*
543, 544	72.45	female	"
545, 546	72.50	male	"
547, 548	72.49	female	"
549, 550	72.48	female	"
551, 552	72.40	female	*C. ascanius*
553	1977.3150	male	"
554	72.39	male	"
555, 556	72.37	male	"
557	1948.501	female	*C. nictitans*
558, 559	1938.7.7.13	male	"
560, 561	1938.7.7.14	female	"
562, 563	72.54	female	*C. mitis*
564, 565	72.90	male	"
566, 567	72.78	female	"
568, 569	72.63	female	"
570, 571	72.66	female	"
572, 573	72.62	female	"
574, 575	72.76	male	"
576, 577	72.68	male	"
578, 579	72.88	male	"
580, 581	72.59	male	"
582, 583	72.87	female	"
584, 585	72.81	female	"
586	72.80	female	"
587	72.52	male	"
588, 589	72.65	male	"
590, 591	72.82	male	"
592, 593	72.85	female	"
594, 595	72.83	female	"
596, 597	72.86	female	"
598, 599	72.53	male	"
600	1930.12.1.7	male	"
601, 602	1930.3.1.6	female	*Colobus badius*
603, 604	1940.108	male	"

Table A.2. (continued)

specimen no.	reference no.	sex	species
605, 606	82.212	female	*Colobus badius*
607	1930.8.1.2	male	"
608, 609	72.133	male	"
610, 611	72.132	female	"
612, 613	1968.7.25.1	male	"
614, 615	1850.11.13.1	female	"
616, 617	40.109	female	*C. preussi*
618	1930.8.1.13	male	*C. angolensis*
619, 620	1938.4.21.2	female	"
621	1972.158	female	"
622, 623	72.135	female	*C. guezera*
624, 625	72.160	male	"
626, 627	1904.12.6.1	male	"
628, 629	72.134	male	"
630, 631	72.140	female	"
632, 633	72.150	female	"
634, 635	72.148	female	"
636, 637	72.149	male	"
638, 639	72.141	male	"
640	72.139	male	"
641, 642	72.138	female	"
643, 644	72.153	female	"
645	1930.12.15.1	male	*C. satanus*
646	1856.12.29.1	male	"
647	1392.a	female	*C. polykomas*
648, 649	1948.5.4.1	male	*Gorilla gorilla*
650	1951.9.27.11	female	"
651, 652	78.1226	male	"
653, 654	1948.12.20.2	female	"
655	1948.3.3.12	female	"
656	1949.12.30.2	male	"
657, 658	1948.3.31.1	female	"
659, 660	1948.436	male	"
661	1976.440	female	"
662, 663	1976.439	female	"
664, 665	1989.328	male	"
666, 667	1861.7.29.4	female	"
668	1916.11.1.1	female	"
669, 670	1864.12.11.1	female	"
671, 672	1948.4.1.1	female	"

Table A.3. Model II analysis of variance – *Homo*, conventional data

	variable	among	within	reliability (%)
females distal	*P*	3204.549	49.1879	96.98
	A	121.088	2.1123	96.57
females proximal	*P*	5078.904	192.1334	92.71
	A	218.060	11.2963	90.15
males distal	*P*	1981.476	123.4916	88.27
	A	127.310	3.8994	94.06
males proximal	*P*	1253.640	142.1063	79.64
	A	129.710	7.2591	89.40

Table A.4. Model II analysis of variance – *Homo*, conventional data (digitizing reliability only)

	variable	among	within	reliability (%)
females distal	*P*	4857.816	5.7166	99.65
	A	241.167	1.4276	98.24
females proximal	*P*	7304.835	9.2564	99.62
	A	375.504	1.6991	98.65
males distal	*P*	5899.131	9.9323	99.50
	A	321.387	1.5369	98.58
males proximal	*P*	5950.308	11.3065	99.43
	A	319.854	1.8353	98.30

Table A.1. Model II analysis of variance – *Homo*, Fourier data

(a) *Homo* females

(i) distal

	X1	Y1	X2	Y2	X3	Y3	X4	Y4	X5	Y5	X6	Y6	X7	Y7	X8	Y8	X9	Y9	X10	Y10
among	130.31	33.21	0.39	3.47	2.69	0.76	0.50	0.97	0.75	0.51	0.20	0.07	0.21	0.28	0.08	0.13	0.06	0.13	0.03	0.04
within	2.10	0.46	0.04	0.44	0.07	0.30	0.04	0.10	0.04	0.03	0.04	0.01	0.02	0.01	0.01	0.03	0.01	0.01	0.01	0.01
rel %	96.82	97.24	81.00	77.40	94.65	43.90	85.23	81.99	89.29	89.89	66.39	74.81	83.81	92.43	76.81	63.16	68.73	89.67	64.17	60.23

	X11	Y11	X12	Y12	X13	Y13	X14	Y14	X15	Y15	X16	Y16	X17	Y17	X18	Y18	X19	Y19	X20	Y20
among	0.01	0.04	0.01	0.02	0.01	0.01	0.00	0.01	0.01	0.00	0.00	0.00	0.00	0.00	0.00	0.00	0.00	0.00	0.00	0.00
within	0.00	0.00	0.00	0.00	0.00	0.00	0.00	0.00	0.00	0.00	0.00	0.00	0.00	0.00	0.00	0.00	0.00	0.00	0.00	0.00
rel %	56.06	80.52	56.18	74.56	77.50	24.98	42.64	64.15	71.14	19.92	41.41	25.09	25.63	81.29	26.14	15.70	51.76	33.82	20.05	39.19

	X21	Y21	X22	Y22	X23	Y23	X24	Y24	X25	Y25	X26	Y26	X27	Y27	X28	Y28	X29	Y29	X30	Y30
among	0.00	0.00	0.00	0.00	0.00	0.00	0.00	0.00	0.00	0.00	0.00	0.00	0.00	0.00	0.00	0.00	0.00	0.00	0.00	0.00
within	0.00	0.00	0.00	0.00	0.00	0.00	0.00	0.00	0.00	0.00	0.00	0.00	0.00	0.00	0.00	0.00	0.00	0.00	0.00	0.00
rel %	54.31	64.31	32.48	22.68	35.89	10.35	8.79	37.82	70.45	33.96	−9.80	−8.77	34.70	29.76	0.87	−13.80	26.39	28.15	−11.71	10.77

(ii) proximal

	X1	Y1	X2	Y2	X3	Y3	X4	Y4	X5	Y5	X6	Y6	X7	Y7	X8	Y8	X9	Y9	X10	Y10
among	207.68	27.43	1.29	6.64	3.76	2.82	0.91	0.85	0.61	0.78	0.12	0.09	0.12	0.26	0.03	0.04	0.07	0.09	0.02	0.02
within	7.38	1.71	0.13	0.43	0.11	0.19	0.09	0.10	0.04	0.13	0.02	0.04	0.02	0.02	0.02	0.02	0.01	0.01	0.01	0.00
rel %	93.14	88.25	81.40	87.95	94.51	87.21	82.29	78.78	89.07	72.35	67.28	42.08	67.53	83.62	29.34	29.82	64.74	75.62	21.80	67.79

	X11	Y11	X12	Y12	X13	Y13	X14	Y14	X15	Y15	X16	Y16	X17	Y17	X18	Y18	X19	Y19	X20	Y20
among	0.03	0.03	0.01	0.01	0.01	0.01	0.01	0.01	0.01	0.01	0.00	0.01	0.01	0.00	0.00	0.00	0.00	0.00	0.00	0.00
within	0.01	0.01	0.01	0.01	0.00	0.00	0.00	0.00	0.00	0.00	0.00	0.00	0.00	0.00	0.00	0.00	0.00	0.00	0.00	0.00
rel %	59.68	60.60	34.26	51.57	62.79	55.57	68.94	68.78	59.62	53.97	35.98	61.93	42.11	−15.49	22.92	34.24	49.71	54.21	7.24	32.27

	X21	Y21	X22	Y22	X23	Y23	X24	Y24	X25	Y25	X26	Y26	X27	Y27	X28	Y28	X29	Y29	X30	Y30
among	0.00	0.00	0.00	0.00	0.00	0.00	0.00	0.00	0.00	0.00	0.00	0.00	0.00	0.00	0.00	0.00	0.00	0.00	0.00	0.00
within	0.00	0.00	0.00	0.00	0.00	0.00	0.00	0.00	0.00	0.00	0.00	0.00	0.00	0.00	0.00	0.00	0.00	0.00	0.00	0.00
rel %	45.88	11.59	9.58	9.95	15.43	48.26	3.88	19.81	32.44	10.82	4.29	28.64	13.43	52.58	−3.92	0.42	14.31	41.49	−17.25	23.09

Table A.5. (continued)

(b) *Homo* males

(i) distal

	X1	Y1	X2	Y2	X3	Y3	X4	Y4	X5	Y5	X6	Y6	X7	Y7	X8	Y8	X9	Y9	X10	Y10
among	75.69	27.34	0.38	6.09	1.09	2.71	0.21	0.81	0.47	0.61	0.12	0.15	0.13	0.15	0.07	0.07	0.06	0.05	0.06	0.04
within	5.95	1.49	0.11	0.52	0.14	0.33	0.04	0.08	0.03	0.04	0.01	0.03	0.01	0.04	0.01	0.01	0.01	0.01	0.01	0.01
rel %	85.42	89.69	55.84	84.33	76.74	78.40	67.95	81.67	86.80	88.27	78.55	68.46	83.46	60.07	72.94	72.46	68.07	74.30	81.54	61.35

	X11	Y11	X12	Y12	X13	Y13	X14	Y14	X15	Y15	X16	Y16	X17	Y17	X18	Y18	X19	Y19	X20	Y20
among	0.02	0.04	0.02	0.01	0.02	0.01	0.01	0.01	0.01	0.00	0.00	0.00	0.01	0.00	0.00	0.00	0.00	0.00	0.00	0.00
within	0.01	0.00	0.01	0.00	0.01	0.00	0.00	0.00	0.00	0.00	0.00	0.00	0.00	0.00	0.00	0.00	0.00	0.00	0.00	0.00
rel %	55.85	83.35	57.83	49.86	77.80	52.99	48.26	41.60	39.54	28.12	24.55	-2.09	43.93	50.89	-18.46	15.03	31.03	-10.18	14.80	39.52

	X21	Y21	X22	Y22	X23	Y23	X24	Y24	X25	Y25	X26	Y26	X27	Y27	X28	Y28	X29	Y29	X30	Y30
among	0.00	0.00	0.00	0.00	0.00	0.00	0.00	0.00	0.00	0.00	0.00	0.00	0.00	0.00	0.00	0.00	0.00	0.00	0.00	0.00
within	0.00	0.00	0.00	0.00	0.00	0.00	0.00	0.00	0.00	0.00	0.00	0.00	0.00	0.00	0.00	0.00	0.00	0.00	0.00	0.00
rel %	28.73	4.04	43.80	28.17	26.71	2.53	17.72	-9.35	25.17	23.27	22.10	19.91	16.41	54.29	32.60	-9.18	5.49	19.94	14.03	-15.35

(ii) proximal

	X1	Y1	X2	Y2	X3	Y3	X4	Y4	X5	Y5	X6	Y6	X7	Y7	X8	Y8	X9	Y9	X10	Y10
among	42.55	18.36	0.50	3.95	0.55	2.95	0.39	0.66	0.27	0.51	0.05	0.16	0.14	0.04	0.06	0.07	0.05	0.03	0.02	0.03
within	5.24	1.52	0.09	0.49	0.09	0.43	0.03	0.12	0.02	0.07	0.01	0.02	0.01	0.02	0.00	0.01	0.01	0.01	0.01	0.00
rel %	78.08	84.75	69.23	77.78	72.43	74.70	83.92	68.57	83.70	76.86	55.28	77.83	85.53	34.63	88.03	70.02	80.89	41.37	62.53	71.73

	X11	Y11	X12	Y12	X13	Y13	X14	Y14	X15	Y15	X16	Y16	X17	Y17	X18	Y18	X19	Y19	X20	Y20
among	0.03	0.02	0.01	0.01	0.01	0.01	0.01	0.00	0.01	0.01	0.00	0.00	0.00	0.00	0.00	0.00	0.00	0.00	0.00	0.00
within	0.00	0.01	0.00	0.00	0.00	0.00	0.00	0.00	0.00	0.00	0.00	0.00	0.00	0.00	0.00	0.00	0.00	0.00	0.00	0.00
rel %	84.47	51.28	58.58	38.13	71.80	70.77	47.87	6.15	59.33	24.71	58.75	15.01	10.42	16.70	37.66	-2.77	53.80	7.25	25.36	37.38

	X21	Y21	X22	Y22	X23	Y23	X24	Y24	X25	Y25	X26	Y26	X27	Y27	X28	Y28	X29	Y29	X30	Y30
among	0.00	0.00	0.00	0.00	0.00	0.00	0.00	0.00	0.00	0.00	0.00	0.00	0.00	0.00	0.00	0.00	0.00	0.00	0.00	0.00
within	0.00	0.00	0.00	0.00	0.00	0.00	0.00	0.00	0.00	0.00	0.00	0.00	0.00	0.00	0.00	0.00	0.00	0.00	0.00	0.00
rel %	47.22	-29.75	-3.35	6.68	44.11	39.07	15.48	40.02	17.32	8.24	12.91	46.55	14.30	36.50	33.08	-35.28	37.27	7.81	39.06	34.87

Table A.5. (continued)

(c) *Homo* males proximal (digitizing error only)

	X1	Y1	X2	Y2	X3	Y3	X4	Y4	X5	Y5	X6	Y6	X7	Y7	X8	Y8	X9	Y9	X10	Y10
among	220.27	64.07	1.89	8.83	3.64	5.50	0.66	1.61	0.93	0.87	0.22	0.33	0.24	0.28	0.14	0.15	0.10	0.13	0.06	0.05
within	0.75	0.22	0.01	0.03	0.01	0.02	0.00	0.01	0.00	0.00	0.00	0.00	0.00	0.00	0.00	0.00	0.00	0.00	0.00	0.00
rel %	98.99	98.98	98.93	98.87	98.99	98.96	98.95	98.96	98.98	98.76	98.91	98.91	98.92	98.89	98.93	98.93	98.90	98.85	96.67	98.75

Table A.2. Power values for Fourier amplitudes

(a) *Homo* females

(i) power – distal

	X1	Y1	X2	Y2	X3	Y3	X4	Y4	X5	Y5	X6	Y6	X7	Y7	X8	Y8	X9	Y9	X10	Y10
power	5735.97	1451.89	1.71	16.56	44.32	5.31	0.97	3.01	3.57	4.23	0.30	0.13	0.36	0.58	0.16	0.16	0.10	0.15	0.05	0.07

	X11	Y11	X12	Y12	X13	Y13	X14	Y14	X15	Y15	X16	Y16	X17	Y17	X18	Y18	X19	Y19	X20	Y20
power	0.03	0.04	0.02	0.02	0.01	0.02	0.01	0.01	0.01	0.01	0.01	0.01	0.00	0.00	0.00	0.00	0.00	0.00	0.00	0.00

	X21	Y21	X22	Y22	X23	Y23	X24	Y24	X25	Y25	X26	Y26	X27	Y27	X28	Y28	X29	Y29	X30	Y30
power	0.00	0.00	0.00	0.00	0.00	0.00	0.00	0.00	0.00	0.00	0.00	0.00	0.00	0.00	0.00	0.00	0.00	0.00	0.00	0.00

(ii) cumulative power as percentage of total – distal

	X1	X2	X3	X4	X5	X6	X7	X8	X9	X10
cumulative %	99.11	99.14	99.90	99.92	99.98	99.99	99.99	100	100	100

	Y1	Y2	Y3	Y4	Y5	Y6	Y7	Y8	Y9	Y10
cumulative %	97.92	99.06	99.43	99.63	99.92	99.93	99.97	99.98	99.97	99.99

(iii) power – proximal

	X1	Y1	X2	Y2	X3	Y3	X4	Y4	X5	Y5	X6	Y6	X7	Y7	X8	Y8	X9	Y9	X10	Y10
power	5092.33	1430.18	4.36	15.93	37.75	6.95	1.33	2.84	4.54	1.66	0.19	0.31	0.69	0.39	0.11	0.12	0.16	0.18	0.05	0.03

	X11	Y11	X12	Y12	X13	Y13	X14	Y14	X15	Y15	X16	Y16	X17	Y17	X18	Y18	X19	Y19	X20	Y20
power	0.04	0.06	0.03	0.02	0.01	0.02	0.01	0.01	0.01	0.01	0.01	0.01	0.00	0.00	0.00	0.00	0.00	0.00	0.00	0.00

	X21	Y21	X22	Y22	X23	Y23	X24	Y24	X25	Y25	X26	Y26	X27	Y27	X28	Y28	X29	Y29	X30	Y30
power	0.00	0.00	0.00	0.00	0.00	0.00	0.00	0.00	0.00	0.00	0.00	0.00	0.00	0.00	0.00	0.00	0.00	0.00	0.00	0.00

(iv) cumulative power as percentage of total – proximal

	X1	X2	X3	X4	X5	X6	X7	X8	X9	X10
cumulative %	99.05	99.14	99.86	99.89	99.97	99.98	99.99	99.99	100	100

	Y1	Y2	Y3	Y4	Y5	Y6	Y7	Y8	Y9	Y10
cumulative %	98.02	99.13	99.62	99.81	99.92	99.94	99.97	99.98	99.99	99.99

Table A.6. (continued)

(b) *Homo* males

(i) power – distal

	X1	Y1	X2	Y2	X3	Y3	X4	Y4	X5	Y5	X6	Y6	X7	Y7	X8	Y8	X9	Y9	X10	Y10
power	6976.15	1728.21	1.35	16.97	53.50	7.14	0.89	2.95	4.15	5.02	0.26	0.21	0.42	0.67	0.16	0.16	0.11	0.16	0.06	0.07

	X11	Y11	X12	Y12	X13	Y13	X14	Y14	X15	Y15	X16	Y16	X17	Y17	X18	Y18	X19	Y19	X20	Y20
power	0.04			0.03	0.02	0.00	0.02	0.01	0.01	0.01	0.01	0.01	0.01	0.00	0.00	0.00	0.00	0.00	0.00	0.00

	X21	Y21	X22	Y22	X23	Y23	X24	Y24	X25	Y25	X26	Y26	X27	Y27	X28	Y28	X29	Y29	X30	Y30
power	0.00	0.00	0.00	0.00	0.00	0.00	0.00	0.00	0.00	0.00	0.00	0.00	0.00	0.00	0.00	0.00	0.00	0.00	0.00	0.00

(ii) cumulative power as percentage of total – distal

	X1	X2	X3	X4	X5	X6	X7	X8	X9	X10
cumulative %	99.14	99.16	99.91	99.92	99.98	99.99	99.99	100	100	100

	Y1	Y2	Y3	Y4	Y5	Y6	Y7	Y8	Y9	Y10
cumulative %	98.08	99.05	99.46	99.63	99.92	99.93	99.97	99.98	99.99	99.99

(iii) power – proximal

	X1	Y1	X2	Y2	X3	Y3	X4	Y4	X5	Y5	X6	Y6	X7	Y7	X8	Y8	X9	Y9	X10	Y10
power	6088.76	1598.03	2.80	15.61	46.90	6.90	0.95	2.32	5.46	1.83	0.18	0.30	0.39	0.38	0.12	0.12	0.24	0.19	0.06	0.04

	X11	Y11	X12	Y12	X13	Y13	X14	Y14	X15	Y15	X16	Y16	X17	Y17	X18	Y18	X19	Y19	X20	Y20
power	0.07	0.06	0.03	0.02	0.02	0.02	0.01	0.01	0.01	0.01	0.01	0.01	0.01	0.01	0.00	0.00	0.00	0.00	0.00	0.00

	X21	Y21	X22	Y22	X23	Y23	X24	Y24	X25	Y25	X26	Y26	X27	Y27	X28	Y28	X29	Y29	X30	Y30
power	0.00	0.00	0.00	0.00	0.00	0.00	0.00	0.00	0.00	0.00	0.00	0.00	0.00	0.00	0.00	0.00	0.00	0.00	0.00	0.00

(iv) cumulative power as percentage of total – proximal

	X1	X2	X3	X4	X5	X6	X7	X8	X9	X10
cumulative %	99.06	99.11	99.87	99.88	99.97	99.97	99.99	99.99	100	100

	Y1	Y2	Y3	Y4	Y5	Y6	Y7	Y8	Y9	Y10
cumulative %	98.28	99.25	99.67	99.81	99.93	99.94	99.97	99.98	99.99	99.99

Table A.6. (continued)

(c) *Cercopithecus* females

(i) power – distal

	X1	Y1	X2	Y2	X3	Y3	X4	Y4	X5	Y5	X6	Y6	X7	Y7	X8	Y8	X9	Y9	X10	Y10
power	252.71	94.66	0.03	0.26	1.43	0.10	0.03	0.03	0.16	0.05	0.01	0.00	0.03	0.01	0.00	0.00	0.01	0.00	0.00	0.00

	X11	Y11	X12	Y12	X13	Y13	X14	Y14	X15	Y15	X16	Y16	X17	Y17	X18	Y18	X19	Y19	X20	Y20
power	0.00	0.00	0.00	0.00	0.00	0.00	0.00	0.00	0.00	0.00	0.00	0.00	0.00	0.00	0.00	0.00	0.00	0.00	0.00	0.00

	X21	Y21	X22	Y22	X23	Y23	X24	Y24	X25	Y25	X26	Y26	X27	Y27	X28	Y28	X29	Y29	X30	Y30
power	0.00	0.00	0.00	0.00	0.00	0.00	0.00	0.00	0.00	0.00	0.00	0.00	0.00	0.00	0.00	0.00	0.00	0.00	0.00	0.00

(ii) cumulative power as percentage of total – distal

	X1	X2	X3	X4	X5	X6	X7	X8	X9	X10
cumulative %	99.34	99.35	99.90	99.92	99.98	99.98	99.99	99.99	100	100

	Y1	Y2	Y3	Y4	Y5	Y6	Y7	Y8	Y9	Y10
cumulative %	99.51	99.79	99.90	99.93	99.97	99.98	99.99	99.99	99.99	99.99

(iii) power – proximal

	X1	Y1	X2	Y2	X3	Y3	X4	Y4	X5	Y5	X6	Y6	X7	Y7	X8	Y8	X9	Y9	X10	Y10
power	256.46	120.63	0.03	0.16	1.14	0.07	0.02	0.02	0 12	0.06	0.01	0.01	0.01	0.01	0.00	0.00	0.00	0.00	0.00	0.00

	X11	Y11	X12	Y12	X13	Y13	X14	Y14	X15	Y15	X16	Y16	X17	Y17	X18	Y18	X19	Y19	X20	Y20
power	0.00	0.00	0.00	0.00	0.00	0.00	0.00	0.00	0.00	0.00	0.00	0.00	0.00	0.00	0.00	0.00	0.00	0.00	0.00	0.00

	X21	Y21	X22	Y22	X23	Y23	X24	Y24	X25	Y25	X26	Y26	X27	Y27	X28	Y28	X29	Y29	X30	Y30
power	0.00	0.00	0.00	0.00	0.00	0.00	0.00	0.00	0.00	0.00	0.00	0.00	0.00	0.00	0.00	0.00	0.00	0.00	0.00	0.00

(iv) cumulative power as percentage of total – proximal

	X1	X2	X3	X4	X5	X6	X7	X8	X9	X10
cumulative %	99.48	99.49	99.93	99.94	99.99	99.99	100	100	100	100

	Y1	Y2	Y3	Y4	Y5	Y6	Y7	Y8	Y9	Y10
cumulative %	99.70	99.84	99.91	99.93	99.98	99.98	99.99	99.99	100	100

Table A.6. (continued)

(d) *Cercopithecus* males

(i) power – distal

	X1	Y1	X2	Y2	X3	Y3	X4	Y4	X5	Y5	X6	Y6	X7	Y7	X8	Y8	X9	Y9	X10	Y10
power	365.28	141.89	0.07	0.44	1.99	0.12	0.07	0.10	0.23	0.07	0.03	0.01	0.04	0.01	0.01	0.01	0.01	0.01	0.01	0.00

	X11	Y11	X12	Y12	X13	Y13	X14	Y14	X15	Y15	X16	Y16	X17	Y17	X18	Y18	X19	Y19	X20	Y20
power	0.00	0.00	0.00	0.00	0.00	0.00	0.00	0.00	0.00	0.00	0.00	0.00	0.00	0.00	0.00	0.00	0.00	0.00	0.00	0.00

	X21	Y21	X22	Y22	X23	Y23	X24	Y24	X25	Y25	X26	Y26	X27	Y27	X28	Y28	X29	Y29	X30	Y30
power	0.00	0.00	0.00	0.00	0.00	0.00	0.00	0.00	0.00	0.00	0.00	0.00	0.00	0.00	0.00	0.00	0.00	0.00	0.00	0.00

(ii) cumulative power as percentage of total – distal

	X1	X2	X3	X4	X5	X6	X7	X8	X9	X10
cumulative %	99.33	99.35	99.89	99.91	99.97	99.98	99.99	99.99	100	100

	Y1	Y2	Y3	Y4	Y5	Y6	Y7	Y8	Y9	Y10
cumulative %	99.43	99.73	99.83	99.91	99.96	99.97	99.98	99.99	99.99	99.99

(iii) power – proximal

	X1	Y1	X2	Y2	X3	Y3	X4	Y4	X5	Y5	X6	Y6	X7	Y7	X8	Y8	X9	Y9	X10	Y10
power	377.90	179.67	0.08	0.32	1.59	0.17	0.06	0.07	0.17	0.10	0.02	0.02	0.02	0.01	0.01	0.01	0.01	0.00	0.00	0.00

	X11	Y11	X12	Y12	X13	Y13	X14	Y14	X15	Y15	X16	Y16	X17	Y17	X18	Y18	X19	Y19	X20	Y20
power	0.00	0.00	0.00	0.00	0.00	0.00	0.00	0.00	0.00	0.00	0.00	0.00	0.00	0.00	0.00	0.00	0.00	0.00	0.00	0.00

	X21	Y21	X22	Y22	X23	Y23	X24	Y24	X25	Y25	X26	Y26	X27	Y27	X28	Y28	X29	Y29	X30	Y30
power	0.00	0.00	0.00	0.00	0.00	0.00	0.00	0.00	0.00	0.00	0.00	0.00	0.00	0.00	0.00	0.00	0.00	0.00	0.00	0.00

(iv) cumulative power as percentage of total – proximal

	X1	X2	X3	X4	X5	X6	X7	X8	X9	X10
cumulative %	99.48	99.51	99.92	99.94	99.98	99.99	99.99	100	100	100

	Y1	Y2	Y3	Y4	Y5	Y6	Y7	Y8	Y9	Y10
cumulative %	99.58	99.78	99.88	99.92	99.97	99.98	99.99	99.99	99.99	100

Table A.6. (continued)

(e) *Colobus* females

(i) power – distal

	X1	Y1	X2	Y2	X3	Y3	X4	Y4	X5	Y5	X6	Y6	X7	Y7	X8	Y8	X9	Y9	X10	Y10
power	467.45	166.80	0.12	0.53	2.79	0.22	0.11	0.05	0.31	0.11	0.03	0.01	0.04	0.03	0.01	0.01	0.01	0.01	0.00	0.00

	X11	Y11	X12	Y12	X13	Y13	X14	Y14	X15	Y15	X16	Y16	X17	Y17	X18	Y18	X19	Y19	X20	Y20
power	0.00	0.00	0.00	0.00	0.00	0.00	0.00	0.00	0.00	0.00	0.00	0.00	0.00	0.00	0.00	0.00	0.00	0.00	0.00	0.00

	X21	Y21	X22	Y22	X23	Y23	X24	Y24	X25	Y25	X26	Y26	X27	Y27	X28	Y28	X29	Y29	X30	Y30
power	0.00	0.00	0.00	0.00	0.00	0.00	0.00	0.00	0.00	0.00	0.00	0.00	0.00	0.00	0.00	0.00	0.00	0.00	0.00	0.00

(ii) cumulative power as percentage of total – distal

	X1	X2	X3	X4	X5	X6	X7	X8	X9	X10
cumulative %	99.27	99.30	99.89	99.91	99.98	99.98	99.99	99.99	100	100

	Y1	Y2	Y3	Y4	Y5	Y6	Y7	Y8	Y9	Y10
cumulative %	99.41	99.72	99.87	99.90	99.97	99.97	99.99	99.99	99.99	100

(iii) power – proximal

	X1	Y1	X2	Y2	X3	Y3	X4	Y4	X5	Y5	X6	Y6	X7	Y7	X8	Y8	X9	Y9	X10	Y10
power	489.95	214.49	0.09	0 40	2.54	0.18	0.05	0.11	0.31	0.13	0.02	0.02	0.04	0.02	0.01	0.01	0.01	0.01	0.00	0.00

	X11	Y11	X12	Y12	X13	Y13	X14	Y14	X15	Y15	X16	Y16	X17	Y17	X18	Y18	X19	Y19	X20	Y20
power	0.00	0.00	0.00	0.00	0.00	0.00	0.00	0.00	0.00	0.00	0.00	0.00	0.00	0.00	0.00	0.00	0.00	0.00	0.00	0.00

	X21	Y21	X22	Y22	X23	Y23	X24	Y24	X25	Y25	X26	Y26	X27	Y27	X28	Y28	X29	Y29	X30	Y30
power	0.00	0.00	0.00	0.00	0.00	0.00	0.00	0.00	0.00	0.00	0.00	0.00	0.00	0.00	0.00	0.00	0.00	0.00	0.00	0.00

(iv) cumulative power as percentage of total – proximal

	X1	X2	X3	X4	X5	X6	X7	X8	X9	X10
cumulative %	99.37	99.39	99.91	99.92	99.98	99.99	99.99	100	100	100

	Y1	Y2	Y3	Y4	Y5	Y6	Y7	Y8	Y9	Y10
cumulative %	99.57	99.76	99.86	99.91	99.97	99.98	99.99	99.99	99.99	100

Table A.6. (continued)

(f) *Colobus* males

(i) power – distal

	X1	Y1	X2	Y2	X3	Y3	X4	Y4	X5	Y5	X6	Y6	X7	Y7	X8	Y8	X9	Y9	X10	Y10
power	554.95	194.53	0.10	0.47	3.12	0.50	0.08	0.07	0.30	0.13	0.03	0.01	0.04	0.03	0.01	0.01	0.01	0.01	0.01	0.00

	X11	Y11	X12	Y12	X13	Y13	X14	Y14	X15	Y15	X16	Y16	X17	Y17	X18	Y18	X19	Y19	X20	Y20
power	0.01	0.00	0.00	0.00	0.00	0.00	0.00	0.00	0.00	0.00	0.00	0.00	0.00	0.00	0.00	0.00	0.00	0.00	0.00	0.00

	X21	Y21	X22	Y22	X23	Y23	X24	Y24	X25	Y25	X26	Y26	X27	Y27	X28	Y28	X29	Y29	X30	Y30
power	0.00	0.00	0.00	0.00	0.00	0.00	0.00	0.00	0.00	0.00	0.00	0.00	0.00	0.00	0.00	0.00	0.00	0.00	0.00	0.00

(ii) cumulative power as percentage of total – distal

	X1	X2	X3	X4	X5	X6	X7	X8	X9	X10
cumulative %	99.34	99.36	99.91	99.93	99.98	99.98	99.99	99.99	100	100

	Y1	Y2	Y3	Y4	Y5	Y6	Y7	Y8	Y9	Y10
cumulative %	99.32	99.58	99.86	99.90	99.97	99.97	99.99	99.99	99.99	99.99

(iii) power – proximal

	X1	Y1	X2	Y2	X3	Y3	X4	Y4	X5	Y5	X6	Y6	X7	Y7	X8	Y8	X9	Y9	X10	Y10
power	563.65	239.13	0.04	0.30	2.78	0.33	0.04	0.11	0.30	0.14	0.03	0.01	0.04	0.02	0.01	0.00	0.01	0.01	0.00	0.00

	X11	Y11	X12	Y12	X13	Y13	X14	Y14	X15	Y15	X16	Y16	X17	Y17	X18	Y18	X19	Y19	X20	Y20
power	0.00	0.00	0.00	0.00	0.00	0.00	0.00	0.00	0.00	0.00	0.00	0.00	0.00	0.00	0.00	0.00	0.00	0.00	0.00	0.00

	X21	Y21	X22	Y22	X23	Y23	X24	Y24	X25	Y25	X26	Y26	X27	Y27	X28	Y28	X29	Y29	X30	Y30
power	0.00	0.00	0.00	0.00	0.00	0.00	0.00	0.00	0.00	0.00	0.00	0.00	0.00	0.00	0.00	0.00	0.00	0.00	0.00	0.00

(iv) cumulative power as percentage of total – proximal

	X1	X2	X3	X4	X5	X6	X7	X8	X9	X10
cumulative %	99.42	99.43	99.92	99.93	99.98	99.99	99.99	100	100	100

	Y1	Y2	Y3	Y4	Y5	Y6	Y7	Y8	Y9	Y10
cumulative %	99.60	99.73	99.87	99.91	99.97	99.98	99.99	99.99	99.99	100

Table A.6. (continued)

(g) *Gorilla* females

(i) power – distal

	X1	Y1	X2	Y2	X3	Y3	X4	Y4	X5	Y5	X6	Y6	X7	Y7	X8	Y8	X9	Y9	X10	Y10
power	3092.17	676.73	0.20	2.93	23.42	4.70	0.24	0.26	2.19	0.66	0.13	0.05	0.39	0.17	0.06	0.02	0.10	0.06	0.03	0.01

	X11	Y11	X12	Y12	X13	Y13	X14	Y14	X15	Y15	X16	Y16	X17	Y17	X18	Y18	X19	Y19	X20	Y20
power	0.03	0.02	0.01	0.01	0.01	0.01	0.01	0.01	0.00	0.00	0.00	0.00	0.00	0.00	0.00	0.00	0.00	0.00	0.00	0.00

	X21	Y21	X22	Y22	X23	Y23	X24	Y24	X25	Y25	X26	Y26	X27	Y27	X28	Y28	X29	Y29	X30	Y30
power	0.00	0.00	0.00	0.00	0.00	0.00	0.00	0.00	0.00	0.00	0.00	0.00	0.00	0.00	0.00	0.00	0.00	0.00	0.00	0.00

(ii) cumulative power as percentage of total – distal

	X1	X2	X3	X4	X5	X6	X7	X8	X9	X10
cumulative %	99.14	99.15	99.90	99.91	99.97	99.98	99.99	99.99	100	100

	Y1	Y2	Y3	Y4	Y5	Y6	Y7	Y8	Y9	Y10
cumulative %	98.53	99.04	99.80	99.84	99.94	99.95	99.98	99.98	99.99	99.99

(ii) power – proximal

	X1	Y1	X2	Y2	X3	Y3	X4	Y4	X5	Y5	X6	Y6	X7	Y7	X8	Y8	X9	Y9	X10	Y10
power	3422.38	909.49	0.26	2.53	22.68	5.19	0.27	0.44	1.86	0.96	0.13	0.06	0.24	0.28	0.06	0.04	0.05	0.06	0.03	0.02

	X11	Y11	X12	Y12	X13	Y13	X14	Y14	X15	Y15	X16	Y16	X17	Y17	X18	Y18	X19	Y19	X20	Y20
power	0.02	0.02	0.01	0.01	0.01	0.01	0.01	0.00	0.00	0.01	0.00	0.00	0.00	0.00	0.00	0.00	0.00	0.00	0.00	0.00

	X21	Y21	X22	Y22	X23	Y23	X24	Y24	X25	Y25	X26	Y26	X27	Y27	X28	Y28	X29	Y29	X30	Y30
power	0.00	0.00	0.00	0.00	0.00	0.00	0.00	0.00	0.00	0.00	0.00	0.00	0.00	0.00	0.00	0.00	0.00	0.00	0.00	0.00

(iv) cumulative power as percentage of total – proximal

	X1	X2	X3	X4	X5	X6	X7	X8	X9	X10
cumulative %	99.26	99.26	99.92	99.93	99.98	99.99	99.99	100	100	100

	Y1	Y2	Y3	Y4	Y5	Y6	Y7	Y8	Y9	Y10
cumulative %	98.99	99.24	99.80	99.84	99.94	99.95	99.98	99.98	99.99	99.99

Table A.6. (continued)

(h) *Gorilla* males

(i) power – distal

	X1	Y1	X2	Y2	X3	Y3	X4	Y4	X5	Y5	X6	Y6	X7	Y7	X8	Y8	X9	Y9	X10	Y10
power	5969.66	1570.93	1.44	12.56	36.95	9.97	1.53	0.41	3.44	0.91	0.52	0.17	0.82	0.21	0.12	0.10	0.21	0.12	0.04	0.02

	X11	Y11	X12	Y12	X13	Y13	X14	Y14	X15	Y15	X16	Y16	X17	Y17	X18	Y18	X19	Y19	X20	Y20
power	0.06	0.06	0.03	0.01	0.02	0.02	0.02	0.06	0.01	0.01	0.01	0.01	0.01	0.01	0.01	0.00	0.01	0.00	0.00	0.00

	X21	Y21	X22	Y22	X23	Y23	X24	Y24	X25	Y25	X26	Y26	X27	Y27	X28	Y28	X29	Y29	X30	Y30
power	0.00	0.00	0.00	0.00	0.00	0.00	0.00	0.00	0.00	0.00	0.00	0.00	0.00	0.00	0.00	0.00	0.00	0.00	0.00	0.00

(ii) cumulative power as percentage of total – distal

	X1	X2	X3	X4	X5	X6	X7	X8	X9	X10
cumulative %	99.25	99.27	99.89	99.91	99.97	99.98	99.99	99.99	100	100

	Y1	Y2	Y3	Y4	Y5	Y6	Y7	Y8	Y9	Y10
cumulative %	98.52	99.22	99.87	99.89	99.95	99.96	99.98	99.98	99.99	99.99

(iii) power – proximal

	X1	Y1	X2	Y2	X3	Y3	X4	Y4	X5	Y5	X6	Y6	X7	Y7	X8	Y8	X9	Y9	X10	Y10
power	5665.85	1605.76	0.37	5.20	33.34	10.74	0.66	1.00	2.16	1.69	0.41	0.19	0.22	0.35	0.19	0.06	0.03	0.12	0.08	0.05

	X11	Y11	X12	Y12	X13	Y13	X14	Y14	X15	Y15	X16	Y16	X17	Y17	X18	Y18	X19	Y19	X20	Y20
power	0.02	0.02	0.03	0.02	0.01	0.02	0.01	0.01	0.01	0.01	0.00	0.00	0.01	0.00	0.00	0.00	0.01	0.00	0.00	0.00

	X21	Y21	X22	Y22	X23	Y23	X24	Y24	X25	Y25	X26	Y26	X27	Y27	X28	Y28	X29	Y29	X30	Y30
power	0.00	0.00	0.00	0.00	0.00	0.00	0.00	0.00	0.00	0.00	0.00	0.00	0.00	0.00	0.00	0.00	0.00	0.00	0.00	0.00

(iv) cumulative power as percentage of total – proximal

	X1	X2	X3	X4	X5	X6	X7	X8	X9	X10
cumulative %	99.34	99.35	99.93	99.94	99.98	99.99	99.99	100	100	100

	Y1	Y2	Y3	Y4	Y5	Y6	Y7	Y8	Y9	Y10
cumulative %	98.83	99.13	99.79	99.85	99.95	99.96	99.98	99.98	99.99	99.99

Table A.7. Means and standard deviations – conventional data

(a) *Homo* females

	mean	sd
P – distal	567.1137	40.2402
A – distal	135.2736	8.9660
P – proximal	541.2152	49.3452
A – proximal	130.2134	11.1705
ln*P* – distal	6.3381	0.0707
ln*A* – distal	4.9051	0.0659
ln*P* – proximal	6.2897	0.0916
ln*A* – proximal	4.8655	0.0859

(b) *Homo* males

	mean	sd
P – distal	622.7800	44.3439
A – distal	148.5515	10.3503
P – proximal	586.2255	44.5358
A – proximal	140.0680	10.2087
ln*P* – distal	6.4316	0.0738
ln*A* – distal	4.9984	0.0723
ln*P* – proximal	6.3708	0.0773
ln*A* – proximal	4.9395	0.0730

(c) *Cercopithecus* females

	mean	sd
P – distal	121.3802	10.7052
A – distal	31.1552	2.6177
P – proximal	126.2356	11.3685
A – proximal	33.1665	2.7662
ln*P* – distal	4.7950	0.0895
ln*A* – distal	3.4355	0.0845
ln*P* – proximal	4.8342	0.0892
ln*A* – proximal	3.4980	0.0862

(d) *Cercopithecus* males

	mean	sd
P – distal	145.7877	23.4991
A – distal	37.3495	6.2593
P – proximal	151.0930	24.0502
A – proximal	40.0057	6.4449
ln*P* – distal	4.9677	0.1774
ln*A* – distal	3.6046	0.1852
ln*P* – proximal	5.0042	0.1718
ln*A* – proximal	3.6746	0.1773

Table A.7. (cont.)

(e) *Colobus* females

	mean	sd
P – distal	164.9323	14.6075
A – distal	41.8296	4.0146
P – proximal	172.1018	17.7502
A – proximal	44.8999	5.2605
ln*P* – distal	5.1018	0.0882
ln*A* – distal	3.7292	0.0956
ln*P* – proximal	5.1428	0.1051
ln*A* – proximal	3.7977	0.1190

(f) *Colobus* males

	mean	sd
P – distal	178.4626	17.9530
A – distal	45.3624	4.5931
P – proximal	183.5446	18.9290
A – proximal	47.8082	5.1384
ln*P* – distal	5.1793	0.1053
ln*A* – distal	3.8095	0.1067
ln*P* – proximal	5.2072	0.1054
ln*A* – proximal	3.8615	0.1097

(g) *Gorilla* females

	mean	sd
P – distal	404.2534	54.5060
A – distal	95.3726	14.4106
P – proximal	432.1927	39.8379
A – proximal	105.8465	9.6942
ln*P* – distal	5.9942	0.1268
ln*A* – distal	4.5479	0.1423
ln*P* – proximal	6.0651	0.0892
ln*A* – proximal	4.6583	0.0868

(h) *Gorilla* males

	mean	sd
P – distal	572.8949	54.7442
A – distal	139.2545	13.4046
P – proximal	558.2696	64.5210
A – proximal	138.2480	14.8968
ln*P* – distal	6.3466	0.0970
ln*A* – distal	4.9321	0.0981
ln*P* – proximal	6.3187	0.1183
ln*A* – proximal	4.9237	0.1102

Table A.8. Means and standard deviations – Fourier data

(a) *Homo* females – distal

	*X*1	*Y*1	*X*2	*Y*2	*X*3	*Y*3	*X*4	*Y*4	*X*5	*Y*5
mean	106.82	53.73	1.70	5.47	9.35	3.09	1.29	2.34	2.60	2.85
sd	7.937	4.175	0.741	1.805	1.073	1.041	0.533	0.739	0.609	0.588

	ln*X*1	ln*Y*1	ln*X*2	ln*Y*2	ln*X*3	ln*Y*3	ln*X*4	ln*Y*4	ln*X*5	ln*Y*5
mean	4.668	3.981	0.420	1.623	2.229	1.064	0.1523	0.794	0.925	1.023
sd	0.0739	0.0770	0.5055	0.4550	0.1147	0.3797	0.4880	0.3562	0.2715	0.2310

(b) *Homo* females – proximal

	*X*1	*Y*1	*X*2	*Y*2	*X*3	*Y*3	*X*4	*Y*4	*X*5	*Y*5
mean	100.48	53.28	2.80	5.38	8.61	3.52	1.50	2.29	2.96	1.75
sd	9.424	4.725	0.923	1.716	1.160	1.241	0.631	0.674	0.572	0.522

	ln*X*1	ln*Y*1	ln*X*2	ln*Y*2	ln*X*3	ln*Y*3	ln*X*4	ln*Y*4	ln*X*5	ln*Y*5
mean	4.606	3.972	0.9648	1.621	2.144	1.186	0.291	0.779	1.064	0.5074
sd	0.0937	0.0891	0.3938	0.3795	0.1373	0.3996	0.5399	0.3204	0.2140	0.3378

(c) *Homo* males – distal

	*X*1	*Y*1	*X*2	*Y*2	*X*3	*Y*3	*X*4	*Y*4	*X*5	*Y*5
mean	117.81	58.60	1.52	5.59	10.28	3.59	1.25	2.25	2.82	3.11
sd	8.598	4.763	0.628	1.644	1.132	1.189	0.471	0.923	0.577	0.598

	ln*X*1	ln*Y*1	ln*X*2	ln*Y*2	ln*X*3	ln*Y*3	ln*X*4	ln*Y*4	ln*X*5	ln*Y*5
mean	4.766	4.067	0.330	1.673	2.324	1.212	0.145	0.7180	1.015	1.114
sd	0.0754	0.0827	0.4310	0.3245	0.1158	0.3884	0.4103	0.4531	0.2213	0.2115

(d) *Homo* males – proximal

	*X*1	*Y*1	*X*2	*Y*2	*X*3	*Y*3	*X*4	*Y*4	*X*5	*Y*5
mean	110.02	56.35	2.23	5.32	9.62	3.46	1.30	2.03	3.26	1.84
sd	8.569	4.622	0.793	1.715	1.102	1.354	0.469	0.734	0.558	0.539

	ln*X*1	ln*Y*1	ln*X*2	ln*Y*2	ln*X*3	ln*Y*3	ln*X*4	ln*Y*4	ln*X*5	ln*Y*5
mean	4.698	4.028	0.723	1.618	2.257	1.146	0.187	0.628	1.164	0.562
sd	0.0795	0.0815	0.4321	0.3384	0.1214	0.4800	0.4070	0.4322	0.1937	0.3201

Table A.8. (continued)

(e) *Cercopithecus* females – distal

	X1	Y1	X2	Y2	X3	Y3	X4	Y4	X5	Y5
mean	22.39	13.71	0.23	0.64	1.67	0.40	0.23	0.21	0.55	0.29
sd	2.083	1.187	0.110	0.334	0.269	0.188	0.113	0.110	0.125	0.103

	ln X1	ln Y1	ln X2	ln Y2	ln X3	ln Y3	ln X4	ln Y4	ln X5	ln Y5
mean	3.104	2.614	−1.614	−0.608	0.499	−1.035	−1.653	−1.758	−0.627	−1.315
sd	0.0949	0.0873	0.6076	0.6146	0.1723	0.5175	0.6472	0.6748	0.2636	0.3757

(f) *Cercopithecus* females – proximal

	X1	Y1	X2	Y2	X3	Y3	X4	Y4	X5	Y5
mean	22.58	15.47	0.22	0.51	1.50	0.35	0.20	0.19	0.48	0.34
sd	1.757	1.447	0.111	0.241	0.192	0.160	0.092	0.103	0.094	0.100

	ln X1	ln Y1	ln X2	ln Y2	ln X3	ln Y3	ln X4	ln Y4	ln X5	ln Y5
mean	3.114	2.734	−1.718	−0.837	0.395	−1.167	−1.765	−1.841	−0.744	−1.115
sd	0.0792	0.0952	0.7708	0.6551	0.1264	0.4950	0.6009	0.6714	0.2065	0.2826

(g) *Cercopithecus* males – distal

	X1	Y1	X2	Y2	X3	Y3	X4	Y4	X5	Y5
mean	26.70	16.56	0.33	0.82	1.96	0.44	0.33	0.37	0.66	0.36
sd	4.221	3.122	0.178	0.457	0.371	0.224	0.158	0.254	0.173	0.149

	ln X1	ln Y1	ln X2	ln Y2	ln X3	ln Y3	ln X4	ln Y4	ln X5	ln Y5
mean	3.271	2.787	−1.288	−0.378	0.653	−0.950	−1.276	−1.264	−0.459	−1.125
sd	0.1727	0.2101	0.7174	0.6672	0.2067	0.5422	0.6437	0.8499	0.2940	0.4663

(h) *Cercopithecus* males – proximal

	X1	Y1	X2	Y2	X3	Y3	X4	Y4	X5	Y5
mean	27.16	18.69	0.37	0.74	1.74	0.50	0.32	0.32	0.55	0.41
sd	4.312	3.185	0.182	0.327	0.412	0.299	0.154	0.216	0.205	0.159

	ln X1	ln Y1	ln X2	ln Y2	ln X3	ln Y3	ln X4	ln Y4	ln X5	ln Y5
mean	3.288	2.911	−1.184	−0.441	0.522	−0.877	−1.305	−1.376	−0.685	−0.995
sd	0.1695	0.1926	0.7079	0.5987	0.2568	0.6862	0.6712	0.7263	0.4242	0.5047

Table A.8. (continued)

(i) *Colobus* females – distal

	X1	Y1	X2	Y2	X3	Y3	X4	Y4	X5	Y5
mean	30.48	18.14	0.40	0.93	2.35	0.58	0.39	0.28	0.78	0.46
sd	2.491	2.201	0.293	0.446	0.245	0.333	0.256	0.123	0.155	0.114

	ln X1	ln Y1	ln X2	ln Y2	ln X3	ln Y3	ln X4	ln Y4	ln X5	ln Y5
mean	3.414	2.891	−1.172	−0.218	0.849	0.769	−1.161	−1.404	−0.274	−0.816
sd	0.0825	0.1187	0.7455	0.6210	0.1053	0.7432	0.6853	0.5774	0.2076	0.2710

(j) *Colobus* females – proximal

	X1	Y1	X2	Y2	X3	Y3	X4	Y4	X5	Y5
mean	31.18	20.49	0.31	0.79	2.25	0.57	0.26	0.39	0.77	0.51
sd	2.827	3.052	0.286	0.422	0.179	0.226	0.155	0.245	0.143	0.109

	ln X1	ln Y1	ln X2	ln Y2	ln X3	ln Y3	ln X4	ln Y4	ln X5	ln Y5
mean	3.436	3.009	−1.428	−0.372	0.807	−0.634	−1.492	−1.118	−0.277	−0.708
sd	0.0924	0.1507	0.6951	0.5698	0.0795	0.3579	0.5283	0.6236	0.1862	0.2473

(k) *Colobus* males – distal

	X1	Y1	X2	Y2	X3	Y3	X4	Y4	X5	Y5
mean	33.16	19.58	0.34	0.86	2.46	0.93	0.36	0.35	0.74	0.50
sd	3.316	2.413	0.281	0.457	0.452	0.386	0.206	0.153	0.232	0.140

	ln X1	ln Y1	ln X2	ln Y2	ln X3	ln Y3	ln X4	ln Y4	ln X5	ln Y5
mean	3.496	2.967	−1.369	−0.273	0.883	−0.182	−1.151	−1.139	−0.354	−0.739
sd	0.1040	0.1298	0.8609	0.5271	0.1877	0.5019	0.5041	0.4407	0.3415	0.3122

(l) *Colobus* males – proximal

	X1	Y1	X2	Y2	X3	Y3	X4	Y4	X5	Y5
mean	33.41	21.68	0.27	0.71	2.32	0.74	0.25	0.39	0.75	0.52
sd	3.435	2.908	0.119	0.330	0.429	0.341	0.135	0.254	0.186	0.132

	ln X1	ln Y1	ln X2	ln Y2	ln X3	ln Y3	ln X4	ln Y4	ln X5	ln Y5
mean	3.504	3.068	−1.396	−0.472	0.827	−0.429	−1.541	−1.224	−0.321	−0.688
sd	0.1039	0.1350	0.4827	0.5940	0.1821	0.5602	0.5986	0.8660	0.2505	0.2689

Table A.8. (continued)

(m) *Gorilla* females – distal

	X1	Y1	X2	Y2	X3	Y3	X4	Y4	X5	Y5
mean	78.01	36.24	0.56	2.21	6.78	3.04	0.62	0.61	2.05	1.10
sd	10.232	6.533	0.286	1.008	0.955	0.435	0.314	0.397	0.450	0.352

	ln X1	ln Y1	ln X2	ln Y2	ln X3	ln Y3	ln X4	ln Y4	ln X5	ln Y5
mean	4.349	3.576	−0.733	0.683	1.906	1.103	−0.608	−0.744	0.693	0.049
sd	0.1232	0.1717	0.6278	0.5140	0.1328	0.1311	0.5237	0.7992	0.2210	0.3022

(n) *Gorilla* females – proximal

	X1	Y1	X2	Y2	X3	Y3	X4	Y4	X5	Y5
mean	82.41	42.44	0.64	2.09	6.70	3.13	0.69	0.85	1.92	1.31
sd	7.585	4.348	0.309	0.862	0.670	0.771	0.266	0.412	0.233	0.465

	ln X1	ln Y1	ln X2	ln Y2	ln X3	ln Y3	ln X4	ln Y4	ln X5	ln Y5
mean	4.408	3.744	−0.539	0.661	1.898	1.115	−0.431	−0.291	0.643	0.212
sd	0.0899	0.0961	0.4845	0.3971	0.1004	0.2408	0.3753	0.5692	0.1214	0.3538

(o) *Gorilla* males – distal

	X1	Y1	X2	Y2	X3	Y3	X4	Y4	X5	Y5
mean	108.89	55.72	1.34	4.08	8.57	4.44	1.38	0.88	2.60	1.27
sd	9.663	6.425	1.107	3.092	0.680	0.477	1.144	0.190	0.311	0.480

	ln X1	ln Y1	ln X2	ln Y2	ln X3	ln Y3	ln X4	ln Y4	ln X5	ln Y5
mean	4.687	4.014	−0.117	0.955	2.146	1.486	0.063	−0.144	0.951	0.174
sd	0.0901	0.1176	1.0473	1.2034	0.0768	0.1073	1.0150	0.2260	0.1175	0.4050

(p) *Gorilla* males – proximal

	X1	Y1	X2	Y2	X3	Y3	X4	Y4	X5	Y5
mean	105.82	56.41	0.81	3.04	8.11	4.56	1.00	1.29	2.05	1.76
sd	12.304	5.776	0.286	1.137	0.984	0.899	0.591	0.615	0.374	0.566

	ln X1	ln Y1	ln X2	ln Y2	ln X3	ln Y3	ln X4	ln Y4	ln X5	ln Y5
mean	4.656	4.028	−0.273	1.046	2.087	1.498	−0.149	0.162	0.702	0.522
sd	0.1190	0.1045	0.4052	0.3932	0.1226	0.2084	0.5759	0.4433	0.1929	0.2980

Table A.9. Covariance-correlation matrices – conventional data

(a) *Homo*

(i) females distal (raw)

1619.2722	0.9296
335.3881	**80.3887**

(ii) females distal (ln *)

4.9948	0.9311
4.3359	**4.3419**

(iii) females proximal (raw)

2434.9449	0.9743
537.0616	**124.7790**

(vi) females proximal (ln*)

8.3838	0.9742
7.6651	**7.3835**

(v) males distal (raw)

1966.3776	0.9359
429.5349	**107.1292**

(vi) males distal (ln *)

5.4452	0.9430
5.0307	**5.2270**

(vii) males proximal (raw)

1983.4359	0.9433
433.7741	**106.6175**

(viii) males proximal (ln*)

5.9686	0.9428
5.3736	**5.4433**

(b) *Cercopithecus*

(i) females distal (raw)

114.6008	0.9746
27.3112	**6.8521**

(ii) females distal (ln*)

8.0125	0.9727
7.3597	**7.1448**

(iii) females proximal (raw)

95.6826	0.9834
25.7733	**7.1792**

(vi) females proximal (ln*)

6.3667	0.9850
6.5036	**6.8468**

(v) males distal (raw)

552.2059	0.9840
144.7265	**39.1783**

(vi) males distal (ln*)

31.4610	0.9862
32.4008	**34.3084**

(vii) males proximal (raw)

583.9174	0.9931
154.6554	**41.5367**

(viii) males proximal (ln*)

29.7581	0.9937
30.3889	**31.4274**

NB variances in bold on diagonal, covariance lower left, correlation upper right
*variances/covariances for ln variables $\times 10^{-3}$

Table A.9. (continued)

(c) *Colobus*

(i) females distal (raw)

213.3785	0.9897
58.0374	**16.1172**

(ii) females distal (ln*)

7.7828	0.9888
8.3428	**9.1467**

(iii) females proximal (raw)

315.0692	0.9935
92.7721	**27.6732**

(iv) females proximal (ln*)

11.0518	0.9939
12.4293	**14.1518**

(v) males distal (raw)

322.3106	0.9654
79.6052	**21.0966**

(vi) males distal (ln*)

11.0829	0.9688
10.0880	**11.3796**

(vii) males proximal (raw)

358.3086	0.9327
93.6332	**26.4032**

(viii) males proximal (ln*)

11.1151	0.9675
11.1921	**12.0395**

(d) *Gorilla*

(i) females distal (raw)

2970.9066	0.9844
77.3248	**207.6659**

(ii) females distal (ln*)

16.0854	0.9815
17.7183	**20.2599**

(iii) females proximal (raw)

1587.0566	0.9692
374.2931	**93.9779**

(iv) females proximal (ln*)

7.9641	0.9662
7.4839	**7.5333**

(v) males distal (raw)

2996.9241	0.9810
719.8784	**179.6846**

(vi) males distal (ln*)

9.3997	0.9809
9.3312	**9.6268**

(vii) males proximal (raw)

4162.9585	0.9967
957.9651	**221.9145**

(viii) males proximal (ln*)

13.9934	0.9968
12.9905	**12.1377**

NB variances in bold on diagonal, covariance lower left, correlation upper right
*variances/covariances for ln variables $\times 10^{-3}$

Table A.10. Covariance-correlation matrices – Fourier data

(a) *Homo*

(i) females distal (raw)

62.9961	0.5294	0.1211	0.0207	0.8599	0.2502	−0.1501	0.3712	0.4951	0.5836
17.5417	**17.4267**	0.4150	0.0761	0.2181	0.0587	0.1669	0.1591	0.0523	0.2877
0.7115	1.2830	**0.5484**	0.3556	0.0358	0.0466	0.4541	0.1734	0.0368	−0.1285
0.2971	0.5734	0.4752	**3.2570**	−0.1620	0.3842	0.7960	0.0372	−0.3599	−0.1343
7.3235	0.9769	0.0285	−0.3136	**1.1513**	−0.0225	−0.4422	0.4653	0.7964	0.5105
2.0676	0.2550	0.0360	0.7221	−0.0251	**1.0844**	0.2734	−0.2501	−0.3648	0.1114
−0.6345	0.3709	0.1791	0.7649	−0.2527	0.1516	**0.2836**	−0.1369	−0.5502	−0.1902
2.1775	0.4908	0.0949	0.0495	0.3690	−0.1924	−0.0539	**0.5461**	0.4060	0.2698
2.3922	0.1330	0.0166	−0.3954	0.5202	−0.2312	−0.1783	0.1827	**0.3705**	0.0377
2.7242	0.7064	−0.0560	−0.1426	0.3222	0.0682	−0.0596	0.1172	0.0135	**0.3459**

(ii) females distal (ln*)

5.4573	0.5317	0.1222	0.0953	0.8518	0.2122	−0.1384	0.3673	0.3918	0.5512
3.0239	**5.9265**	0.3953	0.1429	0.2179	0.0409	0.1642	0.1858	−0.0197	0.2793
4.5651	15.3856	**255.5633**	0.5080	0.0063	0.0571	0.5516	0.1579	−0.0630	−0.1063
3.2023	5.0042	116.8571	**207.0224**	−0.0686	0.2810	0.8008	0.0863	−0.2300	−0.1169
7.2181	1.9240	0.3676	−3.5797	**13.1575**	−0.0491	−0.3876	0.4605	0.7467	0.4864
5.9527	1.1958	10.9550	48.5533	−2.1384	**144.1783**	0.1960	−0.2570	−0.3680	0.0726
−4.9902	6.1668	136.0609	177.7875	−21.6974	36.3204	**238.1149**	−0.1077	−0.4663	−0.1903
9.6665	5.0959	28.4384	13.9872	18.8155	−34.7645	−18.7289	**126.8951**	0.3899	0.2278
7.8577	−0.4114	−8.6481	−28.4109	23.2534	−37.9410	−61.7815	37.7076	**73.7169**	−0.0051
9.4082	4.9683	−12.4205	−12.2906	12.8891	6.3688	−21.4555	18.7495	−0.3204	**53.3780**

(iii) females proximal (raw)

88.8017	0.7921	0.1990	−0.0489	0.9243	0.0180	−0.0266	0.6018	0.7561	0.6294
35.2709	**22.3256**	0.3627	0.0712	0.5917	−0.0027	0.1573	0.4765	0.5669	0.4248
1.7311	1.5819	**0.8518**	0.6396	0.1121	0.2211	0.8340	0.1065	0.1807	0.0961
−0.7914	0.5769	1.0128	**2.9438**	−0.1920	0.5484	0.8482	−0.2662	−0.2244	−0.3411
10.1008	3.2421	0.1200	−0.3821	**1.3448**	−0.1275	−0.1775	0.6052	0.8569	0.6971
0.2108	−0.0160	0.2532	1.1676	−0.1834	**1.5397**	0.3273	−0.1945	−0.1963	−0.2235
−0.1581	0.4693	0.4860	0.9189	−0.1299	0.2564	**0.3987**	−0.3034	−0.0933	−0.3091
3.8207	1.5171	0.0662	−0.3077	0.4729	−0.1626	−0.1291	**0.4540**	0.4110	0.6753
4.0746	1.5319	0.0954	−0.2201	0.5683	−0.1393	−0.0337	0.1584	**0.3270**	0.4059
3.0946	1.0473	0.0463	−0.3054	0.4218	−0.1447	−0.1018	0.2374	0.1211	**0.2722**

(iv) females proximal (ln*)

8.7799	0.7933	0.1989	−0.0946	0.9225	−0.0313	−0.0698	0.6290	0.7400	0.6019
6.6238	**7.9403**	0.3643	0.0145	0.5930	−0.0667	0.1093	0.5230	0.5471	0.4076
7.3403	12.7844	**155.0993**	0.6166	0.1182	0.1763	0.8111	0.1519	0.1547	0.0414
−3.3642	0.4915	92.1653	**144.0374**	−0.1867	0.5173	0.8719	−0.2583	−0.1911	−0.3158
11.8697	7.2560	6.3919	−9.7311	**18.8581**	−0.1521	−0.1611	0.6264	0.8514	0.6806
−1.1717	−2.3741	27.7490	78.4478	−8.3450	**159.6524**	0.3312	−0.2118	−0.2169	−0.2210
−3.5317	5.2585	172.4824	178.6733	−11.9457	71.4527	**291.5419**	−0.2698	−0.0936	−0.2487
18.8823	14.9300	19.1685	−31.4059	27.5592	−27.1172	−46.6799	**102.6499**	0.4476	0.6142
14.8391	10.4333	13.0390	−15.5231	25.0204	−18.5424	−10.8179	30.6872	**45.7934**	0.4100
19.0503	12.2698	5.5119	−40.4831	31.5692	−29.8224	−45.3569	66.4689	29.63416	**114.0989**

NB variances in bold on diagonal, covariance lower left, correlation upper right

*variances/covariances for ln variables $\times 10^{-3}$

Table A.10. (continued)

(v) males distal (raw)

73.9245	0.6362	0.1158	0.1504	0.8582	0.2570	−0.1165	0.2941	0.6003	0.4470
26.0524	**22.6867**	0.1318	0.1196	0.2714	0.0975	0.1383	0.0584	0.0977	0.2702
0.6250	0.3939	**0.3938**	0.4791	0.1322	0.1095	0.3833	0.2576	−0.0094	0.0997
2.1263	0.9371	0.4944	**2.7038**	0.0702	0.1814	0.7129	0.2428	−0.1225	−0.0492
8.3492	1.4625	0.0938	0.1491	**1.2803**	0.0345	−0.3260	0.4121	0.8547	0.4113
2.6281	0.5522	0.0817	0.3547	0.0464	**1.4140**	0.3335	−0.0635	−0.2273	0.0138
−0.4712	0.3099	0.1132	0.5516	−0.1736	0.0187	**0.2214**	−0.1385	−0.4637	−0.0840
2.3339	0.2568	0.1492	0.3685	0.4304	−0.0697	−0.0602	**0.8519**	0.3044	0.1435
2.9780	0.2684	−0.0339	−0.1162	0.5580	−0.1559	−0.1259	0.1621	**0.3329**	0.0573
2.2985	0.7697	0.0374	−0.0484	0.2784	0.0098	−0.0024	0.0792	0.0198	**0.3577**

(vi) males distal (ln*)

5.6838	0.6680	0.0672	0.1484	0.8598	0.2397	−0.1036	0.2476	0.6074	0.4834
4.1663	**6.8440**	0.1011	0.1213	0.3208	0.1125	0.1410	0.0503	0.1475	0.3077
2.1831	3.6056	**185.7131**	0.4059	0.0637	0.0352	0.3254	0.1546	−0.0525	0.0500
3.6299	3.2575	56.7634	**105.3083**	0.0695	0.1821	0.7248	0.2553	0.0728	−0.0580
7.5062	3.0729	3.1767	2.6123	**13.4097**	0.0060	−0.3188	0.3892	0.8613	0.4655
7.0182	3.6135	5.9001	22.9575	0.2687	**150.8609**	0.0978	−0.0963	−0.2587	0.0303
−3.2055	4.7873	57.5445	96.5066	−15.1485	15.5892	**168.3526**	−0.1375	−0.4419	−0.0603
8.4563	1.8839	30.1837	37.5348	20.4171	−16.9386	−25.5559	**205.2690**	0.3427	0.0923
10.1343	2.7000	−5.0059	−5.2260	22.0744	−22.2373	−40.1363	34.3595	**48.9849**	0.1281
7.7104	5.3849	4.5550	−3.9850	11.4026	2.4859	−5.2298	8.8451	5.9972	**44.7529**

(vii) males proximal (raw)

73.4215	0.6700	0.2982	0.1831	0.8613	0.1362	0.0939	0.4185	0.5582	0.5822
26.5317	**21.3583**	0.0778	0.0875	0.2831	0.2361	−0.0605	0.2979	0.0490	0.3118
2.0273	0.2851	**0.6294**	0.4714	0.3878	0.1020	0.6505	0.3412	0.3125	0.1999
2.6916	0.6935	0.6414	**2.9420**	0.1005	0.5306	0.7761	−0.1422	−0.1457	−0.0515
8.1305	1.4413	0.3390	0.1899	**1.2138**	−0.1427	0.1150	0.4185	0.8264	0.6581
1.5809	1.4776	0.1096	1.2325	−0.2129	**1.8340**	0.2767	−0.2210	−0.3561	−0.1802
0.3769	−0.1310	0.2419	0.6239	0.0594	0.1756	**0.2197**	−0.2523	0.0586	−0.0519
2.6301	1.0099	0.1985	−0.1789	0.3382	−0.2195	−0.0867	**0.5381**	0.2437	0.4036
2.6686	0.1264	0.1383	−0.1394	0.5080	−0.2691	0.0153	0.0997	**0.3113**	0.3506
2.6864	0.7761	0.0854	−0.0476	0.3905	−0.1315	−0.0131	0.1594	0.1054	**0.2900**

(viii) males proximal (ln*)

6.3118	0.6615	0.2775	0.1479	0.8642	0.0312	0.0482	0.3849	0.5783	0.5777
4.2821	**6.6387**	0.0594	0.0721	0.2801	0.1749	−0.1018	0.2726	0.0668	0.2776
9.5275	2.0905	**186.6964**	0.4064	0.3614	−0.0031	0.5366	0.3733	0.2528	0.2275
3.9770	1.9874	59.4107	**114.4919**	0.0665	0.4751	0.7787	−0.0873	−0.1484	−0.0535
8.3347	2.7703	18.9567	2.7317	**14.7353**	−0.2026	0.0839	0.3815	0.8379	0.6663
1.1902	6.8418	−0.6406	77.1777	−11.8068	**230.4366**	0.2330	−0.2463	−0.3431	−0.2211
1.5576	−3.3748	94.3741	107.2431	4.1446	45.5232	**165.6823**	−0.2125	0.0057	−0.4320
13.2158	9.5983	69.7093	−12.7733	20.0154	−51.0930	−37.3862	**186.7800**	0.1893	0.3789
8.9009	1.0542	21.1626	−9.7260	19.7049	−31.9073	0.4486	15.8474	**37.5362**	0.3791
14.6892	7.2403	31.4576	−5.7991	25.8878	−33.9775	−5.6279	52.4145	23.5068	**102.4388**

NB variances in bold on diagonal, covariance lower left, correlation upper right
*variances/covariances for ln variables $\times 10^{-3}$

Table A.10. (continued)

(b) *Cercopithecus*

(i) females distal (raw)

4.3399	0.7284	0.1075	0.1246	0.8889	−0.0562	0.0146	0.4468	0.7367	0.4160
1.8011	1.4087	0.0180	0.1473	0.3935	−0.1279	0.1054	0.2647	0.2812	0.3803
0.0246	0.0023	0.0121	0.7804	0.1280	0.0111	0.7810	0.0566	0.0750	0.0649
0.0868	0.0584	0.0287	0.1117	0.1152	−0.1037	0.8890	−0.0154	0.1083	0.0878
0.4984	0.1257	0.0038	0.0104	0.0724	−0.2247	−0.0304	0.5002	0.9043	0.4681
−0.0220	−0.0285	0.0002	−0.0065	−0.0114	0.0353	−0.1204	−0.3580	−0.4769	−0.2842
0.0034	0.0141	0.0097	0.0336	−0.0009	−0.0026	0.0128	−0.0517	0.0063	0.0255
0.1028	0.0347	0.0007	−0.0006	0.0149	−0.0074	−0.0006	0.0122	0.5296	0.2930
0.1925	0.0419	0.0010	0.0045	0.0305	−0.0112	0.0001	0.0073	0.0157	0.2512
0.0894	0.0466	0.0007	0.0030	0.0130	−0.0055	0.0003	0.0033	0.0033	0.0106

(ii) females distal (ln*)

9.0077	0.7115	0.2229	0.2022	0.8873	−0.0057	0.0406	0.3625	0.7122	0.3698
5.8972	7.6269	0.1224	0.1573	0.3733	−0.1099	0.0850	0.1746	0.2513	0.3157
12.8519	6.4933	369.1868	0.8281	0.2063	0.0661	0.6629	−0.0380	0.1497	0.0814
11.7979	8.4455	3.0927	377.7682	0.1982	−0.0454	0.7892	−0.0957	0.1610	0.1030
14.5109	5.6173	21.5960	20.9939	29.6925	−0.1725	0.0248	0.4484	0.8997	0.4155
−0.2819	−4.9649	20.7797	−14.4480	−15.3829	267.7923	−0.0860	−0.3289	−0.4177	−0.3170
2.4941	4.8018	2.6070	313.9171	2.7622	−28.7952	418.8752	−0.1599	0.0373	0.0622
23.2123	102.8892	−15.5808	−39.6801	52.1371	−114.8482	−69.8510	455.3072	0.5051	0.2446
17.8150	5.7853	23.9772	26.0740	40.8608	−56.9681	6.3632	89.8305	69.4661	0.2419
13.1872	11.5401	18.5777	23.7779	26.9019	−61.6415	15.1316	62.0136	23.9499	141.1649

(iii) females proximal (raw)

3.8060	0.7898	0.2099	−0.0429	0.6558	0.1066	−0.0673	0.2148	0.4790	0.3166
2.0071	2.0929	0.2016	−0.1533	0.1241	−0.0563	−0.1646	0.1797	0.1866	0.0830
0.0408	0.0329	0.0123	0.7355	0.1528	−0.0704	0.6172	0.3315	0.0914	0.3174
−0.0181	−0.0535	0.0196	0.0581	0.1423	0.0889	0.9156	0.0141	0.0136	0.3446
0.2209	0.0344	0.0032	0.0066	0.0368	−0.0631	0.1245	0.0678	0.7567	0.5965
0.0300	−0.0131	−0.0013	0.0034	−0.0019	0.0257	0.0666	−0.0388	−0.5225	0.0283
−0.0108	−0.0218	0.0063	0.0202	0.0022	0.0010	0.0084	−0.1081	0.0422	0.3329
0.0388	0.0268	0.0038	0.0003	0.0013	−0.0006	−0.0010	0.0106	−0.0942	0.0537
0.0794	0.0255	0.0010	0.0003	0.0137	−0.0079	0.0004	−0.0009	0.0089	0.2321
0.0559	0.0121	0.0035	0.0083	0.0115	0.0005	0.0031	0.0006	0.0022	0.0101

(iv) females proximal (ln*)

6.2746	0.8099	0.2006	0.0631	0.6406	0.0798	−0.0283	0.1483	0.4438	0.2924
6.1088	9.0674	0.1460	−0.0910	0.1385	−0.0895	−0.1702	0.1288	0.1814	0.0994
12.2479	10.7154	594.1686	0.7876	0.1745	0.0035	0.5893	0.3293	0.0666	0.4119
3.2748	−5.6776	3.9773	429.1471	0.2141	0.0999	0.8800	0.1172	0.1213	0.3474
6.4154	1.6672	17.0078	17.7359	15.9858	−0.0618	0.1614	0.0390	0.7251	0.5444
3.1270	−4.2205	1.3274	32.3913	−3.8674	245.0017	0.1339	−0.0677	−0.5019	0.0265
−1.3447	−9.7379	272.9606	346.3963	12.2639	39.8317	361.0461	−0.0086	0.0663	0.3250
7.8887	8.2334	170.4412	51.5677	3.3092	−22.5016	−3.4856	450.7674	−0.1217	0.0308
7.2578	3.5659	10.6000	16.4040	18.9271	−51.2926	8.2283	−16.8735	42.6243	0.1503
6.5443	2.6745	89.7041	64.3076	19.4489	3.7024	55.1780	5.8380	8.7652	79.8378

NB variances in bold on diagonal, covariance lower left, correlation upper right
*variances/covariances for ln variables $\times 10^{-3}$

Table A.10. (continued)

(v) males distal (raw)

17.8163	0.8760	0.3818	0.5881	0.8130	0.1578	0.5689	0.2761	0.6321	0.3617
11.5450	**9.7488**	0.2792	0.4521	0.4610	−0.0059	0.5933	−0.0291	0.3516	0.2860
0.2863	0.1549	**0.0316**	0.7743	0.3182	0.3261	0.6880	0.2853	0.0911	0.1733
1.1343	0.6450	0.0629	**0.2088**	0.4927	0.3401	0.7369	0.1977	0.2108	0.1727
1.2724	0.5337	0.0210	0.0835	**0.1375**	0.1250	0.2914	0.4573	0.8542	0.4417
0.1490	−0.0041	0.0130	0.0348	0.0104	**0.0500**	0.2215	0.2985	−0.2094	0.0327
0.3797	0.2930	0.0193	0.0532	0.0171	0.0078	**0.0250**	0.2090	0.1050	0.1433
0.2960	−0.0231	0.0129	0.0229	0.0431	0.0170	0.0084	**0.0645**	0.3335	0.0675
0.4611	0.1897	0.0028	0.0166	0.0547	−0.0081	0.0029	0.0146	**0.0299**	0.1860
0.2269	0.1327	0.0046	0.0117	0.0243	0.0011	0.0034	0.0025	0.0048	**0.0221**

(vi) males distal (ln*)

29.8262	0.8923	0.2793	0.5335	0.8217	0.1189	0.5425	0.2422	0.6522	0.3286
32.3750	**44.1410**	0.2259	0.4537	0.4910	0.0288	0.5525	0.0304	0.3849	0.2869
34.5964	34.0460	**514.6029**	0.7293	0.2362	0.0633	0.5501	0.1817	0.0966	0.0763
61.4760	63.6061	349.1009	**445.2144**	0.4355	0.0920	0.7662	0.2192	0.2578	0.1366
29.0063	21.3193	35.0156	60.0540	**42.7069**	0.0467	0.3442	0.4123	0.8834	0.3797
11.1371	3.2780	24.6184	33.2914	5.2368	**294.0218**	0.1245	−0.0109	−0.2423	0.0230
60.3067	74.7115	254.0118	329.0670	45.7791	43.4465	**414.2921**	0.3135	0.2552	0.1179
35.5469	5.4318	110.7570	124.3016	72.4149	−5.0259	171.4867	**722.3635**	0.3775	0.0391
33.1220	23.7755	20.3766	50.5844	53.6789	−38.6373	43.3081	94.3371	**86.4587**	0.1991
26.4639	28.1122	25.5386	42.5193	36.5937	5.8255	35.4044	15.4914	27.3047	**217.4789**

(vii) males proximal (raw)

18.5961	0.9131	0.0547	0.0843	0.7828	0.1742	0.2478	0.4654	0.5460	0.5609
12.5424	**10.1473**	0.0534	0.0381	0.5072	0.0694	0.2554	0.4375	0.3143	0.4292
0.0428	0.0309	**0.0330**	0.6106	−0.1070	0.2915	0.6683	0.2461	−0.2201	−0.1030
0.1188	0.0396	0.0362	**0.1067**	0.0182	0.1911	0.8245	−0.1090	−0.1207	−0.0085
1.3916	0.6661	−0.0080	0.0025	**0.1700**	−0.0035	0.0289	0.3347	0.8630	0.6976
0.2243	0.0660	0.0158	0.0186	−0.0004	**0.0892**	0.1475	0.1336	−0.3158	0.1036
0.1646	0.1253	0.0187	0.0415	0.0018	0.0068	**0.0237**	0.1436	−0.0690	−0.0912
0.4340	0.3014	0.0097	−0.0077	0.0298	0.0086	0.0048	**0.0468**	0.3292	0.1591
0.4820	0.2050	−0.0082	−0.0081	0.0728	−0.0193	−0.0022	0.0146	**0.0419**	0.4370
0.3858	0.2180	−0.0030	0.0004	0.0459	0.0049	−0.0022	0.0055	0.0143	**0.0254**

(viii) males proximal (ln*)

28.7347	0.9221	0.0596	0.1273	0.7425	0.1588	0.3614	0.3569	0.4597	0.6427
30.1043	**37.0971**	0.0689	0.0918	0.4783	0.0775	0.3624	0.3386	0.2277	0.5641
7.1464	9.3966	**501.1745**	0.5784	−0.0727	0.1785	0.6105	0.3618	−0.2018	−0.0056
12.9172	10.5825	245.1439	**358.4535**	0.0439	0.1585	0.8346	0.0301	−0.1119	0.0359
32.3238	23.6572	−13.2214	6.7471	**65.9562**	−0.0432	0.1455	0.2275	0.8594	0.6800
18.4759	10.2479	86.7092	65.1057	−7.6078	**470.8310**	0.1260	0.0516	−0.3762	0.0646
41.1159	46.8523	290.0513	335.3539	25.0719	58.0418	**450.4442**	0.1846	−0.0569	0.1382
43.9355	47.3608	186.0128	13.0748	42.4433	25.7273	90.0005	**527.5356**	0.1789	0.1363
33.0583	18.6025	−60.5989	−28.4235	93.6307	−109.5082	−16.2099	55.1109	**179.9778**	0.4067
54.9916	54.8408	−2.0093	10.8354	88.1442	22.3772	46.8138	49.9771	87.0859	**254.7472**

NB variances in bold on diagonal, covariance lower left, correlation upper right

*variances/covariances for ln variables $\times 10^{-3}$

Table A.10. (continued)

(c) *Colobus*

(i) females distal (raw)

6.2067	0.8648	0.4575	0.2857	0.6874	−0.3348	0.3781	0.2868	0.6765	0.3820
4.7418	**4.8441**	0.7442	0.4487	0.2937	−0.4966	0.6696	0.2441	0.5897	0.0804
3.3424	0.4804	**0.0860**	0.8392	−0.2134	−0.3316	0.9455	0.2026	0.1294	−0.2136
0.3178	0.4409	0.1099	**0.1993**	−0.2116	0.1822	0.8361	0.2229	−0.1770	0.0081
0.4192	0.1582	−0.0153	−0.0231	**0.0599**	−0.2347	−0.2410	0.1040	0.7289	0.7127
−0.2780	−0.3644	−0.0324	0.0028	−0.0191	**0.1111**	−0.3622	0.1231	−0.7413	0.0893
0.2415	0.3778	0.0711	0.0957	−0.0151	−0.0313	**0.0657**	0.1947	0.1211	−0.1699
0.0875	0.0658	0.0073	0.0122	0.0031	0.0050	0.0061	**0.0150**	0.0430	−0.0630
0.2612	0.2011	0.0059	−0.0122	0.0276	−0.0383	0.0048	0.0008	**0.0240**	0.3534
0.1087	0.0202	−0.0072	0.0004	0.0199	0.0034	−0.0050	−0.0009	0.0063	**0.0131**

(ii) females distal (ln*)

6.8003	0.8751	0.3352	0.1746	0.7004	−0.3379	0.2700	0.3709	0.6786	0.3976
8.5650	**14.0879**	0.5667	0.2640	0.3311	−0.4901	0.4896	0.3767	0.6062	0.0852
20.6078	50.1464	**555.7677**	0.8383	−0.2638	−0.1560	0.8495	0.2221	−0.0813	−0.2578
8.9405	19.4585	388.0895	**385.6204**	−0.1849	0.1029	0.8109	0.1463	−0.2582	0.0370
6.0809	4.1381	−20.7072	−12.0912	**11.0857**	−0.1298	−0.2247	0.1201	0.7258	0.7406
−20.7055	−43.2320	−86.4544	47.4755	−15.0849	**552.3171**	−0.2485	−0.0355	−0.6386	0.1972
15.2597	39.8294	434.0203	345.0979	−16.2114	−126.5491	**469.6955**	0.1907	−0.0021	−0.1246
17.6578	25.8130	95.5937	52.4618	7.3034	−15.2207	75.4799	**333.3626**	0.0795	−0.0779
11.6167	14.9363	−12.5860	−33.2825	15.8634	−105.4615	−0.2922	9.5249	**43.0936**	0.3649
8.8861	2.7397	−52.0766	6.2217	21.1304	39.7202	−23.1371	12.1957	20.5284	**73.4412**

(iii) females proximal (raw)

7.9905	0.9413	0.0920	0.1152	0.5470	−0.0119	0.1793	0.1591	0.3685	0.2247
8.1197	**9.3128**	0.0102	0.0359	0.3653	−0.0353	0.1370	0.0355	0.2943	0.3594
0.0743	0.0089	**0.0816**	0.7492	0.2198	−0.0052	0.6727	0.6211	0.0952	−0.0806
0.1374	0.0462	0.0903	**0.1781**	0.0322	0.1883	0.8616	0.6106	−0.0687	−0.3063
0.2760	0.1990	0.0112	0.0024	**0.0319**	−0.4641	0.0619	−0.0529	0.8552	0.1824
−0.0076	−0.0224	−0.0003	0.0180	−0.0188	**0.0513**	0.1913	0.5148	−0.5183	−0.2382
0.0785	0.0647	0.0298	0.0563	0.0017	0.0067	**0.0240**	0.5406	−0.0183	−0.0289
0.1104	0.0266	0.0436	0.0632	−0.0023	0.0286	0.0205	**0.0602**	−0.1422	−0.3964
0.1494	0.1288	0.0039	−0.0042	0.0219	−0.0168	−0.0004	−0.0050	**0.0206**	0.0773
0.0692	0.1195	−0.0025	−0.0141	0.0035	−0.0059	−0.0005	−0.0106	0.0012	**0.0119**

(iv) females proximal (ln*)

8.5348	0.9458	−0.0153	0.1970	0.5571	−0.0614	0.2023	0.0999	0.3816	0.2303
13.1668	**22.7077**	−0.1068	0.1297	0.3871	−0.0743	0.1643	−0.0169	0.3020	0.3583
−0.9819	−11.1813	**483.1023**	0.5760	0.1620	0.0011	0.3424	0.3618	0.0397	−0.1156
10.3724	11.1336	228.1187	**324.7185**	0.0540	0.1245	0.6931	0.4031	0.0181	−0.3858
4.0938	4.6403	8.9567	2.4487	**6.3218**	−0.4342	0.0981	−0.1139	0.8689	0.1728
−2.0312	−4.0061	0.2706	25.3861	−12.3625	**128.0847**	0.1401	0.3969	−0.5293	−0.1846
9.8740	13.0796	125.7284	208.6629	4.1225	26.4831	**279.1516**	0.3093	0.0403	0.0104
5.7539	−1.5910	156.8088	143.2485	−5.6484	88.5759	101.9157	**388.9221**	−0.1984	−0.3748
6.5654	8.4772	5.1384	1.9226	12.8741	−35.2786	3.9631	−23.0436	**34.6879**	0.0237
5.2621	13.3524	−19.8677	−54.3747	3.3998	−16.3391	1.3537	−57.8153	1.0927	**61.1731**

NB variances in bold on diagonal, covariance lower left, correlation upper right
*variances/covariances for ln variables $\times 10^{-3}$

Table A.10. (continued)

(v) males distal (raw)

10.9939	0.6861	−0.0037	−0.0069	0.7688	−0.3581	0.1474	0.1900	0.7214	0.6319
5.4892	**5.8235**	0.1073	−0.1351	0.1021	−0.2310	0.2995	0.2520	0.1905	0.3087
−0.0035	0.0727	**0.0788**	0.8124	−0.0655	−0.3725	0.8852	0.1137	0.0467	−0.0972
−0.0105	−0.1491	0.1043	**0.2090**	0.1233	−0.2034	0.7323	−0.1321	0.1121	0.0973
1.1513	0.1113	−0.0083	0.0255	**0.2040**	−0.4834	0.0166	0.1505	0.9221	0.6257
−0.4586	−0.2154	−0.0404	−0.0359	−0.0843	**0.1492**	−0.4998	−0.4109	−0.6822	−0.2359
0.1008	0.1491	0.0513	0.0691	0.0015	−0.0398	**0.0425**	0.3658	0.1966	0.1358
0.0961	0.0928	0.0049	−0.0092	0.0104	−0.0242	0.0115	**0.0233**	0.3803	0.2278
0.5545	0.1065	0.0030	0.0119	0.0965	−0.0611	0.0094	0.0135	**0.0537**	0.5413
0.2930	0.1042	−0.0038	0.0062	0.0395	−0.0127	0.0039	0.0049	0.0175	**0.0196**

(vi) males distal (ln*)

10.8101	0.7138	−0.1704	−0.0886	0.7555	−0.4301	−0.0282	0.1807	0.7021	0.5817
9.6314	**16.8408**	−0.0528	−0.2100	0.1269	−0.3228	0.2038	0.2295	0.2054	0.2733
−15.2537	−5.9040	**741.0834**	0.5910	−0.1224	−0.3615	0.5862	−0.0554	−0.1441	−0.2615
−4.8546	−14.3624	268.1783	**277.8490**	0.1045	−0.1919	0.6193	−0.1442	0.0231	0.1645
14.7417	3.0903	−19.7777	10.3425	**35.2232**	−0.5061	−0.1223	0.1338	0.9209	0.5868
−22.4408	−21.0217	−156.1683	−50.7795	−47.6717	**251.8843**	−0.5304	−0.3948	−0.6592	−0.3058
−1.4792	13.3347	254.3866	164.5467	−11.5670	−134.1900	**254.1042**	0.3030	0.0152	0.1218
8.2793	13.1259	−21.0157	−33.5025	11.0642	−87.3119	67.3001	**194.2085**	0.3413	0.2540
24.9274	9.1022	−42.3662	4.1657	59.0181	−112.9801	2.6084	51.3604	**116.6123**	0.5071
18.8818	11.0729	−70.2806	27.0757	34.3798	−47.9070	19.1703	34.9463	54.0627	**97.4534**

(vii) males proximal (raw)

11.7992	0.6603	0.0362	0.3324	0.6044	0.4845	0.0076	0.3102	0.3178	0.7552
6.5951	**8.4555**	0.2496	0.2698	−0.1651	0.2248	0.3947	0.3228	−0.3869	0.3944
0.0148	0.0861	**0.0141**	0.4655	−0.2144	0.2684	0.2031	−0.1380	−0.2019	−0.1219
0.3762	0.2586	0.0182	**0.1086**	0.0926	0.4148	0.3140	−0.4858	0.0790	−0.0270
0.8903	−0.2059	−0.0109	0.0131	**0.1839**	0.1976	−0.3173	0.0740	0.8986	0.6749
0.5673	0.2228	0.0109	0.0466	0.0289	**0.1162**	−0.1867	−0.0370	−0.0004	0.0993
0.0035	0.1549	0.0033	0.0140	−0.0184	−0.0086	**0.0182**	0.0913	−0.2181	0.0855
0.2707	0.2385	−0.0042	−0.0407	0.0081	−0.0032	0.0031	**0.0645**	−0.1137	0.4359
0.2028	−0.2090	−0.0045	0.0048	0.0716	−0.0000	−0.0055	−0.0054	**0.0345**	0.4913
0.3419	0.1512	−0.0019	−0.0012	0.0381	0.0045	0.0015	0.0146	0.0120	**0.0174**

(viii) males proximal (ln*)

10.8031	0.6912	−0.0572	0.1984	0.5643	0.4731	−0.1062	0.4317	0.2359	0.7983
9.7008	**18.2306**	0.1213	0.1267	−0.1636	0.2103	0.2778	0.3795	−0.4004	0.4585
−2.8687	7.9063	**232.9889**	0.2456	−0.2112	0.2842	0.2337	−0.1278	−0.2003	−0.1400
12.2504	10.1585	70.4338	**352.8691**	0.0406	0.3737	0.2177	−0.4361	0.0315	−0.1481
10.6805	−4.0220	−18.5635	4.3963	**33.1580**	0.1960	−0.4016	0.1185	0.8581	0.6662
27.5509	15.9089	76.8609	124.3696	19.9959	**313.8595**	−0.1963	0.0357	−0.0326	0.0946
−6.6095	22.4554	67.5264	77.3997	−43.7737	−65.8300	**358.3504**	−0.0893	−0.2970	−0.0253
38.8551	44.3743	−53.4013	−224.3063	18.6785	17.3091	−46.2918	**749.8884**	−0.1348	0.4997
6.1430	−13.5444	−24.2155	4.6881	39.1430	−4.5752	−44.5442	−29.2500	**62.7539**	0.4269
22.3075	16.6438	−18.1643	−23.6453	32.6138	14.2525	−4.0707	116.3497	28.7487	**72.2839**

NB variances in bold on diagonal, covariance lower left, correlation upper right

*variances/covariances for ln variables $\times 10^{-3}$

Table A.10. (continued)

(d) *Gorilla*

(i) females distal (raw)

104.6844	0.9291	−0.4335	−0.2168	0.9302	−0.2947	−0.1056	0.2493	0.8089	0.3969
62.1038	**42.6824**	−0.6090	−0.4223	0.7539	−0.1259	−0.2004	0.3808	0.5973	0.3827
−1.2678	−1.1374	**0.0817**	0.9454	−0.3441	0.3188	0.8212	−0.2741	−0.3573	−0.0384
−2.2353	−2.7802	0.2724	**1.0156**	−0.1542	0.3270	0.9047	−0.1812	−0.2045	0.0228
9.0890	4.7035	−0.0939	−1.4838	**0.9120**	−0.5618	−0.1896	0.0554	0.9567	0.4189
−1.3109	−0.3575	0.0396	0.1432	−0.2333	**0.1890**	0.5760	0.2530	−0.7357	−0.1719
−0.3401	−0.4119	0.0739	0.2869	−0.0570	0.0788	**0.0990**	0.1086	−0.3328	0.0537
1.0129	0.9881	−0.0311	−0.0725	0.0210	0.0437	0.0136	**0.1577**	−0.1183	0.1889
3.7280	1.7578	−0.0460	−0.0929	0.4116	−0.1441	−0.0472	−0.0212	**0.2029**	0.2674
1.4307	0.8809	−0.0039	0.0081	0.1410	−0.0263	0.0060	0.0264	0.0424	**0.1241**

(ii) females distal (ln*)

15.1772	0.9141	−0.5260	−0.2360	0.9110	−0.3056	−0.0617	0.2299	0.7252	0.3982
19.3315	**29.4697**	−0.6603	−0.4372	0.7012	−0.1066	−0.1982	0.3997	0.4815	0.3368
−40.6795	−71.1642	**394.1060**	0.9042	−0.4458	0.3702	0.7767	−0.3576	−0.4661	0.0124
−14.9465	−38.5740	291.7594	**264.1798**	−0.1788	0.3457	0.9156	−0.2779	−0.2692	0.0992
14.9090	15.9906	−37.1753	−12.2056	**17.6475**	−0.6075	−0.1290	0.0462	0.9296	0.4655
−4.9346	−2.3992	30.4666	23.2895	−10.5785	**17.1812**	0.4953	0.0871	−0.8129	−0.2381
−3.9781	−17.8199	255.3579	246.4615	−8.9777	33.9996	**274.2974**	−0.1255	−0.3078	0.0602
22.6364	54.8325	−179.4091	−114.1446	4.9071	9.1283	−52.5411	**638.6750**	−0.1437	0.2410
19.7410	18.2647	−64.6558	−30.5711	27.2892	−23.5450	−35.6238	−25.3787	**48.8281**	0.3220
14.8245	17.4693	2.3602	15.4055	1.8687	−9.4292	9.5265	58.2014	21.5040	**91.3128**

(iii) females proximal (raw)

57.5283	0.7683	0.6369	0.7416	0.8597	0.8074	0.7032	0.8071	0.1204	0.7467
25.3376	**18.9041**	0.8386	0.8533	0.3563	0.5759	0.8823	0.7092	−0.2410	0.5502
1.4906	1.1250	**0.0952**	0.9183	0.3347	0.4457	0.8449	0.4717	−0.1125	0.5396
4.8472	3.1970	0.2442	**0.7426**	0.4663	0.5149	0.8995	0.6238	0.0312	0.4686
4.3712	1.0385	0.0692	0.2694	**0.4494**	0.6462	0.3531	0.5956	0.4859	0.6202
4.7170	1.9299	0.1060	0.3420	0.3338	**0.5939**	0.4536	0.6446	−0.2987	0.8357
1.4201	1.0214	0.0694	0.2064	0.0630	0.0931	**0.0709**	0.7456	−0.1430	0.4803
2.5211	1.2699	0.0599	0.2214	0.1644	0.2046	0.0818	**0.1696**	−0.0777	0.6239
0.2127	−0.2441	−0.0081	0.0063	0.0759	−0.0536	−0.0089	−0.0075	**0.0543**	−0.3023
2.6332	1.1122	0.0774	0.1877	0.1933	0.2994	0.0595	0.1195	−0.0327	**0.2161**

(iv) females proximal (ln*)

8.0914	0.7377	0.5094	0.6793	0.8792	0.7753	0.6098	0.7999	0.1335	0.6660
6.3798	**9.2439**	0.7762	0.8190	0.3512	0.4654	0.8325	0.6086	−0.2328	0.3965
22.2014	36.1623	**234.7810**	0.8932	0.2563	0.1890	0.8113	0.2753	−0.0025	0.2763
24.2608	31.2642	171.8401	**157.6540**	0.4461	0.3546	0.8987	0.5453	0.1107	0.2804
7.9432	3.3913	12.4748	17.7896	**10.0868**	0.6750	0.3062	0.6807	0.4656	0.6029
16.7928	10.7742	22.0561	33.8999	16.3233	**57.9810**	0.2588	0.6002	−0.2671	0.8043
20.5834	30.0383	147.5272	133.9147	11.5390	23.3825	**140.8306**	0.5889	−0.0621	0.2985
40.9551	33.3061	75.9327	123.2407	38.9140	82.2669	125.7964	**323.9981**	0.0843	0.5379
1.4584	−2.7175	−0.0001	5.3373	5.6784	−7.8128	−2.8308	5.8305	**14.7480**	−0.3095
21.1947	13.4877	47.3573	39.3910	21.4238	68.5172	39.6369	108.3263	−13.2986	**125.1656**

NB variances in bold on diagonal, covariance lower left, correlation upper right
*variances/covariances for ln variables $\times 10^{-3}$

Table A.10. (continued)

(v) males distal (raw)

93.3819	0.8690	0.5601	0.5764	0.6941	0.6220	0.5774	0.5693	0.6787	0.0965
53.9516	**41.2799**	0.6618	0.6100	0.2797	0.3622	0.6376	0.1828	0.4353	0.1109
5.9896	4.7058	**1.2248**	0.9690	−0.0298	−0.0022	0.9892	0.1151	−0.1735	0.3785
17.2261	12.1196	3.3164	**9.5635**	0.0748	0.1677	0.9591	0.2295	−0.0454	0.5128
4.5597	1.2217	−0.0224	0.1572	**0.4622**	0.7591	0.0140	0.8219	0.8163	0.0092
2.8702	1.1112	−0.0011	0.2476	0.2464	**0.2280**	0.0187	0.7614	0.3954	0.2349
6.3818	4.6856	1.2523	3.3925	0.0109	0.0102	**1.3084**	0.1680	−0.0091	0.2884
1.0438	0.2228	0.0242	0.1346	0.1060	0.0690	0.0365	**0.0360**	0.5304	0.1701
2.0426	0.8709	−0.0060	−0.0438	0.1728	0.0588	−0.0032	0.0313	**0.0970**	−0.1701
0.4475	0.3419	0.2010	0.7608	0.0030	0.0538	0.1583	0.0155	−0.0254	**0.2302**

(vi) males distal (ln*)

8.1120	0.8741	0.3979	0.4528	0.7085	0.6342	0.5105	0.5460	0.6853	0.0422
9.2561	**13.8240**	0.4447	0.3523	0.3129	0.4006	0.4262	0.1892	0.4640	0.0692
37.5306	54.7586	**1096.9098**	0.9251	−0.0285	0.0216	0.9503	0.2321	−0.1002	0.7275
49.0710	49.4823	1165.8939	**1448.1020**	0.1968	0.2759	0.9747	0.5433	−0.0429	0.7439
4.8001	2.8254	−2.2958	18.1838	**5.8971**	0.7516	0.1861	0.7552	0.8010	−0.0682
6.1278	5.0538	2.4300	35.6166	6.1920	**11.5103**	0.1801	0.7603	0.3701	0.1647
46.6665	50.8659	1010.2198	1190.5295	14.5062	19.6143	**1030.2822**	0.4750	0.0189	0.6257
11.1154	5.0293	54.9520	147.7713	13.1071	18.4356	108.9724	**51.0866**	0.4132	0.2422
7.2534	6.4107	−12.3312	−6.0681	7.2289	4.6656	2.2491	10.9752	**13.8101**	−0.2686
1.5399	3.2971	308.5592	362.5350	−2.1224	7.1573	257.1990	22.1740	−12.7852	**164.0136**

(vii) males proximal (raw)

151.3885	0.9555	0.3105	0.7045	0.9157	0.6533	0.7551	0.3006	0.4302	0.6239
67.9110	**33.3674**	0.3436	0.7230	0.8017	0.5683	0.8031	0.4189	0.3137	0.6193
1.0923	0.5676	**0.0818**	0.8292	0.1028	0.2356	0.6553	0.4089	−0.0706	−0.4697
9.8523	4.7468	0.2695	**1.2920**	0.4832	0.4618	0.9039	0.5928	0.0149	0.0593
11.0936	4.5597	0.0289	0.5408	**0.9695**	0.4807	0.4973	−0.0564	0.7191	0.6748
7.2256	2.8505	0.0606	0.4718	0.4254	**0.8079**	0.4319	0.3077	−0.1101	0.3454
5.4894	2.7412	0.1107	0.6071	0.2893	0.2294	**0.3491**	0.7317	−0.0240	0.1878
2.2740	1.4877	0.0719	0.4143	−0.0341	0.1700	0.2658	**0.3780**	−0.5995	0.0012
1.9776	0.6769	−0.0075	0.0063	0.2645	−0.0370	−0.0053	−0.1377	**0.1396**	0.3312
4.3444	2.0245	−0.0760	0.0381	0.3760	0.1757	0.0628	0.0004	0.0700	**0.3203**

(viii) males proximal (ln*)

14.1515	0.9578	0.2454	0.7038	0.9241	0.6698	0.8391	0.2275	0.4398	0.6156
11.9112	**10.9287**	0.2905	0.7181	0.8229	0.5887	0.8535	0.3082	0.3506	0.6257
11.8276	12.3064	**164.2109**	0.8252	0.0607	0.1974	0.5126	0.2487	−0.0919	−0.4677
32.9271	29.5208	131.4961	**154.6493**	0.5079	0.5227	0.8222	0.4102	0.0500	0.07840
13.4800	10.5482	3.0160	24.4916	**15.0354**	0.4885	0.6673	−0.0807	0.7133	0.6375
16.6052	12.8245	16.6717	42.8358	12.4817	**43.4241**	0.4501	0.3042	−0.1393	0.3492
57.4797	51.3863	119.6269	186.2086	47.1256	54.0150	**331.6590**	0.4840	0.1997	0.3361
11.9976	14.2818	44.6822	71.5000	−4.3848	28.0986	123.5510	**196.5003**	−0.6054	0.0665
10.0910	7.0696	−7.1839	3.7961	16.8690	−5.6001	22.1771	−51.7575	**37.2008**	0.2790
21.8231	19.4915	−56.4763	9.1877	23.2953	21.6829	57.6880	8.7856	16.0350	**88.8067**

NB variances in bold on diagonal, covariance lower left, correlation upper right
*variances/covariances for ln variables $\times 10^{-3}$

Table A.11. Principal component analyses – conventional data

(a) *Homo*

(i) females

	distal				proximal			
	raw		ln		raw		ln	
	U_1	U_2	U_1	U_2	U_1	U_2	U_1	U_2
P	0.9790	0.2041	0.7332	0.6800	0.9764	0.2159	0.7298	0.6837
A	0.2041	−0.9790	0.6800	−0.7332	0.2159	−0.9764	0.6837	−0.7298
l*	1689.1907	10.4701	9.0166	0.3201	2553.6954	6.0284	15.5650	0.2022
%	99.38	0.62	96.57	3.43	99.76	0.24	98.73	1.27

(ii) males

	distal				proximal			
	raw		ln		raw		ln	
	U_1	U_2	U_1	U_2	U_1	U_2	U_1	U_2
P	0.9767	0.2147	0.7147	0.6994	0.9767	0.2148	0.7242	0.6896
A	0.2147	−0.9767	0.6994	−0.7147	0.2148	−0.9767	0.6896	−0.7242
l*	2060.8147	12.6922	10.3680	0.3042	2078.8409	11.2125	11.0860	0.3259
%	99.39	0.61	97.15	2.85	99.46	0.54	97.15	2.85

(b) *Cercopithecus*

(i) females

	distal				proximal			
	raw		ln		raw		ln	
	U_1	U_2	U_1	U_2	U_1	U_2	U_1	U_2
P	0.9276	0.2342	0.7276	0.6860	0.9654	0.2607	0.6939	0.7200
A	0.2324	−0.9726	0.6860	−0.7276	0.2607	−0.9654	0.7200	−0.6939
l*	121.1280	0.3249	14.9511	0.2061	102.6411	0.2208	13.1148	0.0987
%	99.73	0.26	98.64	1.36	99.79	0.21	99.25	0.75

(ii) males

	distal				proximal			
	raw		ln		raw		ln	
	U_1	U_2	U_1	U_2	U_1	U_2	U_1	U_2
P	0.9672	0.2540	0.6914	0.7225	0.9666	0.2563	0.6973	0.7167
A	0.2540	−0.9672	0.7225	−0.6914	0.2563	−0.9666	0.7167	−0.6973
l*	590.2173	1.1669	65.3168	0.4526	624.9169	0.5371	60.9930	0.1924
%	99.80	0.20	99.31	0.69	99.91	0.09	99.69	0.31

*eigenvalues for ln variables $\times 10^{-3}$

Table A.11. (continued)

(c) *Colobus*

(i) females

	distal				proximal			
	raw		ln		raw		ln	
	U_1	U_2	U_1	U_2	U_1	U_2	U_1	U_2
P	0.9648	0.2628	0.6777	0.7353	0.9592	0.2827	0.6619	0.7496
A	0.2628	−0.9648	0.7353	−0.6777	0.2827	−0.9592	0.7496	−0.6619
*l**	229.1872	0.3086	16.8354	0.0941	342.4144	0.3280	25.1274	0.0762
%	99.87	0.13	99.44	0.56	99.90	0.10	99.70	0.30

(ii) males

	distal				proximal			
	raw		ln		raw		ln	
	U_1	U_2	U_1	U_2	U_1	U_2	U_1	U_2
P	0.9706	0.2407	0.7023	0.7119	0.9672	0.2540	0.6924	0.7215
A	0.2407	−0.9706	0.7119	−0.7023	0.2540	−0.9672	0.7215	−0.6924
*l**	342.0546	1.3526	22.1124	0.3501	382.9011	1.8107	22.7789	0.3756
%	99.61	0.39	98.44	1.56	99.53	0.47	98.38	1.62

(d) *Gorilla*

(i) females

	distal				proximal			
	raw		ln		raw		ln	
	U_1	U_2	U_1	U_2	U_1	U_2	U_1	U_2
P	0.9676	0.2524	0.6645	0.7473	0.9731	0.2303	0.7172	0.6969
A	0.2524	−0.9676	0.7473	−0.6645	0.2303	−0.9731	0.6969	−0.7172
*l**	3172.5699	6.0026	36.0135	0.3318	1675.6318	5.4028	15.2357	0.2617
%	99.81	0.19	99.09	0.91	99.68	0.32	98.31	1.69

(ii) males

	distal				proximal			
	raw		ln		raw		ln	
	U_1	U_2	U_1	U_2	U_1	U_2	U_1	U_2
P	0.9722	0.2340	0.7028	0.7114	0.9745	0.2243	0.7319	0.6815
A	0.2340	−0.9722	0.7114	−0.7028	0.2243	−0.9745	0.6815	−0.7319
*l**	3170.2128	6.3959	18.8452	0.1813	4383.4760	1.3970	26.0892	0.0419
	99.80	0.20	99.05	0.95	99.97	0.03	99.84	0.16

*eigenvalues for ln variables $\times 10^{-3}$

Table A.12. Principal component analyses – Fourier data

(a) *Homo* females

(i) distal (raw)

	U_1	U_2	U_3	U_4	U_5	U_6	U_7	U_8	U_9	U_{10}
X1	0.9401	0.2979	0.0343	0.0295	0.0168	0.0413	0.0511	0.1290	0.0441	0.0477
Y1	0.3166	−0.9352	−0.0931	0.0125	0.0326	0.0025	−0.0904	−0.0764	−0.0227	−0.0286
X2	0.0156	−0.0905	0.1175	−0.2257	−0.7836	−0.1747	0.4900	−0.0161	0.1843	0.0892
Y2	0.0065	−0.0672	0.9049	−0.2710	0.1664	0.1326	−0.1048	−0.1635	0.1141	0.0851
X3	0.1050	0.1257	−0.1022	−0.2612	−0.1489	0.0549	−0.1495	−0.6205	−0.1155	−0.6698
Y3	0.0292	0.0276	0.2859	0.7322	−0.3128	−0.3645	−0.3000	−0.1834	−0.1610	−0.0151
X4	−0.0072	−0.0557	0.2153	−0.0196	−0.0052	0.0497	0.3032	0.3768	−0.7847	−0.3130
Y4	0.0323	0.0208	−0.0149	−0.4337	0.1067	−0.8192	−0.2851	0.2083	−0.0450	−0.0321
X5	0.0336	0.0598	−0.1312	−0.2774	−0.2772	0.2018	−0.3831	−0.2071	−0.5004	0.5863
Y5	0.0405	0.0186	−0.0401	0.0695	0.3856	−0.3167	0.5529	−0.5511	−0.2077	0.3001
l	70.0822	11.8533	3.7793	1.1068	0.4203	0.3404	0.2330	0.1493	0.0380	0.0075
%	79.63	13.47	4.29	1.26	0.48	0.39	0.26	0.17	0.04	0.01

(ii) distal (ln)

	U_1	U_2	U_3	U_4	U_5	U_6	U_7	U_8	U_9	U_{10}
X1	0.0004	0.0466	0.1367	0.0117	0.0029	0.1552	0.0902	0.4353	0.4810	0.7252
Y1	0.0272	0.0430	0.0350	0.0465	−0.0773	0.0768	0.0350	0.8395	−0.4786	−0.2170
X2	0.5290	0.4835	−0.0637	0.6816	−0.0280	0.0134	−0.1098	−0.0663	0.0116	0.0126
Y2	0.5470	−0.0396	0.2284	−0.4479	0.3506	0.2144	−0.5236	0.0071	−0.0549	0.0164
X3	−0.0364	0.1247	0.1845	−0.0051	0.1094	0.2585	0.1311	0.1686	0.6423	−0.6419
Y3	0.1503	−0.5026	0.7100	0.3434	0.1036	−0.2126	0.1993	−0.0489	−0.0677	−0.0127
X4	0.6119	−0.1665	−0.2588	−0.2889	−0.2095	−0.1895	0.6335	−0.0153	0.0338	−0.0233
Y4	−0.0018	0.5765	0.4581	−0.3585	−0.2939	−0.4880	0.0651	−0.0198	−0.0098	−0.0017
X5	−0.1381	0.3607	0.1217	−0.4777	0.6386	0.2678	0.4913	−0.1384	−0.2867	0.1070
Y5	−0.0529	0.0480	0.3067	−0.0167	−0.5563	0.7083	0.0250	−0.2252	−0.1892	0.0476
l	0.5410	0.2159	0.1200	0.1137	0.0596	0.0423	0.0235	0.0051	0.0021	0.0001
%	48.16	19.22	10.69	10.12	5.31	3.77	2.09	0.46	0.18	0.01

(iii) proximal (raw)

	U_1	U_2	U_3	U_4	U_5	U_6	U_7	U_8	U_9	U_{10}
X1	0.9117	0.3538	0.1287	0.0077	0.0599	0.0033	0.1264	0.0584	0.0005	0.0639
Y1	0.3923	−0.8651	−0.2790	−0.0923	0.0163	0.0014	−0.0797	−0.0477	−0.0116	−0.0479
X2	0.0211	−0.1539	0.2457	0.4023	−0.6754	−0.2843	0.2087	0.0445	−0.3598	0.2041
Y2	−0.0053	−0.2494	0.7634	0.2631	0.3314	0.3052	−0.2569	−0.0507	−0.0315	0.1150
X3	0.1011	0.1456	−0.0262	0.1481	−0.1370	−0.1362	−0.5881	−0.3218	−0.2759	−0.6189
Y3	0.0014	−0.0510	0.4445	−0.8166	−0.3251	−0.1250	−0.0612	−0.0392	0.0430	−0.0671
X4	0.0002	−0.1108	0.2261	0.2337	−0.0422	−0.2372	0.3598	0.0083	0.6301	−0.5453
Y4	0.0394	0.0296	−0.0817	0.0607	−0.4797	0.6674	−0.2131	0.4420	0.2276	−0.1380
X5	0.0417	0.0354	−0.0421	0.1069	−0.0893	−0.4353	−0.5811	0.1224	0.5064	0.4210
Y5	0.0312	0.0480	−0.0674	0.0434	−0.2564	0.3172	0.0765	−0.8211	0.2936	0.2400
l	105.6019	7.6890	3.9626	1.0330	0.4013	0.2964	0.1431	0.1075	0.0198	0.0050
%	88.55	6.45	3.32	0.87	0.34	0.25	0.12	0.09	0.02	0.00

(iv) proximal (ln)

	U_1	U_2	U_3	U_4	U_5	U_6	U_7	U_8	U_9	U_{10}
X1	0.0142	0.1398	0.0912	0.0188	0.1904	0.0732	0.0636	0.4758	0.3812	0.7445
Y1	−0.0070	0.1207	0.0373	0.0631	0.1070	0.0126	0.1195	0.7874	−0.4771	−0.3265
X2	−0.4131	0.4298	−0.0963	0.2871	−0.1025	−0.5587	−0.4764	0.0367	0.0433	0.0080
Y2	−0.4703	−0.0457	0.0961	−0.0739	−0.0811	0.7003	−0.5057	0.0381	−0.0856	0.0222
X3	0.0411	0.2137	0.1081	−0.0265	0.3345	0.1287	−0.0423	0.1055	0.6896	−0.5686
Y3	−0.2688	−0.2866	0.8776	0.0563	0.0660	−0.2391	0.0922	−0.0412	−0.0186	−0.0153
X4	−0.7011	0.1332	−0.2280	−0.2002	0.0604	0.0134	0.6213	−0.0854	0.0372	−0.0130
Y4	0.1305	0.5225	0.2546	0.5251	−0.3811	0.3263	0.3090	−0.1475	−0.0237	0.0004
X5	0.0470	0.2782	0.0442	0.1385	0.8032	0.0882	−0.0468	−0.3248	−0.3537	0.1166
Y5	0.1526	0.5321	0.2669	−0.7543	−0.1580	−0.0610	−0.0703	−0.0585	−0.1224	0.0360
l	0.5605	0.2280	0.1275	0.0461	0.0383	0.0319	0.0087	0.0051	0.0022	0.0001
%	53.46	21.74	12.16	4.40	3.65	3.05	0.83	0.48	0.21	0.01

Table A.12. (continued)

(b) *Homo* males

(i) distal (raw)

	U_1	U_2	U_3	U_4	U_5	U_6	U_7	U_8	U_9	U_{10}
X1	0.9171	0.3565	0.0190	0.0288	0.0620	0.0072	0.0494	0.1403	0.0528	0.0426
Y1	0.3807	−0.9139	0.0267	−0.0269	−0.0597	−0.0343	−0.0358	−0.1038	−0.0322	−0.0248
X2	0.0088	−0.0100	−0.1887	−0.0612	−0.1565	0.3950	−0.8250	0.2717	0.1479	0.0597
Y2	0.0281	−0.0081	−0.9294	−0.1486	0.1725	−0.0988	0.1106	−0.1922	0.1324	0.0843
X3	0.0974	0.1571	0.0444	−0.2314	−0.0376	−0.0379	−0.2852	−0.6125	−0.1769	−0.6478
Y3	0.0311	0.0388	−0.1836	0.8801	−0.3172	−0.0553	−0.0922	−0.2171	−0.1728	0.0019
X4	−0.0037	−0.0414	−0.1995	−0.0080	0.1825	0.1806	0.0748	0.4212	−0.8030	−0.2544
Y4	0.0270	0.0593	−0.1215	−0.3237	−0.8956	−0.0433	0.2198	0.1143	−0.1039	0.0038
X5	0.0337	0.0769	0.0878	−0.1966	0.0279	−0.3156	−0.2988	−0.2971	−0.4817	0.6608
Y5	0.0284	0.0140	0.0402	−0.0316	−0.0067	0.8333	0.2652	−0.3972	−0.0896	0.2566
l	86.0378	12.2233	2.9765	1.4652	0.6638	0.3439	0.2855	0.1268	0.0352	0.0092
%	82.60	11.73	2.86	1.41	0.64	0.33	0.27	0.12	0.03	0.01

(ii) distal (ln)

	U_1	U_2	U_3	U_4	U_5	U_6	U_7	U_8	U_9	U_{10}
X1	0.0067	0.0473	0.0670	0.0211	0.2379	0.0270	0.1489	0.3208	0.5281	0.7290
Y1	0.0234	0.0078	0.0226	0.0053	0.1477	−0.0525	0.1968	0.8802	−0.3143	−0.2491
X2	0.5675	0.1877	−0.2106	0.7682	−0.0842	0.0030	0.0291	−0.0078	−0.0054	0.0085
Y2	0.4977	0.0596	0.0753	−0.3132	0.2210	0.3843	−0.6592	0.1125	−0.0310	0.0149
X3	−0.0202	0.1279	0.0563	0.0456	0.3674	0.1119	0.1199	−0.0276	0.6527	−0.6239
Y3	0.1585	−0.2369	0.9257	0.1866	−0.0198	0.0356	0.1194	−0.0767	−0.0716	−0.0103
X4	0.6117	−0.2917	−0.1608	−0.4373	0.0664	−0.1891	0.5114	−0.1473	0.0014	−0.0147
Y4	0.1297	0.8564	0.2356	−0.2725	−0.2515	−0.1994	0.1291	−0.0155	−0.0085	0.0055
X5	−0.1140	0.2528	−0.0319	0.0493	0.5309	0.5140	0.3666	−0.2489	−0.4033	0.1207
Y5	−0.0068	0.0634	0.0500	0.0800	0.6170	−0.7038	−0.2499	−0.1380	−0.1655	0.0455
l	0.3070	0.2422	0.1459	0.1210	0.0547	0.0418	0.0156	0.0059	0.0010	0.0001
%	32.84	25.90	15.60	12.94	5.85	4.47	1.66	0.63	0.11	0.01

(iii) proximal (raw)

	U_1	U_2	U_3	U_4	U_5	U_6	U_7	U_8	U_9	U_{10}
X1	0.9165	0.3540	0.0171	0.0886	0.0399	0.0338	0.0621	0.1268	0.0037	0.0623
Y1	0.3816	−0.9063	0.0349	−0.1277	0.0108	−0.0609	−0.0307	−0.0933	−0.0015	−0.0449
X2	0.0239	0.0549	−0.1563	−0.3773	−0.6124	−0.5151	−0.0294	0.2577	0.3420	0.0715
Y2	0.0336	0.0363	−0.8134	−0.4122	0.2414	0.2620	0.0239	−0.1504	0.0887	0.0894
X3	0.0952	0.1759	0.0691	−0.1524	−0.0229	−0.1464	−0.2384	−0.5717	0.1265	−0.7143
Y3	0.0240	−0.0887	−0.5040	0.7442	−0.3576	−0.1051	−0.1021	−0.1670	−0.0706	−0.0379
X4	0.0038	0.0268	−0.1729	−0.1732	0.0326	−0.3031	−0.1979	0.2833	−0.8295	−0.2787
Y4	0.0332	0.0109	0.1078	−0.1989	−0.6570	0.6038	0.1917	−0.1783	−0.2874	−0.0149
X5	0.0297	0.0909	0.0911	−0.1002	0.0118	−0.3875	0.1395	−0.6471	−0.2654	0.5600
Y5	0.0328	0.0326	0.0611	−0.0833	−0.0611	0.1487	−0.9327	0.0245	−0.1140	0.2790
l	85.7839	10.7669	3.9020	1.1427	0.5224	0.3115	0.1773	0.1154	0.0302	0.0058
%	83.48	10.48	3.80	1.11	0.51	0.30	0.17	0.11	0.03	0.01

(iv) proximal (ln)

	U_1	U_2	U_3	U_4	U_5	U_6	U_7	U_8	U_9	U_{10}
X1	0.0052	0.0663	0.0564	0.1358	0.0014	0.1907	0.0506	0.4413	0.4788	0.7149
Y1	0.0022	0.0223	0.0822	0.0615	−0.0199	0.0399	0.0592	0.8526	−0.4235	−0.2777
X2	0.3325	0.6033	−0.0485	−0.2243	0.6276	−0.1852	0.2101	0.0186	0.0090	0.0038
Y2	0.4818	0.0908	−0.0179	0.0398	−0.5239	0.0976	0.6773	−0.0982	−0.0710	0.0171
X3	−0.0115	0.1313	0.0175	0.2281	0.0421	0.3531	0.0523	0.0717	0.6364	−0.6253
Y3	0.5430	−0.3539	0.6906	0.1206	0.2265	0.0610	−0.1713	−0.0616	−0.0132	−0.0061
X4	0.5559	0.1851	−0.4159	0.0457	−0.2691	0.0289	−0.6353	0.0685	0.0070	−0.0063
Y4	−0.2011	0.5698	0.5614	−0.3059	−0.3969	0.1021	−0.2332	−0.0560	−0.0269	0.0050
X5	−0.0605	0.1529	−0.0863	0.2407	0.2157	0.7942	−0.0176	−0.2035	−0.4178	0.1378
Y5	−0.0961	0.3132	0.1206	0.8401	−0.0420	−0.3844	−0.0234	−0.1006	−0.1037	0.0384
l	0.3739	0.3177	0.1581	0.0861	0.0587	0.0306	0.0183	0.0064	0.0016	0.0001
%	35.55	30.21	15.04	8.19	5.58	2.91	1.74	0.61	0.15	0.01

Table A.12. (continued)

(c) *Cercopithecus* females

(i) distal (raw)

	U_1	U_2	U_3	U_4	U_5	U_6	U_7	U_8	U_9	U_{10}
X1	0.8987	0.4004	0.0103	0.0698	0.0356	0.0008	0.0293	0.0654	0.1248	0.0717
Y1	0.4247	−0.8937	0.0367	−0.0312	−0.0061	0.0001	−0.0130	−0.0638	−0.1059	−0.0559
X2	0.0046	0.0130	−0.2509	0.0608	−0.0880	−0.2531	0.7914	−0.4787	−0.0357	0.0681
Y2	0.0203	−0.0342	−0.9204	0.0563	0.0057	0.0560	−0.3430	−0.1086	0.1092	0.0599
X3	0.0970	0.1775	−0.0339	−0.2818	−0.2187	0.1434	−0.1171	−0.3080	−0.4523	−0.7050
Y3	−0.0065	0.0257	0.0649	0.8695	−0.1580	−0.1421	−0.1681	−0.0680	−0.4011	−0.0100
X4	0.0019	−0.0222	−0.2868	0.0124	0.0571	−0.0626	0.3769	0.7862	−0.3066	−0.2363
Y4	0.0208	0.0234	0.0145	−0.2221	−0.0739	−0.9352	−0.2563	0.0455	−0.0170	−0.0368
X5	0.0370	0.0800	−0.0236	−0.2817	0.2747	0.0540	−0.0731	−0.0872	−0.7060	0.5679
Y5	0.0194	−0.0060	−0.0107	−0.1515	−0.9132	0.1030	0.0023	0.1532	−0.0427	0.3266
l	5.2593	0.5758	0.1277	0.0423	0.0089	0.0081	0.0042	0.0020	0.0009	0.0002
%	87.20	9.55	2.12	0.73	0.15	0.13	0.07	0.03	0.02	0.00

(ii) distal (ln)

	U_1	U_2	U_3	U_4	U_5	U_6	U_7	U_8	U_9	U_{10}
X1	0.0140	0.0549	0.0503	0.0961	0.0358	0.2164	0.0967	0.4565	0.2835	0.7992
Y1	0.0109	0.0301	0.0001	0.0636	0.0471	0.0633	0.0045	0.8482	−0.3369	−0.3946
X2	0.5434	0.0745	0.3265	0.3221	−0.3872	−0.4087	0.4143	0.0142	0.0011	−0.0046
Y2	0.5860	0.0691	0.0396	0.1000	−0.1388	0.2907	−0.7318	−0.0293	−0.0137	0.0081
X3	0.0223	0.1303	0.0563	0.1794	0.0223	0.4372	0.2079	0.0235	0.7160	−0.4463
Y3	−0.0050	−0.4230	0.7905	−0.0010	0.3974	0.1584	−0.0097	−0.0617	−0.0957	−0.0108
X4	0.5861	0.0049	−0.2415	−0.5123	0.4953	0.0183	0.2997	0.0035	0.0123	−0.0035
Y4	−0.1237	0.8300	0.4110	−0.2866	0.1158	−0.1357	−0.1136	−0.0013	0.0037	−0.0014
X5	0.0252	0.2322	−0.0119	0.1213	0.1443	0.6614	0.3681	−0.2354	−0.5253	0.0734
Y5	0.0318	0.2167	−0.1842	0.6939	0.6240	−0.1589	−0.0445	−0.1063	−0.0897	0.0257
l	0.9907	0.5601	0.2388	0.1305	0.1056	0.0619	0.0485	0.0081	0.0014	0.0001
%	46.17	26.10	11.13	6.08	4.92	2.88	2.26	0.38	0.07	0.00

(iii) proximal (raw)

	U_1	U_2	U_3	U_4	U_5	U_6	U_7	U_8	U_9	U_{10}
X1	0.7872	0.5906	0.0464	0.0468	0.0334	0.0811	0.0107	0.1083	0.0068	0.0873
Y1	0.6146	−0.7720	−0.0659	−0.0276	−0.0475	−0.0643	0.0085	−0.0912	−0.0095	−0.0079
X2	0.0112	0.0028	−0.3382	−0.0615	0.3286	−0.0184	−0.8647	0.1016	0.1163	−0.0438
Y2	−0.1011	0.0669	−0.8754	0.0303	−0.0711	0.1444	0.2514	−0.0609	−0.3639	0.0533
X3	0.0422	0.2051	−0.0248	−0.3415	−0.1543	−0.3218	−0.0347	−0.3599	−0.1042	−0.7550
Y3	0.0033	0.0518	−0.0161	0.8534	−0.1290	−0.1561	−0.1426	−0.4481	0.0494	−0.0650
X4	−0.0047	0.0230	−0.3073	−0.0006	−0.1405	0.0600	0.2048	0.0888	0.8985	−0.1563
Y4	0.0101	0.0046	−0.0221	0.0066	0.8841	−0.1540	0.3276	−0.2795	0.0921	−0.0100
X5	0.0169	0.0548	0.0132	−0..3727	−0.1583	0.1827	−0.1320	−0.7318	0.1507	0.4727
Y5	0.0111	0.0495	−0.1295	−0.0922	−0.1294	−0.8829	0.0268	0.1183	0.0448	0.3990
l	4.6688	0.5517	0.0712	0.0322	0.0121	0.0082	0.0028	0.0014	0.0011	0.0002
%	87.27	10.31	1.33	0.60	0.23	0.15	0.05	0.03	0.02	0.00

(iv) proximal (ln)

	U_1	U_2	U_3	U_4	U_5	U_6	U_7	U_8	U_9	U_{10}
X1	0.0099	0.0172	0.0012	0.0490	0.1256	0.1924	0.1811	0.4578	0.2997	0.7824
Y1	0.0010	0.0300	−0.0217	0.0739	0.0466	0.0795	0.1774	0.8257	−0.1524	−0.4982
X2	0.6503	0.1626	−0.1395	0.6560	−0.1608	−0.1138	0.2290	−0.0963	0.0173	−0.0022
Y2	0.5666	−0.2016	−0.0005	−0.2283	−0.1012	0.4098	−0.6261	0.1266	−0.0002	−0.0020
X3	0.0251	−0.0045	−0.0420	0.0068	0.3324	0.3400	0.1575	−0.1682	0.7634	−0.3681
Y3	0.0345	−0.1652	0.9300	0.2123	0.0719	0.1785	0.0994	−0.0596	−0.1046	−0.0150
X4	0.4558	−0.3243	0.0633	−0.5691	0.0792	−0.3426	0.4851	−0.1069	0.0071	−0.0003
Y4	0.1853	0.8932	0.2122	−0.3376	0.0820	0.0255	0.0041	−0.0119	−0.0369	−0.0004
X5	0.0143	−0.0253	−0.2503	−0.0404	0.2408	0.6482	0.3759	−0.2254	−0.5124	0.0464
Y5	0.1091	−0.0297	−0.0421	0.1581	0.8714	−0.3002	−0.2827	0.0202	−0.1701	0.0421
l	1.1968	0.4763	0.2563	0.1549	0.0726	0.0405	0.0251	0.0094	0.0020	0.0000
%	53.57	21.32	11.47	6.94	3.25	1.81	1.13	0.42	0.09	0.00

Table A.12. (continued)

(d) *Cercopithecus* males

(i) distal (raw)

	U_1	U_2	U_3	U_4	U_5	U_6	U_7	U_8	U_9	U_{10}
X1	0.8135	0.5447	0.0743	0.0159	0.0660	0.0543	0.0045	0.0886	0.1202	0.0782
Y1	0.5762	−0.7984	−0.0283	0.0208	−0.0629	−0.0415	−0.0092	−0.0983	−0.0969	−0.0670
X2	0.0125	0.0270	−0.3171	0.0196	−0.1937	−0.2190	0.7923	−0.2463	0.3522	−0.0132
Y2	0.0501	0.0865	−0.8707	−0.2762	−0.0415	0.0757	−0.3424	−0.1457	−0.0824	0.0539
X3	0.0518	0.1866	0.1068	−0.2841	−0.0511	−0.2520	0.0489	−0.2540	−0.4049	−0.7572
Y3	0.0046	0.0565	−0.2181	0.6680	0.5547	−0.0552	0.1213	−0.1920	−0.3749	−0.0134
X4	0.0184	−0.0104	−0.2281	0.0650	−0.2014	−0.0375	0.2696	0.8239	−0.3766	−0.0894
Y4	0.0089	0.1202	−0.0011	0.5584	−0.7516	−0.0828	−0.2503	−0.1836	−0.0724	−0.0170
X5	0.0187	0.0691	0.1525	−0.2695	−0.1745	0.1424	0.2614	−0.2844	−0.6271	0.5530
Y5	0.0101	0.0146	0.0264	−0.0843	0.0790	−0.9201	−0.1848	0.0763	−0.0209	0.3142
l	26.1745	1.6616	0.1650	0.0531	0.0370	0.0212	0.0099	0.0061	0.0055	0.0007
%	93.03	5.91	0.59	0.19	0.13	0.08	0.04	0.02	0.02	0.00

(ii) distal (ln)

	U_1	U_2	U_3	U_4	U_5	U_6	U_7	U_8	U_9	U_{10}
X1	0.0873	0.0073	0.0163	0.1780	0.0314	0.2328	0.1888	0.3695	0.3170	0.7822
Y1	0.0825	0.0552	−0.0063	0.2135	0.0942	0.1068	0.2272	0.7777	−0.3012	−0.4208
X2	0.5085	0.3321	−0.1589	−0.4756	−0.5138	−0.0712	0.3316	0.0263	−0.0043	0.0019
Y2	0.5249	0.2830	−0.0480	0.0852	0.1428	0.3603	−0.6922	0.0076	−0.0740	0.0006
X3	0.0963	−0.0537	−0.0104	0.1927	−0.0617	0.3953	0.1884	−0.1210	0.7332	−0.4503
Y3	0.0500	0.0964	0.9671	−0.0481	−0.1244	0.1435	0.0623	−0.0518	−0.0892	−0.0061
X4	0.4861	0.1374	0.0924	0.2679	0.5456	−0.4805	0.3042	−0.1957	0.0713	−0.0005
Y4	0.4351	−0.8736	0.0649	−0.1244	−0.0860	−0.0619	−0.0934	0.0858	−0.0247	−0.0025
X5	0.0965	−0.1090	−0.1548	0.2355	0.0263	0.5511	0.4096	−0.4128	−0.4992	0.0876
Y5	0.0688	0.0224	−0.0067	0.7122	−0.6170	−0.2904	−0.1240	−0.0613	−0.0534	0.0241
l	1.2404	0.6288	0.2984	0.2497	0.1978	0.0968	0.0708	0.0258	0.0024	0.0001
%	44.13	22.37	10.61	8.88	7.04	3.44	2.52	0.92	0.08	0.00

(iii) proximal (raw)

	U_1	U_2	U_3	U_4	U_5	U_6	U_7	U_8	U_9	U_{10}
X1	0.8109	0.5486	0.0283	0.0441	0.0125	0.0136	0.0398	0.1012	0.0080	0.0910
Y1	0.5817	−0.7925	−0.0237	−0.0364	0.0104	−0.1142	−0.0354	−0.1051	0.0029	−0.0790
X2	0.0019	−0.0015	0.3369	−0.0664	−0.3764	−0.0667	0.8055	−0.2622	0.1355	−0.0020
Y2	0.0043	0.0308	0.7090	−0.4995	0.1122	−0.1405	−0.3341	0.0463	0.3121	0.0585
X3	0.0551	0.2329	−0.2323	−0.2550	0.0225	−0.4442	−0.0371	−0.2489	0.0256	−0.7496
Y3	0.0080	0.0613	0.4258	0.7471	0.1046	−0.2349	−0.1984	−0.3729	−0.0607	−0.0925
X4	0.0075	−0.0060	0.3003	−0.1990	−0.1303	0.1457	−0.0345	0.0174	−0.8986	−0.1517
Y4	0.0191	0.0069	−0.0232	0.1213	−0.8735	−0.1901	−0.3333	0.2598	0.0811	−0.0111
X5	0.0186	0.1002	−0.2297	−0.2552	−0.1614	−0.0660	−0.2301	−0.7416	−0.0944	0.4791
Y5	0.0160	0.0429	−0.0618	−0.0160	0.1675	−0.7938	0.1754	0.2984	−0.2385	0.3986
l	27.7210	1.2227	0.1582	0.0916	0.0427	0.0206	0.0121	0.0068	0.0038	0.0007
%	94.68	4.18	0.54	0.31	0.15	0.07	0.04	0.02	0.01	0.00

(iv) proximal (ln)

	U_1	U_2	U_3	U_4	U_5	U_6	U_7	U_8	U_9	U_{10}
X1	0.0495	0.1010	0.0133	0.1795	0.0299	0.0336	0.1993	0.5024	0.1947	0.7892
Y1	0.0530	0.1004	0.0074	0.1546	0.0368	0.2088	0.2475	0.7160	−0.2945	−0.5074
X2	0.5761	0.0029	0.0138	−0.3422	−0.7116	−0.1647	0.1059	0.0774	−0.0026	−0.0003
Y2	0.4630	−0.2405	−0.2736	0.1212	0.2763	−0.1790	−0.6857	0.2440	−0.0117	−0.0034
X3	0.0225	0.1828	−0.0528	0.2986	−0.0397	−0.2956	0.0945	0.0580	0.8112	−0.3387
Y3	0.2011	−0.3446	0.8135	0.3324	0.0728	−0.2228	0.0617	−0.0510	−0.0841	−0.0135
X4	0.5585	−0.1025	−0.2912	0.1868	0.3471	0.2206	0.5259	−0.3343	−0.0190	0.0026
Y4	0.2978	0.7576	0.3575	−0.2570	0.3231	0.0883	−0.1666	−0.0587	0.0096	−0.0021
X5	−0.0565	0.3447	−0.2177	0.2979	−0.0137	−0.7155	0.1379	−0.0876	−0.4470	0.0576
Y5	0.0607	0.2579	−0.0141	0.6501	−0.4279	0.4367	−0.2855	−0.2013	−0.0984	0.0377
l	1.1125	0.5647	0.4707	0.3716	0.1673	0.1015	0.0624	0.0206	0.0035	0.0002
%	38.69	19.64	16.37	12.92	5.82	3.53	2.17	0.72	0.12	0.01

Table A.12. (continued)

(e) *Colobus* females

(i) distal (raw)

	U_1	U_2	U_3	U_4	U_5	U_6	U_7	U_8	U_9	U_{10}
X1	0.7499	0.6141	0.1424	0.0613	0.0955	0.1311	0.0143	0.0463	0.0341	0.0813
Y1	0.6521	−0.6683	−0.2222	−0.2039	−0.1177	−0.1189	−0.0517	0.0011	−0.0415	−0.0687
X2	0.0554	−0.2021	0.2531	0.1643	0.2005	0.2733	0.1756	−0.6943	0.4827	−0.0644
Y2	0.0522	−0.2136	0.7777	0.3111	−0.1726	−0.1473	−0.3704	0.0599	−0.2198	0.0980
X3	0.0401	0.2005	−0.0879	0.2216	−0.2588	−0.3717	−0.0033	−0.2855	−0.1461	−0.7703
Y3	−0.0437	0.1046	0.4069	−0.8110	−0.1373	−0.0722	0.2544	−0.1978	−0.1770	−0.0681
X4	0.0421	−0.1805	0.2245	0.2496	0.1735	0.0597	0.7781	0.3892	−0.1403	−0.2066
Y4	0.0105	0.0066	0.0646	−0.0842	0.6964	−0.6894	−0.0652	0.0171	0.1505	0.0348
X5	0.0317	0.0336	−0.1799	0.2265	−0.0703	−0.2435	0.2976	−0.4736	−0.5252	0.5111
Y5	0.0091	0.0699	0.0360	0.0579	−0.5489	−0.4368	0.2572	0.1248	0.5873	0.2677
l	10.4427	0.8718	0.2029	0.0719	0.0149	0.0108	0.0050	0.0032	0.0013	0.0002
%	89.83	7.50	1.75	0.62	0.13	0.09	0.04	0.03	0.01	0.00

(ii) distal (ln)

	U_1	U_2	U_3	U_4	U_5	U_6	U_7	U_8	U_9	U_{10}
X1	0.0243	0.0324	0.0445	0.1025	0.1475	0.1610	0.1618	0.5371	0.2433	0.7512
Y1	0.0571	0.0643	0.0529	0.0495	0.1550	0.2628	0.0967	0.6841	−0.4461	−0.4668
X2	0.6282	−0.0553	−0.0392	−0.4009	0.5239	0.3024	−0.2022	−0.1670	0.0718	0.1119
Y2	0.4841	−0.2717	−0.1126	0.3055	0.1158	−0.6948	0.2421	0.0959	−0.1046	−0.0074
X3	−0.0198	0.0346	0.0245	0.2269	0.1733	0.0842	0.2362	0.0842	0.7988	−0.4558
Y3	−0.1462	−0.9340	0.0571	−0.0289	−0.0536	0.2777	0.1440	−0.0323	−0.0174	−0.0056
X4	0.5698	0.0405	−0.0908	0.2231	−0.7068	0.3345	0.0218	0.0040	0 0610	−0.0055
Y4	0.1376	0.0108	0.9833	0.0300	−0.0475	−0.0842	−0.0406	−0.0452	−0.0096	0.0043
X5	−0.0060	0.1972	0.0330	0.2799	0.2302	0.3077	0.6825	−0.4279	−0.2778	0.0893
Y5	−0.0412	−0.0608	−0.0177	0.7427	0.2605	0.1814	−0.5662	−0.1144	−0.0801	0.4334
l	1.2991	0.5958	0.3187	0.1107	0.0681	0.0431	0.0055	0.0026	0.0017	0.0000
%	53.13	24.36	13.03	4.53	2.79	1.76	0.23	0.11	0.07	0.00

(iii) proximal (raw)

	U_1	U_2	U_3	U_4	U_5	U_6	U_7	U_8	U_9	U_{10}
X1	0.6777	0.6765	0.2483	0.0489	0.0551	0.0897	0.0444	0.0113	0.0280	0.0713
Y1	0.7349	−0.6322	−0.2195	−0.0272	−0.0444	−0.0703	−0.0196	−0.0198	−0.0160	−0.0583
X2	0.0035	0.1643	−0.4196	−0.3042	−0.6207	0.4018	−0.0186	−0.3454	0.1902	0.0431
Y2	0.0077	0.2494	−0.7342	−0.1251	0.5228	−0.1031	0.0113	−0.0953	−0.2952	0 0524
X3	0.0199	0.1201	0.1058	−0.3638	−0.1134	−0.2049	−0.4330	−0.0058	−0.2791	−0.7221
Y3	−0.0014	0.0345	−0.1181	0.7224	−0.0360	0.0616	−0.6015	−0.3089	0.0035	−0.0255
X4	0.0060	0.0657	−0.2499	−0.0446	0.1299	0.0600	−0.2932	0.5851	0.6817	−0.1328
Y4	0.0057	0.1677	−0.2855	0.3474	−0.5308	−0.4524	0.2578	0.4119	−0.2102	−0.0537
X5	0.0117	0.0379	0.0719	−0.3184	−0.1183	−0.5968	−0.4123	−0.1163	0.1105	0.5710
Y5	0.0080	−0.0627	0 0286	−0.1021	−0.0980	0.4524	−0.3541	0.5002	−0.5259	0.3440
l	16.8106	0.5570	0.2444	0.0797	0.0330	0.0145	0.0132	0.0071	0.0029	0.0003
%	94.64	3.14	1.38	0.45	0.19	0.08	0.07	0.04	0.02	0.00

(iv) proximal (ln)

	U_1	U_2	U_3	U_4	U_5	U_6	U_7	U_8	U_9	U_{10}
X1	0.0122	0.0005	0.0454	0.0674	0.0581	0.3580	0.1218	0.3389	0.4319	0.7386
Y1	0.0024	−0.0096	0.0902	0.0782	0.0997	0.6147	0.0793	0.5703	−0.3131	−0.4102
X2	0.6025	−0.4787	−0.5783	−0.2037	0.1189	−0.0313	0.0775	0.1020	−0.0190	0.0019
Y2	0.5205	−0.1349	0.3792	0.1834	−0.5825	0.2795	−0.2358	−0.2454	0.0098	0.0076
X3	0.0049	−0.0517	0.0023	0.1033	0.0712	0.1302	0.2709	−0.1460	0.7797	−0.5119
Y3	0.0864	0.3726	0.0299	−0.8034	−0.2294	0.1977	0.3201	−0.1141	−0.0142	−0.0002
X4	0.3866	−0.0669	0.6710	−0.1497	0.4800	−0.3211	0.1311	0.1505	−0.0008	−0.0063
Y4	0.4497	0.7573	−0.2416	0.3099	0.2413	0.0320	−0.0745	−0.0696	−0.0109	−0.0052
X5	−0.0091	−0.1238	0.0274	0.3148	0.0980	0.1696	0.7331	−0.4259	−0.3264	0.1453
Y5	−0.0818	−0.1331	0.0346	−0.2015	0.5266	0.4754	−0.4257	−0.4959	−0.0183	0.0544
l	0.8806	0.3132	0.2559	0.1050	0.1025	0.0414	0.0284	0.0091	0.0014	0.0004
%	50.68	18.03	14.73	6.04	5.90	2.39	1.63	0.52	0.08	0.00

Table A.12. (continued)

(f) *Colobus* males

(i) distal (raw)

	U_1	U_2	U_3	U_4	U_5	U_6	U_7	U_8	U_9	U_{10}
X1	0.8429	0.4992	0.0424	0.0921	0.0210	0.1028	0.0638	0.0924	0.0095	0.0801
Y1	0.5302	−0.8308	−0.0315	−0.0348	−0.0411	−0.0949	−0.0757	−0.0788	0.0063	−0.0622
X2	0.0025	−0.0242	−0.4632	0.0602	0.1978	0.5992	0.2167	−0.5787	0.0196	−0.0279
Y2	−0.0058	0.0535	−0.7466	0.3939	−0.1762	−0.3496	−0.2246	0.1280	0.1855	0.1736
X3	0.0720	0.2168	−0.0516	−0.2255	−0.0836	−0.3175	−0.2738	−0.4107	0.1584	−0.7196
Y3	−0.0353	−0.0314	0.3304	0.8151	0.3078	−0.0538	−0.1955	−0.2003	−0.1597	−0.1506
X4	0.1139	−0.0280	−0.3279	−0.0350	0.3552	0.0260	0.1673	0.4762	−0.5297	−0.4776
Y4	0.0091	−0.0104	−0.0257	−0.2082	0.8114	−0.1133	−0.1923	0.0964	0.4671	0.1416
X5	0.0367	0.0869	−0.0718	−0.2677	0.1301	−0.1516	−0.4774	−0.3052	−0.6355	0.3865
Y5	0.2100	0.0285	−0.0090	0.0036	0.1564	−0.5992	0.6977	−0.3098	−0.1082	0.1440
l	14.5981	2.4914	0.3169	0.1375	0.0221	0.0182	0.0075	0.0029	0.0023	0.0005
%	82.96	14.16	1.80	0.78	0.13	0.10	0.04	0.02	0.01	0.00

(ii) distal (ln)

	U_1	U_2	U_3	U_4	U_5	U_6	U_7	U_8	U_9	U_{10}
X1	0.0094	0.0969	0.0264	0.1008	0.0135	0.1531	0.3677	0.2847	0.3903	0.7665
Y1	0.0001	0.0789	−0.0478	−0.0130	−0.1329	0.2559	0.4699	0.6786	−0.2493	−0.4059
X2	−0.8036	−0.2613	−0.3582	0.2083	0.2381	0.2116	0.0636	−0.0819	−0.0445	0.0040
Y2	−0.3801	−0.0533	0.7477	−0.0612	0.2585	−0.3113	−0.1436	0.3237	−0.0235	0.0119
X3	0.0057	0.1825	0.1111	0.2876	0.1782	−0.0113	0.2238	−0.1486	0.7274	−0.4883
Y3	0.2481	−0.5841	0.1727	−0.3232	0.3997	0.1303	0.4656	−0.2556	−0.0609	−0.0231
X4	−0.3831	0.2316	0.1675	−0.5425	−0.5096	0.0153	0.3155	−0.3330	0.0796	−0.0212
Y4	−0.0194	0.4692	−0.3274	−0.5456	0.5870	−0.0971	−0.0631	0.1210	0.0442	−0.0042
X5	0.0049	0.4219	0.0928	0.4016	0.1933	−0.2771	0.4476	−0.3233	−0.4743	0.0894
Y5	0.0286	0.2950	0.3516	0.0450	0.1597	0.8160	−0.2203	−0.1718	−0.1300	0.0141
l	1.0400	0.4280	0.2047	0.1659	0.0800	0.0456	0.0193	0.0106	0.0017	0.0001
%	52.10	21.44	10.26	8.31	4.01	2.29	0.97	0.53	0.09	0.01

(iii) proximal (raw)

	U_1	U_2	U_3	U_4	U_5	U_6	U_7	U_8	U_9	U_{10}
X1	0.7891	0.5877	0.0109	0.0193	0.0107	0.0979	0.0023	0.0165	0.0711	0.1285
Y1	0.6110	−0.7743	0.0184	−0.0412	0.0374	−0.0846	0.0025	0.0122	−0.0620	−0.1120
X2	0.0038	−0.0172	−0.1434	−0.0011	−0.2052	−0.4974	0.7103	0.0496	0.3433	0.2545
Y2	0.0270	0.0076	−0.7004	−0.3932	−0.4378	0.2736	0.0831	−0.1237	−0.2294	−0.1128
X3	0.0344	0.2076	0.1457	−0.2817	0.0206	−0.3949	0.0600	−0.0832	0.0130	−0.8295
Y3	0.0347	0.0492	−0.5020	0.7451	0.2008	−0.3177	−0.1841	0.0054	−0.1314	−0.1916
X4	0.0057	−0.0350	−0.0317	−0.1663	−0.4374	−0.2850	−0.6328	0.1425	0.5133	0.1152
Y4	0.0212	−0.0071	0.4425	0.3484	−0.7526	0.1647	0.1397	0.0462	−0.2203	−0.1365
X5	0.0021	0.0851	0.0442	−0.2344	−0.0164	−0.4184	−0.1004	0.5350	−0.6389	0.2365
Y5	0.0214	0.0266	0.1283	−0.0700	−0.0770	−0.3475	−0.1450	−0.8162	−0.2877	0.2843
l	16.9999	3.5174	0.1566	0.0830	0.0271	0.0123	0.0101	0.0030	0.0023	0.0004
%	81.68	16.90	0.75	0.40	0.13	0.06	0.05	0.01	0.01	0.00

(iv) proximal (ln)

	U_1	U_2	U_3	U_4	U_5	U_6	U_7	U_8	U_9	U_{10}
X1	0.0094	0.0969	0.0264	0.1008	0.0135	0.1531	0.3677	0.2847	0.3903	0.7665
Y1	0.0001	0.0789	−0.0478	−0.0130	−0.1329	0.2559	0.4699	0.6786	−0.2493	−0.4059
X2	−0.8036	−0.2613	−0.3582	0.2083	0.2381	0.2116	0.0636	−0.0819	−0.0445	0.0040
Y2	−0.3801	−0.0533	0.7477	−0.0612	0.2585	−0.3113	−0.1436	0.3237	−0.0235	0.0119
X3	0.0057	0.1825	0.1111	0.2876	0.1782	−0.0113	0.2238	−0.1486	0.7274	−0.4883
Y3	0.2481	−0.5841	0.1727	−0.3232	0.3997	0.1303	0.4656	−0.2556	−0.0609	−0.0231
X4	−0.3831	0.2316	0.1675	−0.5425	−0.5096	0.0153	0.3155	−0.3330	0.0796	−0.0212
Y4	−0.1942	0.4692	−0.3275	−0.5456	0.5870	−0.0971	−0.0631	0.1210	0.0442	−0.0042
X5	0.0049	0.4219	0.0928	0.4016	0.1933	−0.2771	0.4476	−0.3233	−0.4743	0.0894
Y5	0.0286	0.2950	0.3516	0.0450	0.1597	0.8160	−0.2203	−0.1718	−0.1300	0.0141
l	0.8960	0.4470	0.4096	0.2013	0.1137	0.1018	0.0296	0.0043	0.0020	0.0001
%	40.62	20.27	18.57	9.13	5.16	4.62	1.34	0.20	0.09	0.00

Table A.12. (continued)

(g) *Gorilla* females

(i) distal (raw)

	U_1	U_2	U_3	U_4	U_5	U_6	U_7	U_8	U_9	U_{10}
X1	0.8477	0.4863	0.0542	0.0896	0.0735	0.0972	0.0450	0.0326	0.1308	0.0493
Y1	0.5240	−0.7937	−0.1730	−0.0890	−0.1323	−0.1531	−0.0415	−0.0488	−0.1076	−0.0311
X2	−0.0117	0.0729	−0.1900	−0.0729	−0.0827	−0.0787	0.8542	−0.3948	−0.2005	0.1201
Y2	−0.2356	0.2880	−0.7777	−0.1337	−0.1696	−0.3142	−0.3451	−0.2143	0.0172	−0.0327
X3	0.0712	0.1644	0.2178	−0.2519	−0.0502	−0.0260	−0.1030	−0.1246	−0.6204	−0.6654
Y3	−0.0092	−0.0754	−0.3543	0.3521	0.0689	0.7804	−0.0969	−0.1092	−0.3290	0.0376
X4	−0.0036	0.0478	−0.3117	0.0064	0.0472	−0.1014	0.2643	0.8626	−0.2684	−0.0449
Y4	0.0096	−0.0672	−0.1066	−0.0778	0.9597	−0.1699	−0.0337	−0.1256	−0.0999	0.0350
X5	0.0286	0.0960	0.2057	−0.0398	−0.1037	−0.1826	−0.2378	−0.0184	−0.5846	0.7095
Y5	0.1171	0.0044	−0.0496	−0.8751	0.0157	0.4243	−0.0032	0.0841	0.1182	0.1742
l	144.0872	4.9128	0.8564	0.1236	0.1200	0.0416	0.0039	0.0023	0.0010	0.0003
%	95.96	3.27	0.57	0.08	0.08	0.23	0.00	0.00	0.00	0.00

(ii) distal (ln)

	U_1	U_2	U_3	U_4	U_5	U_6	U_7	U_8	U_9	U_{10}
X1	0.0491	0.0039	0.2729	0.1443	0.0037	0.2428	0.3034	0.0171	0.6314	0.5895
Y1	0.1013	0.1925	0.2801	0.2076	0.2570	0.3910	0.5064	−0.4724	−0.3867	−0.1407
X2	−0.5780	0.2511	−0.2526	−0.4520	−0.1148	0.5477	0.1196	0.0788	−0.0305	0.0107
Y2	−0.4599	0.2783	0.1919	0.0497	−0.2933	−0.6158	0.4262	−0.1573	−0.0080	−0.0008
X3	0.0391	−0.0257	0.3221	0.0533	−0.1936	0.1669	0.1359	0.3101	0.3834	−0.7512
Y3	−0.0410	0.0695	−0.1454	0.1540	0.4724	−0.1152	0.3770	0.7175	−0.2310	0.0432
X4	−0.4080	0.3683	0.2593	0.5463	0.2300	0.1289	−0.5122	0.0125	−0.0080	−0.0061
Y4	0.5173	0.8303	−0.1063	−0.0463	−0.1631	0.0338	0.0181	0.0341	−0.0196	0.0066
X5	0.0616	−0.1194	0.4573	0.0083	−0.5444	0.1577	−0.0858	0.3583	−0.5000	0.2565
Y5	0.0251	0.1198	0.5778	−0.6341	0.4453	−0.1587	−0.1578	0.0065	0.0023	0.0253
l	0.9944	0.5369	0.1343	0.0792	0.0300	0.0092	0.0057	0.0011	0.0001	0.0000
%	55.53	29.98	7.50	4.42	1.67	0.51	0.32	0.06	0.01	0.00

(iii) proximal (raw)

	U_1	U_2	U_3	U_4	U_5	U_6	U_7	U_8	U_9	U_{10}
X1	0.8872	0.4300	0.0436	0.0629	0.0126	0.0190	0.1057	0.0116	0.0832	0.0573
Y1	0.4390	−0.8759	−0.0533	0.1265	0.0635	−0.0128	−0.1010	0.0059	−0.0695	−0.0446
X2	0.0260	−0.0542	0.0996	−0.2866	0.1375	−0.3110	0.1280	−0.8654	0.1470	0.0417
Y2	0.0816	−0.1134	0.4416	−0.8027	−0.1266	0.1194	−0.0853	0.2776	0.1624	−0.0132
X3	0.0619	0.1543	0.1846	−0.0067	0.1176	−0.1863	−0.4934	−0.0753	−0.4158	−0.6839
Y3	0.0720	0.0571	−0.7004	−0.4245	0.0980	0.4283	−0.1821	−0.1497	−0.2650	0.0437
X4	0.0244	−0.0447	0.0893	−0.1126	−0.2953	−0.0580	0.6285	−0.0030	−0.6994	−0.0456
Y4	0.0399	−0.0031	−0.0510	0.0973	−0.9102	0.0536	−0.3073	−0.2312	0.0833	0.0136
X5	0.0011	0.0473	0.3312	0.0738	0.1224	0.0255	−0.4182	−0.0833	−0.4473	0.6964
Y5	0.0404	0.0271	−0.3814	−0.2137	−0.0822	−0.8145	−0.1183	0.2922	−0.0232	0.1895
l	71.5142	6.6741	0.3196	0.1807	0.0627	0.0586	0.0100	0.0030	0.0010	0.0004
%	90.73	8.47	0.41	0.23	0.08	0.07	0.01	0.00	0.00	0.00

(iv) proximal (ln)

	U_1	U_2	U_3	U_4	U_5	U_6	U_7	U_8	U_9	U_{10}
X1	0.0931	0.0536	0.0369	0.1451	0.0434	0.0775	0.4136	0.3337	0.3287	0.7535
Y1	0.1023	−0.0298	0.0050	−0.0693	0.1104	−0.2450	0.3635	0.6879	−0.4581	−0.2873
X2	0.4653	−0.5668	0.2334	0.1533	−0.3429	−0.4168	0.1834	−0.2452	0.0330	−0.0018
Y2	0.4414	−0.2784	−0.0973	0.3243	0.3565	0.2003	−0.5845	0.3179	0.0506	0.0244
X3	0.0746	0.0858	0.0388	0.3235	−0.0865	0.3038	0.3249	0.1104	0.5701	−0.5817
Y3	0.1658	0.2470	0.3640	0.2718	0.6701	−0.0750	0.2528	−0.3874	−0.1894	−0.0237
X4	0.4114	−0.2094	−0.1793	−0.6140	0.1632	0.4958	0.2736	−0.1659	−0.0498	−0.0243
Y4	0.5566	0.6191	−0.4308	0.0138	−0.1919	−0.2743	−0.0486	−0.0806	0.0162	0.0002
X5	0.0002	−0.0115	−0.1733	0.5058	−0.3413	0.4885	0.1588	−0.1314	−0.5545	0.0942
Y5	0.2436	0.3191	0.7436	−0.1845	−0.3235	0.2501	−0.2229	0.1639	−0.0859	0.0264
l	0.6680	0.2524	0.1015	0.0268	0.0185	0.0104	0.0037	0.0011	0.0002	0.0000
%	61.70	23.31	9.37	2.48	1.71	0.96	0.34	0.10	0.02	0.00

Table A.12. (continued)

(h) *Gorilla* males

(i) distal (raw)

	U_1	U_2	U_3	U_4	U_5	U_6	U_7	U_8	U_9	U_{10}
X1	0.8293	0.4866	0.2262	0.0564	0.0127	0.0135	0.1292	0.0105	0.0216	0.0597
Y1	0.5224	−0.5501	−0.6344	−0.0787	−0.0080	−0.0030	−0.1006	−0.0353	−0.0360	−0.0547
X2	0.0617	−0.2304	0.1842	0.2792	0.2331	−0.3322	−0.1424	0.6481	−0.2836	0.3818
Y2	0.1716	−0.5638	0.6741	−0.2046	−0.0978	0.2851	−0.1289	−0.1857	0.0795	0.0903
X3	0.0338	0.1721	0.0658	−0.1379	0.1470	0.1117	−0.6465	−0.0074	−0.5374	−0.4528
Y3	0.0228	0.0773	0.0232	−0.4565	−0.6262	−0.3125	−0.2059	0.4169	0.2532	−0.1203
X4	0.0642	−0.2140	0.2123	0.4671	−0.0674	−0.4269	0.1698	−0.0583	0.1012	−0.6765
Y4	0.0077	0.0352	0.0345	−0.0578	−0.0710	−0.6550	−0.2338	−0.6018	−0.1336	0.3541
X5	0.0163	0.0639	−0.0185	0.0751	0.4512	−0.0453	−0.5043	0.0211	0.7275	−0.0085
Y5	0.0053	−0.0533	0.0810	−0.6452	0.5558	−0.2911	0.3717	0.0654	−0.0361	−0.1921
l	132.1942	9.1507	6.0353	0.3155	0.0842	0.0168	0.0144	0.0006	0.0000	0.0000
%	89.43	6.19	4.08	0.21	0.06	0.01	0.01	0.00	0.00	0.00

(ii) distal (ln)

	U_1	U_2	U_3	U_4	U_5	U_6	U_7	U_8	U_9	U_{10}
X1	0.0217	0.0902	0.1171	0.3607	0.1586	0.1566	0.1398	0.2974	−0.7651	0.3233
Y1	0.0251	−0.0084	0.1567	0.5055	0.4810	0.0546	−0.3231	0.3933	0.3173	−0.3536
X2	0.5392	−0.6406	0.1624	0.2380	−0.0112	−0.2147	−0.1072	−0.3701	−0.1435	−0.0251
Y2	0.6305	0.4037	−0.2884	−0.1901	0.2811	0.4069	−0.1788	−0.2019	−0.0476	−0.0231
X3	0.0052	0.1543	0.0266	0.2347	−0.1997	0.1563	0.4892	−0.2042	−0.1778	−0.7371
Y3	0.0103	0.2001	−0.0723	0.3249	0.3952	−0.2520	0.5432	−0.3252	0.3194	0.3558
X4	0.5320	0.1747	0.4130	−0.1491	−0.2691	−0.1785	0.3124	0.4930	0.2115	0.0626
Y4	0.0527	0.5119	−0.0765	0.2153	−0.2168	−0.6541	−0.3881	−0.1289	−0.1838	−0.0842
X5	−0.0029	0.1305	0.1318	0.4902	−0.5424	0.4542	−0.1784	−0.1776	0.2709	0.2968
Y5	0.1572	−0.2122	−0.8077	0.2282	−0.2338	−0.0828	0.1348	0.3748	0.0741	0.0137
l	3.5567	0.1427	0.1039	0.0269	0.0081	0.0030	0.0018	0.0004	0.0000	0.0000
%	92.54	3.71	2.70	0.70	0.21	0.08	0.05	0.01	0.00	0.00

(iii) proximal (raw)

	U_1	U_2	U_3	U_4	U_5	U_6	U_7	U_8	U_9	U_{10}
X1	0.9046	0.3802	0.0773	0.0240	0.0974	0.0532	0.0130	0.0946	−0.0255	0.0925
Y1	0.4122	−0.8385	−0.2728	−0.0592	−0.1937	0.1358	−0.0287	−0.0438	0.0254	−0.0889
X2	0.0068	−0.0470	0.2108	0.1319	−0.2501	0.1095	−0.0254	−0.3682	0.5514	0.6490
Y2	0.0598	−0.1703	0.6674	0.3562	−0.1916	−0.5480	−0.1153	0.0581	−0.1721	−0.1089
X3	0.0653	0.2002	−0.2027	0.2283	−0.0534	−0.1676	−0.2031	−0.4075	0.4932	−0.6172
Y3	0.0426	0.1097	0.2727	−0.7967	−0.3979	−0.0522	0.0062	−0.2887	−0.0730	−0.1653
X4	0.0335	−0.1222	0.2600	0.1174	0.2649	0.1896	0.7825	−0.3798	−0.0443	−0.1946
Y4	0.0147	−0.2084	0.3234	−0.1861	0.6847	0.1810	−0.5077	−0.2393	0.0120	−0.0150
X5	0.0113	0.1014	−0.1830	0.2848	−0.2044	0.1691	−0.2255	−0.5742	−0.6415	0.1119
Y5	0.0261	0.0187	−0.3292	−0.1879	0.3344	−0.7460	0.1511	−0.2638	−0.0535	0.3027
l	184.5283	2.7357	1.0238	0.5271	0.1864	0.0776	0.0148	0.0003	0.0000	0.0000
%	97.59	1.45	0.54	0.28	0.10	0.04	0.01	0.00	0.00	0.00

(iv) proximal (ln)

	U_1	U_2	U_3	U_4	U_5	U_6	U_7	U_8	U_9	U_{10}
X1	0.1159	0.1405	0.0763	0.0975	0.0874	0.2105	0.1768	0.4900	0.7897	−0.0676
Y1	0.1059	0.1143	0.0477	0.0621	−0.0367	0.0946	0.6947	0.0384	−0.3019	−0.6197
X2	0.3558	−0.6214	0.2436	0.0884	−0.1934	−0.0750	0.3989	0.1048	−0.0503	0.4520
Y2	0.4674	−0.1560	0.1886	0.3612	−0.3601	0.1878	−0.4738	−0.1594	0.0554	−0.4162
X3	0.0829	0.1726	0.1437	0.0496	0.0742	0.3538	−0.2240	0.6790	−0.5231	0.1574
Y3	0.1375	0.1089	−0.0258	0.6983	0.6253	0.0168	0.0721	−0.2273	−0.0574	0.1718
X4	0.6966	0.3011	0.1300	−0.4477	0.2947	−0.3383	−0.0564	−0.0445	−0.1423	0.1151
Y4	0.3383	−0.0509	−0.8502	−0.0782	−0.0774	0.3594	0.0652	−0.0391	−0.0167	0.1134
X5	0.0014	0.1779	0.3686	−0.2576	0.0178	0.7044	0.1187	−0.4505	0.0467	0.2245
Y5	0.0698	0.6246	−0.0085	0.2922	−0.5782	−0.2014	0.1597	−0.0542	−0.0119	0.3407
l	0.6172	0.1930	0.1712	0.0454	0.0184	0.0096	0.0017	0.0000	0.0000	0.0000
%	58.41	18.27	16.20	4.30	1.74	0.91	0.16	0.00	0.00	0.00

Table A.13. Principal component analyses omitting outliers – conventional data

(a) *Homo* females proximal (omitting 87)

	U_1	U_2
P	0.7302	0.6833
A	0.6833	−0.7302
I^*	15.1457	0.2040

(b) *Gorilla* females proximal (omitting 671, 672)

	U_1	U_2
P	0.7979	0.6027
A	0.6027	−0.7979
I^*	5.1615	0.1911

Table A.14. Principal component analyses omitting outliers – Fourier data

(a) *Homo* females proximal (omitting 87)

	U_1	U_2	U_3	U_4	U_5	U_6	U_7	U_8	U_9	U_{10}
X1	0.9177	0.3377	0.1288	0.0062	0.0639	0.0002	0.1251	0.0577	0.0005	0.0639
Y1	0.3761	−0.8715	−0.2772	−0.0985	0.0241	0.0011	−0.0798	−0.0530	−0.0130	−0.0482
X2	0.0232	−0.1606	0.2466	0.3869	−0.6917	0.2589	0.2112	0.0645	−0.3568	0.2040
Y2	−0.0104	−0.2479	0.7639	0.2674	0.3357	−0.2952	−0.2568	−0.0577	−0.0330	0.1147
X3	0.1039	0.1434	−0.0264	0.1497	−0.1563	0.1258	−0.5826	−0.3238	−0.2772	−0.6198
Y3	−0.0027	−0.0458	0.4441	−0.8234	−0.3116	0.1177	−0.0607	−0.0407	0.0425	−0.0671
X4	−0.0004	−0.1125	0.2265	0.2315	−0.0510	0.2361	0.3592	0.0093	0.6317	−0.5440
Y4	0.0444	0.0230	−0.0812	0.0437	−0.4477	−0.6804	−0.2162	0.4533	0.2340	−0.1366
X5	0.0431	0.0335	−0.0421	0.1061	−0.1048	0.4321	−0.5836	0.1089	0.5058	0.4220
Y5	0.0324	0.0468	−0.0674	0.0414	−0.2619	−0.3330	0.0894	−0.8139	0.2883	0.2398
l	89.8128	7.6061	4.0004	1.0278	0.3919	0.2983	0.1443	0.1056	0.0198	0.0050
%	86.85	7.36	3.87	0.99	0.38	0.29	0.14	0.10	0.02	0.00

(b) *Gorilla* females proximal (omitting 671, 672)

	U_1	U_2	U_3	U_4	U_5	U_6	U_7	U_8	U_9	U_{10}
X1	0.9822	0.0941	0.0634	0.0177	0.0187	0.0156	0.1096	0.0032	0.0771	0.0590
Y1	0.1058	−0.9494	0.0824	−0.1889	0.0336	−0.1827	−0.0637	0.0279	−0.0639	−0.0402
X2	0.0061	−0.0666	−0.2634	0.2093	−0.2121	−0.2379	0.1726	−0.8651	0.0467	0.0205
Y2	0.0516	−0.2045	−0.7387	0.4430	0.0753	0.3297	−0.1187	0.2250	0.1852	−0.0165
X3	0.1196	0.0907	0.0158	0.2208	−0.1031	−0.1809	−0.5020	−0.0203	−0.3931	−0.6915
Y3	0.0554	0.1510	−0.5077	−0.5998	0.4729	−0.1624	−0.1186	−0.1107	−0.2797	0.0465
X4	0.0099	−0.0648	−0.0943	0.0227	−0.2200	0.3217	0.5402	0.0723	−0.7324	−0.0310
Y4	0.0438	−0.0406	0.0300	−0.4144	−0.3643	0.6774	−0.3862	−0.2758	0.0828	−0.0109
X5	0.0315	−0.0131	0.1255	0.3127	0.0726	−0.0171	−0.4749	−0.0756	−0.4210	0.6865
Y5	0.0311	0.0808	−0.3011	−0.2131	−0.7261	−0.4235	−0.0862	0.3171	0.0166	0.2040
l	26.5250	3.9965	0.1943	0.1660	0.0657	0.0458	0.0091	0.0030	0.0009	0.0005
%	85.55	12.89	0.63	0.53	0.21	0.15	0.03	0.01	0.00	0.00

(c) *Gorilla* males distal (omitting 656)

	U_1	U_2	U_3	U_4	U_5	U_6	U_7	U_8	U_9	U_{10}
X1	0.8065	0.1380	0.4822	0.1891	0.1955	0.1219	0.0574	0.0172	0.0574	0.0481
Y1	0.5485	−0.5336	−0.5414	−0.2128	−0.2160	−0.1029	−0.0893	0.0111	−0.0765	−0.0692
X2	0.0700	0.2220	−0.2885	0.2471	−0.2548	0.0145	0.1071	−0.0076	0.1189	0.8430
Y2	0.1932	0.7584	−0.3075	−0.2825	−0.0490	−0.2537	−0.2329	0.2018	0.0400	−0.2229
X3	0.0265	0.0347	0.2266	0.0399	−0.1825	−0.6328	0.1307	−0.2183	−0.6629	0.0851
Y3	0.0201	0.0080	0.2098	−0.7704	0.0083	−0.0454	0.2009	−0.4350	0.2798	0.2281
X4	0.0712	0.2481	−0.3609	0.1777	0.0871	0.3574	0.4034	−0.6022	−0.2166	−0.2528
Y4	0.0060	0.0280	0.0381	−0.1535	−0.2749	0.0895	0.7652	0.5372	−0.0458	−0.1203
X5	0.0135	−0.0291	0.0445	0.3529	−0.3495	−0.4393	0.1570	−0.2420	0.6245	−0.2900
Y5	0.0090	0.0850	0.2597	−0.0584	−0.7805	0.4227	−0.3044	−0.1106	−0.1355	−0.1035
l	146.9014	6.9610	1.5230	0.1349	0.0514	0.0169	0.0055	0.0000	0.0000	0.0000
%	94.41	4.47	0.99	0.08	0.04	0.01	0.00	0.00	0.00	0.00

Table A.15. Covariance-correlation matrices – conventional data (normalized)

(a) *Homo*

(i) females distal (raw)

1.7969	−0.9998
−7.5564	**31.7917**

(ii) females distal (ln*)

1.8988	−0.9991
−33.6022	**595.7819**

(iii) females proximal (raw)

1.2457	−0.9999
−5.1656	**21.4263**

(iv) females proximal (ln*)

1.3182	−0.9996
−22.6769	**390.3831**

(v) males distal (raw)

1.6843	−0.9999
−7.0463	**29.4863**

(vi) males distal (ln*)

1.7807	−0.9995
−31.1800	**546.5191**

(vii) males proximal (raw)

1.8669	−0.9999
−7.7722	**32.3637**

(viii) males proximal (ln*)

1.9748	−0.9996
−34.2410	**594.1948**

(b) *Cercopithecus*

(i) females distal (raw)

1.5780	−0.9999
−6.1371	**23.8737**

(ii) females distal (ln*)

1.6824	−0.9996
−25.4573	**385.5215**

(iii) females proximal (raw)

0.8329	−1.0000
−3.1390	**11.8303**

(iv) females proximal (ln*)

0.8916	−0.9999
−12.6644	**179.9230**

(v) males distal (raw)

3.3542	−0.9998
−13.1793	**51.8041**

(vi) males distal (ln)*

3.5719	−0.9992
−55.1850	**853.8849**

(vii) males proximal (raw)

1.5829	−0.9999
−6.0294	**22.9706**

(viii) males proximal (ln*)

1.6922	−0.9996
−24.5591	**356.7055**

NB variances in bold on diagonal, covariance lower left, correlation upper right
*variances/covariances for ln variables $\times 10^{-3}$

Table A.15. (continued)

(c) *Colobus*

(i) females distal (raw)

0.8193	−1.0000
−3.2463	**12.8645**

(ii) females distal (ln*)

0.8715	−0.9998
−13.6854	**214.9887**

(iii) females proximal (raw)

1.3002	−1.0000
−4.9943	**19.1869**

(iv) females proximal (ln*)

1.3883	−0.9998
−20.4901	**302.5265**

(v) males distal (raw)

2.4139	−1.0000
−9.5124	**37.4912**

(vi) males distal (ln*)

2.5696	−0.9997
−39.9169	**620.4924**

(vii) males proximal (raw)

2.8410	−0.9999
−1.0976	**42.4161**

(viii) males proximal (ln*)

3.0316	−0.9996
−45.2727	**676.6152**

(d) *Gorilla*

(i) females distal (raw)

2.2608	−0.9999
−9.7269	**41.8590**

(ii) females distal (ln*)

2.3833	−0.9995
−44.1399	**818.3427**

(iii) females proximal (raw)

1.5744	−0.9999
−6.4561	**26.4779**

(iv) females proximal (ln*)

1.6681	−0.9998
−28.0585	**472.1898**

(v) males distal (raw)

1.0621	−0.9999
−4.3764	**18.0345**

(vi) males distal (ln*)

1.1247	−0.9998
−19.0995	**324.4732**

(vii) males proximal (raw)

0.4726	−1.0000
−1.9075	**7.6990**

(viii) males proximal (ln*)

0.5017	−0.9999
−8.1722	**133.1579**

NB variances in bold on diagonal, covariance lower left, correlation upper right
*variances/covariances for ln variables $\times 10^{-3}$

Table A.16. Covariance-correlation matrices – Fourier data (normalized)

(a) *Homo*

(i) females distal

0.1641	−0.9959	−0.3749	−0.1428	0.7432	0.1291	−0.3677	0.1011	0.3916	0.2287
−0.3326	**0.6795**	0.3440	0.0800	−0.7301	−0.1530	0.3215	−0.1269	−0.3720	−0.2168
−0.0292	0.0545	**0.0369**	0.3506	−0.1841	−0.0013	0.4643	0.1219	−0.0464	−0.2851
−0.0285	0.0325	0.0332	**0.2431**	−0.3446	0.3866	0.8169	0.0126	−0.4319	−0.2451
0.0530	−0.1059	−0.0062	−0.0299	**0.0310**	−0.3212	−0.6223	0.3136	0.8040	0.2021
0.0139	−0.0336	−0.0001	0.0508	−0.0151	**0.0711**	0.2926	−0.3559	−0.5323	−0.0203
−0.0214	0.0381	0.0128	0.0579	−0.0158	0.0112	**0.0207**	−0.1211	−0.5636	−0.2498
0.0076	−0.0193	0.0043	0.0011	0.0102	−0.0175	−0.0032	**0.0341**	0.2885	0.1246
0.0226	−0.0437	−0.0013	−0.0303	0.0201	−0.0202	−0.0115	0.0076	**0.0203**	−0.2317
0.0124	−0.0240	−0.0074	−0.0162	0.0048	−0.0007	−0.0048	0.0031	−0.0044	**0.0180**

(ii) females proximal

0.1279	−0.9955	−0.3312	−0.2883	0.7796	−0.0362	−0.3590	0.1793	0.3303	0.3342
−0.2416	**0.4607**	0.2742	0.2118	−0.7639	−0.0175	0.2963	−0.1696	−0.3119	−0.3116
−0.0292	0.0459	**0.0608**	0.6217	−0.2103	0.1925	0.8379	−0.0165	−0.0191	−0.1442
−0.0504	0.0702	0.0749	**0.2387**	−0.4488	0.5691	0.8428	−0.3608	−0.3983	−0.4620
0.0462	−0.0859	−0.0859	−0.0363	**0.0274**	−0.3501	−0.4433	0.3275	0.7135	0.5211
−0.0045	−0.0042	0.0167	0.0977	−0.0204	**0.1235**	0.3278	−0.3027	−0.3658	−0.3363
−0.0226	0.0354	0.0364	0.0725	−0.0129	0.0203	**0.0310**	−0.4020	−0.2269	−0.4119
0.0103	−0.0185	−0.0007	−0.0284	0.0087	−0.0171	−0.0114	**0.0259**	0.0985	0.5356
0.0139	−0.0249	−0.0006	−0.0229	0.0139	−0.0151	−0.0047	0.0019	**0.0138**	0.0934
0.0148	−0.0261	−0.0044	−0.0279	0.0107	−0.0146	−0.0090	0.0107	0.0014	**0.0153**

(iii) males distal

0.1260	−0.9971	−0.0982	−0.0651	0.7879	0.1142	−0.3339	0.2160	0.5572	0.1159
−0.2602	**0.5401**	0.0524	0.0104	−0.7933	−0.1248	0.3046	−0.2430	−0.5511	−0.1141
−0.0052	0.0057	**0.0221**	0.4615	0.0072	0.1187	0.3945	0.2047	−0.1091	−0.0021
−0.0090	0.0030	0.0268	**0.1529**	−0.1214	0.1682	0.7299	0.1932	−0.2702	−0.1827
0.0490	−0.1022	0.0002	−0.0083	**0.0307**	−0.2820	−0.5088	0.3590	0.8495	0.1724
0.0114	−0.0258	0.0050	0.0185	−0.0139	**0.0791**	0.0964	−0.1369	−0.4475	−0.1241
−0.0140	0.0265	0.0069	0.0338	−0.0106	0.0032	**0.0140**	−0.1577	−0.5437	−0.0841
0.0161	−0.0376	0.0064	0.0159	0.0132	−0.0081	−0.0039	**0.0442**	0.2239	0.0345
0.0240	−0.0491	−0.0020	−0.0128	0.0181	−0.0153	−0.0078	0.0057	**0.0147**	−0.1603
0.0054	−0.0110	−0.0000	−0.0094	0.0040	−0.0046	−0.0013	0.0010	−0.0025	**0.0172**

(iv) males proximal

0.1440	−0.9965	0.1980	−0.1354	0.8681	−0.2075	0.0958	0.0924	0.6184	0.3233
−0.2880	**0.5800**	−0.2425	−0.0549	−0.8678	0.1710	−0.1456	−0.0937	−0.6056	−0.3207
0.0147	−0.0361	**0.0383**	0.4212	0.3035	0.0279	0.6312	0.2920	0.2331	0.0890
−0.0022	−0.0177	0.0349	**0.1796**	−0.0927	0.5030	0.7732	−0.2391	−0.2771	−0.1856
0.0606	−0.1215	0.0109	−0.0072	**0.0338**	−0.4419	0.0530	0.1992	0.8318	0.4961
−0.0263	0.0435	0.0018	0.0711	−0.0271	**0.1114**	0.2553	−0.3255	−0.4952	−0.3341
0.0043	−0.0132	0.0146	0.0391	0.0012	0.0101	**0.0141**	−0.3035	0.0042	−0.1391
0.0061	−0.0124	0.0099	−0.0176	0.0064	−0.0189	−0.0063	**0.0302**	0.0788	0.2809
0.0299	−0.0588	0.0058	−0.0150	0.0195	−0.0211	0.0001	0.0017	**0.0162**	0.1697
0.0149	−0.0297	0.0021	−0.0095	0.0111	−0.0135	−0.0020	0.0059	0.0026	**0.0147**

NB variances in bold on diagonal, covariance lower left, correlation upper right

Table A.16. (continued)

(b) *Cercopithecus*

(i) females distal

0.2494	−0.9985	0.1074	−0.0158	0.8993	0.4318	−0.1262	0.2463	0.6987	0.0413
−0.4182	**0.7035**	−0.1350	−0.0153	−0.9008	−0.0405	0.0991	−0.2583	−0.7001	−0.0489
0.0073	−0.0154	**0.0185**	0.7837	0.0873	0.0780	0.7888	−0.0134	0.0073	0.0125
−0.0032	−0.0052	0.0427	**0.1607**	0.0497	−0.0465	0.8892	−0.0959	0.0371	0.0323
0.0985	−0.1658	0.0026	0.0044	**0.0481**	−0.3365	−0.0978	0.3705	0.8676	0.3002
0.0051	−0.0081	0.0025	−0.0044	−0.0176	**0.0568**	−0.0501	−0.3993	−0.5984	−0.3335
−0.0086	0.0114	0.0147	0.0488	−0.0029	−0.0016	**0.0187**	−0.1203	−0.0468	−0.0081
0.0153	−0.0269	−0.0002	−0.0048	0.0101	−0.0118	−0.0020	**0.0154**	0.4352	0.1738
0.0439	−0.0739	0.0001	0.0019	0.0240	−0.0180	−0.0008	0.0068	**0.0158**	0.0666
0.0023	−0.0046	0.0002	0.0014	0.0073	−0.0088	−0.0001	0.0024	0.0009	**0.0124**

(ii) females proximal

0.2094	−0.9992	−0.0282	0.2155	0.8812	0.2680	0.2029	−0.0018	0.4276	0.3148
−0.3130	**0.4686**	0.0088	−0.2391	−0.8877	−0.2634	−0.2243	0.0071	−0.4351	−0.3328
−0.0016	0.0008	**0.0164**	0.7470	0.0404	−0.0830	0.6435	0.3337	−0.0001	0.2679
0.0298	−0.0494	0.0289	**0.0912**	0.2475	0.1139	0.9276	0.0659	0.0604	0.3495
0.0761	−0.1147	0.0010	0.0141	**0.0356**	−0.0948	0.2388	−0.0584	0.6973	0.5501
0.0231	−0.0339	−0.0020	0.0065	−0.0034	**0.0354**	0.1084	0.0850	−0.5970	−0.0023
0.0105	−0.0174	0.0093	0.0318	0.0051	0.0023	**0.0129**	−0.0394	0.0877	0.3478
−0.0001	0.0006	0.0049	0.0023	−0.0013	−0.0018	−0.0005	**0.0133**	−0.1919	0.0341
0.0192	−0.0293	−0.0000	0.0018	0.0129	−0.0110	0.0010	−0.0022	**0.0097**	0.1500
0.0160	−0.0252	0.0038	0.0117	0.0115	−0.0000	0.0044	0.0004	0.0016	**0.0123**

(iii) males distal

0.4629	−0.9983	0.1118	0.1103	0.9381	0.2995	−0.2207	0.5444	0.6363	0.1818
−0.7848	**1.3352**	−0.1215	−0.1231	−0.9329	−0.3060	0.2140	−0.5536	−0.6265	−0.1808
0.0126	−0.0232	**0.0273**	0.7062	0.0512	0.1801	0.6206	0.2277	−0.0991	0.0318
0.0293	−0.0556	0.0456	**0.1525**	0.0367	0.1939	0.6652	0.0840	−0.1550	−0.0540
0.1746	−0.2949	0.0023	0.0039	**0.0749**	0.0631	−0.2908	0.4589	0.7904	0.3344
0.0485	−0.0842	0.0071	0.0180	0.0041	**0.0567**	0.0229	0.1098	−0.3493	0.0204
−0.0205	0.0338	0.0140	0.0355	−0.0109	0.0007	**0.0187**	0.1411	−0.2776	−0.1357
0.0897	−0.1550	0.0091	0.0079	0.0304	0.0063	0.0047	**0.0587**	0.3290	0.0146
0.0633	−0.1059	−0.0024	−0.0089	0.0316	−0.0122	−0.0055	0.0117	**0.0214**	0.0260
0.0170	−0.0287	0.0007	−0.0029	0.0126	0.0007	−0.0026	0.0005	0.0005	**0.0189**

(iv) males proximal

0.3625	−0.9987	−0.0402	0.1024	0.8581	0.2101	−0.0809	−0.0303	0.6279	0.1783
−0.5504	**0.8377**	0.0359	−0.1068	−0.8516	−0.2156	0.0776	0.0327	−0.6308	−0.1631
−0.0045	0.0061	**0.0348**	0.6850	−0.2622	0.2874	0.7418	0.1413	−0.3413	−0.1585
0.0206	−0.0326	0.0426	**0.1112**	−0.0711	0.2348	0.8371	−0.1731	−0.2005	−0.1029
0.1501	−0.2265	−0.0142	−0.0069	**0.0844**	−0.1786	−0.2706	−0.0246	0.8566	0.4566
0.0358	−0.0559	0.0152	0.0222	−0.0147	**0.0802**	0.1711	0.0378	−0.4442	−0.1005
−0.0075	0.0109	0.0212	0.0428	−0.0121	0.0074	**0.0235**	−0.0072	−0.3034	−0.1967
−0.0031	0.0051	0.0045	−0.0099	−0.0012	0.0018	−0.0002	**0.0292**	0.0720	−0.0462
0.0662	−0.1011	−0.0111	−0.0117	0.0436	−0.2201	−0.0081	0.0022	**0.0306**	0.1969
0.0146	−0.0202	−0.0040	−0.0047	0.0180	−0.0039	−0.0041	−0.0011	0.0047	**0.0184**

NB variances in bold on diagonal, covariance lower left, correlation upper right

Table A.16. (continued)

(c) *Colobus*

(i) females distal

0.1935	−0.9978	−0.7823	−0.3563	0.8513	0.5298	−0.7325	−0.0717	−0.0198	0.5370
−0.3218	**0.5374**	0.7562	0.3185	−0.8510	−0.5299	0.7058	0.0757	0.0205	−0.5586
−0.0785	0.1264	**0.0520**	0.7869	−0.7990	−0.3151	0.9310	0.1546	−0.2375	−0.4651
−0.0576	0.0858	0.0659	**0.1350**	−0.5109	0.1145	0.7876	0.2034	−0.5235	−0.1069
0.0685	−0.1142	−0.0333	−0.0344	**0.0335**	0.1118	−0.7280	−0.1477	0.4563	0.7142
0.0750	−0.1250	−0.0231	0.0135	0.0066	**0.1036**	−0.3461	0.1423	−0.7266	0.1745
−0.0656	0.1054	0.0432	0.0589	−0.0271	−0.0227	**0.0415**	0.1709	−0.1768	−0.3634
−0.0034	0.0059	0.0037	0.0079	−0.0029	0.0049	0.0037	**0.0113**	−0.1420	−0.1358
−0.0009	0.0016	−0.0059	−0.0210	0.0091	−0.0255	−0.0039	−0.0016	**0.0119**	0.2317
0.0235	−0.0407	−0.0105	−0.0039	0.0130	0.0056	−0.0074	−0.0014	0.0025	**0.0099**

(ii) females proximal

0.2945	−0.9959	0.1275	0.1392	0.8179	0.2630	−0.0039	0.2367	0.3082	−0.0307
−0.4618	**0.7257**	−0.1582	−0.1595	−0.8253	−0.2596	−0.0166	−0.2600	−0.3196	0.0339
0.0160	−0.0311	**0.0531**	0.7181	0.1675	−0.0350	0.6648	0.6101	0.1057	−0.1039
0.0267	−0.0480	0.0585	**0.1247**	0.0128	0.1303	0.8520	0.5800	−0.0684	−0.3522
0.0808	−0.1279	0.0703	0.0008	**0.0331**	−0.1423	−0.0715	−0.0569	0.7253	0.1975
0.0280	−0.0434	−0.0016	0.0090	−0.0051	**0.0385**	0.1379	0.4606	−0.4857	−0.0573
−0.0003	−0.0018	0.0193	0.0378	−0.0016	0.0034	**0.0158**	0.5200	−0.1167	−0.0716
0.0255	−0.0439	0.0279	0.0406	−0.0021	0.0179	0.0130	**0.0394**	−0.1807	−0.3831
0.0190	−0.0309	0.0028	−0.0027	0.0150	−0.0104	−0.0017	−0.0041	**0.0129**	−0.0388
−0.0016	0.0028	−0.0023	−0.0121	0.0035	−0.0011	−0.0088	−0.0076	−0.0004	**0.0095**

(iii) males distal

0.3853	−0.9993	−0.1674	0.1712	0.9335	−0.0303	−0.2591	−0.1140	0.6329	0.3432
−0.6787	**1.1975**	0.1586	−0.1887	−0.9302	0.0213	0.2422	0.1043	−0.6278	−0.3526
−0.0227	0.0379	**0.0478**	0.7996	−0.1507	−0.1602	0.8794	0.0857	−0.0798	−0.2141
0.0412	−0.0801	0.0678	**0.1503**	0.1382	0.0865	0.7079	−0.1393	−0.0092	0.0210
0.1679	−0.2949	−0.0095	0.0155	**0.0839**	−0.3347	−0.1638	0.0358	0.8387	0.4248
−0.0066	0.0081	−0.0122	0.0117	−0.0338	**0.1217**	−0.3135	−0.3271	−0.6889	−0.1579
−0.0247	0.0408	0.0296	0.0422	−0.0073	−0.0168	**0.0236**	0.3325	0.0391	−0.0135
−0.0084	0.0135	0.0022	−0.0064	0.0012	−0.0135	0.0061	**0.0141**	0.3216	0.1258
0.0627	−0.1097	−0.0028	−0.0006	0.0388	−0.0384	0.0010	0.0061	**0.0255**	0.3425
0.0204	−0.0370	−0.0045	0.0008	0.0118	−0.0053	−0.0002	0.0014	0.0052	**0.0092**

(iv) males proximal

0.5652	−0.9981	−0.2380	−0.0241	0.9548	−0.2104	−0.5046	−0.0941	0.8340	0.3582
−0.8936	**1.4179**	0.2427	0.0102	−0.9555	−0.2142	0.4736	0.0784	−0.8426	−0.3758
−0.0161	0.0259	**0.0081**	0.4271	−0.2277	0.1938	0.1509	−0.1746	−0.1379	−0.2724
−0.0044	0.0029	0.0092	**0.0580**	−0.0852	0.3117	0.3193	−0.6254	−0.0024	−0.3098
0.2248	−0.3563	−0.0064	−0.0064	**0.0981**	−0.0389	−0.3861	−0.0937	0.9329	0.4735
0.0397	−0.0641	0.0044	0.0189	−0.0031	**0.0632**	−0.2688	−0.1122	−0.1550	−0.1593
−0.0382	0.0568	0.0014	0.0077	−0.0122	−0.0068	**0.0102**	0.9326	−0.2083	−0.0276
−0.0138	0.0182	−0.0306	−0.0294	−0.0057	−0.0055	0.0000	**0.0381**	−0.2124	0.3798
0.0938	−0.1501	−0.0019	−0.0001	0.0437	−0.0058	−0.0031	−0.0062	**0.0224**	0.3890
0.0227	−0.0378	−0.0021	−0.0063	0.0125	−0.0034	−0.0002	0.0063	0.0049	**0.0071**

NB variances in bold on diagonal, covariance lower left, correlation upper right

Table A.16. (continued)

(d) *Gorilla*

(i) females distal

0.1263	−0.9987	0.6940	0.6534	0.8346	0.1163	0.3212	−0.3448	0.5747	0.0135
−0.2969	**0.6999**	−0.7135	−0.6738	−0.8273	−0.1181	−0.3490	0.3471	−0.5669	−0.0218
0.0277	−0.0671	**0.0127**	0.9651	0.2903	0.5231	0.8393	−0.1616	−0.0546	0.1279
0.0922	−0.0224	0.0431	**0.1575**	0.2399	0.4766	0.9058	−0.1306	−0.0702	0.0995
0.0468	−0.1092	0.0052	0.0105	**0.0249**	−0.3821	−0.1366	−0.4568	0.8953	0.1790
0.0095	−0.0228	0.0136	0.0437	−0.0139	**0.0534**	0.5527	0.2107	−0.6931	−0.0669
0.0138	−0.0354	0.0114	0.0435	−0.0026	0.0155	**0.0147**	0.1217	−0.3975	0.0603
−0.0177	0.0419	−0.0026	−0.0075	−0.0104	0.0070	0.0021	**0.0208**	−0.5337	0.1154
0.0221	−0.0512	−0.0007	−0.0030	0.0153	−0.0173	−0.0520	−0.0083	**0.0117**	−0.0287
0.0006	−0.0021	0.0017	0.0046	0.0033	−0.0018	0.0009	0.0019	−0.0004	**0.0137**

(ii) females proximal

0.1445	−0.9995	−0.4728	−0.3191	0.9263	0.3892	−0.4417	0.1126	0.3460	0.2807
−0.2928	**0.5938**	0.4560	0.3069	−0.9261	−0.3940	0.4370	−0.1121	−0.3410	−0.2932
−0.0157	0.0307	**0.0076**	0.8770	−0.4627	0.0284	0.7615	0.2030	−0.3776	0.2884
−0.0283	0.0551	0.0179	**0.0542**	−0.3615	0.1043	0.8343	0.4229	−0.3033	0.1634
0.0486	−0.0986	−0.0056	−0.0116	**0.0191**	0.0847	−0.5467	−0.1126	0.6359	0.0879
0.0284	−0.0583	0.0005	0.0047	0.0022	**0.0368**	−0.0120	0.3703	−0.6440	0.7128
−0.0120	0.0240	0.0047	0.0138	−0.0054	−0.0002	**0.0051**	0.5908	−0.4641	0.1785
0.0051	−0.0103	0.0021	0.0118	−0.0019	0.0085	0.0050	**0.0144**	−0.4605	0.4222
0.0114	−0.0229	−0.0029	−0.0061	0.0076	−0.0108	−0.0029	−0.0048	**0.0076**	−0.6189
0.0134	−0.0283	0.0032	0.0048	0.0015	0.0171	0.0016	0.0063	−0.0067	**0.0157**

(iii) males distal

0.1090	−0.9970	−0.4222	−0.2788	0.9206	0.5549	−0.3505	0.7087	0.5363	0.0980
−0.2175	**0.4367**	0.3549	0.2092	−0.8923	−0.5329	0.2801	−0.7254	−0.5016	−0.1107
−0.0355	0.0598	**0.0650**	0.9644	−0.6715	−0.5506	0.9876	−0.1036	−0.5917	0.2994
−0.0666	0.1000	0.1779	**0.5231**	−0.5464	−0.3357	0.9543	0.0416	−0.6285	0.4420
0.0504	−0.0978	−0.0284	−0.0655	**0.2749**	0.6253	−0.6370	0.5490	0.6501	0.0999
0.0187	−0.0360	−0.0144	−0.0248	0.0106	**0.0105**	−0.5276	0.6063	0.0298	0.2490
−0.0305	0.0487	0.0663	0.1818	−0.0278	−0.0142	**0.0694**	−0.3740	−0.5934	0.2100
0.0100	−0.0205	−0.0011	0.0013	0.0039	0.0026	−0.0004	**0.0018**	0.2330	0.1859
0.0109	−0.0204	−0.0093	−0.0280	0.0066	0.0002	−0.0096	0.0006	**0.0038**	−0.2524
0.0040	−0.0091	0.0095	0.0396	0.0021	0.0032	0.0069	0.0010	−0.0019	**0.0153**

(iv) males proximal

0.0444	−0.9994	−0.1514	0.1349	0.5468	0.2783	0.1494	−0.2518	0.1533	0.1329
−0.0867	**0.1695**	0.1289	−0.1530	−0.5371	−0.2935	−0.1551	0.2578	−0.1460	−0.1205
−0.0022	0.0036	**0.0047**	0.7688	−0.4553	0.1034	0.4506	0.2676	−0.2125	−0.8312
0.0067	−0.0149	0.0124	**0.0557**	−0.4716	0.1329	0.8266	0.4498	−0.4600	−0.3631
0.0124	−0.0238	−0.0033	−0.0120	**0.0116**	−0.3572	−0.4873	−0.7867	0.8496	0.2639
0.0116	−0.0239	0.0014	0.0062	−0.0076	**0.0391**	−0.4312	0.1845	−0.6194	−0.0610
0.0041	−0.0083	0.0040	0.0254	−0.0068	−0.0011	**0.0169**	0.5736	−0.4867	−0.1207
−0.0077	0.0015	0.0026	0.0154	−0.0123	0.0053	0.0108	**0.0211**	−0.8093	−0.1934
0.0030	−0.0055	−0.0013	−0.0099	0.0084	−0.0112	−0.0058	−0.0108	**0.0084**	−0.0082
0.0032	−0.0057	−0.0066	−0.0099	0.0033	−0.0014	−0.0018	−0.0032	−0.0001	**0.0134**

NB variances in bold on diagonal, covariance lower left, correlation upper right

Table A.17. Principal component analyses – conventional data (normalized)

(a) *Homo*

	females				males			
	distal		proximal		distal		proximal	
	U_1	U_2	U_1	U_2	U_1	U_2	U_1	U_2
P	0.2312	0.9729	0.2344	0.9721	0.2324	0.9726	0.2335	0.9724
A	−0.9729	0.2312	−0.9721	0.2344	−0.9726	0.2324	−0.9724	0.2335
I^*	33.5878	0.0000	22.6718	0.0000	31.1702	0.0000	34.2302	0.0000
%	100.00	0.00	100.00	0.00	100.00	0.00	100.00	0.00

(b) *Cercopithecus*

	females				males			
	distal		proximal		distal		proximal	
	U_1	U_2	U_1	U_2	U_1	U_2	U_1	U_2
P	0.2490	0.9685	0.2565	0.9666	0.2466	0.9691	0.2539	0.9672
A	−0.9685	0.2490	−0.9666	0.2565	−0.9691	0.2466	−0.9672	0.2539
I^*	25.4513	0.0000	12.6632	0.0000	55.1571	0.0000	24.5533	0.0000
%	100.00	0.00	100.00	0.00	100.00	0.00	100.00	0.00

(c) *Colobus*

	females				males			
	distal		proximal		distal		proximal	
	U_1	U_2	U_1	U_2	U_1	U_2	U_1	U_2
P	0.2447	0.9696	0.2519	0.9678	0.2459	0.9693	0.2505	0.9681
A	−0.9696	0.2447	−0.9678	0.2519	−0.9693	0.2459	−0.9681	0.2505
I^*	13.6837	0.0000	20.4869	0.0000	39.9048	0.0000	45.2566	0.0000
%	100.00	0.00	100.00	0.00	100.00	0.00	100.00	0.00

(d) *Gorilla*

	females				males			
	distal		proximal		distal		proximal	
	U_1	U_2	U_1	U_2	U_1	U_2	U_1	U_2
P	0.2263	0.9740	0.2369	0.9715	0.2358	0.9718	0.2405	0.9707
A	−0.9740	0.2263	−0.9715	0.2369	−0.9718	0.2358	−0.9707	0.2405
I^*	44.1193	0.0000	28.0521	0.0000	19.0965	0.0000	8.1716	0.0000
%	100.00	0.00	100.00	0.00	100.00	0.00	100.00	0.00

Table A.18. Principal component analyses – Fourier data (normalized)

(a) *Homo*

(i) females distal

	U_1	U_2	U_3	U_4	U_5	U_6	U_7	U_8	U_9	U_{10}
X1	0.4318	0.0116	0.0235	0.0004	0.0531	0.0541	0.0565	0.0140	0.4928	0.7489
Y1	−0.8775	−0.1206	0.0137	−0.0223	−0.0017	−0.0653	−0.1262	0.0505	0.2825	0.3350
X2	−0.0774	0.1114	−0.2331	0.8296	−0.1618	0.4189	0.0351	−0.1712	−0.0513	0.0653
Y2	−0.0819	0.9078	−0.2546	−0.1764	0.1082	−0.0560	−0.1910	−0.1136	−0.0450	0.0838
X3	0.1429	−0.0998	−0.2557	0.1321	0.0430	−0.1021	−0.6359	0.1246	0.5525	−0.3864
Y3	0.0333	0.2734	0.7337	0.3141	−0.3433	−0.3274	−0.1853	0.1654	0.0202	−0.0010
X4	−0.0599	0.2144	−0.0214	0.0147	0.0583	0.2602	0.4070	0.7860	0.2398	−0.1942
Y4	0.0254	−0.0149	−0.4418	−0.0875	−0.7816	−0.3614	0.2198	0.0468	0.0603	0.0239
X5	0.0626	−0.1234	−0.2757	0.2335	0.2323	−0.3679	−0.2600	0.4958	−0.4949	0.3204
Y5	0.0339	−0.0524	0.0689	−0.3188	−0.4138	0.6025	−0.4721	0.2151	−0.2470	0.1593
l	0.8767	0.2798	0.0763	0.0296	0.0256	0.0165	0.0105	0.0027	0.0006	0.0004
%	66.48	21.22	5.79	2.24	1.94	1.25	0.80	0.20	0.00	0.00

(ii) females proximal

	U_1	U_2	U_3	U_4	U_5	U_6	U_7	U_8	U_9	U_{10}
X1	0.4354	0.1181	0.0199	0.0459	0.0183	0.0924	0.0282	0.0070	0.1807	0.8668
Y1	−0.8118	−0.3205	−0.0700	−0.0329	0.0104	−0.1048	−0.0642	0.0201	0.1739	0.4317
X2	−0.1323	0.2158	0.4693	−0.6241	0.2976	0.2418	0.0635	0.3642	−0.1964	0.0630
Y2	−0.2787	0.7508	0.2629	0.3193	−0.3078	−0.2688	−0.0632	0.0368	−0.1003	0.0717
X3	0.1702	−0.0369	0.1626	−0.1379	0.1214	−0.5708	−0.3054	0.3218	0.6065	−0.1377
Y3	−0.0693	0.4576	−0.7635	−0.4162	0.1292	−0.0635	−0.0378	−0.0422	0.0754	0.0014
X4	−0.1111	0.2134	0.2522	−0.0196	0.2517	0.3265	−0.0037	−0.6363	0.5364	−0.1249
Y4	0.0518	−0.0900	0.1104	−0.4833	−0.6771	−0.1795	0.4273	−0.2241	0.1414	0.0013
X5	0.0579	−0.0548	0.1246	−0.1078	0.4190	−0.6113	0.1123	−0.4825	−0.3967	0.1206
Y5	0.0638	−0.0733	0.0690	−0.2599	−0.2958	0.0860	−0.8350	−0.2689	−0.2232	0.0631
l	0.6493	0.3121	0.0832	0.0350	0.0228	0.0119	0.0085	0.0016	0.0004	0.0002
%	57.72	27.74	7.40	3.11	2.02	1.05	0.76	0.14	0.04	0.02

(iii) males distal

	U_1	U_2	U_3	U_4	U_5	U_6	U_7	U_8	U_9	U_{10}
X1	0.4246	0.0229	0.0323	0.0627	0.0076	0.0591	0.1085	0.0020	0.1179	0.8860
Y1	−0.8804	0.0493	−0.0321	−0.0699	0.0331	−0.0297	−0.1219	0.0668	0.1050	0.4292
X2	−0.0112	−0.1821	−0.0520	−0.1628	−0.3973	−0.8215	0.2723	−0.1592	−0.0479	0.0551
Y2	−0.0172	−0.9182	−0.2074	0.1580	0.0743	0.1094	−0.2182	−0.1243	−0.0693	0.0566
X3	0.1705	0.0672	−0.2401	−0.0575	0.0050	−0.2747	−0.5940	0.2181	0.6520	−0.0669
Y3	0.0369	−0.2242	0.8686	−0.3132	0.0507	−0.0796	−0.2337	0.1793	0.0001	0.0117
X4	−0.0478	−0.2063	−0.0073	0.1920	−0.1527	0.0626	0.4566	0.7931	0.2187	−0.0747
Y4	0.0648	−0.1004	−0.3159	−0.8949	0.0530	0.2231	0.1469	0.1029	−0.0074	0.0138
X5	0.0835	0.0985	−0.1979	0.0180	0.2988	−0.3055	−0.3042	0.4728	−0.6589	0.1051
Y5	0.0185	0.0597	−0.0325	−0.0154	−0.8471	0.2828	−0.3486	0.1086	−0.2468	0.0554
l	0.6957	0.1748	0.0862	0.0373	0.0192	0.0166	0.0086	0.0020	0.0006	0.0002
%	66.82	16.79	8.28	3.58	1.85	1.60	0.83	0.19	0.06	0.02

(iv) males proximal

	U_1	U_2	U_3	U_4	U_5	U_6	U_7	U_8	U_9	U_{10}
X1	0.4323	0.0193	0.0912	0.0344	0.0159	0.0624	0.1089	0.0411	0.1897	0.8657
Y1	−0.8691	0.0626	−0.1166	−0.0046	−0.0617	−0.0671	−0.0940	0.0257	0.1721	0.4240
X2	0.0568	−0.1539	−0.3836	−0.5889	−0.5384	−0.0305	0.2663	−0.3356	−0.0531	0.0450
Y2	0.0127	−0.8199	−0.4009	0.2272	0.2655	0.0151	−0.1580	−0.0938	−0.0676	0.0784
X3	0.1875	0.0668	−0.1517	−0.0206	−0.1308	−0.3145	−0.5347	−0.1060	0.7107	−0.1367
Y3	−0.0858	−0.4897	0.7460	−0.3731	−0.1101	−0.1219	−0.1507	0.0747	0.0419	0.0071
X4	0.0183	−0.1772	−0.1724	0.0489	−0.2928	−0.0029	0.2829	0.8376	0.2377	−0.1108
Y4	0.0230	0.1102	−0.2090	−0.6699	0.5607	0.2409	−0.2060	0.2819	0.0194	0.0153
X5	0.0932	0.0890	−0.1007	0.0272	−0.3930	0.0261	−0.6590	0.2543	−0.5423	0.1560
Y5	0.0477	0.0635	−0.0846	−0.0940	0.2276	−0.9044	0.1343	0.1172	−0.2631	0.0836
l	0.7649	0.2438	0.0751	0.0354	0.0205	0.0121	0.0080	0.0020	0.0004	0.0002
%	65.81	20.98	6.46	3.04	1.76	1.04	0.68	0.17	0.04	0.01

Table A.18. (continued)

(b) *Cercopithecus*

(i) females distal

	U_1	U_2	U_3	U_4	U_5	U_6	U_7	U_8	U_9	U_{10}
X1	0.4984	0.0309	0.0493	0.0278	0.0624	0.0300	0.0449	0.0382	0.5660	0.6472
Y1	−0.8378	0.0085	−0.0756	−0.0165	0.0286	−0.0151	−0.0725	−0.1650	0.3996	0.3145
X2	0.0173	−0.2557	0.0664	−0.0212	−0.2725	0.7918	−0.4731	−0.0309	−0.0341	0.0488
Y2	0.0043	−0.9210	0.0149	−0.0074	0.0548	−0.3478	−0.1113	0.0999	−0.0193	0.0693
X3	0.1999	−0.0202	−0.2946	−0.2391	0.0971	−0.1048	−0.2978	−0.4826	0.4788	−0.4944
Y3	0.0040	0.0327	0.8647	−0.1390	−0.1618	−0.1732	−0.0599	−0.4147	−0.0056	−0.0073
X4	−0.0143	−0.2881	0.1007	0.0768	−0.0381	0.3767	0.7949	−0.2839	0.1599	−0.1713
Y4	0.0332	0.0266	−0.2174	0.1083	−0.9297	−0.2549	0.0592	−0.0279	0.0713	0.0217
X5	0.0901	−0.0098	−0.2808	0.2735	0.1042	−0.0495	−0.0696	−0.6874	−0.4543	0.3757
Y5	0.0066	−0.0096	−0.1627	−0.9108	−0.0760	0.0261	0.1551	−0.0397	−0.2283	0.2443
l	1.0015	0.1884	0.0744	0.0122	0.0117	0.0064	0.0028	0.0014	0.0004	0.0001
%	77.07	14.50	5.72	0.94	0.90	0.50	0.21	0.11	0.03	0.01

(ii) females proximal

	U_1	U_2	U_3	U_4	U_5	U_6	U_7	U_8	U_9	U_{10}
X1	0.5387	0.0827	0.0353	0.0547	0.0813	0.0085	0.0905	0.0420	0.2230	0.7952
Y1	−0.8071	−0.0730	−0.0269	−0.0360	−0.0643	0.0252	−0.1038	0.0096	0.2805	0.4969
X2	0.0027	−0.3188	0.0751	0.3513	−0.0237	−0.8656	0.0607	0.1018	0.0729	−0.0106
Y2	0.0972	−0.8818	0.0186	−0.0998	0.1263	0.2302	−0.0368	−0.3568	−0.0478	0.0530
X3	0.1994	−0.0067	−0.3413	−0.1384	−0.3266	0.0095	−0.3740	−0.1091	0.7166	−0.2290
Y3	0.0575	−0.0211	0.8545	−0.0824	−0.1877	−0.1180	−0.4539	0.0302	0.0543	−0.0138
X4	0.0344	−0.3097	0.0048	−0.1465	0.0358	0.1764	0.0715	0.9066	0.1259	−0.0781
Y4	−0.0010	−0.0374	−0.0243	0.8834	−0.0672	0.3665	−0.2672	0.0820	−0.0108	−0.0231
X5	0.0512	0.0194	−0.3650	−0.1785	0.1570	−0.1282	−0.7317	0.1327	−0.4531	0.1805
Y5	0.0462	−0.1026	−0.1070	−0.0515	−0.8946	0.0327	0.1351	0.0370	−0.3553	0.1611
l	0.7182	0.1076	0.0439	0.0159	0.0112	0.0043	0.0018	0.0014	0.0003	0.0001
%	79.39	11.89	4.85	1.75	1.24	0.47	0.20	0.16	0.04	0.01

(iii) males distal

	U_1	U_2	U_3	U_4	U_5	U_6	U_7	U_8	U_9	U_{10}
X1	0.4932	0.0275	0.0138	0.0489	0.0368	0.0426	0.0767	0.0444	0.7362	0.4477
Y1	−0.8384	−0.0094	−0.0427	−0.0288	−0.0602	−0.1218	−0.0569	−0.1870	0.4776	0.1559
X2	0.0153	−0.2980	−0.0552	−0.1320	−0.2475	0.8491	−0.3275	0.0313	0.0067	−0.0008
Y2	0.0360	−0.9016	−0.1534	0.1707	0.0697	−0.3142	−0.1005	−0.1299	0.0033	0.0506
X3	0.1861	0.0757	−0.2517	0.1710	−0.2545	0.0139	0.1056	−0.4643	0.3146	−0.6902
Y3	0.0520	−0.1432	0.8775	−0.0701	−0.0620	0.0527	0.1570	−0.4119	−0.0290	−0.0227
X4	−0.0207	−0.2411	−0.0797	−0.1869	−0.0216	0.1981	0.8666	0.3091	−0.0110	−0.1176
Y4	0.0985	−0.0369	−0.1418	−0.9272	−0.1028	−0.2332	−0.1071	−0.1759	0.0410	−0.0017
X5	0.0672	0.1043	−0.3335	0.0671	0.1460	0.1958	0.2641	−0.6556	−0.3275	0.4500
Y5	0.0186	0.0289	−0.0183	0.1298	−0.9099	−0.2085	0.0744	0.0610	−0.1470	0.2817
l	1.8985	0.1796	0.0603	0.0439	0.0203	0.0113	0.0060	0.0057	0.0011	0.0005
%	85.24	8.06	2.71	1.97	0.91	0.51	0.27	0.26	0.05	0.02

(iv) males proximal

	U_1	U_2	U_3	U_4	U_5	U_6	U_7	U_8	U_9	U_{10}
X1	0.5316	0.0150	0.0317	0.0069	0.0336	0.0588	0.1577	0.0192	0.3835	0.7343
Y1	−0.8083	−0.0370	−0.0586	−0.0105	−0.1413	−0.0481	−0.0768	−0.0075	0.3638	0.4256
X2	−0.0080	0.3582	−0.0868	0.3683	−0.0084	0.7493	−0.3772	0.1514	0.0406	−0.0051
Y2	0.0297	0.7276	−0.4512	−0.1261	−0.1080	−0.3829	0.0213	0.2907	−0.0707	0.0446
X3	0.2233	−0.2218	−0.2828	−0.0233	−0.4464	−0.1040	−0.2942	0.0101	0.6184	−0.0078
Y3	0.0492	0.3814	0.7689	−0.0890	−0.2738	−0.2014	−0.3404	−0.1282	0.0712	−0.0078
X4	−0.0119	0.3108	−0.1768	0.1239	0.0601	0.0438	0.2053	−0.8827	0.1450	−0.0943
Y4	−0.0049	−0.0372	0.0924	0.8931	−0.1625	−0.3282	0.2115	0.1142	−0.0176	−0.0136
X5	0.1004	−0.2058	−0.2615	0.1232	0.0241	−0.2601	−0.6893	−0.2724	−0.3826	0.3163
Y5	0.0225	−0.0756	−0.0706	−0.1077	−0.8138	0.2397	0.2493	−0.0965	−0.3986	0.1646
l	1.2803	0.1706	0.0829	0.0327	0.0221	0.0120	0.0063	0.0043	0.0011	0.0003
%	79.39	10.58	5.14	2.03	1.37	0.74	0.39	0.27	0.07	0.02

Table A.18. (continued)

(c) *Colobus*

(i) females distal

	U_1	U_2	U_3	U_4	U_5	U_6	U_7	U_8	U_9	U_{10}
X1	0.4713	0.0637	0.0940	0.0905	0.1400	0.0458	0.1157	0.0266	0.5626	0.6360
Y1	−0.7825	−0.1653	−0.2419	−0.0544	−0.1587	0.0823	0.0653	−0.0761	0.4106	0.2970
X2	−0.2034	0.2551	0.1863	0.1118	0.3010	−0.1549	−0.7564	0.3558	0.1814	−0.0111
Y2	−0.1668	0.7732	0.3477	−0.1276	−0.1812	0.3665	0.1053	−0.2107	−0.0817	0.0882
X3	0.1698	−0.1242	0.2364	−0.1039	−0.4195	0.0157	−0.2034	−0.2862	0.5784	−0.5051
Y3	0.1855	0.4420	−0.7729	−0.0751	−0.1613	−0.2581	−0.1874	−0.1885	0.0610	−0.0147
X4	−0.1719	0.2275	0.2422	0.1391	0.1403	−0.7799	0.4117	−0.0909	0.1415	−0.1220
Y4	−0.0101	0.0603	−0.0425	0.9038	−0.3899	0.0909	0.0216	0.1229	−0.0370	−0.0179
X5	0.0007	−0.1985	0.2254	0.0413	−0.2189	−0.2852	−0.3905	−0.5782	−0.3250	0.4317
Y5	0.0589	0.0069	0.1114	−0.3251	−0.6404	−0.2609	0.0147	0.5894	−0.1001	0.2064
l	0.8631	0.1702	0.0668	0.0109	0.0100	0.0038	0.0028	0.0015	0.0004	0.0001
%	76.41	15.07	5.91	0.96	0.89	0.34	0.24	0.13	0.03	0.01

(ii) females proximal

	U_1	U_2	U_3	U_4	U_5	U_6	U_7	U_8	U_9	U_{10}
X1	0.5276	0.0651	0.0310	0.0702	0.0171	0.1080	0.0260	0.0706	0.6139	0.5631
Y1	−0.8294	−0.0524	−0.0104	0.0007	−0.0231	−0.0706	0.0136	−0.0158	0.3260	0.4438
X2	0.0405	−0.4370	−0.2642	−0.6369	−0.2984	0.1792	0.4291	0.1549	0.0499	−0.0125
Y2	0.0636	−0.7860	−0.1035	0.5217	0.2580	−0.0621	0.0482	−0.2930	0.0426	−0.0290
X3	0.1461	0.0707	−0.3562	−0.0875	−0.1936	−0.4478	−0.0766	−0.2476	−0.4880	0.5439
Y3	0.0504	−0.0679	0.7471	0.0008	−0.3951	−0.4405	0.2878	0.0319	−0.0191	0.0193
X4	0.0049	−0.2561	−0.0203	0.1004	−0.2375	−0.0604	−0.5233	0.7569	−0.1055	0.0768
Y4	0.0534	−0.3186	0.3445	−0.5324	0.4456	−0.0852	−0.4759	−0.2325	0.0027	0.0851
X5	0.0356	0.0428	−0.3327	−0.0971	0.1472	−0.7265	−0.0008	0.1028	0.4336	−0.3587
Y5	−0.0039	0.0766	−0.0602	−0.0815	−0.6628	0.1185	−0.4729	−0.4302	0.2736	−0.2168
l	1.0539	0.1826	0.0549	0.0249	0.0143	0.0086	0.0055	0.0021	0.0003	0.0001
%	78.23	13.55	4.08	1.85	1.06	0.64	0.41	0.16	0.02	0.01

(iii) males distal

	U_1	U_2	U_3	U_4	U_5	U_6	U_7	U_8	U_9	U_{10}
X1	0.4792	0.0279	0.0263	0.0413	0.1257	0.0326	0.1376	0.0176	0.2215	0.8259
Y1	−0.8451	−0.0079	−0.0676	0.0570	−0.0751	−0.1061	0.2076	0.0159	0.2199	0.4116
X2	−0.2587	−0.4441	−0.1197	−0.1561	0.5865	0.2806	0.5646	0.0058	−0.0465	−0.1405
Y2	0.0575	−0.8472	0.0555	0.1819	−0.3349	−0.2385	−0.1239	0.1483	−0.1592	0.1050
X3	0.2104	0.0265	−0.2236	0.0371	−0.2923	−0.3150	0.4275	0.1973	0.6351	−0.3065
Y3	−0.0121	−0.0347	0.8982	−0.2464	−0.0657	−0.1227	0.2215	−0.2053	0.1303	−0.0608
X4	−0.0278	−0.2832	−0.1527	−0.3398	0.0169	0.2360	−0.4421	−0.4800	0.5457	−0.0267
Y4	−0.0091	0.0171	−0.1255	−0.8539	−0.0770	−0.1922	−0.0628	0.4138	−0.1542	0.1137
X5	0.0797	0.0383	−0.2829	−0.1435	−0.1499	−0.4139	0.2911	−0.7023	−0.3397	0.0654
Y5	0.0265	0.0157	−0.0387	−0.1018	−0.6356	0.6883	0.2966	−0.0379	−0.1334	0.0471
l	1.6755	0.1980	0.1487	0.0150	0.0117	0.0057	0.0021	0.0018	0.0004	0.0001
%	81.38	9.62	7.22	0.73	0.57	0.28	0.10	0.09	0.02	0.00

(iv) males proximal

	U_1	U_2	U_3	U_4	U_5	U_6	U_7	U_8	U_9	U_{10}
X1	0.5190	0.0046	0.0256	0.1511	0.0730	0.2005	0.0473	0.3987	0.2866	0.6467
Y1	−0.8226	−0.0240	−0.0420	0.1171	−0.0948	0.0684	0.0843	0.1741	0.3680	0.3475
X2	−0.0149	0.1220	−0.0300	−0.1254	−0.7017	0.5515	−0.0574	0.2449	−0.3250	−0.0529
Y2	−0.0027	0.6771	−0.3837	−0.4983	0.2207	0.1621	0.1772	−0.1208	0.1503	0.0487
X3	0.2076	−0.1637	−0.2564	−0.1894	−0.3773	−0.1002	0.1552	0.0671	0.6996	−0.4400
Y3	0.0356	0.5629	0.7024	0.0926	−0.2624	−0.2517	−0.0277	−0.0700	0.2040	−0.1954
X4	−0.0334	0.0265	−0.1495	−0.3889	−0.1029	−0.5436	−0.5138	0.4945	−0.0728	0.0686
Y4	−0.0116	−0.4046	0.4578	−0.7031	0.0759	0.2374	−0.0440	−0.1431	0.2043	0.0770
X5	0.0875	−0.0659	−0.2414	−0.0130	−0.4086	−0.1813	−0.2462	−0.6733	0.0339	0.4632
Y5	0.0219	−0.1164	0.0151	−0.2114	−0.2234	−0.4080	0.7775	0.0920	−0.2738	0.1915
l	2.0944	0.0958	0.0589	0.0191	0.0073	0.0068	0.0040	0.0017	0.0003	0.0002
%	91.52	4.18	2.57	0.83	0.32	0.30	0.17	0.07	0.01	0.01

Table A.18. (continued)

(d) *Gorilla*

(i) females distal

	U_1	U_2	U_3	U_4	U_5	U_6	U_7	U_8	U_9	U_{10}
X1	0.3643	0.1029	0.1136	0.0220	0.0167	0.2231	0.2831	0.1774	0.6584	0.4981
Y1	−0.8606	−0.1964	−0.1550	−0.0496	−0.0387	0.1031	0.2434	−0.0907	0.2944	0.1674
X2	0.0897	−0.1799	−0.0751	−0.0183	−0.0733	−0.9141	0.2616	−0.0658	0.0664	0.1883
Y2	0.3031	−0.6839	−0.5100	−0.0413	0.0619	0.2582	0.2931	0.0016	−0.1166	−0.0930
X3	0.1280	0.2508	−0.1099	0.0874	−0.1911	0.0230	0.2697	−0.6143	0.3573	−0.5349
Y3	0.0399	−0.4900	0.7464	−0.1448	−0.2812	0.1008	0.0503	−0.2902	−0.0597	0.0262
X4	0.0538	−0.2779	−0.1698	0.0515	0.1446	−0.0748	−0.7602	−0.3487	0.3776	0.1403
Y4	−0.0506	−0.1156	0.2051	0.8431	0.4426	−0.0062	0.1457	−0.0960	−0.0696	0.0081
X5	0.0568	0.2387	−0.1563	−0.0720	0.0381	0.1355	0.1114	−0.5914	−0.4223	0.5915
Y5	0.0042	−0.0151	−0.1814	0.4978	−0.8094	0.0514	−0.1391	0.1173	−0.0694	0.1526
l	0.9367	0.1341	0.0329	0.0180	0.0123	0.0006	0.0005	0.0002	0.0001	0.0000
%	82.50	11.81	2.89	1.58	1.08	0.05	0.05	0.01	0.01	0.00

(ii) females proximal

	U_1	U_2	U_3	U_4	U_5	U_6	U_7	U_8	U_9	U_{10}
X1	0.4328	0.0074	0.0370	0.0405	0.0526	0.0673	0.0936	0.3447	0.2901	0.7685
Y1	−0.8772	−0.0503	−0.0896	0.0034	0.0056	−0.1217	0.0692	0.2589	0.1859	0.3142
X2	−0.0474	0.2258	0.1475	−0.2132	−0.3044	0.1206	0.8655	0.1238	0.0005	0.0886
Y2	−0.0880	0.7034	0.5695	−0.2046	0.1403	−0.0926	0.2531	−0.1814	0.0548	0.0545
X3	0.1456	−0.1077	0.1761	−0.1241	−0.1807	−0.5125	0.0330	0.4091	0.5338	−0.4147
Y3	0.0869	0.4423	−0.6377	−0.2918	0.4151	−0.1970	−0.0709	0.2640	−0.1067	−0.0877
X4	−0.0371	0.1851	0.1181	0.2100	−0.0625	0.5842	0.1833	0.6448	−0.1431	−0.3020
Y4	0.0139	0.2921	−0.0219	0.8706	0.0752	−0.3226	−0.2150	−0.0041	−0.0049	−0.0025
X5	0.0336	−0.2026	0.3036	−0.0905	0.0336	−0.4383	0.0075	0.3331	−0.7314	0.1351
Y5	0.0418	0.2894	−0.3165	−0.0135	−0.8180	−0.1364	0.2953	−0.0457	−0.1625	0.1034
l	0.7710	0.0728	0.0361	0.0103	0.0068	0.0013	0.0004	0.0002	0.0001	0.0000
%	85.77	8.09	4.01	1.15	0.76	0.14	0.04	0.02	0.01	0.00

(iii) males distal

	U_1	U_2	U_3	U_4	U_5	U_6	U_7	U_8	U_9	U_{10}
X1	0.2773	0.3293	0.0143	0.0366	0.0526	0.0217	0.1247	0.4309	0.0132	0.7801
Y1	−0.5172	−0.7101	−0.1194	0.0243	−0.0136	−0.0231	−0.1071	0.2793	0.0442	0.3483
X2	−0.2629	0.1429	0.2394	0.2774	0.2391	−0.2406	−0.2756	−0.5117	−0.4554	0.3406
Y2	−0.6954	0.5658	−0.1968	−0.1240	−0.3237	0.1315	0.0171	0.1322	−0.0278	−0.0393
X3	0.1670	0.0963	−0.1775	0.2249	−0.0445	0.1273	−0.8819	0.2653	0.0372	−0.1141
Y3	0.0653	0.0331	−0.4262	−0.6539	0.1118	−0.2649	−0.2344	−0.3551	0.2621	0.2303
X4	−0.2584	0.1703	0.4272	0.0087	0.5468	−0.1540	−0.0790	0.1537	0.5987	−0.1033
Y4	0.0176	0.0420	−0.0298	−0.1525	0.0549	−0.7500	0.0154	0.4514	−0.3800	−0.2446
X5	0.0504	−0.0004	0.1107	0.3390	−0.6265	−0.4851	−0.0122	−0.1733	0.4473	0.1102
Y5	−0.0334	0.0758	−0.6933	0.5380	0.3551	−0.1258	0.2396	−0.0554	0.1293	−0.0630
l	0.7807	0.4513	0.0203	0.0066	0.0014	0.0011	0.0007	0.0001	0.0000	0.0000
%	61.86	35.76	1.61	0.52	0.11	0.08	0.05	0.00	0.00	0.00

(iv) males proximal

	U_1	U_2	U_3	U_4	U_5	U_6	U_7	U_8	U_9	U_{10}
X1	0.4436	0.0244	0.0234	0.0610	0.0894	0.0138	0.1037	0.0395	0.8795	0.0652
Y1	−0.8685	−0.0262	−0.0346	−0.0503	−0.1060	0.0084	0.0588	−0.0962	0.4577	−0.0885
X2	−0.0160	−0.1667	0.0658	−0.3263	0.0751	0.0089	−0.1105	−0.5008	0.0045	0.7697
Y2	0.0858	−0.7313	0.3134	−0.2228	−0.3721	0.3595	0.0761	0.1176	0.0131	−0.1500
X3	0.1181	0.2698	0.1896	−0.1018	−0.0382	0.3354	−0.2822	−0.6725	0.0319	−0.4692
Y3	0.1333	−0.2025	−0.8524	−0.2319	−0.1934	−0.0774	0.1706	−0.2376	0.0018	−0.1786
X4	0.0440	−0.3590	0.2218	0.3044	−0.0380	−0.7520	−0.1462	−0.3468	0.0085	−0.1997
Y4	−0.0794	−0.3466	−0.1324	0.4917	0.6094	0.3806	0.2299	−0.2020	−0.0662	−0.0101
X5	0.0248	0.2242	0.2524	−0.2408	0.0150	−0.0570	0.8851	−0.1645	−0.1022	−0.0561
Y5	0.0286	0.1523	−0.0516	0.6174	−0.6517	0.1960	0.1505	−0.1663	−0.0279	0.2791
l	0.2244	0.0888	0.0414	0.0177	0.0098	0.0023	0.0001	0.0000	0.0000	0.0000
%	58.34	23.09	10.77	4.61	2.55	0.60	0.03	0.00	0.00	0.00

Table A.19. Kolmogorov-Smirnov Z – conventional data

(a) *Homo*

	P	*A*	ln*P*	ln*A*
females distal	0.876	0.662	0.761	0.674
females proximal	0.910	0.791	0.911	0.869
males distal	0.793	1.037	0.891	1.190
males proximal	0.747	0.794	0.898	0.706

(b) *Cercopithecus*

	P	*A*	ln*P*	ln*A*
females distal	0.624	0.543	0.534	0.518
females proximal	0.591	0.672	0.592	0.745
males distal	1.232	[a]1.425	1.344	[b]1.517
males proximal	0.664	0.835	0.901	1.078

[a]significant at $p = 0.035$ [b]significant at $p = 0.020$

(c) *Colobus*

	P	*A*	ln*P*	ln*A*
females distal	0.613	0.564	0.580	0.632
females proximal	0.767	0.569	0.819	0.647
males distal	0.878	0.784	0.962	0.823
males proximal	0.692	0.626	0.777	0.709

(d) *Gorilla*

	P	*A*	ln*P*	ln*A*
females distal	0.771	0.659	0.664	0.585
females proximal	0.614	0.923	0.544	0.852
males distal	0.616	0.506	0.649	0.493
males proximal	0.803	0.721	0.825	0.718

Table A.20. Kolmogorov-Smirnov $Z - |x|$, conventional data

(a) *Homo*

	Z
females distal	0.875
females proximal	0.926
males distal	0.810
males proximal	0.756

(b) *Cercopithecus*

	Z
females distal	0.605
females proximal	0.636
males distal	1.264
males proximal	0.676

(c) *Colobus*

	Z
females distal	0.597
females proximal	0.760
males distal	0.915
males proximal	0.686

(d) *Gorilla*

	Z
females distal	0.759
females proximal	0.615
males distal	0.613
males proximal	0.794

Table A.21. Size variances, *F*-ratios and 95% confidence intervals – conventional data

(a) *Homo*, distal

	s^2	$F_{m,f}$	95% CI
male	2060.48	1.27	0.91 to 1.78
female	1618.06		

(b) *Homo*, proximal

	s^2	$F_{f,m}$	95% CI
male	2077.93	1.23	0.83 to 1.81
female	2552.79		

(c) *Cercopithecus*, distal

	s^2	$F_{m,f}$	95% CI
male	590.18	*4.87	2.75 to 8.63
female	121.08		

*significant at $p = 0.00$

(d) *Cercopithecus*, proximal

	s^2	$F_{m,f}$	95% CI
male	624.90	*6.09	3.44 to 10.77
female	102.64		

*significant at $p = 0.00$

(e) *Colobus*, distal

	s^2	$F_{m,f}$	95% CI
male	342.05	1.49	0.65 to 3.57
female	229.11		

(f) *Colobus*, proximal

	s^2	$F_{m,f}$	95% CI
male	383.00	1.12	0.49 to 2.68
female	342.09		

Table A.21. (continued)

(g) *Gorilla*, distal

	s^2	$F_{f,m}$	95% CI
male	3170.10	1.00	0.24 to 3.20
female	3170.91		

(h) *Gorilla*, proximal

	s^2	$F_{m,f}$	95% CI
male	4382.23	2.62	0.64 to 8.38
female	1675.52		

Table A.22. Single-classification analysis of variance for mean size difference – conventional data

(a) *Homo*, distal

	female	male
n_i	102	101
ΣY	59469.44	64666.46
$\hat{Y}_i$	583.03	640.26
Σy_i^2	170494.13	206047.81
$\hat{Y}_{grand}$	611.51	

source of variation	df	SS	MS	*F*	95% CI
among sexes	1	166205.61	166205.61	*88.72	45.35 to 69.10
within sexes	201	376541.95	1873.34		

*significant at $p = 0.00$

(b) *Homo*, proximal

	female	male
n_i	106	99
ΣY	59006.53	59673.49
$\hat{Y}_i$	556.67	602.76
Σy_i^2	268043.13	203636.88
$\hat{Y}_{grand}$	578.93	

source of variation	df	SS	MS	*F*	95% CI
among sexes	1	108776.85	108776.85	*46.82	32.81 to 59.38
within sexes	203	471680.00	2323.55		

*significant at $p = 0.00$

(c) *Cercopithecus*, distal

	female	male
n_i	49	49
ΣY	6140.50	7374.50
$\hat{Y}_i$	125.32	150.50
Σy_i^2	5811.63	28328.88
$\hat{Y}_{grand}$	137.91	

source of variation	df	SS	MS	*F*	95% CI
among sexes	1	15538.24	15538.24	*43.69	17.62 to 32.75
within sexes	96	34140.51	355.63		

*significant at $p = 0.00$

Table A.22. (continued)

(d) *Cercopithecus*, proximal

	female	male
n_i	49	50
ΣY	6350.88	7827.01
$\hat{Y}_i$	129.61	156.54
Σy_i^2	4926.94	30619.97
$\hat{Y}_{grand}$	143.21	

source of variation	df	SS	MS	F	95% CI
among sexes	1	17947.75	17947.75	*48.98	19.29 to 34.57
within sexes	97	35546.91	366.46		

*significant at $p = 0.00$

(e) *Colobus*, distal

	female	male
n_i	26	21
ΣY	4424.03	3866.96
$\hat{Y}_i$	170.16	184.14
Σy_i^2	5727.75	6841.05
$\hat{Y}_{grand}$	176.40	

source of variation	df	SS	MS	F	95% CI
among sexes	1	2272.37	2272.37	*8.14	4.11 to 23.86
within sexes	45	12568.79	279.31		

*significant at $p = 0.0065$

(f) *Colobus*, proximal

	female	male
n_i	26	21
ΣY	4624.47	3983.13
$\hat{Y}_i$	177.86	189.67
Σy_i^2	8552.19	7659.95
$\hat{Y}_{grand}$	183.14	

source of variation	df	SS	MS	F	95% CI
among sexes	1	1620.00	1620.00	*4.50	0.59 to 23.02
within sexes	45	16212.14	360.27		

*significant at $p = 0.0394$

Table A.22. (continued)

(g) *Gorilla*, distal

	female	male
n_i	16	9
ΣY	6645.76	5306.23
$\bar{Y}_i$	415.36	589.58
Σy_i^2	47563.71	25360.83
$\bar{Y}_{grand}$	478.08	

source of variation	df	SS	MS	*F*	95% CI
among sexes	1	174833.83	174833.83	*55.14	125.68 to 222.76
within sexes	23	72924.53	3170.63		

*significant at $p = 0.00$

(h) *Gorilla*, proximal

	female	male
n_i	16	9
ΣY	7119.54	5176.21
$\bar{Y}_i$	444.97	575.13
Σy_i^2	25132.83	35057.84
$\hat{Y}_{grand}$	491.83	

source of variation	df	SS	MS	*F*	95% CI
among sexes	1	97589.16	97589.16	*37.29	86.06 to 174.26
within sexes	23	60190.67	2616.99		

*significant at $p = 0.00$

Table A.23. Kolmogorov-Smirnov Z – |x|, Fourier data

(a) *Homo*

	Z
females distal	0.760
females proximal	0.932
males distal	0.893
males proximal	0.686

(b) *Cercopithecus*

	Z
females distal	0.570
females proximal	0.666
males distal	*1.421
males proximal	0.768

*significant at $p = 0.035$

(c) *Colobus*

	Z
females distal	0.486
females proximal	0.721
males distal	0.804
males proximal	0.714

(d) *Gorilla*

	Z
females distal	0.709
females proximal	0.640
males distal	0.624
males proximal	0.779

Table A.24. Size variances, *F*-ratios and 95% confidence intervals – Fourier data

(a) *Homo*, distal

	s^2	*F*	95% CI
male	85.82	1.25	0.89 to 1.75
female	68.88		

(b) *Homo*, proximal

	s^2	*F*	95% CI
male	85.06	1.23	0.83 to 1.81
female	104.55		

(c) *Cercopithecus*, distal

	s^2	*F*	95% CI
male	26.02	*5.04	2.84 to 8.93
female	5.17		

*significant at $p = 0.00$

(d) *Cercopithecus*, proximal

	s^2	*F*	95% CI
male	27.64	*5.93	3.35 to 10.47
female	4.66		

*significant at $p = 0.00$

(e) *Colobus*, distal

	s^2	*F*	95% CI
male	14.53	1.43	0.62 to 3.42
female	10.14		

(f) *Colobus*, proximal

	s^2	*F*	95% CI
male	17.03	1.07	0.47 to 2.56
female	15.86		

Table A.24. (continued)

(g) *Gorilla*, distal

	s^2	*F*	95% CI
male	128.43	1.10	0.27 to 3.52
female	141.59		

(h) *Gorilla*, proximal

	s^2	*F*	95% CI
male	183.51	2.58	0.81 to 10.58
female	71.01		

Table A.25. Single-classification analysis of variance for mean size difference – Fourier data

(a) *Homo*, distal

	female	male
n_i	102	101
ΣY	12268.39	13363.97
$\hat{Y}_i$	120.28	132.32
Σy_i^2	6956.97	8581.97
$\hat{Y}_{grand}$	126.27	

source of variation	df	SS	MS	*F*	95% CI
among sexes	1	7354.40	7354.40	*95.13	9.60 to 14.47
within sexes	201	15538.93	77.31		

*significant at $p = 0.00$

(b) *Homo*, proximal

	female	male
n_i	106	99
ΣY	12128.61	12307.46
$\hat{Y}_i$	114.42	124.32
Σy_i^2	10977.51	8335.92
$\hat{Y}_{grand}$	119.20	

source of variation	df	SS	MS	*F*	95% CI
among sexes	1	5014.14	5014.14	*52.70	7.21 to 12.59
within sexes	203	19313.43	95.14		

*significant at $p = 0.00$

(c) *Cercopithecus*, distal

	female	male
n_i	49	49
ΣY	1290.71	1545.66
$\hat{Y}_i$	26.34	31.54
Σy_i^2	247.93	1249.17
$\hat{Y}_{grand}$	28.94	

source of variation	df	SS	MS	*F*	95% CI
among sexes	1	663.28	663.28	*42.53	3.62 to 6.79
within sexes	96	1497.10	15.59		

*significant at $p = 0.00$

Table A.25. (continued)

(d) *Cercopithecus*, proximal

	female	male
n_i	49	50
ΣY	1344.48	1653.18
$\bar{Y}_i$	27.44	33.06
Σy_i^2	223.68	1345.25
$\bar{Y}_{grand}$	30.28	

source of variation	df	SS	MS	F	95% CI
among sexes	1	783.05	783.05	*48.41	4.02 to 7.23
within sexes	97	1568.93	16.17		

*significant at $p = 0.00$

(e) *Colobus*, distal

	female	male
n_i	26	21
ΣY	925.55	811.89
$\bar{Y}_i$	35.60	38.66
Σy_i^2	253.45	29.20
$\bar{Y}_{grand}$	37.00	

source of variation	df	SS	MS	F	95% CI
among sexes	1	109.00	109.00	*9.02	1.01 to 5.12
within sexes	45	544.06	12.09		

*significant at $p = 0.0043$

(f) *Colobus*, proximal

	female	male
n_i	26	21
ΣY	973.26	839.33
$\bar{Y}_i$	37.43	39.97
Σy_i^2	396.43	340.97
$\bar{Y}_{grand}$	38.57	

source of variation	df	SS	MS	F	95% CI
among sexes	1	74.65	74.65	*4.56	0.14 to 4.93
within sexes	45	737.01	16.38		

*significant at $p = 0.0382$

Table A.25. (continued)

(g) *Gorilla*, distal

	female	male
n_i	16	9
ΣY	1383.26	1105.99
$\hat{Y}_i$	86.45	122.89
Σy_i^2	2123.80	1027.47
$\hat{Y}_{grand}$	99.57	

source of variation	df	SS	MS	*F*	95% CI
among sexes	1	7646.05	7646.05	*55.81	26.34 to 46.52
within sexes	23	3151.27	137.01		

*significant at $p = 0.00$

(h) *Gorilla*, proximal

	female	male
n_i	16	9
ΣY	1489.42	1083.38
$\hat{Y}_i$	93.09	120.38
Σy_i^2	1065.22	147.6226
$\hat{Y}_{grand}$	102.91	

source of variation	df	SS	MS	*F*	95% CI
among sexes	1	4288.81	4288.81	*38.94	18.24 to 36.33
within sexes	23	2533.29	110.14		

*significant at $p = 0.00$

Table A.26. Kolmogorov-Smirnov $Z - u_1, u_2$

(a) *Homo*

		Z
females distal	u_1	0.759
	u_2	0.541
females proximal	u_1	0.648
	u_2	0.684
males distal	u_1	0.813
	u_2	0.746
males proximal	u_1	0.743
	u_2	0.421

(b) *Cercopithecus*

		Z
females distal	u_1	0.568
	u_2	0.686
females proximal	u_1	0.743
	u_2	0.729
males distal	u_1	0.364
	u_2	0.523
males proximal	u_1	0.761
	u_2	0.582

(c) *Colobus*

		Z
females distal	u_1	0.917
	u_2	0.575
females proximal	u_1	0.680
	u_2	0.797
males distal	u_1	0.757
	u_2	0.907
males proximal	u_1	0.361
	u_2	0.501

(d) *Gorilla*

		Z
females distal	u_1	0.713
	u_2	0.639
females proximal	u_1	0.775
	u_2	0.779
males distal	u_1	0.592
	u_2	0.540
males proximal	u_1	0.622
	u_2	0.555

Table A.27. Shape variances, *F*-ratios and 95% confidence intervals – u_1, u_2

(a) ***Homo*, distal**

		$s^{2\,a}$	*F*	95% CI
u_1	male	6.9566	1.26	0.90 to 1.76
	female	8.7673		
u_2	male	1.7480	*1.60	1.14 to 2.24
	female	2.7978		

*significant at $p = 0.0097$

(b) ***Homo*, proximal**

		$s^{2\,a}$	*F*	95% CI
u_1	male	7.6491	1.18	0.80 to 1.75
	female	6.4934		
u_2	male	2.4380	1.28	0.86 to 1.88
	female	3.1205		

(c) ***Cercopithecus*, distal**

		$s^{2\,a}$	*F*	95% CI
u_1	male	18.9850	*1.90	1.07 to 3.37
	female	10.0146		
u_2	male	1.7959	1.05	0.59 to 1.86
	female	1.8841		

*significant at $p = 0.0141$

(d) ***Cercopithecus*, proximal**

		$s^{2\,a}$	*F*	95% CI
u_1	male	12.8025	*1.78	1.01 to 3.14
	female	7.1822		
u_2	male	1.7060	1.59	0.90 to 2.81
	female	1.0756		

*significant at $p = 0.0238$

[a]variances $\times 10^{-5}$

Table A.27. (continued)

(e) *Colobus*, distal

		$s^{2\,a}$	F	95% CI
u_1	male	16.7550	1.94	0.84 to 4.64
	female	8.6306		
u_2	male	1.9802	1.16	0.50 to 2.78
	female	1.7018		

(f) *Colobus*, proximal

		$s^{2\,a}$	F	95% CI
u_1	male	16.7550	1.59	0.69 to 3.81
	female	10.5392		
u_2	male	1.9802	1.08	0.47 to 2.59
	female	1.8257		

(g) *Gorilla*, distal

		$s^{2\,a}$	F	95% CI
u_1	male	7.8072	1.20	0.29 to 3.84
	female	9.3674		
u_2	male	4.5128	*3.36	1.05 to 13.78
	female	1.3412		

*significant at $p = 0.0206$

(h) *Gorilla*, proximal

		$s^{2\,a}$	F	95% CI
u_1	male	2.2437	3.44	0.84 to 11.00
	female	7.7098		
u_2	male	0.8881	1.22	0.38 to 5.00
	female	0.7276		

[a]variances $\times 10^{-5}$

Table A.28. Single-classification analysis of variance for mean shape differences – Fourier data

(a) *Homo*, distal

	u_1		u_2	
	female	male	female	male
n_i	102	101	102	101
ΣY [a]	4.9389	131.4070	−104.9658	7.3117
$\hat{Y}_i$ [a]	0.0484	1.3011	−1.0291	0.0724
Σy_i^2 [a]	0.8855	0.6957	2.8258	1.7480
$\hat{Y}_{grand}$ [a]	0.6717		−0.4811	

	source of variation	df	SS [b]	MS [b]	F	95% CI
u_1	among sexes	1	7.9622	7.9622	1.01	−1.20 to 3.71
	within sexes	201	1581.15	7.8664		
u_2	among sexes	1	6.1562	6.1562	2.71	−2.19 to 2.42
	within sexes	201	457.38	2.2755		

(b) *Homo*, proximal

	u_1		u_2	
	female	male	female	male
n_i	106	99	106	99
ΣY [a]	0.6018	177.4921	199.2140	73.6250
$\hat{Y}_i$ [a]	0.0057	1.7928	1.8793	0.7436
Σy_i^2 [a]	6.8180	7.4960	3.2765	2.3892
$\hat{Y}_{grand}$ [a]	0.8688		1.3309	

	source of variation	df	SS [b]	MS [b]	F	95% CI
u_1	among sexes	1	16.3492	16.3492	2.32	−0.53 to 4.10
	within sexes	203	1431.4	7.0512		
u_2	among sexes	1	6.6026	6.6026	2.37	−3.08 to 0.80
	within sexes	203	566.57	2.7910		

[a] sums, means and sums of squares $\times 10^{-3}$
[b] sums of squares and mean squares $\times 10^{-5}$

Table A.28. (continued)

(c) *Cercopithecus*, distal

	u_1		u_2	
	female	male	female	male
n_i	49	49	49	49
ΣY [a]	27.9282	−74.1625	42.0060	−83.9188
$\hat{Y}_i$ [a]	0.5699	−1.5135	0.8572	−1.7126
Σy_i^2 [a]	4.8069	9.1127	0.9043	0.8620
$\hat{Y}_{grand}$ [a]	−0.4718		−0.4277	

	source of variation	df	SS [b]	MS [b]	F	95% CI
u_1	among sexes	1	10.6344	10.6344	0.73	−6.35 to 3.31
	within sexes	96	1391.96	14.4996		
u_2	among sexes	1	16.1795	16.1795	*8.79	−4.29 to −0.85
	within sexes	96	176.63	1.8399		

*significant at $p = 0.0038$

(d) *Cercopithecus*, proximal

	u_1		u_2	
	female	male	female	male
n_i	49	50	49	50
ΣY [a]	60.4962	−70.5319	60.2279	73.8298
$\hat{Y}_i$ [a]	1.2346	−1.4106	1.2291	1.4765
Σy_i^2 [a]	3.4474	6.2732	0.5163	0.8359
$\hat{Y}_{grand}$ [a]	−0.0992		1.3541	

	source of variation	df	SS [b]	MS [b]	F	95% CI
u_1	among sexes	1	17.3161	17.3161	1.73	−6.64 to 1.35
	within sexes	97	972.06	10.0212		
u_2	among sexes	1	0.1515	0.1515	0.11	−1.24 to 1.74
	within sexes	97	135.22	1.3940		

[a] sums, means and sums of squares $\times 10^{-3}$
[b] sums of squares and mean squares $\times 10^{-5}$

Table A.28. (continued)

(e) *Colobus*, distal

	u_1		u_2	
	female	male	female	male
n_i	26	21	26	21
ΣY^a	103.7259	−7.6317	−71.6259	−26.3202
$\bar{Y}_i{}^a$	3.9894	−0.3634	−2.7548	−1.2533
$\Sigma y_i^{2\,a}$	2.1576	3.3509	0.4254	0.3960
$\bar{Y}_{grand}{}^a$	2.0349		−2.0840	

	source of variation	df	SS[b]	MS[b]	F	95% CI
u_1	among sexes	1	22.0111	22.0111	1.80	−10.89 to 2.18
	within sexes	45	550.85	12.2411		
u_2	among sexes	1	2.6191	2.6191	1.43	−1.02 to 4.03
	within sexes	45	82.14	1.8253		

(f) *Colobus*, proximal

	u_1		u_2	
	female	male	female	male
n_i	26	21	26	21
ΣY^a	4.0872	16.0521	44.4656	−13.0737
$\bar{Y}_i{}^a$	0.1572	0.7643	1.7102	−0.6225
$\Sigma y_i^{2\,a}$	2.6348	4.1887	0.4564	0.1915
$\bar{Y}_{grand}{}^a$	0.4285		0.6679	

	source of variation	df	SS[b]	MS[b]	F	95% CI
u_1	among sexes	1	0.4282	0.4282	0.03	−6.21 to 7.42
	within sexes	45	682.35	15.1633		
u_2	among sexes	1	6.3214	6.3214	4.39	−4.90 to 0.24
	within sexes	45	64.79	1.4398		

[a]sums, means and sums of squares × 10^{-3}
[b]sums of squares and mean squares × 10^{-5}

Table A.28. (continued)

(g) *Gorilla*, distal

	u_1		u_2	
	female	male	female	male
n_i	16	9	16	9
ΣY^a	−44.4103	−4.3516	−17.7863	2.5811
$\bar{Y}_i{}^a$	−2.7756	−0.4835	−1.1116	0.2867
$\Sigma y_i^{2\,a}$	1.4051	0.6245	0.2011	0.3663
$\bar{Y}_{grand}{}^a$	−1.9505		−0.6082	

	source of variation	df	SS[b]	MS[b]	*F*	95% CI
u_1	among sexes	1	3.0261	3.0261	0.34	−5.81 to 10.39
	within sexes	23	202.96	8.8243		
u_2	among sexes	1	1.1262	1.1262	0.46	−2.86 to 5.66
	within sexes	23	56.74	2.4670		

(h) *Gorilla*, proximal

	u_1		u_2	
	female	male	female	male
n_i	16	9	16	9
ΣY^a	−24.3213	−6.6889	57.8083	−0.5947
$\bar{Y}_i{}^a$	−1.5200	−0.7432	3.6130	−0.0661
$\Sigma y_i^{2\,a}$	1.1564	0.1794	0.1091	0.0710
$\bar{Y}_{grand}{}^a$	−1.2404		3.0994	

	source of variation	df	SS[b]	MS[b]	*F*	95% CI
u_1	among sexes	1	0.1251	0.1251	0.02	−5.79 to 7.35
	within sexes	23	133.58	5.8078		
u_2	among sexes	1	9.4404	9.4404	*12.05	−6.09 to −1.27
	within sexes	23	18.0148	0.7833		

*significant at $p = 0.0021$

[a]sums, means and sums of squares $\times 10^{-3}$
[b]sums of squares and mean squares $\times 10^{-5}$

Table A.29. Major axis regressions (male and female combined)

(a) *Homo*

(i) correlation-covariance matrices

2561.5920	0.9537	**2714.4781**	0.9678
566.0272	**137.5208**	597.3756	**140.3673**

(ii) major axis regressions

	proximal		distal	
	U_1	U_2	U_1	U_2
P	0.9762	0.2167	0.9765	0.2156
A	0.2167	−0.9762	0.2156	−0.9765
l*	2687.2474	11.8655	2846.3551	8.4902

(iii) slopes, intercepts and their 95% confidence limits

	a	a_1	a_2	c	c_1	c_2
distal	0.22	0.23	0.21	9.83	4.00	15.60
proximal	0.22	0.23	0.21	10.73	6.22	15.17

(b) *Cercopithecus*

(i) correlation-covariance matrices

480.4334	0.9874	**510.2661**	0.9943
123.3185	**32.4691**	134.7156	**35.9728**

(ii) major axis regressions

	proximal		distal	
	U_1	U_2	U_1	U_2
P	0.9685	0.2490	0.9668	0.2554
A	0.2490	−0.9685	0.2554	−0.9668
l*	512.1375	0.7650	545.8590	0.3799

(iii) slopes, intercepts and their 95% confidence limits

	a	a_1	a_2	c	c_1	c_2
distal	0.26	0.27	0.25	−0.09	−1.20	1.02
proximal	0.26	0.27	0.26	0.06	−0.73	0.85

(c) *Colobus*

(i) correlation-covariance matrices

302.3342	0.9798	**360.0871**	0.9799
78.2247	**21.0838**	99.5340	**28.6554**

(ii) major axis regressions

	proximal		distal	
	U_1	U_2	U_1	U_2
P	0.9680	0.2511	0.9637	0.2672
A	0.2511	−0.9680	0.2672	−0.9637
l^*	322.6268	0.7912	387.6812	1.0613

(iii) slopes, intercepts and their 95% confidence limits

	a	a_1	a_2	c	c_1	c_2
distal	0.26	0.28	0.24	−0.91	−3.65	1.79
proximal	0.28	0.29	0.26	−2.94	−5.95	0.05

(d) *Gorilla*

(i) correlation-covariance matrices

9681.3821	0.9949	**6194.4564**	0.9935
2499.3136	**651.8350**	1533.6738	**384.6732**

(ii) major axis regressions

	proximal		distal	
	U_1	U_2	U_1	U_2
P	0.9682	0.2501	0.9706	0.2405
A	0.2501	0.9682	0.2405	−0.9706
l^*	10327.0105	6.2066	6574.4622	4.6674

(iii) slopes, intercepts and their 95% confidence limits

	a	a_1	a_2	c	c_1	c_2
distal	0.26	0.27	0.25	−8.93	−14.18	−3.68
proximal	0.25	0.26	0.24	−0.83	−6.66	4.99

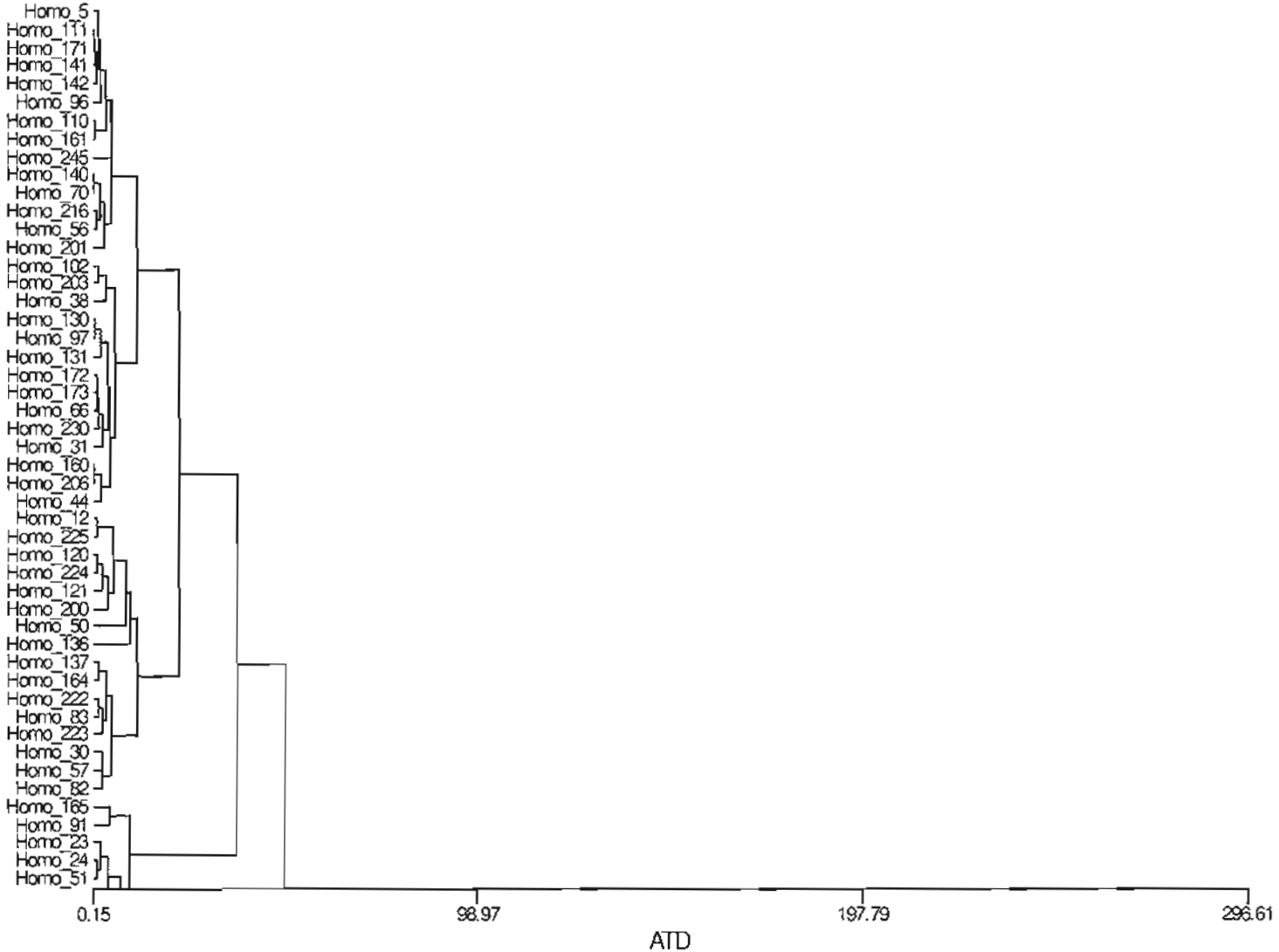

Figure A.1. Tree diagram from UPGMA cluster analysis – females distal, conventional data (letters refer to clusters in text)

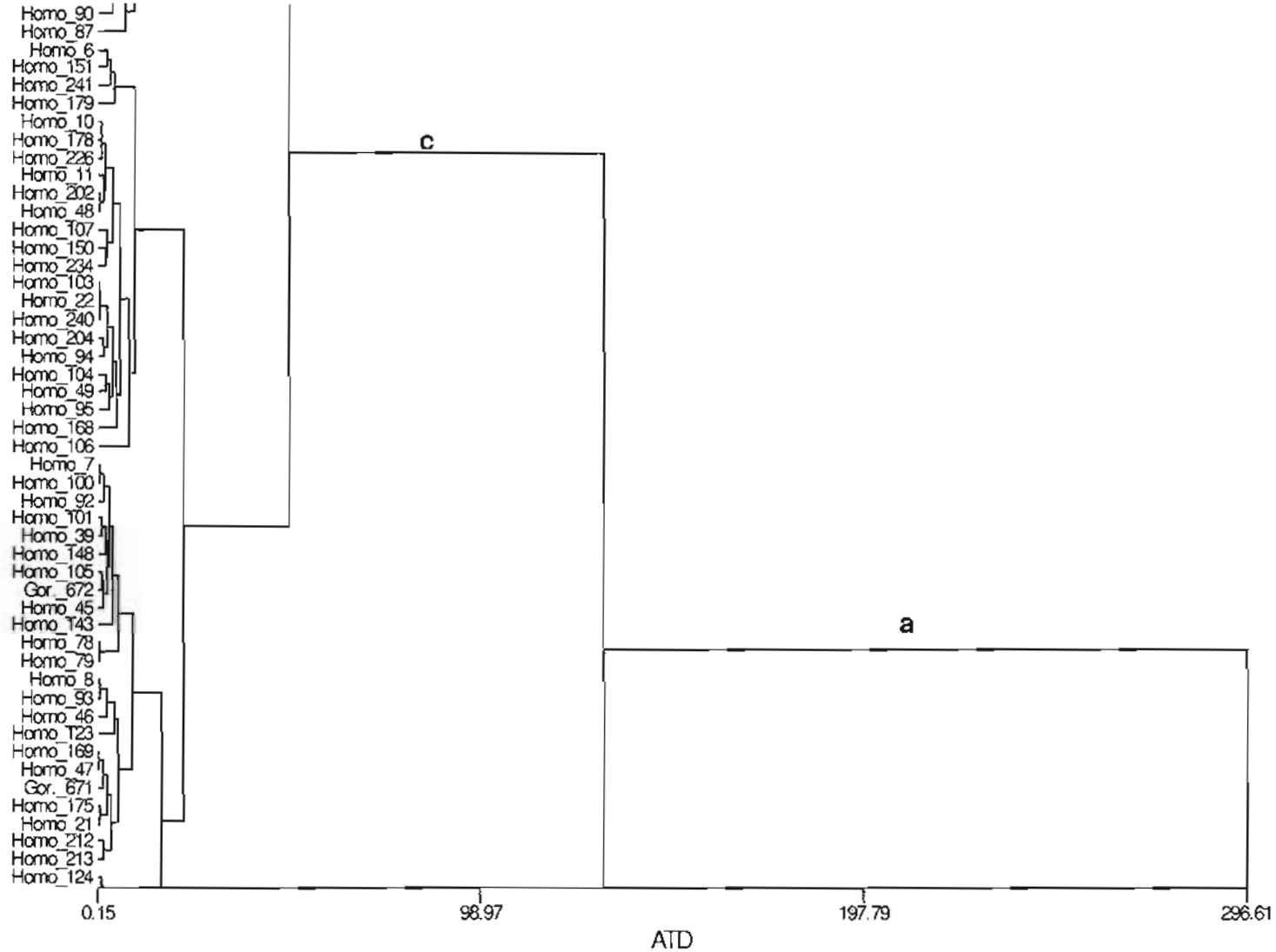

Figure A.1. (continued)

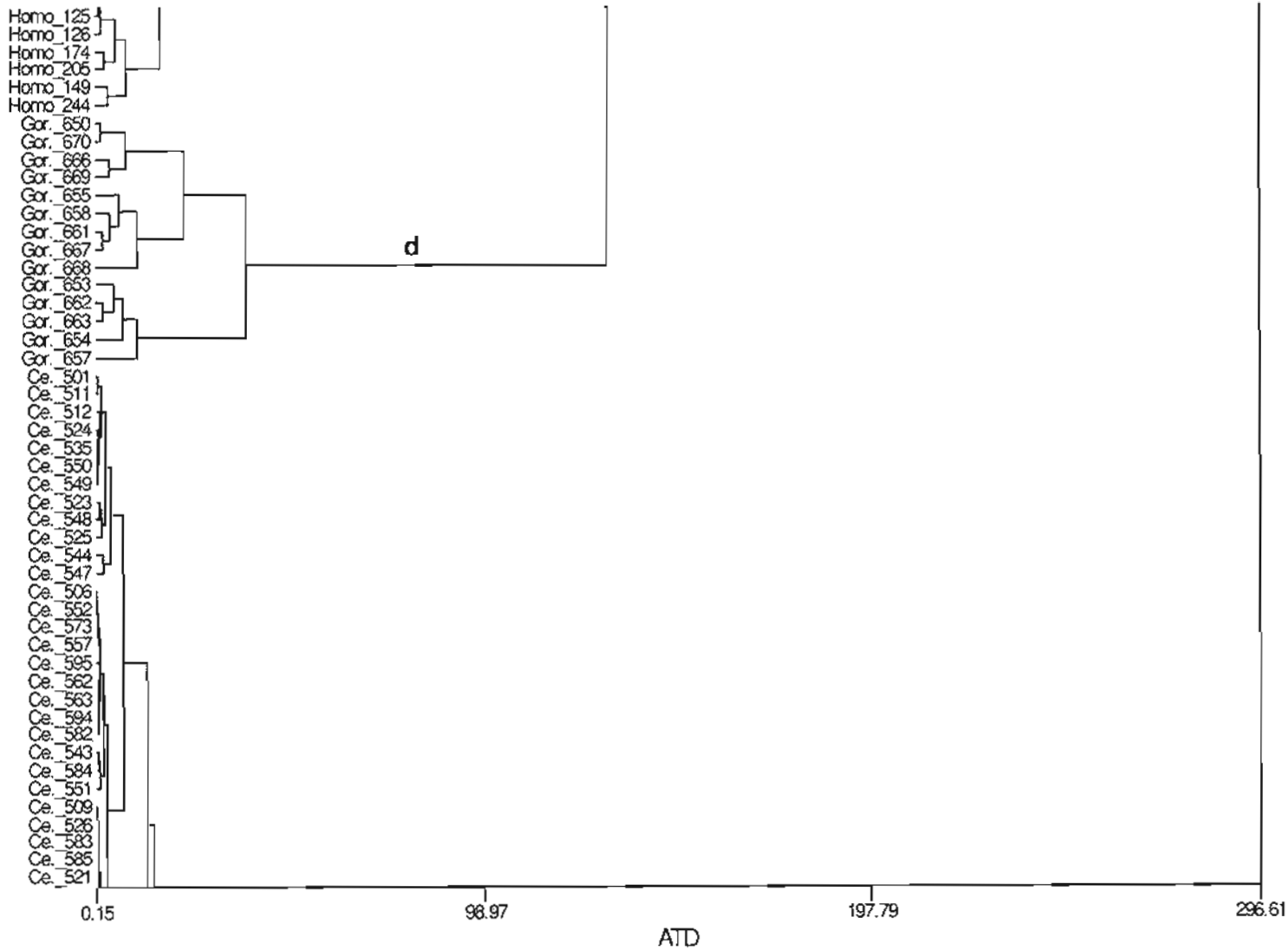

Figure A.1. (continued)

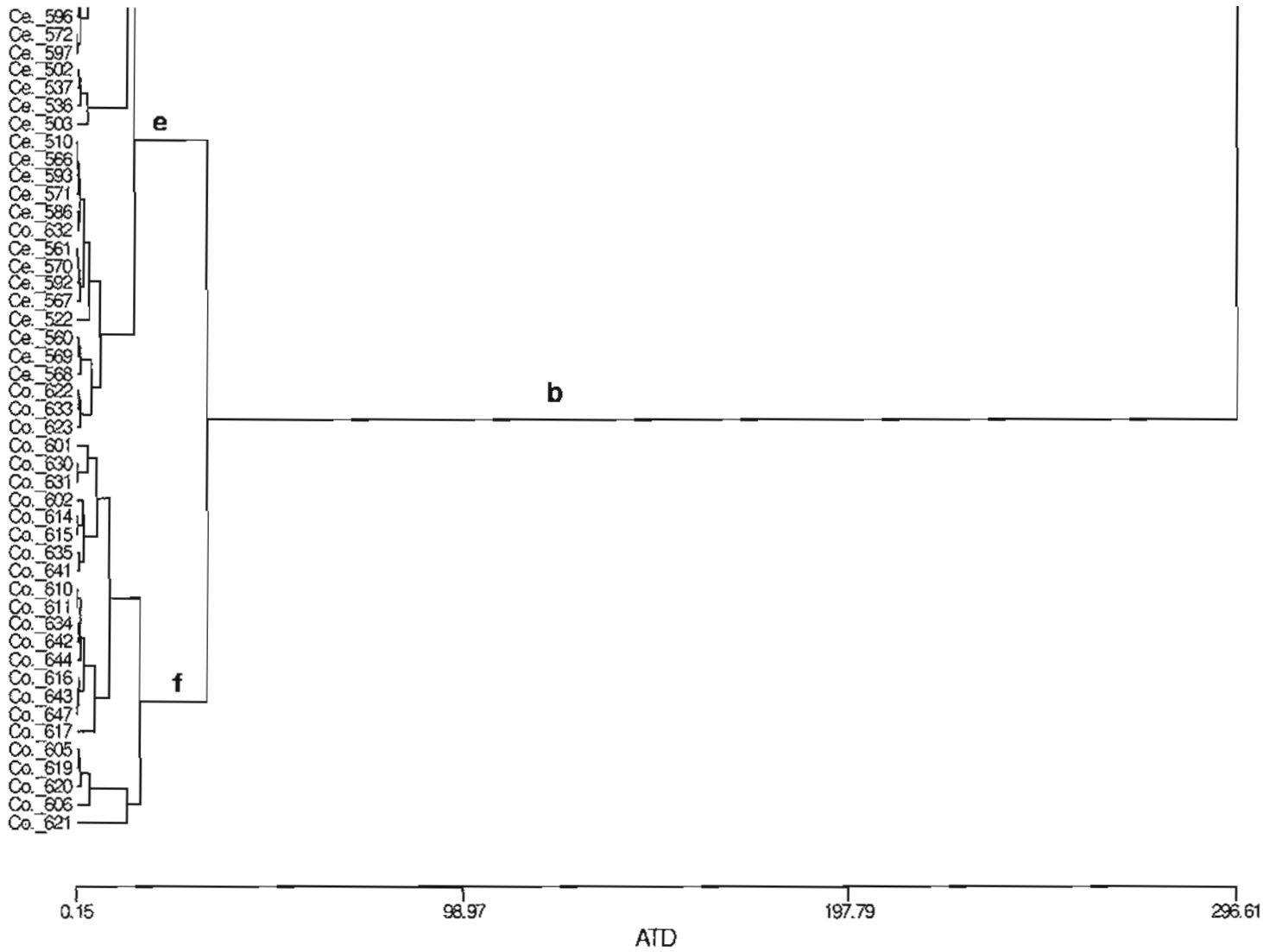

Figure A.1. (continued)

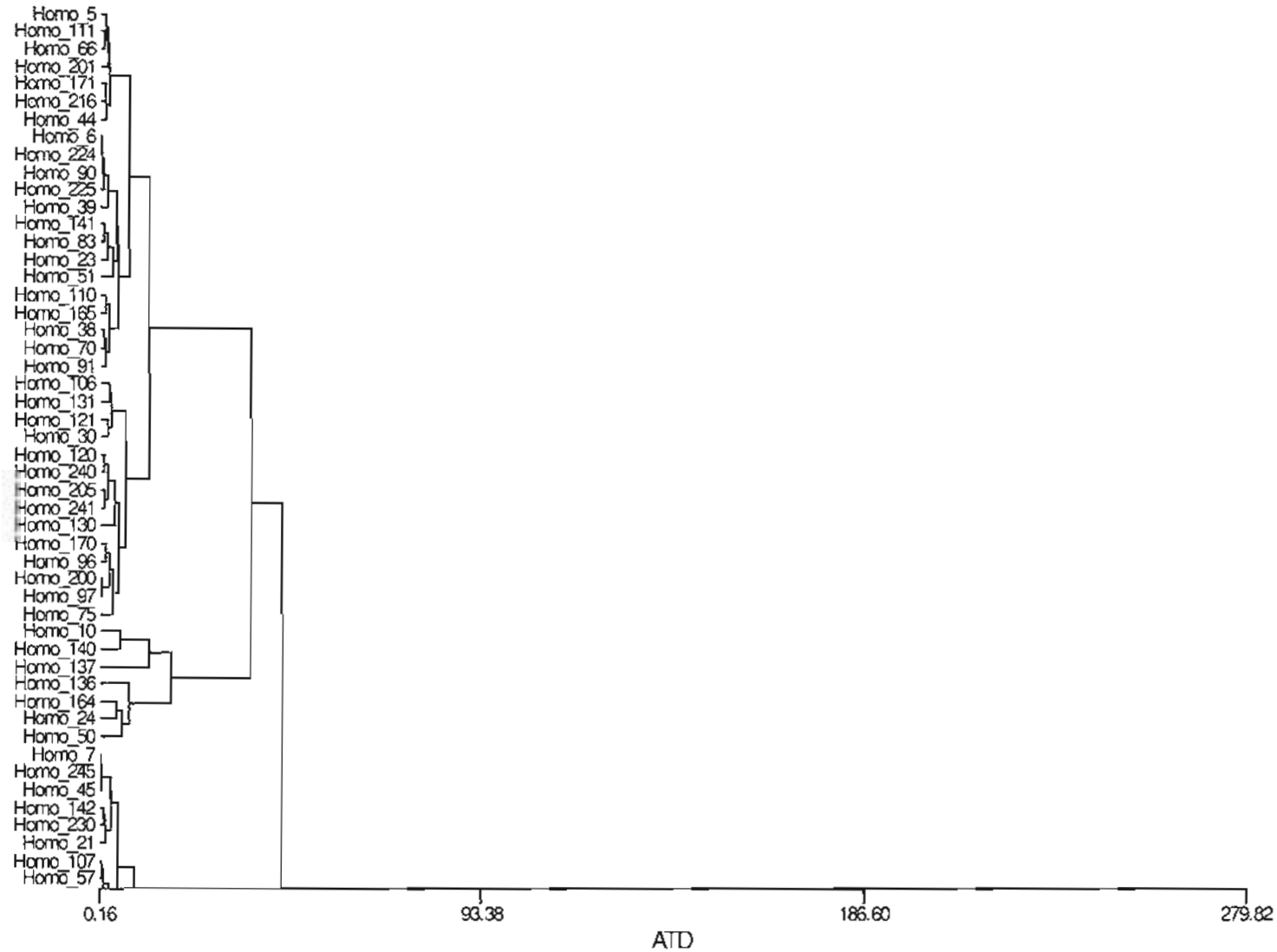

Figure A.2. Tree diagram from UPGMA cluster analysis – females proximal, conventional data (letters refer to clusters in text)

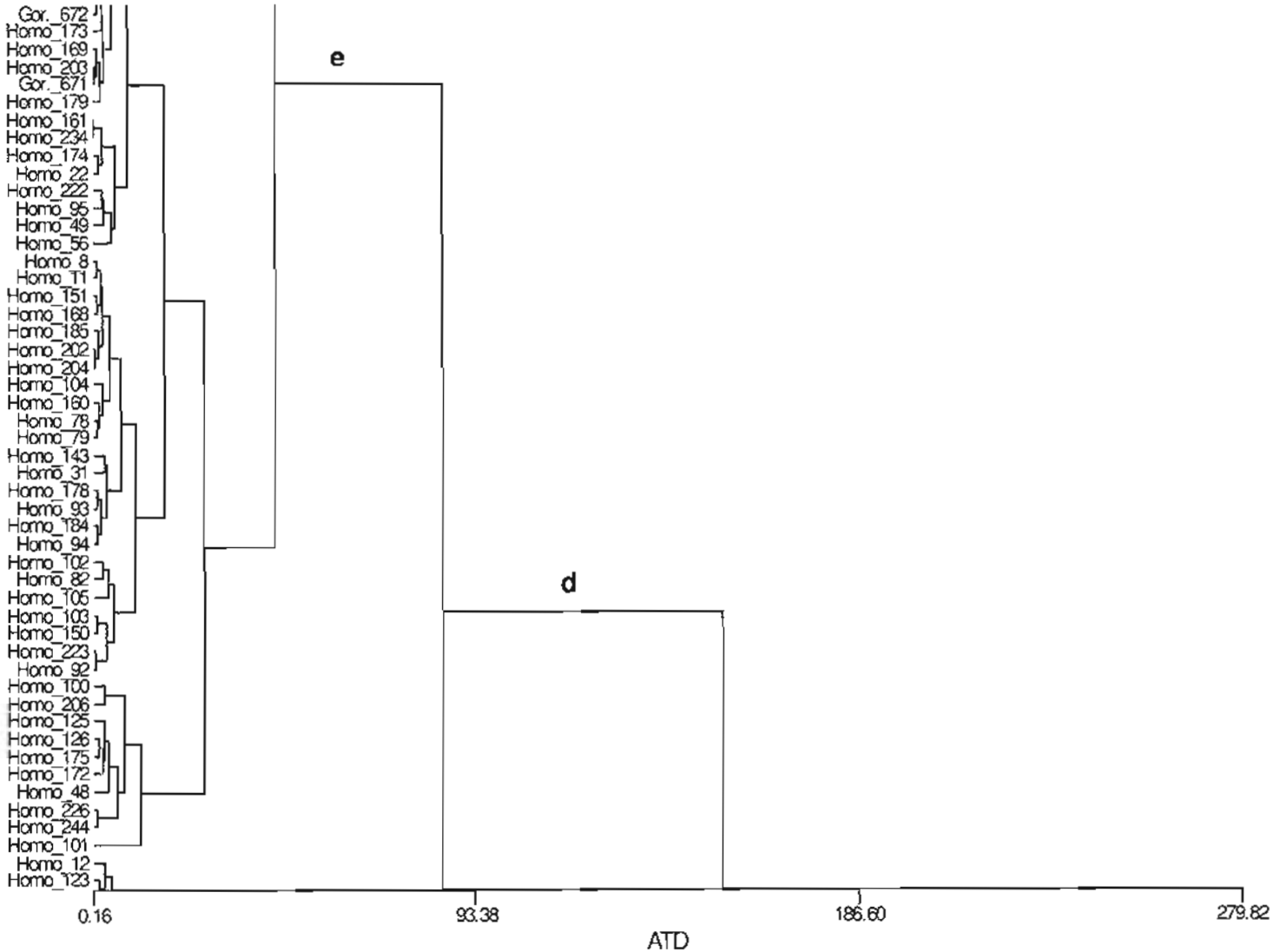

Figure A.2. (continued)

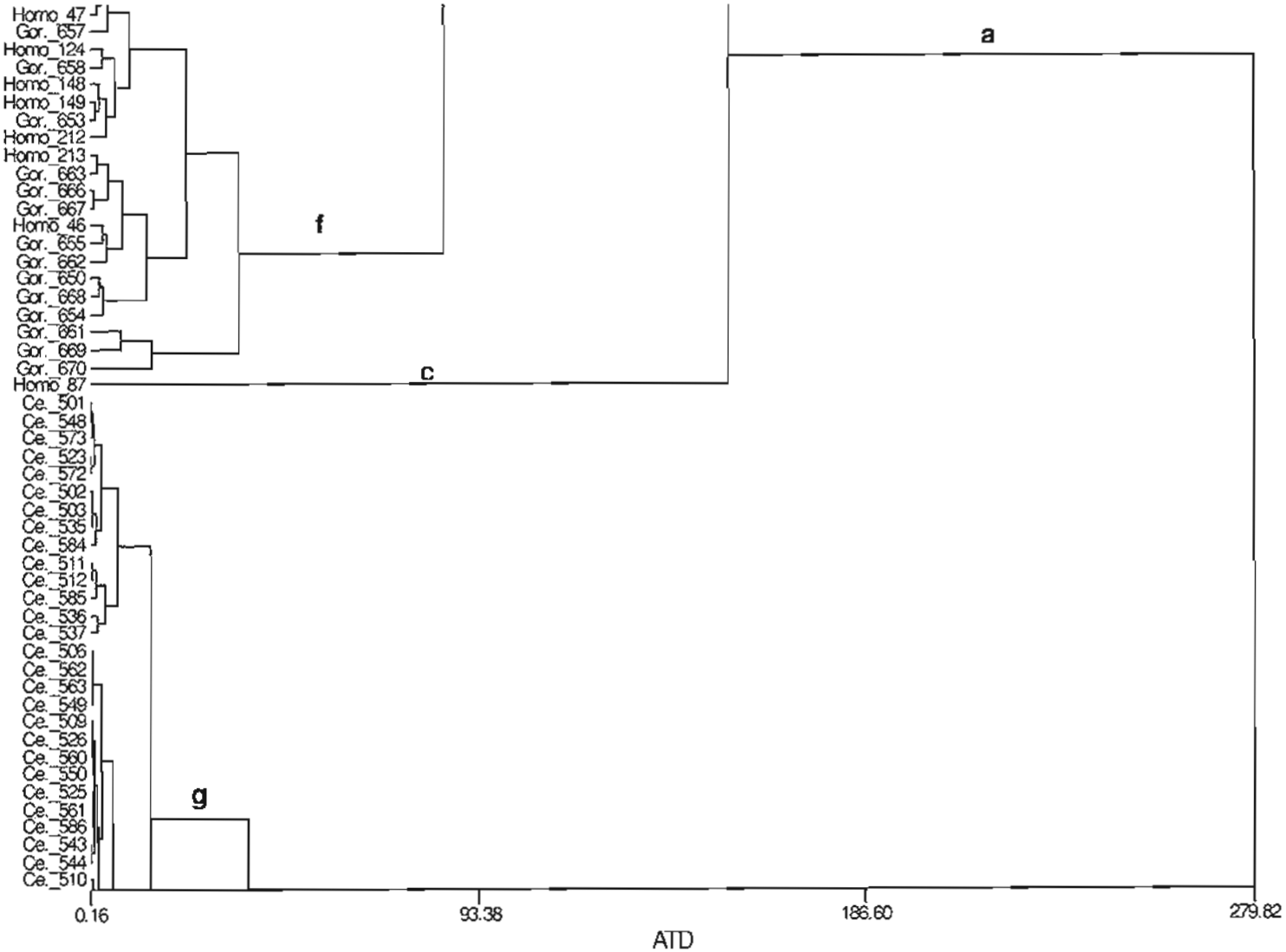

Figure A.2. (continued)

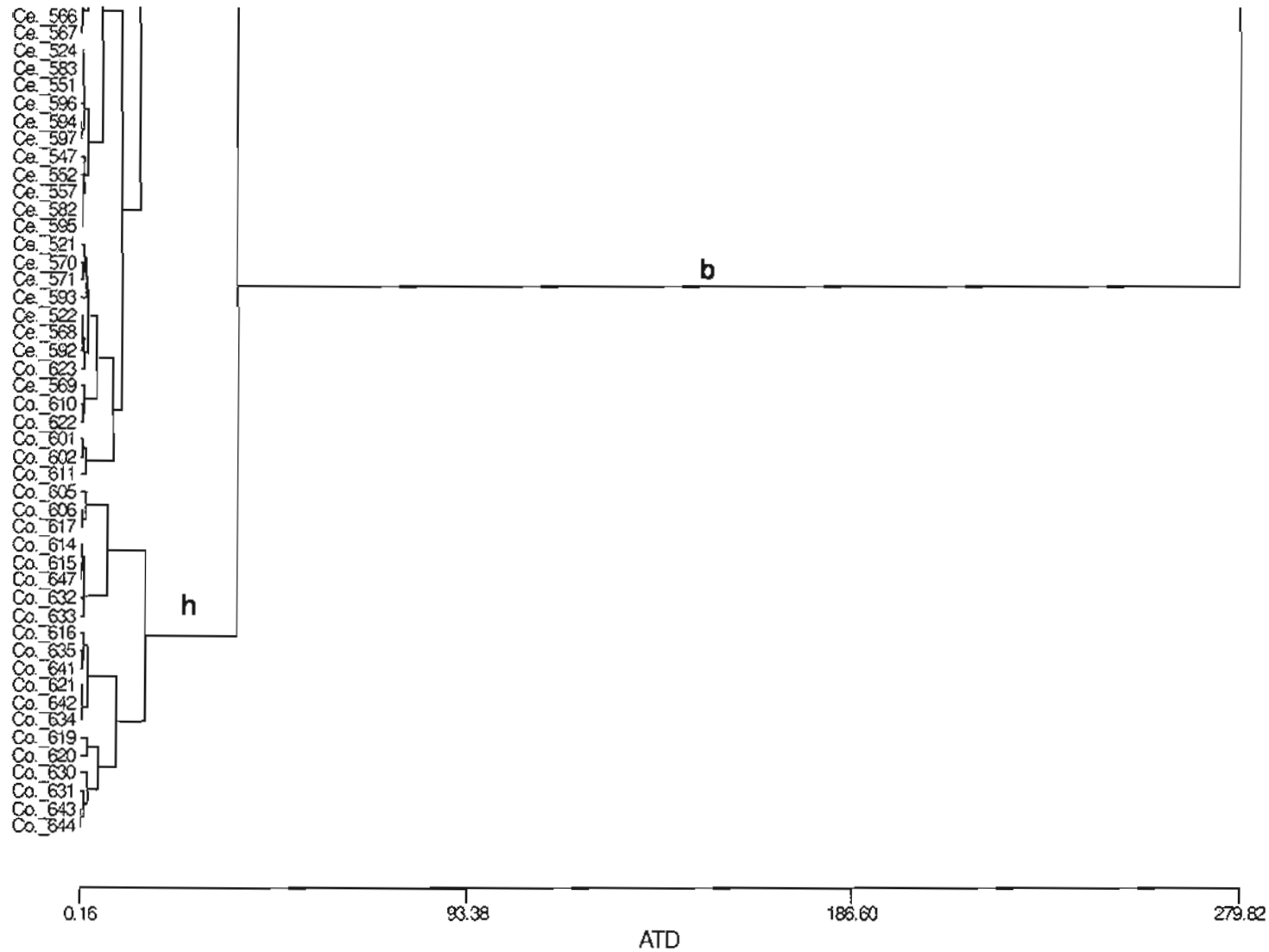

Figure A.2. (continued)

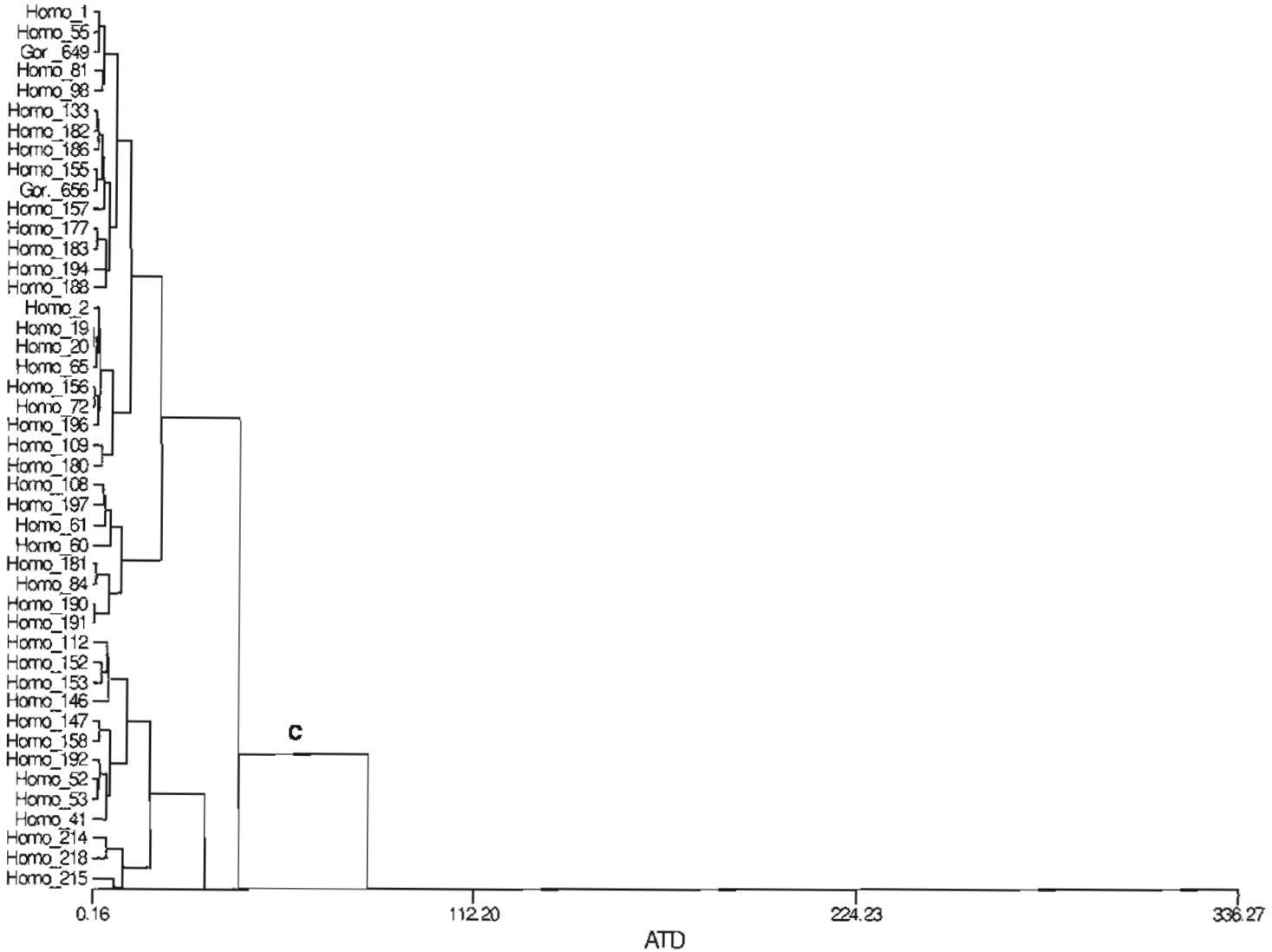

Figure A.3. Tree diagram from UPGMA cluster analysis – males distal, conventional data (letters refer to clusters in text)

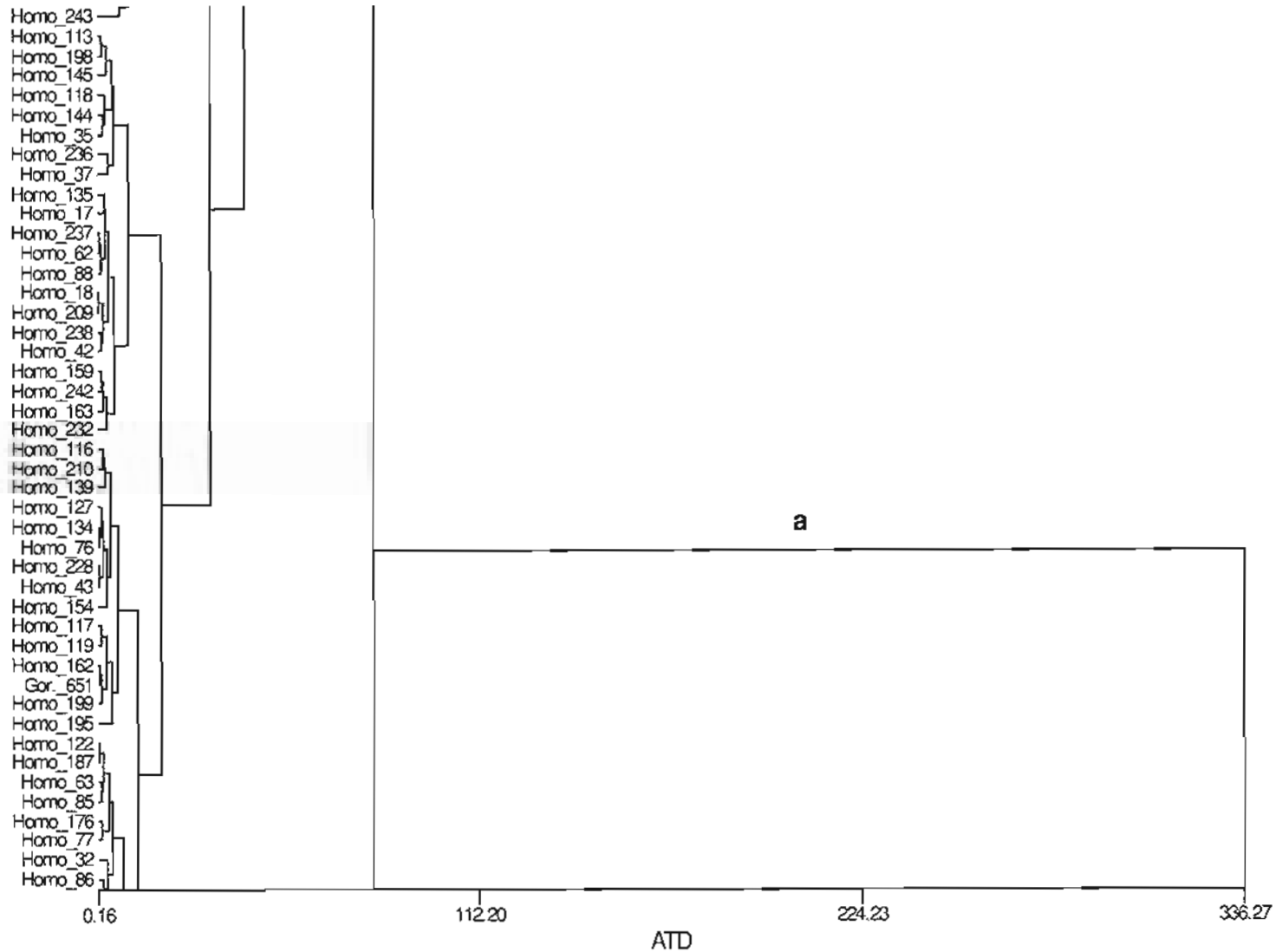

Figure A.3. (continued)

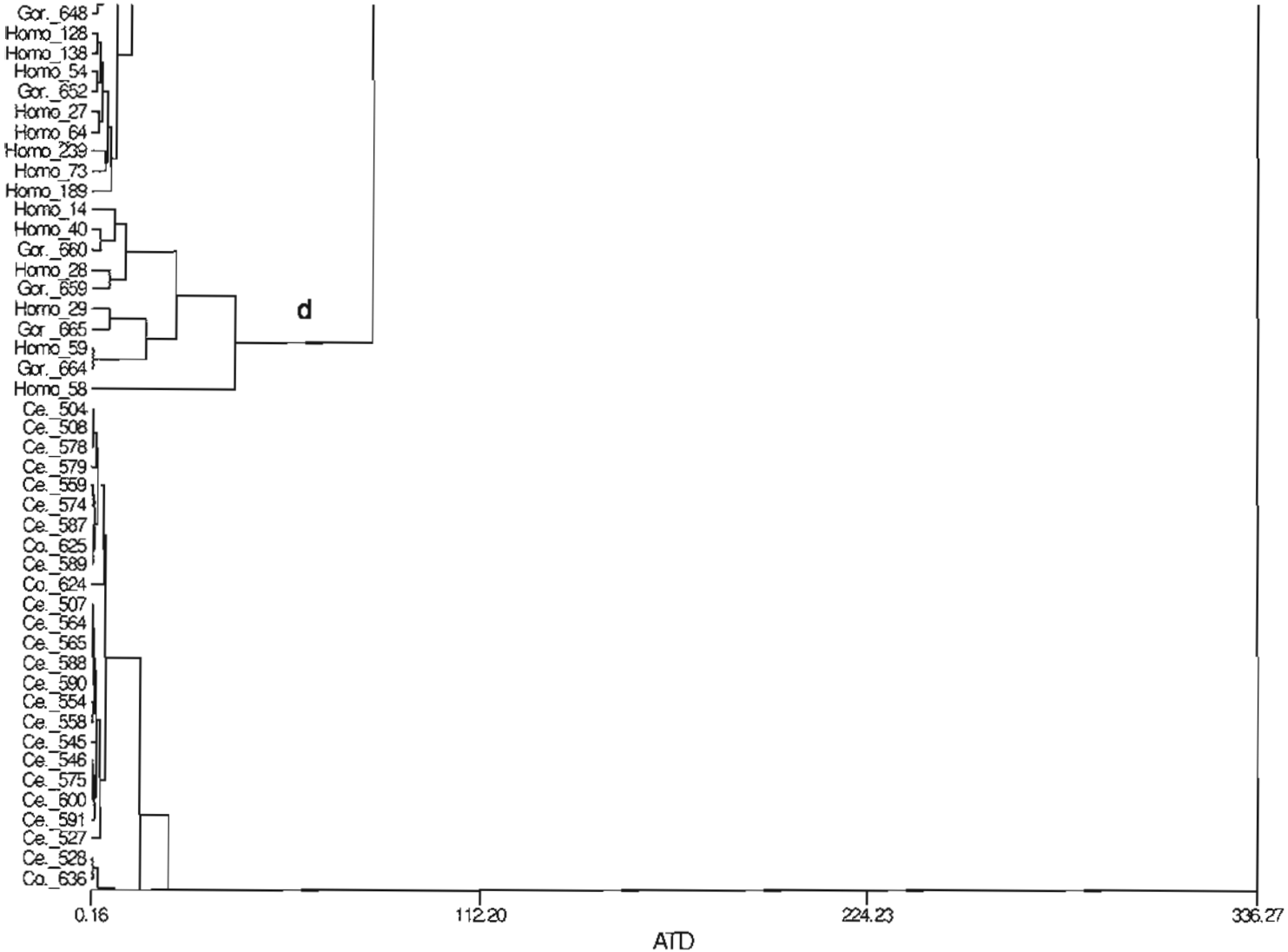

Figure A.3. (continued)

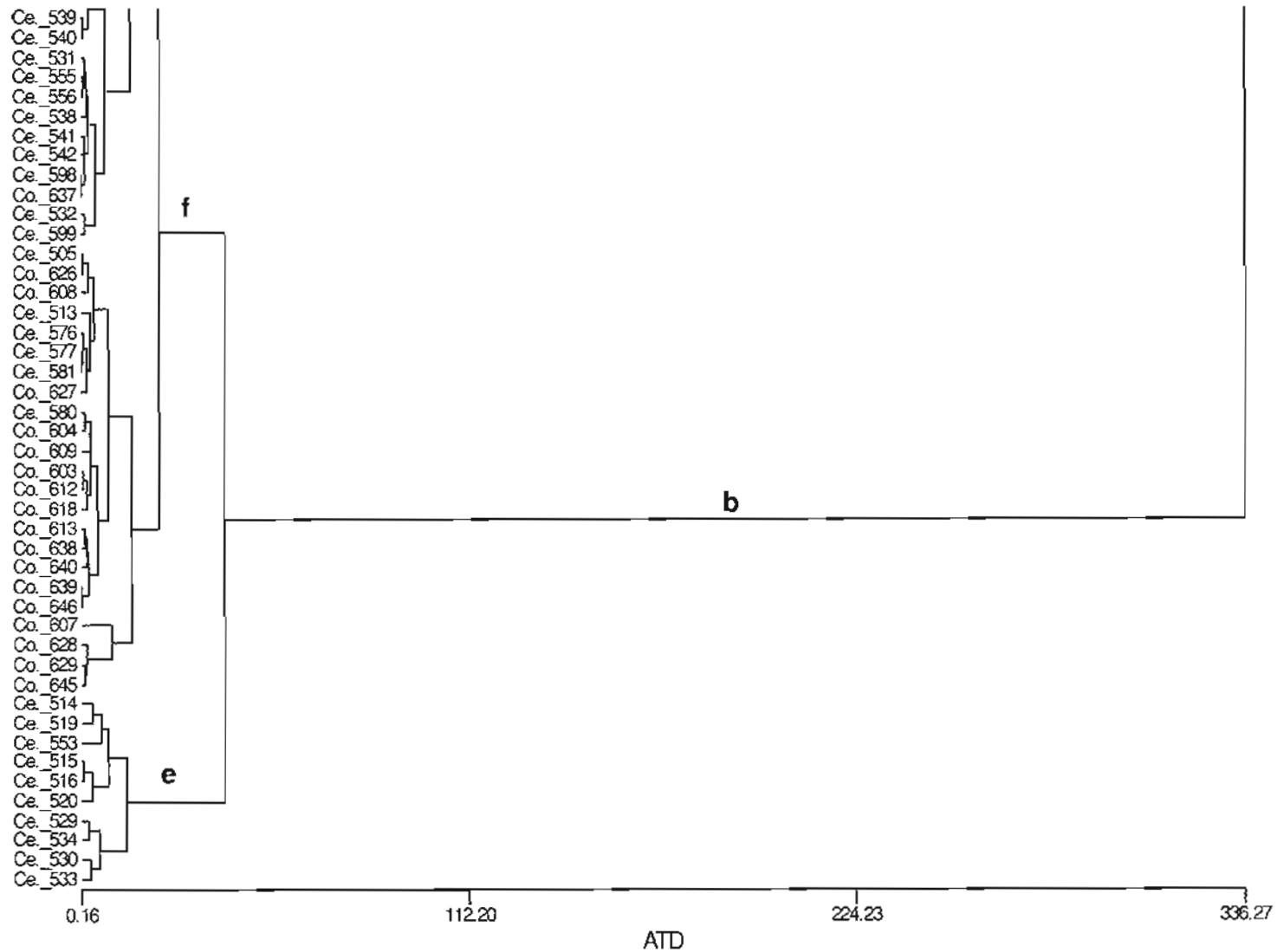

Figure A.3. (continued)

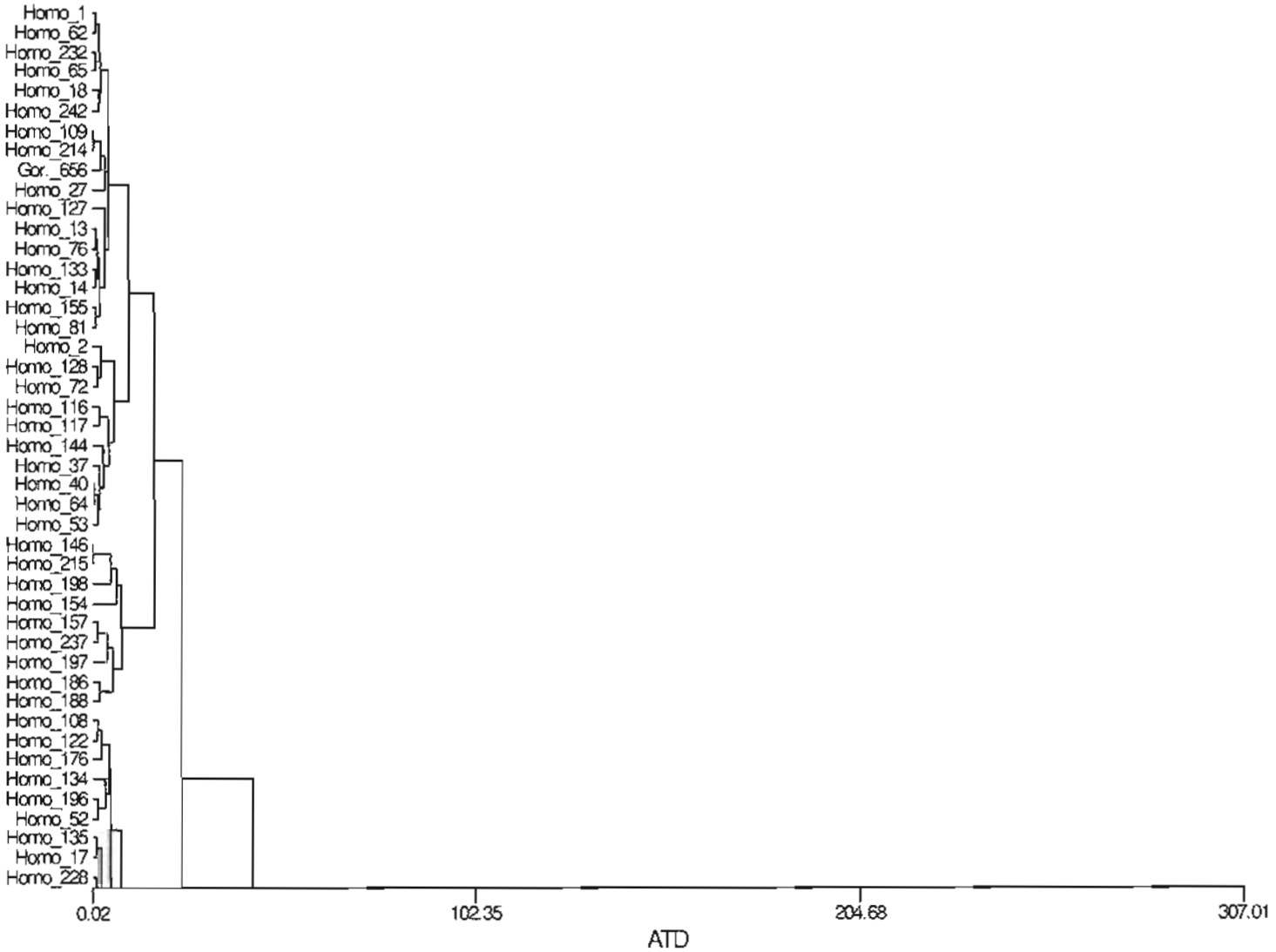

Figure A.4. Tree diagram from UPGMA cluster analysis – males proximal, conventional data (letters refer to clusters in text)

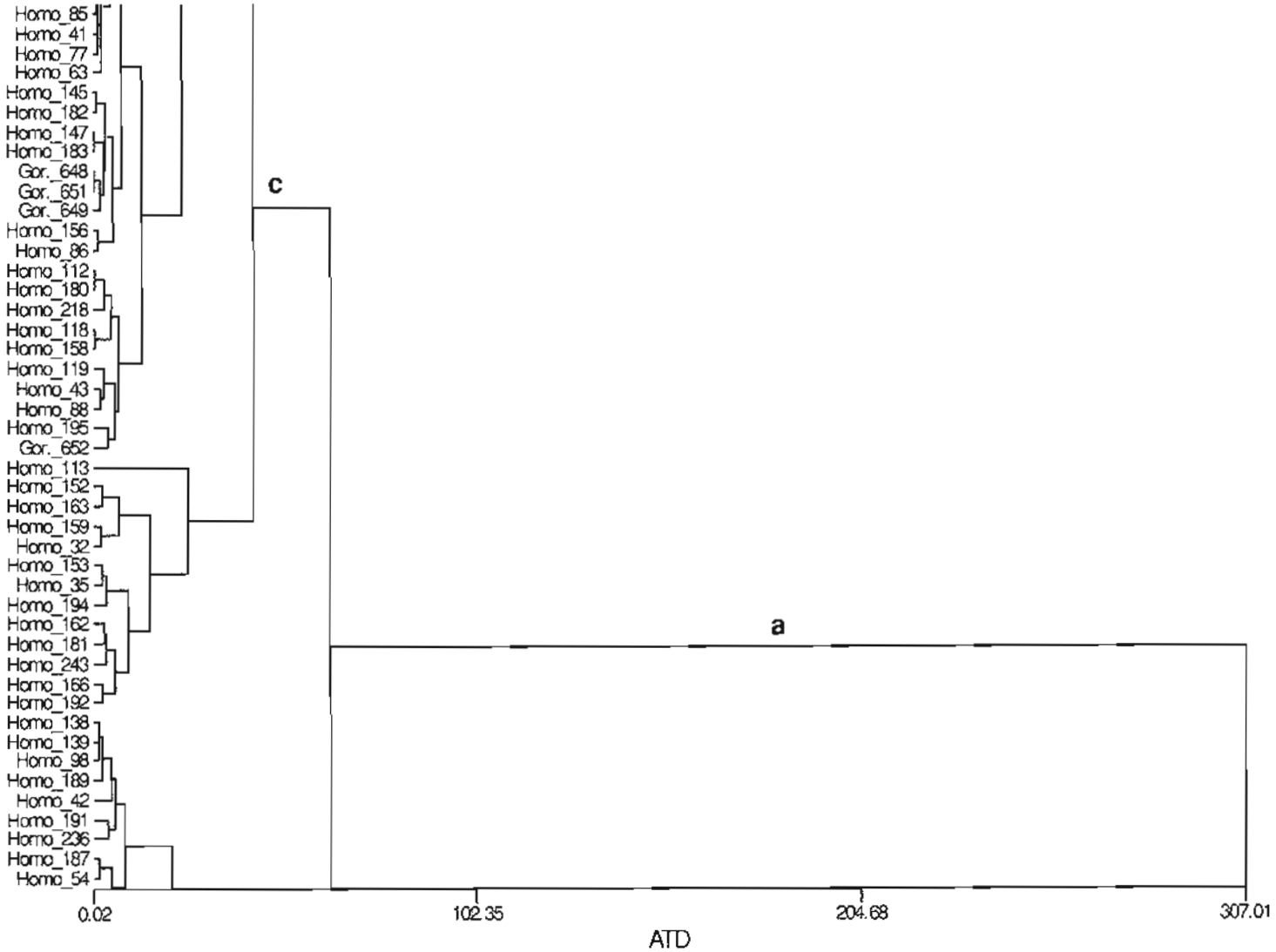

Figure A.4. (continued)

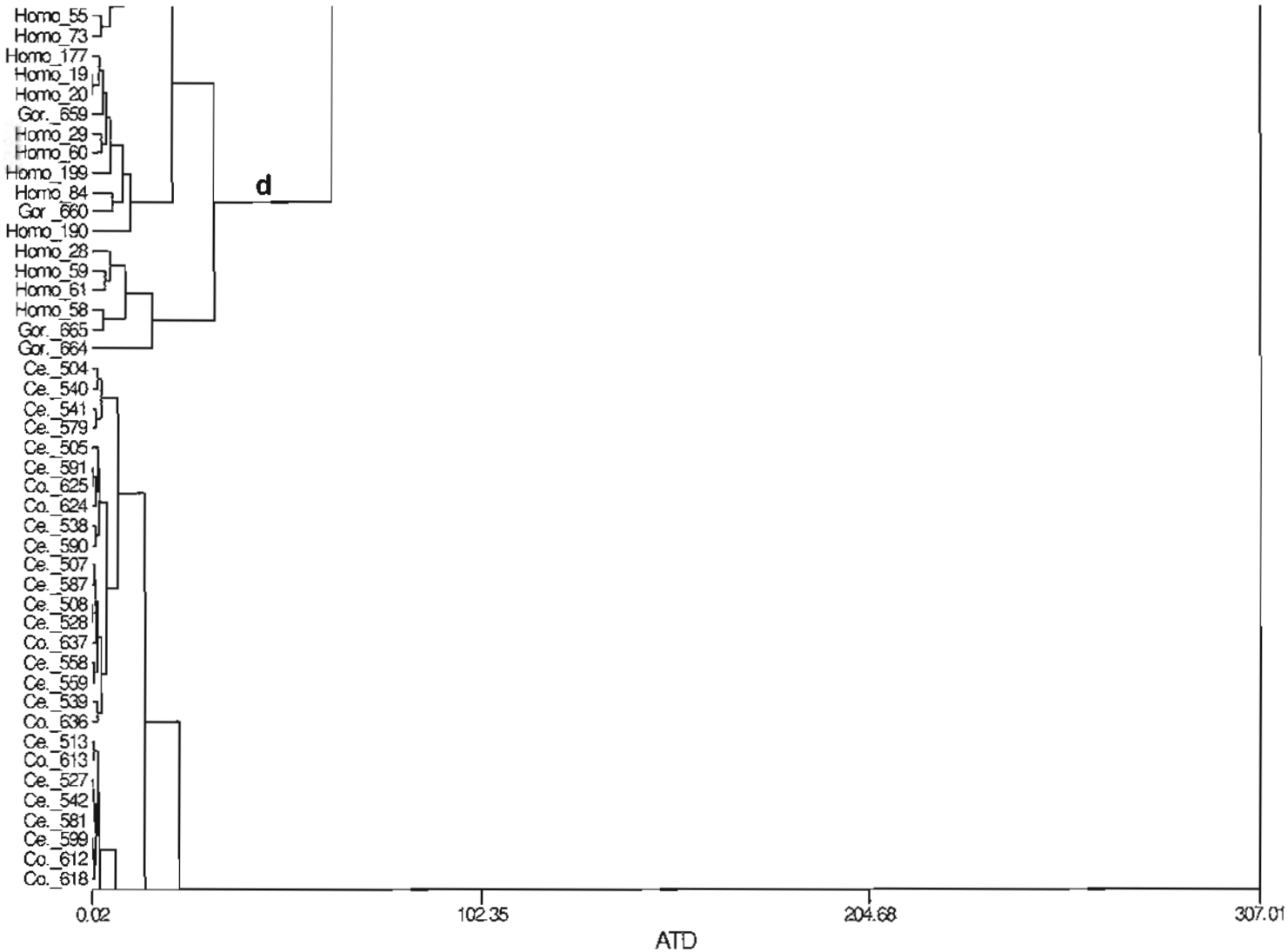

Figure A.4. (continued)

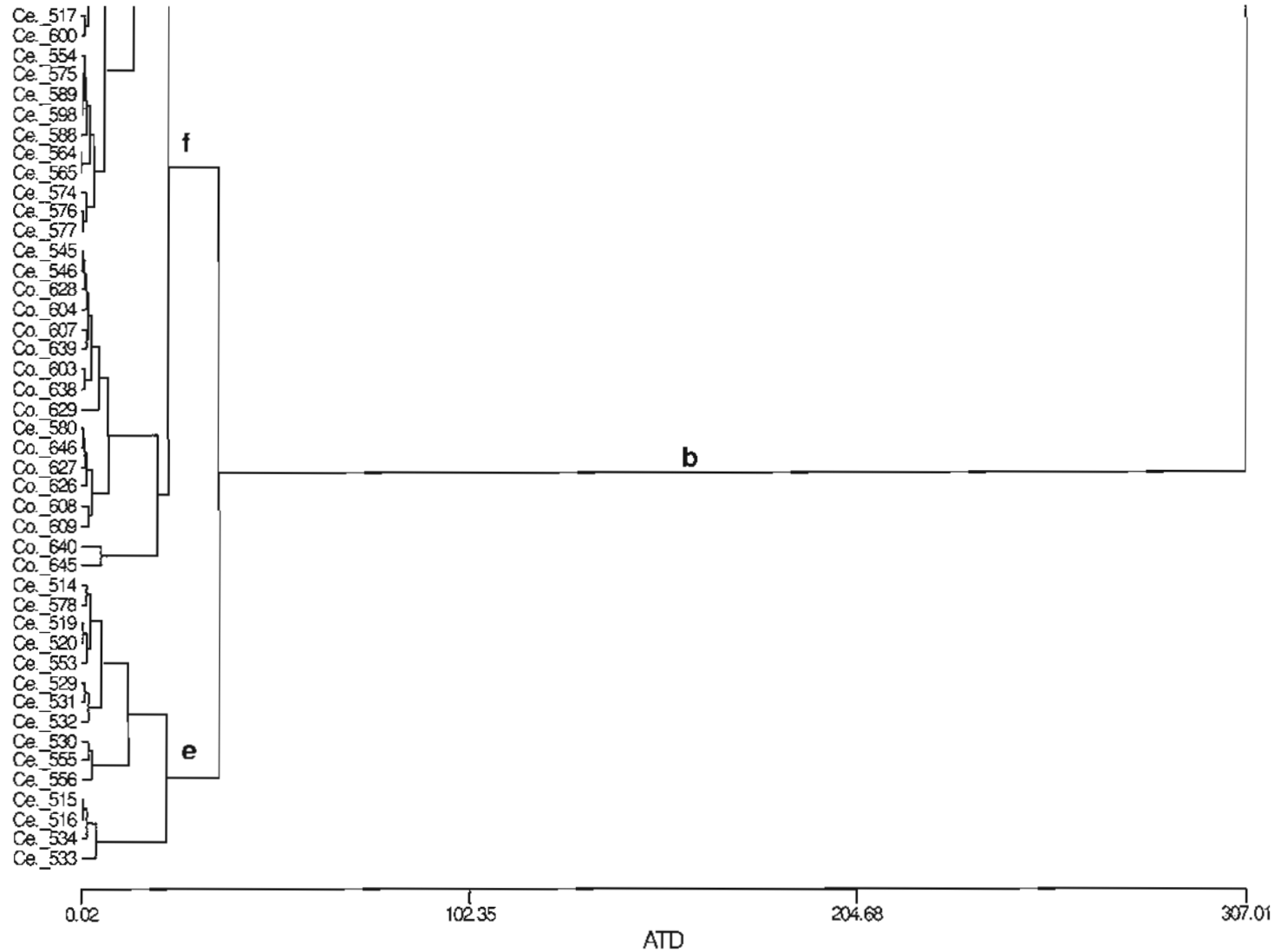

Figure A.4. (continued)

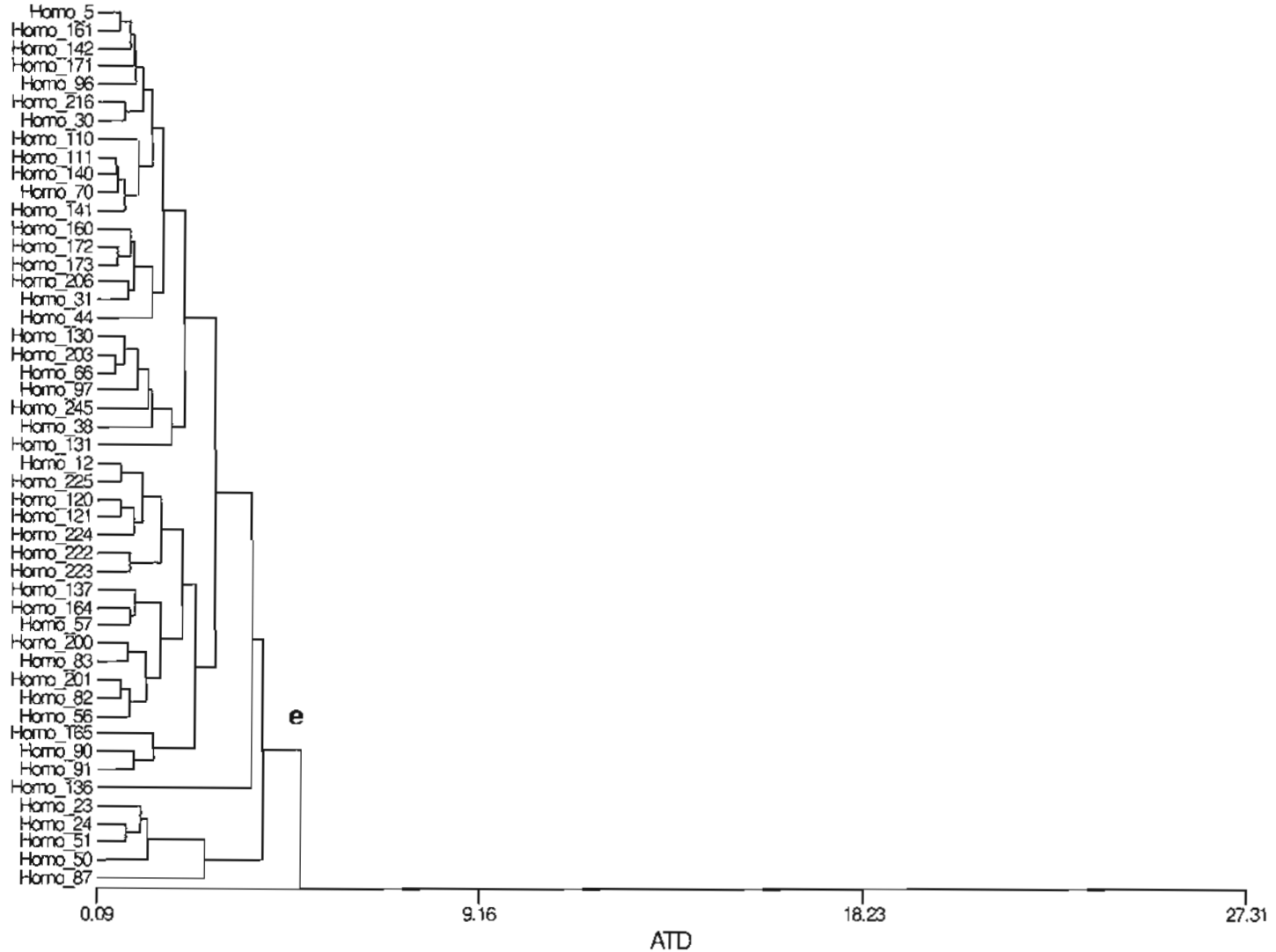

Figure A.5. Tree diagram from UPGMA cluster analysis – females distal, Fourier data (letters refer to clusters in text)

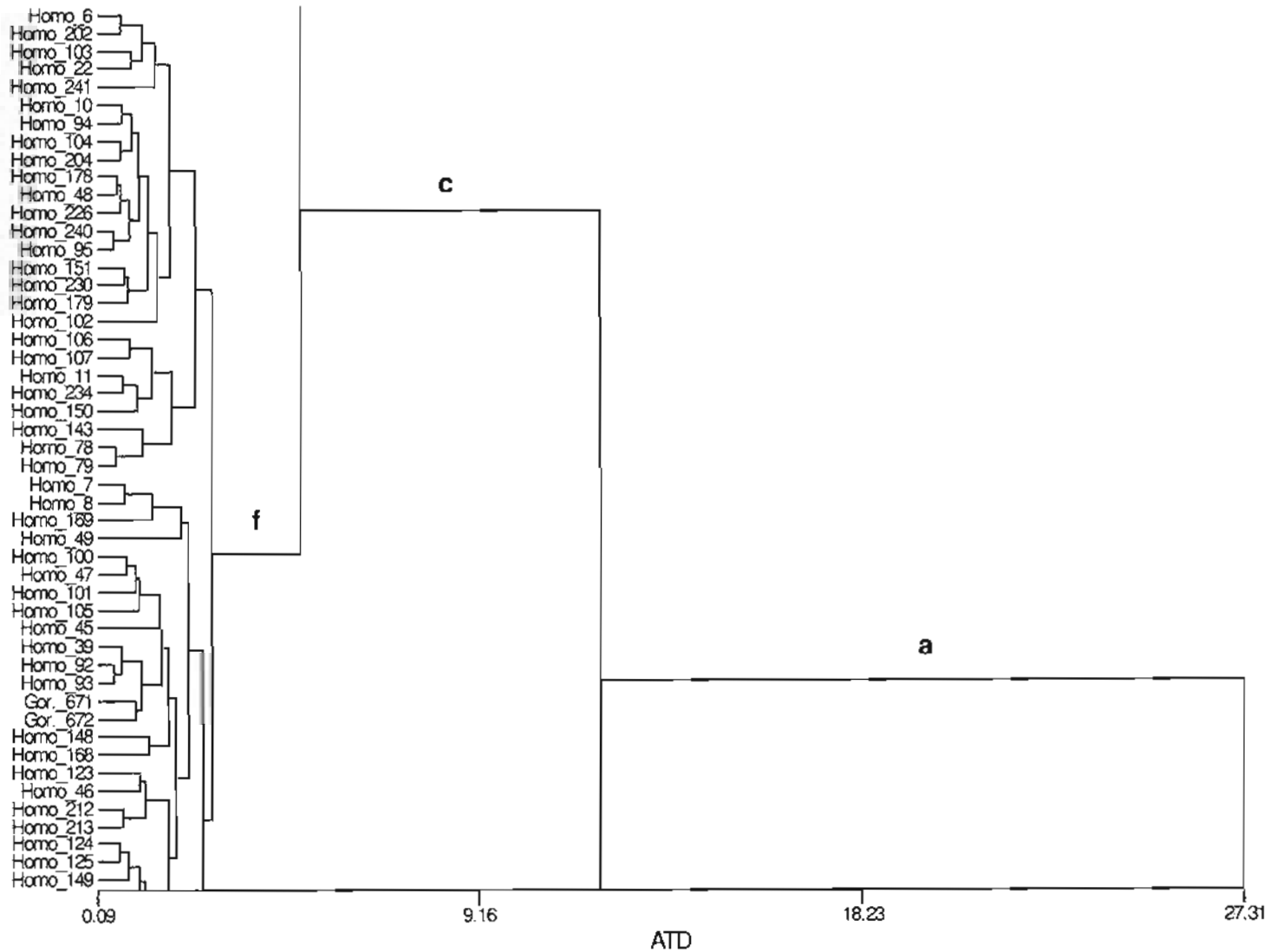

Figure A.5. (continued)

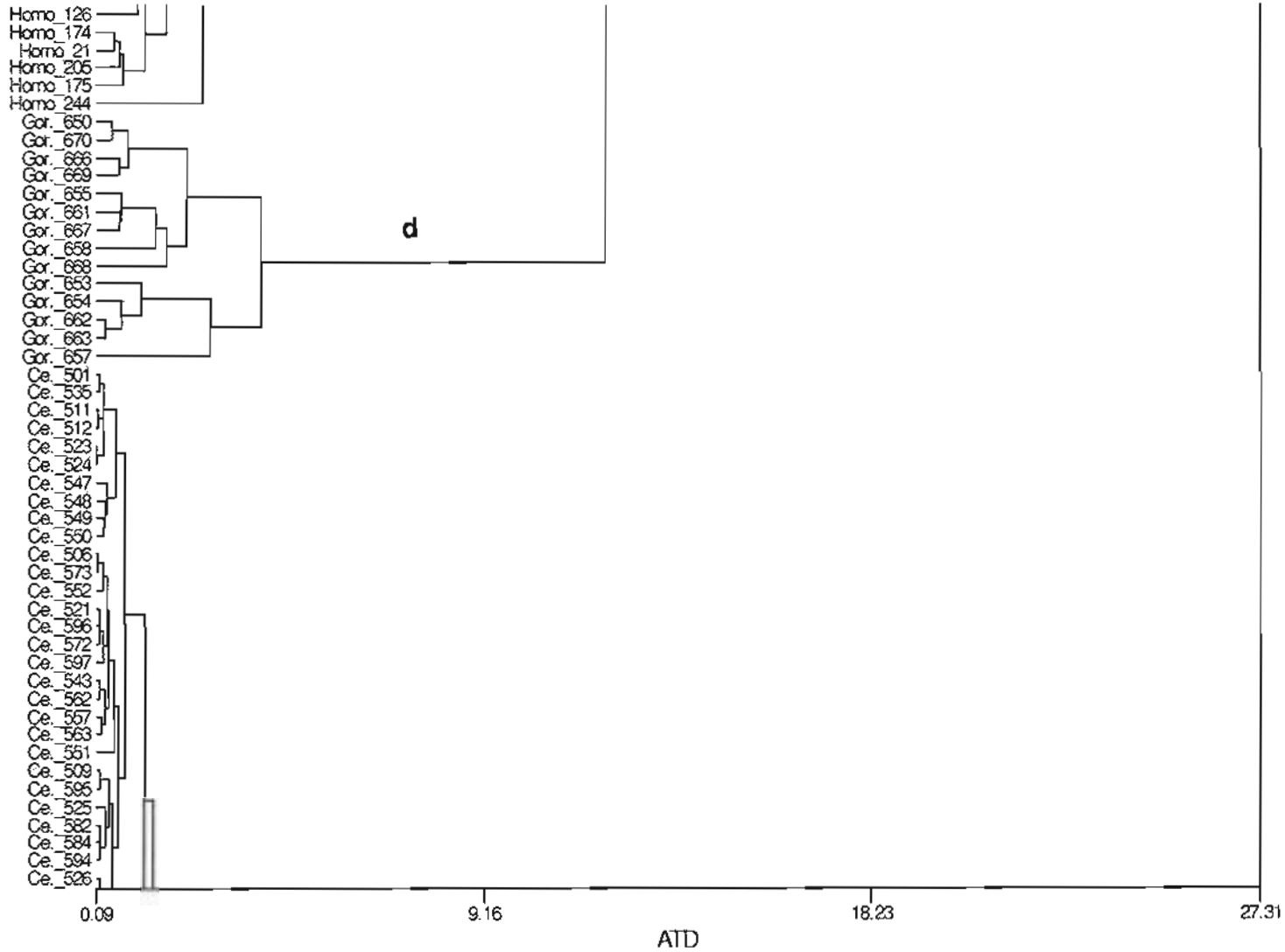

Figure A.5. (continued)

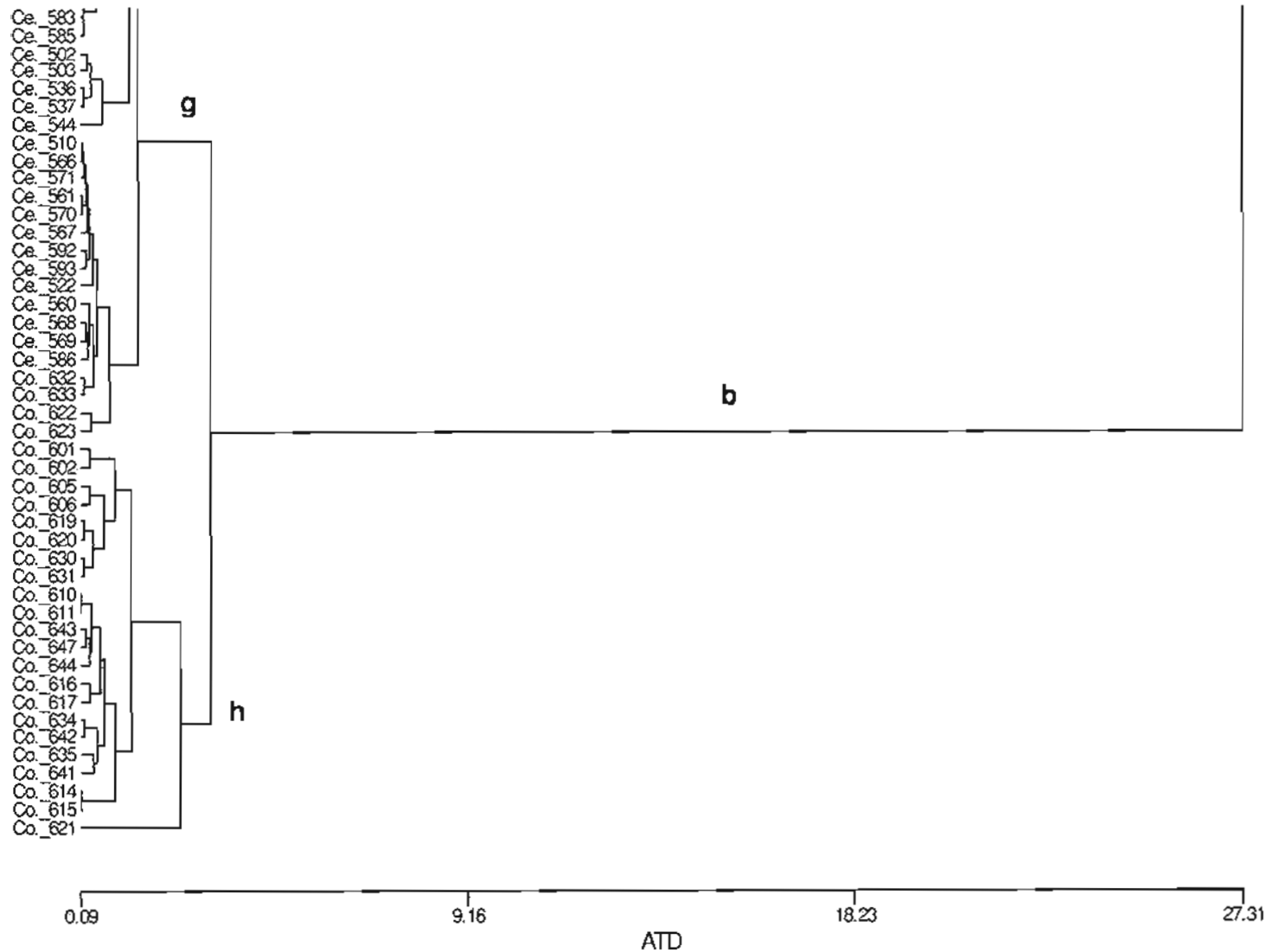

Figure A.5. (continued)

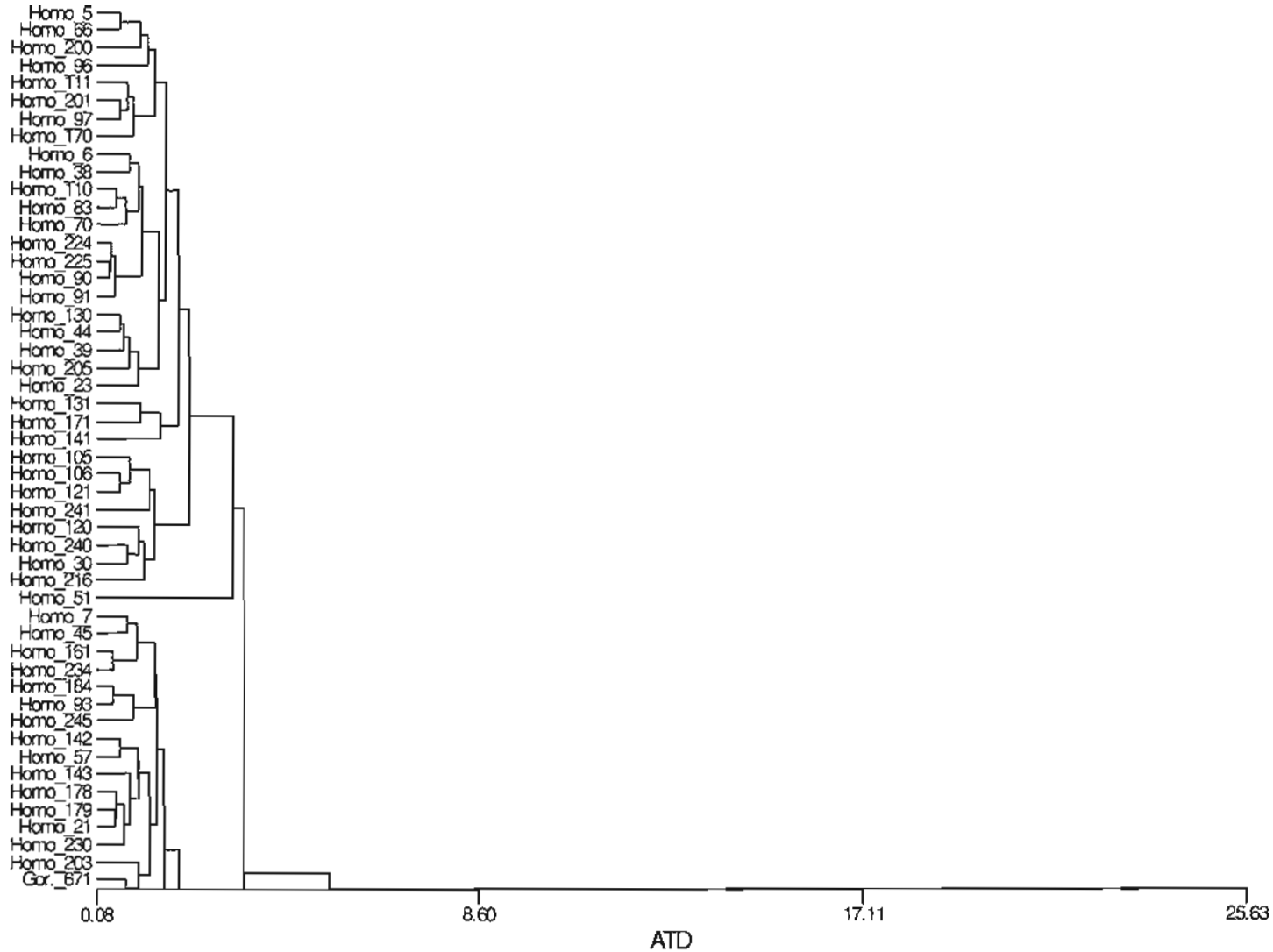

Figure A.6. Tree diagram from UPGMA cluster analysis – females proximal, Fourier data (letters refer to clusters in text)

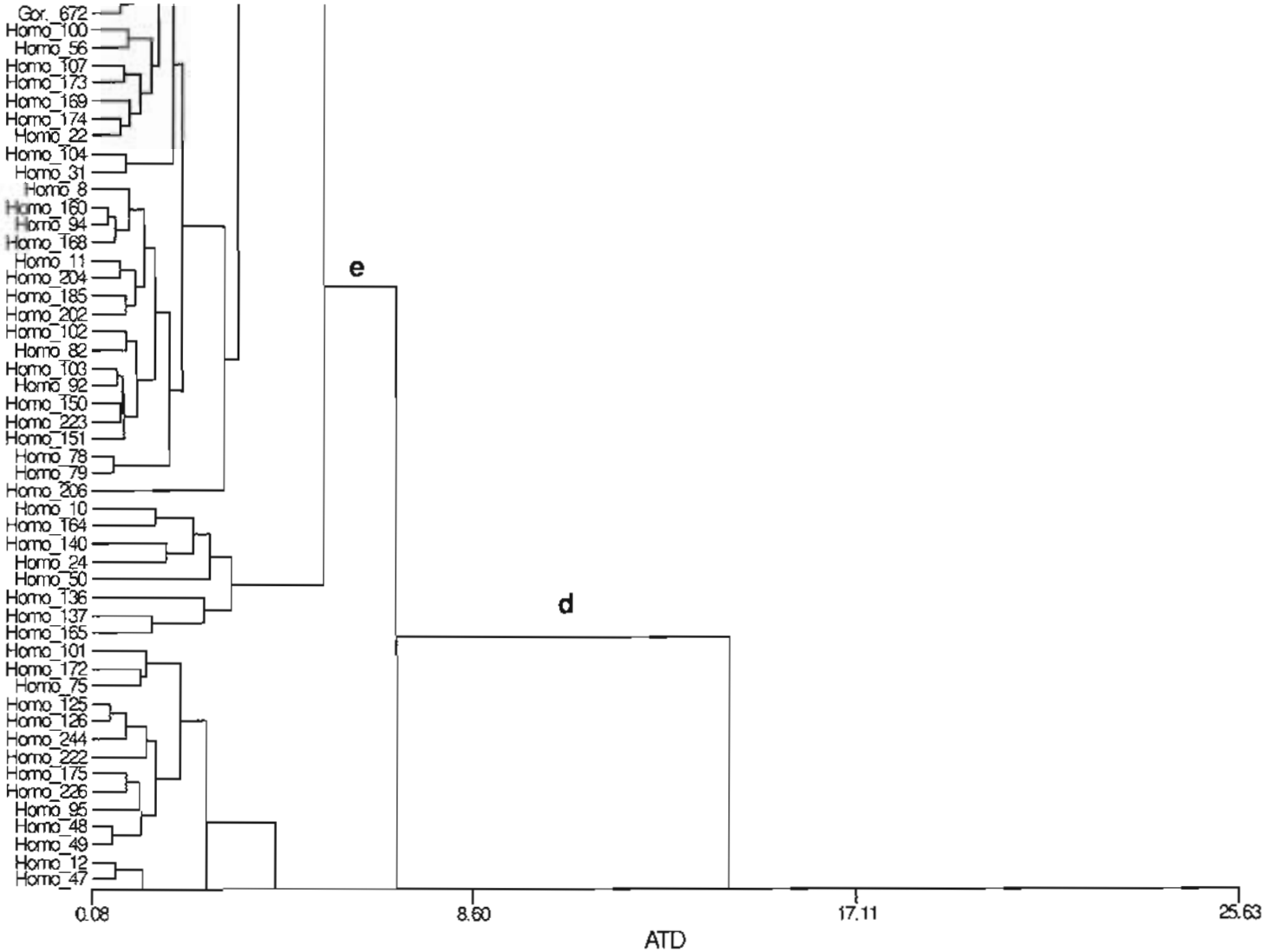

Figure A.6. (continued)

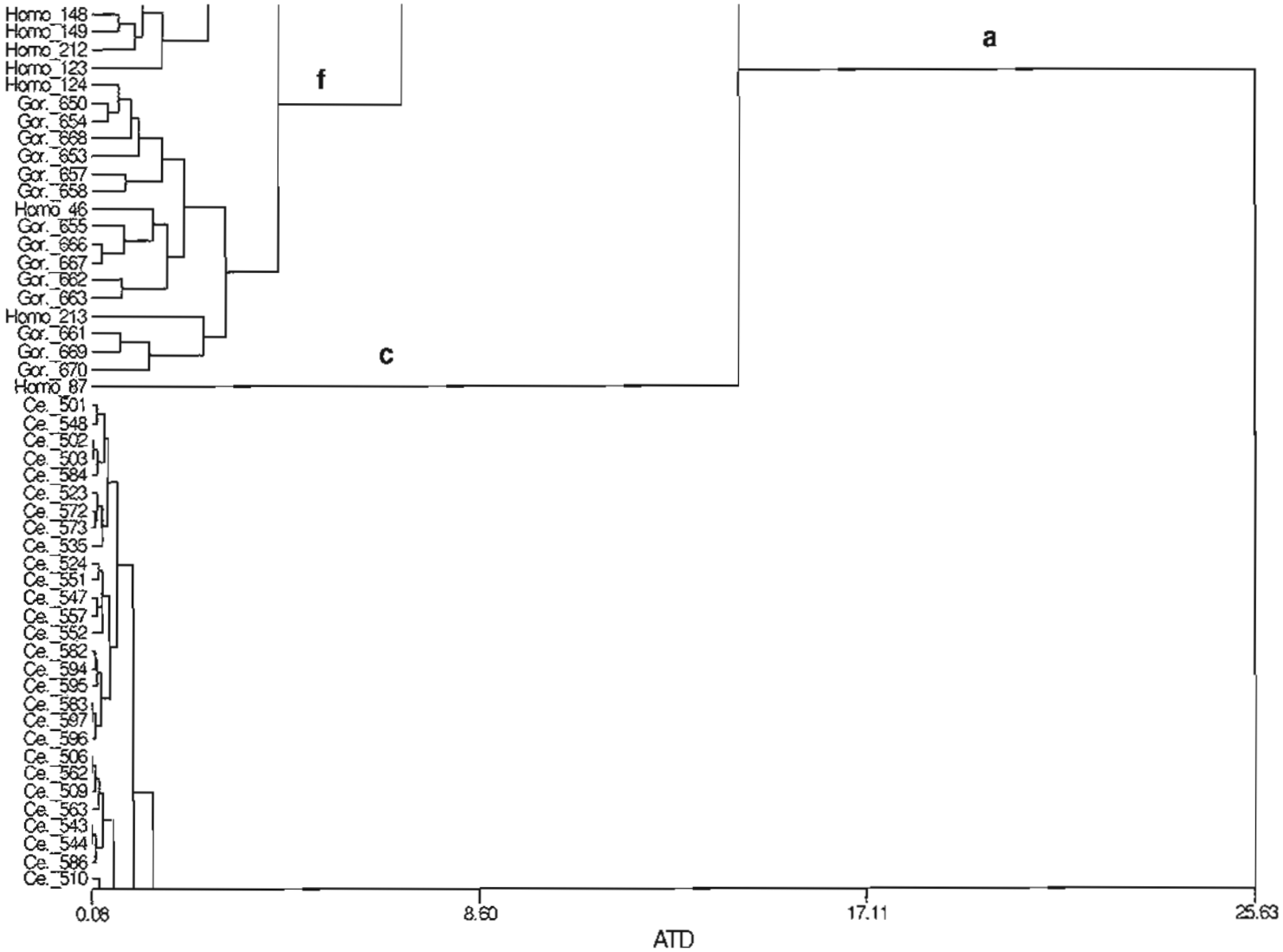

Figure A.6. (continued)

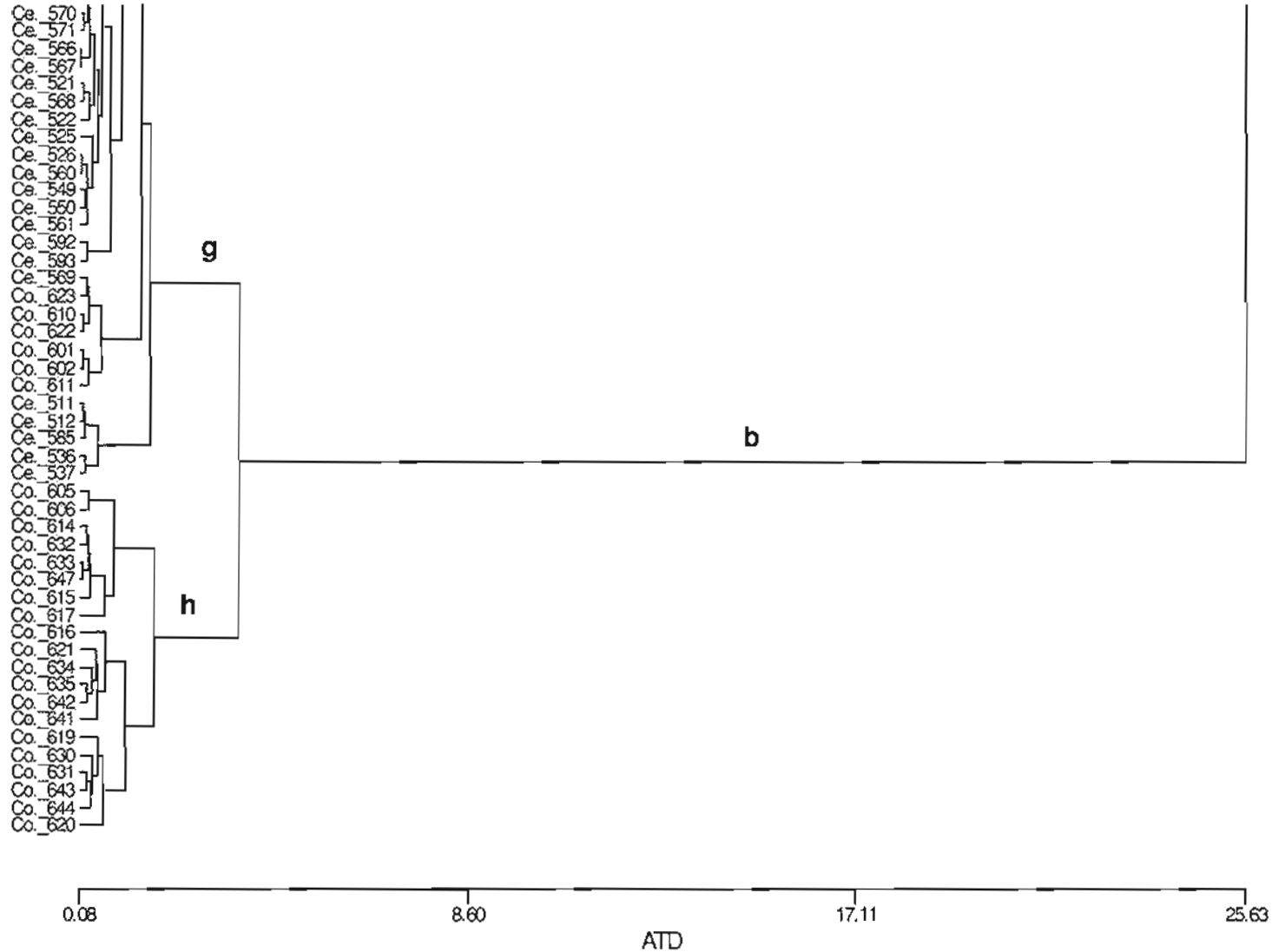

Figure A.6. (continued)

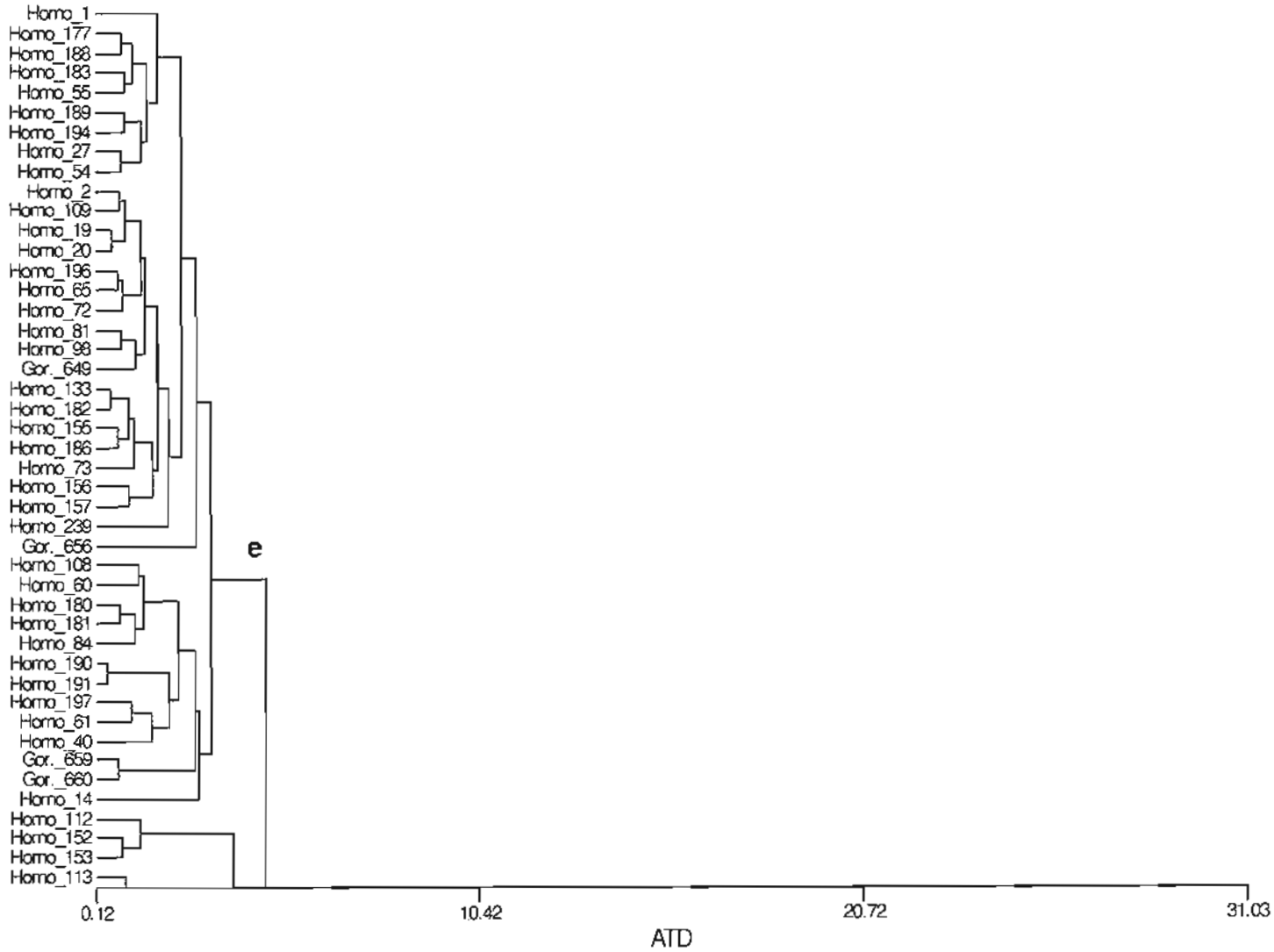

Figure A.7. Tree diagram from UPGMA cluster analysis – males distal, Fourier data (letters refer to clusters in text)

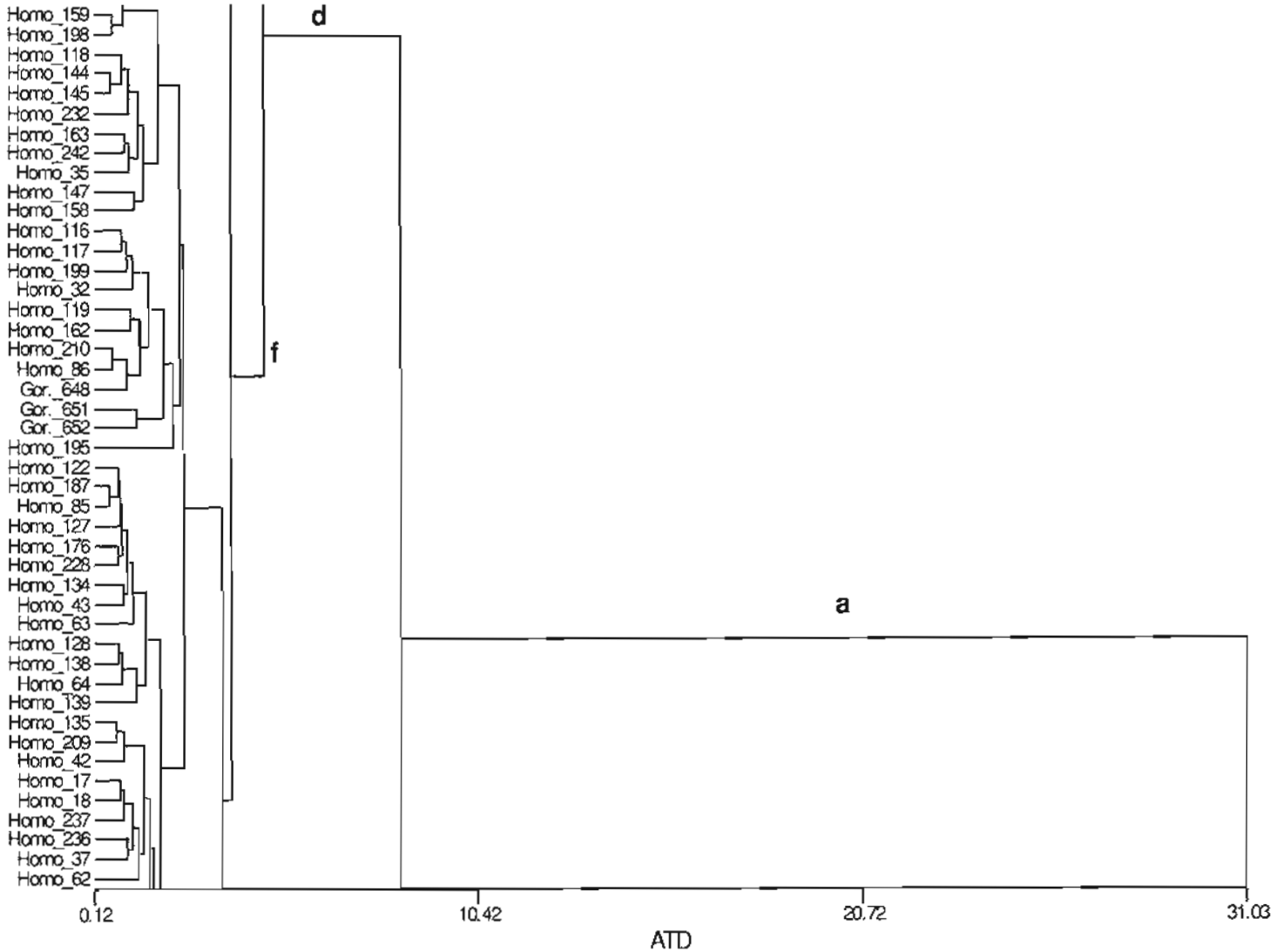

Figure A.7. (continued)

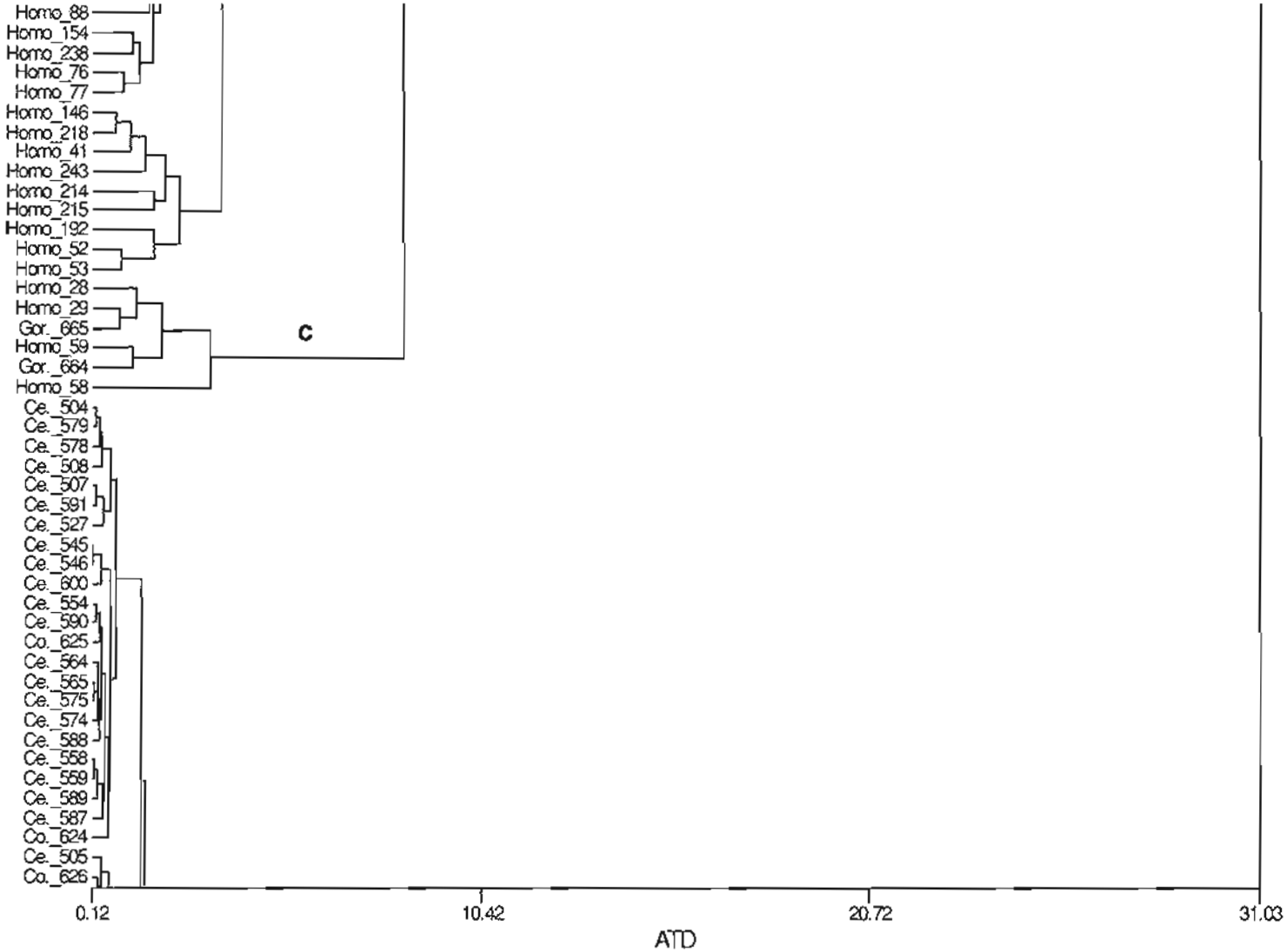

Figure A.7. (continued)

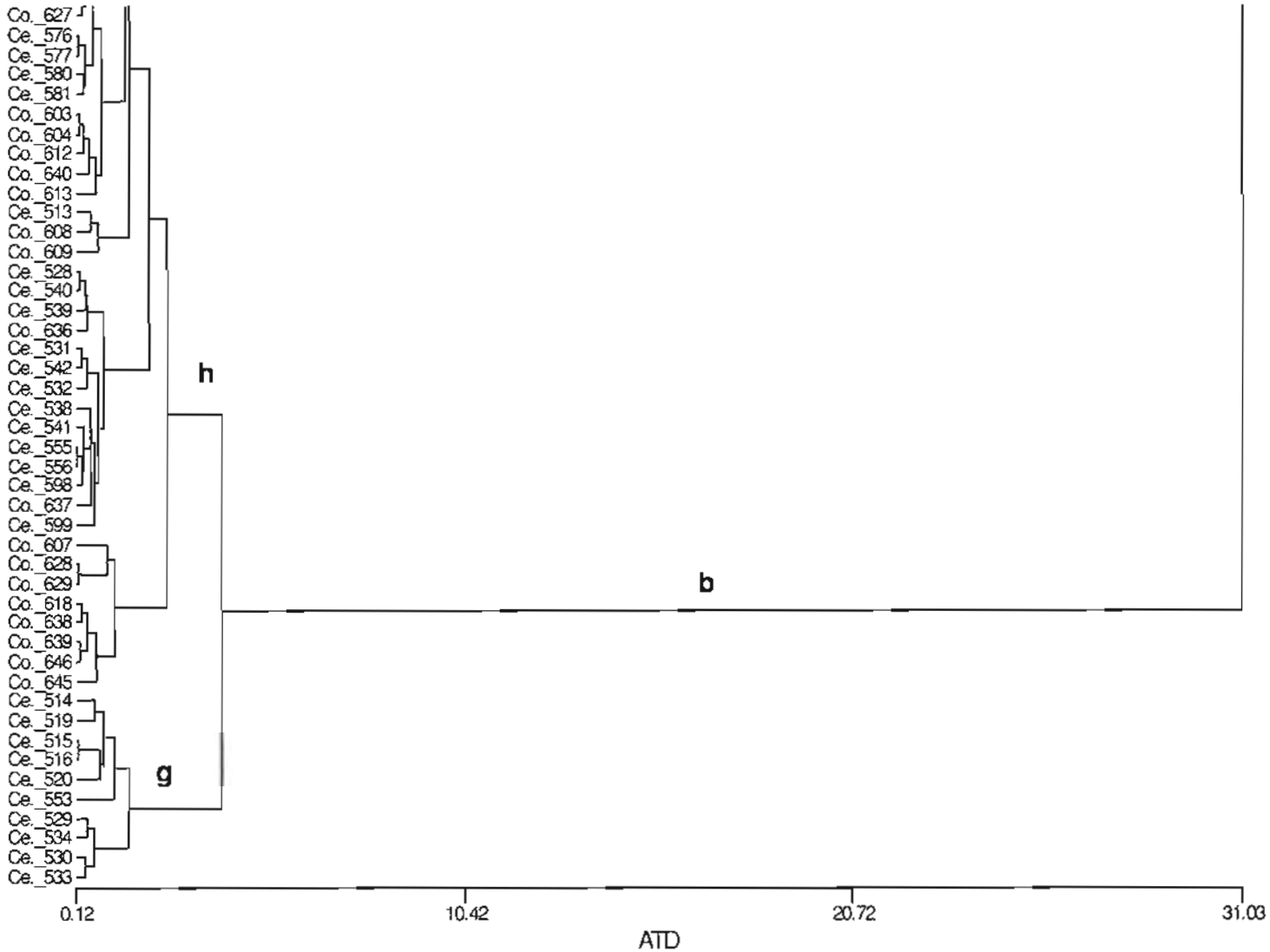

Figure A.7. (continued)

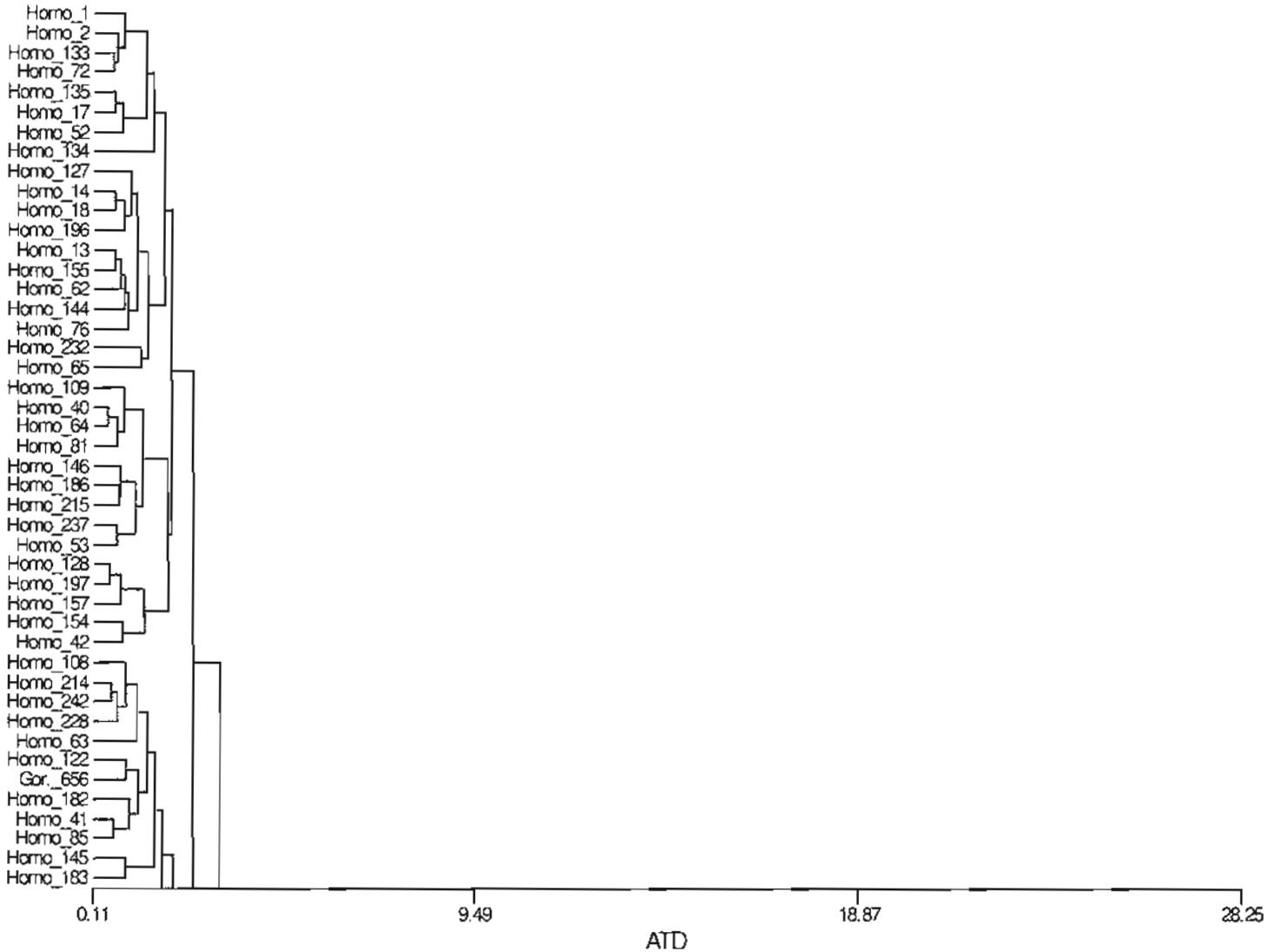

Figure A.8. Tree diagram from UPGMA cluster analysis – males proximal, Fourier data

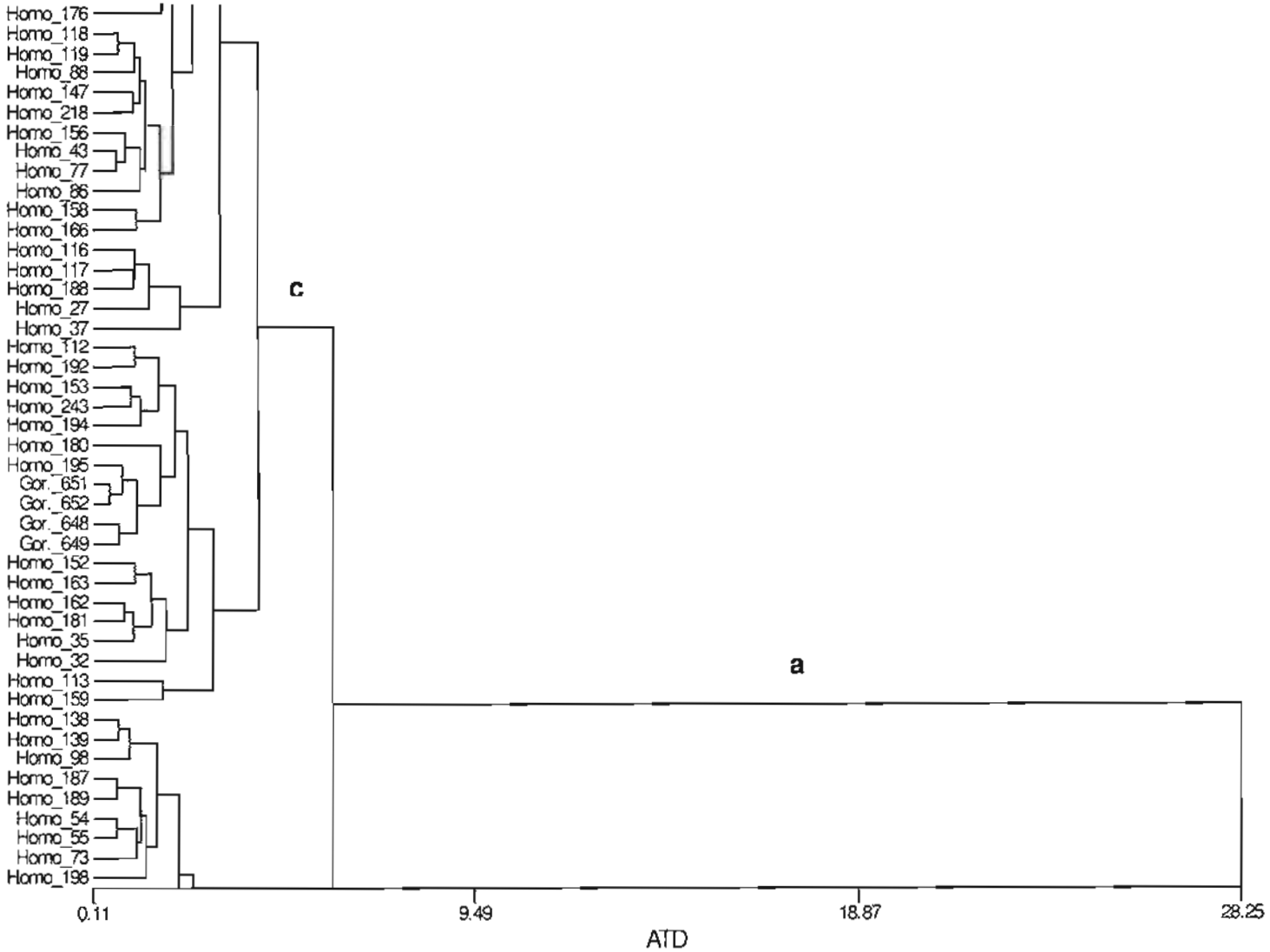

Figure A.8. (continued)

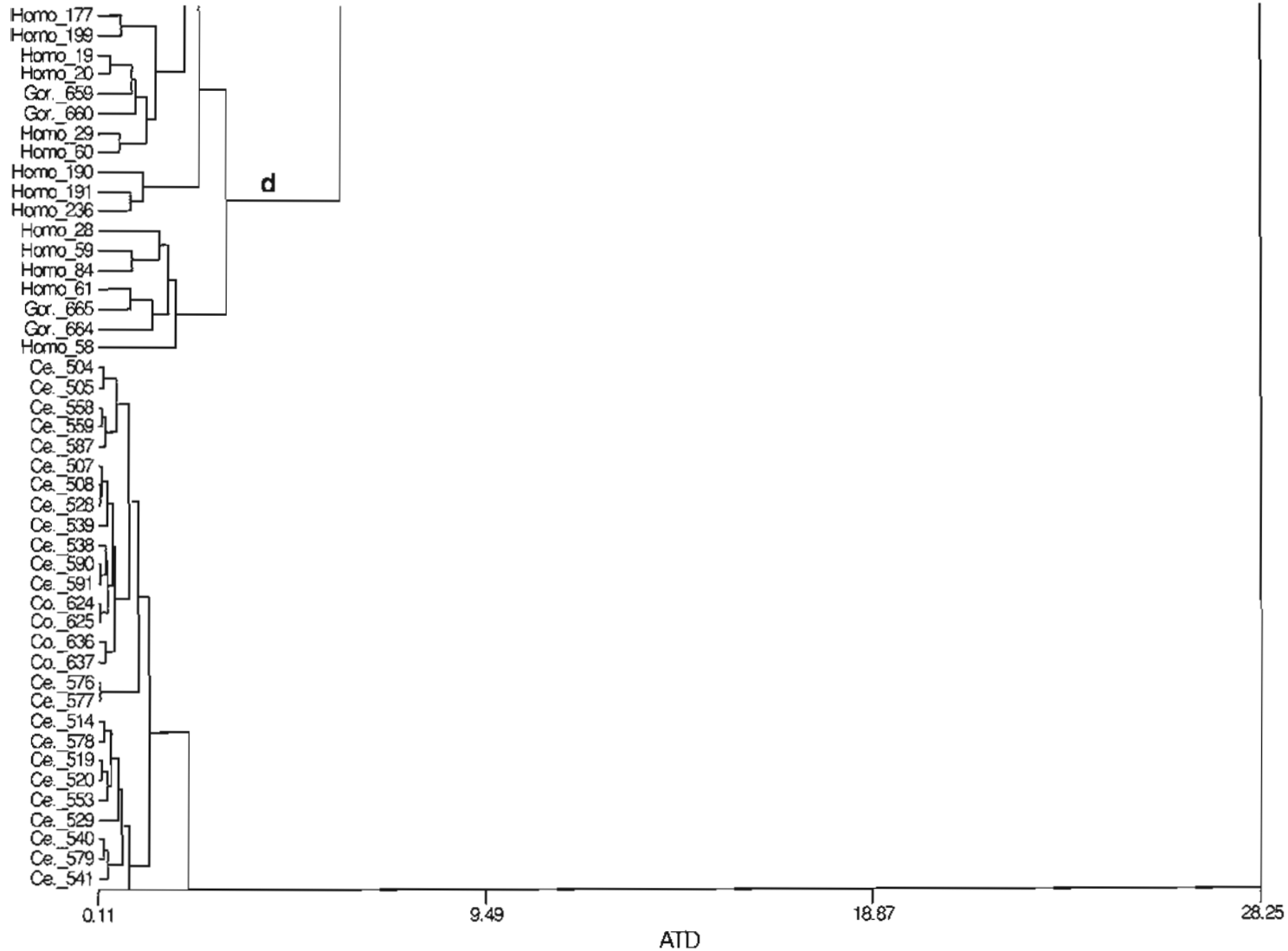

Figure A.8. (continued)

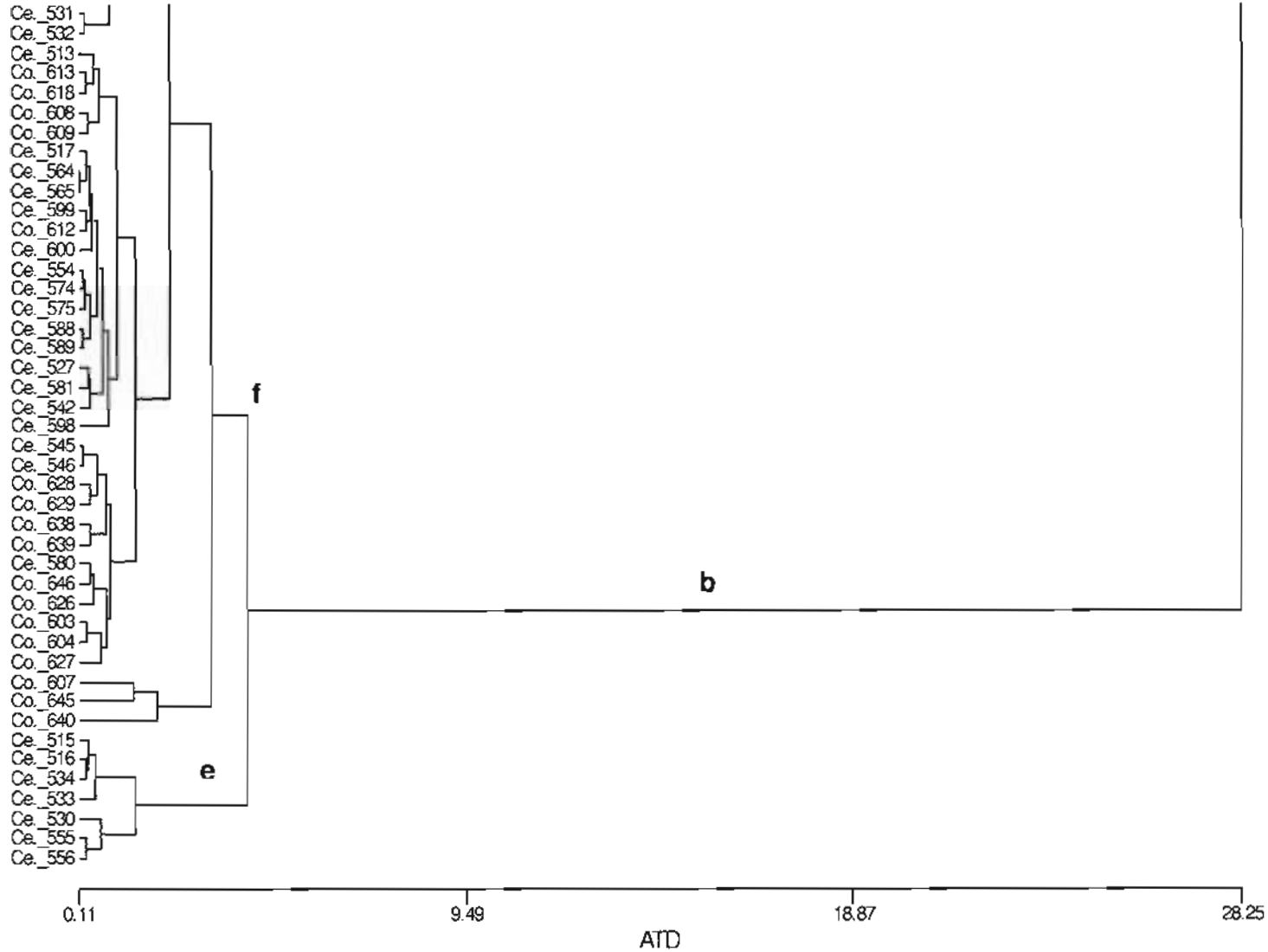

Figure A.8. (continued)

References

Aglietti, P, Insall, J and Cerulli, G (1983): Patellar pain and incongruence I: measurements of incongruence. *Clinical Orthopaedics and Related Research* 176: 217-24.

Ahmed, AM, Burke, DL and Hyder, A (1987): Force analysis of the patellar mechanism. *Journal of Orthopaedic Research* 5: 69-85.

Ahmed, AM, Burke, DL and Yu, A (1983): In-vitro measurement of static pressure distribution in synovial joints - part II: retropatellar surface. *Journal of Biomechanical Engineering* 105: 226-36.

Aiello, LC (1981): The allometry of primate body proportions. *Symposia of the Zoological Society of London* 48: 331-58.

Aiello, LC (1992): Allometry and the analysis of size and shape in human evolution. *Journal of Human Evolution* 22: 127-47.

Aiello, L and Dean, C (1990): An Introduction to Human Evolutionary Anatomy. London: Academic Press.

Aiello, LC and Wheeler, P (1995): The expensive-tissue hypothesis. The brain and the digestive system in human and primate evolution. *Current Anthropology* 36: 199-221.

Alberch, P (1982): Developmental constraints in evolutionary processes. In Bonner, JT (ed.): Evolution and Development. Berlin: Springer-Verlag.

Albrecht, GH, Gelvin, BR and Hartman, SE (1993): Ratios as a size adjustment in morphometrics. *American Journal of Physical Anthropology* 91: 441-68.

Aldenderfer, MS and Blashfield, RK (1984): Cluster Analysis. Beverly Hills: Sage Publications.

Alexander, RM (1977): Allometry of the limbs of antelopes (Bovidae). *Journal of Zoology London* 183: 125-46.

Alexander, RM (1980): Forces in animal joints. *Engineering in Medicine* 9: 93-7.

Alexander, RM (1981): Analysis of force platform data to obtain joint forces. In Dowson, D and Wright, V (eds.): An Introduction to the Bio-mechanics of Joints and Joint Replacement. London: Mechanical Engineering Publications.

Alexander, RM (1985a): Body support, scaling, and allometry. In Hildebrand, M, Bramble, DM, Liem, KF and Wake, DB (eds.): Functional Vertebrate Morphology. Cambridge: Harvard University Press.

Alexander, RM (1985b): The maximum forces exerted by animals. *Journal of Experimental Biology* 115: 231-8.

Alexander, RM and Dimery, NJ (1985): The significance of sesamoids and retro-articular processes for the mechanics of joints. *Journal of Zoology London* 205: 357-71.

Alexander, RM, Jayes, AS, Maloiy, GMO and Wathuta, EM (1979): Allometry of the limb bones of mammals from shrews (Sorex) to elephant (Loxodonta). *Journal of Zoology London* 189: 305-14.

Alexander, RM, Jayes, AS, Maloiy, GMO and Wathuta, EM (1981): Allometry of the leg muscles of mammals. *Journal of Zoology London* 194: 539-52.

Alexander, RMcN and Ker, RF (1990): The architecture of leg muscles. In Winters, JM and Woo, SLY (eds.): Multiple Muscle Systems: Biomechanics and Movement Organization. New York: Springer-Verlag.

Allison, DB, Paultre, F, Goran, MI, Poehlman, ET and Heymsfield, SB (1995): Statistical considerations regarding the use of ratios to adjust data. *International Journal of Obesity* 19: 644-52.

Amis, AA and Farahmand, F (1996): Extensor mechanism of the knee. *Current Orthopaedics* 10: 102-9.

Amtmann, E (1979): Biomechanical interpretation of form and structure of bones: role of genetics and function in growth and remodeling. In Morbeck, ME, Preuschoft, H and Gomberg, N (eds.): Environment, Behavior, and Morphology: Dynamic Interactions in Primates. New York: Gustav Fisher.

Anapol, F, Turner, TR and Mott, CS (1995): Postcranial proportions of *Cercopithecus aethiops* and *C. mitis*. *American Journal of Physical Anthropology* Supplement 20: 57.

Andersen, H (1961): Histochemical studies on the histogenesis of the knee joint and superior tibio-fibular joint in human foetuses. *Acta Anatomica* 46: 279-303.

Anderson, CM (1986): Predation and primate evolution. *Primates* 27: 15-39.

Anderson, JY and Trinkaus, E (1998): Patterns of sexual, bilateral and interpopulational variation in human femoral neck-shaft angles. *Journal of Anatomy* 192: 279-85.

Anderson, TW (1958): An Introduction to Multivariate Statistical Analysis. New York: John Wiley & Sons.

Anemone, RL (1993): The functional anatomy of the hip and thigh in primates. In Gebo, DL (ed.): Postcranial Adaptations in Nonhuman Primates. DeKalb: Northern Illinois University Press.

Armitage, P and Berry, G (1994): Statistical Methods in Medical Research (3rd ed.). Oxford: Blackwell Scientific Publications.

Arsuaga, JL and Carretero, JM (1994): Multivariate analysis of the sexual dimorphism of the hip bone in a modern human population and in early hominids. *American Journal of Physical Anthropology* 93: 241-57.

Ashton, EH, Healy, MJR, Oxnard, CE and Spence, TF (1965): The combination of locomotor features of the primate shoulder girdle by canonical analysis. *Journal of Zoology London* 147: 406-29.

Ashton, EH and Oxnard, CE (1964): Locomotor patterns in primates. *Proceedings of the Zoological Society of London* 145: 1-28.

Atchley, WR, Gaskins, CT and Anderson, D (1976): Statistical properties of ratios. I. Empirical results. *Systematic Zoology* 25: 137-48.

Atchley, WR and Hall, BK (1991): A model for development and evolution of complex morphological structures. *Biological Reviews* 66: 101-57.

Augat, P, Reeb, H and Claes, LE (1996): Prediction of fracture load at different skeletal sites by geometric properties of the cortical shell. *Journal of Bone and Mineral Research* 11: 1356-63.

Baba, H (1975): On the squatting facets of primates. Contemporary Primatology. 5th International Congress on Primatology, Nagoya 1974.

Bailey, RC and Byrnes, J (1990): A new, old method for assessing measurement error in both univariate and multivariate morphometric studies. *Systematic Zoology* 39: 124-30.

Bardeen, CR (1905): Studies of the development of the human skeleton. *American Journal of Anatomy* 4: 265-99.

Beaupré, GS, Orr, TE and Carter, DR (1990): An approach for time-dependent bone modeling and remodeling – theoretical development. *Journal of Orthopaedic Research* 8: 651-61.

Bennet-Clark, HC (1977): Scale effects in jumping animals. In Pedley, TJ (ed.): Scale Effects in Animal Locomotion. London: Academic Press.

Bennett, KA (1981): On the expression of sex dimorphism. *American Journal of Physical Anthropology* 56: 59-61.

Bennett, MB (1996): Allometry of the leg muscles of birds. *Journal of Zoology London* 238: 435-43.

Bennett, WF, Doherty, N, Hallisey, MJ and Fulkerson, JP (1993): Insertion orientation of terminal vastus lateralis obliquus and vastus medialis obliquus muscle fibers in human knees. *Clinical Anatomy* 6: 129-34.

Biegert, J and Maurer, R (1972): Rumpfskelettlänge, allometrien und körperproportionen bei catarrhinen primaten. *Folia Primatologica* 17: 142-56.

Biewener, AA (1982): Bone strength in small mammals and bipedal birds: do safety factors change with body size? *Journal of Experimental Biology* 98: 289-301.

Biewener, AA (1983): Allometry of quadrupedal locomotion: the scaling of duty factor, bone curvature and limb orientation to body size. *Journal of Experimental Biology* 105: 147-71.

Biewener, AA (1989): Scaling body support in mammals: limb posture and muscle mechanics. *Science* 245: 45-8.

Biewener, AA (1990): Biomechanics of mammalian terrestrial locomotion. *Science* 250: 1097-103.

Bishop, RED (1977): On the mechanics of the human knee. *Engineering in Medicine* 6: 46-52.

Bishop, RED and Denham, RA (1977): A note on the ratio between tensions in the quadriceps tendon and infra-patellar ligament. *Engineering in Medicine* 6: 53-4.

Bissell, AF and Ferguson, RA (1975): The jackknife - toy, tool or two-edged weapon? *Statistician* 24: 79-100.

Blackith, RE (1960): A synthesis of multivariate techniques to distinguish patterns of growth in grasshoppers. *Biometrics* 16: 28-40.

Blauth, M and Tillmann, B (1983): Stressing on the human femoro-patellar joint. I. Components of a vertical and horizontal tensile bracing system. *Anatomy and Embryology* 168: 117-23.

Bookstein, FL (1986): Size and shape spaces for landmark data in two dimensions. *Statistical Science* 1: 181-242.

Bookstein, FL (1989): "Size and shape": a comment on semantics. *Systematic Zoology* 38: 173-80.

Bookstein, FL (1990): Introduction and overview: geometry and biology. In Rohlf, FJ and Bookstein, FL (eds.): Proceedings of the Michigan Morphometrics Workshop. Ann Arbor: University of Michigan Museum of Zoology.

Bookstein, FL (1991): Morphometric Tools for Landmark Data: Geometry and Biology. Cambridge: Cambridge University Press.

Bookstein, FL (1996a): Biometrics, biomathematics and the morphometric synthesis. *Bulletin of Mathematical Biology* 58: 313-65.

Bookstein, FL (1996b): Combining the tools of geometric morphometrics. In Marcus, LF, Corti, M, Loy, A, Naylor, GJP and Slice, DE (eds.): Advances in Morphometrics. New York: Plenum.

Bookstein, FL, Strauss, RE, Humphries, JM, Chernoff, B, Elder, RL and Smith, GR (1982): A comment on the use of Fourier methods in systematics. *Systematic Zoology* 31: 85-92.

Bose, K, Kanagasuntheram, R and Osman, MBH (1980): Vastus medialis oblique: an anatomic and physiologic study. *Orthopedics* 3: 880-3.

Boyce, AJ (1969): Mapping diversity: a comparative study of some numerical methods. In Cole, AJ (ed.): Numerical Taxonomy. London: Academic Press.

Brattström, H (1964): Shape of the intercondylar groove normally and in recurrent dislocation of the patella. A clinical and X-ray investigation. *Acta Orthopaedica Scandinavica* Supplement 68.

Brattström, H and Ahlgren, SA (1960): Patellar shape and degenerative changes in the femoro-patellar joint. *Acta Orthopaedica Scandinavica* 29: 153-4.

Brown, TD and Ferguson, AB (1980): Mechanical property distributions in the cancellous bone of the human proximal femur. *Acta Orthopaedica Scandinavica* 51: 429-37.

Buff, H-U, Jones, LC and Hungerford, DS (1988): Experimental determination of forces transmitted through the patello-femoral joint. *Journal of Biomechanics* 21: 17-23.

Burkus, JK, Ganey, TM and Ogden, JA (1993): Development of the cartilage canals and the secondary center of ossification in the distal chondroepiphysis of the prenatal human femur. *Yale Journal of Biology and Medicine* 66: 193-202.

Burr, DB and Martin, RB (1992): Mechanisms of bone adaptation to the mechanical environment. *Triangle* 31: 59-76.

Burr, DB, Piotrowski, G, Martin, RB and Cook, PN (1982): Femoral mechanics in the lesser bushbaby (*Galago senegalensis*): structural adaptations to leaping in primates. *Anatomical Record* 202: 419-29.

Burr, DB, Piotrowski, G and Miller, GJ (1981): Structural strength of the macaque femur. *American Journal of Physical Anthropology* 54: 305-19.

Burr, DB, Schaffler, MB, Yang, KH, Lukoschek, M, Sivaneri, N, Blaha, JD and Radin, EL (1989a): Skeletal change in response to altered strain environments: is woven bone a response to elevated strain? *Bone* 10: 223-33.

Burr, DB, Schaffler, MB, Yang, KH, Wu, DD, Lukoschek, M, Kandzari, D, Sivaneri, N, Blaha, JD and Radin, EL (1989b): The effects of altered strain environments on bone tissue kinetics. *Bone* 10: 215-21.

Campbell, NA and Atchley, WR (1981): The geometry of canonical variate analysis. *Systematic Zoology* 30: 268-80.

Caplan, AI and Boyan, BD (1994): Endochondral bone formation: the lineage cascade. In Hall, BK (ed.): Bone (vol. 8). Mechanisms of Bone Development and Growth. Boca Raton: CRC Press.

Carey, EJ, Zeit, W and McGrath, BF (1927): Studies in the dynamics of histogenesis XII. The regeneration of the patellae of dogs. *American Journal of Anatomy* 40: 127-58.

Carpenter, JE, Kasman, R and Matthews, LS (1994): Fractures of the patella. In Schafer, M (ed.): Instructional Course Lectures. American Academy of Orthopaedic Surgeons.

Carter, DR and Hayes, WC (1976): Bone compressive strength: the influence of density and strain rate. *Science* 194: 1174-6.

Carter, DR, van der Meulen, MCH and Beaupré, GS (1996): Mechanical factors in bone growth and development. *Bone* 18: 5S-10S.

Carter, DR, Wong, M and Orr, TE (1991): Musculoskeletal ontogeny, phylogeny, and functional adaptation. *Journal of Biomechanics* 24: 3-16.

Cheverud, JM (1996): Developmental integration and the evolution of pleiotropy. *American Zoologist* 36: 44-50.

Cheverud, JM, Dow, MM and Leutenegger, W (1985): The quantitative assessment of phylogenetic constraints in comparative analyses: sexual dimorphism in body weight among primates. *Evolution* 39: 1335-51.

Clarke, GM (1998): The genetic basis of developmental stability. V. Inter- and intra-individual character variation. *Heredity* 80: 562-7.

Cliff, N (1987): Analyzing Multivariate Data. San Diego: Harcourt Brace Jovanovich.

Clutton-Brock, TH, Harvey, PH and Rudder, B (1977): Sexual dimorphism, socionomic sex ratio and body weight in primates. *Nature* 269: 797-800.

Collard, M and Wood, B (2000): How reliable are human phylogenetic hypotheses? *Proceedings of the National Academy of Science USA* 97: 5003-6.

Conlan, T, Garth, WP and Lemons, JE (1993): Evaluation of the medial soft-tissue restraints of the extensor mechanism of the knee. *Journal of Bone and Joint Surgery* 75A: 682-93.

Cooper, RR and Misol, S (1970): Tendon and ligament insertion. A light and electron microscopic study. *Journal of Bone and Joint Surgery* 52A: 1-20.

Corruccini, RS (1975): Morphometric affinities in the forelimb of Anthropoid primates. *Zeitschrift für Morphologie und Anthropology* 67: 19-31.

Corruccini, RS (1977): Relative growth and shape analysis. *Homo* 28: 222-6.

Corruccini, RS (1987): Shape in morphometrics: comparative analyses. *American Journal of Physical Anthropology* 73: 289-303.

Corruccini, RS (1995): Of ratios and rationality. *American Journal of Physical Anthropology* 96: 189-91.

Crampton, JS (1995): Elliptic Fourier shape analysis of fossil bivalves: some practical considerations. *Lethaia* 28: 179-86.

Cross, MJ and Waldrop, J (1975): The patella index as a guide to the understanding and diagnosis of patellofemoral instability. *Clinical Orthopaedics and Related Research* 110: 174-6.

Currey, JD (1977): Problems of scaling in the skeleton. In Pedley, TJ (ed.): Scale Effects in Animal Locomotion. London: Academic Press.

Currey, J (1984): The Mechanical Adaptations of Bones. Princeton: Princeton University Press.

Currey, JD (2003): How well are bones designed to resist fracture? *Journal of Bone and Mineral Research* 18: 591-8.

Currier, DP (1990): Elements of Research in Physical Therapy (3rd ed.). Baltimore: Williams & Wilkins.

Daegling, DJ and Jungers, WL (2000): Elliptical Fourier analysis of symphyseal shape in great ape mandibles. *Journal of Human Evolution* 39: 107-22.

Dahhan, P, Delepine, G and Larde, D (1981): The femoropatellar joint. *Anatomia Clinica* 3: 23-39.

Darroch, JN and Mosimann, JE (1985): Canonical and principal components of shape. *Biometrika* 72: 241-52.

Davis, JC (1986): Statistics and Data Analysis in Geology (2nd ed.). New York: John Wiley & Sons.

Dellanini, L, Hawkins, D, Martin, RB and Stover, S (2003): An investigation of the interactions between lower-limb bone morphology, limb inertial properties and limb dynamics. *Journal of Biomechanics* 36: 913-9.

Demes, B and Günther, MM (1989): Biomechanics and allometric scaling in primate locomotion and morphology. *Folia Primatologica* 53: 125-41.

Demes, B and Jungers, WL (1989): Functional differentiation of long bones in lorises. *Folia Primatologica* 52: 58-69.

Demes, B, Jungers, WL and Selpein, K (1991): Body size, locomotion, and long bone cross-sectional geometry in Indriid primates. *American Journal of Physical Anthropology* 86: 537-47.

DePalma, AF (1954): Diseases of the Knee. Philadelphia: J.B. Lippincott Company.

DeVore, I and Washburn, SL (1963): Baboon ecology and human evolution. In Howell, FC and Bourlière, F (eds.): African Ecology and Human Evolution. London: Methuen & Co.

de Vriese, B (1909): Recherches sur l'anatomie comparée de la rotule. *Bulletin de l'Académie Royale de Médecine* : 155-219.

Diaz, G, Cappai, C, Setzu, MD, Sirigu, S and Diana, A (1997): Elliptic Fourier descriptors of cell and nuclear shapes. In Lestrel (ed.): Fourier Descriptors and their Applications in Biology. Cambridge: Cambridge University Press.

Dixson, AF (1981): The Natural History of the Gorilla. London: Weidenfeld and Nicolson.

Dobbie, RP and Ryerson, S (1942): The treatment of fractured patella by excision. *American Journal of Surgery* 55: 339-73.

Doran, DM (1993): Sex differences in adult chimpanzee positional behaviour: the influence of body size on locomotion and posture. *American Journal of Physical Anthropology* 91: 99-115.

Doran, DM (1997): Ontogeny of locomotion in mountain gorillas and chimpanzees. *Journal of Human Evolution* 32: 323-44.

Doskocil, M (1985): Formation of the femoropatellar part of the human knee joint. *Folia Morphologica* 33: 38-47.

Drachman, DB and Sokoloff, L (1966): The role of movement in embryonic joint development. *Developmental Biology* 14: 401-20.

Duda, GN, Brand, D, Freitag, S, Lierse, W and Schneider, E (1996): Variability of femoral muscle attachments. *Journal of Biomechanics* 29: 1185-90.

Dye, SF (1987): An evolutionary perspective of the knee. *Journal of Bone and Joint Surgery* 69A: 976-83.

Dye, SF (1993): Patellofemoral anatomy. In Fox, JM and Del Pizzo, W (eds.): The Patellofemoral Joint. New York: McGraw-Hill.

Ebert, TA and Russell, MP (1994): Allometry and model II non-linear regression. *Journal of Theoretical Biology* 168: 367-72.

Eckstein, F, Merz, B, Schön, M, Jacobs, CR and Putz, R (1999): Tension and bending, but not compression alone determine the functional adaptation of subchondral bone in incongruous joints. *Anatomy and Embryology* 199: 85-97.

Efron, B and Gong, G (1983): A leisurely look at the bootstrap, the jackknife, and cross-validation. *American Statistician* 37: 36-48.

Ehrlich, R, Pharr, RB and Healy-Williams, N (1983): Comments on the validity of Fourier descriptors in systematics: a reply to Bookstein et al. *Systematic Zoology* 32: 202-6.

Elias, SG, Freeman, MAR and Gokcay, I (1990): A correlative study of the geometry and anatomy of the distal femur. *Clinical Orthopaedics and Related Research* 260: 98-103.

Epker, BN and Frost, HM (1965): A histological study of remodeling at the periosteal, haversian canal, cortical endosteal, and trabecular endosteal surfaces in human rib. *Anatomical Record* 152: 129-36.

Erlebacher, A, Filvaroff, EH, Gitelman, SE and Derynck, R (1995): Toward a molecular understanding of skeletal development. *Cell* 80: 371-8.

Evans, EJ, Benjamin, M and Pemberton, DJ (1990): Fibrocartilage in the attachment zones of the quadriceps tendon and patellar ligament of man. *Journal of Anatomy* 171: 155-62.

Evans, EJ, Benjamin, M and Pemberton, DJ (1991): Variations in the amount of calcified tissue at the attachments of the quadriceps tendon and patellar ligament in man. *Journal of Anatomy* 174: 145-51.

Fabry, G, Cheng, LX and Molenaers, G (1994): Normal and abnormal torsional development in children. *Clinical Orthopaedics and Related Research* 302: 22-6.

Fairbairn, DJ (1997): Allometry for sexual size dimorphism: pattern and process in the coevolution of body size in males and females. *Annual Review of Ecology and Systematics* 28: 659-87.

Fairbank, JCT, Pynsent, PB, van Poortvliet, JA and Phillips, H (1984): Mechanical factors in the incidence of knee pain in adolescents and young adults. *Journal of Bone and Joint Surgery* 66B: 685-93.

Farahmand, F, Senavongse, W and Amis, AA (1998): Quantitative study of the quadriceps muscles and trochlear groove geometry related to instability of the patellofemoral joint. *Journal of Orthopaedic Research* 16: 136-43.

Faulkner, KG, Cummings, SR, Black, D, Palermo, L, Glüer, CC and Genant, HK (1993): Simple measurement of femoral geometry predicts hip fracture: the study of osteoporotic fractures. *Journal of Bone and Mineral Research* 8: 1211-7.

Fay, JM, Carroll, R, Kerbis Peterhans, JC and Harris, D (1995): Leopard attack on and consumption of gorillas in the Central African Republic. *Journal of Human Evolution* 29: 93-9.

Ferber, R, Davis, IM and Williams, DS (2003): Gender differences in lower extremity mechanics during running. *Clinical Biomechanics* 18: 350-7.

Ferrario, VF, Sforza, C, Serrao, G, Frattini, T and Del Favero, C (1994): Shape of the human corpus callosum. Elliptic Fourier analysis on midsagittal magnetic resonance scans. *Investigative Radiology* 29: 677-81.

Ferson, S, Rohlf, FJ and Koehn, RK (1985): Measuring shape variation of two-dimensional outlines. *Systematic Zoology* 34: 59-68.

Ficat, P, Ficat, C and Bailleux, A (1975): Syndrome d'hyperpression externe de la rotule (SHPE). *Revue de Chirurgie Orthopédique* 61: 39-59.

Fleagle, JG (1976): Locomotion and posture of the Malayan siamang and implications for hominoid evolution. *Folia Primatologica* 26: 245-69.

Fleagle, JG (1985): Size and adaptation in primates. In Jungers, WL (ed.): Size and Scaling in Primate Biology. New York: Plenum Press.

Fleagle, JG (1988): Primate Adaptation and Evolution. San Diego: Academic Press.

Fleagle, JG and Mittermeier, RA (1980): Locomotor behavior, body size, and comparative ecology of seven Surinam monkeys. *American Journal of Physical Anthropology* 52: 301-14.

Fleiss, JL (1986): The Design and Analysis of Clinical Experiments. New York: John Wiley & Sons.

Flessa, KW and Bray, RG (1977): On the measurement of size-independent morphological variability: an example using successive populations of a Devonian spirifed brachiopod. *Paleobiology* 3: 350-9.

Flury, B (1988): Common Principal Components and Related Multivariate Models. New York: John Wiley & Sons.

Flury, B and Riedwyl, H (1988): Multivariate Statistics. A Practical Approach. London: Chapman and Hall.

Foottit, RG and Sorensen, JT (1992): Ordination methods: their contrast to clustering and cladistic techniques. In Sorensen, JT and Foottit, R (eds.): Ordination in the Study of Morphology, Evolution and Systematics of Insects: Applications and Quantitative Genetic Rationales. Amsterdam: Elsevier.

Foster, DW and Kaesler, RL (1988): Shape analysis. Ideas from the ostracoda. In McKinney, ML (ed.): Heterochrony in Evolution. A Multidisciplinary Approach. New York: Plenum Press.

Fox, JC and Keaveny, TM (2001): Trabecular eccentricity and bone adaptation. *Journal of Theoretical Biology* 212: 211-21.

Francis, AJ (1980): Introducing Structures. Oxford: Pergamon Press.

Frankel, VH and Burstein, AH (1965): Load capacity of tubular bone. In Kenedi, RM (ed.): Biomechanics and Related Bio-engineering Topics. Oxford: Pergamon Press.

Frost, HM (1979): A chondral modeling theory. *Calcified Tissue International* 28: 181-200.

Frost, HM (1983): A determinant of bone architecture. The minimum effective strain. *Clinical Orthopaedics and Related Research* 175: 286-92.

Frost, HM (1990a): Skeletal structural adaptations to mechanical usage (SATMU): 1. Redefining Wolff's Law: The bone modeling problem. *Anatomical Record* 226: 403-13.

Frost, HM (1990b): Skeletal structural adaptations to mechanical usage (SATMU): 2. Redefining Wolff's Law: The remodelling problem. *Anatomical Record* 226: 414-22.

Frost, HM (1990c): Skeletal structural adaptations to mechanical usage (SATMU): 3. The hyaline cartilage modeling problem. *Anatomical Record* 226: 423-32.

Frost, HM (1994): Wolff's Law and bone's functional adaptations to mechanical usage: an overview for clinicians. *Angle Orthodontist* 64: 175-88.

Frost, HM (1997): Why do marathon runners have less bone than weight lifters? A vital-biomechanical view and explanation. *Bone* 20: 183-9.

Fu, FH, Seel, MJ and Berger, RA (1993): Patellofemoral biomechanics. In Fox, JM and Del Pizzo, W (eds.): The Patellofemoral Joint. New York: McGraw-Hill.

Fulkerson, JP (1997): Disorders of the Patellofemoral Joint (3rd ed.). Baltimore: Williams & Wilkins.

Fulkerson, JP and Cautilli, RA (1993): Chronic patellar instability: subluxation and dislocation. In Fox, JM and Del Pizzo, W (eds.): The Patellofemoral Joint. New York: McGraw-Hill.

Fulkerson, JP and Gossling, HR (1980): Anatomy of the knee joint lateral retinaculum. *Clinical Orthopaedics and Related Research* 153: 183-8.

Galileo Galilei (1638): Two New Sciences. Translated by Drake, S (1974). Madison: University of Wisconsin Press.

Gambaryan, PP (1974): How Mammals Run: Anatomical Adaptations. New York: John Wiley & Sons.

Gardner, E and O'Rahilly, R (1968): The early development of the knee joint in staged human embryos. *Journal of Anatomy* 102: 289-99.

Garn, SM, Rohmann, CG, Wagner, B and Ascoli, W (1967): Continuing bone growth throughout life: a general phenomenon. *American Journal of Physical Anthropology* 26: 313-8.

Gautier-Hion, A and Gautier, JP (1985): Sexual dimorphism, social units and ecology among sympatric forest guenons. In Ghesquiere, J, Martin, RD and Newcombe, F (eds.): Human Sexual Dimorphism. London: Taylor & Francis.

Gere, JM and Timoshenko, SP (1997): Mechanics of Materials (4th ed.). Boston: PWS Publishing Company.

Giardina, CR and Kuhl, FP (1977): Accuracy of curve approximation by harmonically related vectors with elliptical loci. *Computer Graphics and Image Processing* 6: 277-85.

Gibson, LJ (1985): The mechanical behaviour of cancellous bone. *Journal of Biomechanics* 18: 317-28.

Gijzen, A and Tijskens, J (1971): Growth in weight of the lowland gorilla and of the mountain gorilla. *International Zoo Yearbook* 11: 183-93.

Gnanadesikan, R and Wilk, MB (1969): Data analytic methods in multivariate statistical analysis. In Krishnaiah, PR (ed.): Multivariate Analysis - II. New York: Academic Press.

Godfrey, L, Sutherland, M, Boy, D and Gomberg, N (1991): Scaling of limb joint surface areas in anthropoid primates and other animals. *Journal of Zoology London* 223: 603-25.

Goldstein, SA, Coale, E, Weiss, APC, Grossnickle, M, Meller, B and Matthews, LS (1986): Patellar surface strain. *Journal of Orthopaedic Research* 4: 372-7.

Goodfellow, J, Hungerford, DS and Zindel, M (1976): Patello-femoral joint mechanics and pathology 1. Functional anatomy of the patello-femoral joint. *Journal of Bone and Joint Surgery* 58B: 287-90.

Gould, SJ (1966): Allometry and size in ontogeny and phylogeny. *Biological Reviews* 41: 587-640.

Gould, SJ (1971): Geometric similarity in allometric growth: a contribution to the problem of scaling in the evolution of size. *American Naturalist* 105: 113-36.

Gould, SJ (1975): On the scaling of tooth size in mammals. *American Zoologist* 15: 351-62.

Gould, SJ and Lewontin, RC (1979): The spandrels of San Marco and the Panglossian paradigm: a critique of the adaptationist programme. *Proceedings of the Royal Society of London, Biology* 205: 581-98.

Gower, JC (1967): Multivariate analysis and multidimensional geometry. *Statistician* 17: 13-28.

Gower, JC (1987): Introduction to ordination techniques. In Legendre, P and Legendre, L (eds.): Developments in Numerical Ecology. Berlin: Springer-Verlag.

Gray, DJ and Gardner, E (1950): Prenatal development of the human knee and superior tibiofibular joints. *American Journal of Anatomy* 86: 235-88.

Grelsamer, RP, Proctor, CS and Bazos, AN (1994): Evaluation of patellar shape in the sagittal plane. A clinical analysis. *American Journal of Sports Medicine* 22: 61-6.

Grine, FE, Jungers, WL and Schultz, J (1996): Phenetic affinities among early *Homo* crania from East and South Africa. *Journal of Human Evolution* 30: 189-225.

Grood, ES, Suntay, WJ, Noyes, FR and Butler, DL (1984): Biomechanics of the knee-extension exercise. Effect of cutting the anterior cruciate ligament. *Journal of Bone and Joint Surgery* 66A: 725-34.

Guerra, JP, Arnold, MJ and Gajdosik, RL (1994): Q angle: effects of isometric quadriceps contraction and body position. *Journal of Orthopedic and Sports Physical Therapy* 19: 200-4.

Günther, MM, Ishida, H, Kumakura, H and Nakano, Y (1991): The jump as a fast mode of locomotion in arboreal and terrestrial biotopes. *Zeitschrift für Morphologie und Anthropology* 78: 341-72.

Haines, RW (1947): The development of joints. *Journal of Anatomy* 81: 33-51.

Halbrecht, JL and Jackson, DW (1993): Acute dislocation of the patella. In Fox, JM and Del Pizzo, W (eds.): The Patellofemoral Joint. New York: McGraw-Hill.

Hall, BK and Herring, SW (1990): Paralysis and growth of the musculoskeletal system in the embryonic chick. *Journal of Morphology* 206: 45-56.

Hall-Craggs, ECB (1965): An analysis of the jump of the Lesser Galago (*Galago senegalensis*). *Journal of Zoology London* 147: 20-9.

Hallén, LG and Lindahl, O (1965): Rotation in the knee-joint in experimental injury to the ligaments. *Acta Orthopaedica Scandinavica* 36: 400-7.

Hallén, LG and Lindahl, O (1966): The "screw-home" movement in the knee joint. *Acta Orthopaedica Scandinavica* 37: 97-106.

Hallgrímsson, B, Willmore, K and Hall, BK (2002): Canalization, developmental stability, and morphological integration in primate limbs. *Yearbook of Physical Anthropology* 45: 131-58.

Hallisey, MJ, Doherty, N, Bennett, WF and Fulkerson, JP (1987): Anatomy of the junction of the vastus lateralis tendon and the patella. *Journal of Bone and Joint Surgery* 69A: 545-9.

Hamrick, MW (1999): A chondral modeling theory revisited. *Journal of Theoretical Biology* 201: 201-8.

Han, SM (1999): Ultrasound velocity and attenuation in relation to maximum trabecula stress in the patella. *Medical Engineering and Physics* 21: 541-6.

Harris, HA and Russell, AE (1933): The atypical growth in cartilage as the fundamental factor in dwarfism and achondroplasia. *Proceedings of the Royal Society of Medicine* 26: 779-87.

Harrison, GA, Tanner, JM, Pilbeam, DR and Baker, PT (1988): Human Biology. An Introduction to Human Evolution, Variation, Growth and Adaptability (3rd ed.). Oxford: Oxford University Press.

Harrison, MJS (1988): A new species of guenon (genus *Cercopithecus*) from Gabon. *Journal of Zoology London* 215: 561-75.

Hartman, JL, Garvik, B and Hartwell, L (2001): Principles for the buffering of genetic variation. *Science* 291: 1001-4.

Harvey, PH, Kavanagh, M and Clutton-Brock, TH (1978): Sexual dimorphism in primate teeth. *Journal of Zoology London* 186: 475-85.

Harvey, PH and Pagel, MD (1991): The Comparative Method in Evolutionary Biology. Oxford: Oxford University Press.

Haxton, H (1944): The patellar index in mammals. *Journal of Anatomy* 78: 106-7.

Hayes, WC, Swenson, LW and Schurman, DJ (1978): Axisymmetric finite element analysis of the lateral tibial plateau. *Journal of Biomechanics* 11: 21-33.

Hayes, WC and Snyder, B (1981): Toward a quantitative formulation of Wolff's Law in trabecular bone. In Cowin, SC (ed.): Mechanical Properties of Bone. New York: American Society of Mechanical Engineers.

Healy-Williams, N, Ehrlich, R and Full, WE (1997): Closed-form Fourier analysis: a procedure for extracting ecological information from foraminiferal test morphology. In Lestrel, PE (ed.): Fourier Descriptors and their Applications in Biology. Cambridge: Cambridge University Press.

Heegaard, J, Leyvraz, PF, Curnier, A, Rakotomanana, L and Huiskes, R (1995): The biomechanics of the human patella during passive knee flexion. *Journal of Biomechanics* 28: 1265-79.

Heegaard, J, Leyvraz, PF, Van Kampen, A, Rakotomanana, L, Rubin, PJ and Blankevoort, L (1994): Influence of soft structures on patellar three-dimensional tracking. *Clinical Orthopaedics and Related Research* 299: 235-43.

Hefzy, MS, Jackson, WT, Saddemi, SR and Hsieh, YF (1992): Effects of tibial rotations on patellar tracking and patello-femoral contact areas. *Journal of Biomedical Engineering* 14: 329-43.

Hehne, HJ (1990): Biomechanics of the patellofemoral joint and its clinical relevance. *Clinical Orthopaedics and Related Research* 258: 73-85.

Heiple, KG and Lovejoy, CO (1971): The distal femoral anatomy of Australopithecus. *American Journal of Physical Anthropology* 35: 75-84.

Henneberg, M (1998): Evolution of the human brain: is bigger better? *Clinical and Experimental Pharmacology and Physiology* 25: 745-9.

Hens, SM, Konigsberg, LW and Jungers, WL (1998): Estimation of African ape body length from femur length. *Journal of Human Evolution* 34: 401-11.

Hey Groves, EW (1931): A note on the extension apparatus of the knee joint. *British Journal of Surgery* 24: 747-8.

Hildebrand, M (1988): Analysis of Vertebrate Structure (3rd ed.). New York: John Wiley & Sons.

Hinchliffe, JR and Johnson, DR (1983): Growth of cartilage. In Hall, BK (ed.): Cartilage. Volume 2. Development, Differentiation, and Growth. London: Academic Press.

Hirokawa, S (1991): Three-dimensional mathematical model analysis of the patellofemoral joint. *Journal of Biomechanics* 24: 659-71.

Hopkins, JW (1966): Some considerations in multivariate allometry. *Biometrics* 22: 747-60.

Horton, MG and Hall, TL (1989): Quadriceps femoris muscle angle: normal values and relationships with gender and selected skeletal measures. *Physical Therapy* 69: 897-901.

Hosseini, A and Hogg, DA (1991): The effects of paralysis on skeletal development in the chick embryo. I. General effects. *Journal of Anatomy* 177: 159-68.

Houston, CS and Zaleski, WA (1967): The shape of vertebral bodies and femoral necks in relation to activity. *Radiology* 89: 59-66.

Huberti, HH and Hayes, WC (1984): Patellofemoral contact pressures. The influence of Q-angle and tendofemoral contact. *Journal of Bone and Joint Surgery* 66A: 715-24.

Huberti, HH, Hayes, WC, Stone, JL and Shybut, GT (1984): Force ratios in the quadriceps tendon and ligamentum patellae. *Journal of Orthopaedic Research* 2: 49-54.

Humphrey, LT (1998): Growth patterns in the modern human skeleton. *American Journal of Physical Anthropology* 105: 57-72.

Hungerford, DS and Barry, M (1979): Biomechanics of the patellofemoral joint. *Clinical Orthopaedics and Related Research* 199: 9-15.

Hungerford, DS and Lennox, DW (1983): Rehabilitation of the knee in disorders of the patellofemoral joint: relevant biomechanics. *Orthopedic Clinics of North America* 14: 397-402.

Huxley, JS (1932): Problems of Relative Growth. London: Methuen & Co.

Huxley, JS and Teissier, G (1936): Terminology of relative growth. *Nature* 137: 780-1.

Igbigbi, PS and Msamati, BC (2002): Tibiofemoral angle in Malawians. *Clinical Anatomy* 15: 293-6.

Insall, J, Falvo, KA and Wise, DW (1976): Chondromalacia patellae. A prospective study. *Journal of Bone and Joint Surgery* 58A: 1-8.

Isbell, LA (1990): Sudden short-term increase in mortality of vervet monkeys (*Cercopithecus aethiops*) due to leopard predation in Amboseli National Park, Kenya. *American Journal of Primatology* 21: 41-52.

Iwamoto, J, Yeh, JK and Aloia, JF (1999): Differential effect of treadmill exercise on three cancellous bone sites in the young growing rat. *Bone* 24: 163-9.

Iwasaki, M, Le, AX and Helms, JA (1997): Expression of indian hedgehog, bone morphogenetic protein 6 and gli during skeletal morphogenesis. *Mechanisms of Development* 69: 197-202.

Jee, WSS (1983): The skeletal tissues. In Weiss, L (ed.): Histology. Cell and Tissue Biology. New York: Macmillan Press.

Jee, WSS and Frost, HM (1992): Skeletal adaptations during growth. *Triangle* 31: 77-88.

Jee, WSS, Li, XJ and Schaffler, MB (1981): Adaptation of diaphyseal structure with aging and increased mechanical usage in the adult rat: a histomorphometrical and biomechanical study. *Anatomical Record* 230: 332-8.

Johnson, DR (1997): Fourier descriptors and shape differences: studies on the upper vertebral column of the mouse. In Lestrel, PE (ed.): Fourier Descriptors and their Applications in Biology. Cambridge: Cambridge University Press.

Johnson, KA, Muir, P, Nicoll, RG and Roush, JK (2000): Asymmetric adaptive modeling of central tarsal bones in racing greyhounds. *Bone* 27: 257-63.

Jolicoeur, P (1963a): The degree of generality of robustness in *Martes americana*. *Growth* 27: 1-27.

Jolicoeur, P (1963b): The multivariate generalization of the allometry equation. *Biometrics* 19: 497-9.

Jolicoeur, P (1968): Interval estimation of the slope of the major axis of a bivariate normal distribution in the case of a small sample. *Biometrics* 24: 679-82.

Jolicoeur, P (1990): Bivariate allometry: interval estimation of the slopes of the ordinary and standardized normal major axes and structural relationship. *Journal of Theoretical Biology* 144: 275-85.

Jolicoeur, P and Heusner, AA (1971): The allometry equation in the analysis of the standard oxygen consumption and body weight of the white rat. *Biometrics* 27: 841-55.

Jolicoeur, P and Mosimann, JE (1960): Size and shape variation in the Painted Turtle. A principal component analysis. *Growth* 24: 339-54.

Jolicoeur, P and Mosimann, JE (1968): Intervalles de confiance pour la pente de l'axe majeur d'une distribution normale didimensionnelle. *Biométrie-Praximétrie* 9: 121-40.

Jolliffe, IT (1986): Principal Component Analysis. New York: Springer-Verlag.

Jo-Osvatic, A, Nikolic, V, Hudec, M, Percac, S and Subaric, M (1993): Developmental biomechanics of the patella. *Periodicum Biologorum* 95: 179-80.

Jungers, WL (1979): Locomotion, limb proportions, and skeletal allometry in lemurs and lorises. *Folia Primatologica* 32: 8-28.

Jungers, WL (1984): Aspects of size and scaling in primate biology with special reference to the locomotor skeleton. *Yearbook of Physical Anthropology* 27: 73-97.

Jungers, WL (1988): Relative joint size and hominoid locomotor adaptations with implications for the evolution of hominid bipedalism. *Journal of Human Evolution* 17: 247-65.

Jungers, WL (1990): Problems and methods in reconstructing body size in fossil primates. In Damuth, J and MacFadden, BJ (eds.): Body Size in Mammalian Paleobiology. Estimation and Biological Implications. Cambridge: Cambridge University Press.

Jungers, WL and Burr, DB (1994): Body size, long bone geometry and locomotion in quadrupedal monkeys. *Zeitschrift für Morphologie und Anthropology* 80: 89-97.

Jungers, WL, Cole, TM and Owsley, DW (1988): Multivariate analysis of relative growth in the limb bones of Arikara Indians. *Growth, Development & Aging* 52: 103-7.

Jungers, WL, Falsetti, AB and Wall, CE (1995): Shape, relative size, and size-adjustments in morphometrics. *Yearbook of Physical Anthropology* 38: 137-61.

Jungers, WJ, Jouffroy, FK and Stern, JT (1980): Gross structure and function of the quadriceps femoris in *Lemur fulvus*: an analysis based on telemetered electromyography. *Journal of Morphology* 164: 287-99.

Jungers, WL and Minns, RJ (1979): Computed tomography and biomechanical analysis of fossil long bones. *American Journal of Physical Anthropology* 50: 285-90.

Jungers, WL and Susman, RL (1984): Body size and skeletal allometry in African apes. In Susman, RL (ed.): The Pygmy Chimpanzee. Evolutionary Biology and Behavior. New York: Plenum Press.

Kaplan, EB (1957): Surgical approach to the lateral (peroneal) side of the knee joint. *Surgery, Gynecology and Obstetrics* March: 346-56.

Kaplan, EB (1962): Some aspects of functional anatomy of the human knee joint. *Clinical Orthopaedics and Related Research* 23: 18-29.

Karp, SJ, Schipani, E, St-Jacques, B, Hunzelman, J, Kronenberg, H and McMahon, AP (2000): Indian hedgehog coordinates endochondral bone growth and morphogenesis via Parathyroid Hormone related-Protein-dependent and –independent pathways. *Development* 127: 543-8.

Kaufer, H (1971): Mechanical function of the patella. *Journal of Bone and Joint Surgery* 53A: 1551-60.

Kaufer, H (1979): Patellar biomechanics. *Clinical Orthopaedics and Related Research* 144: 51-4.

Kendall, MG and Stuart, A (1973): The Advanced Theory of Statistics (3rd ed.). London: Griffin.

Kern, HM and Straus, WL (1949): The femur of *Plesianthropus transvaalensis*. *American Journal of Physical Anthropology* 7: 53-77.

Kernozek, TW and Greer, NL (1993): Quadriceps angle and rearfoot motion: relationships in walking. *Archives of Physical Medicine and Rehabilitation* 74: 407-10.

Key, C and Ross, C (1999): Sex differences in energy expenditure in non-human primates. *Proceedings of the Royal Society of London, Biology* 266: 2479-85.

Kim, YJ, Sah, RLY, Grodzinsky, AJ, Plaas, AHK and Sandy, JD (1994): Mechanical regulation of cartilage biosynthetic behavior: physical stimuli. *Archives of Biochemistry and Biophysics* 311: 1-12.

Kimura, DK (1992): Symmetry and scale dependence in functional relationship regression. *Systematic Biology* 41: 233-41.

King, CA, Iscan, MY and Loth, SR (1998): Metric and comparative analysis of sexual dimorphism in the Thai femur. *Journal of Forensic Sciences* 43: 954-8.

Klingenberg, CP (1996): Multivariate allometry. In Marcus, LF, Corti, M, Loy, A, Naylor, GJP and Slice, DE (eds.): Advances in Morphometrics. New York: Plenum Press.

Klingenberg, CP (1998): Heterochrony and allometry: the analysis of evolutionary change in ontogeny. *Biological Reviews* 73: 79-123.

Klingenberg, CP, Leamy, LJ, Routman, EJ and Cheverud, JM (2001): Genetic architecture of mandible shape in mice: effects of quantitative trait loci analyzed by geometric morphometrics. *Genetics* 157: 785-802.

Kronenberg, HM, Lee, K, Lanske, B and Segre, GV (1997): Parathyroid hormone-related protein and Indian hedgehog control the pace of cartilage differentiation. *Journal of Endocrinology* 154: S39-45.

Kuhl, FP and Giardina, CR (1982): Elliptic Fourier features of a closed contour. *Computer Graphics and Image Processing* 18: 236-58.

Kuhry, B and Marcus, LF (1977): Bivariate linear models in allometry. *Systematic Zoology* 26: 201-9.

Lague, MR (2003): Patterns of joint size dimorphism in the elbow and knee of catarrhine primates. *American Journal of Physical Anthropology* 120: 278-97.

Lague, MR and Jungers, WL (1996): Morphometric variation in Plio-Pleistocene hominid distal humeri. *American Journal of Physical Anthropology* 101: 401-27.

Lague, MR and Jungers, WL (1999): Patterns of sexual dimorphism in the hominoid distal humerus. *Journal of Human Evolution* 36: 379-99.

Lamont, JC (1910): Note on the influence of posture on the facets of the patella. *Journal of Anatomy and Physiology* 44: 149-50.

Lanske, B, Karaplis, AC, Lee, K, Luz, A, Vortkamp, A, Pirro, A, Karperien, M, Defize, LHK, Ho, C, Mulligan, RC, Abou-Samra, AB, Jüppner, H, Segre, GV and Kronenberg, HM (1996): PTH/PTHrP receptor in early development and Indian hedgehog-regulated bone growth. *Science* 273: 663-6.

Lanyon, LE (1981): Locomotor loading and functional adaptation in limb bones. *Symposia of the Zoological Society of London* 48: 305-29.

Lanyon, LE (1987): Functional strain in bone tissue as an objective, and controlling stimulus for adaptive bone remodelling. *Journal of Biomechanics* 20: 1083-93.

Lanyon, LE (1996): Using functional loading to influence bone mass and architecture: objectives, mechanisms, and relationship with estrogen of the mechanically adaptive process in bone. *Bone* 18: 37S-43S.

Lanyon, LE, Goodship, AE, Pye, CJ and MacFie, JH (1982): Mechanically adaptive bone remodelling. *Journal of Biomechanics* 15: 141-54.

Lanyon, LE and Rubin, CT (1985): Functional adaptation in skeletal structures. In Hildebrand, M, Bramble, DM, Liem, KF and Wake, DB (eds.): Functional Vertebrate Morphology. Cambridge: Harvard University Press.

Lazenby, RA (2002): Population variation in second metacarpal sexual size dimorphism. *American Journal of Physical Anthropology* 118: 378-84.

Leamy, L and Bradley, D (1982): Static and growth allometry of morphometric traits in randombred house mice. *Evolution* 36: 1200-12.

Legendre, P and Legendre, L (1998): Numerical Ecology (2nd ed.). Amsterdam: Elsevier.

Leigh, SR (1995): Socioecology and the ontogeny of sexual size dimorphism in anthropoid primates. *American Journal of Physical Anthropology* 97: 339-56.

Leigh, SR and Shea, BT (1996): Ontogeny of body size variation in African apes. *American Journal of Physical Anthropology* 99: 43-65.

Lele, S (1991): Some comments on coordinate-free and scale-invariant methods in morphometrics. *American Journal of Physical Anthropology* 85: 407-14.

Lestrel, PE (1989): Method for analyzing complex two-dimensional forms: elliptical Fourier functions. *American Journal of Human Biology* 1: 149-64.

Lestrel, PE (1989): Some approaches toward the mathematical modeling of the craniofacial complex. *Journal of Craniofacial Genetics and Developmental Biology* 9: 77-91.

Lestrel, PE (1997a): Introduction. In Lestrel, PE (ed.): Fourier Descriptors and their Applications in Biology. Cambridge: Cambridge University Press.

Lestrel, PE (1997b): Introduction and overview of Fourier descriptors. In Lestrel, PE (ed.): Fourier Descriptors and their Applications in Biology. Cambridge: Cambridge University Press.

Lestrel, PE, Bodt, A and Swindler, DR (1993): Longitudinal study of cranial base shape changes in *Macaca nemestrina*. American Journal of Physical Anthropology 91: 117-29.

Lestrel, PE and Kerr, WJS (1993): Quantification of function regulator therapy using elliptical Fourier functions. *European Journal of Orthodontics* 15: 481-91.

Lestrel, PE, Kimbel, WH, Prior, FW and Fleischmann, ML (1977): Size and shape of the hominoid distal femur: Fourier analysis. *American Journal of Physical Anthropology* 46: 281-90.

Leutenegger, W (1978): Scaling of sexual dimorphism in body size and breeding system in primates. *Nature* 272: 610-1.

Leutenegger, W (1982): Sexual dimorphism in nonhuman primates. In Hall, RL (ed.): Sexual Dimorphism in *Homo sapiens*. A Question of Size. New York: Praeger.

Leutenegger, W and Cheverud, JM (1985): Sexual dimorphism in primates. The effects of size. In Jungers, WL (ed.): Size and Scaling in Primate Biology. New York: Plenum Press.

Leutenegger, W and Larson, S (1985): Sexual dimorphism in the postcranial skeleton of New World primates. *Folia Primatologica* 44: 82-95.

Leutenegger, W and Lubach, G (1987): Sexual dimorphism, mating system, and effect of phylogeny in De Brazza's monkey (*Cercopithecus neglectus*). *American Journal of Primatology* 13: 171-9.

LeVeau, BF (1992): Williams & Lissner's Biomechanics of Human Motion (3rd ed.). Philadelphia: W B Saunders.

Levinton, JS (1986): Developmental constraints and evolutionary saltations: a discussion and critique. In Gustafson, JP, Stebbins, GL and Ayala, FJ (eds.): Genetics, Development, and Evolution. New York: Plenum Press.

Lieb, FJ and Perry, J (1968): Quadriceps function. An anatomical and mechanical study using amputated limbs. *Journal of Bone and Joint Surgery* 50A: 1535-48.

Lieberman, DE (1997): Making behavioral and phylogenetic inferences from hominid fossils: considering the developmental influence of mechanical forces. *Annual Review of Anthropology* 26: 185-210.

Lieberman, LS (1982): Normal and abnormal sexual dimorphic patterns of growth and development. In Hall, RL (ed.): Sexual Dimorphism in *Homo sapiens*. A Question of Size. New York: Praeger.

Lin, F, Makhsous, M, Chang, AH, Hendrix, RW and Zhang, LQ (2003): In vivo and non-invasive six degrees of freedom patellar tracking during voluntary knee movement. *Clinical Biomechanics* 18: 401-9.

Lindenfors, P and Tullberg, BS (1998): Phylogenetic analyses of primate size evolution: the consequences of sexual selection. *Biological Journal of the Linnean Society* 64: 413-47.

Lindley, DV (1947): Regression lines and the linear relationship. *Journal of the Royal Statistical Society Supplement* 9: 218-44.

Lindstedt, SL and Calder, WA (1981): Body size, physiological time, and longevity of homeothermic animals. *Quarterly Review of Biology* 56: 1-16.

Liu, J, Mercer, JM, Stam, LF, Gibson, GC, Zeng, ZB and Laurie, CC (1996): Genetic analysis of a morphological shape difference in the male genitalia of *Drosophila simulans* and *D. mauritiana*. *Genetics* 142: 1129-45.

Lohmann, GP (1983): Eigenshape analysis of microfossils: a general morphometric procedure for describing changes in shape. *Mathematical Geology* 15: 659-72.

Lovejoy, CO, Burstein, AH and Heiple, KG (1976): The biomechanical analysis of bone strength: a method and its application to platycnemia. *American Journal of Physical Anthropology* 44: 489-506.

Lovejoy, CO, Heiple, KG and Burstein, AH (1973): The gait of *Australopithecus*. *American Journal of Physical Anthropology* 38: 757-80.

Lovich, JE and Gibbons, JW (1992): A review of techniques for quantifying sexual size dimorphism. *Growth, Development & Aging* 56: 269-81.

Lovy, D (1994-1996): WinDIG. University of Geneva. Version 2.5.

Lowe, BF, Phillips, C, Lestrel, PE and Fields, HW (1994): Skeletal jaw relationships: a quantitative assessment using elliptic Fourier functions. *Angle Orthodontist* 64: 299-310.

Lu, KH (1965): Harmonic analysis of the human face. *Biometrics* 21: 491-505.

Macchiarelli, R and Sperduti, A (1998): Mandibular fossa size variation in past and extant human populations. *Homo* 49: 172-92.

Malkin, SAS (1932): Dislocation of the patella. *British Medical Journal* II: 91-4.

Manaster, BJ (1979): Locomotor adaptations within the *Cercopithecus* genus: a multivariate approach. *American Journal of Physical Anthropology* 50: 169-82.

Mankin, HJ (1962): Localization of tritiated thymidine in articular cartilage in rabbits. I. Growth in immature cartilage. *Journal of Bone and Joint Surgery* 44A: 682-8.

Maquet, PGJ (1984): Biomechanics of the Knee. With Application to the Pathogenesis and the Surgical Treatment of Osteoarthritis (2nd ed.). Berlin: Springer-Verlag.

Marcus, LF (1990): Traditional morphometrics. In Rohlf, FJ and Bookstein, FL (eds.): Proceedings of the Michigan Morphometrics Workshop. Ann Arbor: The University of Michigan Museum of Zoology.

Marini, E, Racugno, W and Borgognini Tarli, SM (1999): Univariate estimates of sexual dimorphism: the effects of intrasexual variability. *American Journal of Physical Anthropology* 109: 501-8.

Martin, RB and Atkinson, PJ (1977): Age and sex-related changes in the structure and strength of the human femoral shaft. *Journal of Biomechanics* 10: 223-31.

Martin, RD and Barbour, AD (1989): Aspects of line-fitting in bivariate allometric analyses. *Folia Primatologica* 53: 65-81.

Martin, RD, Willner, LA and Dettling, A (1994): The evolution of sexual size dimorphism in primates. In Short, RV and Balaban, E (eds.): The Differences between the Sexes. Cambridge: Cambridge University Press.

Masterson, TJ and Hartwig, WC (1998): Degrees of sexual dimorphism in *Cebus* and other New World monkeys. *American Journal of Physical Anthropology* 107: 243-56.

Mattfeldt, T and Mall, G (1987): Statistical methods for growth allometric studies. *Growth* 51: 86-102.

Maynard Smith, J, Burian, R, Kauffman, S, Alberch, P, Campbell, J, Goodwin, B, Lande, R, Raup, D and Wolpert, L (1985): Developmental constraints and evolution. *Quarterly Review of Biology* 60: 265-87.

McDermott, LJ (1943): Development of the human knee joint. *Archives of Surgery* 46: 705-19.

McGraw, WS (1996): Cercopithecid locomotion, support use, and support availability in the Tai Forest, Ivory Coast. *American Journal of Physical Anthropology* 100: 507-22.

McLachlan, JC (1999): Developmental morphologies not directly specified by the genome of the individual. In Chaplain, MAJ, Singh, GD and McLachlan, JC (eds.): On Growth and Form: Spatio-temporal Pattern Formation in Biology. Chichester: John Wiley & Sons.

McLellan, T and Endler, JA (1998): The relative success of some methods for measuring and describing the shape of complex objects. *Systematic Biology* 47: 264-81.

McLeod, KJ, Rubin, CT, Otter, MW and Qin, YX (1998): Skeletal cell stresses and bone adaptation. *American Journal of the Medical Sciences* 316: 176-83.

McMahon, T (1973): Size and shape in biology. Elastic criteria impose limits on biological proportions, and consequently on metabolic rates. *Science* 179: 1201-4.

McMahon, TA (1975): Allometry and biomechanics: limb bones in adult ungulates. *American Naturalist* 109: 547-63.

Merchant, AC (1993): The lateral patellar compression syndrome. In Fox, JM and Del Pizzo, W (eds.): The Patellofemoral Joint. New York: McGraw-Hill.

Mérida-Velasco, JA, Sánchez-Montesimos, I, Espín-Ferra, J, Rodríguez-Vázquez, JF, Mérida-Velasco, JR and Jiménez-Collado, J (1997): Development of the human knee joint. *Anatomical Record* 248: 269-78.

Miller, JA and Gross, MM (1998): Locomotor advantages of Neandertal skeletal morphology at the knee and ankle. *Journal of Biomechanics* 31: 355-61.

Milz, S, Eckstein, F and Putz, R (1995): The thickness of the subchondral plate and its correlation with the thickness of the uncalcified articular cartilage in the human patella. *Anatomy and Embryology* 192: 437-44.

Milz, S, Eckstein, F and Putz, R (1997): Thickness distribution of the subchondral mineralization zone of the trochlear notch and its correlation with the cartilage thickness: an expression of functional adaptation to mechanical stress acting on the humeroulnar joint? *Anatomical Record* 248: 189-97.

Minns, RJ, Birnie, AJM and Abernethy, PJ (1979): A stress analysis of the patella, and how it relates to articular cartilage lesions. *Journal of Biomechanics* 12: 699-711.

Mittermeier, RA and Fleagle, JG (1976): The locomotor and postural repertoires of *Ateles geoffroyi* and *Colobus guereza*, and a reevaluation of the locomotor category semibrachiation. *American Journal of Physical Anthropology* 45: 235-56.

Morrison, DF (1976): Multivariate Statistical Methods (2nd ed.). New York: McGraw-Hill Book Company.

Mosimann, JE (1970): Size allometry: size and shape variables with characterizations of the lognormal and generalized gamma distributions. *Journal of the American Statistical Association* 65: 930-45.

Mosimann, JE and James, FC (1979): New statistical methods for allometry with application to Florida red-winged blackbirds. *Evolution* 33: 444-59.

Mosimann, JE and Malley, JD (1979): Size and shape variables. In Orloci, L, Rao, CR and Stiteler, WM (eds.): Multivariate Methods in Ecological Work. Fairland: International Co-operative Publishing House.

Nakamura, T, Turner, CH, Yoshikawa, T, Slemenda, CW, Peacock, M, Burr, DB, Mizuno, Y, Orimo, H, Ouchi, Y and Johnston, CC (1994): Do variations in hip geometry explain differences in hip fracture risk between Japanese and white Americans? *Journal of Bone and Mineral Research* 9: 1071-6.

Napier, JR and Walker, AC (1967): Vertical clinging and leaping – a newly recognized category of locomotor behaviour of primates. *Folia Primatologica* 6: 204-19.

Nettle, D (2002): Women's height, reproductive success and the evolution of sexual dimorphism in modern humans. *Proceedings of the Royal Society of London, Biology* 269: 1919-23.

Nigg, BM and Grimston, SK (1994): Bone. In Nigg, BM and Herzog, W (eds.): Biomechanics of the Musculo-skeletal System. Chichester: Wiley.

Nordin, M and Frankel, VH (1989): Biomechanics of the knee. In Nordin, M and Frankel, VH (eds.): Basic Biomechanics of the Musculoskeletal system. Philadelphia: Lea & Febiger.

Oates, JF, Whitesides, GH, Davies, AG, Waterman, PG, Green, SM, Dasilva, GL and Mole, S (1990): Determinants of variation in tropical forest biomass: new evidence from West Africa. *Ecology* 71: 328-43.

O'Connor, J, Shercliff, T, FitzPatrick, D, Bradley, J, Daniel, DM, Biden, E and Goodfellow, J (1990): Geometry of the knee. In Daniel, DM, Akeson, WH and O'Connor, JJ (eds.): Knee Ligaments: Structure, Function, Injury, and Repair. New York: Raven Press.

Ogden, JA (1984): Radiology of postnatal skeletal development X. Patella and tibial tuberosity. *Skeletal Radiology* 11: 246-57.

Ogden, JA (1990): Development and maturation of the neuromusculoskeletal system. In Morrissy, RT (ed.): Lovell and Winter's Pediatric Orthopaedics. Philadelphia: J B Lippincott.

Ogden, JA, Grogan, DP and Light, TR (1987): Postnatal Development and Growth of the Musculoskeletal System. In Albright, JA and Brand, RA (eds.): The Scientific Basis of Orthopaedics. Connecticut: Appleton & Lange.

O'Higgins, P (1989): Developments in cranial morphometrics. *Folia Primatologica* 53: 101-24.

O'Higgins, P (1997): Methodological issues in the description of forms. In Lestrel, PE (ed.): Fourier Descriptors and their Applications in Biology. Cambridge: Cambridge University Press.

O'Higgins, P and Dryden, IL (1993): Sexual dimorphism in hominoids: further studies of craniofacial shape differences in *Pan*, *Gorilla* and *Pongo*. *Journal of Human Evolution* 24: 183-205.

Ohtsuki, F, Uetake, T, Adachi, K, Lestrel, PE and Hanihara, K (1997): Fourier analysis of size and shape changes in Japanese skulls. In Lestrel (ed.): Fourier Descriptors and their Applications in Biology. Cambridge: Cambridge University Press.

Olerud, C and Berg, P (1984): The variation of the Q angle with different positions of the foot. *Clinical Orthopaedics and Related Research* 191: 162-5.

O'Rahilly, R and Gardner, E (1975): The timing and sequence of events in the development of the limbs in the human embryo. *Anatomy and Embryology* 148: 1-23.

Outerbridge, RE (1964): Further studies on the etiology of chondromalacia patellae. *Journal of Bone and Joint Surgery* 46B: 179-90.

Oxnard, CE (1971): Tensile forces in skeletal structures. *Journal of Morphology* 134: 425-36.

Oxnard, CE (1978): One biologist's view of morphometrics. *Annual Review of Ecology and Systematics* 9: 219-41.

Oxnard, CE (1979): Some methodological factors in studying the morphological-behavioral interface. In Morbeck, ME, Preuschoft, H and Gomberg, N (eds.): Environment, Behavior, and Morphology: Dynamic Interactions in Primates. New York: Gustav Fisher.

Oxnard, CE (1983a): The Order of Man. A Biomathematical Anatomy of the Primates. Hong Kong: Hong Kong University Press.

Oxnard, CE (1983b): Sexual dimorphisms in the overall proportions of primates. *American Journal of Primatology* 4: 1-22.

Oxnard, CE (1984): Interpretation and testing in multivariate statistical approaches to physical anthropology: the example of sexual dimorphism in the primates. In van Vark, GN and Howells, WW (eds.): Multivariate Statistical Methods in Physical Anthropology. Dordrecht: D. Reidel Publishing Company.

Parsons, FG (1914): The characters of the English thigh-bone. *Journal of Anatomy* 48: 238-67.

Pawlowski, B, Dunbar, RIM and Lipowicz, A (2000): Tall men have more reproductive success. *Nature* 403: 156.

Pead, MJ, Skerry, TM and Lanyon, LE (1988): Direct transformation from quiescence to bone formation in the adult periosteum following a single brief period of bone loading. *Journal of Bone and Mineral Research* 3: 647-56.

Pearson, K and Bell, J (1919): Drapers' Company Research Memoirs Biometric Series X. A Study on the Long Bones of the English Skeleton. Part I. The Femur. London: Cambridge University Press.

Perry, J (1992): Gait Analysis. Normal and Pathological Function. Thorofare: Slack.

Pielou, EC (1984): The Interpretation of Ecological Data. New York: John Wiley & Sons.

Pigliucci, M, Schlichting, CD, Jones, CS and Schwenk, K (1996): Developmental reaction norms: the interactions among allometry, ontogeny and plasticity. *Plant Species Biology* 11: 69-85.

Pimentel, RA (1992): An introduction to ordination, principal components analysis and discriminant analysis. In Sorensen, JT and Foottit, R (eds.): Ordination in the Study of Morphology, Evolution and Systematics of Insects: Applications and Quantitative Genetic Rationales. Amsterdam: Elsevier.

Pirola, CJ, Wang, HM, Strgacich, MI, Kamyar, A, Cercek, B, Forrester, JS, Clemens, TL and Fagin, JA (1994): Mechanical stimuli induce vascular parathyroid hormone-related protein gene expression in vivo and in vitro. *Endocrinology* 134: 2230-6.

Plavcan, JM (2002): Taxonomic variation in the pattern of craniofacial dimorphism in primates. *Journal of Human Evolution* 42: 579-608.

Plavcan, JM and van Schaik, CP (1992): Intrasexual competition and canine dimorphism in anthropoid primates. *American Journal of Physical Anthropology* 87: 461-77.

Polk, JD (2002): Adaptive and phylogenetic influences on musculoskeletal design in cercopithecine primates. *Journal of Experimental Biology* 205: 3399-412.

Pollock, CM and Shadwick, RE (1994): Allometry of muscle, tendon, and elastic energy storage capacity in mammals. *American Journal of Physiology* 266: R1022-31.

Post, D, Goldstein, S and Melnick, D (1978): An analysis of cercopithecoid odontometrics. II. Relations between dental dimorphism, body size dimorphism and diet. *American Journal of Physical Anthropology* 49: 533-44.

Premoli, AC (1996): Leaf architecture of South American *Nothofagus* (Nothofagaceae) using traditional and new methods in morphometrics. *Botanical Journal of the Linnean Society* 121: 25-40.

Prescher, A and Klümpen, T (1995): Does the area of the glenoid cavity of the scapula show sexual dimorphism? *Journal of Anatomy* 186: 223-6.

Preuschoft, H (1970): Functional anatomy of the lower extremity. In Bourne, GH (ed.): The Chimpanzee. Basel: S. Karger.

Preuschoft, H (1979): Motor behavior and shape of the locomotor apparatus. In Morbeck, ME, Preuschoft, H and Gomberg, N (eds.): Environment, Behavior, and Morphology: Dynamic Interactions in Primates. New York: Gustav Fisher.

Preuschoft, H and Tardieu, C (1996): Biomechanical reasons for the divergent morphology of the knee joint and the distal epiphyseal suture in hominoids. *Folia Primatologica* 66: 82-92.

Preuschoft, H and Weinmann, W (1973): Biomechanical investigations of *Limnopithecus* with special reference to the influence exerted by body weight on bone thickness. *American Journal of Physical Anthropology* 38: 241-50.

Prost, JH (1965): A definitional system for the classification of primate locomotion. *American Anthropologist* 67: 1198-214.

Raab, DM, Crenshaw, TD, Kimmel, DB and Smith, EL (1991): A histomorphometric study of cortical bone activity during increased weight-bearing exercise. *Journal of Bone and Mineral Research* 6: 741-9.

Radin, EL, Orr, RB, Kelman, JL, Paul, IL and Rose, RM (1982): Effect of prolonged walking on concrete on the knees of sheep. Journal of Biomechanics 15: 487-92.

Raff, RA (1996): The Shape of Life. Genes, Development, and the Evolution of Animal Form. Chicago: University of Chicago Press.

Rafferty, KL (1998): Structural design of the femoral neck in primates. *Journal of Human Evolution* 34: 361-83.

Rajendran, K (1985): Mechanism of locking at the knee joint. *Journal of Anatomy* 143: 189-94.

Rális, ZA, Rális, HM, Randall, M, Watkins, G and Blake, PD (1976): Changes in shape, ossification and quality of bones in children with spina bifida. *Developmental Medicine and Child Neurology* 18: 29-41.

Ralls, K (1977): Sexual dimorphism in mammals: avian models and unanswered questions. *American Naturalist* 111: 917-38.

Ranta, E, Laurila, A and Elmberg, J (1994): Reinventing the wheel: analysis of sexual dimorphism in body size. *Oikos* 70: 313-21.

Rao, CR (1964): The use and interpretation of principal component analysis in applied research. *Sankhya A*26: 329-58.

Rayner, JMV (1985): Linear relations in biomechanics: the statistics of scaling functions. *Journal of Zoology London* 206: 415-39.

Read, DW and Lestrel, PE (1986): Comment on uses of homologous-point measures in systematics: a reply to Bookstein et al. *Systematic Zoology* 35: 241-53.

Reddi, AH (1994): Cartilage morphogenesis: role of bone and cartilage morphogenetic proteins, homeobox genes and extracellular matrix. *Matrix Biology* 14: 599-606.

Reider, B, Marshall, JL, Koslin, B, Ring, B and Girgis, FG (1981): The anterior aspect of the knee joint. An anatomical study. *Journal of Bone and Joint Surgery* 63A: 351-6.

Remis, M (1995): Effects of body size and social context on the arboreal activities of lowland gorillas in the Central African Republic. *American Journal of Physical Anthropology* 97: 413-33.

Rencher, AC (1995): Methods of Multivariate Analysis. New York: John Wiley & Sons.

Rendel, JM (1979): Canalisation and selection. In Thompson, JN and Thoday, JM (eds.): Quantitative Genetic Variation. New York: Academic Press.

Reyment, RA (1980): On the interpretation of the smallest principal component. *Bulletin of the Geological Institutions of the University of Uppsala* 8: 1-4.

Reyment, RA, Blackith, RE and Campbell, NA (1984): Multivariate Morphometrics (2nd ed.). London: Academic Press.

Reyment, RA and Jöreskog, KG (1993): Applied Factor Analysis in the Natural Sciences (2nd ed.). Cambridge: Cambridge University Press.

Reynolds, JD and Harvey, PH (1994): Sexual selection and the evolution of sex differences. In Short, RV and Balaban, E (eds.): The Differences between the Sexes. Cambridge: Cambridge University Press.

Rice, BJ and Strange, JD (1977): College Algebra. Boston: Prindle, Weber & Schmidt.

Rigal, WM (1962): The use of tritiated thymidine in studies of chondrogenesis. In Lacroix, P and Budy, AM (eds.): Radioisotopes and Bone. Oxford: Blackwell Scientific Publications.

Rincón, PA (2000): Big fish, small fish: still the same species. Lack of morphometric evidence of the existence of two sturgeon species in the Guadalquivir river. *Marine Biology* 136: 715-23.

Ripley, S (1967): The leaping of langurs: a problem in the study of locomotor adaptation. *American Journal of Physical Anthropology* 26: 149-70.

Roach, HI, Baker, JE and Clarke, NMP (1998): Initiation of the bony epiphysis in long bones: chronology of interactions between the vascular system and the chondrocytes. *Journal of Bone and Mineral Research* 13: 950-61.

Rodman, PS (1979): Skeletal differentiation of *Macaca fascicularis* and *Macaca nemestrina* in relation to arboreal and terrestrial quadrupedalism. *American Journal of Physical Anthropology* 51: 51-62.

Rodríguez, JI, Palacios, J, Ruiz, A, Sanchez, M, Alvarez, I and Demiguel, E (1992): Morphological changes in long bone development in fetal akinesia deformation sequence: an experimental study in curarized rat fetuses. *Teratology* 45: 213-21.

Rohlf, FJ (1986-1998): NTSYSpc. Applied Biostatistics Inc. Version 2.02k.

Rohlf, FJ (1986): Relationships among eigenshape analysis, Fourier analysis, and analysis of coordinates. *Mathematical Geology* 18: 845-54.

Rohlf, FJ (1990): Rotational fit (Procrustes) methods. In Rohlf, FJ and Bookstein, FL (eds.): Proceedings of the Michigan Morphometrics Workshop. Ann Arbor: Univeristy of Michigan Museum of Zoology.

Rohlf, FJ and Archie, JW (1984): A comparison of Fourier methods for the description of wing shape in mosquitoes (Diptera: Culicidae). *Systematic Zoology* 33: 302-17.

Rohlf, FJ and Marcus, LF (1993): A revolution in morphometrics. *Trends in Ecology and Evolution* 8: 129-32.

Rohlf, FJ and Sokal, RR (1965): Coefficients of correlation and distance in numerical taxonomy. *University of Kansas Science Bulletin* 45: 3-27.

Rohlf, FJ and Sokal, RR (1981): Comparing numerical taxonomic studies. *Systematic Zoology* 30: 459-90.

Rohlf, FJ and Sokal, RR (1995): Statistical Tables (3rd ed.). New York: WH Freeman and Company.

Rollinson, J and Martin, RD (1981): Comparative aspects of primate locomotion, with special reference to arboreal cercopithecines. *Symposia of the Zoological Society of London* 48: 377-427.

Rose, MD (1973): Quadrupedalism in primates. *Primates* 14: 337-57.

Ross, WD and Ward, R (1982): Human proportionality and sexual dimorphism. In Hall, RL (ed.): Sexual Dimorphism in *Homo sapiens*. A Question of Size. New York: Praeger.

Rubin, CT and Lanyon, LE (1984): Dynamic strain similarity in vertebrates; an alternative to allometric limb bone scaling. *Journal of Theoretical Biology* 107: 321-7.

Rubin, CT and Lanyon, LE (1987): Osteoregulatory nature of mechanical stimuli: function as a determinant for adaptive remodeling in bone. *Journal of Orthopaedic Research* 5: 300-10.

Rubin, C, Turner, AS, Mallinckrodt, C, Jerome, C, McLeod, K and Bain, S (2002): Mechanical strain, induced noninvasively in the high-frequency domain, is anabolic to cancellous bone, but not cortical bone. *Bone* 30: 445-52.

Ruff, C (1987): Sexual dimorphism in human lower limb bone structure: relationship to subsistence strategy and sexual division of labor. *American Journal of Physical Anthropology* 16: 391-416.

Ruff, C (1988): Hindlimb articular surface allometry in Hominoidea and *Macaca*, with comparisons to diaphyseal scaling. *Journal of Human Evolution* 17: 687-714.

Ruff, C (1990): Body mass and hindlimb bone cross-sectional and articular dimensions in anthropoid primates. In Damuth, J and MacFadden, BJ (eds.): Body Size in Mammalian Paleobiology. Estimation and Biological Implications. Cambridge: Cambridge University Press.

Ruff, CB (1995): Biomechanics of the hip and birth in early *Homo*. *American Journal of Physical Anthropology* 98: 527-74.

Ruff, CB (2000): Biomechanical analyses of archaeological human skeletons. In Katzenberg, MA and Saunders, SR (eds.): Biological Anthropology of the Human Skeleton. New York: Wiley-Liss.

Ruff, CB (2002): Long bone articular and diaphyseal structure in Old World monkeys and apes. I: Locomotor effects. *American Journal of Physical Anthropology* 119: 305-42.

Ruff, CB and Hayes, WC (1982): Subperiosteal expansion and cortical remodeling of the human femur and tibia with aging. *Science* 217: 945-8.

Ruff, CB and Hayes, WC (1983a): Cross-sectional geometry of Pecos Pueblo femora and tibiae - a biomechanical investigation: I. Method and general patterns of variation. *American Journal of Physical Anthropology* 60: 359-81.

Ruff, CB and Hayes, WC (1983b): Cross-sectional geometry of Pecos Pueblo femora and tibiae - a biomechanical investigation: II. Sex, age, and side differences. *American Journal of Physical Anthropology* 60: 383-400.

Ruff, CB and Runestad, JA (1992): Primate limb bone structural adaptations. *Annual Review of Anthropology* 21: 407-33.

Ruff, CB, Trinkaus, E, Walker, A and Larsen, CS (1993): Postcranial robusticity in *Homo*. I: temporal trends and mechanical interpretation. *American Journal of Physical Anthropology* 91: 21-53.

Ruff, CB, Walker, A and Trinkaus, E (1994): Postcranial robusticity in *Homo*. III: ontogeny. *American Journal of Physical Anthropology* 93: 35-54.

Scammon, RE and Calkins, LA (1929): The Development and Growth of the External Dimensions of the Human Body in the Fetal Period. Minneapolis: University of Minnesota Press.

Schaffler, MB, Burr, DB, Jungers, WL and Ruff, CB (1985): Structural and mechanical indicators of limb specialization in primates. *Folia Primatologica* 45: 61-75.

Schmitt, D (1999): Compliant walking in primates. *Journal of Zoology London* 248: 149-60.

Schodek, DL (1980): Structures. Eaglewood Cliffs: Prentice-Hall.

Schutzer, SF, Ramsby, GR and Fulkerson, JP (1986): The evaluation of patellofemoral pain using computerized tomography. A preliminary study. *Clinical Orthopaedics and Related Research* 204: 286-93.

Seal, HL (1964): Multivariate Statistical Analysis for Biologists. London: Methuen and Co.

Seebacher, JR, Inglis, AE, Marshall, JL and Warren, RF (1982): The structure of the posterolateral aspect of the knee. *Journal of Bone and Joint Surgery* 64A: 536-41.

Seiffert, ER and Kappelman, J (2001): Morphometric variation in the hominoid orbital aperture: a case study with implications for the use of variable characters in Miocene catarrhine systematics. *Journal of Human Evolution* 40: 301-18.

Seim, E and Sæther, BE (1983): On rethinking allometry: which regression model to use? *Journal of Theoretical Biology* 104: 161-8.

Shea, BT (1981): Relative growth of the limbs and trunk in the African apes. *American Journal of Physical Anthropology* 56: 179-201.

Shea, BT (1983): Allometry and heterochrony in the African apes. *American Journal of Physical Anthropology* 62: 275-89.

Shea, BT (1985a): Bivariate and multivariate growth allometry: statistical and biological considerations. *Journal of Zoology London* 206: 367-90.

Shea, BT (1985b): Ontogenetic allometry and scaling. A discussion based on the growth and form of the skull in African apes. In Jungers, WL (ed.): Size and Scaling in Primate Biology. New York: Plenum Press.

Shea, BT (1985c): The ontogeny of sexual dimorphism in the African apes. *American Journal of Primatology* 8: 183-8.

Shefelbine, SJ, Tardieu, C and Carter, DR (2002): Development of the femoral bicondylar angle in hominid bipedalism. *Bone* 30: 765-70.

Sinclair, D and Dangerfield, P (1998): Human Growth after Birth (6th ed.). Oxford: Oxford University Press.

Smillie, IS (1971): Injuries of the Knee Joint (4th ed.). Edinburgh: Churchill Livingstone.

Smit, TH and Burger, EH (2000): Is BMU-coupling a strain-regulated phenomenon? A finite element analysis. *Journal of Bone and Mineral Research* 15: 301-7.

Smith, RJ (1980): Rethinking allometry. *Journal of Theoretical Biology* 87: 97-111.

Smith, RJ (1999): Statistics of sexual size dimorphism. *Journal of Human Evolution* 36: 423-59.

Smith, RJ and Jungers, WL (1997): Body mass in comparative primatology. *Journal of Human Evolution* 32: 523-59.

Smith, RJ and Leigh, SR (1998): Sexual dimorphism in primate neonatal body mass. *Journal of Human Evolution* 34: 173-201.

Smith-Gill, SJ (1983): Developmental plasticity: developmental conversion versus phenotypic modulation. *American Zoologist* 23: 47-55.

Sneath, PHA and Sokal, RR (1973): Numerical Taxonomy. San Francisco: WH Freeman and Company.

Sokal, RR and Rohlf, FJ (1962): The comparison of dendrograms by objective methods. *Taxon* 11: 33-40.

Sokal, RR and Rohlf, FJ (1995): Biometry (3rd ed.). New York: WH Freeman and Company.

Solursh, M (1983): Cell-cell interactions and chondrogenesis. In Hall, BK (ed.): Cartilage. Volume 2. Development, Differentiation, and Growth. London: Academic Press.

Sprent, P (1968): Linear relationships in growth and size studies. *Biometrics* 24: 639-56.

Sprent, P (1969): Models in Regression and Related Topics. London: Methuen & Co.

Sprent, P (1972): The mathematics of size and shape. *Biometrics* 28: 23-37.

Sprent, P and Dolby, GR (1980): The geometric mean functional relationship. *Biometrics* 36: 547-50.

SPSS Inc (1989-1999): SPSS for Windows. Version 10.0.5.

Stanford, CB, Wallis, J, Matama, H and Goodall, J (1994): Patterns of predation by chimpanzees on red colobus monkeys in Gombe National Park, 1982-1991. *American Journal of Physical Anthropology* 94: 213-28.

Stern, JT (1971a): Functional interpretation of the differences between primates with regard to the musculus biceps femoris and musculi vasti. Proceedings of the Third International Congress of Primatology, Zurich 1970.

Stern, JT (1971b): Functional myology of the hip and thigh of cebid monkeys and its implications for the evolution of erect posture. *Bibliotheca Primatologica* 14: 1-318.

Stern, JT and Oxnard, CE (1973): Primate locomotion: some links with evolution and morphology. *Primatologia* 4: 1-93.

Steudel, K (1981): Sexual dimorphism and allometry in primate ossa coxae. *American Journal of Physical Anthropology* 55: 209-15.

Steudel, K (1982): Allometry and adaptation in the catarrhine postcranial skeleton. *American Journal of Physical Anthropology* 59: 431-41.

St-Jacques, B, Hammerschmidt, M and McMahon, AP (1999): Indian hedgehog signaling regulates proliferation and differentiation of chondrocytes and is essential for bone formation. *Genes & Development* 13: 2072-86.

Strasser, E (1992): Hindlimb proportions, allometry, and biomechanics in old world monkeys (primates, Cercopithecidae). *American Journal of Physical Anthropology* 87: 187-213.

Struhsaker, TT (1969): Correlates of ecology and social organization among African cercopithecines. *Folia Primatologica* 11: 80-118.

Swartz, SM (1989): The functional morphology of weight bearing: limb joint surface area allometry in anthropoid primates. *Journal of Zoology London* 218: 441-60.

Tague, RG (1992): Sexual dimorphism in the human bony pelvis, with a consideration of the Neandertal pelvis from Kebara cave, Israel. *American Journal of Physical Anthropology* 88: 1-21.

Tanaka, H (1999): Numerical analysis of the proximal humeral outline: bilateral shape differences. *American Journal of Human Biology* 11: 343-57.

Tardieu, C (1993): L'angle bicondylaire du fémur est-il homologue chez l'homme et les primates non humains? Réponse ontogénétique. *Bulletins et Mémoires de la Société d'Anthropologie de Paris* 5: 159-68.

Tardieu, C and Damsin, JP (1997): Evolution of the angle of obliquity of the femoral diaphysis during growth - correlations. *Surgical and Radiologic Anatomy* 19: 91-7.

Tardieu, C and Preuschoft, H (1996): Ontogeny of the knee joint in humans, great apes and fossil hominids: pelvi-femoral relationships during postnatal growth in humans. *Folia Primatologica* 66: 68-81.

Tardieu, C and Trinkaus, E (1994): Early ontogeny of the human femoral bicondylar angle. *American Journal of Physical Anthropology* 95: 183-95.

Taylor, AB (1997): Relative growth, ontogeny, and sexual dimorphism in *Gorilla* (*Gorilla gorilla gorilla* and *G. g. beringei*): evolutionary and ecological considerations. *American Journal of Primatology* 43: 1-31.

Thompson, DW (1946): On Growth and Form. Cambridge: Cambridge University Press.

Thorogood, P (1983): Morphogenesis of cartilage. In Hall, BK (ed.): Cartilage. Volume 2. Development, Differentiation, and Growth. London: Academic Press.

Tickle, C (1994): On making a skeleton. *Nature* 368: 587-8.

Torday, JS and Sanchez-Esteban, J (1998): Paracrine mediators of mechanotransduction in lung development. *American Journal of the Medical Sciences* 316: 205-8.

Trinkaus, E (1983): The Shanidar Neandertals. New York: Academic Press.

Trinkaus, E (2000): Human patellar articular proportions: recent and Pleistocene patterns. *Journal of Anatomy* 196: 473-83.

Trinkaus, E, Churchill, SE and Ruff, CB (1994): Postcranial robusticity in *Homo*. II: humeral bilateral asymmetry and bone plasticity. *American Journal of Physical Anthropology* 93: 1-34.

Trinkaus, E and Rhoads, ML (1999): Neandertal knees: power lifters in the Pleistocene? *Journal of Human Evolution* 37: 833-59.

Turner, TR, Anapol, F and Jolly, CJ (1997): Growth, development, and sexual dimorphism in vervet monkeys (*Cercopithecus aethiops*) at four sites in Kenya. *American Journal of Physical Anthropology* 103: 19-35.

Urban, JPG (1994): The chondrocyte: a cell under pressure. *British Journal of Rheumatology* 33: 901-8.

van Dam, J (1996): Stephanodonty in fossil murids. A landmark-based morphometric approach. In Marcus, LF, Corti, M, Loy, A, Naylor, GJP and Slice, DE (eds.): Advances in Morphometrics. New York: Plenum Press.

van der Eerden, BCJ, Emons, J, Ahmed, S, van Essen, JW, Lowik, CWGM, Wit, JM and Karperien, M (2002): Evidence for genomic and nongenomic actions in estrogen in growth plate regulation in female and male rats at the onset of sexual maturation. *Journal of Endocrinology* 175: 277-88.

van der Meulen, MCH, Beaupré, GS and Carter, DR (1993): Mechanobiologic influences in long bone cross-sectional growth. *Bone* 14: 635-42.

van der Meulen, MCH, Jepsen, KJ and Mikic, B (2001): Understanding bone strength: size isn't everything. *Bone* 29: 101-4.

van Eijden, TMGJ, de Boer, W and Weijs, WA (1985): The orientation of the distal part of the quadriceps femoris muscle as a function of the knee flexion-extension angle. *Journal of Biomechanics* 10: 803-9.

van Eijden, TMGJ, Weijs, WA, Kouwenhoven, E and Verburg, J (1987): Forces acting on the patella during maximal voluntary contraction of the quadriceps femoris muscle at different knee flexion/extension angles. *Acta Anatomica* 129: 310-4.

Vilensky, JA and Gankiewicz, E (1990): Effects of growth and speed on hindlimb joint angular displacement patterns in vervet monkeys (*Cercopithecus aethiops*). *American Journal of Physical Anthropology* 81: 441-9.

Vortkamp, A, Lee, K, Lanske, B, Segre, GV, Kronenberg, HM and Tabin, CJ (1996): Regulation of rate of cartilage differentiation by Indian hedgehog and PTH-related protein. *Science* 273: 613-21.

Waddington, CH (1942): Canalization of development and the inheritance of acquired characters. *Nature* 150: 563-5.

Waddington, CH (1957): The Strategy of the Genes. London: George Allen & Unwin.

Waddington, CH (1959): Canalization of development and genetic assimilation of acquired characters. *Nature* 183: 1654-5.

Wagner, GP and Altenberg, L (1996): Complex adaptations and the evolution of evolvability. *Evolution* 50: 967-76.

Walji, AH and Fasana, FV (1983): Structural and functional organization of the suprapatella in two Cercopithecines. *Journal of Morphology* 176: 113-9.

Wallis, GA (1996): Bone growth: coordinating chondrocyte differentiation. *Current Biology* 6: 1577-80.

Walmsley, R (1940): The development of the patella. *Journal of Anatomy* 74: 360-8.

Walmsley, T (1933): The vertical axes of the femur and their relations. A contribution to the study of the erect position. *Journal of Anatomy* 67: 284-300.

Wanner, JA (1977): Variations in the anterior patellar groove of the human femur. *American Journal of Physical Anthropology* 47: 99-102.

Ward, CV, Ruff, CB, Walker, A, Teaford, MF, Rose, MD and Nengo, IO (1995): Functional morphology of *Proconsul* patellas from Rusinga Island, Kenya, with implications for other Miocene-Pliocene catarrhines. *Journal of Human Evolution* 29: 1-19.

Warren, LF and Marshall, JL (1979): The supporting structures and layers on the medial side of the knee. *Journal of Bone and Joint Surgery* 61A: 56-62.

Watts, DP (1996): Comparative socio-ecology of gorillas. In McGrew, WC, Marchant, LF and Nishida, T (eds.): Great Ape Societies. Cambridge: Cambridge University Press.

Weinstabl, R, Scharf, W and Firbas, W (1989): The extensor apparatus of the knee joint and its peripheral vasti: anatomic investigation and clinical relevance. *Surgical and Radiologic Anatomy* 11: 17-22.

Wiberg, G (1941): Roentgenographic and anatomic studies on the femoropatellar joint. With special reference to chondromalacia patellae. *Acta Orthopaedica Scandinavica* 12: 319-410.

Williams, EJ (1959): Regression Analysis. New York: John Wiley & Sons.

Williams, PL, Warwick, R, Dyson, M and Bannister, LH (1989): Gray's Anatomy (37th ed.). Edinburgh: Churchill Livingstone.

Willner, LA and Martin, RD (1985): Some basic principles of mammalian sexual dimorphism. In Ghesquiere, J, Martin, RD and Newcombe, F (eds.): Human Sexual Dimorphism. London: Taylor & Francis.

Wolpert, L (1982): Cartilage morphogenesis in the limb. In Bellairs, R, Curtis, A and Dunn, G (eds.): Cell Behaviour. Cambridge: Cambridge University Press.

Wolpoff, MH (1983): Lucy's lower limbs: long enough for Lucy to be fully bipedal? *Nature* 304: 59-61.

Wood, BA (1976): The nature and basis of sexual dimorphism in the primate skeleton. *Journal of Zoology London* 180: 15-34.

Wood, B (1985): Sexual dimorphism in the hominid fossil record. In Ghesquiere, J, Martin, RD and Newcombe, F (eds.): Human Sexual Dimorphism. London: Taylor & Francis.

Wood, CG and Lynch, JM (1996): Sexual dimorphism in the craniofacial skeleton of modern humans. In Marcus, LF, Corti, M, Loy, A, Naylor, GJP and Slice, DE (eds.): Advances in Morphometrics. New York: Plenum Press.

Woodland, LH and Francis, RS (1992): Parameters and comparisons of the quadriceps angle of college-age men and women in the supine and standing positions. *American Journal of Sports Medicine* 20: 208-11.

Yamagiwa, J (2001): Factors influencing the formation of ground nests by eastern lowland gorillas in Kahuzi-Biega National Park: some evolutionary implications of nesting behavior. *Journal of Human Evolution* 40: 99-109.

Yamaguchi, GT and Zajac, FE (1989): A planar model of the knee joint to characterize the knee extensor mechanism. *Journal of Biomechanics* 22: 1-10.

Young, IT, Walker, JE and Bowie, JE (1974): An analysis technique for biological shape. *Medinfo* 74: 843-9.

Zeiss, J, Saddemi, SR and Ebraheim, NA (1992): MR imaging of the quadriceps tendon: normal layered configuration and its importance in cases of tendon rupture. *American Journal of Roentgenology* 159: 1031-4.